

NUREG/CR-0030
SAND76-0587
RT

POOR ORIGINAL

PARC (Plutonium Accident Resistant Container) Program Research, Design, and Development

John A. Andersen, Thomas A. Duffey, Stephen A. Dupree, Robert H. Nilson

Printed July 1978



Sandia Laboratories

POOR ORIGINAL

Prepared for
U. S. NUCLEAR REGULATORY COMMISSION

1567 035

7912140

526,

NOTICE

This report was prepared as an account of work sponsored by an agency of the United States Government. Neither the United States Government nor any agency thereof, or any of their employees, makes any warranty, expressed or implied, or assumes any legal liability or responsibility for any third party's use, or the results of such use, of any information, apparatus, product or process disclosed in this report, or represents that its use by such third party would not infringe privately owned rights.

The views expressed in this report are not necessarily those of the U.S. Nuclear Regulatory Commission.

Available from
National Technical Information Service
Springfield, VA 22161

NUREG/CR-0030
SAND76-0587
RT

PARC (PLUTONIUM ACCIDENT RESISTANT CONTAINER) PROGRAM
RESEARCH, DESIGN, AND DEVELOPMENT

John A. Andersen
Thomas A. Duffey
Stephen A. Dupree
Robert H. Nilson

Manuscript Submitted: May 1978
Date Published: July 1978

Sandia Laboratories
Albuquerque, NM 87185
operated by
Sandia Corporation
for the
U.S. Department of Energy

Prepared for

Division of Safeguards, Fuel Cycle, and Environmental Research
Office of Nuclear Regulatory Research
U.S. Nuclear Regulatory Commission
Washington, DC 20555
Under Interagency Agreement DOE 40-550-75
NRC FIN No. A-1141

1567 037

1567 037

ACKNOWLEDGMENTS

The authors are indebted to a number of people who, directly or indirectly, have helped shape this work. They wish to acknowledge especially the contribution of Brian J. Joseph, the PARC program engineering science assistant. Among others are William Lahs, Wait Von Riesenmann, Ron Pope, Ken Cole, Mike Stone, Will Schmidt, and Steve H. Sutherland, who made many contributions to the program and this text.

ABSTRACT

The PARC (plutonium accident resistant container) project resulted in the design, development, and certification testing of a crashworthy air-transportable plutonium package (shipping container) for certification by the USNRC (Nuclear Regulatory Commission). This PAT-1 (plutonium air transportable) package survives a very severe sequential test program of impact, crush, puncture, slash, burn, and water immersion. There is also an individual hydrostatic pressure test. The package was engineered for a payload mass capacity of 3.15 kg of PuO_2 and a thermal capacity of 25 watts. The design rationale for very high energy absorption (impact, crush, puncture, and slash protection) with residual high-level fire protection, resulted in a reasonably small air-transportable package, advancing the packaging state-of-art. Optimization design iterations were utilized in the areas of impact energy absorption and stress and thermal analysis. Package test results are presented in relation to radioactive materials containment acceptance criteria, shielding and criticality standards.

1567 039

CONTENTS

	<u>Page</u>
CHAPTER 1 GENERAL INFORMATION	17
1.1 Introduction	17
1.2 Package Description	17
1.2.1 General	17
1.2.2 Packaging	18
1.2.3 Operational Features	22
1.2.4 Contents of Packaging	23
CHAPTER 2 STRUCTURAL CRITERIA, DESIGN, ANALYSIS, TESTS, AND RESULTS	25
2.1 Summary of Design and Acceptance Criteria	25
2.1.1 Prevailing Design Criteria	25
2.1.2 Other Design Criteria	27
2.1.3 Acceptance Criteria	27
2.2 Design and Analysis	28
2.2.1 Structural Design Description	28
2.2.2 Mass Properties	30
2.2.3 Mechanical Properties of Materials Used	30
2.2.4 Chemical and Galvanic Design Considerations	30
2.2.5 Positive Closure	31
2.2.6 Lifting Devices	31
2.2.7 Tiedowns	31
2.2.8 Load Resistance per 10 CFR 71.32a	32
2.2.9 External Pressure per 10 CFR 71.32b	32
2.2.10 Pressure per 10 CFR 71 Appendix A3	32
2.2.11 Compression per 10 CFR 71 Appendix A10	32
2.2.12 Containment Vessel Stress Analyses	32
2.2.13 Terminal Free-Fall Analysis	37
2.3 Test Program Requirements	37
2.3.1 NRC Qualification Tests	38
2.3.2 Normal Conditions of Transport per 10 CFR 71 Appendix A	40
2.3.3 Hypothetical Accident Conditions per 10 CFR 71 Appendix B	40
2.4 Test Program Results - Summary	40
2.4.1 NRC Qualification Criteria	40
2.4.2 Normal Conditions of Transport: 10 CFR 71 Appendix A	41
2.4.3 Hypothetical Accident Conditions: 10 CFR 71 Appendix B	42

CONTENTS (Cont)

	<u>Page</u>
2.5 Test Program Results - Detailed	42
2.5.1 NRC Qualification Criteria (Sequential Tests)	42
2.5.2 Individual Hydrostatic Tests	76
2.5.3 Summary of Acceptance Criteria Results of NRC Qualification Testing	82
2.5.4 Normal Conditions of Transport Tests per 10 CFR 71 Appendix A	83
2.5.5 Hypothetical Accident Conditions Tests per 10 CFR 71 Appendix B	92
2.6 Test Facilities	98
2.7 List of Appendices	99
References	99
APPENDIX 2A -- Package Impact Analysis	101
APPENDIX 2B -- Properties of Principle Materials Used in the PAT-1 Package	112
APPENDIX 2C -- Package Load Resistance per 10 CFR 71.32a	117
APPENDIX 2D -- External Pressure per 10 CFR 71.32b	123
APPENDIX 2E -- Pressure Analysis per 10 CFR 71 Appendix A3	125
APPENDIX 2F -- Compression analysis per 10 CFR 71 Appendix A10	137
APPENDIX 2G -- Terminal Free Fall	141
APPENDIX 2H -- Test Protocol	143
APPENDIX 2I -- Characterization of Surrogate UO ₂	155
APPENDIX 2J -- Test Facility Descriptions	157
CHAPTER 3 THERMAL EVALUATION	165
3.1 Summary	165
3.2 Thermal Properties of Materials	166
3.3 Technical Specifications	168
3.4 Thermal Evaluation for Normal Conditions of Transport	168
3.4.1 Thermal Models	170
3.4.2 Maximum Temperatures	178
3.4.3 Minimum Temperatures	178
3.4.4 Maximum Internal Pressure	178
3.4.5 Maximum Thermal Stresses	178
3.4.6 Evaluation of Package Performance for Normal Conditions of Transport	179
3.5 10 CFR 71 -- Thermal Accident Evaluation	179
3.5.1 Thermal Models	179
3.5.2 Package Conditions and Environment	183
3.5.3 Package Temperatures	183
3.5.4 Maximum Internal Pressure	183

CONTENTS (Cont)

	<u>Page</u>	
3.5.5	Maximum Thermal Stresses	183
3.5.6	Evaluation of Package Performance for the 10 CFR 71 Accident Conditions	183
3.6	NRC Qualification Criteria -- Thermal Accident Evaluation	184
3.6.1	Thermal Models	184
3.6.2	Package Conditions and Environment	189
3.6.3	Package Temperatures	191
3.6.4	Maximum Internal Pressure	191
3.6.5	Maximum Thermal Stresses	191
3.6.6	Evaluation of Package Performance for NRC Qualification Criteria Thermal Conditions	191
APPENDIX 3A	-- Test of Establish Thermal Resistance Values of PAT-1 Components	193
	References	199
CHAPTER 4	CONTAINMENT	201
4.1	Summary	201
4.2	Containment Boundary	202
4.2.1	TB-1 Containment Vessel	202
4.2.2	PC-1 Product Can	202
4.2.3	Closure	203
4.3	Requirements for Normal Conditions of Transport 10 CFR 71	203
4.3.1	Release of Radioactive Contents	203
4.3.2	Pressurization of Containment Vessel	205
4.4	Requirements for Accident Conditions of Transport 10 CFR 71	206
4.4.1	Release of Radioactive Contents	206
4.4.2	Pressurization of Containment Vessel	207
4.5	Requirements for NRC Qualification Criteria	209
4.5.1	Release of Radioactive Contents	209
4.5.2	Pressurization of Containment Vessel	211
	References	212
APPENDIX 4A	-- IAEA (A2) Quantity Containment Requirements	213
APPENDIX 4B	-- Application and Characterization of Surrogate UO ₂ Powder	215
APPENDIX 4C	-- Post-NRC-Qualification-Test Uranium Detection Measurements, Internal to TB-1 Containment Vessel	217

CONTENTS (Cont)

	<u>Page</u>
CHAPTER 5 RADIATION SHIELDING EVALUATION	221
5.1 Summary	221
5.2 Introduction	221
5.3 Source Definition	222
5.4 Shielding Calculations	223
5.5 Results	234
References	239
APPENDIX 5A -- Derivation of Worst-Case Source Terms for the PAT-1	241
CHAPTER 6 CRITICALITY EVALUATION	251
6.1 Summary	251
6.2 Introduction	252
6.3 Calculational Model	252
6.4 Benchmark Calculations	259
6.5 Results of Criticality Calculations	262
References	265
APPENDIX 6A -- Effect of Oxide Density on Neutron Self-Multiplication in the PAT-1	267
APPENDIX 6B -- Effect of Water Inside a TB-1 on Neutron Self-Multiplication in the PAT-1	259
APPENDIX 6C -- Criticality Analysis of Arrays of Bare TB-1's	273
APPENDIX 6D -- Tests of the Convergence of KENO Criticality Results	277
CHAPTER 7 OPERATING PROCEDURES	281
7.1 Procedures for Loading the PAT-1 Package	281
7.1.1 Loading of PuO ₂ Into the PC-1 Product Can	281
7.1.2 Loading the PC-1 Into the TB-1 Containment Vessel	281
7.1.3 Loading the TB-1 Containment Vessel Into the AQ-1 Overpack	282
7.1.4 Loading the AQ-1 Overpack Onto a Packing Skid	283
7.1.5 Replacement Operations for Copper Seal	284
7.2 Procedures for Unloading the Package	284
APPENDIX 7A -- Operating Procedures for Loading of PuO ₂ Into the PC-1 Product Can	287
APPENDIX 7B -- Loading the PC-1 Product Can Into the TB-1 Containment Vessel	289
APPENDIX 7C -- Loading the TB-1 Containment Vessel Into the AQ-1 Overpack	295
CHAPTER 8 ACCEPTANCE TESTS AND MAINTENANCE PROGRAM	305
8.1 Acceptance Tests to be Performed Prior to First Use of Each Package	305
8.1.1 Visual Inspection	305

CONTENTS (Cont)

	<u>Page</u>
8.1.2 Structural, Pressure, and Leak-Rate Tests of the TB-1 Containment Vessel	306
8.1.3 Leak Testing of PC-1 Product Can	306
3.2 Tests to Verify Proper Assembly Prior to Each Shipment	307
8.2.1 PC-1 Product Can	307
8.2.2 TB-1 Containment Vessel	307
8.3 Periodic Test and Maintenance	307
8.3.1 TB-1 Containment Vessel	307
8.3.2 PC-1 Product Can	307
8.3.3 Replacement of Gaskets on Containment Vessel	307
CHAPTER 9 QUALITY ASSURANCE	309
9.1 Discussion	309
9.2 Quality Assurance Program	309
9.2.1 Organization	310
9.2.2 Design Control	310
9.2.3 Procurement Document Control	312
9.2.4 Instructions, Procedures, and Drawings	312
9.2.5 Document Control	312
9.2.6 Control of Purchased Material	312
9.2.7 Identification and Control of Material Parts and Components	313
9.2.8 Control of Special Processes	313
9.2.9 Inspection	313
9.2.10 Test Control	313
9.2.11 Control of Measuring and Test Equipment	314
9.2.12 Handling and Related Functions	314
9.2.13 Inspection, Test, and Operating Status	314
9.2.14 Nonconforming Materials, Parts, or Components (in service)	314
9.2.15 Corrective Action	314
9.2.16 Quality Assurance Records	314
9.2.17 Audits	314
9.3 Certification of Compliance	314
APPENDIX 9A -- Hierarchical Index to PAT-1 Specification and Drawing System	315
APPENDIX 9B -- Certification of Compliance	395

ILLUSTRATIONS

<u>Figure</u>	<u>Page</u>
1. 2. 1-1. The PAT-1 Air Transportable Package	18
1. 2. 2-1. Cutaway of PAT-1 Package	19
1. 2. 2-2. The TB-1 Containment Vessel	21
1. 2. 2-3. TB-1 Disassembled	22
1. 2. 3-1. PAT-1 Package on Pallet	23
2. 2. 12. 3-1. Containment Vessel	35
2. 5. 1. 1-1. Top (0°) Impact	45
2. 5. 1. 1-2. Top (0°) Impact	45
2. 5. 1. 1-3. Postimpact Radiograph Showing TB-1 Containment Vessel (Top End (0°) Impact)	46
2. 5. 1. 1-4. Postimpact Package Measurements -- Top (0°) Impact	47
2. 5. 1. 1-5. Top Corner (30°) Impact	48
2. 5. 1. 1-6. Top Corner (30°) Impact	48
2. 5. 1. 1-7. Postimpact Radiograph Showing TB-1 Containment Vessel (Top Corner 30° Impact)	49
2. 5. 1. 1-8. Postimpact Package Measurements After Top Corner (30°) Impact	50
2. 5. 1. 1-9. Side (90°) Impact	52
2. 5. 1. 1-10. Side (90°) Impact	52
2. 5. 1. 1-11. Postimpact Package Measurements -- Side (90°) Impact	53
2. 5. 1. 1-12. Postimpact Radiograph Showing TB-1 Containment Vessel (Side (180°) Impact)	54
2. 5. 1. 1-13. Bottom Corner (150°) Impact	55
2. 5. 1. 1-14. Bottom Corner (150°) Impact	55
2. 5. 1. 1-15. Postimpact Measurements -- Bottom Corner (150°) Impact	56
2. 5. 1. 1-16. Postimpact Radiograph Showing TB-1 Containment Vessel (Bottom Corner (150°) Impact)	57
2. 5. 1. 1-17. Bottom (180°) Impact	58
2. 5. 1. 1-18. Bottom (180°) Impact	58
2. 5. 1. 1-19. Postimpact Measurements -- Bottom (180°) Impact	59
2. 5. 1. 1-20. Postimpact Radiograph Showing TB-1 Containment Vessel (Bottom End (180°) Impact)	60
2. 5. 1. 2-1. Crush Test	61
2. 5. 1. 2-2. Crush Test	62
2. 5. 1. 2-3. Crush Test	62
2. 5. 1. 3-1. Puncture Test on Top-End-Impacted PAT-1	63
2. 5. 1. 3-2. Puncture Test on Top-Corner-Impacted PAT-1	63
2. 5. 1. 3-3. Puncture Test on Side-Impacted PAT-1	63
2. 5. 1. 3-4. Puncture Test on Bottom-Corner-Impacted PAT-1	63
2. 5. 1. 3-5. Puncture Test on Bottom-End-Impacted PAT-1	64

1567 045

ILLUSTRATIONS (Cont)

<u>Figure</u>	<u>Page</u>
2.5.1.4-1. Slash Test	64
2.5.1.4-2. Slash Test	64
2.5.1.4-3. Slash Test	65
2.5.1.4-4. Slash Test	65
2.5.1.5-1. Preburn Appearance of Top-End-Impacted PAT-1	66
2.5.1.5-2. Preburn Appearance of Top-Corner-Impacted PAT-1	66
2.5.1.5-3. Preburn Appearance of Side-Impacted PAT-1	66
2.5.1.5-4. Preburn Appearance of Bottom-Corner-Impacted PAT-1	67
2.5.1.5-5. Preburn Appearance of Bottom-End-Impacted PAT-1	67
2.5.1.5-6. Burn Test	68
2.5.1.6-1. Postimmersion Test of Top-End-Impacted PAT-1	69
2.5.1.6-2. Immersion Test on Top-Corner-Impacted PAT-1	69
2.5.1.6-3. Immersion Test on Side-Impacted PAT-1	69
2.5.1.6-4. Postimmersion Test on Bottom-Corner-Impacted PAT-1	70
2.5.1.6-5. Postimmersion Test on Bottom-End-Impacted PAT-1	70
2.5.1.7-1. Disassembly of Top-End-Impacted PAT-1	71
2.5.1.7-2. AQ-1 Bottom Removed Showing Charred Redwood and Load Spreader	71
2.5.1.7-3. Top View of Load Spreader	71
2.5.1.7-4. Load Spreader Showing Redwood and Internal Plug (Circular Plate Load Spreader Removed)	71
2.5.1.7-5. Internal (Charred Redwood) Plug Removed Showing TB-1	72
2.5.1.7-6. TB-1 Removed from AQ-1	72
2.5.1.7-7. Bottom View of TB-1	72
2.5.1.7-8. Disassembly of Top-Corner-Impacted PAT-1	72
2.5.1.7-9. Disassembled Top-Corner-Impacted PAT-1	73
2.5.1.7-10. Disassembly of Side-Impacted PAT-1	73
2.5.1.7-11. Posttest TB-1 - Top View	73
2.5.1.7-12. Posttest TB-1 - Bottom View	73
2.5.1.7-13. Disassembly of Bottom-Corner-Impacted PAT-1	74
2.5.1.7-14. Load Spreader Showing Charred Redwood, Load Spreader, and Top of TB-1	74
2.5.1.7-15. Disassembled Bottom-Corner-Impacted PAT-1	74
2.5.1.7-16. TB-1 Removed From AQ-1	74
2.5.1.7-17. Disassembly of Bottom-End-Impacted PAT-1	75
2.5.1.7-18. Bottom-End-Impacted PAT-1 With Top Removed Showing Charred Redwood and Load Spreader	75
2.5.1.7-19. Load Spreader Disc Removed Showing Charred Redwood and Top of TB-1	75
2.5.1.7-20. TB-1 Removed From AQ-1	75

ILLUSTRATIONS (Cont)

<u>Figure</u>	<u>Page</u>
2.5.2.1-1. Hydrostatic Test Chamber and TB-1	77
2.5.2.1-2. Posthydrostatic Test	77
2.5.2.2-1. Cold (-40°F) Impact of Prototype PAT Package	78
2.5.2.2-2. Radiograph of Cold (-40°F) Impacted Prototype PAT Package	79
2.5.2.2-3. Hot (200°F) Impacted Prototype PAT Package	80
2.5.2.2-4. Radiograph of Hot (200°F) Impacted PAT Package	81
2.5.4.2-1. PAT-1 After 215°F Environment for 48 hours	84
2.5.4.5-1. PAT-1 Secured for Horizontal Transportation Vibration Test	86
2.5.4.5-2. PAT-1 Secured for Vertical Transportation Vibration Test	86
2.5.4.6-1. PAT-1 Being Subjected to Water Spray Test	87
2.5.4.7-1. Damage From 4-ft Drop Test	88
2.5.4.7-2. Damage From 4-ft Drop Test	88
2.5.4.7-3. Damage From 4-ft Drop Test	88
2.5.4.9-1. Slight Dimple Resulting From 10 CFR 71. A. 8 Penetration Test	89
2.5.4.10-1. Compression Test	90
2.5.4.10-2. Compression Test	90
2.5.4.11-1. Disassembled TB-1 Following 10 CFR 71. A Tests	91
2.5.5.2-1. Damage From 30-ft Side Drop	93
2.5.5.2-2. Damage Resulting From 30-ft Side, Top Corner, and Bottom Corner Drops	93
2.5.5.2-3. Damage Resulting From 30-ft Side, Top Corner, Bottom Corner, Bottom, and Top End Drops	94
2.5.5.3-1. Impression on PAT-1 From Puncture Test	95
2.5.5.5-1. Water Immersion Test	96
2.5.5.6-1. Sectioned PAT-1 Showing 3-in. Char Depth	97
2.5.5.6-2. Sectioned PAT-1 Showing Char Depth and Essentially Unaffected Internal Redwood	97
2.5.5.6-3. Disassembled TB-1, Post 10 CFR 71 Test, Showing Roll Crimp Closure and Epoxy Overbonding Intact	98
2A-1. PAT-1 Impact Analysis	101
2A-2. Typical Load-Deflection Behavior for Redwood	104
2A-3. Static Crush Testing of Redwood	104
2A-4. Simplified PAT-1 Cross Section (not to scale) Showing Impact Surface	106
2A-5. Simplified PAT Cross Section (not to scale) Showing Initially Undeformed Regions A and B	108
2A-6. Impact Energy Balance	109
2B-1. Specific Energy to Lockup	115
2B-2. A Typical Load-Displacement Curve (at room temperature)	116
2B-3. Average Crush Stress for Redwood as a Function of Temperature	116
2C-1. Simple Beam Bending Model	118
2C-2. Simple Beam Undergoing Pure Bending	119

1567 047

ILLUSTRATIONS (Cont)

<u>Figure</u>		<u>Page</u>
2D-1.	PAT-1 Plutonium Air Transportable Package	123
2D-2.	Critical Stress Locations for 25-psi External Pressure Acting on TB Containment Vessel	124
2E-1.	TB-1 Containment Vessel	125
2E-2.	Internal Generalized Stresses at Cylinder-Head Intersection	126
2E-3.	Simply Supported, Uniformly Loaded Circular Plate-Load Case a.	128
2E-4.	Unsupported Plate Subjected to a Uniform Edge Moment	130
2E-5.	Membrane Stresses Due to Internal Pressure	132
2E-6.	Uniform Radial Shear on a Long Cylinder	133
2E-7.	Uniform Radial Edge Moment on a Long Cylinder	133
2E-8.	Graph of Resultant Hoop Stresses as a Function of Axial Distance	135
2E-9.	Maximum Values of Outside and Inner Surfaces	135
2F-1.	PAT-1 (Plutonium Air Transportable) Package Showing Load-Carrying End Ring	137
2F-2.	Detail of Container End Connection	138
2F-3.	Uniform Radial Edge Moment Induced by Axial Compressive-Loading of Container Flange	139
2G-1.	Terminal Velocity as a Function of Altitude and Initial Velocity for a Tumbling PAT-1	142
2J-1.	Rocket Pulldown Cable Facility	158
2J-2.	Rocket Pulldown Facility	158
2J-3.	Top (0°) Impact Test	159
2J-4.	Top Corner (30°) Impact Test	159
2J-5.	Side (90°) Impact Test	159
2J-6.	Bottom Corner (150°) Impact Test	160
2J-7.	Bottom Corner (180°) Impact Test	160
2J-8.	Static Test Machine	161
2J-9.	Puncture Test Facility	161
2J-10.	Slash Test Facility	163
3. 2-1.	Charring Data from Reference 3	167
3. 4-1.	Schematic of Numerical Model Used to Assess Solar Heating	168
3. 4-2.	Schematic of Internal Heat Flow Path	169
3. 4. 1. 2-1.	Results of Thermal Test (Solid Lines) and Comparison with Numerical Calculation (Symbols)	175
3. 4. 1. 2-2.	Daily Thermal Cycle of PAT-1 Subjected to Solar Radiation	176
3. 4. 1. 2-3.	Temperature Distribution in Redwood Overpack Just Before Sundown (Most Severe Case)	177
3. 4. 1. 2-4.	Temperature of PAT Redwood -- Severe Normal Environment	177
3. 5. 1. 2-1.	Luminous Flame Zone	182
3. 5. 1. 2-2.	Internal Package Conditions	182
3. 5. 1. 2-3.	Char Depth	182

ILLUSTRATIONS (Cont)

<u>Figure</u>	<u>Page</u>
3.6.1.2-1. Flame Temperature at Package Level	186
3.6.1.2-2. AQ-1 Drum Temperature	187
3.6.1.2-3. AQ-1 Drum Temperature	187
3.6.1.2-4. Flame Temperature at Package Level	187
3.6.1.2-5. Flame Temperature 1-hr Below Package Level	187
3.6.1.2-6. AQ-1 Drum Temperature	188
3.6.1.2-7. AQ-1 Drum Temperature	188
3.6.1.2-8. Flame Temperature at Package Level	188
3.6.1.2-9. AQ-1 Drum Temperature	188
3.6.2.2-1. Steel-Tub Burn Pit	190
3.6.2.2-2. Noncombustible Fence Surrounds Chimney	190
3.6.2.2-3. Storage Tanks for Water and JP-4 Fuel	190
4.2.3-1. Cross Section of TB-1 Seals	203
4C-1. First Opening of TB-1 Containment Vessel	218
4C-2. Product Can From Top-End-Impact Sequence	218
4C-3 - 4-10. Series Showing TB-1 Disassembly and Details of PC-1 Condition	219
5.4-1. One-Dimensional Model of the PAT-1 (Normal Operation)	224
5.4-2. Two-Dimensional Discrete-Ordinates Model of the PAT-1 (Normal Operation) in an Air-Over-Ground Geometry	226
5.4-3. Picture Printout of the MORSE Monte Carlo Model of the PAT-1	229
5A-1. Calculated Thermal Power Emitted by Pu Samples Consisting Initially of Pure Isotopes	242
5A-2. Calculated Gamma-Ray Energy-Emission Rate From Samples of Pu Consisting Initially of Pure Isotopes	242
5A-3. Calculated Neutron-Emission Rate From Samples of Pu Consisting Initially of Pure Isotopes	242
5A-4. Maximum PAT-1 Payload and Corresponding Neutron and Gamma Ray Energy Emission Rates for Case 2 PuO ₂ as a Function of Shelf Life	249
6.3-1. KENO Geometry Models for the PAT-1 and the TB-1, Normal Operating Conditions	254
6.3-2. Postaccident KENO Calculational Model for the PAT-1	256
6.3-3. Finite Array of 768 Impact-Damage PAT-1's, Redwood Replaced With Air, Externally Water Reflected	257
6.5-1. Calculational Model for an Infinite Array of Postaccident PAT-1 Packages	263
6.5-2. Calculational Model for Infinite Array of Impact-Damaged PAT-1's in Which the TB-1's are Arranged in Clusters of Eight	264
6B-1. Neutron Multiplication in the PAT-1, Normal Operation	270
6C-1. Neutron Multiplication in a Single TB-1	274
6C-2. Effect of Pitch on Neutron Self-Multiplication in Rectangular Arrays of TB-1's	275
6C-3. Neutron Self-Multiplication of a Worst-Case Finite Array of Bare TB-1's	276

ILLUSTRATIONS (Cont)

<u>Figure</u>		<u>Page</u>
7.1. 4 ¹	Shipping Configuration	283
7B-1 - 7B-6.	Parts for Loading PC-1 Product Can	290
7C-1 - 7C-14.	Loading Procedure for TB-1 Containment Vessel Into the AQ-1	296

CHAPTER 1
GENERAL INFORMATION

1.1 Introduction

This report describes the Plutonium Accident Resistant Container (PARC) program supporting research and the design, development and certification testing of the Plutonium Air Transportable (PAT) package and provides the necessary information to be considered by the USNRC (Nuclear Regulatory Commission) for a Safety Analysis Report (SAR) of the package.

The PAT package is designed primarily for the safe transport of plutonium oxide in powder form.

The package is resistant to severe accidents, especially the crash of high-speed jet aircraft. The package is designed to withstand such environments as hydrocarbon-fueled fires, extreme crushing, puncturing and slashing loads, and deep underwater immersion with no escape of contents. The accident environments may be imposed upon the package singly or sequentially.

The package meets the 10 CFR 71* Fissile Class I requirements with a cargo of 3.15 kg of $^{239}\text{PuO}_2$, or with any other isotopic form of plutonium oxide, not to exceed 25 watts (W) of thermal activity.

This report presents design and operational descriptions including evaluations and analyses, test results, maintenance, and quality assurance information.

1.2 Package Description

1.2.1 General

The PAT-1 package has a gross weight of approximately 500 lb (227 kg) when loaded with 3.15 kg of PuO_2 . The package measures 24-1/2 in. (62 cm) outside diameter and 42-1/2 in. (108 cm) in height. Its external appearance is a right circular cylinder of smooth stainless steel as shown in Figure 1.2.1-1.

Engineering drawings and specifications for the package are included in Appendix 9A. Material lists; dimensions; and material, process, and acceptance specifications are included on the drawings or in the specification documents.

* Title 10 of the Code of Federal Regulations Part 71 contains the rules and regulations of the NRC for the transportation of nuclear material. In referring to these and other regulations in the Code of Federal Regulations, an abbreviated form is used: "10 CFR 71.35(a)" meaning "Paragraph (a) of Section 71.35 of part 71 of Title 10 in the Code of Federal Regulations."

POOR ORIGINAL



Figure 1.2.1-1. The PAT-1 Air Transportable Package

1.2.2 Packaging

The PAT-1 package comprises three basic parts: (1) a stainless-steel containment vessel (designated TB-1); (2) a protective overpack assembly of redwood with an imbedded aluminum cylinder and aluminum discs, and a double-walled outer stainless-steel drum (designated as the AQ-1); and (3) a special product can (designated the PC-1) within the containment vessel, TB-1. The TB-1 serves as the containment vessel for the purpose of 10 CFR 71 and the NRC qualification criteria. The PC-1 provides the secondary containment as required by 10 CFR 71, Part 42.

Figure 1.2.2-1, a cutaway illustration of the PAT-1 package, shows its essential elements.

The outer drum assembly of the AQ-1 overpack consists of an outside 65-gal drum that is fully lined with an inside drum, both made of stainless steel. The inside drum has a cylindrical center section, which is bonded (fixed) to the outside drum, and separate end sections. The corners of the inside drum sections are rounded. The drum covers have integral skirt-extension members which, upon assembly, fit between the center and end sections of the inner drum. The C-ring cover clamp has a skirt extension that overlaps a region of the outside drum. Twenty-three 3/8-in. -diam bolts pass through these five layers of sheet metal (i. e., the C-clamp extension, the outside drum, the inner liner central section, the cover extension skirt, and the top or bottom end sections of the inner liner) and fasten into nut plates secured inside the inner end sections. Although the top C-ring can be removed by removing the draw bolt provided, the bottom C-ring is welded shut.

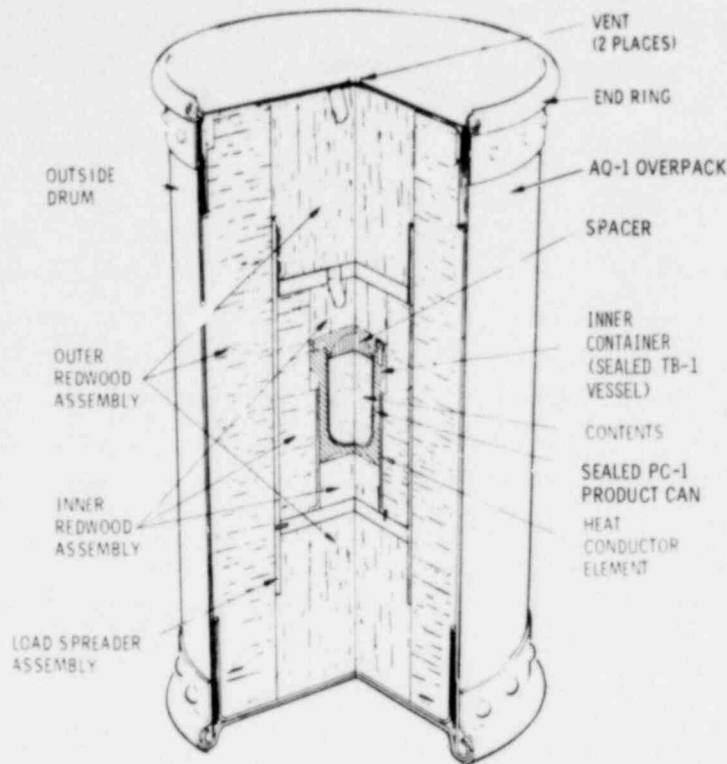


Figure 1.2.2-1. Cutaway of PAT-1 Package

The three wooden elements of the grain-oriented outer redwood assembly are fabricated from clear, select, kiln-dried redwood to take advantage of the specific energy absorption of this material and its fire-resistant characteristics. The elements are a large removable plug with longitudinally oriented grain, a hollow outer cylinder with essentially radial grain orientation fabricated as a series of wedges of wood arranged in a ring, and a large fixed plug with longitudinally oriented grain. The removable plug affords access to the AQ-1 interior. The outer redwood cylinder is bonded to the inner drum; the large fixed plug is bonded to the wooden outer cylinder and to the inner drum; and the large fixed plug is bonded to adjacent load-spreader members.

The bonding agent used to join the major subassemblies of wooden elements to adjacent metal or wooden elements is a polyester-flexibilized epoxy adhesive which has resilience over a wide temperature range. When impact forces cause deformations, this bond acts in unison with the wooden elements and their adjacent metal members.

The outer redwood cylinder affects the flow of heat between the interstitial load-spreader assembly and the outer containment-vessel assembly. The thickness of redwood utilized in the outer redwood cylinder does not significantly impede the outward conduction of any internal decay heat generated by the PuO_2 contents in the inner vessel. The dissipation of heat is accomplished

in conjunction with the load spreaders, using them as thermal conduction members. The outer redwood cylinder is sufficiently thick, however, to provide prolonged thermal protection from external high temperatures generated in a fire environment. This protection is afforded by a charring of the redwood which decreases its thermal conductivity.

The interstitial load-spreader assembly consists of a longitudinally oriented aluminum load-spreader tube, 24 in. (61 cm) long, 0.5 in. (1.27 cm) thick with an outside diameter of 12 in. (30 cm), and a complementary pair of aluminum discs 1 in. (2.54 cm) thick and 11 in. (28 cm) in diameter. One disc is removable to afford access to the TB-1 vessel; the other is bonded to adjacent members. The load spreaders distribute dynamic inertial compressive loading from a relatively small area of the vessel, the inner heat-conductor tube, and the inner grain-oriented redwood assemblies, into a relatively large area-loading of shock-absorbing material. The extension of the load-spreader tube beyond the two discs is a design feature that aids in performance of the load spreaders in the case of a corner impact (i. e., an impact that is neither axial nor lateral in principal attitude). In a side or lateral impact, the tube is the principal load spreader. In an end or longitudinal impact, the removable disc is the principal forward load spreader and the fixed disc is the principal aft load spreader. In a corner impact of severe magnitude, the extended region of the tube (beyond the location of either disc) buckles or deforms inward, constricting the possible passage of the discs in an outward direction. The entire protective redwood assembly is confined by means of the outer drum assembly, with the interstitial load-spreader assembly confining the inner redwood assemblies.

A removable redwood plug with longitudinal grain orientation, a hollow inner redwood cylinder that has radial grain orientation from fabrication as a series of wedges arranged in a ring, and a fixed redwood plug with longitudinal grain orientation constitute the inner redwood assembly.

The inner heat-conductor tube, made of copper, conducts internal decay heat from the TB-1 containment vessel. The conduction path leads from the contents to the product can, to the TB-1 containment vessel, to the copper tube, into the fixed disc, and into the aluminum load-spreader tube. The inner conductor tube, the disc, and the load-spreader tube are mechanically connected to insure an effective heat conductive path. From the large outside surface area of the tube, internally generated heat is conducted through the hollow outer redwood cylinder to the outer drum assembly, thence to an exchange with ambient air.

The containment vessel, TB-1, shown in more detail in Figures 1.2.2-2 and 1.2.2-3, consists of a body, a lid secured by bolts, a copper gasket, and an O-ring. The vessel body and lid are fabricated from PH13-8Mo precipitation-hardened stainless steel. The H1075 steel's temper enhances ductility while preserving high strength from low to high temperatures. The TB body and lid are designed with approximately hemispherical end shapes and cylindrical side wall shaped to resist deformation from either external or internal loads or pressures. The lid is hermetically

sealed to the body by the use of a ductile copper gasket in conjunction with knife-edge sealing beads on both the body and lid and with a pattern of bolts. The sealing surfaces are arranged to afford handling protection to the knife-edge sealing beads. The lid has a pilot diameter region of great structural shear strength which fits closely into the mating internal diameter of the body. This limits possible radial motion between these parts, especially motion that would be induced from deformations resulting from accidental crash, crush, or puncture loads. This pilot diameter is also equipped with an O-ring in a groove, as a secondary seal to supplement the upper copper gasket and double knife edges, for containment of contents within the TB-1 containment vessel.

The twelve TB-1 1/2 in.-diam shown in Figure 1.2.2-3, are forged from A-286 stainless steel, with more than 30,000-lb ultimate tensile strength per bolt. This material resists corrosion with the stainless-steel TB body and lid, and provides high-temperature strength to maintain the TB-1 seal at elevated temperatures. The bolts are silver plated to prevent galling of the stainless-steel bolt in the stainless-steel TB-1.

A shock-mitigation spacer within the TB-1 containment vessel is fabricated from aluminum honeycomb (see Figure 1.2.2-3) with axial cell orientation. The honeycomb spacer prevents the flat end of the PC-1 product can from entering into the hollow hemispheric lid in the case of severe impact loads in the axial bottom direction. The spacer also serves as a thermal conductor for any heat generated by the PuO_2 contents.

The TB-1 inner container is highly resistant to seawater corrosion and will withstand the hydrostatic pressures specified in the NRC qualification criteria.

The PC-1 product can (Figure 1.2.2-3), fabricated from stainless steel, is sealed by crimping in a canning machine. The outside cylindrical region of the TB-1 containment vessel limits the possible deflection or permanent change of shape under severe lateral impact loads. The product can provides double containment under normal and accident conditions of transport performance tests as specified by 10 CFR 71.42.

The assemblage of the above described AQ-1 overpack, TB-1 containment vessel, spacer, and PC-1 product can is identified as the PAT-1 package.



Figure 1.2.2-2. The TB-1 Containment Vessel

POOR ORIGINAL

1567 055

POOR ORIGINAL

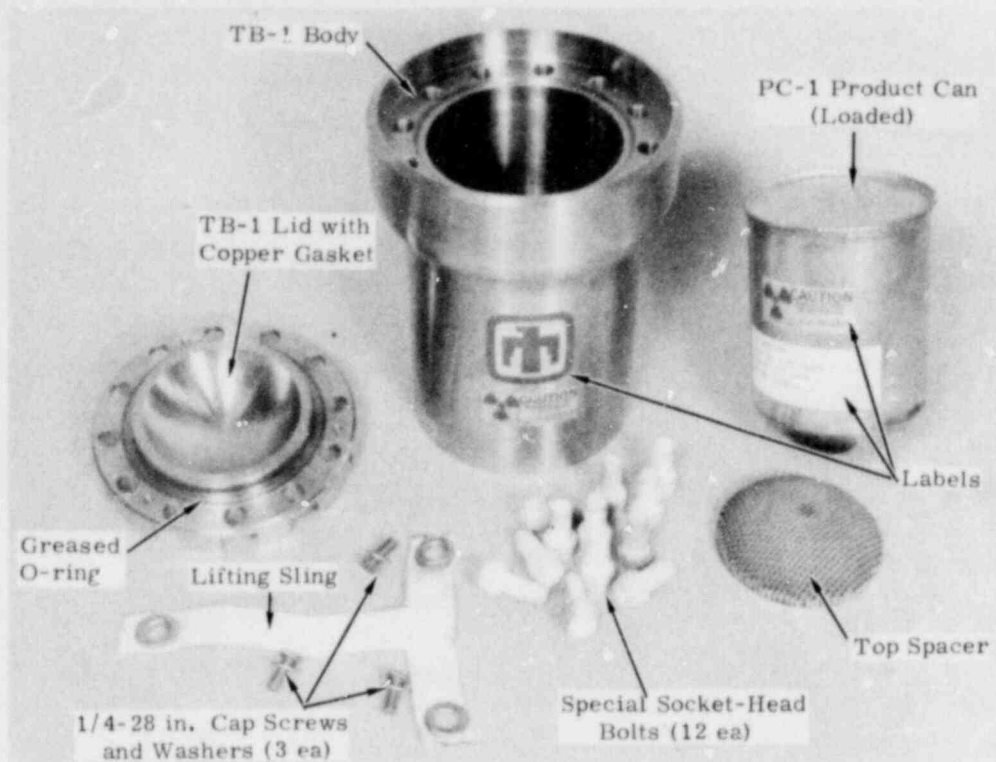


Figure 1. 2. 2-3. TB-1 Disassembled

In both the damaged and undamaged arrays specified in the NRC qualification criteria, the assemblies of packages are subcritical by wide margins. Design considerations to meet impact and thermal protection resulted in a configuration that did not require additional considerations for radiation shielding. The limitations on weight and internal decay heat for contents, expressed as items a through f in Section 1. 2. 4 have satisfied the external radiation limitation of 10 mrem/hr. (refer 49 CFR 173. 393 (i), for all foreseeable mixtures of recycled plutonium.

1. 2. 3 Operational Features

The operational features of the PAT-1 package require only a minimal amount of instruction for assembly, disassembly, handling, and transporting the package. The package can be palletized (Figure 1. 2. 3-1) or it may be handled and transported as an ordinary drum. Ordinary socket wrenches are used to attach or remove the C-ring cover clamp. No tools are necessary after this operation to assemble/disassemble the other AQ-1 removable covers, plugs, load spreaders, and insulation pad, or to insert/remove the TB-1 containment vessel. Hand tools can also be used to assemble/disassemble the TB-1.

POOR ORIGINAL

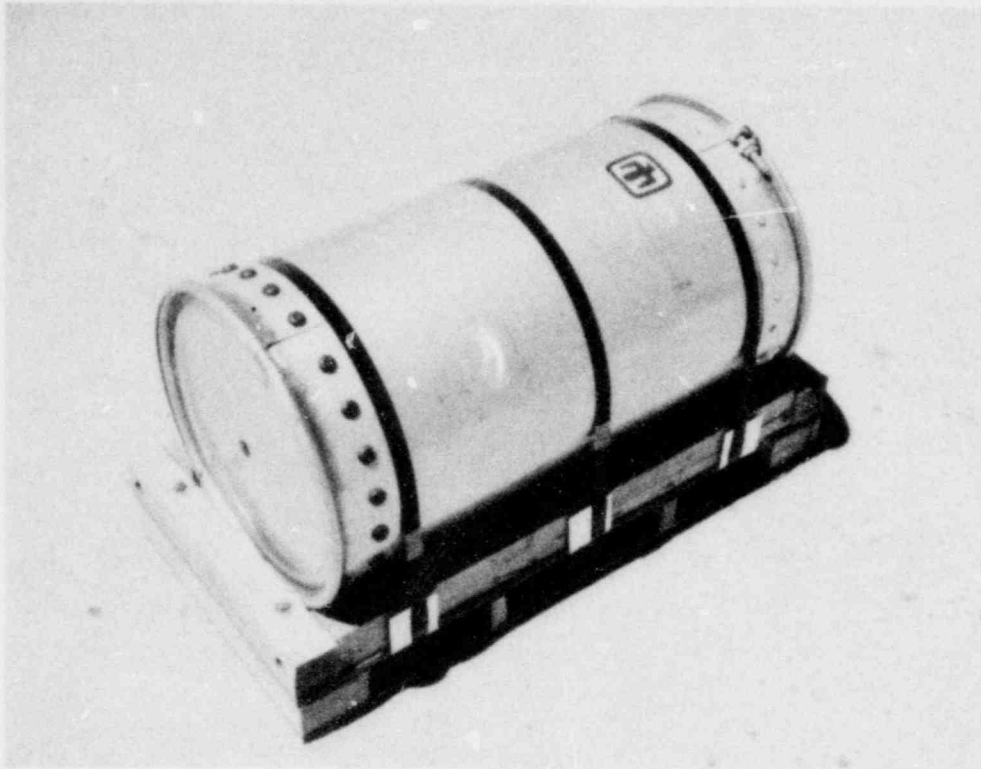


Figure 1.2.3-1. PAT-1 Package on Pallet

The product can is sealed using a commercial canning tool and may be opened with a standard can opener.

The physical operating features which assure TB-1 integrity following the 10 CFR 71 normal and accident condition of transport performance requirements and the NRC qualification criteria are the TB-1 copper gasket, a fluorocarbon O-ring, and the TB-1 structure. These features of the TB-1, when assembled to procedures described in Chapter 7 and acceptance tested and maintained as described in Chapter 8, assure that the TB-1 will meet acceptance criteria with regard to plutonium leakage under normal and accident conditions of transport.

1.2.4 Contents of Packaging

The contents of the PAT-1 package are limited by the following:

- a. Material type: plutonium oxide (PuO_2), including the isotopic, chemical, and physical compositions resulting from plutonium recycling.
- b. Material form: powder.
- c. Material quantity: limited to a maximum mass of 3.15 kg.

820 5021

1567 057

- d. Moisture content: limited to 16 g H₂O (0.5 w/o of full 3.15-kg PuO₂ contents).
- e. Internal decay heat: a restriction of maximum internal decay power of 25 W is imposed; this may be calculated as follows:

$$\begin{aligned} & \frac{\text{watts}}{\text{g}} \text{}^{238}\text{Pu} \times \text{g} \text{}^{238}\text{Pu} + \frac{\text{watts}}{\text{g}} \text{}^{239}\text{Pu} \times \text{g} \text{}^{239}\text{Pu} \\ & + \frac{\text{watts}}{\text{g}} \text{}^{240}\text{Pu} \times \text{g} \text{}^{240}\text{Pu} + \frac{\text{watts}}{\text{g}} \text{}^{241}\text{Pu} \times \text{g} \text{}^{241}\text{Pu} \\ & + \frac{\text{watts}}{\text{g}} \text{}^{242}\text{Pu} \times \text{g} \text{}^{242}\text{Pu} + \frac{\text{watts}}{\text{g}} \text{}^{241}\text{Am} \times \text{g} \text{}^{241}\text{Am} \\ & + \frac{\text{watts}}{\text{g}} \text{ (fission products or other transuranic isotopes)} \end{aligned}$$

$$x \text{ g (fission products or other transuranic isotopes)} \leq 25 \text{ watts.}$$

Note: Due to the increase of decay power with time, the maximum decay power is calculated for the isotopic composition which will exist at the longest storage time, or the peak power period.

- f. Additional permissible packaging: the product may be double bagged and taped in minimal size polyethylene bags as described in Chapter 7.

CHAPTER 2

STRUCTURAL CRITERIA, DESIGN, ANALYSIS, TESTS, AND RESULTS

2.1 Summary of Design and Acceptance Criteria

The PAT structural criteria are the newly emerging very severe NRC accident levels for plutonium shipping packages¹ which are more demanding than the earlier 10 CFR 71 criteria.² These criteria define sequential and individual test conditions for impact, crush, slash, puncture, thermal, and hydrostatic accident environments.¹ The PAT is also designed to be compatible with thermally active contents of up to 25-W output. The postaccident test sequence acceptance or success criteria are essentially no release of PuO₂ ("leaktight" per ANSI N14.5³), or less than an "A2" quantity per IAEA Safety Series No. 6,⁴ maintenance of an effective shield (less than 1 rem/hr at 3 ft), and maintenance of subcriticality.

2.1.1 Prevailing Design Criteria

The required impact test, the required slash test, the required fire test, and the 25-W internal heat source are the predominant design criteria. Design satisfaction of these three conditions with essentially no release of PuO₂ from the inner containment vessel produced a package that satisfied the other design criteria of crush, puncture, submersion, hydrostatic, heat, cold, pressure, vibration, water spray, drop, penetration, and compression without additional specific design consideration.

2.1.1.1 Impact

The impact condition¹ of 250-knot (129-m/s) minimum velocity, perpendicular to an unyielding target, is very severe for a package that is to be within practical size and weight constraints for commercially feasible air transport and that is to provide a very high degree of protection for its contents. These criteria caused the selection of a packaging material with very high specific energy absorption capability.

It was determined through correlation and analysis⁵⁻¹⁰ that this impact velocity onto an unyielding target is comparable to much higher velocity impacts onto earth and rock, as indicated in Table 2.1.1-I.

Also, the requirement that the impact trajectory be perpendicular to the target means that essentially all of the kinetic energy of the package must be converted into strain (deformation and crushing) energy; this is the most severe trajectory.

1567 059

TABLE 2.1.1-I

Impact Condition Correlation

Target	Yield Ratio, Unyielding Target to Natural Target	Velocity Multipliers for Comparable Deformation		Velocity Multipliers for Weighted Average; Yield and Damage	Approximate Resultant Velocities		
		LLD-1*	6M*		m/s	fps	KTS
Unyielding	1.0	1.0	1.0	1	129	422	250
Soft rock	2.5	1.4	1.4	2	258	844	575
Hard soil	3.4	2.3	2.5	3	387	1266	863

* Existing packages - see References 5, 6, and 7.

The design features which accommodate the impact condition, as well as test descriptions and package test results, all follow in other sections of this chapter.

2.1.1.2 Slash

The slash condition (Reference 1 as amended by letter) requires that a 100-lb (45-kg) structural-steel angle beam be dropped from at least 150 ft (46 m) in such a manner as to slash the package open. Details and results of this test appear later in this section. This criterion increased the package's vulnerability to fire and caused a leveling effect with respect to impact deformation; i. e., the final results obtained from packages with greater or lesser extents of impact damage were essentially similar after the introduction of the slash test into the required sequential criteria.

The design features which accommodate the slash threat and the slash test description and package test results all follow in other sections of this chapter.

2.1.1.3 Fire

The required fire test¹ represents a maximum credible accidental fire which would be associated with a minimal crash environment. However, the PAT package criteria require a maximum credible fire in a sequence that first includes a very high-level crash environment.

This criterion caused the selection of packaging material that exhibited high specific energy absorption and good thermal resistivity in its original condition, and also one with appropriate thermal resistivity following severe deformation.

The design features which accommodate the fire, and test descriptions and results, follow later in this chapter.

2.1.1.4 Internal Heat Source

In order to accommodate a broad spectrum of plutonium oxide powders, relating to radioisotopic activity and the resultant thermal activity, an internal heat design load of 25 W was designated. This criterion caused the incorporation of certain specific design features, calculations, and tests, as reported later.

2.1.2 Other Design Criteria

A number of other design criteria, aside from the prevailing criteria of impact, slash, fire, and internal heat, are required by References 1 (NRC Qualification Criteria), 2 (10 CFR 71), and 11 (Standard Format for SAR). These include extreme temperature considerations, terminal velocity consideration, individual versus sequential testing effects, radioactive contents effects, corrosion considerations, positive closure of the package, and load resistance, external pressure, compression, and internal pressure calculations. These criteria are addressed later in the report.

2.1.3 Acceptance Criteria

In general, the posttest acceptance criteria or standards for the PAT-1 package are:

2.1.3.1 Containment

The containment vessel must not be ruptured in its posttested condition, and the package must provide a sufficient degree of containment to restrict accumulated loss of radioactive contents to not more than an A2 quantity of plutonium in a period of one week. An A2 quantity of plutonium is defined in Table VII of the International Atomic Energy Agency Regulations for the Safe Transport of Radioactive Materials (IAEA Safety Series No. 6).

2.1.3.2 Shielding

The external radiation level must not exceed 1 rem/hr at a distance of 3 feet from the surface of the package in its posttested condition.

2.1.3.3 Subcriticality

A single package and an array of packages must be subcritical in accordance with 10 CFR 71, except that the damaged condition of the package must result from the NRC qualification tests rather than the conditions specified in Appendix B of 10 CFR 71.

2.1.3.4 Hydrostatic

The acceptance criterion following a hydrostatic pressure test is that there be no detectable leakage of water into the containment vessel.

2.2 Design and Analysis

2.2.1 Structural Design Description

A general design description of the PAT-1 package was provided in Chapter 1. Some additional structural design description follows.

The Air Qualified (AQ-1) overpack of the PAT-1 package is designed to experience gross structural deformations during high-velocity impact and slash tests, thereby minimizing damage to the inner containment vessel (TB-1). The primary structural system consists of the double-walled outer stainless-steel drum assembly, two regions of shock-mitigating redwood, the cylindrical and circular interstitial load spreaders, and the inner containment vessel.

Structurally, the drum retains the redwood after high-velocity impact and slash attacks and also provides a fire barrier. The outer drum is reinforced by a stainless-steel inner liner bonded to the outer drum wall with polyester-flexibilized epoxy adhesive. The corners of the inner liner are rounded to lessen the liner's vulnerability to tearing. The closure system for the removable drum lid and the nonremovable drum bottom are specifically designed for increased strength.

The use of redwood as a filler in the drum affords protection to the inner containment vessel in a high-velocity impact and subsequent fire. In this application the grain is oriented parallel with the direction of expected impact, so that the grain is end-on to a target surface that is perpendicular to the direction of motion. Mechanical and thermal characteristics of redwood are presented in Appendix 3A.

Sufficient shock mitigation or packaging material could not be provided to totally protect the inner containment vessel from insult. Therefore, the design permits full deformation of overpack members (double drum, redwood, load spreaders) and minor permanent deformation of the tough inner containment vessel.

A work-energy analysis for kinetic energy absorption in the final PAT design, for side and end impacts, is presented in Appendix 2A. The anisotropy of redwood not parallel or perpendicular to the grain impedes a formal analysis of the corner crash; however, this crash attitude involves the longest path length of protection and test results show excellent response. Also, the tubular load spreader was deliberately designed to extend past the circular load-spreader plates

so that corner crashes would pinch the tube inward, both absorbing energy and restricting outward passage of the inner containment vessel/load-spreader plate.

The initial general design arrangement (material choice, size, location, strength) of the interstitial load spreaders was determined by an iterative optimization work-energy strength-of-materials analysis programmed in Fortran on the CDC-6600 computer. Refinement in the load-spreader design and in the outside drum design ensued throughout the development test program.

The interstitial load spreaders consist of an imbedded aluminum cylinder and two aluminum plates. These load spreaders protect the inner containment vessel and enable the application of a greater surface area of redwood as an energy absorbing material. At impact, the load spreaders undergo large deformations after the redwood has reached its usable crush limit.

The TB-1 inner containment vessel provides a secure inner seal for the nuclear contents and survives an accident without releasing its contents to the environment. It is made of high-strength ductile stainless steel and has a secure sealing mechanism utilizing an O-ring seal and a double knife-edge metallic seal with a copper gasket. The lid of the TB-1 fits down within the body for high shear strength and is secured by twelve 1/2-in. stainless-steel high-strength bolts.

The postcrash slash threat and the postcrash, postslash fire threat are met by the design feature of redwood applied to two zones, sandwiched between two assemblies of metallic containment (the double-wall outside stainless steel drum and the inner aluminum interstitial load spreaders). The fire retardation characteristics of redwood in this application are reported in Chapter 3, Thermal Evaluation. Approximately 1-hr thermal delay protection from a large 1850°F (1010°C) fire is provided by each redwood region in the undamaged package. Total disruption by crash or slash testing of the outer wood region can be tolerated. It has been observed in the test program that the inner wood, although compressed by reaction between the inner containment vessel and the interstitial load spreaders, provides nearly the same thermal protection as the same mass of uncompressed wood.

Additional data are presented under the topics of materials properties and thermal test evaluation.

The 25-W internal heat load was accommodated within the PAT-1 design by the inclusion of a copper tube surrounding a region of the TB-1 containment vessel. This copper tube is mechanically connected to the bottom load-spreader circular plate; this plate is mechanically connected to the aluminum load-spreader tube. Thus, the containment vessel heat load is transmitted to the load-spreader tube which has a much larger surface area. The load-spreader tube is insulated from the outer drums by only one layer of the redwood. The ultimate heat sink is provided by the drum's interaction with the ambient external environment. This heat path results in acceptable internal package temperatures, as demonstrated by the experiments and analyses presented in Chapter 3.

2.2.2 Mass Properties

The weights of the three basic parts of the PAT-1 package are approximately as follows:

	<u>lb</u>	<u>kg</u>
AQ-1 overpack	454.0	206.0
TB-1 containment vessel	37.0	16.8
PC-1 product can (including aluminum fillers)	0.3	0.1
Contents (maximum)	<u>6.8</u>	<u>3.1</u>
Total (nominal)	498.1	226.0

The weight of the AQ-1 overpack varies due to natural variation in the weight of kiln-dried redwood.

Centroid location is on the PAT-1 drum longitudinal centerline approximately 20-3/16 in. (51 cm) up from the bottom surface of the package. Roll moment of inertia is approximately 35,000 lb-in.² (10 kg·m²); the pitch and yaw moment of inertia is approximately 85,000 lb-in.² (25 kg·m²).

The above mass properties are without the optional wooden skid, which is provided to facilitate handling and tiedown. Total weight with the skid is approximately 570 lb (259 kg).

2.2.3 Mechanical Properties of Materials Used

The principal structural and thermal barrier materials used in the design and construction of the PAT-1 package are the 304 stainless-steel drum members, the 6061-T6 tubular aluminum load spreader and the 7075-T6 aluminum load-spreader plates, the PH13-8 Mo stainless steel used for the containment vessel, the A286 stainless steel used for the containment vessel closure bolts, the aluminum honeycomb spacers within the containment vessel, and the redwood impact limiter/thermal barrier material.

The principal mechanical and thermal properties of these materials as used in supporting analyses are reported in Appendix 2B.

2.2.4 Chemical and Galvanic Design Considerations

There are no significant chemical, galvanic, or any other reactions among the PAT-1 package components or between the package and package contents.

Metal-to-metal contact on the exterior of the AQ-1 overpack is limited to the stainless-steel drum and cadmium-plated steel bolts. Contact between the aluminum load-spreader tube and the bottom load-spreader disc is accomplished with cadmium-plated steel spring pins. Contact

between the bottom load-spreader disc and the cadmium-plated copper heat conducting tube is effected by self-tapping cadmium-plated steel screws. These two joints are then encapsulated in moisture-resistant flexibilized epoxy. At the interface between the cadmium-plated copper heat conducting tube and TB-1 containment vessel, the inside diameter of the tube is lined with epoxy-resin fiberglass cloth to prevent scraping of the cadmium plating during TB-1 installation and removal. Metal-to-metal contacts in the TB-1 containment vessel are between PH13-8 Mo martensitic precipitation-hardened stainless steel, silver-plated stainless-steel bolts, and the copper gasket. Within the sealed TB-1, contact is made with the aluminum honeycomb spacer and the sealed stainless-steel PC-1 product can. The plutonium product, which may be double wrapped and taped within polyethylene bags, is contained in the PC-1.

These interfaces present no significant corrosion problem.

2.2.5 Positive Closure

Positive closure of the PAT-1 cover is provided by the skirted C-clamp closure ring with twenty-three 3/8-in. bolts passing through the outer and inner drum construction (including five layers of stainless steel) into internal nut plates, and a 5/8-in. draw bolt passing through the stainless-steel lugs on the clamp ring.

The bottom end of the PAT is similarly secured except that in place of the draw bolt the clamp ring is welded shut to prevent disassembly.

Positive closure of the TB-1 containment vessel is provided by the twelve 1/2-in. -diameter bolts which fasten the lid and body of the vessel.

Positive closure of the PC-1 product can is accomplished by roll crimping, contact adhesive, and flexibilized epoxy overbonding.

2.2.6 Lifting Devices

The simple cylindrical PAT package is pallet-mounted to facilitate forklift handling. Also, any adequate nylon sling may be used for lifting the PAT without pallet; the sling should be cinched so the package does not slip out. The beaded corners at the top and bottom of the AQ tend to restrain slippage through a sling.

2.2.7 Tiedowns

The PAT is provided on a standard pallet to facilitate tiedown on aircraft and other common carrier vehicles. Any approved tiedowns may be used. The PAT is attached to the skid with specified steel banding straps (see Product Specification R00602, provided with PAT drawings in Appendix 9A).

1567 065

2.2.8 Load Resistance per 10 CFR 71.32a

Compliance to this standard for "Type B and Large Quantity Packaging" per 10 CFR 71.32a is demonstrated in the analysis of Appendix 2C. The maximum resulting stress was 143 psi (0.99 MPa) in the alloy 304 stainless-steel drum, which is insignificant.

2.2.9 External Pressure per 10 CFR 71.32b

10 CFR 71.32 (b) requires that the packaging be adequate so that the containment vessel will suffer no loss of contents if subjected to an external pressure of 25 psi (0.17 MPa). The NRC qualification criteria for plutonium air transportable packages requires the package to be submerged and subjected to an external water pressure of at least 600 psi (4.1 MPa) for a period not less than 8 hours. Compliance of the PAT-1 package, specifically the TB-1 containment vessel, with the 25-psi (0.17 MPa) requirement is demonstrated through the 600-psi (4.1 MPa) hydrostatic pressure test reported later.

Also, Appendix 2D is an analysis of the 25-psi (0.17 MPa) condition.

2.2.10 Pressure per 10 CFR 71 Appendix A3

The application of 0.5 times standard atmospheric pressure to the PAT-1 package induces negligible loadings and stresses. An analysis of this condition is presented in Appendix 2E.

2.2.11 Compression per 10 CFR 71 Appendix A10

This requirement relates to a compressive load equal to five times the PAT-1 package weight applied uniformly against the top and bottom of the package. Analytical results are given in Appendix 2F. Test results are given later in this chapter.

2.2.12 Containment Vessel Stress Analyses

2.2.12.1 5000-Psi Hydrostatic Analysis

An elastostatic finite element analysis of the TB-1 containment vessel for hydrostatic pressure load was performed to assess the effects of deep water immersion. The analysis was done using the axisymmetric finite element code TEXGAP.* The finite element mesh and boundary conditions applied are similar to those shown in Figure 2D-2.

Material	PH13-8 Mo Stainless, H1075 Temper
Hydrostatic Pressure	5000 psi (34.5 MPa)
Maximum Stress	631 psi (4.35 MPa)
Minimum Stress	-42,768 psi (-294.9 MPa)

*TEXGAP - the "Texas Grain Analysis Program," E. B. Becker and R. S. Dunham, TICOM Report 73-1, The Texas Institute for Computational Mechanics, The University of Texas at Austin, August 1973.

Assuming a compression yield for PH13-8 Mo equal to the tensile yield, the margin of safety is calculated as

$$M.S. = \frac{150000}{42768} - 1 = 3.5 - 1 = 2.5.$$

2.2.12.2 NMOP (Normal Maximum Operating Pressure) Containment Vessel Stress Analysis

Based upon 10 CFR 71 Appendix A criteria and supporting Sandia tests and calculations as presented in Chapter 3, the normal maximum pressure is found to be 34.3 psi (0.245 MPa) at a temperature of 215°F (102°C).

As discussed in the following section, entitled "Maximum Credible Accident Pressure Analysis," the stress field for the internally pressurized TB-1 containment vessel can be determined by scaling down the results presented in Appendix 2E using the Principle of Linear Superposition. Thus the maximum stresses calculated in Appendix 2E [for 7.35 psi (50 kPa) internal pressure] are simply multiplied by the pressure ratio, 34.3/7.35. The maximum stresses in the TB-1 containment vessel (cylinder portion and end cap) and their locations are thus as follows for 34.3-psi (0.236 MPa) internal pressure.*

$$\text{End cap (outer edge, inside surface): } (\sigma_{rr})_{\max} = 507 \text{ psi (3.5 MPa)}$$

$$(\sigma_{\theta\theta})_{\max} = 153 \text{ psi (1.05 MPa)}$$

$$\text{Cylinder: } (\sigma_{\theta\theta})_{\max} = 155 \text{ psi (1.07 MPa) (occurs 1.25 radii in from end)}$$

$$(\sigma_{zz})_{\max} = 513 \text{ psi (3.54 MPa) (near cap-cylinder intersection)}$$

When the above numbers are compared with the yield stress at 215°F (102°C) of approximately 140 ksi (0.97 GPa) (guaranteed minimum) for the TB-1 containment vessel material, stresses are extremely small. Thus plastic yielding or failure of the vessel itself will not occur during the normal conditions of transport.

The total axial force per bolt is found from the projected area of the end cap by

$$F = \frac{P\pi a^2}{N} \quad (1)$$

*The TB vessel was conservatively modeled for analysis as a cylinder with flat end caps.

where

P = internal pressure

a = inside radius of the cylinder

N = number of bolts

For P = 34.3 psi (0.236 MPa), a = 2.125 in. (5.4 cm), and N = 12 bolts; then F = 40.5 lb (187 N). Compared to the maximum ultimate tensile strength of 30,000 lb (0.13 mN) for the A286 bolts, the loading due to the "normal maximum" pressure is negligible.

Thread shear stress in the weaker PH13-8 Mo material is given by

$$\tau = \frac{F}{\pi d_o l_o}$$

where

F = bolt loading

d_o = thread outer diameter

l = engaged thread length

For F = 40.5 lb (187 N), d_o = 0.5 in. (1.27 cm), and l_o = 0.75 in. (1.9 cm); then τ = 34.4 psi (0.237 MPa). This shear stress is negligible in comparison to the shear failure stress (approximated as one-half the ultimate tensile stress value) of 81,500 psi (562 MPa). Thus bolt or thread failure will not occur under the normal transport conditions.

2.2.12.3 Maximum Credible Accident Pressure Analysis

As developed in Chapters 3 and 4, the maximum credible "accident" pressure occurring within the TB-1 containment vessel shown in Figure 2.2.12.3-1 is 1253 psi (8.6 MPa), with corresponding internal temperature of 1080°F (582°C). A stress analysis of the identical TB-1 pressure vessel subjected to a much lower internal pressure of 7.35 psi (50.7 kPa) was presented in Appendix 2E. Since vessel response is postulated in the linear elastic regime undergoing small deflections, then the Principle of Linear Superposition applies. It is thus possible to scale up the stress fields determined in Appendix 2E simply by multiplying by the ratio of internal pressures,* 1253/7.35. The analysis presented in Appendix 2E is based upon conservative geometric modeling assumptions. Thus, stresses scaled up here from those predictions are conservative, bounding the actual stresses from above.

* Note that 25 percent degradation in elastic modulus at the 1080°F (582°C) internal temperature of the TB-1 does not influence the elastic stress field. This can be seen by examination of the generalized stress (M_o and V_o) and stress equations utilized in Appendix 2E. In particular, for equal moduli in end cap and cylindrical portions of the TB-1, the equations are found to be independent of the elastic modulus.

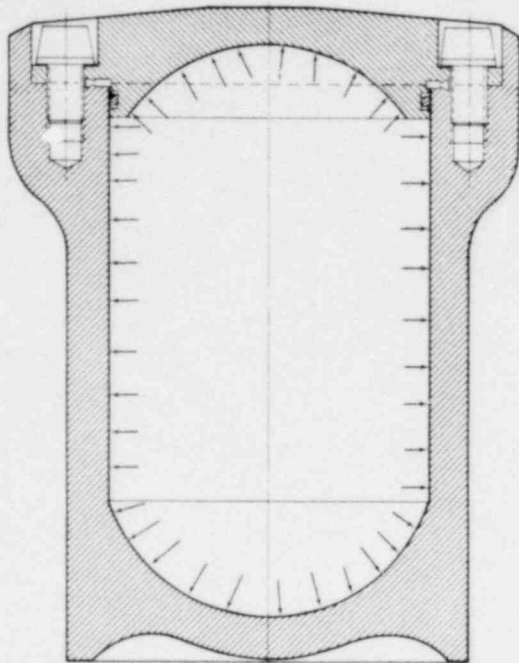


Figure 2.2.12.3-1. Containment Vessel

occurring near the end cap/cylinder intersection on the inner surface. These scaled-up stresses, corresponding to 1253-psi (8.6 MPa) internal pressure, are:

$$(\sigma_{\theta\theta})_{\max} = 5676 \text{ psi (39.1 MPa)}$$

$$(\sigma_{ZZ})_{\max} = 18751 \text{ psi (129 MPa) (Z = 0).}$$

Due to the presence of a biaxial stress state, worst case stresses must be calculated at the same point so that biaxial yielding can be checked using a suitable yield criterion. Since axial stress (at $Z = 0$) is dominant, the hoop stress at $Z = 0$ is calculated using Eq. (15), Appendix 2E, and multiplying by an appropriate scale factor. The resulting worst-case stress state (occurs at $Z = 0$) is then

$$(\sigma_{\theta\theta})_{\max} = 954 \text{ psi (6.6 MPa)}$$

$$(\sigma_{ZZ})_{\max} = 18751 \text{ psi (129 MPa).}$$

Examination of the earlier analysis indicates that the location of maximum stress state in the end cap is on the inner surface near the outer edge of the cap (cap/cylinder intersection). The scaled-up radial and circumferential stresses are found to be

$$(\sigma_{rr})_{\max} = 18513 \text{ psi (0.128 GPa)}$$

$$(\sigma_{\theta\theta})_{\max} = 5591 \text{ psi (38.5 MPa)}$$

at this location for 1253-psi (8.6 MPa) internal pressure.

The maximum stresses for the cylinder in hoop and axial directions occur in different locations, the maximum hoop stress occurring at an axial distance of 1.25 radii from the end, and the maximum axial stress

1567 069

POOR ORIGINAL

These stress values should be compared to the calculated "guaranteed" minimum yield strength of PH13-8 Mo alloy in the H1075 condition at 1080 °F (582 °C) of $\sigma_y = 93,000$ psi (641 MPa).^{*} In particular, based upon an effective stress, σ_{eff} , as calculated from the Von Mises yield condition,^{**}

$$\sigma_{\text{eff}} = \left(\sigma_1^2 + \sigma_2^2 - \sigma_1\sigma_2 \right)^{1/2}$$

the factor of safety on yielding for the end cap is found to be 5.65 and the corresponding factor of safety for the cylindrical portion (at $Z = 0$) is 5.08.

Since pressure is internal, bolt or thread failure (see Figure 2.2.12.3-1) is a possibility.

The total axial force per bolt is found from the projected area by

$$F = \frac{P\pi a^2}{N}$$

where

P = internal pressure

a = inside radius of the cylinder

N = number of bolts.

For $P = 1253$ psi (8.6 MPa), $a = 2.125$ in. (5.4 cm), and $N = 12$ bolts; then $F = 1481$ lb (6.6 kN).

The number should be compared to the maximum ultimate tensile strength of the A286 closure bolts at 1080 °F (582 °C) of 15,327 lb (68 kN).[†] It is seen that bolt tensile failure will not occur (factor of safety of 10.3).

Thread shearing failure is another possibility. Consider the weaker PH13-8 Mo TB-1 vessel material. The shear stress in this material tending to strip out the threads is

$$\tau = \frac{F}{\pi d_o l_o}$$

^{*} This yield value has been conservatively structured from information on extremely similar alloys in Metallic Materials and Elements for Aerospace Vehicle Structures, Vol. 2, September 1977.

^{**} Comparison of the uniaxial yield stress with stress components individually would correspond to a maximum principal stress yield theory. Such a theory does not accurately predict yielding of metals and, hence, is not used here.

[†] Based upon A286 ultimate tensile stress at 1080 °F (582 °C).

where

F = bolt loading

d_o = thread outer diameter

l_o = engaged thread length.

For $F = 1481$ lb (6.6 kN), $d_o = 0.5$ in. (1.27 cm), $l_o = 0.75$ in. (1.9 cm), and $\tau = 1257$ psi (8.7 MPa).

This shear stress should be compared to the shear failure stress, estimated as one-half the guaranteed minimum* tensile ultimate strength at 1080 °F (582 °C) of 100,000 psi (689 MPa) or 50,000 psi (345 MPa). It is seen that thread shearing failure will not occur for the stated accident conditions (factor of safety of 39).

2.2.13 Terminal Free-Fall Analysis

The NRC Qualification Criteria¹ requires confirmation that the required 250 knots (129 m/s) impact velocity is not exceeded by the terminal free-fall velocity of the PAT-1 package.

This was done analytically; results confirm that terminal velocity is less than 250 knots (129 m/s). Additionally, the package was given horizontal velocity vectors of 250 knots (129 m/s) at 10,000 ft (3 km) altitudes, 504 knots (850 fps; 2.6×10^2 m/s) at 12,000 ft (3.7 km) altitude, and Mach 0.9 880 fps (2.7×10^2 m/s) at 35,000 ft (10.7 km) altitude with a free fall. These conditions also result in a terminal velocity (or ground impact velocity) less than 250 knots (129 m/s).

Results are detailed in Appendix 2G.

2.3 Test Program Requirements

Testing of the PAT-1 package required three principal programs. The definitions of these test programs are contained within the NRC Qualification Criteria for Plutonium Package Certification¹ and 10 CFR 71 Appendixes A and B.² A detailed description of package preparation, test plans, test conduct, and data collection, for all three principal test programs, is delineated in Appendix 2H, Test Protocol. The suitability of a surrogate depleted UO_2 powder used in place of PuO_2 powder throughout the test programs is discussed in Appendix 2I. A brief description of the test program follows.

* Conservatively estimated from data on extremely similar alloys in Metallic Materials and Elements for Aerospace Vehicle Structures, Vol. 2, September 1977.

2.3.1 NRC Qualification Tests

2.3.1.1 Sequential Tests

- a. Impact -- The PAT-1 package is impacted at a velocity of not less than 422 fps (129 m/s) onto a flat, essentially unyielding surface, in the orientation expected to result in maximum damage at the conclusion of the test sequence; the impact trajectory is perpendicular to the unyielding target.
- b. Crush -- The PAT-1 package is crushed by applying a static compressive load of 70,000 lb (3.1×10^5 N); the crush force is applied to the package with the edge of a 2-in. (5.1 cm) wide, straight, solid, steel bar. The package rests on a flat, steel, essentially unyielding surface. The length of the bar must be at least as long as the diameter of the package and the longitudinal axis of the bar is parallel to the plane of the flat surface. The load is applied to the bar in a manner that prevents any support or device from contacting the package. The point of application of the compressive load is the orientation expected to result in maximum damage to the package.
- c. Puncture -- The PAT-1 package is punctured by the 10-ft (3-m) drop of a 500-lb (227-kg) steel spike in the orientation expected to result in maximum threat to the inner containment vessel. The spike is in the shape of a frustum of a cone 12 in. (30.5 cm) long, 8 in. (20 cm) base diameter, and 1 in. (2.5 cm) in tip surface diameter. The PAT-1 package rests on an essentially unyielding surface.
- d. Slash -- The PAT-1 package is slashed (ripped and torn) by the 150-ft (46-m) drop of a 100-lb (45-kg) (minimum) structural-steel angle beam with the PAT-1 package firmly imbedded in earth and tilted at an angle of 45 degrees from the vertical free-fall trajectory path of the beam. The area of package impact damage (from the impact test) is in the lowermost position; the beam is to strike approximately the center of the vertical projection of area of the emplaced package. The beam is a structural-steel angle member with equal legs at least 5 in. (12.7 cm) long and 0.5 in. (1.3 cm) thick.

- e. Fire -- The PAT-1 package is burned in a large JP-4 or JP-5 aviation-fuel fire for at least 1 hr. The luminous flames of the fire extend at least 3 ft (1 m) and no more than 10 ft (3 m) beyond the package in all horizontal directions. The position and orientation of the package in relation to the fuel is that which results in maximum damage at the conclusion of the test sequence. After termination of the fire, the package is allowed to cool naturally or may be cooled by water sprinkling, whichever results in maximum damage at the conclusion of the test sequence. The fire-test facility is constructed in such a manner as to produce a minimum temperature of 1850° (1010°C) at the PAT-1 package level throughout the burn.
- f. Immersion -- The PAT-1 package is submerged under water to a depth of at least 3 ft (1 m) for a period of at least 8 hr.

2.3.1.2 Individual Tests

- a. Hydrostatic -- The NRC Qualification Criteria for plutonium air-transportable packages also requires the package to withstand, without detectable water leakage into the containment vessel, water submersion with an external water pressure of at least 600 psi (4.1 MPa) for a period of not less than 8 hr.
- b. Free-Fall -- A further requirement for a free-fall impact is not applicable to the PAT-1 package, since its calculated terminal free-fall velocity, as assessed in paragraph 2.2.13, is less than 422 fps (129 m/s).

2.3.1.3 Other Requirements

The NRC Qualification Criteria also requires demonstration or assessment that the PAT-1 package testing results would not be adversely affected by:

- a. The presence of actual PuO₂ contents.
- b. Ambient water temperatures ranging from +33°F (0.6°C) to +70°F (21°C) for those tests involving water, and ambient atmospheric temperatures ranging from -40°F (-40°C) to +130°F (54°C) for the other qualification tests.

2.3.2 Normal Conditions of Transport per 10 CFR 71 Appendix A

This test sequence consists of:

- a. Heat
- b. Cold
- c. Pressure
- d. Vibration
- e. Water Spray
- f. Free Drop
- g. Corner Drop
- h. Penetration
- i. Compression

Detailed information of test conditions and results follow in paragraph 2.4.

2.3.3 Hypothetical Accident Conditions per 10 CFR 71 Appendix B

This test sequence consists of:

- a. Free Drop
- b. Puncture
- c. Thermal (Fire)
- d. Water Immersion

Detailed information of test conditions and results follow in paragraph 2.4.

2.4 Test Program Results - Summary

2.4.1 NRC Qualification Criteria

The PAT-1 package meets or exceeds the requirements of the NRC Qualification Criteria.¹ This compliance was demonstrated by a test program involving seven packages and one additional containment vessel.

The sequential test requirements were satisfied through the use of five PAT-1 packages, with each package initially impacted at a different principal attitude, followed by an essentially identical test sequence of crush, puncture, slash, fire, immersion, and inspection.

The results were:

- Containment - No detectable release of contents from containment vessel after all tests, 4.5×10^{-5} to 1.7×10^{-7} cm^3/s air leak rates.
- Shielding - Damaged package adequate for < 1 rem/hr at 3 ft (~ 1 m).
- Subcriticality - An infinite array of closely nested damaged packages would be very subcritical.

An individual containment vessel passed the hydrostatic test requirement with no leakage of water.

Two development packages were impact tested to demonstrate compliance with the operating temperature extremes requirement; impact at -40°F (-40°C) and at $+200^\circ\text{F}$ (93°C) indicated satisfaction of the containment, shielding, and subcriticality requirements.

These summary results are tabulated in Table 2.4-I and are detailed in paragraph 2.5.

TABLE 2.4-I
Summary of NRC Qualification Tests, PAT-1 Package

Sandia I. D.	Impact Orientation	Impact Vel. \perp to Unyield Target (fps)	Crush 70,000 (lb)	Puncture 5000 (ft-lb)	Slash 15,000 (ft-lb)	Fire 2200°F Av. 60 minutes (min.)	Immersion	Uranium Detection $\leq 10^{-8}$	cm^3/s (air)
PAT-15XB	Top 0°	442	✓	✓	✓	✓	✓	none	$< 4.6 \times 10^{-6}$
PAT-12XA	Top Corner 30°	451	✓	✓	✓	✓	✓	none	$< 4.5 \times 10^{-5}$ probably $\sim 1.7 \times 10^{-7}$
PAT-11XB	Side 90°	445	✓	✓	✓	✓	✓	none	1.4×10^{-6}
PAT-16XF	Bottom Corner 150°	443	✓	✓	✓	✓	✓	none	$< 5.5 \times 10^{-6}$
PAT-14XF	End 180°	466	✓	✓	✓	✓	✓	none	1.9×10^{-6}

Individual Test: 600 psi hydrostatic; 8 hr -- no detectable water in leakage; $< 10^{-10}$ cm^3/s ;

Other Requirements: Impact at -40°F -- 2.4×10^{-6} cm^3/s ;

Impact at 200°F -- 7×10^{-8} cm^3/s ;

2.4.2 Normal Conditions of Transport: 10 CFR 71 Appendix A

The PAT-1 package meets or exceeds the standards of paragraph 71.35 of 10 CFR 71 when subjected to the normal conditions of transport as specified in Appendix A of 10 CFR 71 (heat, cold, pressure, vibration, water spray, drop, penetration, and compression). This was demonstrated by performing the tests in sequence (not just individually as permitted) on one PAT-1 package.

The results were: the containment vessel was leaktight and there was no release of contents; there was no substantial reduction of package effectiveness or geometric form; the package remained subcritical; there was no reduction of shielding effectiveness; and no apertures were induced in the package.

These summary results are detailed in paragraph 2.5.

2.4.3 Hypothetical Accident Conditions: 10 CFR 71 Appendix B

The PAT-1 package meets or exceeds the standards of paragraph 71.36 of 10 CFR 71 when subjected to the hypothetical accident conditions as specified in Appendix B of 10 CFR 71 (drop, puncture, fire, and immersion). This was demonstrated on one PAT-1 package.

The results were: the containment vessel was leaktight and there was no release of contents; the PC-1 product can within the TB-1 containment vessel did not release contents; there was no substantial or meaningful change of package geometry or effectiveness, no reduction in shielding, and no increased vulnerability to criticality, even with an infinite array of damaged packages.

These summary results are detailed in paragraph 2.5.

2.5 Test Program Results - Detailed

2.5.1 NRC Qualification Criteria (Sequential Tests)

To demonstrate that the PAT-1 package complies with the requirements of the NRC Qualification Criteria, five prototype PAT-1 packages were subjected to the sequence of tests described in paragraph 2.3.1.1.

2.5.1.1 Impact of ≥ 422 fps (129 m/s)

The only intended variable in the five impact tests was the package attitude (orientation) upon impact with the unyielding surface.* Since the impact orientation which would produce maximum package damage at the conclusion of the test sequence could not be conclusively proven by analysis prior to tests, top end, top corner, side, bottom corner, and bottom end impacts were conducted.

*Trajectory path is always perpendicular to surface of unyielding target; package attitude along the trajectory was controlled by individual towing rigs, shown in Appendix 2J.

Table 2.5.1-I summarizes the conditions and results of the five impact tests with emphasis on two factors: the kinetic energy of the inner containment vessel and the final leak rate of that vessel (after the entire sequence including impact, crush, puncture, slash, burn, immersion, and postmortem). This table is presented because the mass of the surrogate UO_2 contents (use of surrogate is specified in the Test Protocol, Appendix 2H; description of surrogate is provided in Appendix 2J) that would physically fit within the PC-1 product can was less than 6.9 lb (3.15 kg). Velocities greater than the requirement were generally obtained in the impact tests, resulting in adequate kinetic energies. A contents payload of 6.9 lb (3.15 kg) was used in all structural analyses (Chapter 2), shielding (Chapter 5), and criticality (Chapter 6) analyses.

- a. Top (0°) Impact -- A PAT-1 package was impacted onto the top end (designated as the 0° orientation) at 442 fps (135 m/s) with an angular error of 2° ($\pm 10^\circ$ is allowed by the Test Protocol, Appendix 2H). The original package length of approximately 43 in. (109 cm) was shortened to 30 in. (76 cm). Health physics monitoring revealed no uranium material on the package exterior. There was no opening through the drum or drum liner, and no exposed redwood. The tubular load spreader imprinted the bottom end but did not penetrate. The postimpact condition is shown in Figures 2.5.1.1-1 and -2. Postimpact radiographs revealed no discernible change in the TB-1 containment vessel, as shown in Figure 2.5.1.1-3. Postimpact package measurements are shown in Figure 2.5.1.1-4.

- b. Top Corner (30°) Impact -- A PAT-1 package was impacted onto the top corner (designated as the 30° orientation) at 451 fps (137 m/s) at an angle of 32° . The clamp ring draw bolt was deliberately impacted. Rebound (second) impact slightly dented the bottom corner. The primary crash indentation essentially transferred the entire top end of the package into the plane perpendicular to the 32° trajectory. A small amount of tearing in the drum covers revealed some interior redwood, but no wood was lost. Health physics monitoring revealed no uranium. The postimpact appearance is shown in Figures 2.5.1.1-5 and -6. Postimpact radiographs revealed no discernible change in the TB-1 containment vessel (Figure 2.5.1.1-7). Postimpact package measurements are shown in Figure 2.5.1.1-8.

1567 077

TABLE 2.5.1-1

PAT-1 Test Conditions, Calculated Kinetic Energy, and Results

Unit I. D.	Impact Orient.	Impact Vel. (fps)	Surrogate UO ₂ (kg) [†]	UO ₂ wt. (lb)	TB-1+PC-1 +UO ₂ (lb)	KE (ft-lb)	% [*] of Goal ^{**}	q [†]
PAT-15XB	Top 0°	442	1.346	2.967	40.267	1.223x10 ⁵	99.85	<4.5x10 ⁻⁶
PAT-12XA	Corner 30°	451	1.048	2.310	39.61	1.253x10 ⁵	103.2	<4.5x10 ⁻⁵
PAT-11XB	Side 90°	445	1.205	2.657	39.957	1.230x10 ⁵	100.4	1.4x10 ⁻⁶
PAT-16XF	Corner 150°	443	1.073	2.366	39.666	1.210x10 ⁵	98.78	<5.5x10 ⁻⁶
PAT-14XB	End 180°	466	1.080	2.381	39.681	1.340x10 ⁵	109.4	1.9x10 ⁻⁶

* Goal is 1,22488x10⁵ ft-lb KE. This is with 6.94 lb UO₂ (3.15 kg), 44.24 lb (20 kg) total weight (TB-1+PC-1+UO₂), and 422 fps impact.

** Average percent of goal in five tests is 102.3.

† q results are TB-1 air leak rates in cm³/s after entire NRC qualification test series of impact perpendicular to unyielding target at stated velocity; 70,000 lb crush; 5,000 ft-lb puncture; 15,000 ft-lb slash; 1 hr 1850°F burn; 3 ft 8 hr underwater; helium mass spectrometer leak check.

POOR ORIGINAL



Figure 2.5.1.1-1. Top (0°) Impact

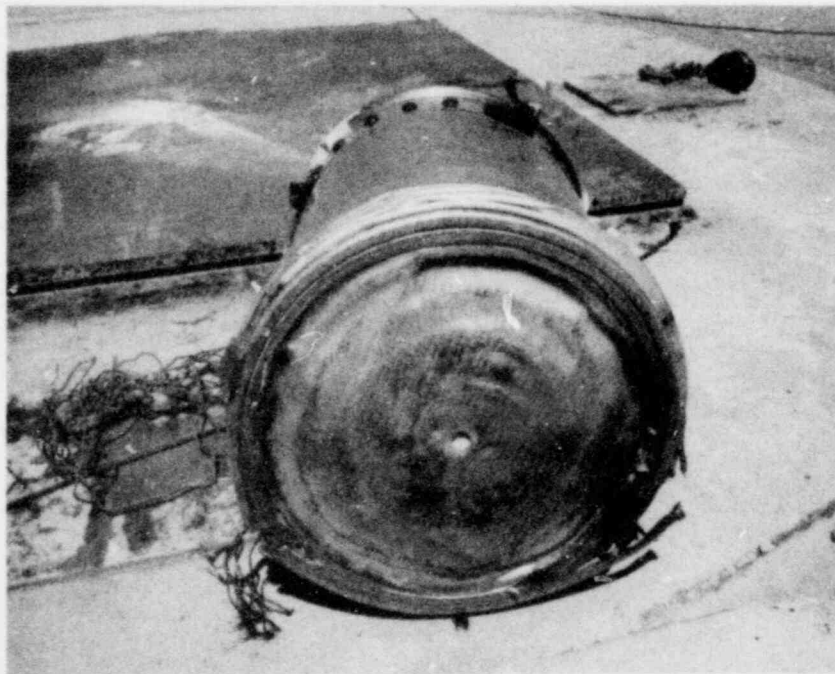


Figure 2.5.1.1-2. Top (0°) Impact

1567 079

POOR ORIGINAL

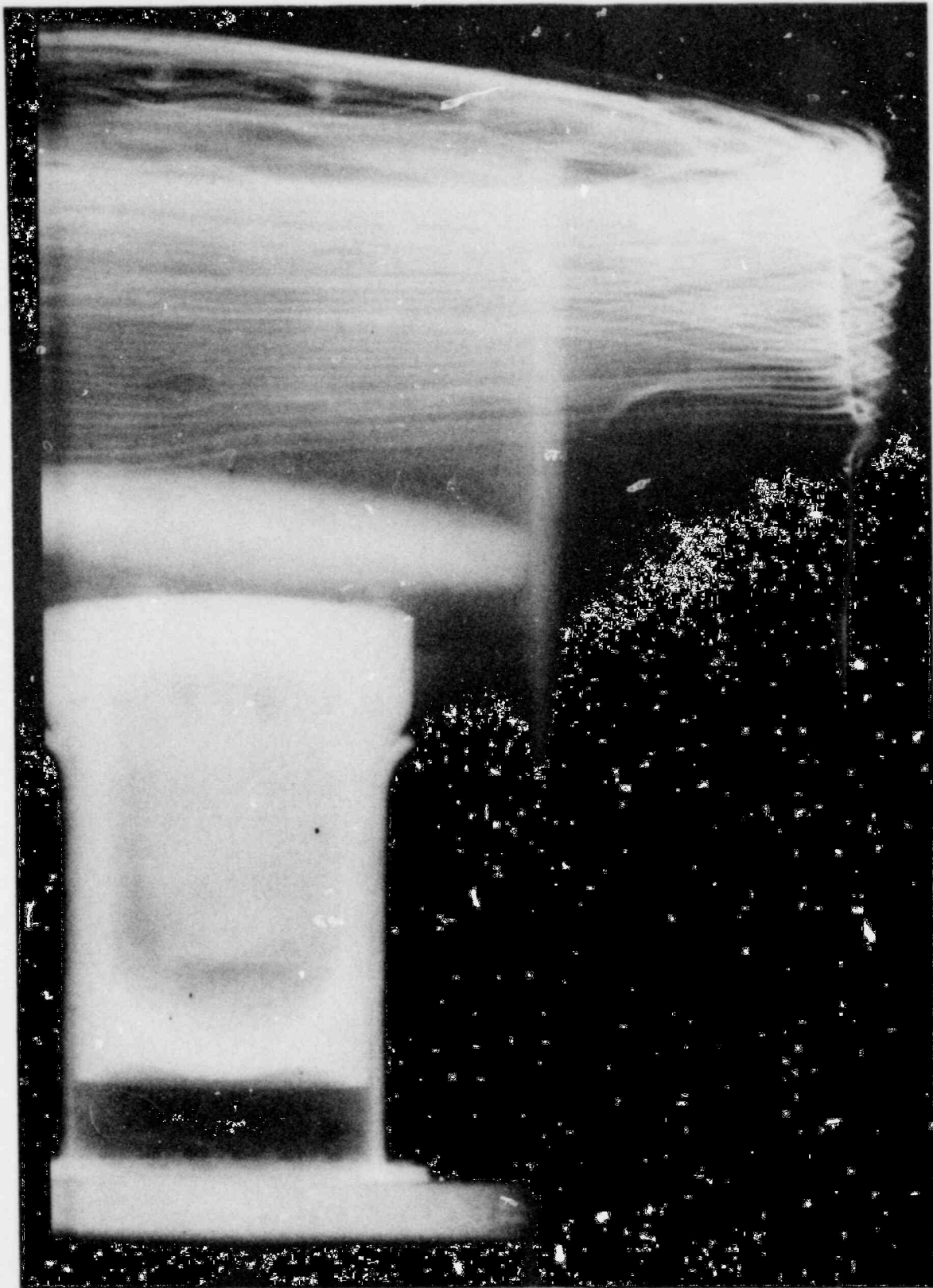


Figure 2.5.1.1-3. Postimpact Radiograph Showing TB-1 Containment Vessel
(Top End (0°) Impact)

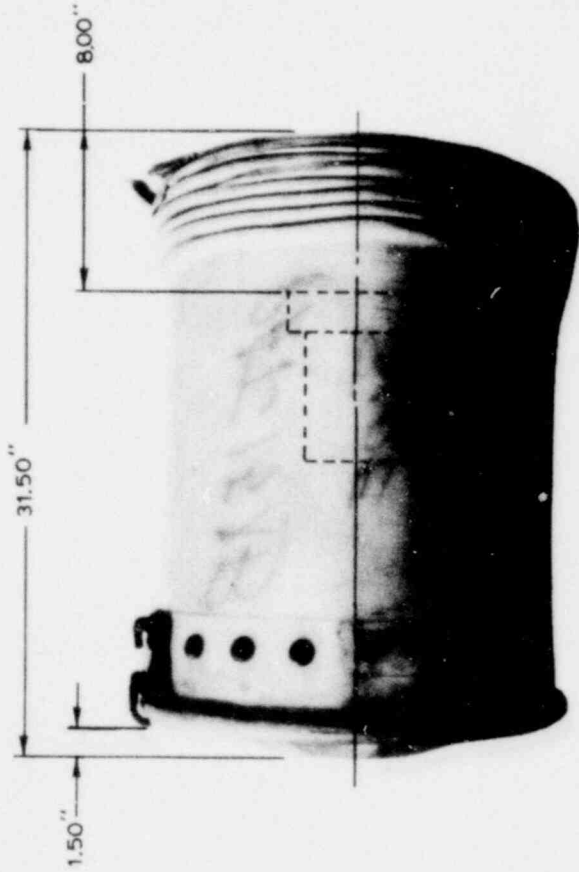
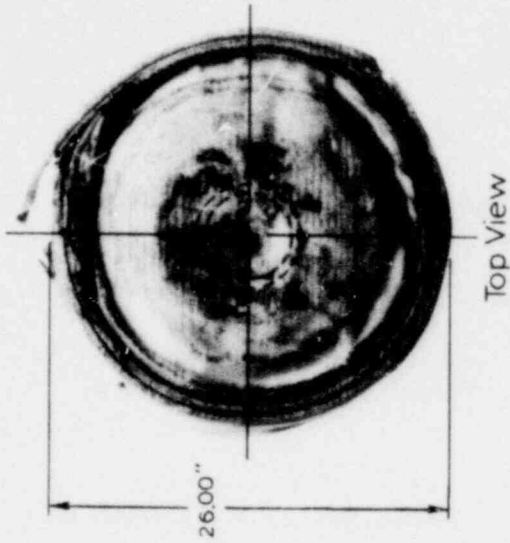
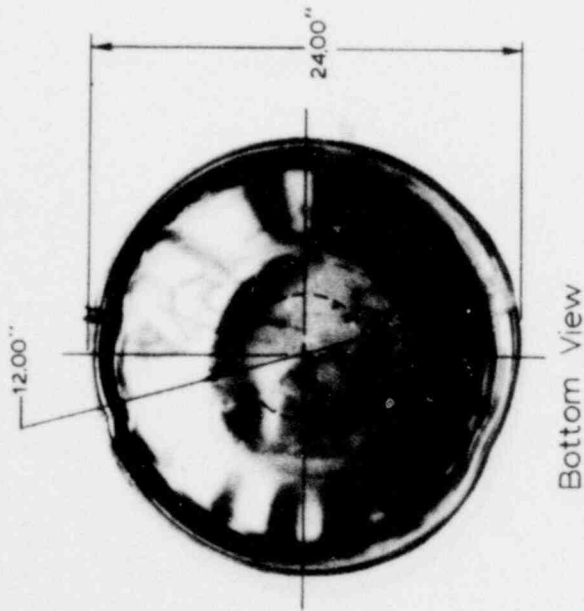


Figure 2.5.1.1-4. Postimpact Package Measurements -- Top (0°) Impact

POOR ORIGINAL



Figure 2.5.1.1-5. Top Corner (30°) Impact



Figure 2.5.1.1-6. Top Corner (30°) Impact

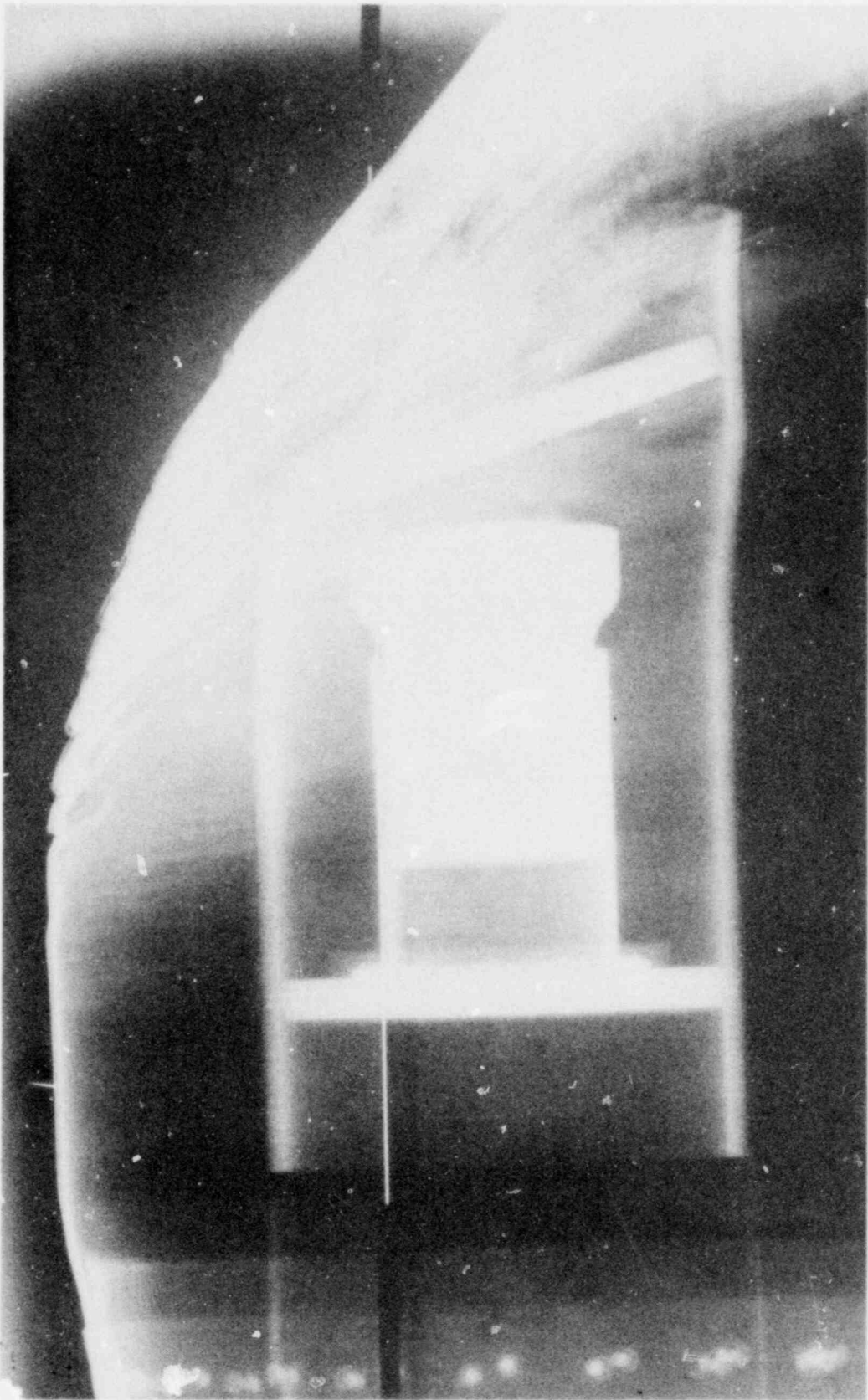


Figure 2.5.1.1-7. Postimpact Radiograph Showing TB-1 Containment Vessel
(Top Corner 30° Impact)

POOR ORIGINAL

1567 083

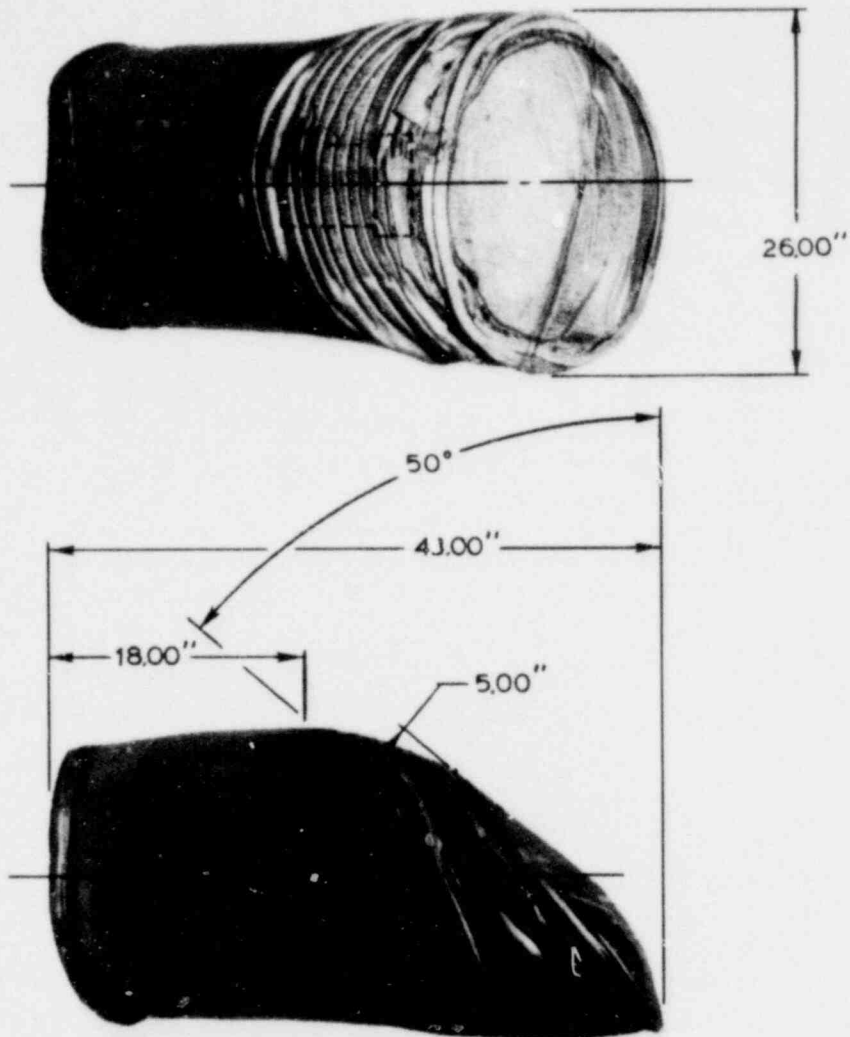


Figure 2.5.1.1-8. Postimpact Package Measurements After Top Corner (30°) Impact

1567 084

- c. Side (90°) Impact -- A PAT-1 package was impacted onto the side (designated as the 90° orientation) at 445 fps (137 m/s) at an angle of 88°. The package was flattened to approximately one-half of the original diameter. The inner drum liner was revealed at the corners, but there was no visible redwood. Health physics monitoring revealed no uranium. The postimpact appearance is shown in Figures 2.5.1.1-9, -10, and -11. Postimpact radiography revealed that this crash attitude is the most threatening to the inner containment vessel, but there was no discernible effect on the inner containment vessel (Figure 2.5.1.1-12).
- d. Bottom Corner (150°) Impact -- A PAT-1 package was impacted onto the bottom corner (designated as the 150° orientation) at 443 fps (135 m/s), with a compound angular error approaching 4° ($\pm 10^\circ$) allowed. The welded joint in the bottom clamp ring was deliberately impacted. A rebound (second) impact slightly dented the top corner. The primary crash indentation essentially transferred the entire bottom end of the package into the plane perpendicular to the 150° trajectory. A tear in the outside drum, in one of the crash-induced corrugations, exposed the bonding material between the drum and the drum liner, but the inner liner was not exposed and therefore there was no exposed redwood. Health physics monitoring revealed no uranium. The postimpact appearance is shown in Figures 2.5.1.1-13, -14, and -15. Postimpact radiography revealed no discernible change in the TB-1 containment vessel, as shown in Figure 2.5.1.1-16.
- e. Bottom (180°) Impact -- A PAT-1 package was impacted onto the bottom end (designated as the 180° orientation) at 466 fps (142 m/s) and with an angular error of 1°. The original package length of approximately 43 in. (109 cm) was reduced to approximately 30 in. (76 cm). There was no opening through the drum or drum liner, and therefore no exposed redwood. The tubular load-spreader imprint in the top end was not as apparent as with the top crash. Health physics monitoring revealed no uranium material on the package exterior. The postimpact appearance is shown in Figures 2.5.1.1-17, -18, and -19. Postimpact radiographs revealed no discernible change in the TB-1 containment vessel, as shown in Figure 2.5.1.1-20.

POOR ORIGINAL

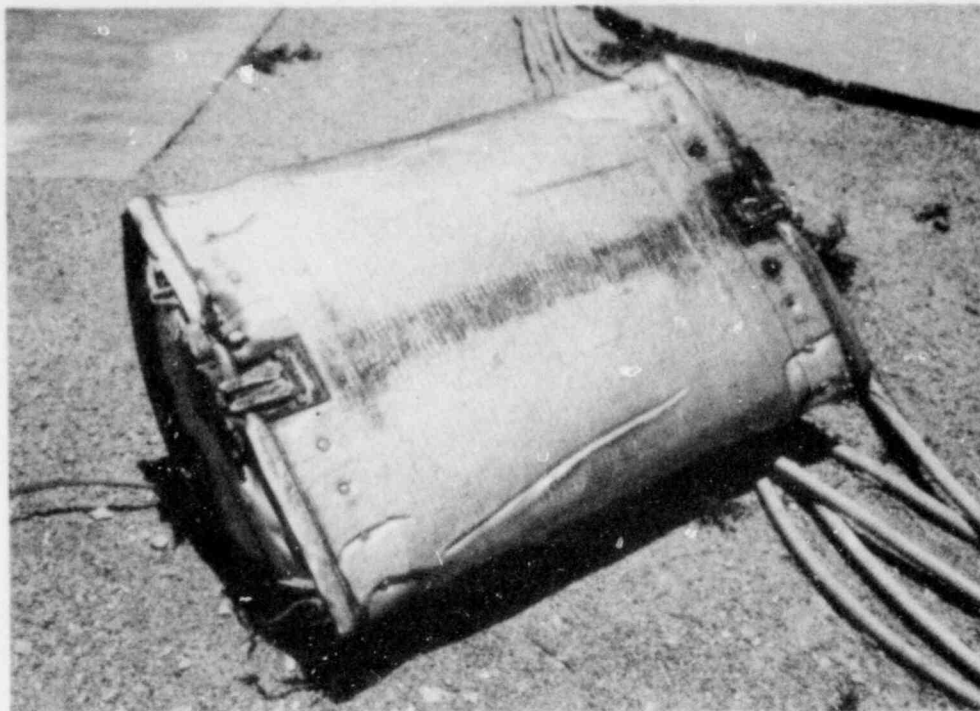


Figure 2.5.1.1-9. Side (90°) Impact

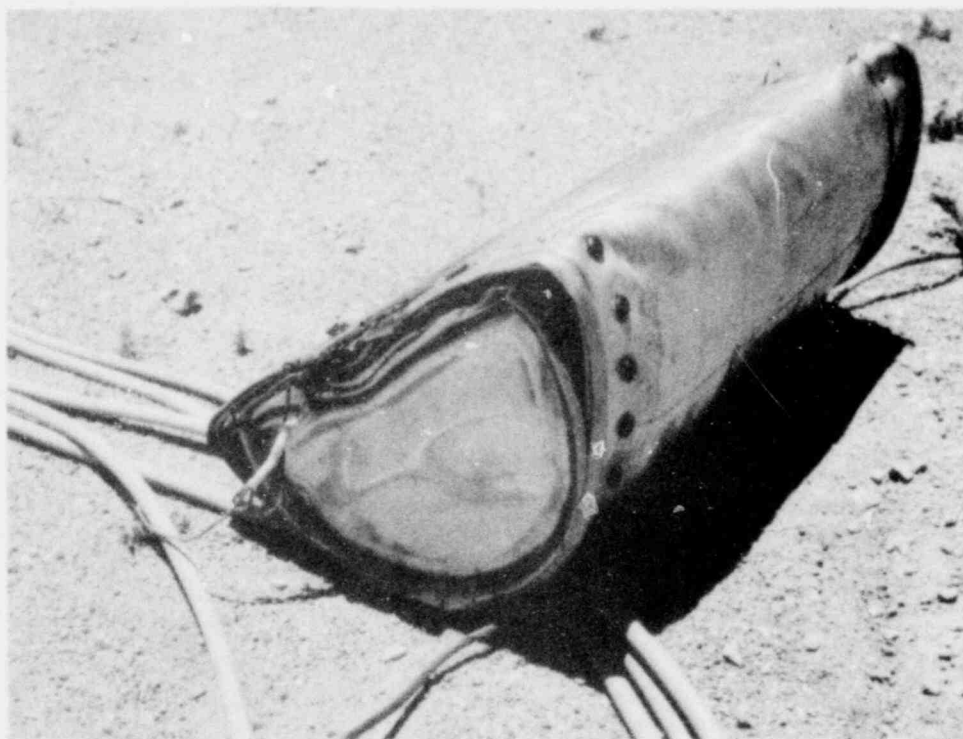
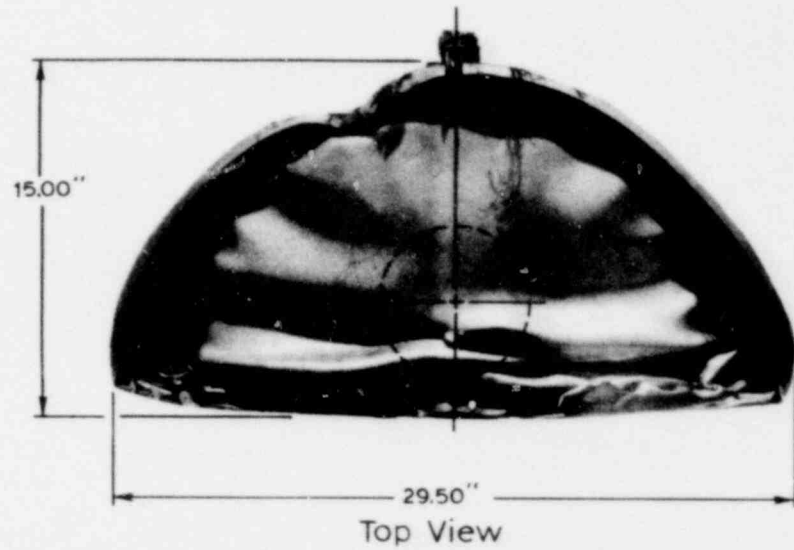
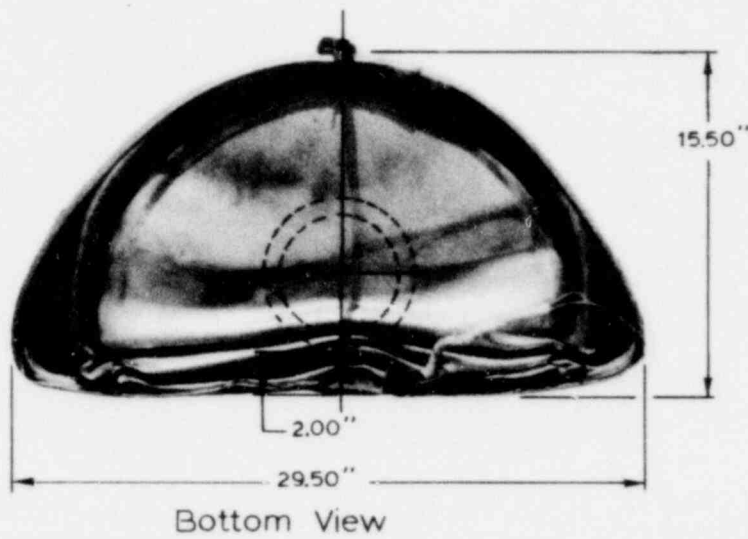


Figure 2.5.1.1-10. Side (90°) Impact



POOR ORIGINAL

1567 087

Figure 2.5.1.1-11. Postimpact Package Measurements--Side (90°) Impact

POOR ORIGINAL

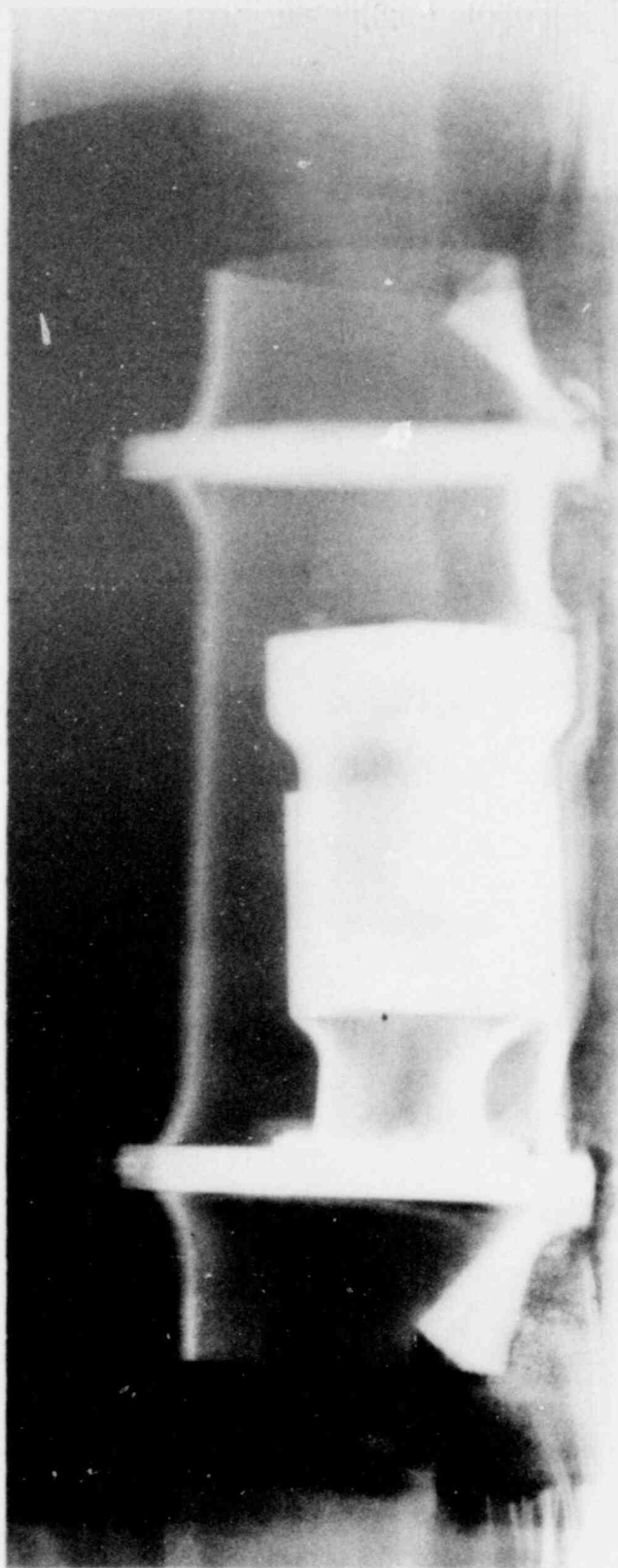


Figure 2.5.1.1-12. Postimpact Radiograph Showing TB-1 Containment Vessel (Side (180°) Impact)

POOR ORIGINAL

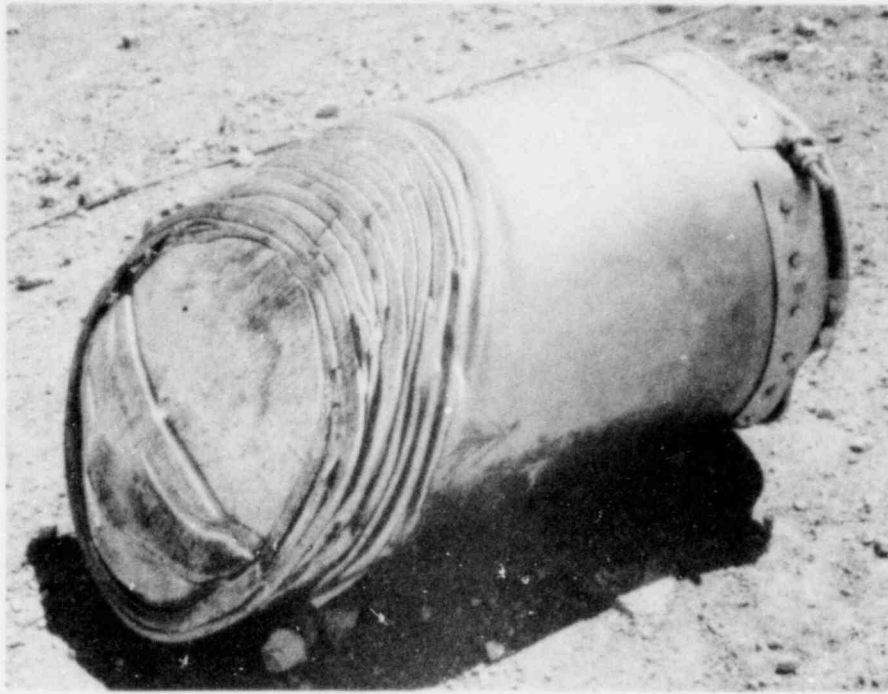


Figure 2.5.1.1-13. Bottom Corner (150°) Impact



Figure 2.5.1.1-14. Bottom Corner (150°) Impact

1567 089

POOR ORIGINAL

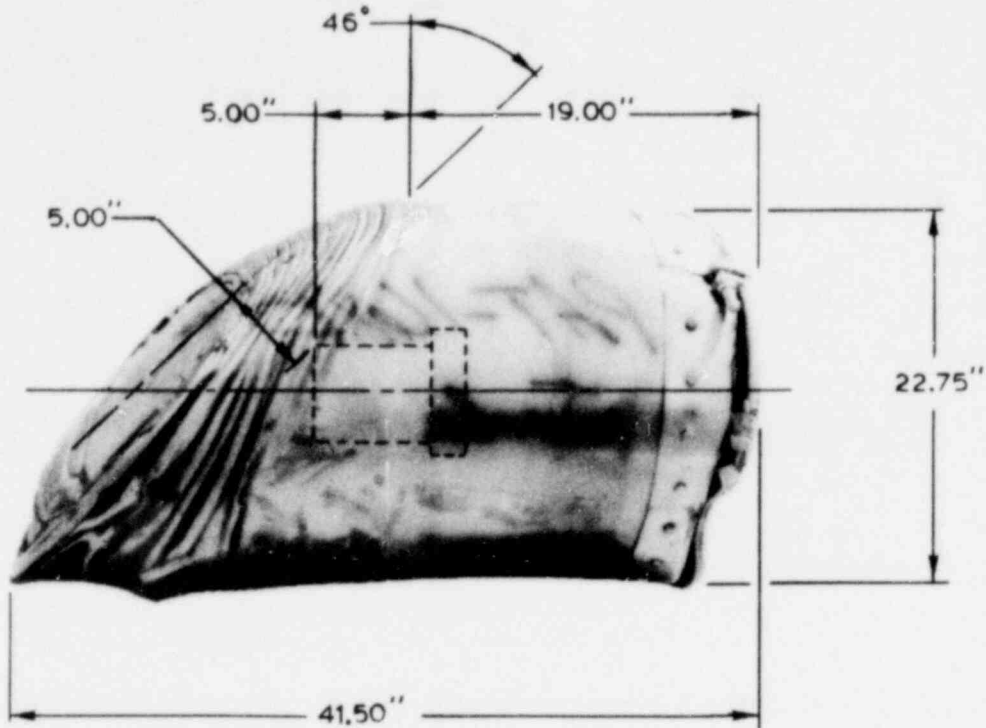


Figure 2.5.1. 1-15. Postimpact Measurements -- Bottom Corner (150°) Impact

POOR ORIGINAL

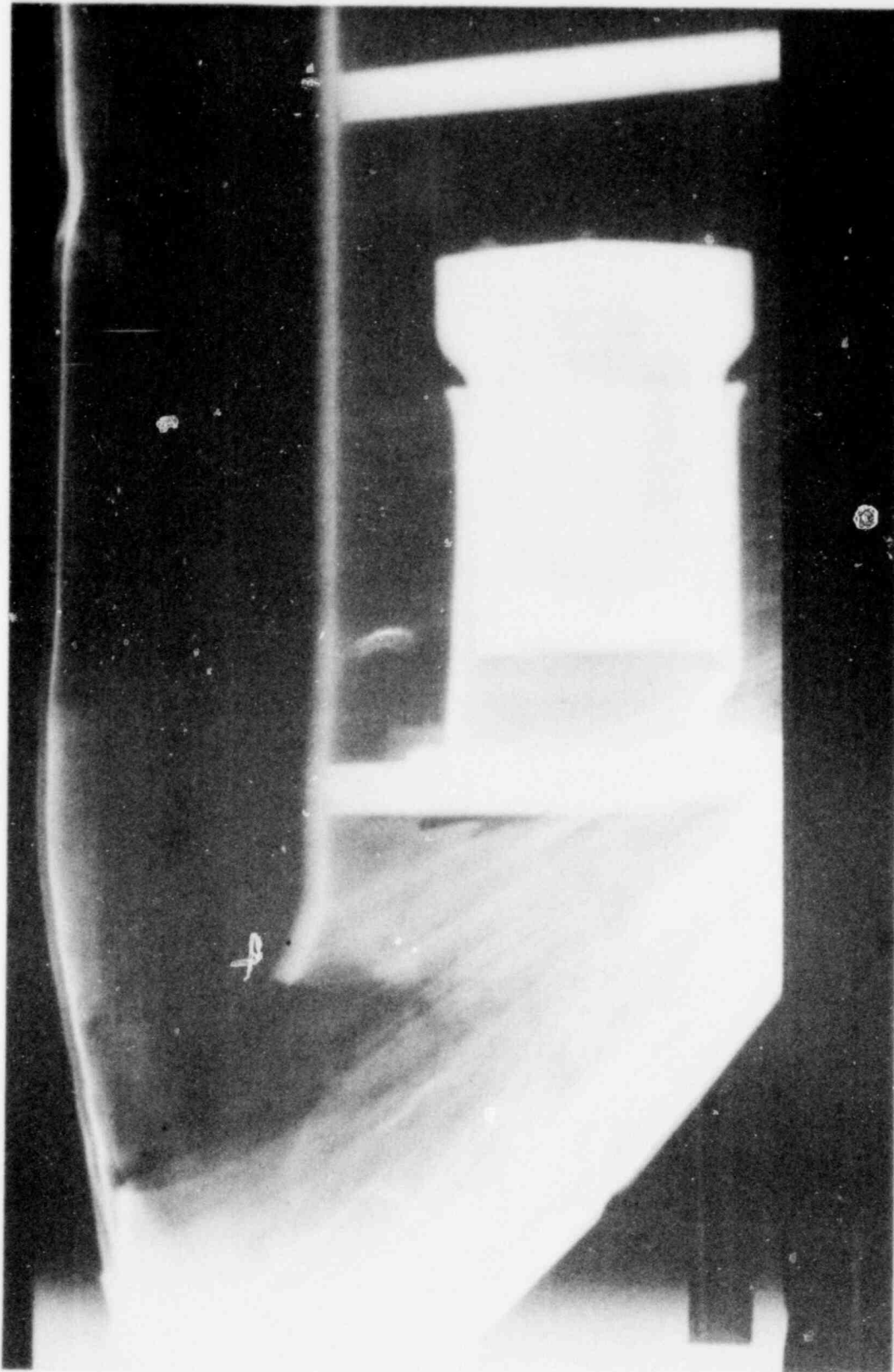


Figure 2.5.1.1-16. Postimpact Radiograph Showing TB-1 Containment Vessel (Bottom Corner (150°) Impact)

1567 091



Figure 2.5.1.1-17. Bottom (180°) Impact

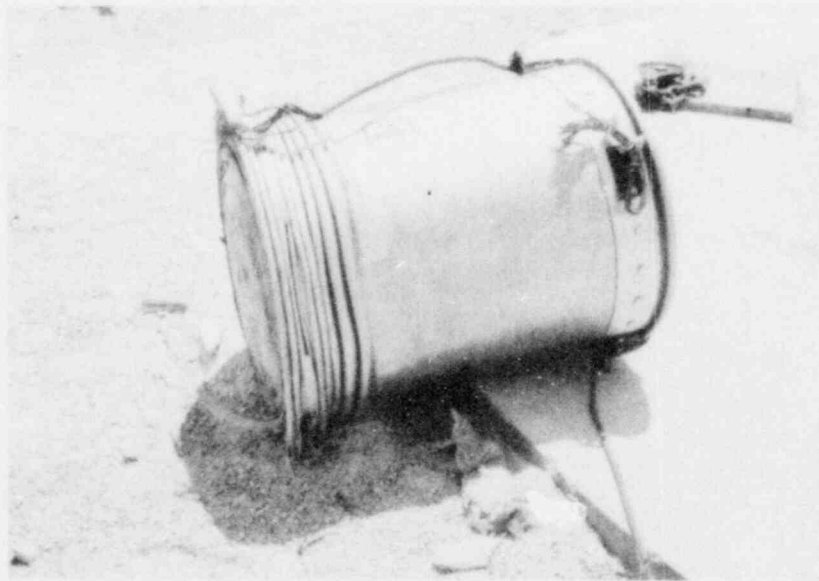


Figure 2.5.1.1-18. Bottom (180°) Impact

POOR ORIGINAL

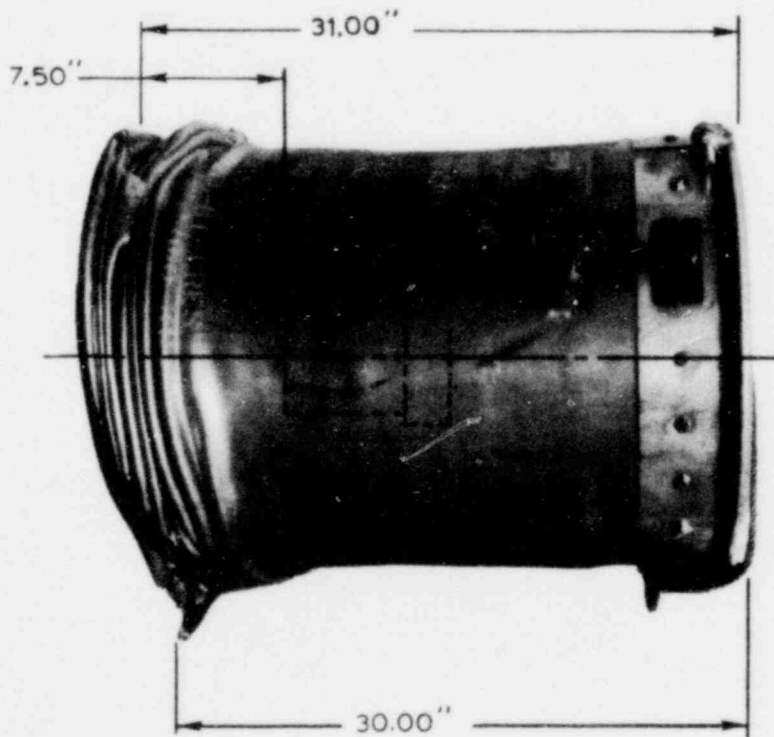
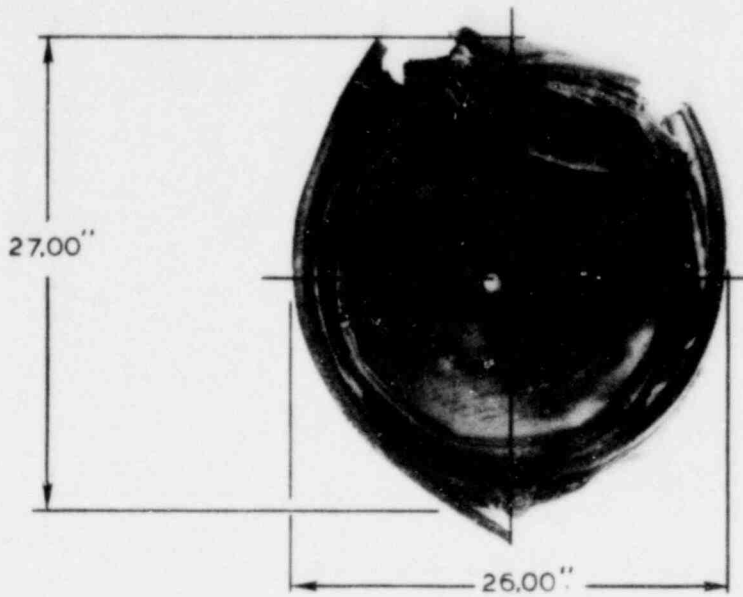


Figure 2.5.1.1-19. Postimpact Measurements -- Bottom (180°) Impact

1567 093

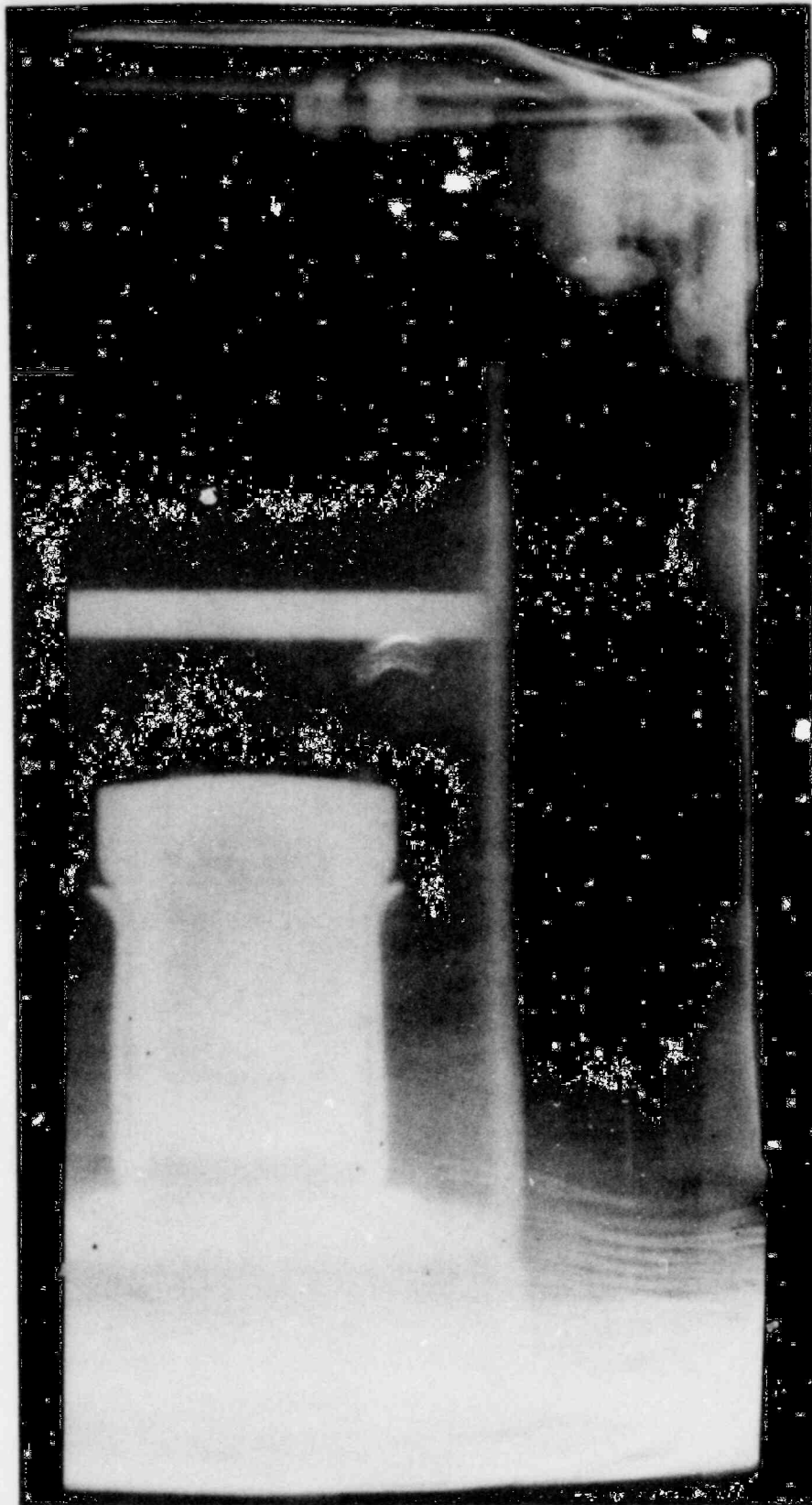


Figure 2.5.1.1-20. Postimpact Radiograph Showing TB-1 Containment Vessel (Bottom End (180°) Impact)

POOR ORIGINAL

1567 094

POOR ORIGINAL

2.5.1.2 Crush

The 70,000-lb (0.311 MN) crush test was applied through a rigid 2-in. (5-cm) wide steel beam to the most vulnerable point on the crashed PAT-1 packages as revealed by radiographs. This test produces negligible effects on the PAT-1 package, as shown in Figures 2.5.1.2-1, -2, and -3.

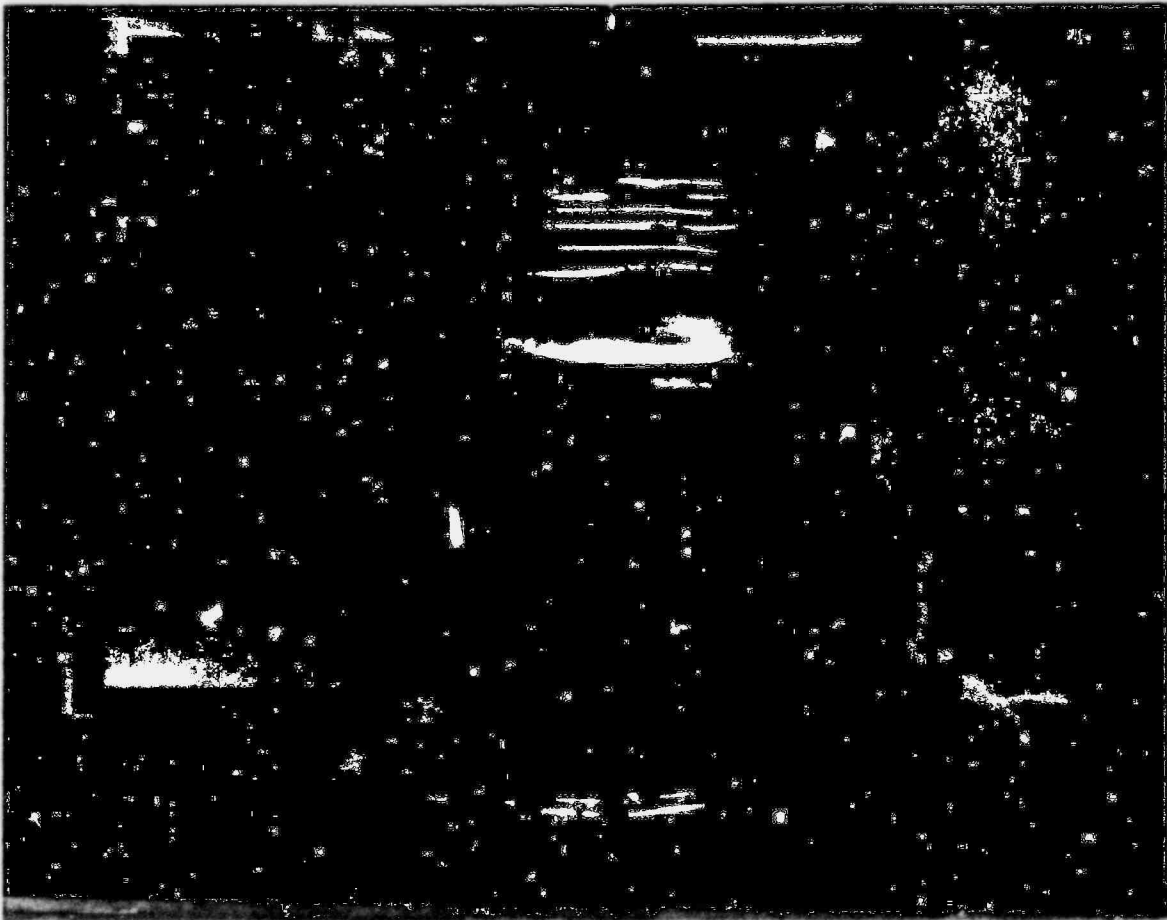


Figure 2.5.1.2-1. Crush Test

1567 095



Figure 2.5.1.2-2. Crush Test

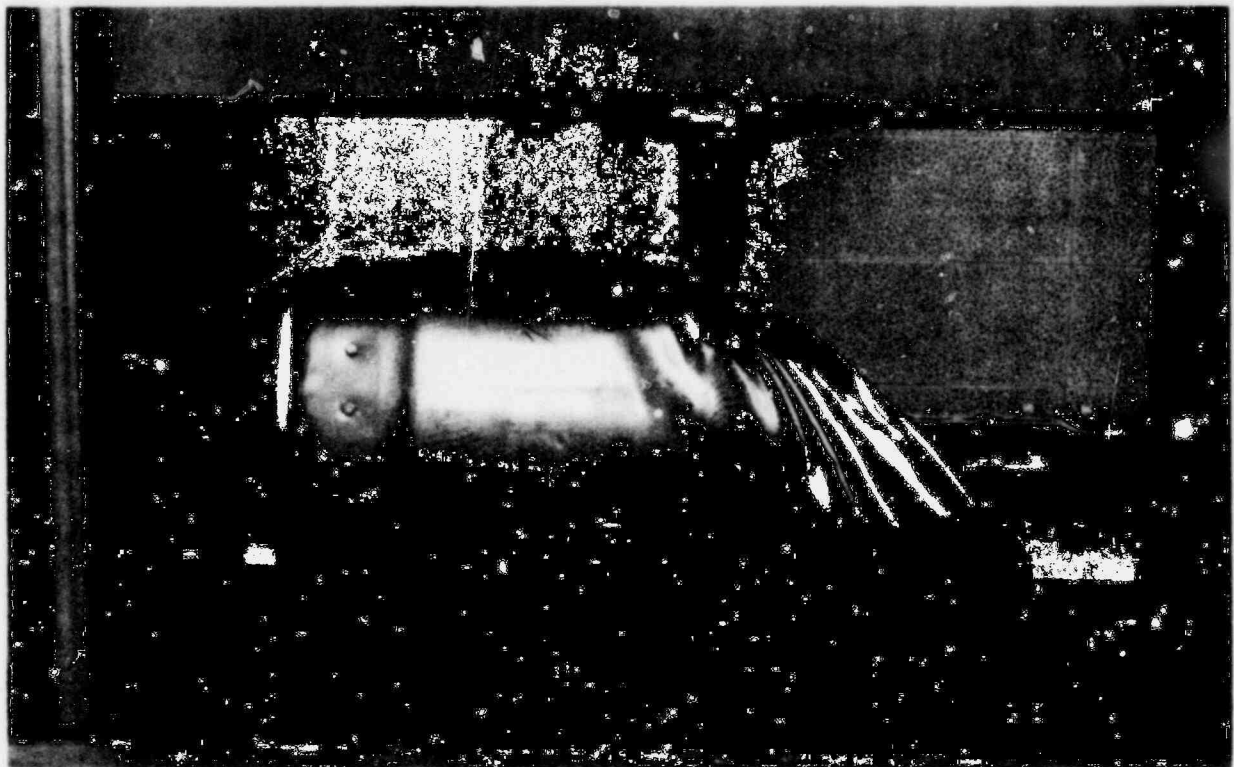


Figure 2.5.1.2-3. Crush Test

2.5.1.3 Puncture

The 10-ft (3-m) drop of the 500-lb (227-kg) steel spike onto the same contact point used for the crush test generally opened a 2-in. (5-cm) diam hole through the drum and drum liner, penetrating into the redwood. On a side-crashed package, penetration was not as great due to the preexisting severe compaction from the crash test. Results of the five packages are shown in Figures 2.5.1.3-1, -2, -3, -4, and -5.

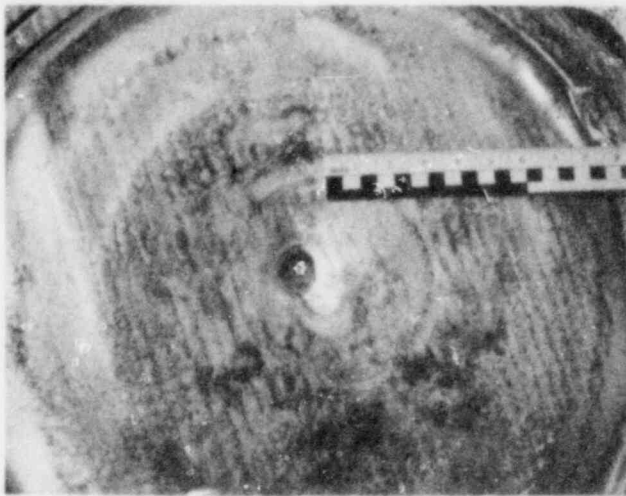


Figure 2.5.1.3-1. Puncture Test on Top-End-Impacted PAT-1

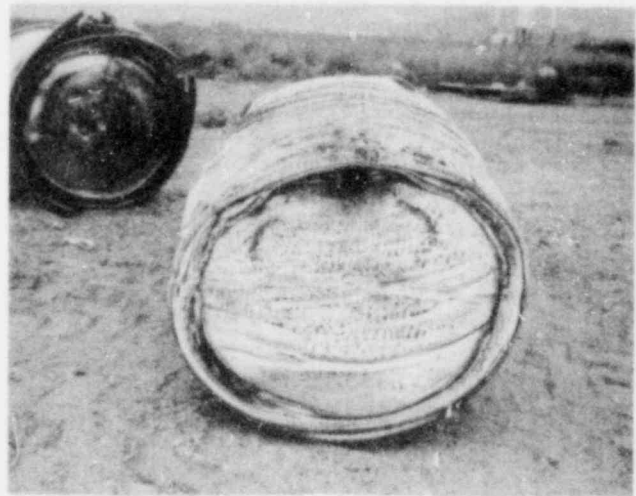


Figure 2.5.1.3-2. Puncture Test on Top-Corner-Impacted PAT-1

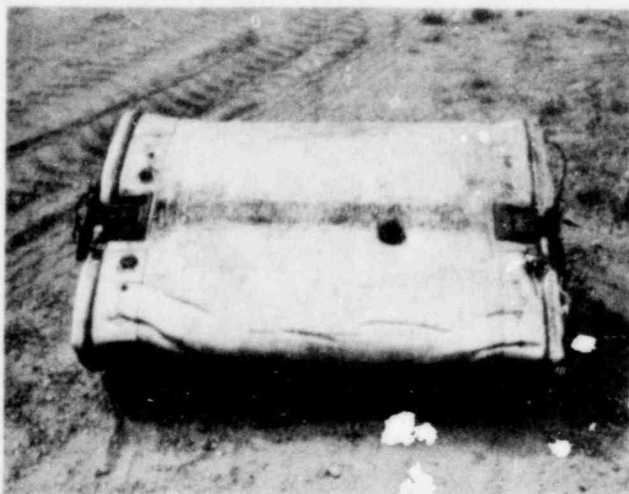


Figure 2.5.1.3-3. Puncture Test on Side-Impacted PAT-1



Figure 2.5.1.3-4. Puncture Test on Bottom-Corner-Impacted PAT-1

POOR ORIGINAL

1567 097

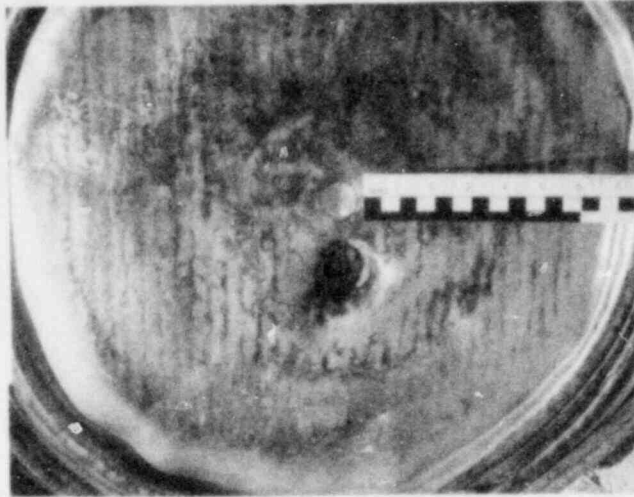


Figure 2.5.1.3-5. Puncture Test on Bottom-End-Impacted PAT-1

2.5.1.4 Slash

The slash test produces a relatively major effect, penetrating the outer stainless-steel PAT-1 drum and the drum liner, generally to a depth of approximately 4 in. (10 cm) along the trajectory path, or about 3 in. (7 cm) of penetration normal to a drum surface. The slash projectile did not reach the load-spreader structure embedded within the PAT-1 outer redwood components. The effects of this double test are shown in Figures 2.5.1.4-1, -2, -3, and -4.

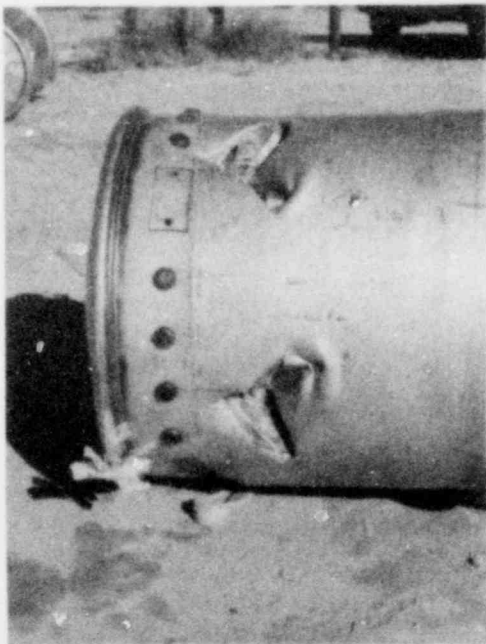


Figure 2.5.1.4-1. Slash Test

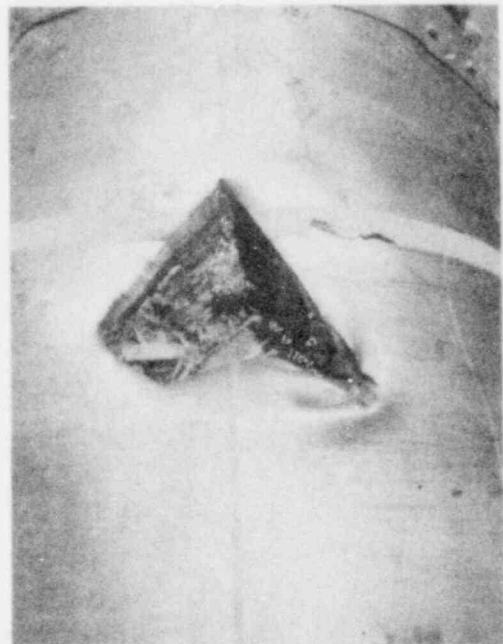


Figure 2.5.1.4-2. Slash Test

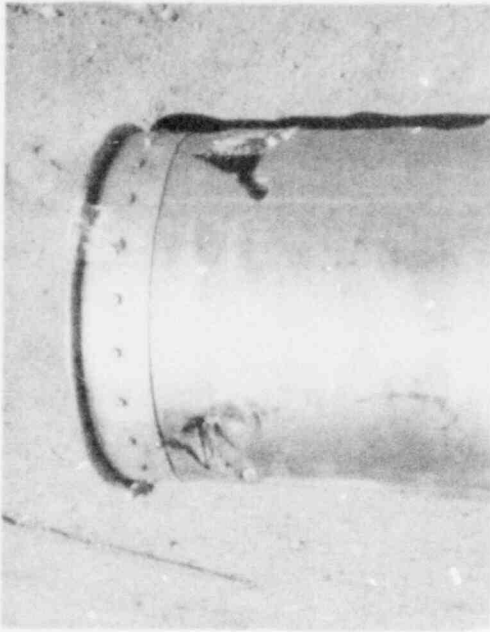


Figure 2.5.1.4-3. Slash Test



Figure 2.5.1.4-4. Slash Test

2.5.1.5 Fire

The 60-minute (minimum) contained JP-4 fire with an enhanced draft typically produced a flame temperature of approximately 2200°F (1200°C) at the level of the PAT-1 package. This test, following the impact, crush, puncture, and slash tests, generally resulted in charring of all the redwood in the PAT-1 package. The AQ-1 aluminum load-spreader elements did not appear to have exceeded the solidus temperature (approximately 1080°F (582°C)). The AQ-1 copper heat-conductor tube was integral. The TB-1 nylon lifting strap was always totally consumed (approximately 500°F (260°C)) char temperature. The chimney was entered shortly after fuel starvation extinguishment of the JP-4 fire and redwood was observed as glowing red coal through the slash holes; charring wood, not exposed aluminum, was always initially observed. The PAT-1 packages required from 1 to 3 days for afterburn temperature to subside to a temperature comfortable for the prolonged touch of a bare hand on the AQ-1 drum. At this time, the wood observed through the slash holes essentially had the appearance of ash.

The preburn appearance of the packages is shown in Figures 2.5.1.5-1, -2, -3, -4, and -5. In-progress appearance of the three fires used to burn the five packages is shown in Figures 2.5.1.5-6a, b, and c. Postburn (and postmortem) appearance of the packages is discussed in paragraph 2.5.1.7.

POOR ORIGINAL

1567 099

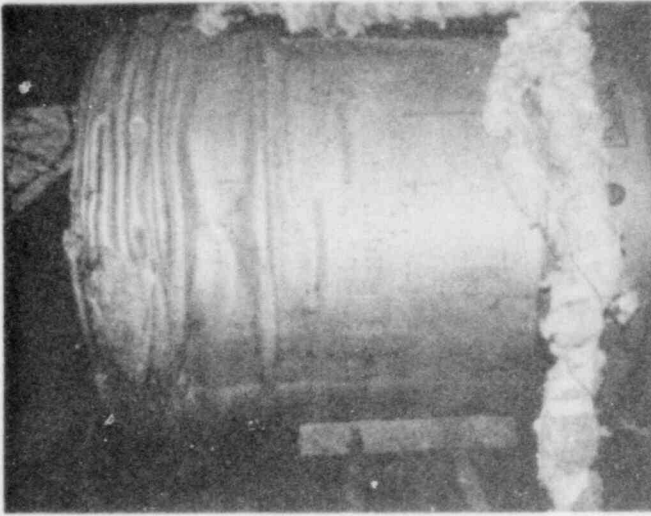


Figure 2.5.1.5-1. Preburn Appearance of Top-End-Impacted PAT-1

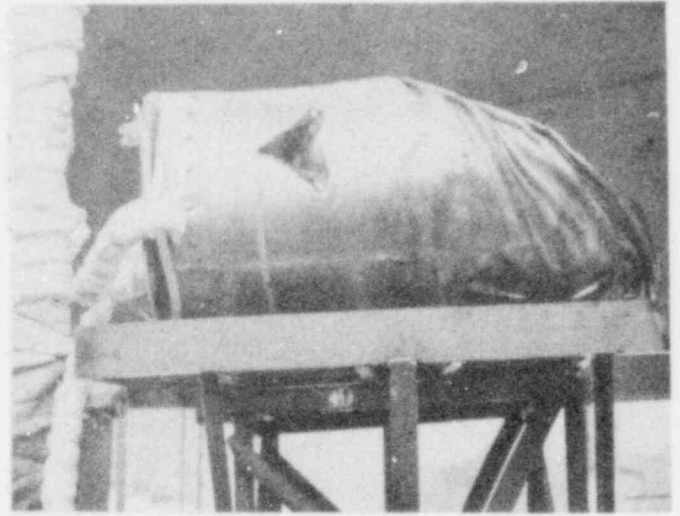


Figure 2.5.1.5-2. Preburn Appearance of Top-Corner-Impacted PAT-1

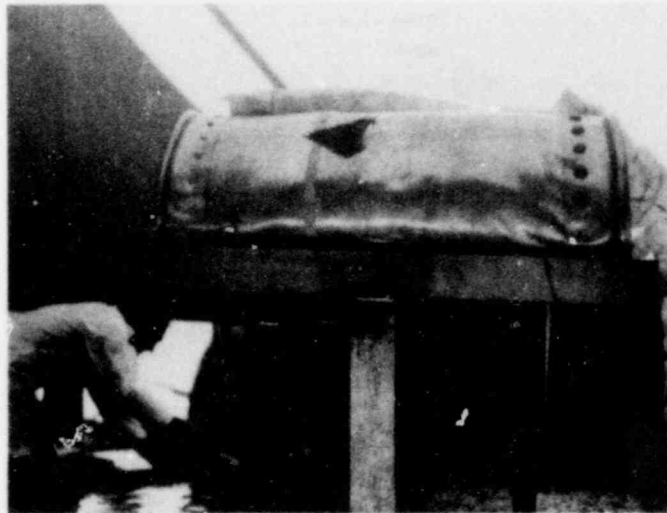


Figure 2.5.1.5-3. Preburn Appearance of Side-Impacted PAT-1

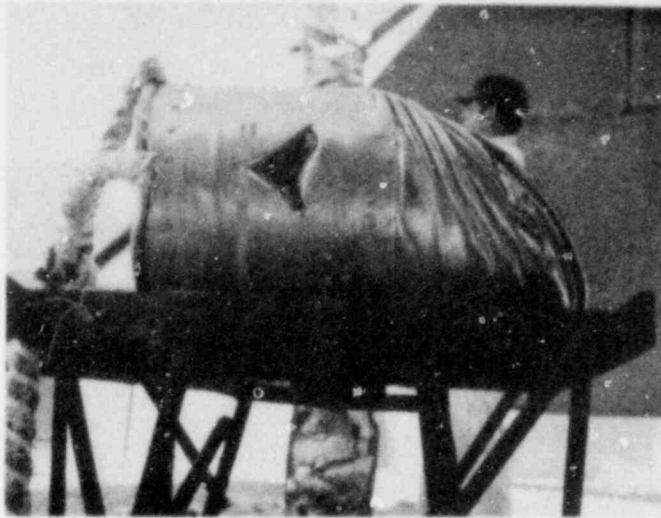


Figure 2.5.1.5-4. Preburn Appearance of Bottom-Corner-Impacted PAT-1

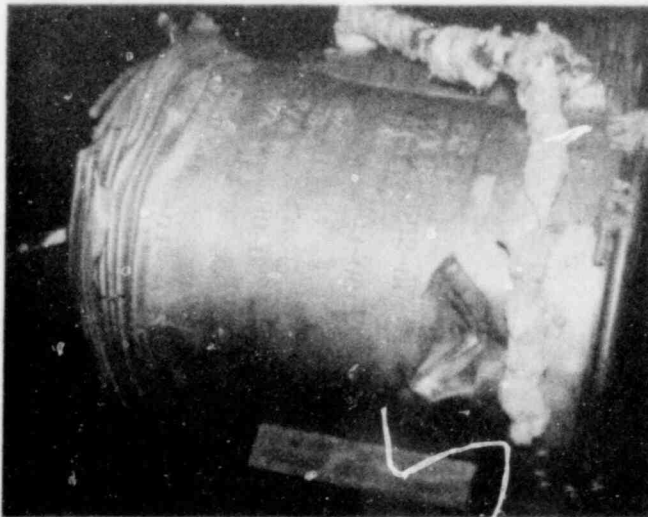


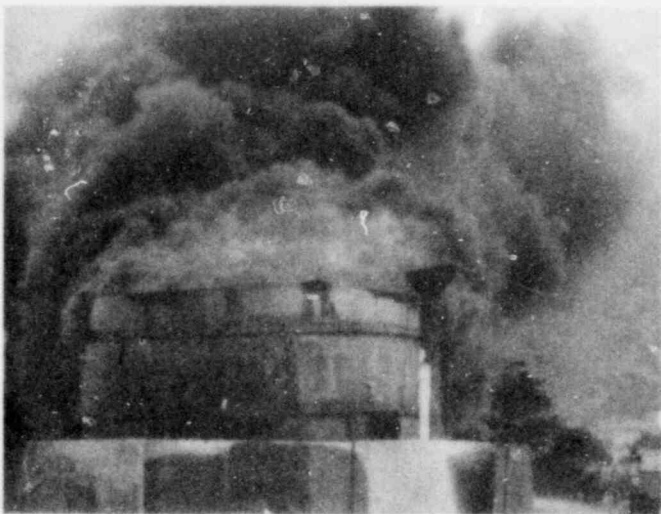
Figure 2.5.1.5-5. Preburn Appearance of Bottom-End-Impacted PAT-1

507 1387
POOR ORIGINAL

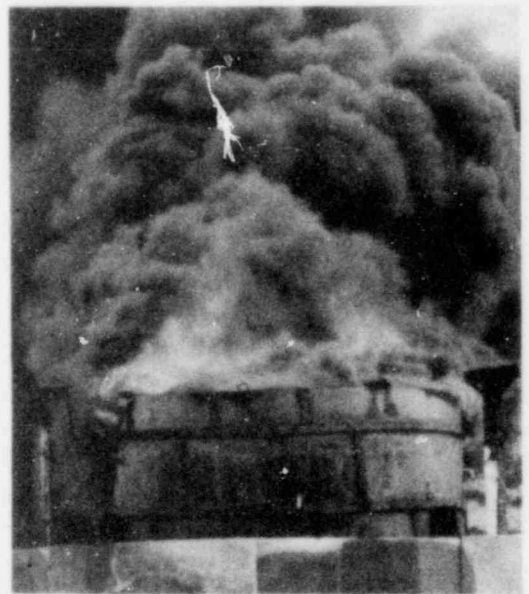
1567 101



a.



b.



c.

Figure 2.5.1.5-6. Burn Test

2.5.1.6 Immersion

The immersion test washed out the redwood ash in the region of the two slash holes in each PAT-1 package, exposing the AQ-1 tubular aluminum load spreader. The immersion test also tended to spread black sooty water onto the TB-1 containment vessel (as observed in following postmortem operations).

The appearance of the vessels after the five immersion tests is shown in Figures 2.5.1.6-1, -2, -3, -4, and -5.

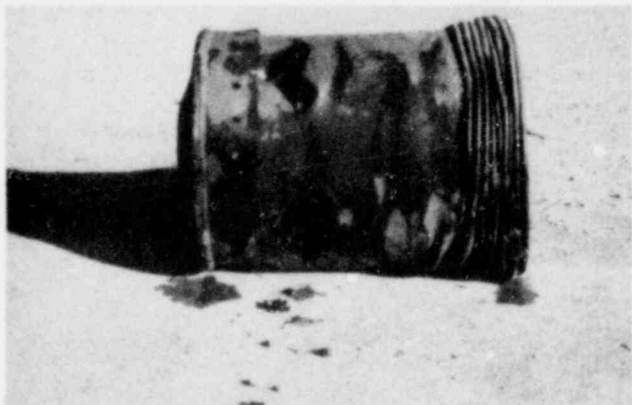


Figure 2.5.1.6-1. Postimmersion Test of Top-End-Impacted PAT-1

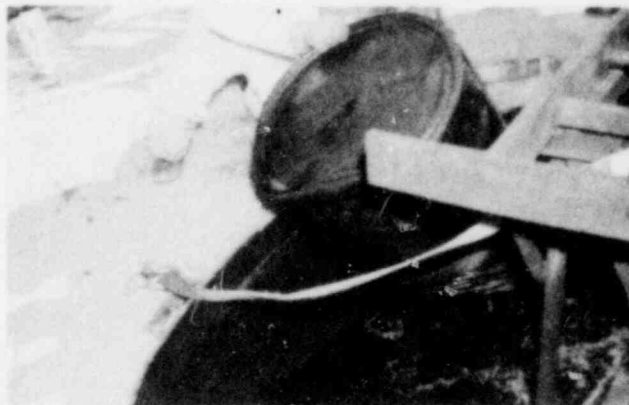


Figure 2.5.1.6-2. Immersion Test on Top-Corner-Impacted PAT-1



Figure 2.5.1.6-3. Immersion Test on Side-Impacted PAT-1

POOR ORIGINAL

1567 103

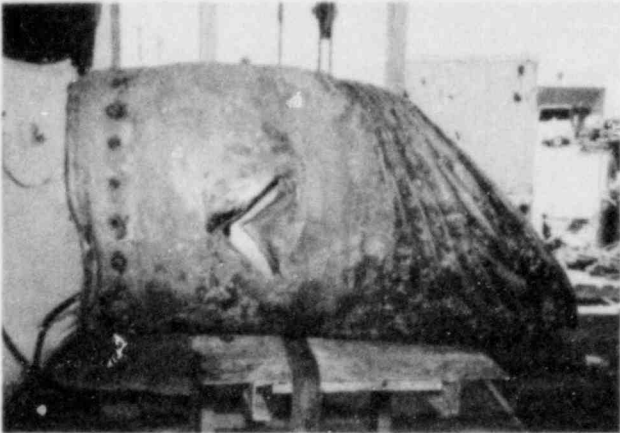


Figure 2.5.1.6-4. Postimmersion Test on Bottom-Corner-Impacted PAT-1

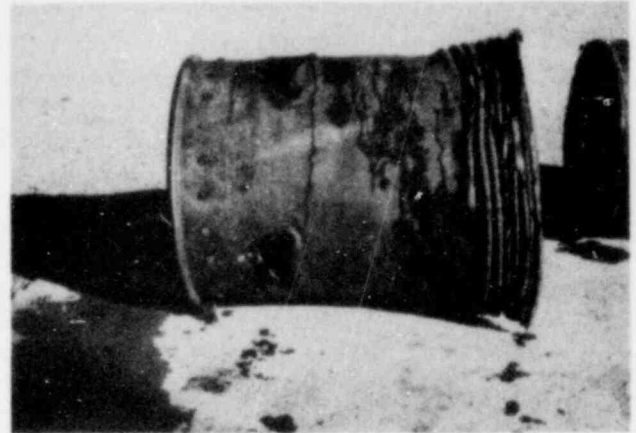


Figure 2.5.1.6-5. Postimmersion Test on Bottom-End-Impacted PAT-1

2.5.1.7 Posttest Summary of Package Damage

Disassembly of the five sequentially tested* PAT-1 packages was accomplished by the use of cutting torches, a large water-cooled machine-fed band saw, and hand tools.

Sequential photographs of the disassembly of the top-impacted PAT-1 package appear as Figures 2.5.1.7-1, -2, -3, -4, -5, -6, and -7. Uranium material was not detected at any point, as measured by a health physics team.

Photographs of the completely disassembled top-corner-impacted PAT-1 package appear as Figures 2.5.1.7-8 and -9.

Sequence photographs of the disassembly of the side-impacted PAT-1 package appear as Figures 2.5.1.7-10, -11, and -12.

The bottom-corner-impacted PAT-1 package postmortem photos appear as Figures 2.5.1.7-13, -14, -15, and -16.

The bottom-end-impacted PAT-1 package postmortem sequence photos appear as Figures 2.5.1.7-17, -18, -19, and -20.

* Impact, crush, puncture, slash, burn, immersion.

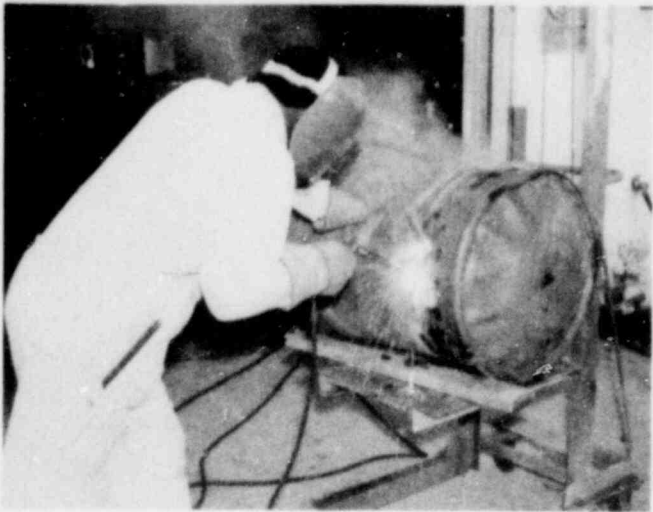


Figure 2.5.1.7-1. Disassembly of Top-End-Impacted PAT-1

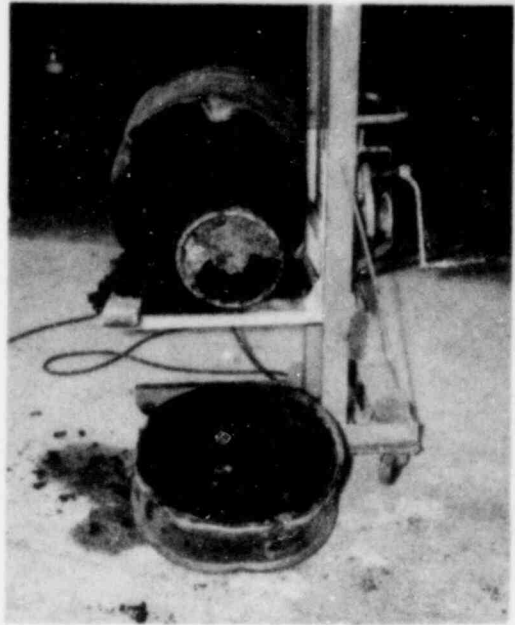


Figure 2.5.1.7-2. AQ-1 Bottom Removed Showing Charred Redwood and Load Spreader



Figure 2.5.1.7-3. Top View of Load Spreader



Figure 2.5.1.7-4. Load Spreader Showing Redwood and Internal Plug (Circular Plate Load Spreader Removed)

POOR ORIGINAL

1567 105

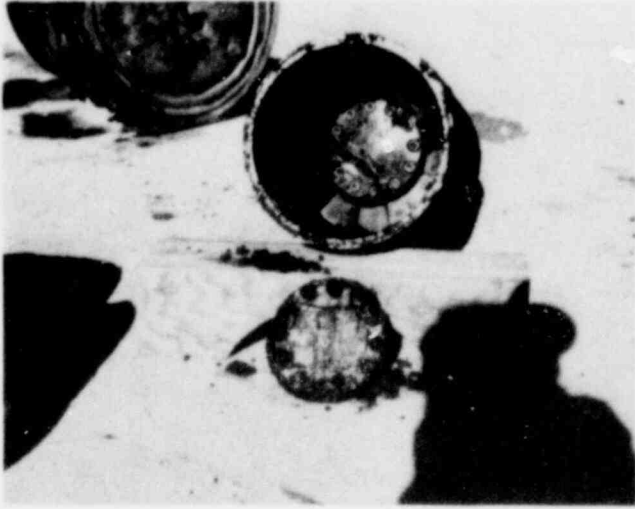


Figure 2.5.1.7-5. Internal (Charred Redwood) Plug Removed Showing TB-1



Figure 2.5.1.7-6. TB-1 Removed From AQ-1



Figure 2.5.1.7-7. Bottom View of TB-1

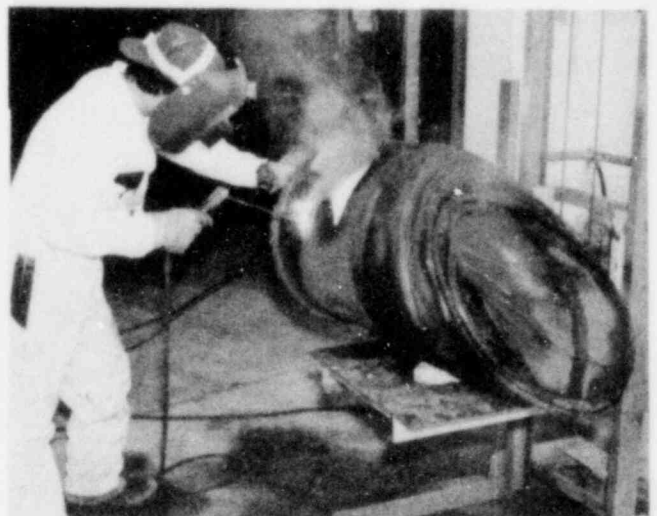


Figure 2.5.1.7-8. Disassembly of Top-Corner-Impacted PAT-1

POOR ORIGINAL

1567 106

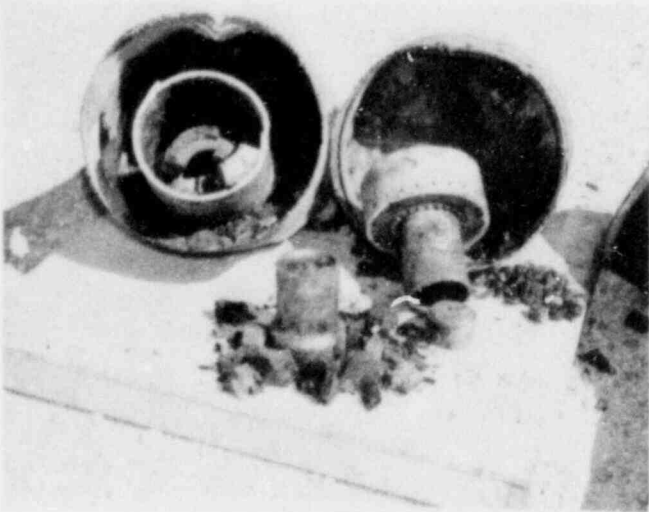


Figure 2.5.1.7-9. Disassembled Top-Corner-Impacted PAT-1



Figure 2.5.1.7-10. Disassembly of Side-Impacted PAT-1

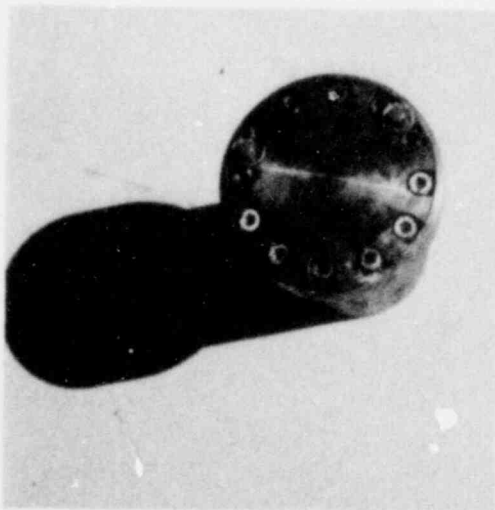


Figure 2.5.1.7-11. Posttest TB-1 - Top View



Figure 2.5.1.7-12. Posttest TB-1 - Bottom View

POOR ORIGINAL

1567 107



Figure 2.5.1.7-13. Disassembly of Bottom-Corner-Impacted PAT-1

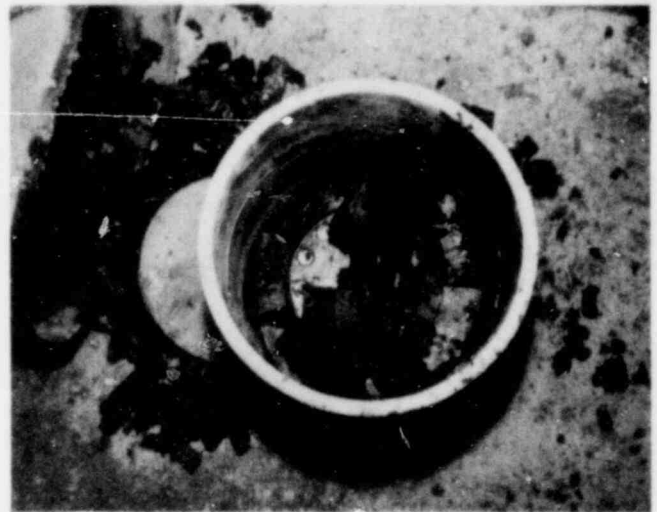


Figure 2.5.1.7-14. Load Spreader Showing Charred Redwood, Load Spreader, and Top of TB-1

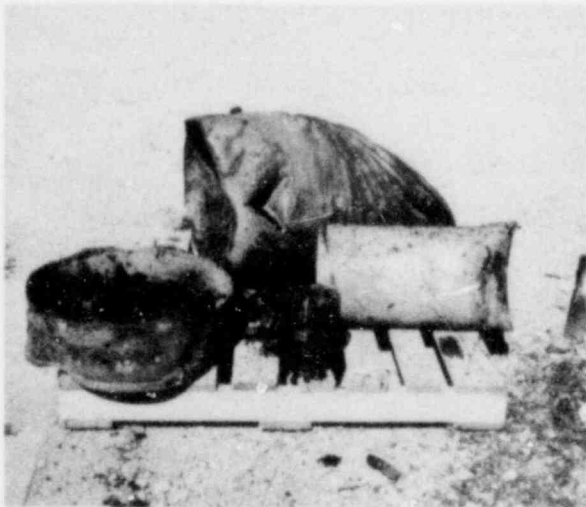


Figure 2.5.1.7-15. Disassembled Bottom-Corner-Impacted PAT-1



Figure 2.5.1.7-16. TB-1 Removed From AQ-1

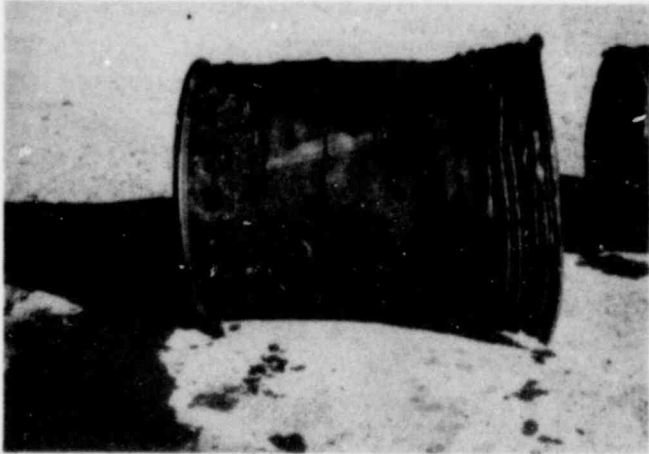


Figure 2.5.1.7-17. Disassembly of Bottom-End-Impacted PAT-1

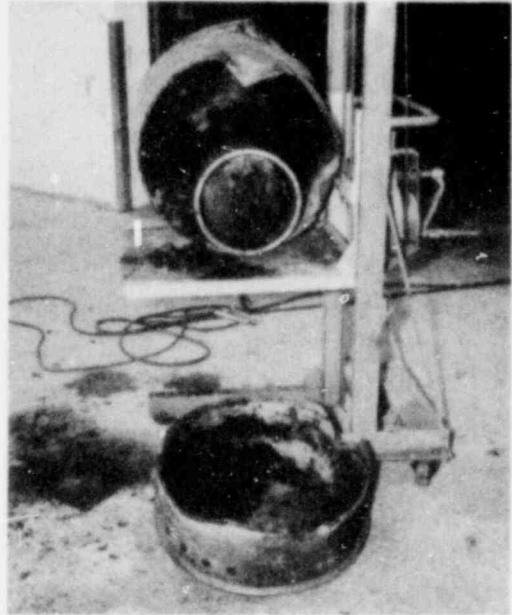


Figure 2.5.1.7-18. Bottom-End-Impacted PAT-1 With Top Removed Showing Charred Redwood and Load Spreader

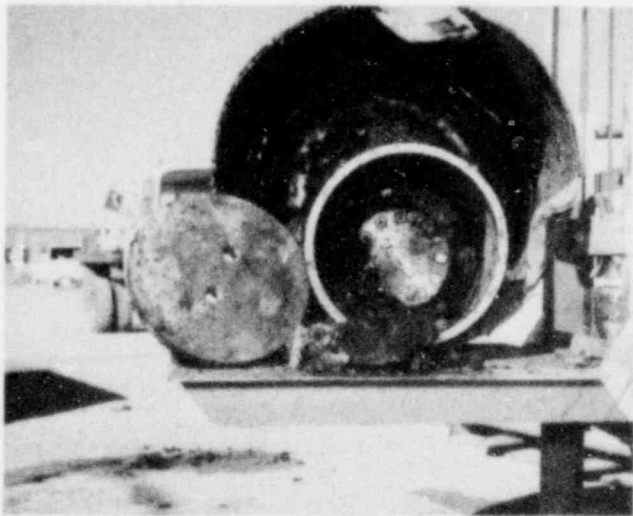


Figure 2.5.1.7-19. Load Spreader Disc Removed Showing Charred Redwood and Top of TB-1



Figure 2.5.1.7-20. TB-1 Removed From AQ-1

POOR ORIGINAL

1567 109

As can be seen in the referenced photos, the TB-1 is charred and blackened by the pyrolysis of the surrounding redwood. Tempilaq, a commercial heat-responding coded lacquer coating, was affected by this pyrolysis and by the water immersion, but still gives rough indications of perhaps 1000°F (~540°C) exposure of the TB-1.

Swipe tests were taken of all TB-1 containment vessels as they emerged from the charcoal during the postmortems; uranium fluorimetry measurements sensitive to 10^{-8} g uranium revealed no uranium on any surface or in any crevice of any TB-1.

The char and contamination on the surface of the TB-1 vessels inhibits the use of highly sensitive mass spectrometer helium leak-detection equipment. Therefore, the vessel exterior is rigorously cleaned with powered wire brushes, solvents, hot vapor-degrease processes, and glass-bead shot peening.

All TB-1 vessels responded favorably to mass spectrometer helium-leak detection (i. e., sufficiently low pressure of deleterious gases to permit helium detection, and positive indication of the presence of helium in a sufficiently small quantity to stay below the saturation level of the instrument). The helium leak-rate readings were converted to air standard by a factor of the square root of their molecular weight ratio. The initial results ranged from a high leak of $< 4.5 \times 10^{-5}$ cm³/s to a low leak of 1.4×10^{-6} cm³/s. Further cleaning of the exterior of the high-leak TB-1 permitted another helium leak-rate measurement, which was 1.7×10^{-7} cm³/s (air).

2.5.2 Individual Hydrostatic Test

2.5.2.1 Individual Hydrostatic Test

A TB-1 containment vessel was subjected to an external pressure of over 600 psi (4.1 MPa) for 25 hr in green-dyed water (Figure 2.5.2.1-1). The helium leak rate of the vessel was $< 10^{-10}$ cm³/s both before and after hydrostatic testing. Following exterior drying, the weight of the TB-1 was identical to its pretest weight. Upon opening of the TB-1, there was no indication of green dye or water inside of the copper seal region (Figure 2.5.2.1-2).



Figure 2.5.2.1-1. Hydrostatic Test Chamber and TB-1

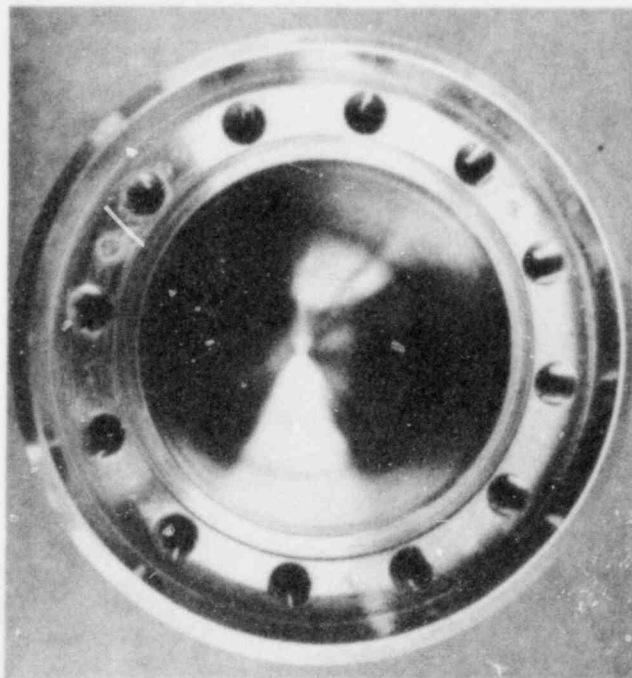


Figure 2.5.2.1-2. Posthydrostatic Test

POOR ORIGINAL 1567 111

2.5.2.2 Impact Tests at Temperature Extremes

- a. Cold -- A prototype PAT package, with construction features that made it a valid comparison to a model PAT-1 package in the side-impact (90°) orientation, was cold soaked at -50°F (-45°C) for more than 48 hr, wrapped with insulating materials, and was side-impacted 2 hr and 15 min. later on a 40°F (4°C) day. Although the external drum would have approached 40°F (4°C) at the time of impact, the bulk temperature of the package at this time was calculated and estimated to be < -40°F (-40°C).

The impact test, at approximately -40°F (-40°C), was conducted perpendicular to the unyielding target on the side (90°) at 433 fps (132 m/s) with 1° error. The package appeared to be slightly less crushed up (Figure 2.5.2.2-1) than similar packages crushed at ambient temperatures. Radiographic inspection (Figure 2.5.2.2-2) revealed slightly more redwood at the point of minimum separation between the outer stainless-steel drum and the TB-1 than usually observed. There was no apparent deformation of the TB-1 containment vessel. This package was then crushed, punctured, burned, and immersed, but not slashed. The posttest-sequence TB leak rate was $2.4 \times 10^{-6} \text{ cm}^3/\text{s}$ air. This leak rate is comparable with the results of similar prototype packages impacted side-on at ambient temperatures, and sequenced through all of the other test environments in a similar manner.



Figure 2.5.2.2-1. Cold (-40°F) Impact of Prototype PAT Package

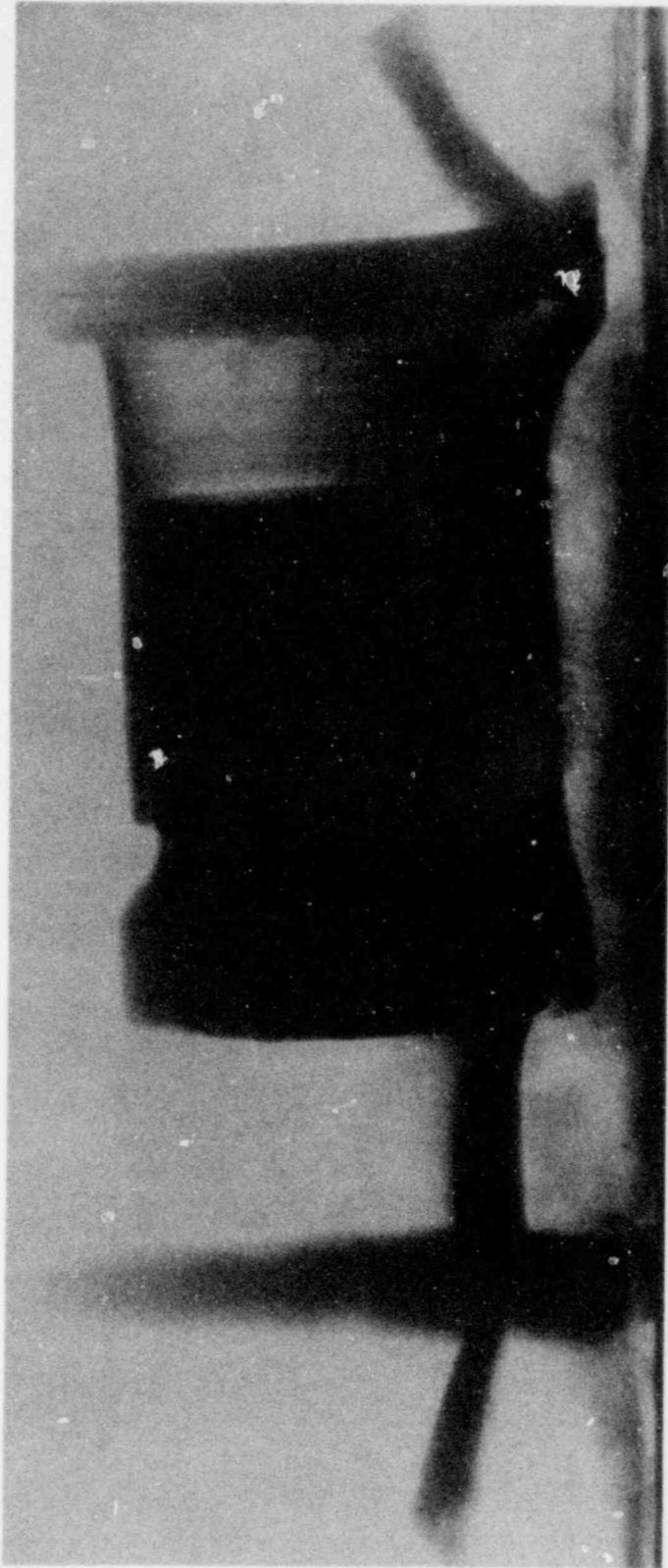


Figure 2.5.2.2-2. Radiograph of Cold (-40°F)
Impacted Prototype PAT
Package

POOR ORIGINAL 1567 113

It is concluded, therefore, that sequential testing at temperatures as low as -40°F (-40°C) will not affect the posttest acceptability of the PAT-1 package, because the impact test is the most severe condition for the cold (stiffer) redwood shock mitigation packaging material.

- b. Hot -- A prototype PAT package, with construction features that made it a valid comparison to a model PAT-1 package in the side-impact (90°) orientation, was hot soaked at $+200^{\circ}\text{F}$ (93°C) for more than 48 hr, wrapped in insulating materials, and then quickly rigged for a side impact perpendicular to the unyielding target. The impact velocity was 424 fps (129 m/s) with $< 1^{\circ}$ error. The bulk temperature at the time of the impact was nearly 200°F (93°C).

The package appeared to be deformed (Figure 2.5.2.2-3) similarly to ambient temperature side-impacted packages. Radiographic inspection revealed slightly less redwood at the point of minimum separation between the TB and the external stainless-steel drum than usually was observed (Figure 2.5.2.2-4). There was no apparent damage to the TB containment vessel. The package was crushed, punctured, burned and immersed, but not slashed; a postmortem was conducted. The post-test-sequence TB leak rate was $7 \times 10^{-8} \text{ cm}^3/\text{s}$. This leak rate is comparable with the results of similar prototype packages impacted at ambient temperature, side-on, and sequenced through all of the other test environments in a similar manner.

It is concluded, therefore, that sequential testing at temperatures as high as 200°F (93°C) will not affect the posttest acceptability of the PAT-1 packages.

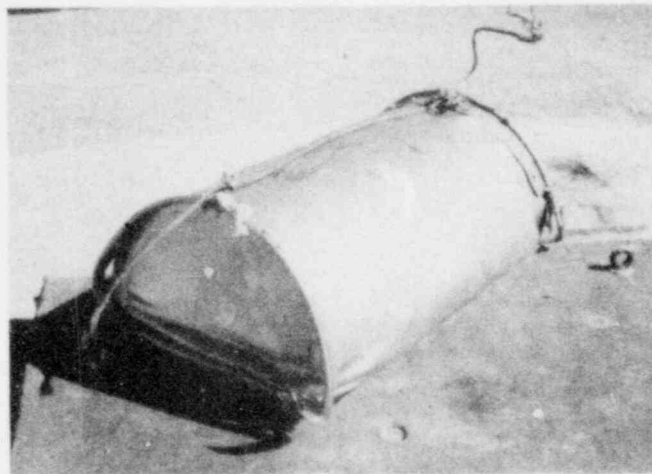


Figure 2.5.2.2-3. Hot (200°F) Impacted Prototype PAT Package

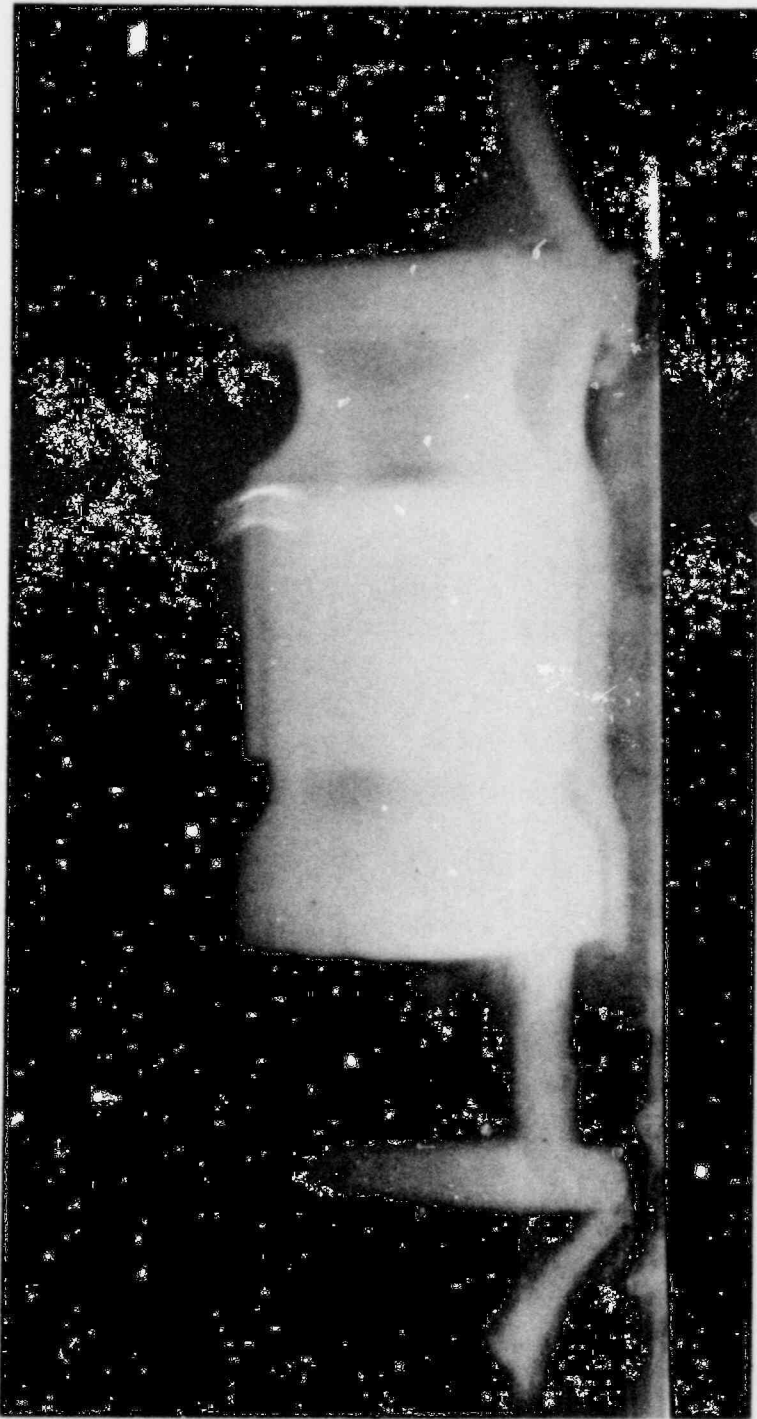


Figure 2.5.2.2-4. Radiograph of Hot (200 °F)
Impacted PAT Package

POOR ORIGINAL 1567 115

2.5.2.3 Relationship of Individual Tests to Sequential Tests

The severe sequence of high velocity (rocket pull-down) impact perpendicular to an unyielding target (reducing the package volume by about 50% in the most severe attitude), followed by 70,000 lb (311 MN) crush, followed by 5,000 ft-lb (6.8 kJ) puncture, followed by 15,000 ft-lb (20.4 kJ) slash (deliberately tearing the double outer drum), followed by a large JP-4 fuel fire of approximately 1850 °F (1010 °C) on the package surface for at least 1 hr, followed by underwater immersion, produces a far greater deteriorating effect on the PAT-1 package than that effect produced by any of those tests singly.

Tests of the prevailing design criteria (paragraph 2.1.1) -- impact, slash, fire, and internal heat source -- were all conducted singly during the PAT-1 development program. Individual impact tests of up to 449 fps (338 mph; 151 m/s) resulted in TB-1 containment vessel leak rates in the 10^{-8} cm³/s range. Individual slash and fire tests had no perceptible effect on the TB-1 containment vessel. The TB-1 containment vessel remained sealed ($< 10^{-10}$ cm³/s leak rate) in individual heating tests with severe internal overpressure test conditions at temperatures up to 800 °F (427 °C) demonstrating that the 200 °F-300 °F (93 °C-149 °C) normal range of temperature with a 25-W internal heat source (see 2.5.4.2 and Chapter 3) is no threat.

The other tests of crush, puncture, and underwater immersion are inconsequential as single tests; that is, they have no perceptible affect on the TB-1 containment vessel.

2.5.3 Summary of Acceptance Criteria Results of NRC Qualification Testing

- a. Containment -- The reported TB-1 containment vessel leak rates (see 2.5.1.7 and Table 2.4-1) -- $\sim 10^{-5}$ to 10^{-7} cm³/s -- and the measured lack of uranium oxide contents escape ($< 10^{-8}$ g) -- demonstrate that far less than an A2 quantity of plutonium oxide could be released. This fact is discussed in Chapter 4, Containment. In fact, it is practical and reasonable to state that there would be no plutonium release.
- b. Shielding -- Biological protection from the effects of ionizing radiation is provided, even by the impacted (crushed-up) PAT-1 package, in infinite arrays. Conservative dimensions of the damaged packages were used in the shielding calculations of Chapter 5. The dose rate, with any specified plutonium contents, is much less than 1 rem/hr at a distance of 3 ft.
- c. Subcriticality -- There is no nuclear fission criticality problem, even with an infinite array of damaged PAT-1 packages. The conservative dimensions of the side-impacted packages as reported in this chapter were used in the criticality calculations of Chapter 6, with very subcritical results.

- d. Water Leakage -- There was no water leakage into the TB-1 containment vessel.
- e. Temperature Extremes -- The extremes of heat and cold, as reported in this chapter, are tolerated by the PAT-1 package.
- f. Individual and Sequential Tests -- The PAT-1 package withstands the stated test threats, whether applied singly or in sequence.

These results are briefly tabulated in Table 2.4-I.

2.5.4 Normal Conditions of Transport Tests per 10 CFR 71 Appendix A

2.5.4.1 Summary and Results

Demonstration that the PAT-1 package complies with the standard for normal conditions of transport has been accomplished primarily by actual PAT-1 package tests. A PAT-1 package was sequentially subjected to all environments stated in 10 CFR 71 Appendix A. Following this test sequence, the TB-1 exhibited an air-leakage rate of $< 10^{-10}$ cm³/s. A leakage rate of 10^{-7} cm³/s or less, based on dry air at 77°F (25°C) and for a pressure differential of 1 atm against a vacuum of 10^{-2} atm or less, is considered to represent leak tightness (reference USNRC Reg. Guide 7.4, which references ANSI 3 N14.5). Therefore, the PAT-1 package meets the 10 CFR 71 containment requirements for normal conditions of transport for all allowable isotopic compositions of plutonium oxide powder ("allowable" is defined in Chapter 1).

Since the geometric form of the PAT-1 package and its TB-1 containment vessel was essentially unchanged after the test series, the following requirements of 10 CFR 71.35 are satisfied: (1) no substantial reduction in the effectiveness of the package occurred, (2) the total effective volume on which nuclear safety was assessed was not reduced by more than 5%, (3) the spacing between the center of the TB-1 containment vessel and the outer surface of the PAT-1 package on which nuclear safety was assessed was not reduced by more than 5%, and (4) no aperture in the outer surface of the package large enough to permit entry of a 4-in. (10.2-cm) cube was evident.

After the sequence of tests, uranium detection measurements were taken from swipes of the PC-1 product can and the internal walls of the TB-1. No release of contents (uranium dioxide used as a surrogate for PuO₂) was detected. This demonstrated compliance with the double containment requirements of 10 CFR 71.42.

2.5.4.2 Heat

A PAT-1 package was subjected to a 215°F (102°C) environment for 48 hr (Figure 2.5.4.2-1). As indicated by the thermal analysis in Chapter 3, a 215°F (102°C) external environment will generate peak PAT-1 package temperatures greater or equal to those which would

occur if the package was exposed to "direct sunlight" at an ambient temperature of 130°F (54°C) in still air with the contents generating a maximum heat output of 25 W. Maximum internal TB-1 pressure was created by adding a surplus 19.3 g of internal water to the PC-1 product can contents, thereby producing a maximum normal operating internal pressure in excess of 34.3 psi (236 kPa) as calculated in Chapter 4. Assessment of the potential for content loss was made after all performance tests were accomplished in sequence (i. e., after the complete sequence of heat, cold, overpressure, vibration, water spray, drops, penetration, and compression). Results of this assessment were stated in the foregoing summary.

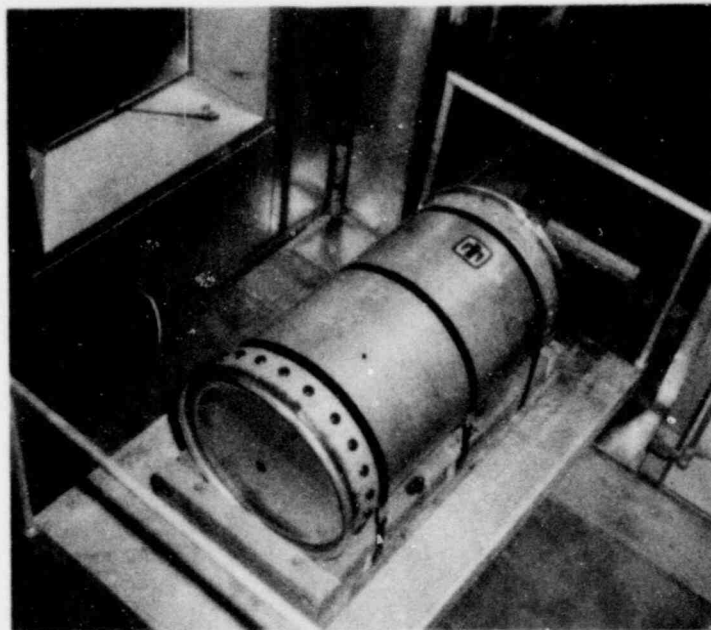


Figure 2.5.4.2-1. PAT-1 After 215°F Environment for 48 Hours

To assess the TB-1 margins of safety for prolonged use at maximum operating temperatures and pressures, a series of thermal threat tests were conducted. Oven tests which sequentially cycled TB-1 temperatures between ambient and 200°F (93°C), 400°F (204°C), 600°F (315°C), 700°F (371°C), and 800°F (427°C), holding each peak temperature for ~ 24 hr, resulted in no detectable helium leakage from the TB-1 ($< 10^{-10}$ cm³/s). A direct exposure of the bare TB-1 to a large JP-4 jet fuel fire at 1850°F (1010°C) (minimum) for slightly over 7 minutes, with the TB-1 rising to 750°F (399°C) in that time, also resulted in no detectable helium leak and no loss of UO₂ (surrogate for PuO₂) powder greater than the 10⁻⁸ g detection capability.

Also, the use of forged PH13-8 Mo stainless steel for the TB-1 body and lid, the use of A286 stainless-steel bolts for the closure, and the use of a copper seal assure that normal maximum temperatures in the 200°F (93°C) to 300°F (149°C) range are no threat to the integrity of the TB-1, due to the negligible effect of this temperature on these materials.

The limitation on internal decay heat of 25 W assures that under the specified assumptions pertaining to normal conditions of transport, the mean redwood temperature will not exceed 182°F (83°C), and the peak redwood temperature will not exceed 225°F (107°C). Combining the observations of Reference 12 ("At a constant moisture content and below about 400°F (204°C), mechanical properties are essentially linearly related to temperature") with the specific findings of Reference 13, no significant degradation of redwood properties is expected over long term exposure to the heat encountered in the PAT-1 package configuration.

The properties of the polyester-flexibilized epoxy used as the bonding agent in the redwood element/redwood element and redwood element/metal joints is such that its adhesive capability following exposure to 225°F (107°C) may be slightly enhanced by the curing action provided to this otherwise room-temperature-cured adhesive system. Therefore, exposure to 225°F (107°C) is not harmful (Reference 14).

2.5.4.3 Cold

Following the heat test, the same PAT-1 package was cold-soaked at -40°F (-40°C) for 48 hr. No degradation of the PAT-1 package was observed and none is expected as a result of operations in a -40°F (-40°C) environment.

The TB-1 containment vessel is fabricated from PH3-8 Mo precipitation-hardened stainless steel which has excellent service characteristics at temperatures well below -40°F (-40°C). The twelve A286 stainless-steel TB-1 closure bolts have been shown by actual test to provide sufficient strength to withstand the impact forces of the NRC qualification criteria at a temperature of -40°F (-40°C).

The redwood and flexibilized epoxy resin bonding agent are also capable of withstanding prolonged exposure to -40°F (-40°C) with no significant loss in heat transfer, fire retardant, or specific energy absorption characteristics.

2.5.4.4 Pressure

The PAT-1 package, specifically the TB-1 containment vessel, must be able to withstand an atmospheric pressure of 0.5 times standard atmospheric pressure. 10 CFR 71.53(b) also requires assurance that the TB-1 containment vessel will not leak at an internal pressure 50% higher than the maximum normal operating pressure prior to first use. To demonstrate compliance with both these requirements, the TB-1 containment vessel with the AQ overpack which was subjected to the heat and cold tests was removed from the AQ-1 package and heated to 255°F (124°C) for 8 hr. Water (19.3 g) was added to the UO₂ surrogate material (which had some initial moisture content) during packaging within the PC-1, assuring an internal PC-1 pressure of at least 51 psi (1.5 times prescribed normal operating pressure of 34 psi) at 255°F

124°C (paragraph 4.2.2). The unit was leak tested before exposure, while hot, and after cool down with a resulting leak rate of $< 10^{-10}$ cm³/s in each case, a value which demonstrates that the container was leaktight. Since this test was conducted in a vacuum, compliance with the 0.5-atm exposure requirement is also demonstrated.

2.5.4.5 Vibration

The TB-1 which was removed from the AQ-1 overpack for the pressure test was re-assembled with the AQ-1, reconstituting the original PAT-1 package. This PAT-1 package, which was subjected to the heat and cold tests per 10 CFR 71 Appendix A, was subjected to the following described transportation vibration environment (see Figures 2.5.4.5-1 and -2).

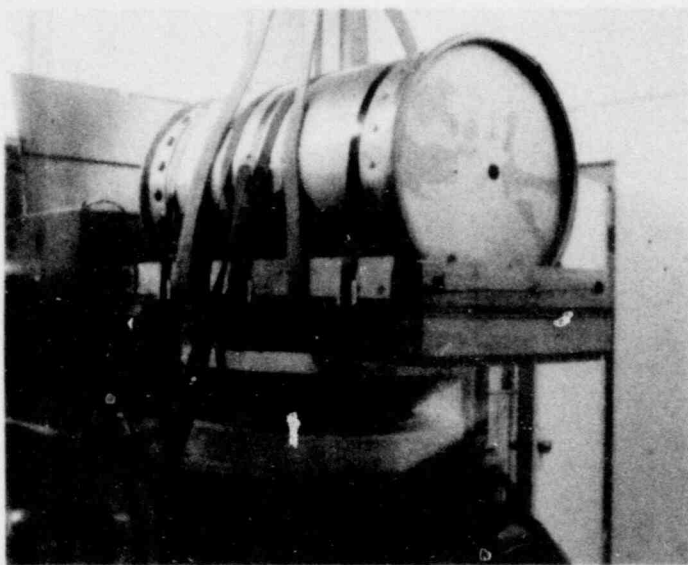


Figure 2.5.4.5-1. PAT-1 Secured for Horizontal Transportation Vibration Test

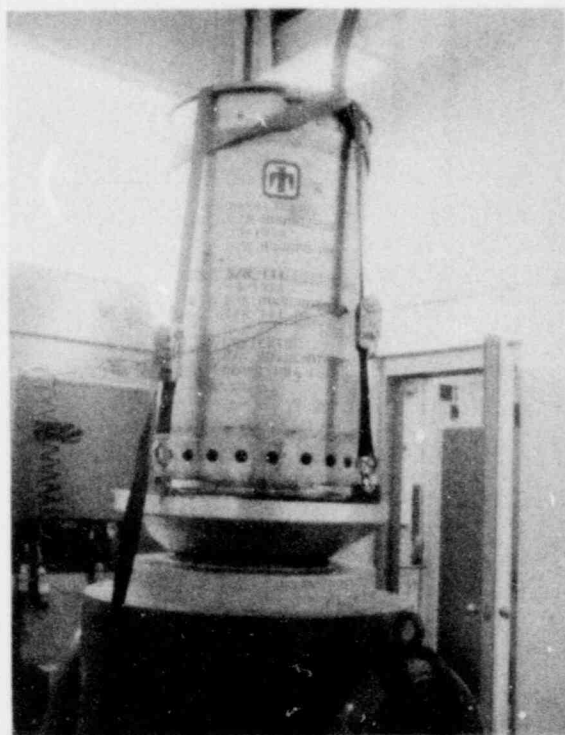


Figure 2.5.4.5-2. PAT-1 Secured for Vertical Transportation Vibration Test

The Sandia Laboratories Environmental Data Bank was utilized to design a specific vibration test for the PAT package. The test definition encompasses road transportation (SFT-Standard Freight Trailer), rail transportation (vibration on railcars and humping shock on cushioned underframe cars), and air transportation (vibration in aircraft).

PAT Package Transportation Shock and Vibration Test:

0.2 g²/Hz -- 30-150 Hz *

6 dB/octave rolloff -- 150-2000 Hz

8-hr duration -- longitudinal axis

8-hr duration -- vertical axis

The rail shock, if tested as a separate entity, would be longitudinal 9 g, 53 ms half-sine pulse. This is negligible in view of the 4-ft (1.2-m) drops for 10 CFR 71 and the 288 mph (129 m/s) (minimum) crash perpendicular to an unyielding target for the NRC criteria, and is therefore not tested.

2.5.4.6 Water Spray

The PAT-1 package (used previously) was subjected to a water spray test in accordance with 10 CFR 71 Appendix A.5. The actual test, shown in Figure 2.5.4.6-1, utilized a 3-in. (7.6-cm) diam fire hose equipped with a fog nozzle, delivering more than 124 gal/min (4.7 x 10² m³). The upper PAT-1 surface was continuously sprayed for more than 30 min, and then the side was also sprayed. 10 CFR 71 requires that the effect of this test not be individually assessed, but that free drops be done within 1-1/2 to 2-1/2 hr later.

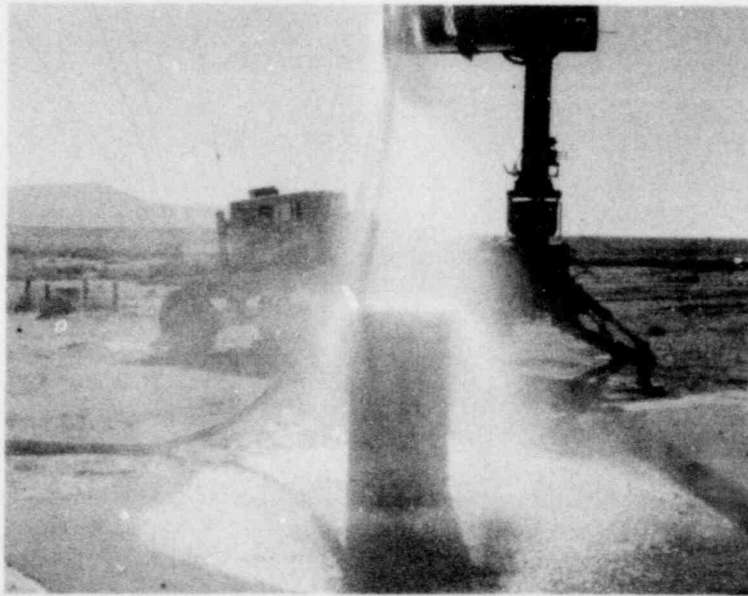


Figure 2.5.4.6-1. PAT-1 Being Subjected to Water Spray Test

* Random vibration levels are specified in g²/Hz units (which are analogous to power levels) versus frequency. The method used to translate this level to an approximate equivalent sinusoidal vibration is to choose the bandwidth of interest and integrate and take the square root. This provides an rms g level that corresponds to sinusoidal motion in that bandwidth.

POOR ORIGINAL

1567 121

2.5.4.7 Free Drop

The PAT-1 package was subjected to a 4-ft (1.2 m) free drop onto an essentially unyielding surface in a side-impact orientation, which was assessed as being the most vulnerable orientation, approximately 1/4 hr after the water spray test. To provide assurance that the PAT-1 has a wide design margin to withstand such drops, the package was also dropped 4 ft (1.2 m) onto its top, top corner, bottom, and bottom corner. Figures 2.5.4.7-1, -2, and -3 provide visual evidence that the effect of these tests on the PAT-1 package are inconsequential with regard to the physical requirements of 10 CFR 71.35.



Figure 2.5.4.7-1. Damage From 4-ft Drop Test

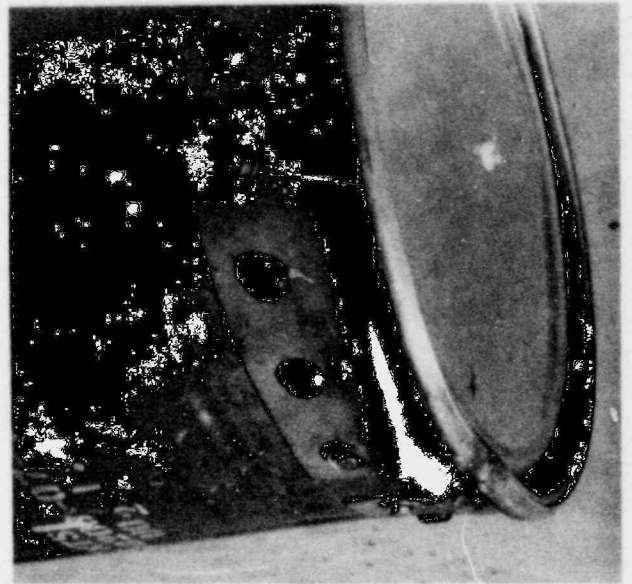


Figure 2.5.4.7-2. Damage From 4-ft Drop Test



Figure 2.5.4.7-3. Damage From 4-ft Drop Test

2.5.4.8 Corner Drop

This requirement applies to packages that weight less than 210 lb (95 kg) and does not apply to the 500-lb (227 kg) PAT-1 package. However, corner drops were performed as discussed in paragraph 2.5.4.7.

2.5.4.9 Penetration

The PAT-1 package was subjected to the penetration test of 10 CFR 71 Appendix A. This test utilizes a 40-in (102-cm) drop of a 13-lb (5.9 kg), 1-1/4-in. (3.2-cm) diam steel cylinder having a hemispherical end. The result on the PAT-1 package was a slight dimple as shown in Figure 2.5.4.9-1.

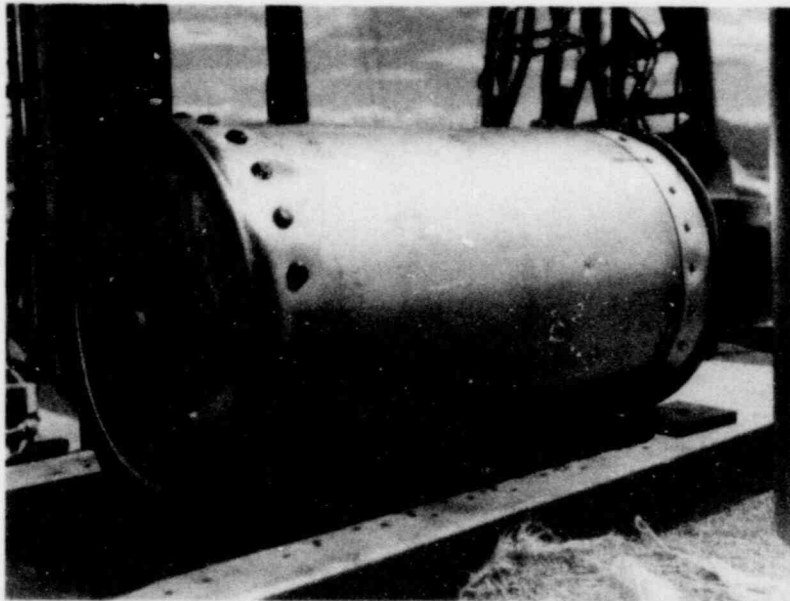


Figure 2.5.4.9-1. Slight Dimple Resulting From 10 CFR 71. A. 8 Penetration Test

2.5.4.10 Compression

The PAT-1 package used in all previous normal condition tests was subjected to the compression test of 10 CFR 71 Appendix A.9. This test requires a compressive load five times the package weight ($5 \times 500 \text{ lb} = 2500 \text{ lb}$) (or 1135 kg) or 2 psi x cross section area [$2 \times (22.5)^2 / 4 = 795 \text{ lb}$] (or 361 kg), whichever is greater. Therefore, a load of 3150 lb, a conveniently available mass, was placed on the top of the PAT-1 package with the package resting on a massive steel plate which in turn rested on a massive concrete block, for a period exceeding 24 hr (see Figure 2.5.4.10-1). There was no apparent or observed effect.

POOR ORIGINAL 1567 123

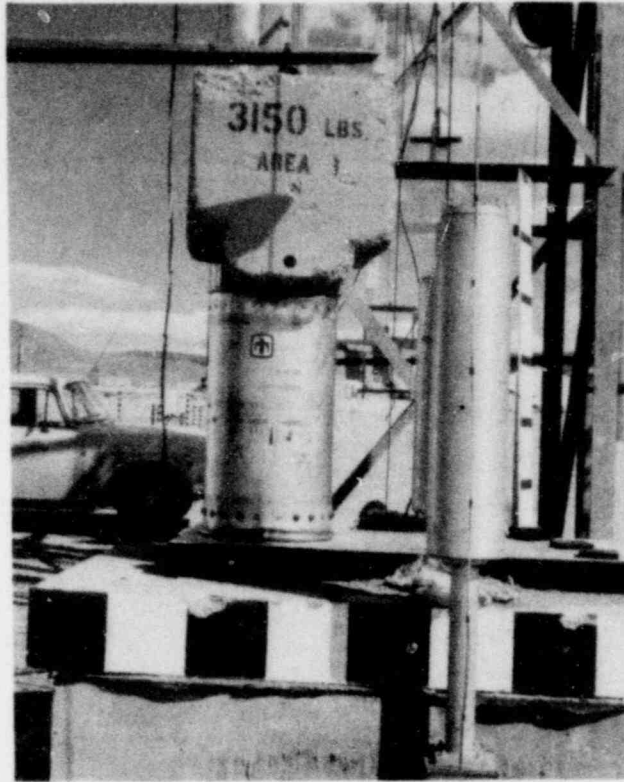


Figure 2.5.4.10-1. Compression Test

This same PAT-1 package was then placed on its side on a concrete pad, and a concrete block weighing 5060 lb (2297 kg) was leaned on the package with the 3150 lb (1430 kg) concrete block also placed over the PAT-1 package for an approximate total load of more than 5600 lb (2542 kg) (see Figure 2.5.4.10-2). There was no apparent or observed effect. Appendix 2F is an analysis of this "normal condition" test.

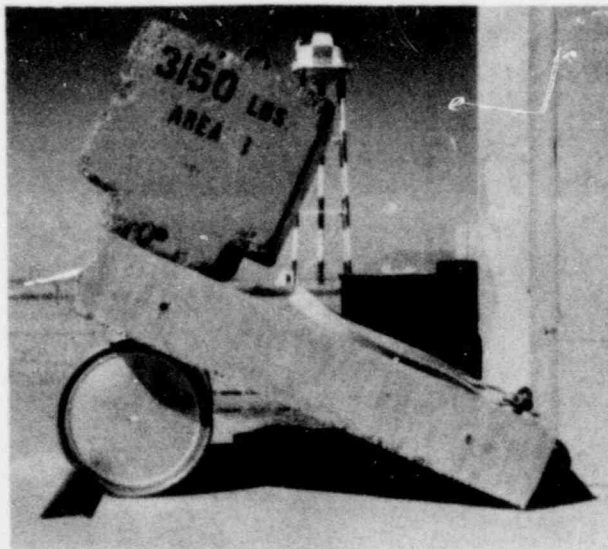


Figure 2.5.4.10-2. Compression Test

2.5.4.11 Posttest Summary of Package Damage

Subjecting the PAT-1 package to the 10 CFR 71 Appendix A normal condition of transport performance tests results in only minor superficial damage to the outer stainless-steel drum and C-clamp drum closure ring. As indicated in 2.5.4.1, the TB-1 containment vessel was leak-tight following this series of 10 CFR 71 tests and the PAT-1 package met the requirements of 10 CFR 71.35. Posttest disassembly of the TB-1 indicated a helium-rich internal atmosphere, thereby validating the leak-rate measurement. Examination of the PC-1 product can revealed that the roll crimp closure and the flexibilized epoxy overbonding remained intact and the can itself was essentially undamaged. These observations are shown in Figure 2.5.4.11-1. Uranium detection measurements were based on swipes of the product can and inner walls of the TB-1. Public health physics radioactivity and uranium fluorimetry detection methods indicated no release of uranium from the product can to the limits of fluorimeter detectability ($\geq 10^{-8}$ g U).



Figure 2.5.4.11-1. Disassembled TB-1 Following 10 CFR 71.A Tests

POOR ORIGINAL

1567 125

2.5.5 Hypothetical Accident Conditions Tests per 10 CFR 71 - Appendix B

2.5.5.1 Summary and Results

Demonstration that the PAT-1 package meets the requirements of 10 CFR 71 Appendix B for accident conditions of transport could be inferred from the package's ability to acceptably withstand the far more severe NRC Qualification Criteria,¹ as detailed in 2.5.1, 2.5.2, and 2.5.3. However, 10 CFR 71.42(b) requires that plutonium in excess of 20 curies per package shall be packaged in a separate inner container which shall not release plutonium when subjected to the normal and accident test conditions specified in 10 CFR 71 Appendices A and B. Primarily to demonstrate that the PC-1 product can comply with this inner container requirement, two PAT-1 packages (including a PC-1 product can loaded with UO₂ surrogate contents) were subjected to the test conditions of 10 CFR 71 Appendix B.

One PAT-1 package for 10 CFR 71 Appendix B testing included a PC-1 product can filled with UO₂ surrogate contents; due to the specific density of the UO₂, the payload in the PC-1 was 1.747 kg. Another PAT-1 package was assembled with 0.606 kg UO₂ and 2.545 kg No. 8 lead shot for a total payload of 3.151 kg in the PC-1 product can. The two packages were both tested in accordance with 10 CFR 71 Appendix B, except that one was dropped 30 ft (~ 10 m) five times (not required, but this tested top, top corner, side, bottom corner, and bottom) and the other was dropped 30 ft (~ 10 m) one time (on the side), as required. The puncture, fire, and immersion tests were essentially identical. Final results were identical, as reported below. The following figures and data used in this report are of the package dropped five times.

Following completion of this test series, the TB-1s, through leak testing and monitoring for uranium release, were found to be leak-tight. The TB-1s were then disassembled and the interior of the TB-1s and exterior of the PC-1 product cans, were monitored for uranium contamination. No contamination was detected; therefore, compliance of the PC-1s with the requirements of 10 CFR 71.42, and the TB-1s with the requirements of 10 CFR 71 Appendix B, was demonstrated.

Since the geometry of the PAT-1 package was not significantly changed, the reduction of shielding resulting from the 10 CFR 71 Appendix B test series is insignificant, and the radiation level at 3 ft (~ 1 m) from the external surface of the package would be limited to the approximately 4 mrem/hr allowable in 10 CFR 71.36(a) (1). The minimally deformed package also meets the requirements for subcriticality as required in 10 CFR 71.36(b) as demonstrated in Chapter 6.

2.5.5.2 Free Drop

A PAT-1 package was subjected to a 30-ft (9.1-m) freefall drop onto an essentially unyielding surface in the side-impact orientation (assessed to be the most vulnerable—Figure 2.5.5.2-1). To provide assurance that the PAT-1 package has a wide design margin to withstand such drops and that all primary impact orientations were tested, this same PAT-1 package was also subjected to similar drops onto its top end, top corner, bottom end, and bottom corner. Figures 2.5.5.2-3 and -3 illustrate the minor denting of the outer stainless-steel drum of the AQ-1 which resulted from these tests. Testing for containment adequacy was performed following the full sequence of the drop, puncture, thermal, and water-immersion tests.



Figure 2.5.5.2-1. Damage From 30-ft Side Drop

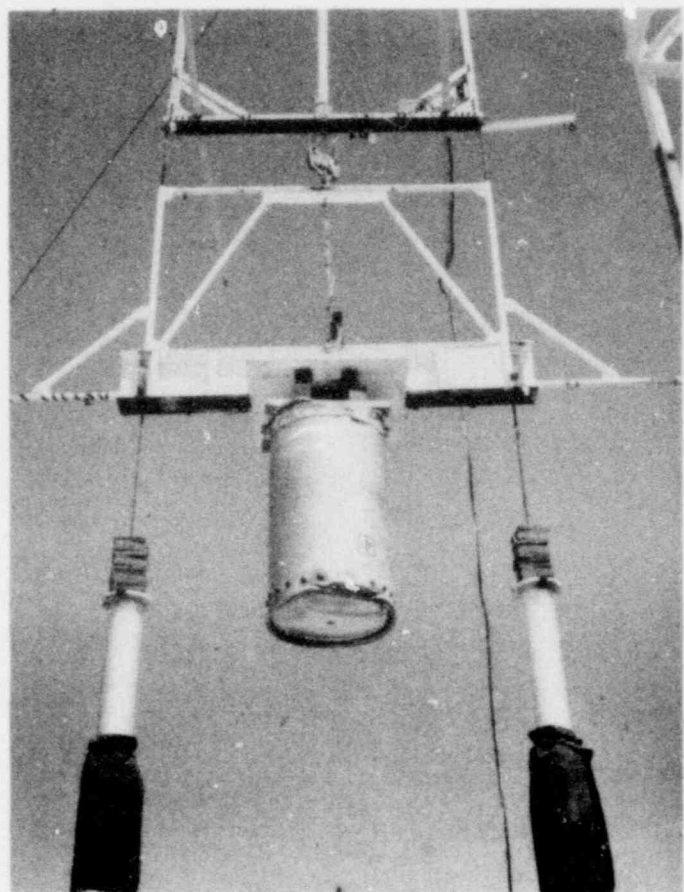


Figure 2.5.5.2-2. Damage Resulting From 30-ft Side, Top Corner, and Bottom Corner Drops

POOR ORIGINAL

1567 127

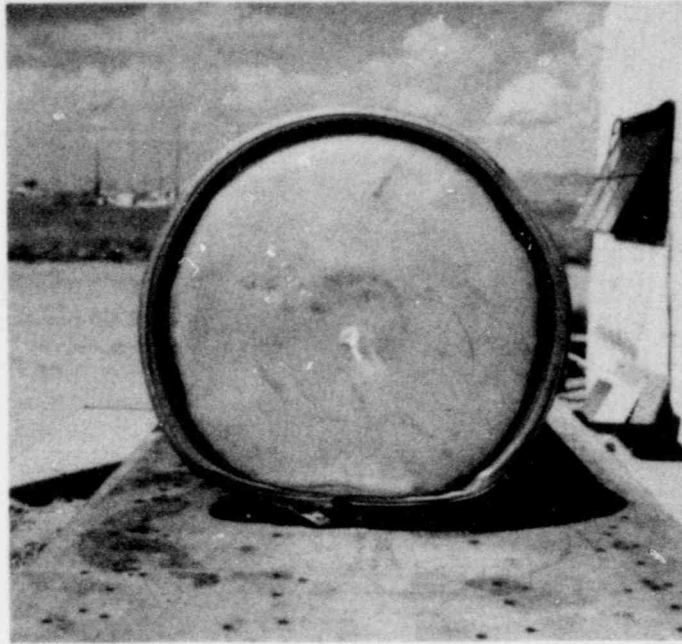


Figure 2.5.5.2-3. Damage Resulting From 30-ft Side, Top Corner, Bottom Corner, Bottom, and Top End Drops

2.5.5.3 Puncture

The impacted PAT-1 package was subjected to a free drop of 40 in. (~ 1 m) onto a 6-in. (15-cm) long, steel bar mounted on an essentially unyielding horizontal surface as defined by 10 CFR 71 Appendix B. 2, and as shown in Figure 2.5.3-1. The point of contact between the bar and the PAT-1 package was chosen at midlength on the cylindrical surface of the package (the point where the minimum dimension of redwood exists between the TB-1 containment vessel and the surface of the AQ-1). The damage to the PAT-1 following this test involved a minor imprint in the outer drum (Figure 2.5.5.3-1); the integrity of the drum was not affected.

2.5.5.4 Thermal (Fire)

The dropped and puncture-tested PAT-1 package was subjected to a fire test which exposed the package to a thermal-radiation environment in excess of that defined in 10 CFR 71 Appendix B.3. The facility used for this test involved the 10-ft (3-m) diam fuel pool and surrounding 16-ft (4.9-m) diam by 10-ft (3-m) tall chimney used to attain the higher temperatures required by the NRC qualification criteria fire test (see Section 3). As indicated by the measurements shown in Table 2.5.5-1, the temperatures within the fire and on the package surface were considerably in excess of the 1475°F (802°C) environment specified in the regulations. Afterburn was permitted to persist until the package was cool to the touch of a bare hand.

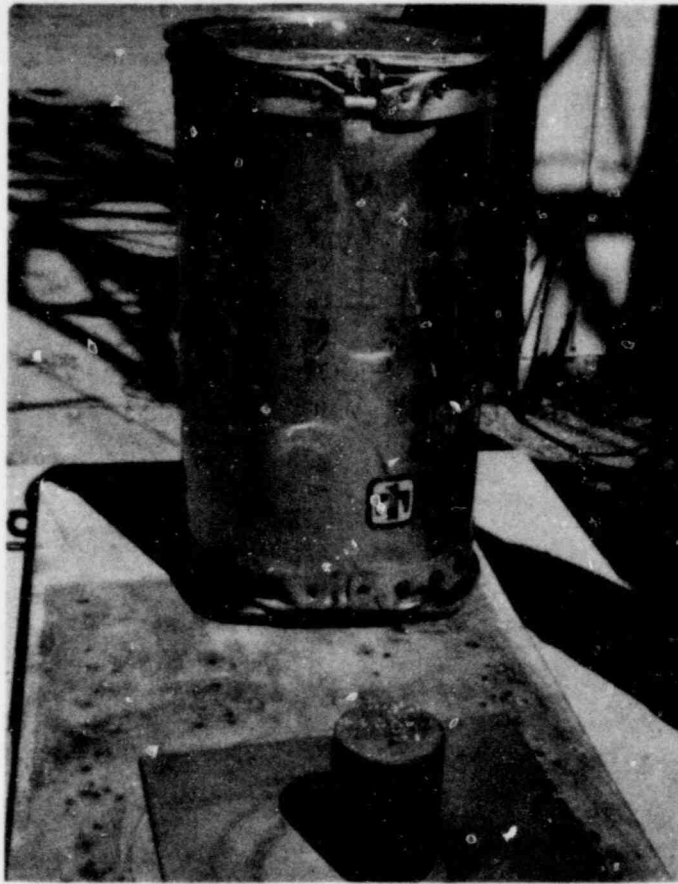


Figure 2.5.5.3-1. Impression on PAT-1 From Puncture Test

TABLE 2.5.5-1

10 CFR 71 Appendix B Burn Test

Observed average temperature on AQ-1 drum	~ 1800 °F
Observed flame temperatures in vicinity of PAT-1	2200 °-2300 °F
Duration of above temperatures	52 minutes
Char depth in outer redwood	3.825 in.
TB-1 temperature	~ 200 °F, > 170 °F, < 210 °F
Cumulative char rate*	< 0.37 ft/hr

* Total char depth observed was divided by 52 minutes; this is a severe assumption for determining the rate because char would persist beyond the 52-minute duration of the JP-4 fire, resulting in a lower char rate calculation.

POOR ORIGINAL 1567 129

2.5.5.5 Water Immersion

The PAT-1 package was then submerged in the water within the basin of the fire-test facility (Figure 2.5.5.5-1). The 6-ft (1.8-m) pool depth assured that all surfaces of the package were immersed under at least 3 ft (1 m) of water. Package immersion continued for a period of approximately 24 hr.

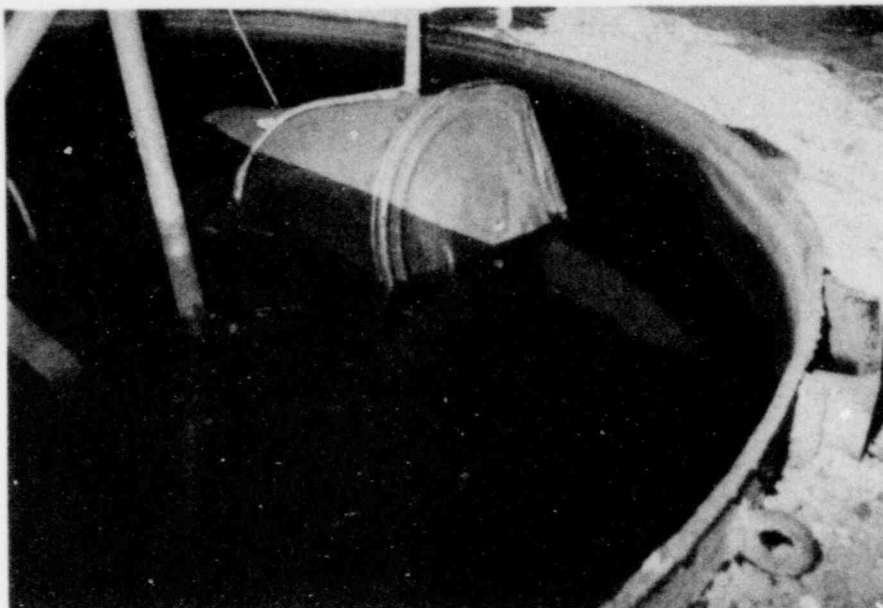


Figure 2.5.5.5-1. Water Immersion Test

2.5.5.6 Posttest Summary of Package Damage

Subjecting the PAT-1 package to the 10 CFR 71 Appendix B accident conditions of transport performance tests results in only minor damage to the outer steel drum and C-clamp drum closure ring and its skirt extension. The outer layer of redwood experienced charring to about 4-in. (10.2-cm) depth (Figure 2.5.5.6-1) while the redwood internal to the load spreader was essentially unaffected (Figure 2.5.5.6-2). The TB-1, except for char residue picked up in the immersion test, showed no visible effects from this series of tests. As indicated in paragraph 2.7.1, the TB-1 containment vessel was leaktight following this series of 10 CFR 71 tests and the PAT-1 package met the requirements of 10 CFR 71.36(a)(1) and 10 CFR 71.36(b). Post-test disassembly of the TB-1 indicated a helium-rich internal atmosphere, therefore validating the leak-test measurement.



Figure 2.5.5.6-1. Sectioned PAT-1 Showing
3-in. Char Depth

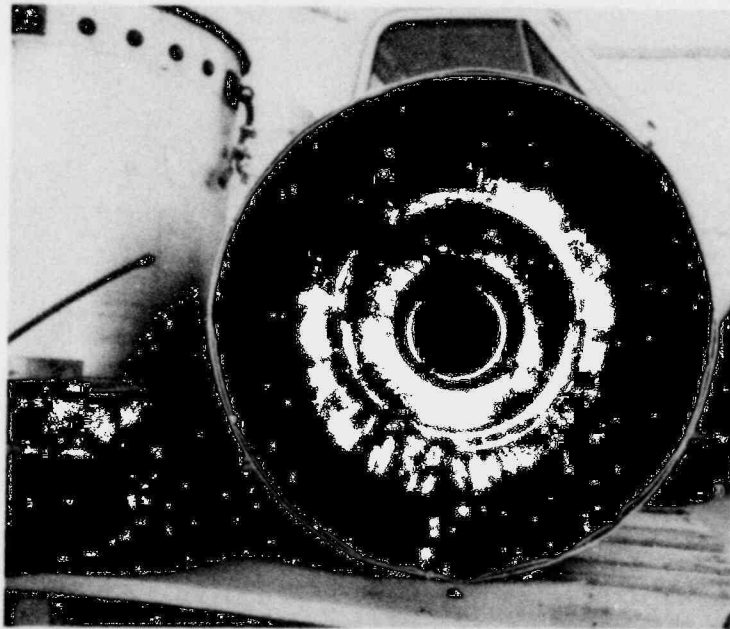


Figure 2.5.5.6-2. Sectioned PAT-1 Showing Char Depth
and Essentially Unaffected Internal
Redwood

POOR ORIGINAL 1567 131

Examination of the PC-1 product can revealed that the roll crimp closure and the flexibilized epoxy overbonding remained intact while the can itself had several minor dents. These observations are shown in Figure 2.5.5.6-3.



Figure 2.5.5.6-3. Disassembled TB-1, Post 10 CFR 71 Test, Showing Roll Crimp Closure and Epoxy Overbonding Intact

Uranium detection measurements were based on swipes of the product can and inner walls of the TB-1. Both health physics radioactivity and uranium fluorimetry detection methods indicated no release of uranium from the product can to the limits of fluorimeter detectability ($\geq 10^{-8}$ g U).

2.6 Test Facilities

The special or major facilities which were utilized to perform the sequential test series include: (1) a rocket pulldown cable facility at which controlled attitude high-velocity impacts onto an unyielding target were performed, (2) a static test machine to accomplish the required package crushing, (3) two tower facilities utilized to perform the puncture and slashing tests, (4) a fire-test facility, and (5) an immersion pool. Appendix 2J describes these facilities and the test and data acquisition methods utilized to assure that the desired test environments were properly produced.

2.7 List of Appendices

Appendix 2A - Package Impact Analysis

2B - Properties of Principal Materials Used in the PAT-1 Package

2C - Package Load Resistance per 10 CFR 71.32

2D - External Pressure per 10 CFR 71.32(b)

2E - Pressure Analysis per 10 CFR 71 Appendix A.3

2F - Compression Analysis per 10 CFR 71 Appendix A.10

2G - Terminal Velocity Analysis

2H - Test Protocol

2I - Surrogate UO_2 Powder Used in Tests

2J - Test Facility Descriptions

References

1. Working Paper-Qualification Criteria for Plutonium Package Certification, Transportation Branch, Assistant Director for Material Safety and Licensing, Division of Fuel Cycle and Material Safety, Office of Material Safety and Standards, U.S. Nuclear Regulatory Commission, Sept 27, 1976, and subsequently amended by letter, Sept 6, 1977.
2. Code of Federal Regulations, Title 10, Part 71, Packaging of Radioactive Materials for Transport and Transportation of Radioactive Materials Under Certain Conditions.
3. ANSI N14.5, Proposed American National Standard Leakage Tests on Packages for Shipment of Radioactive Materials, American National Standards Institute, Inc., Oct 1976.
4. IAEA Safety Series No.6.
5. "Target Correlation Presentation to the National Academy of Engineering, Ad-hoc Committee on the Air Transport of Plutonium," by W. A. Von Riesemann, Sandia Laboratories Design Technology Division 5431, on March 31 and April 1, 1977, documented April 14, 1977.
6. Bonzon, Lloyd L., Final Report on Special Impact Tests of Plutonium Shipping Containers - Description of Test Results, NUREG 766515, Sandia Laboratories, Albuquerque, NM, Feb 1977.
7. Bonzon, L. L., and Schamaun, J. T., "Container Damage Correlation with Impact Velocity and Target Hardness," IAEA-SR-10/21, reprint from "Transport Packaging for Radioactive Materials," IAEA, Vienna, 1976, pp.397-408.
8. Schamaun, J. T., and Von Riesemann, W. A., Effects of Target Rigidity on Impact Behavior of Shipping Containers, SAND76-0207, Sandia Laboratories, Albuquerque, NM, 1976.
9. Shappert, L. B., Bradley, N. C., Evans, J. H., and Jurgensen, M. C., The Obsolete Cask Program: Test Number 2, ORNL-TM-1312, Vol. 16, Oak Ridge National Laboratory, Oak Ridge, TN, April 1975.

10. Waddoups, Ivan G., Air Drop Test of Shielded Radioactive Material Containers, SAND75-0276, Sandia Laboratories, Albuquerque, NM, Sept 1975.
11. Standard Format and Content of Part 71 Applications for Approval of Packaging of Type B, Large Quantity and Fissile Radioactive Material, Second Draft, Sept 1977, U. S. Nuclear Regulatory Commission.
12. Wood Handbook - Wood as an Engineering Material, USDA Agricultural Handbook 72, Rev., 1974.
13. Von Rieseemann, W. A., and Guess, T. R., The Effects of Temperature on the Energy-Absorbing Characteristics of Redwood, SAND77-1589, Sandia Laboratories, Albuquerque, NM, 1977.
14. DeLollis, N. J., Durability of Structural Adhesive Bonds (A Review), Sandia Laboratories, Albuquerque, NM.
15. Memorandum from T. L. Wilson to J. Andersen, "Transportation, Shock, and Vibration Tests for PARC," dated Jan 26, 1977.

APPENDIX 2A

Package Impact Analysis

2A.1 Purpose

The purpose of this appendix is to analyze the capability of the PAT-1 package to survive a 250-knot (approximately 422 fps or 129 m/s) crash on an unyielding target; the definition of survival is related to release of radioactive material, shielding, and criticality as defined by 10 CFR 71, 49 CFR 173, and the new NRC criteria. End-on, side-on, and angular impact configurations will be considered.

A view of the PAT-1 package showing all components is displayed in Figure 2A-1. The basic approach used in the design of the package is to absorb the impact energy by material crushing and plastic work; the aim is to isolate the inner containment vessel from excessive shock.

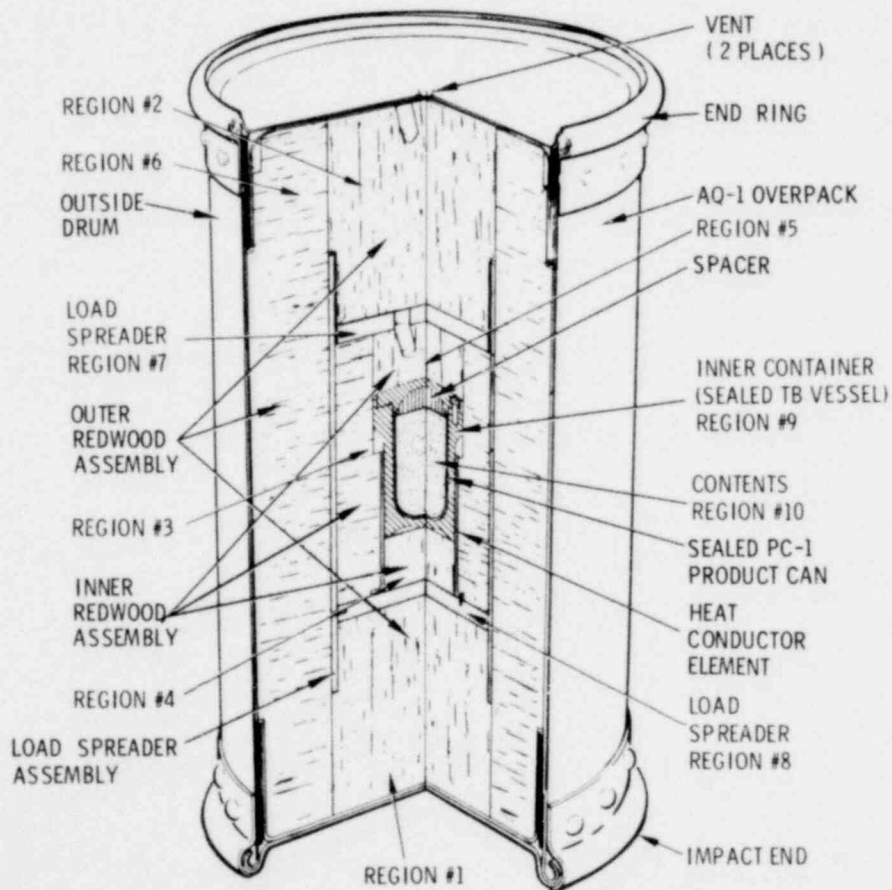


Figure 2A-1. PAT-1 Impact Analysis

The inner containment vessel is treated as a rigid, massive (but fairly small) object, the motion of which must be stopped primarily by the crushing of redwood. A load-spreader assembly surrounds the TB-1 containment vessel to distribute the inertial loading over a larger area of the redwood than would be caused by the projected area of the TB-1 alone.

The following impacts will be considered: end-on, side-on, and corner.

2A.2 End-On Impact

The postulated impact occurs on the package bottom, as shown in Figure 2A-1. At impact, the package bottom suddenly stops and the TB-1 is still moving with the impact velocity of 422 fps (129 m/s). The energy-absorbing redwood consists of a total of six sections: two outer end plugs (Nos. 1 and 2), two inner end plugs (Nos. 4 and 5), an inner hollow cylinder (No. 3), and an outer hollow cylinder (No. 6).

The significant crushing strength of redwood lies in the direction parallel to the grain. Thus the mechanism of absorbing the initial kinetic energy of the TB-1 vessel is crushing of region No. 4 (to approximately 30 percent of its original volume), combined with a similar crushing of region No. 1. Note that the diameter of region No. 1 is greater than the TB-1 vessel. The entire volume of this region is exploited for energy absorption by means of a thick circular plate "load spreader" (No. 1) which transmits the inertial load of the TB-1 vessel to the entire cross section of region No. 1. Region No. 1 is also assumed capable of absorbing energy through crushing to a final volume equal to approximately 30 percent of the initial volume.

The end-on impact situation is modeled as follows:

- a. The behavior of the impact process is taken as uniaxial, one-dimensional stress and deformation. This is appropriate for redwood compressed parallel to the grain, based upon the response of redwood similarly compressed during material property tests performed in support of this program.
- b. The column of material isolating the TB-1 vessel, consisting of regions Nos. 1, 2, 3, 4, and 5 as well as load spreaders Nos. 1 and 2, is assumed at the time of impact to be a rigid body of kinetic energy corresponding to the 422 fps (129 m/s) impact velocity and the total mass of all materials in the column.
- c. The kinetic energy attributed to rigid body motion in paragraph b must be absorbed by permanent deformational energy of the redwood material. It is conservatively assumed that the kinetic energy of the entire column

is fully absorbed by redwood regions Nos. 1 and 4 only; that is, redwood under the TB-1 vessel. Such an assumption does not consider the absorption capability of regions Nos. 2, 3, and 5, and the two load spreaders, and is therefore conservative. If it can be shown here that regions Nos. 1 and 4 are capable of absorbing all the initially available kinetic energy without redwood being compressed beyond the lockup deflection (~ 70%), survival is achieved.

2A.2.1 Discussion of Material Properties

A series of redwood compressive crush tests which were performed is reported in Appendix 2B. All tests were static, crushing the material in a direction parallel to the grain. Crush data were obtained over a range in temperatures from -40°F (-40°C) to 231°F (111°C). Results at room temperature 71°F (22°C) using the sets of complete data provided in Appendix 2B are shown in Table 2A-I. The physical meaning of lockup and associated specific energy can be visualized by examination of Figure 2A-2, a typical load-deflection curve for the redwood tested. The lockup point corresponds to that amount of crushing or deformation beyond which the modulus of the material becomes steep. Beyond this point, large forces can be transmitted through the redwood which may induce plastic deformation to the TB containment vessel. Thus, in subsequent energy-absorption calculations, only energy capacity up to the point of lockup is considered. The area under the load-deflection curve given is the energy absorption capability of the redwood.

TABLE 2A-I
Redwood Crush Data from Reference¹

Specimen No.	Deflection to Lockup (in.)*	Specific Energy to Lockup (ft-lbf/lbm)
12	1.90	22,000
29	1.91	24,300
7	1.88	21,900
15	1.85	21,200
21	1.88	22,500
Averages	1.88	23,380

¹ Personal communication, W. A. Von Riesenmann, Division 5431, Sandia Laboratories, June 8, 1977

* Note that initial specimen length is 3.00 inches. Thus the specimens are crushed to about 37 percent of their original volume.

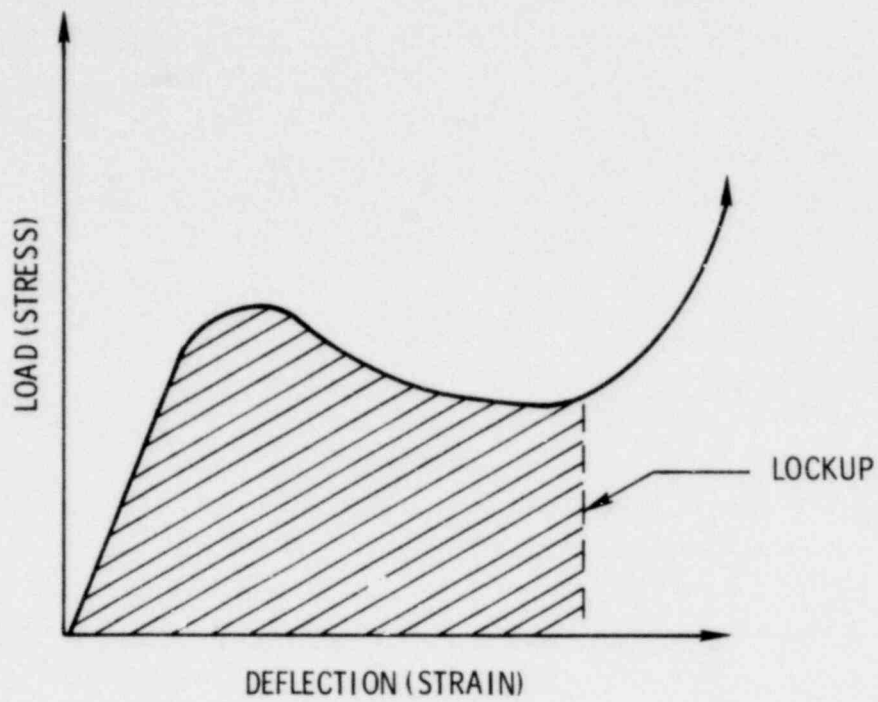


Figure 2A-2. Typical Load-Deflection Behavior for Redwood

A sketch of the specimen geometry and loading is shown in Figure 2A-3 for clarity.

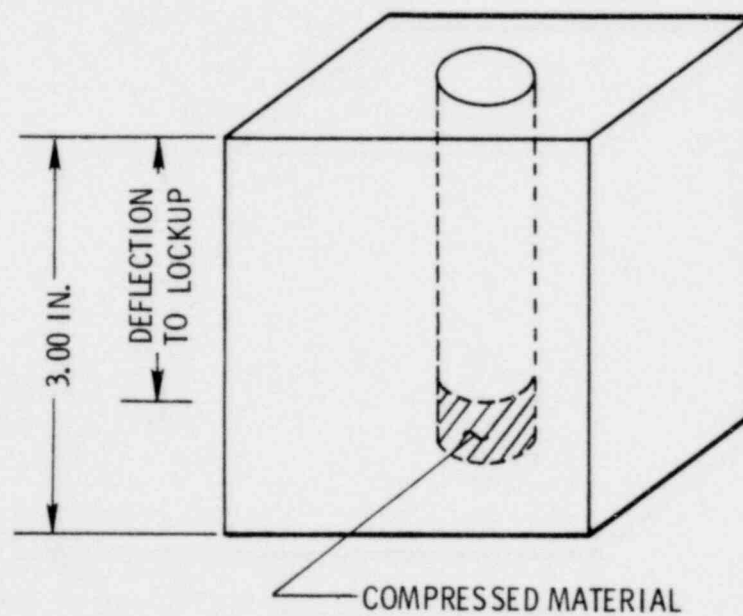


Figure 2A-3. Static Crush Testing of Redwood

2A.2.2 Analysis

The various elements making up the inner vertical column of material are necessary both for calculating kinetic energy on impact as well as for determining total energy absorbed by the permanent crushing mode; this latter information is supplied from the material property tests performed on redwood (see Appendix 2B). Mass information is presented in Table 2A-II.

TABLE 2A-II
Mass Values for PAT Components

Region No.*	Mass (lbm)	Region No.*	Mass (lbm)
1	15.3	6	111.1
2	15.2	7	9.4
3	11.2	8	9.4
4	1.4	9	36.0
5	1.4	10	7.0

* See Figure 2A-1 for region identifications.

The inner column consists of regions 1-5 as well as regions 7-10. The total mass of the inner column from Table 2A-II is then 106.3 lbm (48.3 kg), including the mass of the TB contents. The initial rigid body kinetic energy at the instant of impact is

$$(KE)_{\text{Column}} = \frac{1}{2} Mv^2$$

where

M = total column mass

v = impact velocity

For $v = 422 \text{ ft/s}$ (129 m/s) and $M = 3.30 \text{ slugs}$ (48.22 kg), the total kinetic energy is $2.98 \times 10^5 \text{ ft-lbf}$ ($4.04 \times 10^5 \text{ J}$). To assume that all of this kinetic energy must be absorbed through crushing of only that redwood lying directly beneath the TB-1 containment vessel (that is, regions Nos. 1 and 4) is extremely conservative, and neglects the energy absorbed by the remaining redwood as well as the load spreaders (through plastic deformation). Thus the total redwood mass available for energy absorption is 7.6 kg (16.7 lbm). Based upon the redwood crush data listed in Table 2A-I, the total energy capable of being absorbed by crushing to the point of lockup is simply the product of the above mass and the specific energy, 67 KJ ($22,380 \text{ ft-lbf/lbm}$). Thus, the total energy capacity of redwood pieces Nos. 1 and 4 is 507 KJ ($3.74 \times 10^5 \text{ ft-lbf}$). By comparison to the impact kinetic energy calculated above, there is a 25-percent margin of safety for end-on container impact, assuring survival of the TB-1 containment vessel.

2A.3 Side-On Impact

A simplified cross-sectional view of the PAT-1 package is shown in Figure 2A-4. As in the end-impact situation, the kinetic energy associated with the impact velocity of 422 fps (129 m/s) must be fully absorbed by permanent crushing of the redwood filler material and by plastic deformation of metal components.

Notice in Figure 2A-4* that the primary components of interest to impact response of the package are the inner TB-1 containment vessel, redwood region No. 3, the cylindrical load spreader tube, redwood region No. 6, and the outer drum/liner assembly.

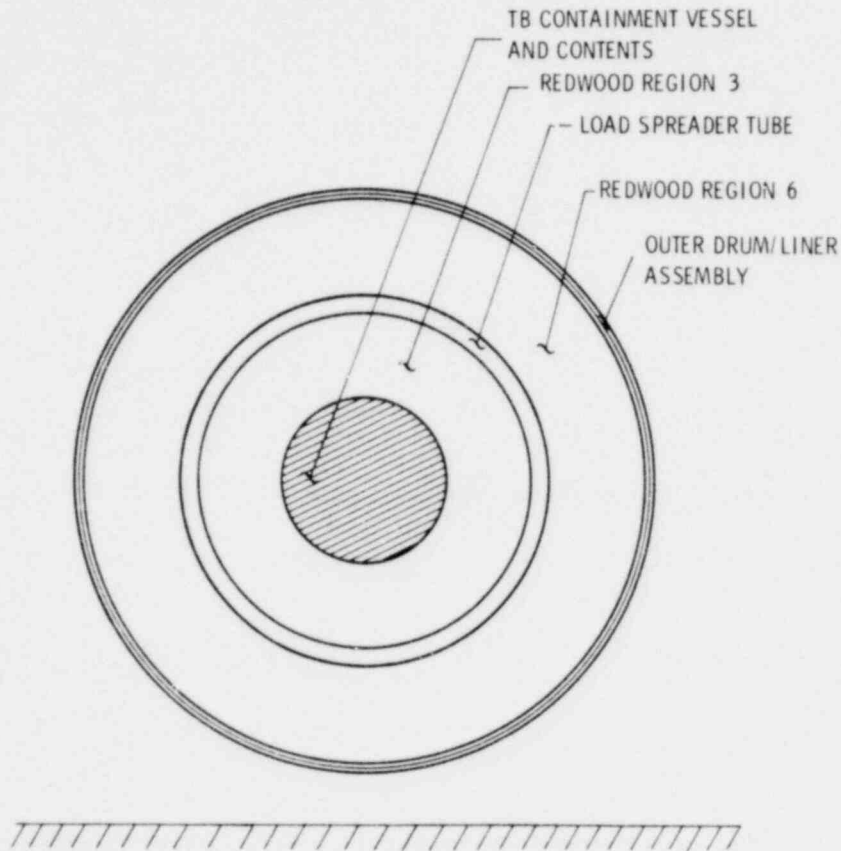


Figure 2A-4. Simplified PAT-1 Cross Section (not to scale) Showing Impact Surface

* Note that the cross section shown is taken near the middle of the PAT-1.

Ideally, the redwood filler should so isolate the TB-1 vessel that it would be fully stopped following impact, with the resultant redwood crush deflection not exceeding the point of material lockup.

A unit length of the cross section is shown in Figure 2A-4. The densities of the respective layers, their areas, and the resulting mass per unit axial length for the PAT-1 near its middle section are indicated in Table 2A-III.

TABLE 2A-III
Mass Properties for Side-On Impact Calculations

Region	Density ₃ (lbm/in. ³)	Cross Section Area (in. ²)	Mass/Unit Length (lbm/in.)
TB Containment Vessel and Contents	--	--	5.06*
Redwood Region No. 3	0.013	63.3	0.82
Load Spreader Tube	0.098	21.5	2.11
Redwood Region No. 6	0.013	267.0	3.47
Outer Drum Assembly	0.029	8.4	2.44
Total Mass/Unit Length =			13.90**

* Estimated from mass of TB-1 vessel and contents divided by TB-1 length.

** This value should be compared to 11.9 lbm/in. based upon total PAT-1 loaded weight divided by total length.

The total rigid body kinetic energy per unit length of the PAT-1 package at a cross section through the TB vessel is

$$KE/\text{Unit Length} = 1/2 mv^2$$

where

m = mass per unit length

v = impact velocity.

For m = 0.432 slugs/in. (0.248 kg/cm) and v = 422 fps (129 m/s), K.E./unit length = 39015 ft lbf/in. (2.1 MJ/m).

This total impact kinetic energy is first assumed entirely absorbed by redwood crushing, thus ignoring the plastic deformation energy in deformed metal components.* Based upon examinations of radiographic data and posttest photographs, redwood and metal materials appeared crushed up to the side of the TB-1 vessel, as indicated in Figure 2A-5. Thus the initial cross-sectional areas of the deformed regions of material are as shown in the shaded area in Figure 2A-5, denoted as region A and region B.

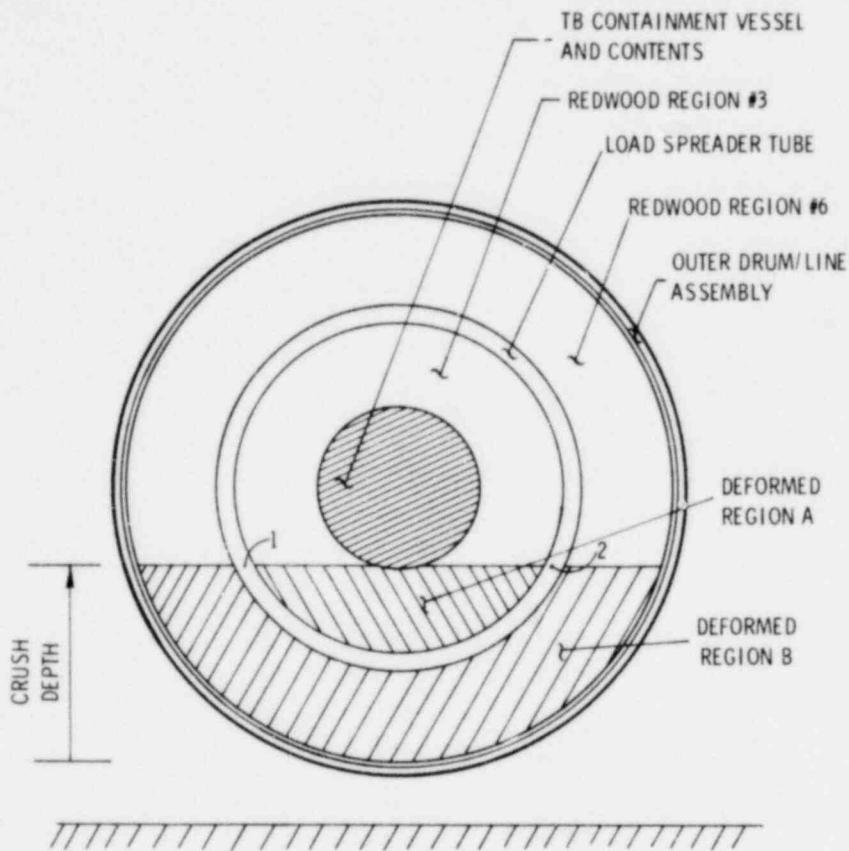


Figure 2A-5. Simplified PAT Cross Section (not to scale) Showing Initially Undeformed Regions A and B

Elementary application of geometric formulas¹ leads to a net redwood initial volume per unit axial length, V , of 118 in.³/in. (7.6×10^{-2} m³/m).

* This assumption subsequently will be shown to be overly conservative and insufficient.

¹ R. S. Burington, Handbook of Mathematical Tables and Formulas, Handbook Publishers, Inc., 1948.

Based upon a redwood density of 0.013 lbm/in.^3 (360 jg/m^3), a specific energy absorption capacity of the redwood per unit length is determined to be $34,502 \text{ ft-lbf/in.}$ (1.842 MJ/m). When this value is compared to the impact kinetic energy calculated above $39,015 \text{ ft-lbf/in.}$ (2.082 MJ/m), it is seen that the container is marginal. Some "bottoming out" will most probably occur and may induce slight plastic deformations in the TB-1 vessel. In fact, such slight localized deformations were observed, although observed leak rates were still well below critical levels.

Next the plastic energy absorption capability of the deformed metal components is included to determine if energy absorbed in these components leads to a net positive margin of safety. In particular, consider the cylindrical load-spreader tube with cross section as indicated in Figure 2A-5. Based upon observations of side-impacted PAT-1 packages, it is reasonable to assume that the load-spreader tube segment between points 1 and 2 undergoes pure membrane compression into the flattened configuration indicated in Figure 2A-6. While it is acknowledged that some ovaling of the load spreader above the flattened region does occur, this is ignored because of the cavity or foundation support effect afforded by the surrounding redwood.

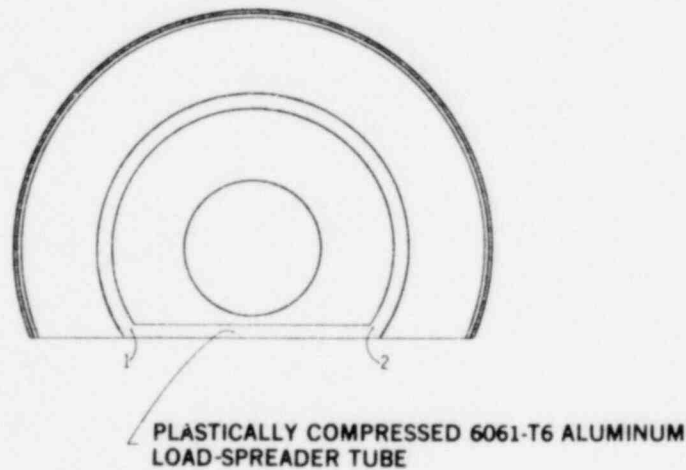


Figure 2A-6. Impact Energy Balance

The 6061-T6 aluminum load-spreader tube material is approximated as rigid, perfectly plastic, with yield stress $\sigma_y = 35,000 \text{ psi}$ (241 MPa).

The average strain experienced in membrane compression by the arc length between 1 and 2 is approximated as

$$\epsilon_{\text{avg}} = \frac{\Delta l}{l_0} = \frac{\text{arc } \widehat{1-2} - \text{chord } \widehat{1-2}}{\text{arc } \widehat{1-2}}$$

1567 143

The energy absorbed per unit axial length is then given by*

$$\epsilon/\text{unit length} = \int_v [\sigma_{ij} d\epsilon_{ij}] dv$$

where

σ_{ij} = stress tensor

ϵ_{ij} = strain tensor

v = volume over which the strain energy density is integrated
(i.e., between points 1 and 2).

For the case of uniaxial stress and uniform strain energy density field (between points 1 and 2),

$$\epsilon/\text{unit length} = \sigma_y \epsilon_{\text{avg}} v_{1-2}$$

where

v_{1-2} = volume per unit axial length between points 1 and 2.

For¹

$$v_{1-2} = 6.21 \text{ in.}^3/\text{in.} \quad (4.01 \text{ mm}^3/\text{m})$$

$$\text{arc } \widehat{1-2} = 10.36 \text{ in.} \quad (26.3 \text{ cm})$$

$$\text{chord } \widehat{1-2} = 9.00 \text{ in.} \quad (22.9 \text{ cm})$$

The average strain (membrane compression) is 13.1%, resulting in plastic energy absorbed per unit length of

$$\epsilon/\text{unit length} = 2380 \text{ ft-lbf/in} \quad (0.127 \text{ MJ/m})$$

Thus total $\epsilon/\text{unit length} = 2380 + 34502 = 36882 \text{ ft-lbf/in.} \quad (1.97 \text{ MJ/m})$. Comparing this value with the impact kinetic energy of 39,015 ft-lbf/in. (2.08 MJ/m) indicates a slight negative margin of safety on impact. Thus, bottoming out of the TB-1 containment vessel and some resulting plastic deformation is anticipated. Selection of the precipitation heat treatment of the PH13-8 Mo material (TB-1) was specifically oriented toward the enhancement of toughness and ductility.

2A.4 Corner Impact

When the PAT-1 package is impacted on its corner, the principal wood grain directions are no longer aligned parallel and perpendicular, respectively, to the direction of impact. As a result, material anisotropy clouds the problem solution. In addition, the inherent asymmetry of this type

* The inner integral is the strain energy density field which is taken as uniform between points 1 and 2.

of impact serves to make any meaningful energy balance analysis unrealistic. The following comments are, however, worthy of note:

- a. Experimentally, the PAT-1 package is shown to withstand without failure impact velocities in excess of the required 422 fps (129 m/s) in an angular, corner-on configuration. This fact alone supports and justifies the PAT-1 package design concept.
- b. Radiographs and postmortems of the deformed PAT-1 package indicate that the TB-1 containment vessel suffers no plastic deformation and has no leakage or loss of contents in corner impact tests.
- c. The observed inward buckling of the ends of the cylindrical load-spreader tube serves to contain, protect, and isolate the TB-1 vessel as well as to absorb impact energy through plastic work due to permanent deformation.
- d. The path length from point of initial impact of the outer container and the isolated TB-1 package is greatest for the corner impact. This greater path length permits greater attenuation and dispersion of impact-generated stress waves as well as providing a longer crush length and resulting greater energy absorption.

It is thus concluded that the PAT-1 package meets corner-impact requirements.

APPENDIX 2B

Properties of Principle Materials Used in the PAT-1 Package*

2B.1 Stainless Steel 304 (Ref. QQ-S-766c and Aerospace Structural Metals Handbook)

Cuter drum, drum liners, product can

$$f_{tu} = 75 \text{ ksi min}$$

$$f_{ty} = 30 \text{ ksi}$$

40% elongation in 2 in.

50% min reduction in area

$$E = 29 \times 10^6 \text{ lb/in.}^2 \text{ (dynamic and low temperature)}$$

$$\mu = 0.26$$

$$\rho = 0.29 \text{ lb/in.}^3$$

2B.2 Aluminum 6061-T6 (Ref. MIL Handbook 5B)

Load-spreader tube

$$f_{tu} = 42 \text{ ksi}$$

$$f_{ty} = 35 \text{ ksi}$$

$$E = 9.9 \times 10^6 \text{ lb/in.}^2$$

$$\mu = 0.33$$

$$\rho = 0.098$$

2B.3 Aluminum 7075-T6 (Ref. MIL Handbook 5B)

Load-spreader plates

$$F_{tu} = 77 \text{ ksi}$$

$$F_{ty} = 70 \text{ ksi}$$

$$E = 10.3 \times 10^6 \text{ lb/in.}^2$$

$$\mu = 0.33$$

$$\rho = 0.101 \text{ lb/in.}^3$$

* In this Appendix, materials references are not in metric units except as noted in paragraph 2B.8.

- 2B.4 Stainless Steel PH13-8 Mo H1075 (Aerospace Structural Metals Handbook and MIL Handbook 5B and Minimum Guarantees From Armco Steel Corp.)
TB inner containment vessel

$$F_{tu} = 163 \text{ ksi}$$

$$F_{ty} = 150 \text{ ksi}$$

$$E = 29.4 \times 10^6 \text{ lb/in.}^2$$

13% elongation in 4D

$$\mu = 0.278$$

$$\rho = 0.279 \text{ lb/in.}^3$$

Note: H1075 temper especially chosen for this specific application to enhance toughness to withstand maximum fire threat bonding high temperature of impacted, crushed, punctured, slashed, and burned package.

- 2B.5 Stainless Steel A286 (Ref. AMS-5731)

TB-1 closure bolts

$$F_{tu} = 180 \text{ ksi min (per heat treatment requirements on drawing R00638)}$$

Minimum ultimate tensile strength = 30,000 lb (per heat treat requirements on drawing R00638)

- 2B.6 Aluminum Honeycomb (Ref. Hexcel Std. for CR III - 1/8 - 5056 - 00X2N-8.1)

Spacers inside TB-1 inner containment vessel

5056 alloy

0.002 in. foil

1/8 in. cell

$$8.1 \text{ lb/ft}^3$$

1700 psi crush strength

- 2B.7 Redwood Impact Limiter Material

Six hollow and solid redwood impact energy adsorbing rings and plugs. Clear, select, kiln-dried redwood per SS-R00602-000.

Reference: W. A. Von Riesemann et al, The Effects of Temperature on the Energy-Absorbing Characteristics of Redwood, SAND77-1589, and SS-R00602, Appendix 9A.

Note: Units (metric/English) are herein used as stated in reference.

Density: Varies between 0.33 and 0.38 g/cm³

Specific Energy Absorbed: 22,380 ft-lbf/lbm (R. T.) (7 kJ/kg)

Specific energy absorbed is obtained under the following conditions and within the following constraints:

- a. Motion of the flat crushing (impact limiter) surface is parallel to the grain. (The surface itself is perpendicular to the grain.)
- b. The above value is an average value of five tests performed at room temperature.
- c. Specimens were statically loaded.
- d. The above value is the average energy absorbed per pound of redwood taken to lockup, a strain corresponding to crushing to approximately 37 percent of original volume.

Note that average specific energy data over a wide range in test temperatures is presented in Figure 2B-1.

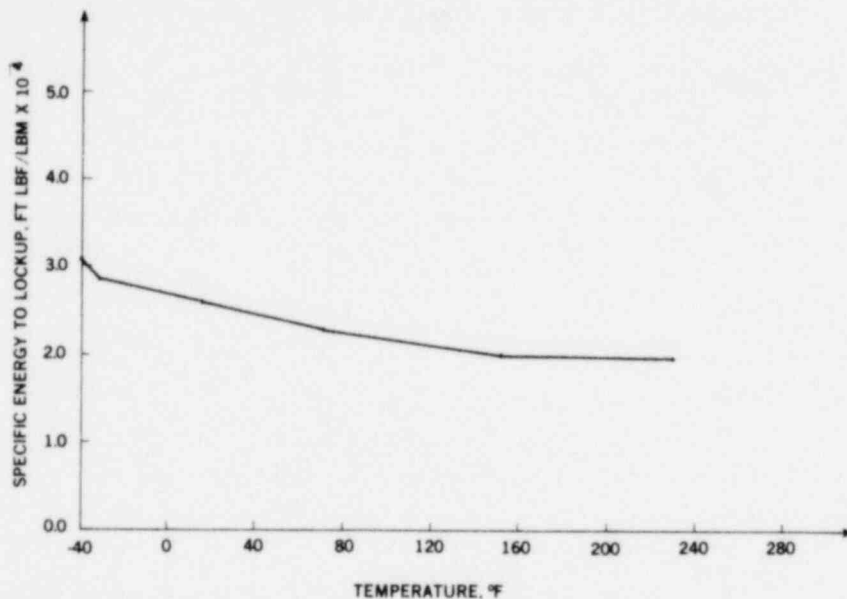


Figure 2B-1. Specific Energy to Lockup

Crush Strength: $f_c = 5380$ psi (R. T.) (37.1 MPa)

This value is the average unit force to lockup for room temperature test conditions. Loading conditions and constraints are listed above. A typical load^{*}-displacement curve (at room temperature) is presented in Figure 2B-2. Finally, the variation in average crush strength with test temperature is indicated in Figure 2B-3.

Details of the test procedure, sample size, etc., are presented in SAND77-1589, Ref. 13 in main text.

^{*}Or stress, since 1 in.² (6.45×10^{-4} m²) platen face was utilized.

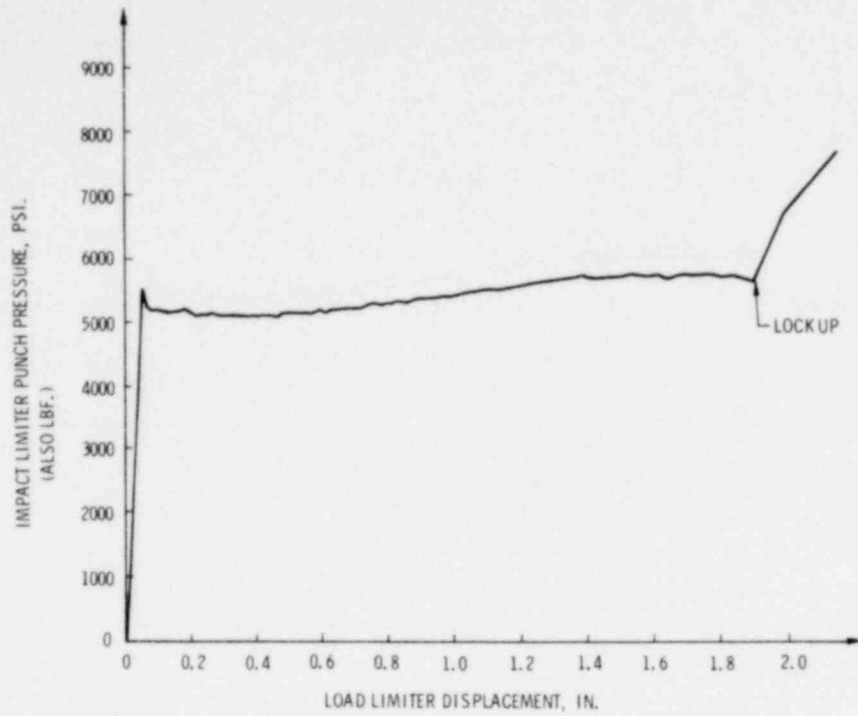


Figure 2B-2. A Typical Load-Displacement Curve (at room temperature)

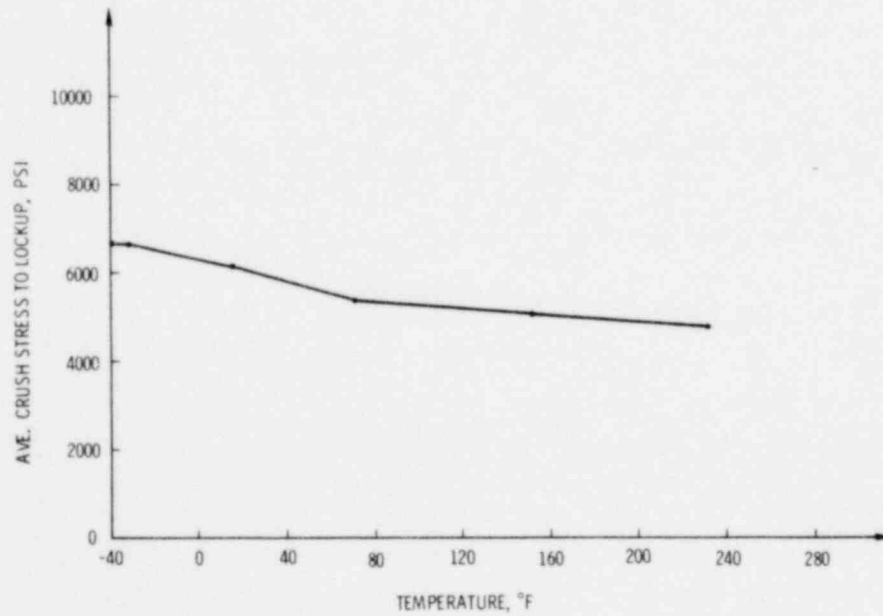


Figure 2B-3. Average Crush Stress for Redwood as a Function of Temperature

APPENDIX 2C

Package Load Resistance per 10 CFR 71.32a

In this analysis, the package is treated as a simple beam supported at both ends and subjected to a uniformly distributed load equal to five times the package weight (as per 10 CFR 71.32 a).

It is assumed for simplicity that the packaging consists of three basic load-carrying components for beam bending:^{*} the outside drum (stainless steel), the inside drum liner (stainless steel), and the outer redwood cylinder with radial-grain orientation. The resulting bending model is taken as shown in Figure 2C-1. Note that the model cross section consists of three concentric hollow bonded circular cylinders, the redwood cylinder defined over $r_a \leq r < r_b$ (region 1), the inner drum defined over $r_b \leq r < r_c$ (region 2), and the outer drum defined over $r_c \leq r \leq r_d$ (region 3). It is necessary to calculate the maximum stress occurring in each of these three cylinders and to check them individually for yielding.

For the simply supported uniformly loaded beam shown in Figure 2C-1, the maximum moment occurs at midspan and can be written¹

$$M_{\max} = \frac{5WL}{8} \quad (1)$$

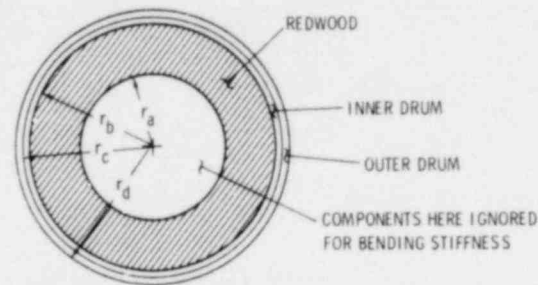
where

W = package weight

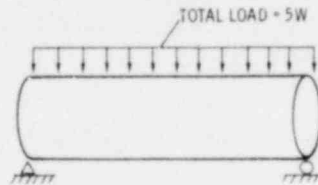
L = package overall length.

^{*} Such an assumption is conservative. The inner assemblies will add slight additional bending stiffness to the PAT package.

¹ R. J. Roark and W. C. Young, Formulas for Stress and Strain, McGraw-Hill Book Company, Inc., New York, 1975.



a. PACKAGE CROSS SECTION AT MIDSPAN



b. ASSUMED LOADING AND BOUNDARY CONDITIONS

Figure 2C-1. Simple Beam Bending Model

The standard beam-stress formula cannot be directly applied to the package because of the presence of materials in the cross section with differing elastic moduli (and hence bending stiffness). The method of equivalent cross sections is not directly applicable since the cross sections are circular rather than rectangular. It is necessary, therefore, to draw upon simple (Bernoulli-Euler) beam theory directly.

Simple beam theory is based upon the assumption that, under pure bending, plane sections perpendicular to the neutral axis remain plane during deformation. This kinematic assumption implies that the nature of the geometric deformation is independent of the stress-strain behavior of the material. Thus bending strain and beam curvature are uniquely related and are independent of the material layers. The strain² is:

$$\epsilon_x = \frac{y}{\rho} \quad (2)$$

where

y = distance off the neutral axis (Figure 2C-2).

ρ = radius of curvature of the neutral axis (Figure 2C-2).

ϵ_x = in-plane bending strain component.

²S. H. Crandall and N. C. Dahl, An Introduction to the Mechanics of Solids, McGraw-Hill Book Company, Inc., New York, 1959.

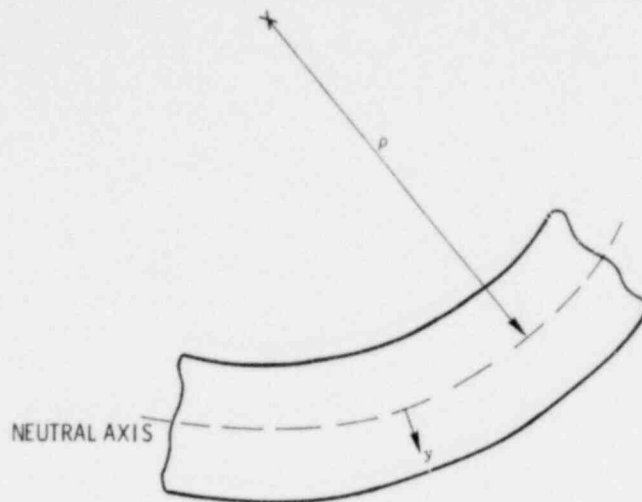


Figure 2C-2. Simple Beam Undergoing Pure Bending

Further, in a given region of the cross section, Hooke's Law reduces (under simple beam theory) to

$$\sigma = \epsilon E \quad (3)$$

where

E = the appropriate elastic modulus.

Now consider one of the hollow sections. The stress is then

$$\sigma = \frac{My}{I} \quad (4)$$

where

M = applied moment

I = area moment of inertia about the neutral axis.

Now each of the three cylinders, acting as a unit under bending, carries some of the total available moment. In the elastic range, the moment-curvature relationship for a single cylinder is

$$\frac{1}{\rho} = \frac{M}{EI} \quad (5)$$

so that the contribution of each of the three cylinders to the total moment is (for some arbitrary but fixed curvature, $1/\rho$), respectively,

$$M_1 = \frac{E_1 I_1}{\rho}; \quad M_2 = \frac{E_2 I_2}{\rho}; \quad M_3 = \frac{E_3 I_3}{\rho}.$$

The total moment at the cross section, M_{\max} , as given by equation (1), is the sum of these three moments,

$$M_{\max} = M_1 + M_2 + M_3 = \frac{1}{\rho} [E_1 I_1 + E_2 I_2 + E_3 I_3] \quad (6)$$

The only unknown in this equation is ρ , the resulting radius of curvature.

Since from equations (2), (3), and (6),

$$\sigma = E \frac{y}{\rho} = \frac{E M_{\max}}{\sum_{i=1}^3 E_i I_i} y \quad (7)$$

and the fact that $I = \pi/4 (r_o^4 - r_i^4)$, where r_o is the outer radius and r_i the inner radius of a given cylinder, it is easily shown that the maximum stresses occurring in each of the three concentric cylinder materials is

Redwood

$$(\sigma_{\max})_1 = \frac{2.5 E_1 W L r_b}{\pi [E_1 (r_b^4 - r_a^4) + E_2 (r_c^4 - r_b^4) + E_3 (r_d^4 - r_c^4)]} \quad (8)$$

Inner Drum

$$(\sigma_{\max})_2 = \frac{2.5 E_2 W L r_c}{\pi [E_1 (r_b^4 - r_a^4) + E_2 (r_c^4 - r_b^4) + E_3 (r_d^4 - r_c^4)]} \quad (9)$$

Outer Drum

$$(\sigma_{\max})_3 = \frac{2.5 E_3 W L r_d}{\pi [E_1 (r_b^4 - r_a^4) + E_2 (r_c^4 - r_b^4) + E_3 (r_d^4 - r_c^4)]} \quad (10)$$

Note that for a single continuous material (i. e., $E_1 = E_2 = E_3$), the equations reduce to the simple beam-bending stress formula.

Consider now the following numerical values:

$$r_a = 6.08 \text{ in. (15.44 cm)}$$

$$r_b = 11.190 \text{ in. (28.42 cm)}$$

$$r_c = 11.250 \text{ in. (28.58 cm)}$$

$$r_d = 11.309 \text{ in. (28.72 cm)}$$

$$W = 500 \text{ lb (2.224 kN)}$$

$$L = 42.5 \text{ in. (108 cm)}$$

$$E_1 = 1.34 \times 10^6 \text{ psi (9.24} \times 10^3 \text{ MPa)}$$

$$E_2 = 29.0 \times 10^6 \text{ psi (2} \times 10^5 \text{ MPa)}$$

$$E_3 = 29.0 \times 10^6 \text{ psi (2} \times 10^5 \text{ MPa)}$$

$$\sigma_{1 \text{ yield}} = 6,900 \text{ psi (47.6 MPa) (proportional limit)}$$

$$\sigma_{2 \text{ yield}} = 30,000 \text{ psi (207 MPa) (yield)}$$

$$\sigma_{3 \text{ yield}} = 30,000 \text{ psi (207 MPa) (yield)}$$

Resulting maximum stresses using equations (8), (9), and (10) are as follows:

$$(\sigma_{\text{max}})_1 = 6.5 \text{ psi (44.8 kPa)}$$

$$(\sigma_{\text{max}})_2 = 142 \text{ psi (979 kPa)}$$

$$(\sigma_{\text{max}})_3 = 143 \text{ psi (986 kPa) .}$$

Comparing these stresses to corresponding material yield values listed above, it is seen that stresses due to the stated bending load are negligible.

APPENDIX 2D

External Pressure per 10 CFR 71.32(b)

10 CFR 71.32(b) requires that the packaging be adequate to assure that the TB-1 containment vessel will suffer no loss of contents if subjected to an external pressure of 25 psi (172 kPa).

In investigating this requirement, it is important to note that the stainless-steel outside drum, end caps, and associated drum liner are not intended to be leak-tight. In fact, the top and bottom end caps are vented, as shown in Figure 2D-1, to assure that no pressure differential can build up across the outer container. Since slight air spaces are present between pieces of redwood, the required 25 psi (172 kPa) pressure produces a significant loading only upon the inner sealed container, also shown in Figure 2D-1. Thus, satisfaction of this external pressure requirement reduces so that the TB-1 containment vessel does not crack open when subjected to a 25 psi (172 kPa) external pressure differential. It would thus be conservative to show that plastic yielding does not occur.

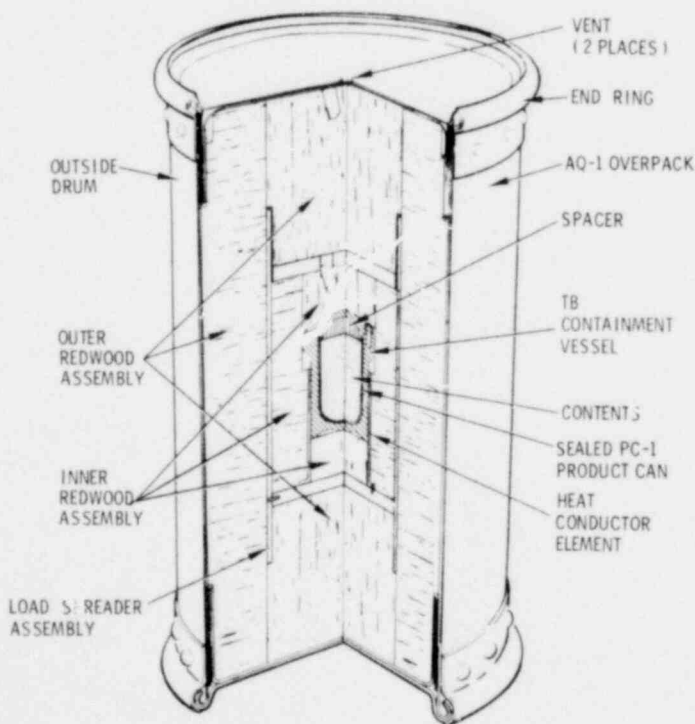


Figure 2D-1. PAT-1 Plutonium Air Transportable Package

In order to satisfy a later requirement (water immersion), an elastostatic analysis of the TB-1 containment vessel subjected to an external hydrostatic pressure of 5000 psi (34.5 MPa) was performed. Since the analysis was linearly elastic in the small deflection regime, the stress field generated in the TB-1 vessel by the 5000 psi (34.5 MPa) loading can be scaled down exactly to the case of 25 psi (172 kPa) external pressure simply by multiplying all stresses by the load ratio, 0.005.

The axisymmetric finite element grid utilized for the TB containment vessel is shown in Figure 2D-2.

Locations of maximum (i. e., tensile) and minimum (compressive) stresses are, as could be anticipated, in the vicinity of the sharp corner. This stress and the extreme tensile and compressive values shown in Figure 2D-2 are insignificant when compared to the yield stress of the PH13-8 Mo TB-1 vessel material of 150,000 psi (1034 MPa). Clearly, the vessel will suffer no loss in contents for the 25 psi (172 kPa) external pressure loading requirement.

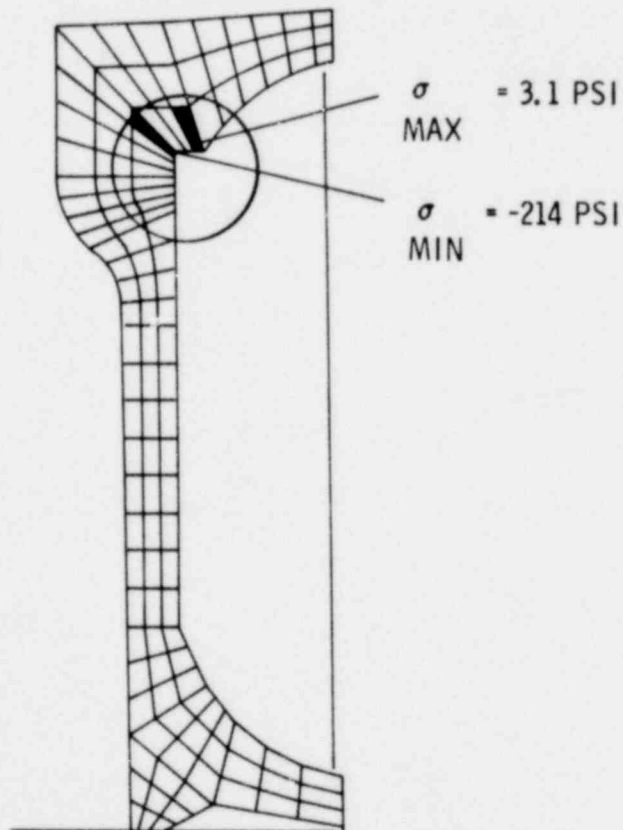


Figure 2D-2. Critical Stress Locations for 25-psi External Pressure Acting on TB Containment Vessel

APPENDIX 2E

Pressure Analysis per 10 CFR 71 Appendix A3

2E.1 General

As required in Appendix A3 in 10 CFR 71, a normal condition of transport is the application of 0.5 times standard atmospheric pressure to the package. The TB-1 containment vessel is sealed and assumed to contain standard atmospheric pressure. The outside drum is purposely vented to prevent buildup of a pressure differential. Because of air spaces between wood layers, the result of shipment of the package in a subatmospheric pressure environment is simply an 0.5 atmospheric 7.35-psi (50.7-kPa) positive pressure differential in the TB-1 containment vessel.

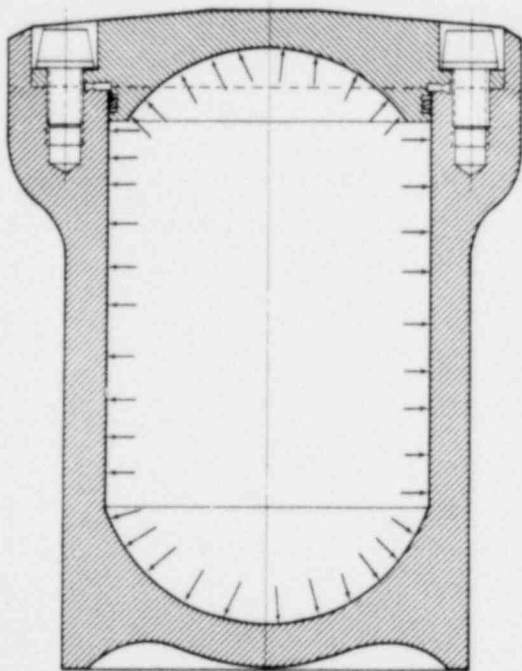


Figure 2E-1. TB-1 Containment Vessel

The cross section of the TB-1 containment vessel subjected to 7.35-psi (50.7-kPa) internal pressure is shown in Figure 2E-1. The problem is most conservatively modeled* by assuming the vessel to be a uniform cylinder with flat ends, a portion of which is shown in Figure 2E-2 along with internal generalized stresses acting at the end cap - cylinder intersection.

Stresses in the cylinder and flat head are found¹ by superposing a number of individual loading cases. The generalized stresses M_o (bending moment per unit circumferential length) and V_o (transverse shear force per unit circumferential length) acting at the cylinder-head intersection are indicated in Figure 2E-2. These generalized

* An alternate procedure is to model the problem using an elastostatic finite element program such as TEXGAP (see Section 2.2.12.1).

¹R. J. Roark, Formulas for Stress and Strain, McGraw-Hill Book Company, Inc., New York, 1965.

stresses are

$$M_o = \frac{\frac{Pr^3\lambda_2^2 D_2}{4D_1(1+\nu)} + \frac{2Pr^2\lambda_2^3 Et_1 D_2}{Et_2(1-\nu/2) [Et_1 + 2rD_2\lambda_2^3(1-\nu)]}}{2\lambda_2 + \frac{2r\lambda_2^2 D_2}{D_1(1+\nu)} - \frac{\lambda_2 Et_1}{Et_1 + 2D_2\lambda_2^3 r(1-\nu)}} \quad (1)$$

and

$$V_o = M_o \left(2\lambda_2 + \frac{2r\lambda_2^2 D_2}{D_1(1+\nu)} \right) - \frac{Pr^3\lambda_2^2 D_2}{4D_1(1+\nu)} \quad (2)$$

where $()_1$ refers to the flat head and $()_2$ refers to the cylinder,

$$D_1 = \frac{E_1 t_1^3}{12(1-\nu_1^2)} ; \quad D_2 = \frac{E_2 t_2^3}{12(1-\nu_2^2)} ; \quad \lambda_2 = \sqrt[4]{\frac{3(1-\nu_2^2)}{r^2 t_2^2}} ;$$

and $(E_1, \nu_1), (E_2, \nu_2)$ denote, respectively, the elastic constants of the flat head and the cylinder. Other terms appearing in Equations (1) and (2) are average radius, r , thickness, t , and internal pressure, P . The stress fields throughout the flat end cap and cylinder can be determined using the generalized stresses M_o and V_o .

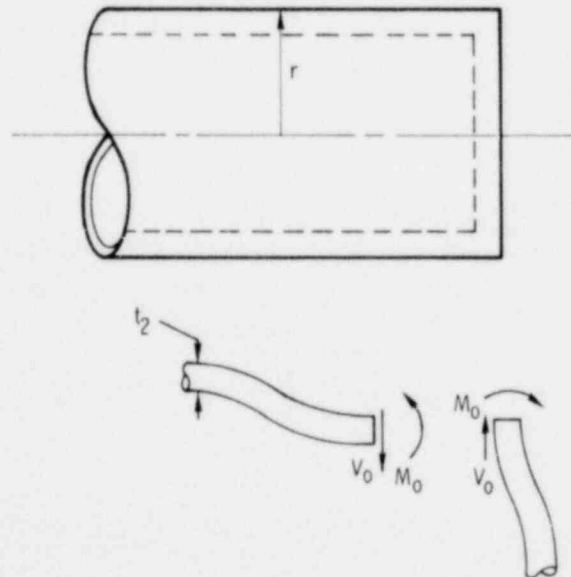


Figure 2E-2. Internal Generalized Stresses at Cylinder-Head Intersection

Consider the following input data* for the TB-1 container:

$$P = 7.35 \text{ psi (50.7 kPa)}$$

$$r = 2.4 \text{ in. (6.1 cm)}$$

$$t_1 = t_2 = 0.55 \text{ in. (1.4 cm)}$$

$$E_1 = E_2 = 29.4 \times 10^6 \text{ psi (2.03} \times 10^5 \text{ MPa)}$$

$$\nu_1 = \nu_2 = 0.278$$

The resulting calculated values of moment and transverse shear are then

$$M_o = 4.741 \text{ in.} \cdot \text{lb/in. (21.09 N} \cdot \text{m/m)}$$

$$V_o = 8.033 \text{ lb/in. (1407 N/m)}$$

2E.2 Stresses in Flat End Cap

The stress field in the flat end cap is obtained by superposition of stresses due to the following:

- Internal pressure, P : The applicable load case is a simply supported, uniformly loaded circular plate.
- Bending moment, M_o : The applicable load case is an unsupported plate subjected to a uniform edge moment.
- Transverse shear force, V_o : The applicable load case is a circular plate subjected to a uniform radial in-plane edge load, V_o , per unit length.

Each of these load cases is now solved individually and later superimposed.

- The uniformly loaded plate is shown in Figure 2E-3. The radial, outer fiber bending stress field in the plate is given by

$$\sigma_{rr} = \frac{3\nu P a^2}{8t^2} \left[\left(\frac{3}{\nu} + 1 \right) \left(1 - \frac{r^2}{a^2} \right) \right] \quad (3)$$

$$\sigma_{\theta\theta} = \frac{3\nu P a^2}{8t^2} \left[\left(\frac{3}{\nu} + 1 \right) - \left(\frac{1}{\nu} + 3 \right) \frac{r^2}{a^2} \right]$$

where r is the radial coordinate and other terms are defined earlier.

* Values appear in SI units in parentheses.

For $P = 7.35 \text{ psi (50.7 MPa)}$

$a = 2.4 \text{ in. (6.1 cm)}$

$t = 0.55 \text{ in. (1.4 cm)}$

$\nu = 0.278$

then the stress field due to transverse pressure loading is

$$\sigma_{rr} = 172 - 29.8 r^2 \text{ psi} \quad (\sigma_{rr} = 1.19 - 318 r^2 \text{ MPa}) \quad (5)$$

$$\sigma_{\theta\theta} = 172 - 16.7 r^2 \text{ psi} \quad (\sigma_{\theta\theta} = 1.19 - 178 r^2 \text{ MPa}). \quad (6)$$

These equations represent bending stresses, and result in tension on the outer plate surface and compression on the inner surface.

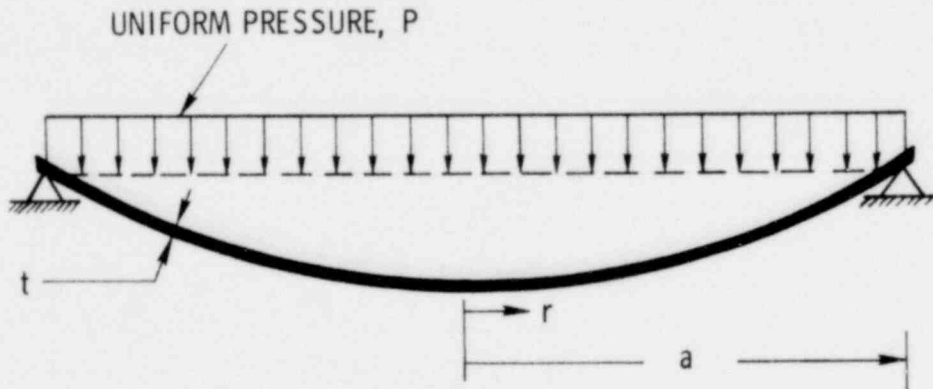


Figure 2E-3. Simply Supported, Uniformly Loaded Circular Plate—Load Case a.

- b. An unsupported plate subjected to a uniform edge moment is shown in Figure 2E-4. The resulting stress field is

$$\sigma_{rr} = \sigma_{\theta\theta} = -\frac{6M_0}{t^2}. \quad (7)$$

For the values of parameters indicated above,

$$\sigma_{rr} = \sigma_{\theta\theta} = -94.0 \text{ psi (-648 kPa)}.$$

This value corresponds to compression on the outside plate surface and tension on the inner surface.

Combining Equations (1), (2), and (4), the superposed (membrane and bending) axial stress (at a point on the container outer wall) can be written

$$\left(\sigma_{ZZ}\right)_{\max} = -\frac{5W}{2\pi at} - \frac{15W\delta}{a(t')^2} \quad (5)$$

Now consider the following input values:

$$\delta = 0.31 \text{ in. (0.79 cm)}$$

$$a = 11.25 \text{ in. (28.6 cm)}$$

$$t' = 0.1196 \text{ in. (0.3 cm)}$$

$$t = 0.059 \text{ in. (0.15 cm)}$$

$$W = 500 \text{ lb (2224 N)}$$

$$\nu = 0.26 .$$

Then the maximum circumferential (hoop) stress is found from Equation (3) to be

$$\left(\sigma_{\theta\theta}\right)_{\max} = 2563 \text{ psi (17.7 MPa)}$$

and the maximum axial stress, from Equation (5), is

$$\left(\sigma_{ZZ}\right)_{\max} = -5190 \text{ psi (-35.8 MPa)} .$$

To determine if plastic yielding occurs under this biaxial state of stress, the Von Mises effective stress is calculated from

$$\sigma_{\text{eff}} = \left[\sigma_{\theta\theta}^2 + \sigma_{ZZ}^2 - \sigma_{\theta\theta}\sigma_{ZZ} \right]^{1/2}$$

or

$\sigma_{\text{eff}} = 6842 \text{ psi (47 MPa)}$. Comparing this value to the 30,000-psi (207-MPa) yield stress of the 304 stainless steel material, it is seen that plastic yielding will not occur when the container is subjected to compressive loading five times its weight.

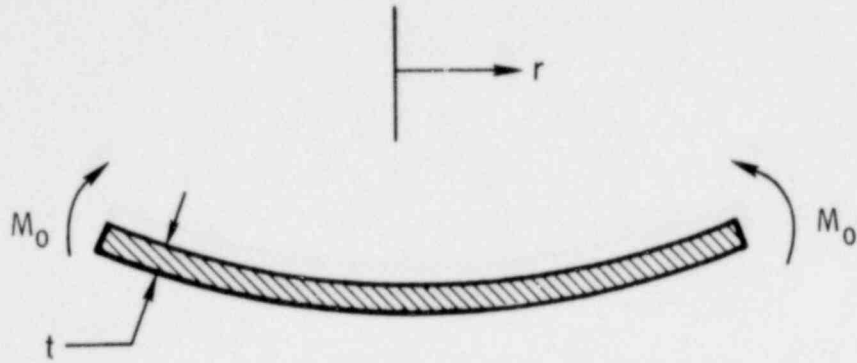


Figure 2E-4. Unsupported Plate Subjected to a Uniform Edge Moment

- c. The uniform transverse shear force, V , induces a tensile uniform radial stress in the plate,

$$\sigma_{rr} = \frac{V_0}{t} \quad (8)$$

or

$$\sigma_{rr} = 14.6 \text{ psi (101 kPa).}$$

This stress is uniform membrane radial tension, i. e., tension on both inner and outer surfaces.

Stress fields will be maximum at the plate center or at the plate edge (plate-cylinder intersection). Cases a, b, and c are superposed (on inner and outer surfaces) at the plate center in Table 2E-I and outer edge in Table 2E-II.

TABLE 2E-I

Extreme Fiber Stresses at Plate Center

Case No.	Outer Surface Stress (psi)		Inner Surface Stress (psi)	
	σ_{rr}	$\sigma_{\theta\theta}$	σ_{rr}	$\sigma_{\theta\theta}$
a	172.0	172.0	-172.0	-172.0
b	- 94.0	- 94.0	94.0	94.0
c	14.6	0	14.6	0
Sum	92.6	78.0	- 63.4	- 78.0

TABLE 2E-II

Extreme Fiber Stresses at Plate Outer Edge

Case No.	Outer Surface Stress (psi)		Inner Surface Stress (psi)	
	σ_{rr}	$\sigma_{\theta\theta}$	σ_{rr}	$\sigma_{\theta\theta}$
a	0	75.8	0	-75.8
b	-94.0	-94.0	94.0	94.0
c	14.6	14.6	14.6	14.6
Sum	-79.4	-3.6	108.6	32.8

Inspection of Tables 2E-I and 2E-II reveals that the maximum stress in the plate is 108.6 psi (749 kPa) (radial stress at cylinder-plate intersection on inner plate surface) and minimum value (i. e., most compressive) is -79.4 psi (-547 kPa) at the same radial location on the outer plate surface. Clearly, these values of stress are completely negligible in comparison to the 150,000 psi (1034 MPa) yield stress of the TB-1 vessel material.

2E.3 Stresses in the Cylinder

The stress field in the cylindrical portion of the pressure vessel is found in a somewhat similar manner by superposing stresses due to the following:

- Internal pressure, P , acting in a closed cylindrical pressure vessel.
- Transverse edge shear force, V_o , per unit circumferential length, acting on the end of a long cylinder.
- Uniform edge moment, M_o , per unit length acting on the end of a semi-infinite cylinder.

Each of these load cases is now solved individually and later superimposed.

- As shown in Figure 2E-5, hoop and axial membrane stresses induced by internal pressure are, respectively,¹

$$\sigma_{\theta\theta} = \frac{Pa}{t} \quad (9)$$

$$\sigma_{ZZ} = \frac{Pa}{2t} \quad (10)$$

¹R. J. Roark, op cit.

where

- P = internal pressure
- a = average cylinder radius
- t = cylinder thickness

For P = 7.35 psi (50.7 kPa); a = 2.4 in. (6.1 cm); and t = 0.55 in. (1.4 cm)

$$\sigma_{\theta\theta} = 32.0 \text{ psi (221 kPa)}$$

$$\sigma_{ZZ} = 16.0 \text{ psi (110 kPa)}$$

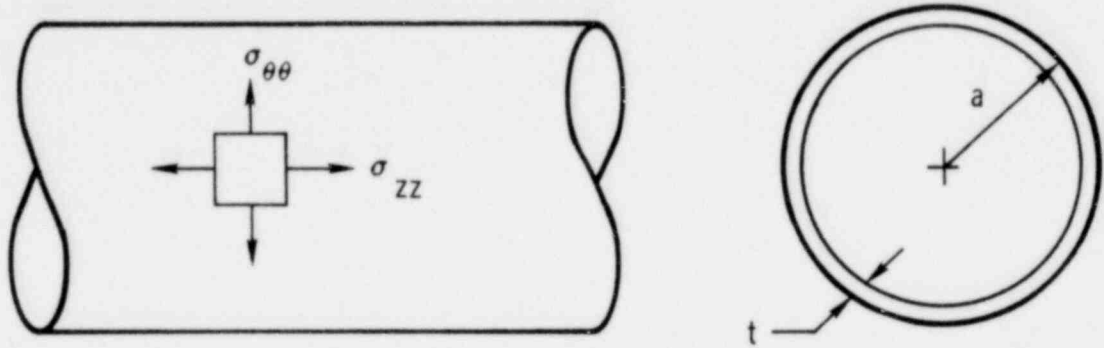


Figure 2E-5. Membrane Stresses Due to Internal Pressure

b. For uniform radial shear loading shown in Figure 2E-6, the hoop stress is

$$\sigma_{\theta\theta} = \frac{-2V_o}{t} \left(\lambda a e^{-\lambda Z} \cos \lambda Z \right) \quad (11)$$

and the axial bending stress is

$$\sigma_{ZZ} = \left(\frac{6}{t^2} \frac{1}{\lambda} V_o e^{-\lambda Z} \sin \lambda Z \right) \quad (12)$$

where

V_o = shear force per unit circumferential length,

$$\lambda = \sqrt{\frac{4}{a^2} \frac{3(1-\nu^2)}{t^2}},$$

ν = Poisson's ratio of the cylinder material,

Z = axial coordinate.

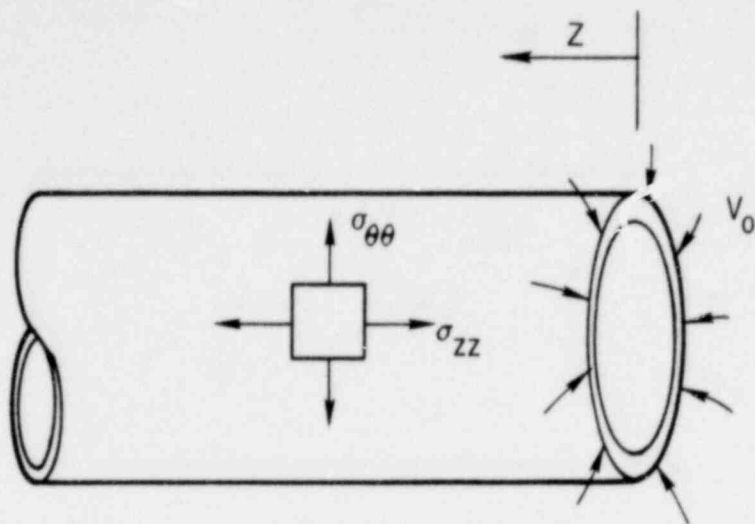


Figure 2E-6. Uniform Radial Shear on a Long Cylinder

- c. Finally, for the uniform edge moment, M_0 , shown in Figure 2E-7, the hoop stress is¹

$$\sigma_{\theta\theta} = \frac{2\lambda^2 a M_0 e^{-\lambda Z} (\cos \lambda Z - \sin \lambda Z)}{t} \quad (13)$$

$$\sigma_{zz} = -\frac{6}{t^2} [M_0 e^{-\lambda Z} (\cos \lambda Z + \sin \lambda Z)] \quad (14)$$

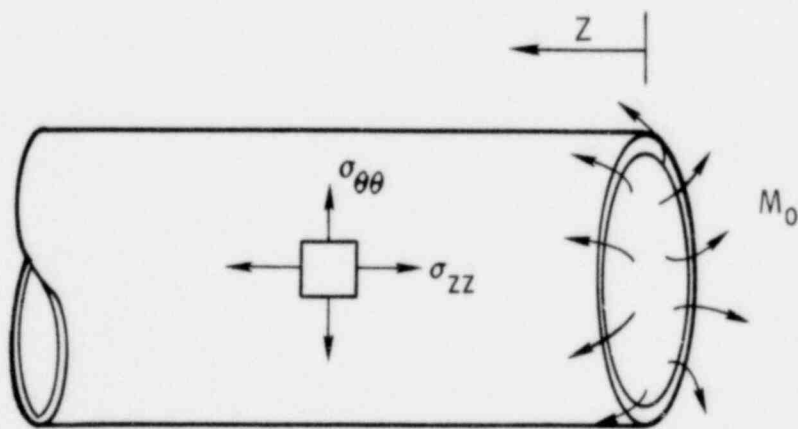


Figure 2E-7. Uniform Radial Edge Moment on a Long Cylinder

¹R. J. Roark, op cit.

The superposition of cases a through c for the cylinder results in the following hoop-stress as a function of the axial coordinate, Z:

$$\sigma_{\theta\theta} = 32 + \left[\left(\frac{2\lambda^2 aM_o - 2V_o\lambda a}{t} \right) \cos \lambda Z - \frac{2\lambda^2 aM_o}{t} \sin \lambda Z \right] e^{-\lambda Z} \text{ psi} . \quad (15)$$

For the TB-1 vessel, the appropriate parameter values are

$$\begin{aligned} \lambda &= 1.122 \text{ in.}^{-1} (44.7/\text{m}) \\ a &= 2.4 \text{ in.} (6.1 \text{ cm}) \\ M_o &= 4.741 \text{ in.-lb/in.} (21.09 \text{ N-m/m}) \\ V_o &= 8.033 \text{ lb/in.} (1407 \text{ N/m}) \\ t &= 0.55 \text{ in.} (1.4 \text{ cm}) \end{aligned}$$

resulting in the following equation for hoop stress.

$$\sigma_{\theta\theta}(Z) = 32 - [26.57 \cos(1.122Z) + 52.08 \sin(1.122Z)] e^{-1.122Z} \text{ psi} . \quad (16)$$

The maximum value of this hoop-stress is found graphically by plotting $\sigma_{\theta\theta}(Z)$ as a function of Z, as shown in Figure 2E-8, resulting in a peak stress of 33.3 psi (230 kPa).

Next, the superposition of axial stresses for the cylinder results in

$$\sigma_{ZZ}(Z) = 16 \pm \frac{6}{t} e^{-\lambda Z} \left\{ \left(\frac{V_o}{\lambda} \right) - M_o \sin \lambda Z - M_o \cos \lambda Z \right\} \text{ psi} \quad (17)$$

where (+) is for outer surface and (-) for inner surface stresses. Using the above parameter values, Equation (17) becomes

$$\sigma_{ZZ} = 16 \pm \left\{ 47.9 \sin(1.122Z) - 94.0 \cos(1.122Z) \right\} e^{-1.122Z} \text{ psi} . \quad (18)$$

Again, the maximum values are found graphically (see Figure 2E-9) to be -78 psi (-538 kPa) on the outside surface and 119 psi (758 kPa) on the inner surface, this time at Z = 0. Clearly, these resultant cylinder stresses are seen to be negligible in comparison to the 150,000-psi (1034-MPa) yield stress of the TB-1 vessel material.

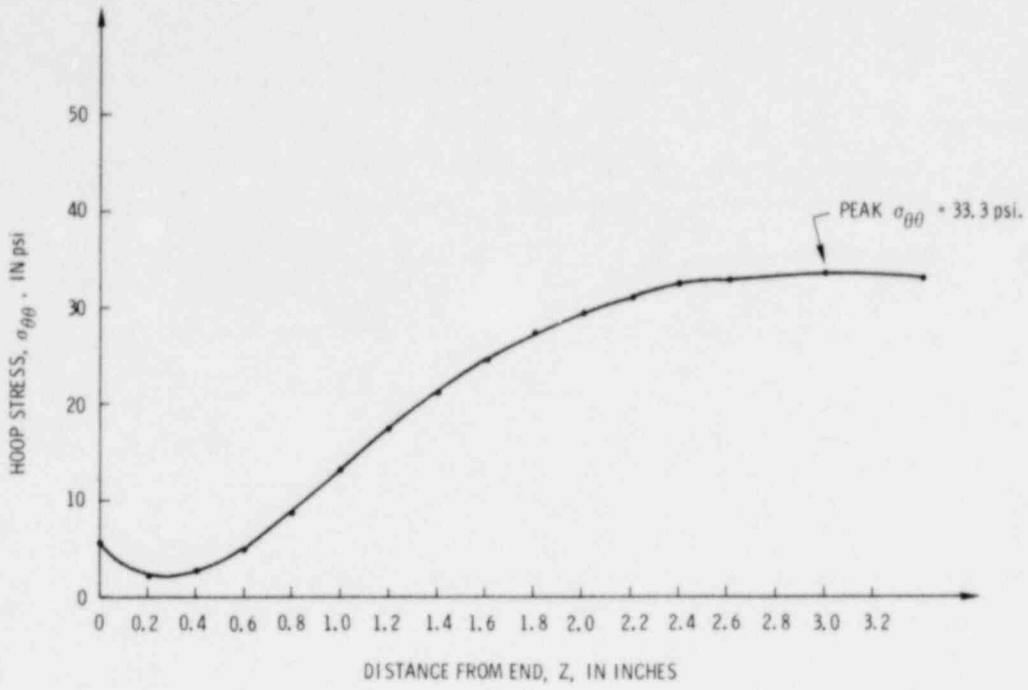


Figure 2E-8. Graph of Resultant Hoop Stresses as a Function of Axial Distance

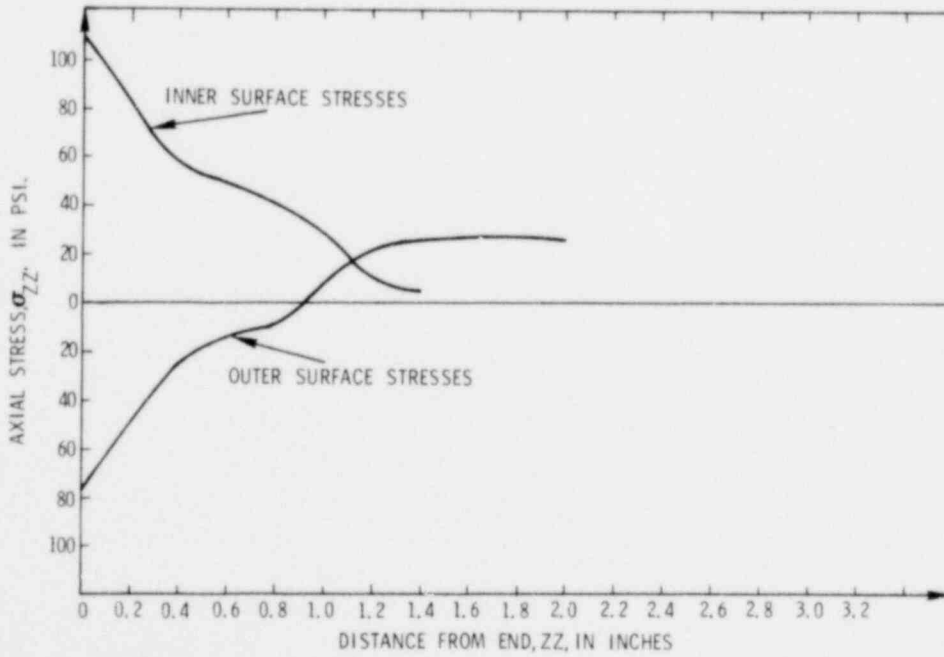


Figure 2E-9. Maximum Values of Outside and Inner Surfaces

Finally, bolt failure in tension is a possibility for positive internal pressure. Based upon the projected area of the end cap, and considering that the load is carried by 12 bolts, it is easily shown that the tensile load per bolt is 11 lb (49 N). Since the A286 stainless-steel TB-1 closure bolts have a minimum ultimate tensile strength of 30,000 lb (133 kN), bolt failure obviously will not occur for 7.35-psi (51-kPa) pressure differential.

It is thus concluded that application of 0.5-atmospheres pressure differential to the container during normal transport induces negligible internal loading of the package.

APPENDIX 2F

Compression Analysis per 10 CFR 71 Appendix A10

2F.1 General

According to 10 CFR 71 Appendix A, 10, it is necessary to determine the effect on the package of a compressive load equal to five times the weight of the package* applied uniformly against the top and bottom of the package in the position in which the package would normally be transported.

The PAT-1 package, as shown in Figure 2F-1, has identical end ring assemblies on top and bottom. When loaded by uniform compression, the entire loading could, in the worst case, be applied over the end rings.

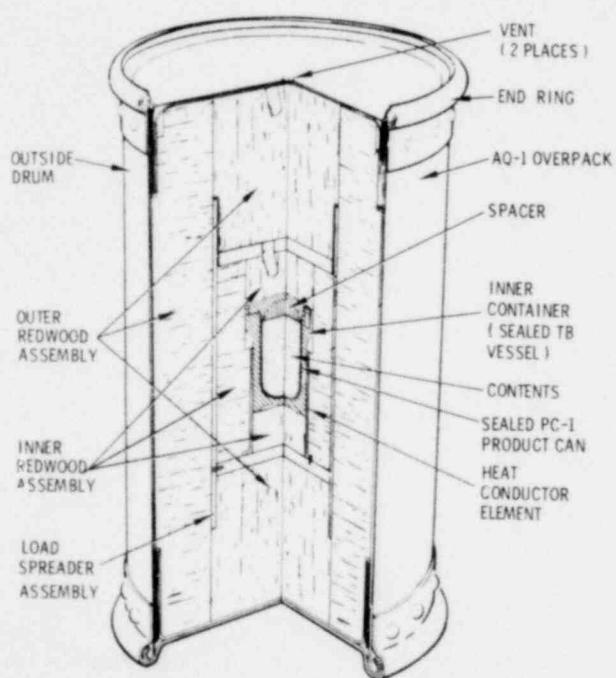


Figure 2F-1. PAT-1 (Plutonium Air Transportable) Package Showing Load-Carrying End Ring

A sketch of the end ring assembly detail (Figure 2F-2), shows that, neglecting the structural stiffness of the inner container and other structural stiffening elements in the vicinity of the container end, the end connection can be conservatively interpreted as consisting of three membrane and bending load-carrying elements: the clamp ring, the outer drum cover, and the outer drum. Also shown in Figure 2F-2 is the loading caused by the compression force requirement. This loading is a circular line load applied with offset, δ . The resultant loading thus can be accurately modeled as a compressive load of magnitude $5W\delta$ applied to the assembly. The solution for stresses is thus obtained by superposing the axial compressive membrane stresses and axial bending stresses generated by compressive load and bending moment, respectively.

*This requirement is more severe than the 2-psi (13.8-kPa) requirement.

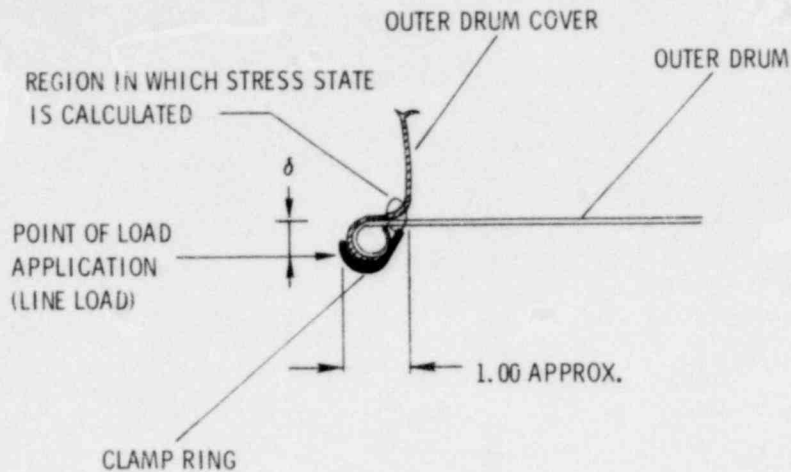


Figure 2F-2. Detail of Container End Connection

2F.2 Axial Compressive Load

It is conservatively assumed that the outer container independently carries the entire $5W$ compressive loading,

$$\left(\sigma_{ZZ}\right)_{5W} = -\frac{5W}{2\pi at} \quad (1)$$

where

a = cylinder radius

t = cylinder thickness

2F.3 Uniform Radial Edge Moment

The loading due to the bending moment induced by the loading offset, δ , is as shown in Figure 2F-3, where the edge moment per unit circumferential length is

$$M_o = \frac{5W\delta}{2\pi a} \quad (2)$$

It can be easily shown¹ that extreme values* of resulting stress for this problem will occur at the end of the cylinder in this problem, i. e., for $Z = 0$ in Figure 2F-3.

The maximum circumferential stress ($Z = 0$) induced in a long cylinder for uniform edge moment, M_o , per unit length is¹

$$\left(\sigma_{\theta\theta}\right)_{\max} = \frac{2\lambda^2 a M_o}{t'} \quad (3)$$

¹R. J. Roark, Formulas for Stress and Strain, McGraw-Hill Book Company, Inc., NY, 1965.

*Bending stiffness afforded by the clamp ring (as well as other structural components already ignored) is conservatively neglected here.

where

$$\lambda = \sqrt[4]{\frac{3(1-\nu^2)}{a^2(t')^2}}$$

ν = Poisson's ratio

t' = thickness of drum and drum cover* and

M_o = is defined by Equation (2).

M_o , UNIFORM EDGE MOMENT
PER UNIT CIRCUMFERENTIAL
LENGTH

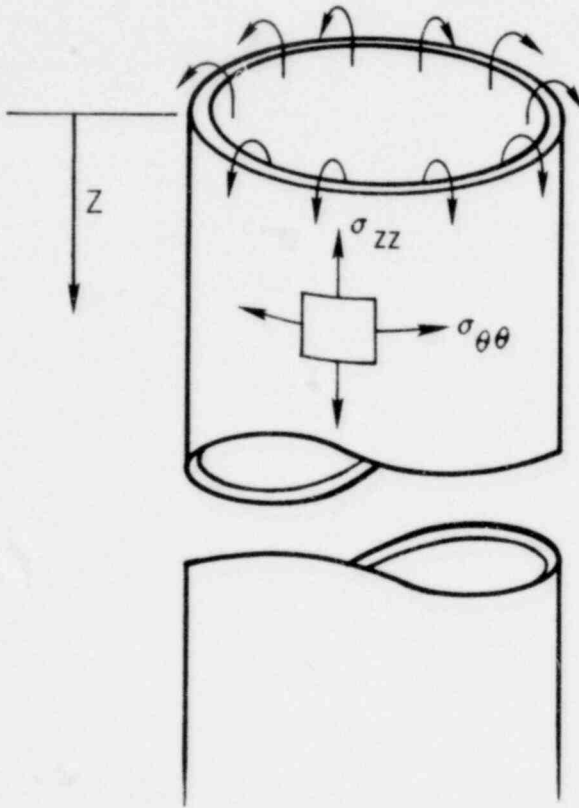


Figure 2F-3. Uniform Radial Edge Moment Induced by Axial Compressive-Loading of Container Flange

Next, the maximum axial bending stress ($Z = 0$) is given by

$$(\sigma_{ZZ}) M_o = - \frac{6 M_o}{(t')^2} \quad (4)$$

* Bending stiffness afforded by the clamp ring (as well as other structural components already ignored) is conservatively neglected here.

APPENDIX 2G
Terminal Free Fall

A falling PAT-1 package was treated aerodynamically as a tumbling right-circular cylinder, with appropriately applied coefficients for the end-on and side-on drag, and appropriate treatment of area.

A digital program was written to process the calculations. Various initial conditions were assumed:

- a. Horizontal cruise at Mach .9 and package release at 35,000 ft (10.7 km)
- b. Vertical free free fall from 35,000 ft (10.7 km)
- c. Horizontal cruise at 422 ft/s (129 m/s) and package release at 10,000 ft (3.05 km)
- d. Horizontal cruise at 850 ft/s (260 m/s) and package release at 12,000 ft (3.66 km)

All results converged to essentially the same value at sea level: 350 fps (107 m/s). This is 83 percent of the USNRC criteria-required minimum crash velocity of 250 KTS, 422 fps (129 m/s). These results are shown in Table 2G-1 and Figure 2G-1.

Table 2G-1
Summary of Terminal Free-Fall Velocity Calculations

Release Altitude (ft)	Release Velocity (ft/s)	Velocity at 5000 feet (ft/s)	Velocity at Sea Level (ft/s)
10,000	422 (250 KTS)	354	347
12,000	850 (503 KTS)	364	348
35,000	0 (Mach = 0)	377	350
35,000	880 (Mach = 0.9)	377	350

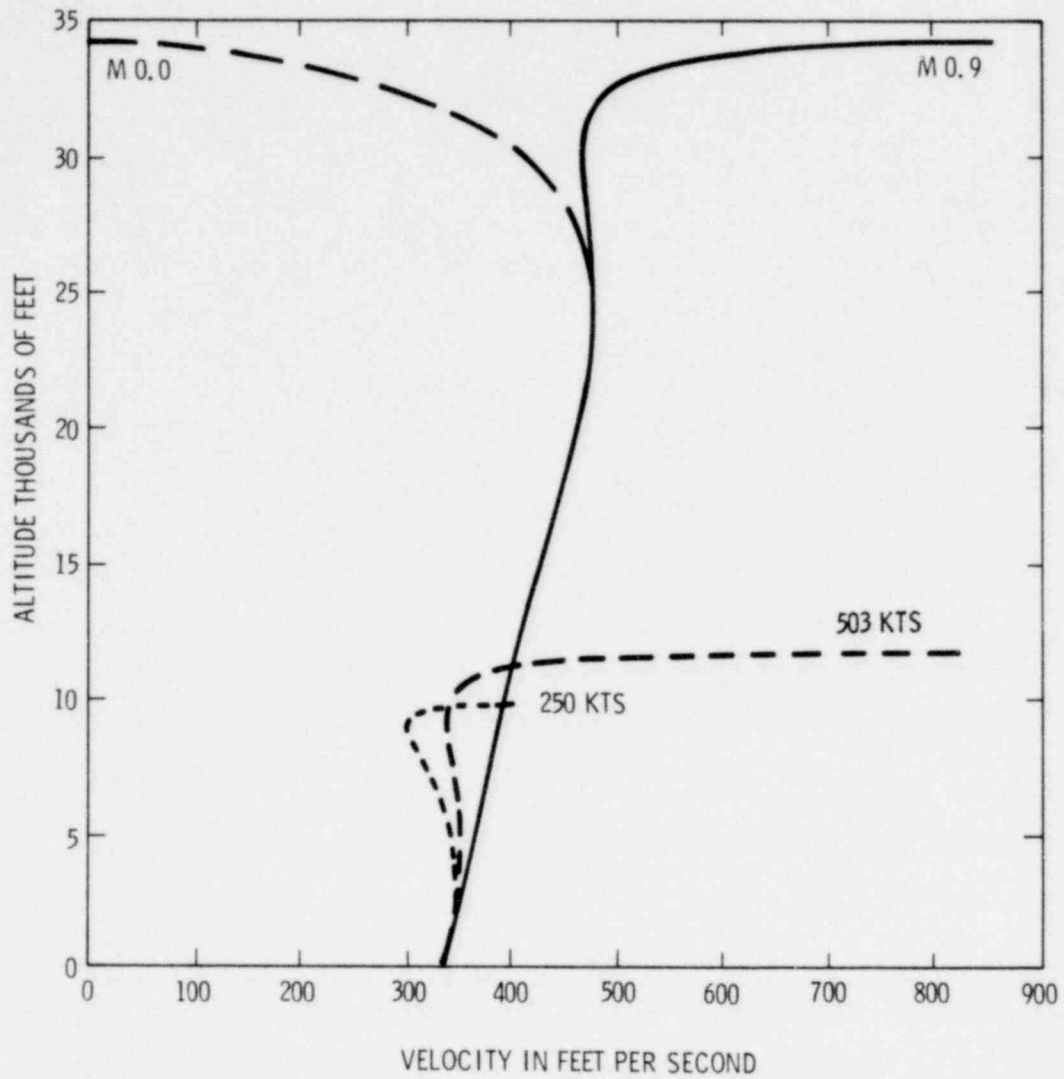


Figure 2G-1. Terminal Velocity as a Function of Altitude and Initial Velocity for a Tumbling PAT-1

APPENDIX 2H

Test Protocol

PAT-1 (Plutonium Air Transportable) Package, Model 1

This test protocol furnishes a description of the equipment, sequential tests, and procedures to be utilized in the qualification testing of the PAT-1 (Plutonium Air Transportable) package. The object of these tests is to demonstrate and assure that the container will conform to or will surpass the qualification criteria set forth by the U.S. Nuclear Regulatory Commission. Data generated from these tests can be evaluated for certification and licensing purposes for the package.

This test program has been formulated to the requirements stipulated in the NRC Qualification Criteria for Plutonium Package Certification, NUREG 360, and Code of Federal Regulations, Title 10, Part 71, dated January 1, 1976.

I. Package Preparation

A. Contents

Surrogate material for plutonium-oxide cargo will be utilized; this surrogate is natural UO_2 sinterable powder, provided by Eldorado Nuclear Ltd., Port Hope, Ontario, Canada, Specification ENL-1, Issue 5. The particle size distribution and the dry process performance of this powder makes it an excellent surrogate for evaluating a potential plutonium-oxide powder leak. 1.0 kg to 1.5 kg of UO_2 will be in each PAT-1, representing the maximum practical quantity which can be accommodated within the space available.

B. PC-1 Inner Sealed Vessel

1. 19.3 g of water will be added to the UO_2 fuel inside the PC-1's used in the 10 CFR 71 tests. This amount of water models the maximum moisture content of the PuO_2 contents (0.5 w/o water) and accounts for internal pressure generated by the decay heat from plutonium-oxide fuel (analysis provided in Chapter 3). For the packages used in testing to the NRC Qualification Criteria, this water need not be added to the UO_2 contents but must be added within the TB-1.

1567 174

2. The UO_2 powder will be wrapped and taped in two plastic bags, and will then be canned in a stainless-steel product can (PC-1) with a rounded bottom replacing a commercial No. 2-1/2 product can. In addition to can crimping, the can will be sealed with an application of room-temperature curing, impact-resistant rubber-modified epoxy sealant. This sealed can is the inner sealed vessel, meeting the containment requirements of 10 CFR 71. A2 (for 10 CFR 71 tests only). For the packages used in testing to the NRC qualification criteria, a prototype stainless steel produce can (without rounded bottom) may be utilized (if PC-1 is unavailable). Safety throughout the NRC qualification criteria testing is not based on the structural integrity of the product can.
3. Swipe tests for total uranium will be performed to verify the absence of UO_2 material on the can exterior prior to commencement of the tests. Fluorimeter analysis sensitive to 10^{-8} g uranium will be utilized.
4. Appropriate markings and radioactive material stickers will be affixed to the PC-1 vessel.

C. TB-1 (Outer Sealed) Containment Vessel

1. The inner sealed vessel, PC-1, with UO_2 contents and the aluminum honeycomb spacer will be placed in the body of the TB vessel.
2. The copper gasket will be correctly installed on the lid.
3. A Viton O-ring, properly lubricated with silicone grease, will be placed in the lid O-ring groove.
4. Remaining free-air space within the TB-1 vessel and lid, principally air space within the honeycomb filler, will be flooded with helium gas.
5. The TB-1 lid and vessel will be mated in such a manner as to entrap the helium gas. The lid will be attached to the body with the twelve 1/2-20 stainless-steel, silver-plated, socket head cap screws, first with all 12 screws hand-tightened, then torqued to 50 ft-lbs in a crisscross pattern, and then to 75 ft-lbs in a crisscross pattern.
6. A helium leak rate test will be performed, using a mass spectrometer with 10^{-10} cm^3/s sensitivity.
7. The nylon lifting strap will be bolted to the lid.
8. Appropriate markings and radioactive material stickers will be affixed to the TB-1 vessel.

D. AQ-1 (Air Qualified) Overpack Assembly.

1. The TB-1 vessel will be fully seated in the AQ-1.
2. The inner removable redwood plug will be seated on top of the TB-1.
3. The removable disc load spreader will be positioned.
4. The outer removable redwood plug will be seated.
5. The inner cover will be installed, aligning the 23-hole pattern with the hole pattern in the outer drum.
6. The 14-in. diameter insulation pad will be positioned on top of the inner cover.
7. The outer cover will be installed, aligning the 23-hole pattern.
8. The skirted clamp ring will be mated, aligning the 23-hole pattern.
9. The twenty-three 3/8-24 bolts will be installed, torquing sufficiently to completely install each bolt.
10. The clamp ring bolt and nut will be installed, tightening both the bolt and the nut, independently and separately. The nut may be placed between the forged ring lugs, tightened against either lug.
11. The 1-in. diameter Caplug will be installed in the lid vent hole.

E. PAT-1 (Plutonium Air Transportable) Package Assembly

1. Appropriate stenciling, labeling, and radioactive contents warning stickers will be affixed to the PAT-1. The contents, TB-1 serial number, AQ-1 serial number, and PAT-1 serial number will appear. Total weight of the PAT-1 will be recorded.
2. Towing hardware for the Sandia Laboratories rocket pulldown test will be affixed to the PAT-1 assembly, as appropriate for the planned impact test.

II. Test Plan -- Packages for NRC Criteria Testing

A. General

Five PAT packages, selected from a group of 16 packages of similar construction (identical models), will comprise the qualification test group.

B. Sequential Tests

1. Impact or Crash Test

- a. 250 knots (422 ft/s; 129 m/s) minimum velocity at impact; will be measured by redundant photometrics.

1567 176

- b. Unyielding target used for all crash tests:
526,000 lb (2.4×10^5 kg mass; 3000 psi (20.7 MPa) concrete, with extensive steel reinforcement, approximately 20 ft (6 m) diam by 11.5 ft (3.5 m) thick, faced with a 10-x 10-ft (3- by 3-m) sheet of battleship armor plate, 3 to 5 inches (7.6 to 12.7 cm) thick, 4 inch (10.1 cm) thick at center. Steel facing is welded to reinforcing members which are embedded in concrete; steel facing is grouted to concrete plug with 12,000 psi (82.7 MPa) expanding metal-filings-filled grout.
 - c. The velocity vector of package motion will be perpendicular to the face of the unyielding target.
 - d. Crash attitudes:
 - (1) Top end PAT-1 impact (defined as 0 degrees attitude)
 - (2) Top corner PAT-1 impact (defined as 30 degrees attitude)
 - (3) Side PAT-1 impact (defined as 90 degrees attitude)
 - (4) Bottom corner PAT-1 impact (defined as 150 degrees attitude)
 - (5) Bottom end PAT-1 impact (defined as 180 degrees attitude)
 Attitude at impact will be measured by redundant photometrics. Attitude will be controlled to within ± 10 degrees.
 - e. The Sandia Laboratories Coyote Test Field rocket pulldown cable test site will be utilized.
 - f. Radiographs will be taken of crashed PAT-1 to locate position of TB-1 with respect to exterior of AQ-1 as a reference for setup of the crush and puncture tests.
2. Static Crush Test
- a. Load will be 70,000 lb (3.1×10^5 N).
 - b. Impact-tested PAT-1 package will be placed at rest on an unyielding surface (steel bed of static test machine), resting on a principal remaining (postcrash) surface.
 - c. Load will be applied perpendicular to unyielding surface through a 2-inch (5-cm) wide mild steel bar, 7-inch (18-cm) deep, longer than contact surface coinciding with PAT-1.
 - d. Loading point of contact will be chosen as most threatening to inner TB-1 vessel (point of minimum dimension of redwood between TB-1 and AQ-1).
 - e. A Tinius-Olsen static test machine will be utilized.
3. Puncture Test
- a. A blunt steel spike will be dropped 10 ft (3 m) onto the crashed and crushed PAT-1 package at the point of contact chosen to be most threatening to the inner TB-1 vessel (point of minimum dimension of redwood between TB-1 and AQ-1).

- b. Mild steel spike will be the shape of the frustum of a right-circular cone, 12 inch (30.5 cm) long, 8 inch (20 cm) diam at the base and 1 inch (2.5 cm) diam at the tip or puncture contact point.
- c. Spike will weigh 500 lb (227 kg) minimum.
- d. The PAT-1 package will rest on an essentially unyielding surface.
- e. A drop-tower crosshead with an explosive cable-cutter release will be utilized to drop the spike onto the package. The Sandia Laboratories Area III 185-ft tower will be utilized.

4. Slash Test

- a. The PAT-1 package is to be firmly restrained and supported in tamped earth such that its longitudinal axis is inclined approximately 45° to the horizontal. The area of the package which made first contact with the impact surface in the crash test is to be in the lowermost position.
- b. The slash projectile will be a structural-steel angle beam at least 6 ft in length with equal legs at least 5-inches long, 0.5 inch thick, and 90° apart. The angle beam ends are perpendicular to the longitudinal axis of the member, providing a relatively sharp three-axis 90° corner for slashing the PAT-1 package. The corner of the angle formed by the intersection of the two legs is to strike the PAT-1 package first, with the 90° angle between the legs approximately evenly bisecting the PAT-1 package longitudinal axis.
- c. The package is to be struck at approximately the center of its vertical projection by the end of the structural-steel angle beam falling from a height of at least 150 ft. The angle beam is to be guided in such a way as to fall end-on, without tumbling.
- d. After one slash test, the PAT-1 package is to be rotated approximately 90° about its longitudinal axis and struck again by the steel angle beam falling as before.
- e. The Sandia Laboratories Area III 300-ft tower will be utilized with a guided drop carriage and photometric instrumentation.

5. Thermal Exposure or Fire Test

- a. JP-4 aviation fuel will be combusted as the heat source.
- b. The burn pit is approximately a 10 ft (3 m) diam steel tub, 6 ft (2 m) deep, set 6 ft (2 m) into the ground. The steel tub has minimum free-board above the ground surface level. The JP-4 will be floated on water to permit flame surface height adjustment.
- c. A chimney, approximately 16 ft (5 m) diam and 10 ft (3 m) tall, fabricated from 1 inch (2.5 cm) thick mild steel plate, is centered over the burn pit. The chimney is suspended on wire ropes and can be lifted to provide draft for the fire.

- d. A 4 ft (1.2 m) high, noncombustible fence is situated about 3 ft (1 m) away from the draft opening (all around the chimney) to lessen the effects of surface wind on flame characteristics when the chimney is lifted for additional draft.
 - e. A stainless-steel stand is situated in the center of the tub, holding the PAT packages approximately 3 ft (1 m) above the JP-4 fuel surface. The stand is lightly constructed and offers no interference with incident heat input to the PAT.
 - f. The water level, the JP-4 fuel level, and the chimney draft are preset to maintain a minimum temperature of 1283 K (1850^oF; 1010^oC) at the median height of a crashed, crushed, punctured, and slashed PAT-1 package, or to maintain the highest possible temperature at the level of the PAT-1 if 1283 K cannot be attained under the particular conditions of a given test (ambient surface winds have greatest effect).
 - g. The PAT-1 packages will be oriented on the stand so the point chosen to be most threatening to the inner TB-1 vessel will face down toward the burning JP-4 fuel.
 - h. A 60-minute minimum supply of fuel will be ignited. Facility warmup time, to achieve 1850^oF (1010^oC) minimum, will not be counted.
 - i. Flame temperature will be measured by thermocouples at levels below, even with, and above the PAT-1. Thermocouples will be attached to the external drum of the PAT-1 to measure surface temperatures. A time versus temperature record will be made from each thermocouple.
 - j. The PAT-1 package will not be artificially cooled (no attempt to extinguish a possible lingering fire within the PAT-1) after the 1 hr burn test. (The package is to cool enough for the bare hand to remain upon it.)
6. Water Immersion Test
- The crashed, crushed, punctured, slashed, and burned PAT-1 package will be immersed in 3 ft (0.9 m) of water (minimum depth to any point on the PAT) for a minimum of 8 hr.
7. Containment Acceptance Test Measurements
- a. The TB-1 vessel will be extracted from the crashed, crushed, punctured, slashed, burned, and immersed PAT-1 package. The TB-1 exterior will be monitored for uranium material release or contamination, using a fluorimeter sensitive to 10⁻⁸ gm uranium.
 - b. A mass spectrometer helium leak-rate test will be conducted on the TB-1 vessel. Leak-rate results will be converted to cm³/s air-leak rate.

C. Individual (Nonsequential) Test: Hydrostatic Pressure

One TB-1 vessel with a clean and dry interior will be randomly selected and assembled in accordance with I.C. 2 through 6 and will be subjected to 600 psi (4.1 MPa) hydrostatic water pressure for 8 hr minimum. The TB-1 interior will then be examined for water. A hydrostatic test vessel will be utilized.

III. 10 CFR 71 Tests

A. General

1. Test Sequence

Although the 10 CFR 71 normal conditions of transport are not required to be sequentially cumulative, they will be applied in sequence on one PAT-1, as described below.

2. Hardware Selection

One PAT-1 package, including surrogate UO_2 contents, a PC-1 sealed product can, a sealed TB-1 containment vessel, an AQ-1 overpack, prepared as described in Part I Package Preparation (above) will be randomly selected for testing in accordance with 10 CFR 71 normal conditions for transport.
with 10 CFR 71 normal conditons for transport.

B. 10 CFR 71 Normal Conditions for Transport

1. Heat

The high-temperature exposure test will be satisfied by a 367 K (200^oF) exposure of PAT-1 for 48 hr (130^oF ambient plus 70^oF addition to account for solar radiation and 25-W decay heat load equals 200^oF); thermal equilibrium occurs in less than 24 hr; 48 hr gives added assurance of reaching thermal equilibrium.

2. Cold

233 K (-40^oF) exposure of PAT-1 for 48 hr (no allowance is taken for internal decay heat contribution).

3. Pressure

a. The separate TB-1 vessel will be removed from the AQ-1 and will be heated to 397 K (225^oF; 124^oC) for 8 hr, and then helium leak rate checked while hot to demonstrate compliance with the 1.5 times maximum normal operating pressure test of 10 CFR 71.53. Chapter 3 includes the analysis that demonstrates that 255^oF produces an internal TB-1 pressure 1.5 times the maximum normal operating pressure.

1567 180

b. The TB-1 vessel will be allowed to cool to ambient temperature and then again be helium leak rate tested. The helium leak-rate tests are conducted in a vacuum vessel, hence the 10 CFR 71 test of 0.5-ATM exposure is satisfied repeatedly.

4. Vibration

The TB-1 and AQ-1 will be reassembled into a PAT-1 configuration in accordance with the earlier described procedure. A comprehensive transportation vibration spectrum exposure of PAT-1 will then be conducted:

0.2 g²/Hz 30-150 Hz

6 dB/octave rolloff 150-2000 Hz

8 hr duration - longitudinal axis

8 hr duration - vertical axis

5. Water Spray

30-minute exposure per 10 CFR 71.

6. Free Drop

Since PAT-1, loaded, will weigh less than 500 lb, PAT-1 will be dropped 4 ft (1.2 m) per 10 CFR 71. Five principal drop attitudes (top, top corner, side, bottom corner, bottom) will be tested. The first of these drops will follow the water spray test by less than 2 hr.

7. Penetration

40-inch (1-m) drop of 13-lb (5.9 kg) rounded spike per 10 CFR 71, onto the most vulnerable point of PAT-1 package.

8. Compression

2500 lb (1138 kg) minimum, 24 hr compression load on ends and side of PAT-1 package, per 10 CFR 71.

9. Containment Acceptance Test Measurements

Acceptance tests of the PAT-1 package following the 10 CFR 71 normal condition tests described above will be in accordance with II. B. 7. a. and b. above (uranium release monitoring and leak rate testing of TB-1 vessel), and also uranium monitoring of the inner sealed vessel (PC-1) by swipe test. After disassembly, the interior of the TB-1 will be monitored for uranium by swipe testing. Swipe tests will have 10⁻⁸ g U sensitivity.

C. 10 CFR 71 Standards for Hypothetical Accidents

1. General

One PAT-1 package, with surrogate UO_2 contents and the containment of the PC-1 sealed inner vessel and the sealed TB-1 containment vessel, and with the assembly of the AQ-1 and PAT-1 as described in Item I above, will be randomly selected for sequential testing in accordance with 10 CFR 71 hypothetical accident conditions.

2. Free Drop

30-ft (9.1-m) freefall onto unyielding target, side of PAT-1 package (most vulnerable attitude), then onto top, top corner, bottom corner, and bottom.

3. Puncture

- a. Crashed and PAT-1 package will be dropped 40 inches (1 m), impacting a blunt steel spike at the point of contact chosen to be most threatening to the inner TB-1 vessel (point of minimum dimension of redwood between TB-1 and AQ-1 outer surface).
- b. Blunt steel spike will be 6-inch (15-cm) diam, 0.25-inch (0.6-cm) corner radius, 10-inches (25.4-cm) minimum length.
- c. Spike will be supported on a large reinforced concrete mass.
- d. A crane, support cable, and explosive cable cutter release will be utilized to drop the package onto the spike.

4. Thermal

1075 K (1475^oF) or greater, 30 minutes or greater, JP-4 jet-fuel fire exposure in facility described in II. B. 5 above. No artificial cooling of PAT-1 for at least 3 hr after the 30-minute exposure (natural extinguishment permitted).

5. Water Immersion

3-ft (0.9 m), 8-hr minimum exposure per II. B. 6 above.

6. Containment Acceptance Test Measurements

Acceptance of the PAT-1 package following the 10 CFR 71 accident condition tests described above will be in accordance with II. B. 7. a and b above (uranium-release monitoring and leak-rate testing of TB-1 vessel), plus uranium-release monitoring of the inner sealed vessel (PC-1 product can) and of the TB-1 vessel interior by swipe test. Swipe tests will have 10^{-8} g-U sensitivity.

IV. Contingency PAT-1 Packages

PAT-1 packages will be available for replacement tests, if required. A possible cause would be undertest or test apparatus failure in the rocket pull-down crash testing, requiring replacement of one or more PAT-1 packages to achieve an acceptable crash (impact) velocity and attitude. Another possible cause would be an underperforming burn test.

V. Substantiating Analyses or Tests

- A. Aerodynamic calculations of a PAT-1 package freefall from the most severe possible high-altitude high-speed transport aircraft accident showed that the terminal velocity is lower than the 250-knot (129 m/s) crash velocity used in the crash testing onto the unyielding target.
- B. Results of development testing of PAT-1 package impacts at low-temperature and high-temperature extremes are presented in Chapter 2 to show compliance with these conditions.
- C. The TB-1 vessel was subjected to a thermal environment which resulted in a vessel temperature and internal pressure that equaled or exceeded the maximum temperature and pressure the vessel experienced in the fire test that was a part of the sequential test series. The TB-1 vessel did not rupture or open in any manner.

VI. Data

Data from the above described tests will consist primarily of the following:

- A. Pretest quality control inspection data or manufacturer's certification on the PAT-1, AQ-1, TB-1, and PC-1 assemblies, including leak-rate test data on the TB-1 vessel before environmental testing.
- B. Photometric data of the impact tests (velocity and attitude).
- C. Postimpact radiographs of PAT-1 showing location of TB-1 with respect to AQ-1.
- D. Laboratory test reports (observed measurements of the crush, puncture, slash, and hydrostatic tests).

- E. Thermocouple data as described herein for the burn (fire) tests.
- F. Health physics swipe test results of TB-1 and PC-1 as required for radiological and uranium (chemistry) monitoring, 10^{-8} g-U sensitivity.
- G. Laboratory standard leak-rate reports of mass spectrometer helium leak-rate testing of TB-1 vessel, converted to air standard, after environmental test sequences.
- H. Posttest observables on TB-1 copper and O-ring seals.
- I. Posttest inspection data on the TB-1.
- J. Posttest observables on the PC-1.
- K. Approximate dimensional descriptions of PATs after test series, prior to destructive opening to recover TBs, describing shape and dimensions of exterior and locating internal TB-1 with respect to the exterior.
- L. Photographic (still and motion picture) coverage of major test events; still photos of PAT-1, AQ-1, TB-1, and PC-1 after tests or test series.

APPENDIX 2I

Characterization of Surrogate UO_2

Depleted sinterable UO_2 powder was used in the PAT-1 qualification tests in place of PuO_2 powder. The depleted UO_2 powder was supplied by Eldorado Nuclear, Ltd., Port Hope, Ontario, Canada, as specified in ENL-1-Issue 5 Depleted Sinterable UO_2 .

The powder was examined by the Nuclear Materials Division, Savannah River Laboratory (SRL), by agitating it in an isoton solution by ultrasonic means and then taking measurements with both an electron-beam microscope and a Coulter counter.

Eldorado reported the bulk density to be $1.00 \pm 0.25 \text{ g/c}^3$ per ASTM-B329 (the 40,000 psi sintered density would be 5 to 6 g/c^3). SRL reported the particle size as:

3.01 μ median

5.59 μ mean

52.74% of population < 1 micron

5.65% of volume < 1 micron

For comparison purposes, SRL reports the following for an oxalate precipitation 239 PuO_2 (direct strike); low (small particle) data group of four measured samples:

28.06 μ median

29.14 μ mean

No particles < 6 μ .

The above data shows that the UO_2 examined was much finer than a certain PuO_2 powder; the PuO_2 powder was typically "briquette-like or straw-like,"¹ whereas the UO_2 powder was more sand-like. Additional information on PuO_2 microstructures may be found in Reference 2, below.

The particle size distribution of the UO_2 used in the PAT-1 qualification tests is given in the following table.

1 Telecon 11/10/77, from James Scarbrough, Savannah River Laboratory Nuclear Materials Divison, to J. A. Andersen, Division 5433, Sandia Laboratories.

2 "Effect of Oxalate Precipitation on PuO_2 Microstructures," 6th International Materials Symposium, Berkeley, California, August 24-27, 1976.

Table 2I-1

Particle Size Distribution of Depleted UO_2 Powder, PAT-1

<u>μ Range</u>	<u>Volume %</u>	<u>Population %</u>
0.63 - 0.79	2.60	33.23
0.79 - 1.00	3.05	19.51
1.00 - 1.26	5.77	18.42
1.26 - 1.59	7.24	11.56
1.59 - 2.00	10.41	8.31
2.00 - 2.52	12.50	5.00
2.52 - 3.17	11.03	2.20
3.17 - 4.00	10.75	1.07
4.00 - 5.04	9.45	0.47
5.04 - 6.35	6.22	0.16
6.35 - 8.00	4.07	0.05
8.00 - 10.08	2.88	0.02
10.08 - 12.7	2.94	0.009
12.70 - 16.00	3.28	0.005
16.00 - 20.16	2.43	0.001
20.16 - 25.40	1.70	0.0006
25.40 - 32.00	2.55	0.0005
32.00 - 40.32	0.0	0.0005
40.32 - 50.80	1.13	-----
	100.00	100.01615

APPENDIX 2J

Test Facility Descriptions

2J.1 Rocket Pulldown Cable Facility

The rocket pulldown cable facility used to accomplish package impact tests consists of a tensioned aerial cable suspended over a canyon between two ridges, a carriage which can be hoisted from a ground-based target up to the aerial cable, an unyielding target, a monorail sled track, a rocket-propelled sled, and control and instrumentation capabilities. The general arrangement is shown in Figures 2J-1 and -2. The PAT-1 package is suspended at a height of approximately 185 ft (56 m) perpendicular to the unyielding target. Rocket sled tow lines (a continuous wire rope used in a loop so there appears to be two tow lines, one on each side of the PAT-1 package) are attached to the PAT-1 by means of towing fittings (Figure 2J-3, -4, -5, -6, and -7) in such a manner that high-speed towing will be stable and the package will impact in a designated attitude. The towlines route vertically downward from the PAT-1 package and pass through pulleys that straddle the unyielding target; the towlines then route horizontally (approximately) to the rocket sled, where they are firmly attached. The rocket sled uses a variable number of 5-in. HVAR (High-Velocity-Aerial-Rocket) motors that have 5000 lb-s impulse. By a combination of adjusting the package height above the target and varying the number of rockets installed on the sled, the desired impact velocities are attained or exceeded.

Operation is accomplished by a firing sequence involving staged rocket ignition and wire rope cutters. Between first- and second-stage rocket ignition, the package suspension wire rope is cut and towing commences. The tow lines are cut to separate the PAT-1 just prior to impact; this action is triggered by sled passage through a breakwire on the monorail track.

The unyielding target is an extensively reinforced 526,000-lb (2.4×10^5 -kg) mass of concrete, approximately 20 ft (6 m) in diameter and 11.5 ft (3.5 m) deep into prepared (tamped) earth, faced with a 10-ft x 10-ft (3- x 3-m) slab of battleship armor plate, 3 to 5 in. (7.6 to 12.7 cm) thick. The steel facing is welded to the alloy steel-concrete reinforcing members and is grouted to the concrete plug with iron-filings-filled cement grout.

Redundant high-speed photometrics are utilized to measure PAT-1 package impact velocity and attitude and to assure that the 422-fps (129 m/s) impact velocity was achieved or exceeded.

1567 187

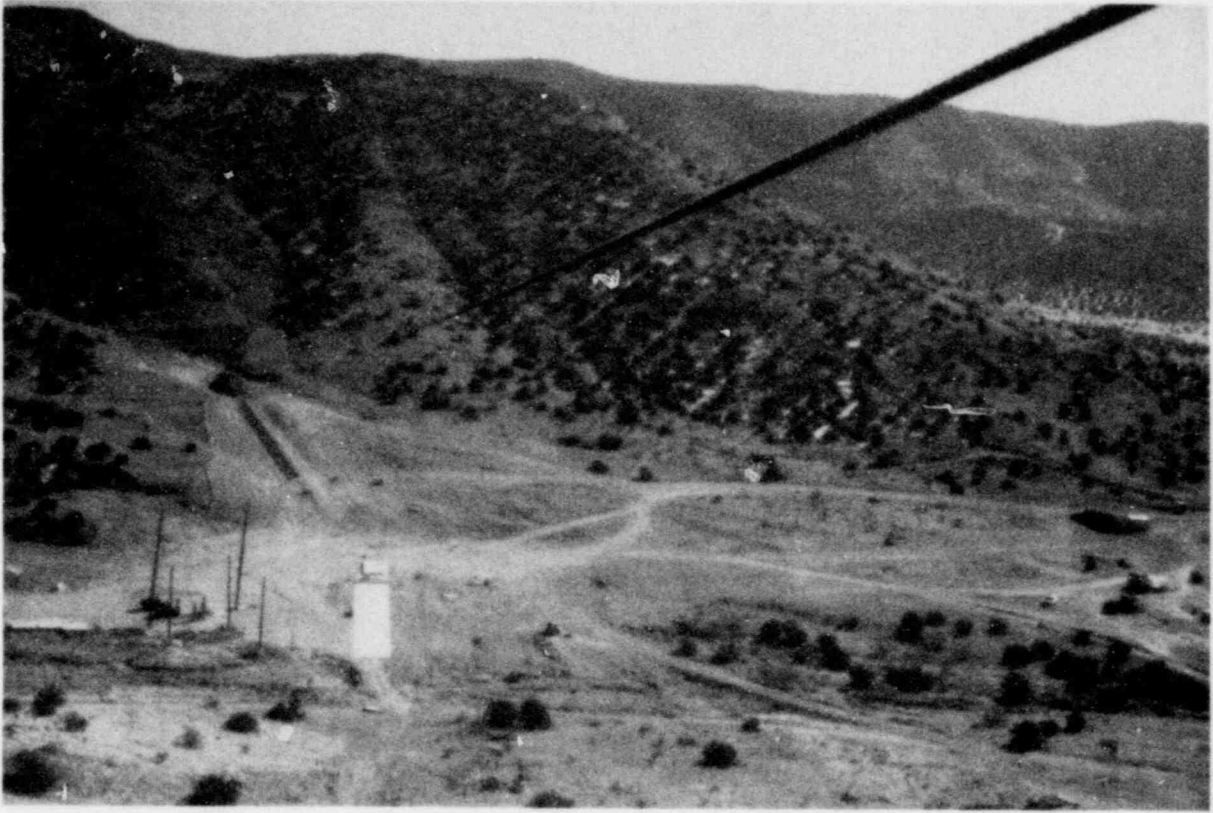


Figure 2J-1. Rocket Pulldown Cable Facility

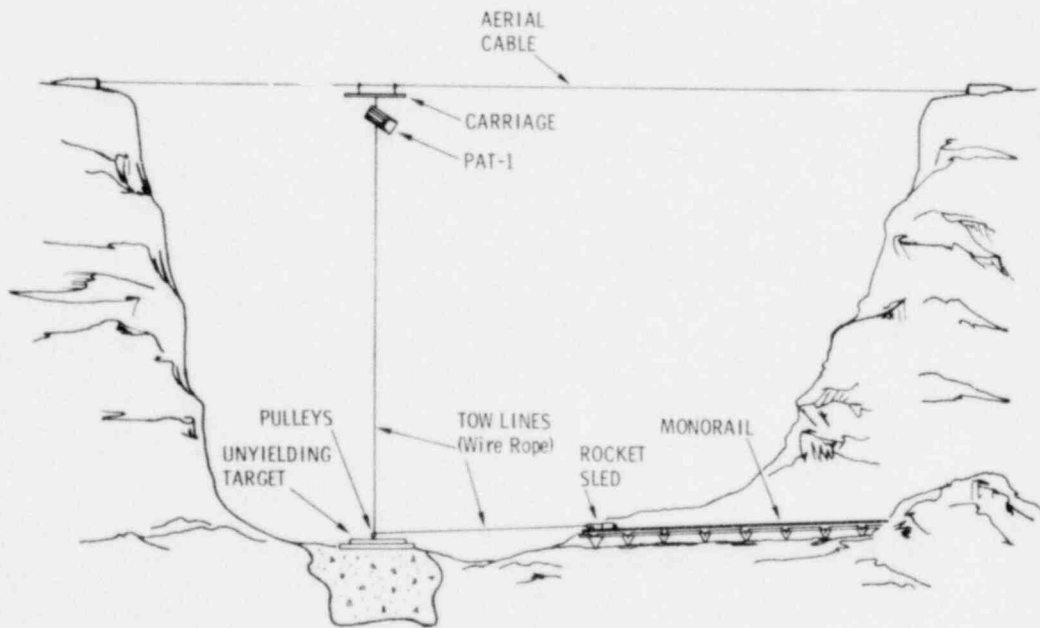


Figure 2J-2. Rocket Pulldown Facility

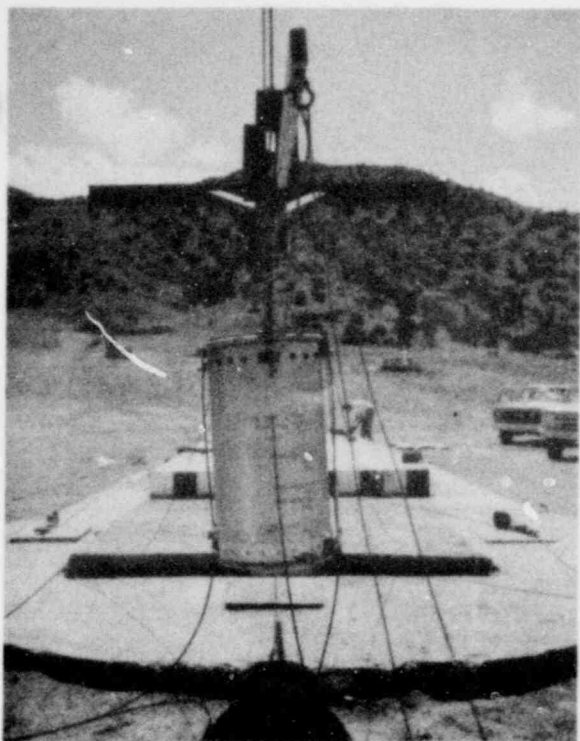


Figure 2J-3. Top (0°) Impact Test

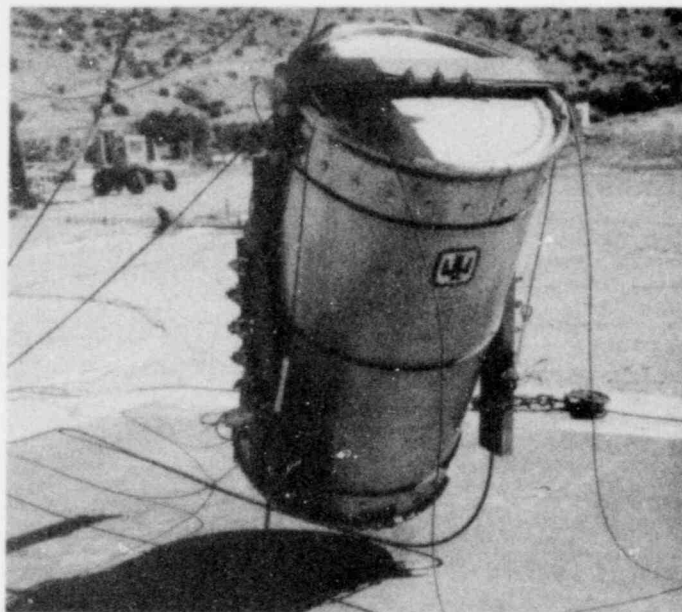


Figure 2J-4. Top Corner (30°) Impact Test

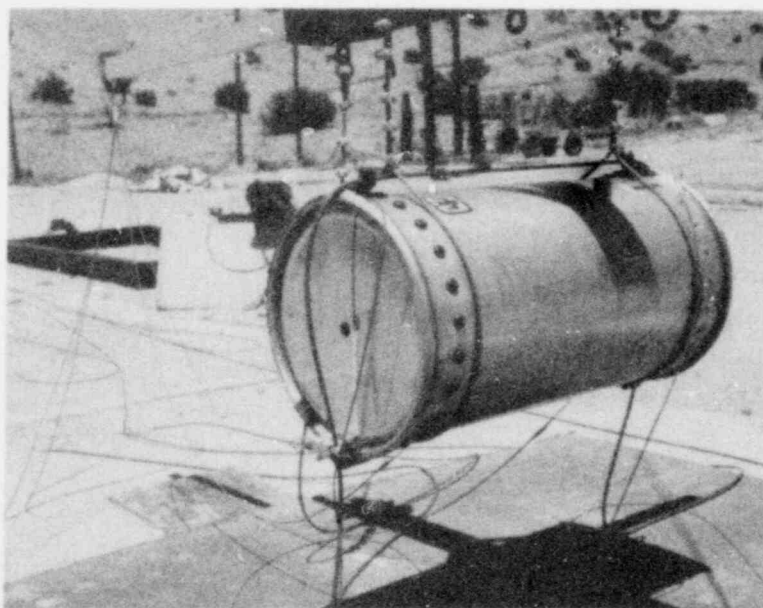


Figure 2J-5. Side (90°) Impact Test

POOR ORIGINAL

1567 189

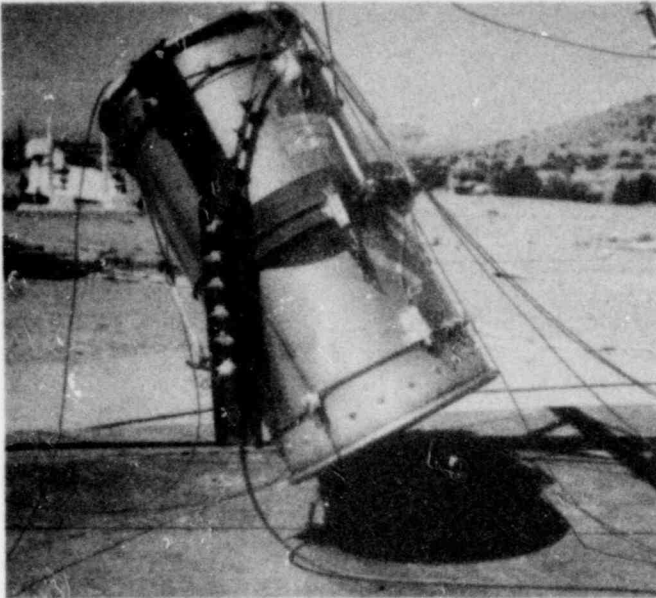


Figure 2J-6. Bottom Corner (150°) Impact Test

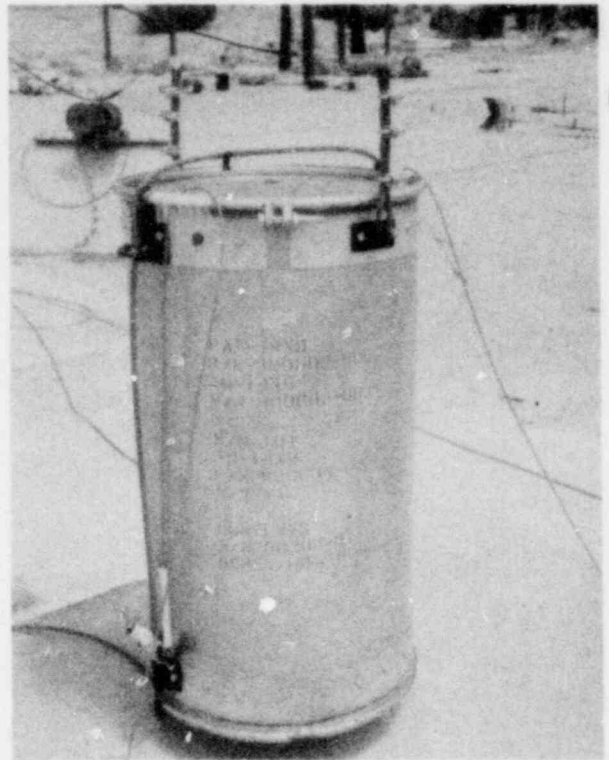


Figure 2J-7. Bottom Corner (180°) Impact Test

2J.2 Static Test Machine

The crush test was accomplished through use of a Tinius Olsen static test machine (Figure 2J-8). Radiographs of the PAT-1 after impact were used to establish that this crush and the subsequent puncture test were performed in a manner to cause maximum package damage (i. e., the distance between the TB-1 containment vessel and the point of applied load were minimized).

2J.3 Drop Tower Facilities

Two drop towers of 185 ft (56 m) and 300 ft (91 m), respectively, were utilized to accomplish the puncture and slashing tests, respectively. Both facilities provided for proper impact location and orientation control of the test probes when impacting the PAT-1 package.

The puncture test involves the dropping of a 500 lb (227 kg) blunt conical probe from a height of 10 ft (3 m) onto a package which is supported on a concrete-backed steel-plate target. A guide tube assured proper impact orientation control of the probe. The PAT-1 package rests on the essentially unyielding support of a massive steel plate and a large block of reinforced concrete. The general arrangement for this test is shown in Figure 2J-9.

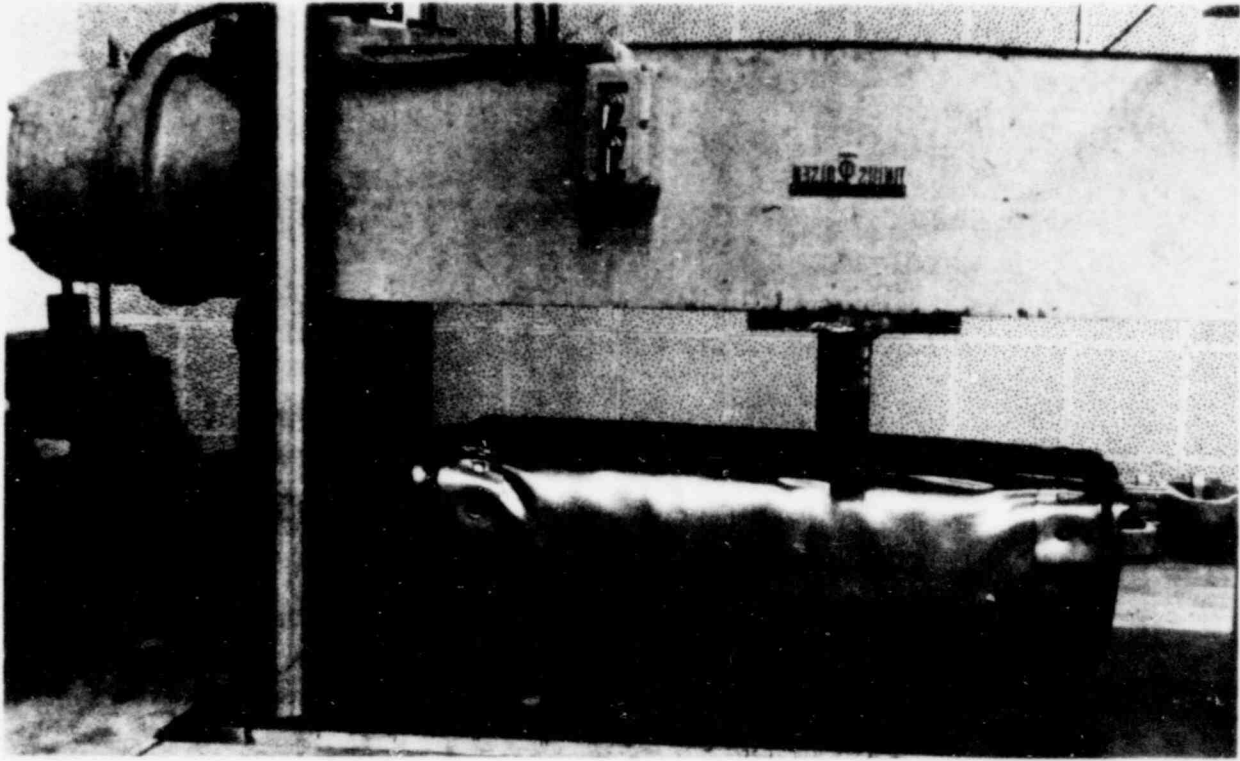


Figure 2J-8. Static Test Machine

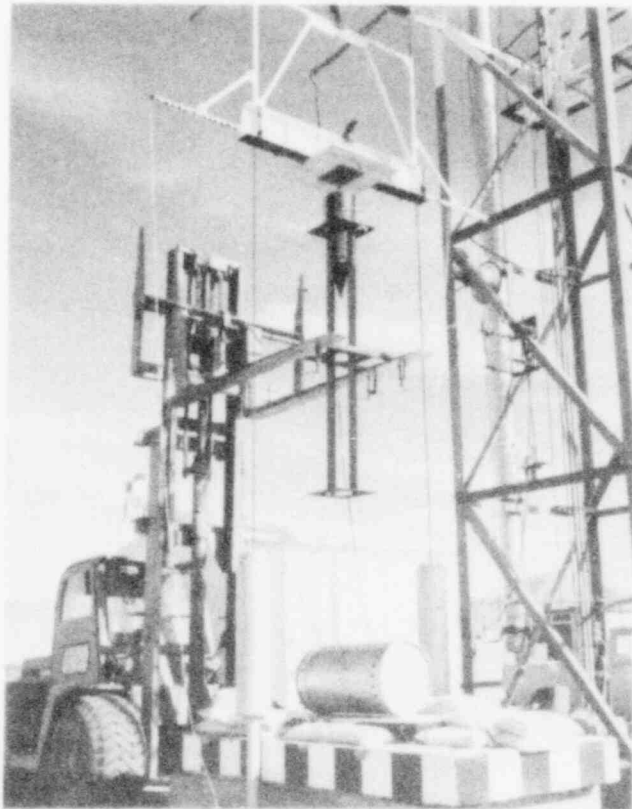


Figure 2J-9. Puncture Test Facility

POOR ORIGINAL

1567 191

The slash test was accomplished by use of a guided carriage on the 300-ft drop tower. The 5-in. leg x 1/2-in. thick x 6-ft long steel angle beam, with squared-off ends, was attached perpendicular to the mounting deck of this guided carriage. The angle beam was oriented so the sharp central corner of the angle impacted the PAT-1 package first, and the 90° angle of the beam approximately bisected a longitudinal plane of the PAT-1. Testing was accomplished by hoisting the carriage with the steel beam to a correct drop height, allowing for friction on the guide wires, and then allowing them to slide down the guide wires toward the PAT-1 package (Figure 2J-10). The steel angle is separated from the carriage just above the PAT-1 package by means of an explosive cable cutter, allowing unrestrained final free-flight into the PAT-1. Impact velocities are determined through photometrics.

2J.4 Fire Test Facility

This facility is described in Chapter 3.

2J.5 Water Immersion Facility

The 10-ft (3-m) diam x 6-ft (1.8-m) deep water tub used to float the JP-4 fuel for the burn test is utilized as the pond for the submersion test. The impacted, crush, punctured, slashed, and burned PAT-1 packages did not require ballast weights to sink to the bottom of the pond.

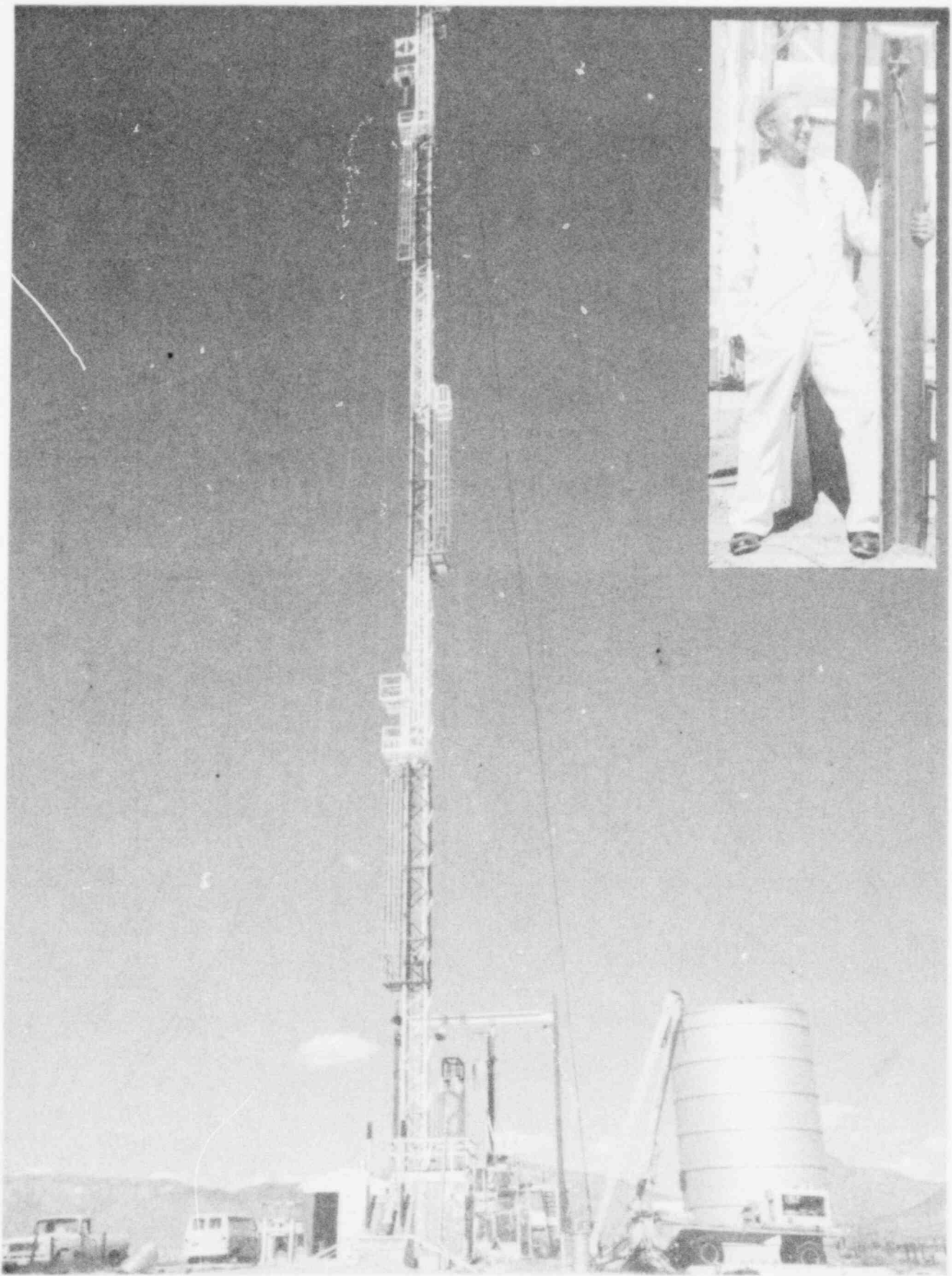


Figure 2J-10. Slash Test Facility

POOR ORIGINAL

1567 193

163-164

CHAPTER 3
THERMAL EVALUATION

3.1 Summary

The PAT-1 package is designed to safely contain its plutonium contents under a variety of normal and accident conditions. This chapter summarizes the thermal evaluations which complement the structural evaluation in Chapter 2 and the containment evaluation in Chapter 4.

The supporting information required for the structural evaluation involved the calculation of extreme PAT-1 package temperatures under specified normal conditions of transport. This information was utilized for four main purposes: (1) to establish the experimental test conditions for the heat test in Chapter 2; (2) to assure that differential thermal expansion of PAT-1 package materials had been properly considered; (3) to assure that the long-term performance of package materials could not significantly degrade over the container's useful life; and (4) to establish test conditions for the pressure test in Chapter 2.

The supporting information required for the containment evaluation involved the assessment of maximum TB-1 containment vessel temperatures and accident environments from which internal containment vessel pressures were calculated. This evaluation of differential pressure across the TB-1 seal was necessary to allow an assessment of maximum credible content leakage to be made for the five PAT-1 packages tested to the NRC Qualification Criteria.

The results of this thermal evaluation under maximum and minimum environmental extremes for normal conditions of transport as specified in 10 CFR 71 Appendix A are shown in Table 3.1-I. The maximum normal operating pressure (MNOP) that will occur within the TB-1 containment vessel is 34.3 psi (236 kPa).

During the sequence of accident environments specified in the NRC qualification criteria, the maximum TB-1 containment vessel temperature and pressure are 1080°F (582°C) and 1253 psi (8.6 MPa), respectively.

1567 194

TABLE 3. 1-1

Summary of PAT-1 Package Temperatures
Normal Operations^o

Location	Maximum (°F)	Minimum (°F)
TB-1 vessel and seals	212	-40
Aluminum load spreader	188	-40
Redwood: Mean	182	-40
Maximum	225	-40
Stainless-steel outer drum:		
Mean	176	-40
Peak	225	-40

Note: Under ambient conditions in the absence of solar heating, the outer drum temperature will exceed ambient by 10°F.

^o As specified by 10 CFR 71, assuming the maximum 25-Watt content decay heat in establishing the maximum temperatures.

3.2 Thermal Properties of Materials

The thermal properties used in this section are shown in Table 3. 2-I, Reference 1.

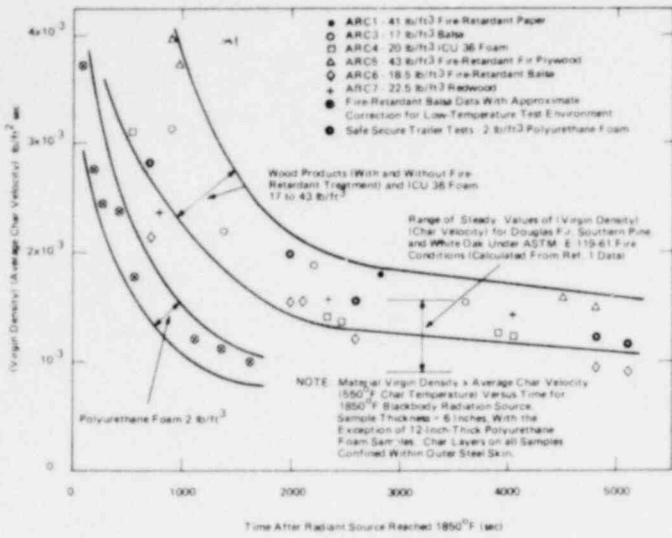
Since the thermal conductivity and specific heat of the redwood assembly are subject to variations due to moisture content and the assembly process (specifically the glued joints), the values stated in Table 3. 2-1 are based on experimental data derived from an actual PAT-1 (AQ-1) assembly (Appendix 3A. 1), and varied slightly from the values given in Reference 2.

TABLE 3. 2-1

Thermal Properties of Materials

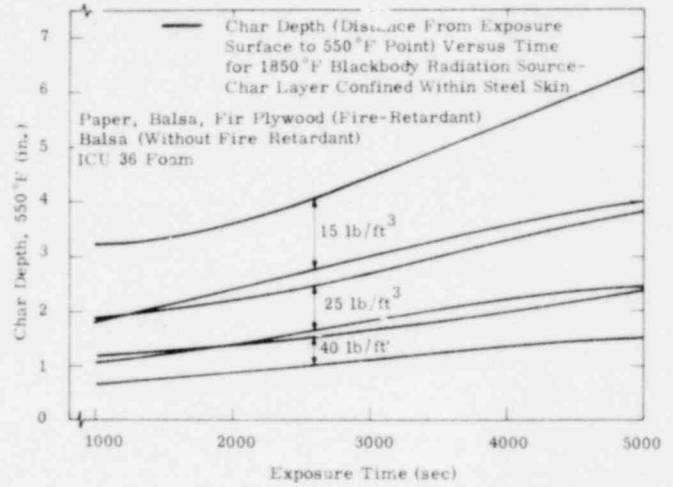
Material	Thermal Conductivity ² k (Btu/hr/ft/°F)	Density ρ (lbm/ft ³)	Specific Heat c (Btu/lbm/°F)	Solar Absorptance/ Emittance α _s /ε
Aluminum honeycomb	N. A.	8.1	0.21	N. A.
Aluminum	90.0	169.0	0.21	N. A.
ETP copper	220.0	558.0	0.09	N. A.
Stainless steel	10.0	500.0	0.11	0.45/0.2 @ 200°F
UO ₂	N. A.	N. A.	0.08	N. A.
Redwood:				
Parallel to grain	0.14(1+0.006T(°F))			
Perpendicular to grain	0.05(1+0.006T(°F))	22.0	0.19(1+0.01T(°F))	N. A.

To assess the thermal protection provided by the redwood under the specified accident environments, reliance was placed on the charring data shown in Figure 3. 2-1.³ The experimental evidence from the five packages subjected to the performance tests of the NRC qualification criteria indicates that an analysis utilizing this data does predict TB-1 temperatures typical of the temperatures actually experienced in the tests.



a. Char Velocity for Various Materials

b. Char Depth vs Time for Charring Materials



c. Char Depth vs Density

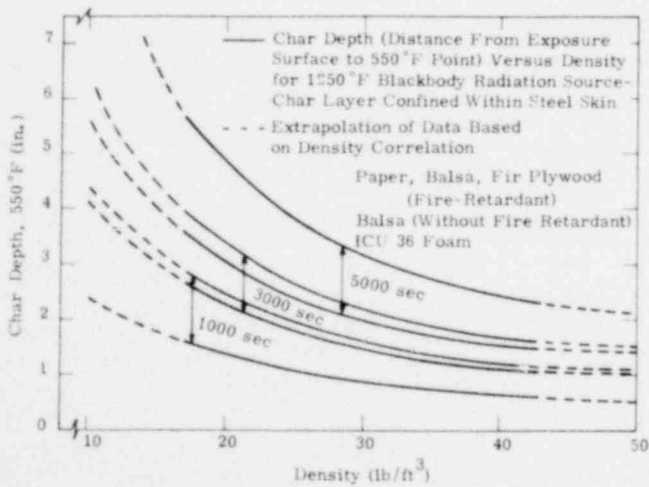


Figure 3.2-1. Charring Data from Reference 3

3.3 Technical Specifications

PAT-1 package detailed specifications are supplied in the drawing and product specification set in an appendix to Chapter 9.

3.4 Thermal Evaluation for Normal Conditions of Transport

Two models were utilized in the thermal evaluation: a simplified steady-state model and a finite difference numerical model. The steady-state model assumed solar heating as a constant value while the finite difference numerical model illustrated in Figure 3.4-1 considers the daily thermal cycle of a PAT-1 package [130°F (54°C) ambient temperature with 16-hr exposure to direct sunlight]. To establish basic input data for both models, a thermal test reported in Appendix 3A.1 was conducted to determine the thermal resistance of PAT-1 components along the heat path from the TB-1 containment vessel, through the copper heat-conducting tube, aluminum load-spreader tube and discs, then through the redwood to the outside stainless-steel drum. A schematic diagram of this heat path is shown in Figure 3.4-2. The thermal resistances determined through this experiment are shown in Table 3.4-I.

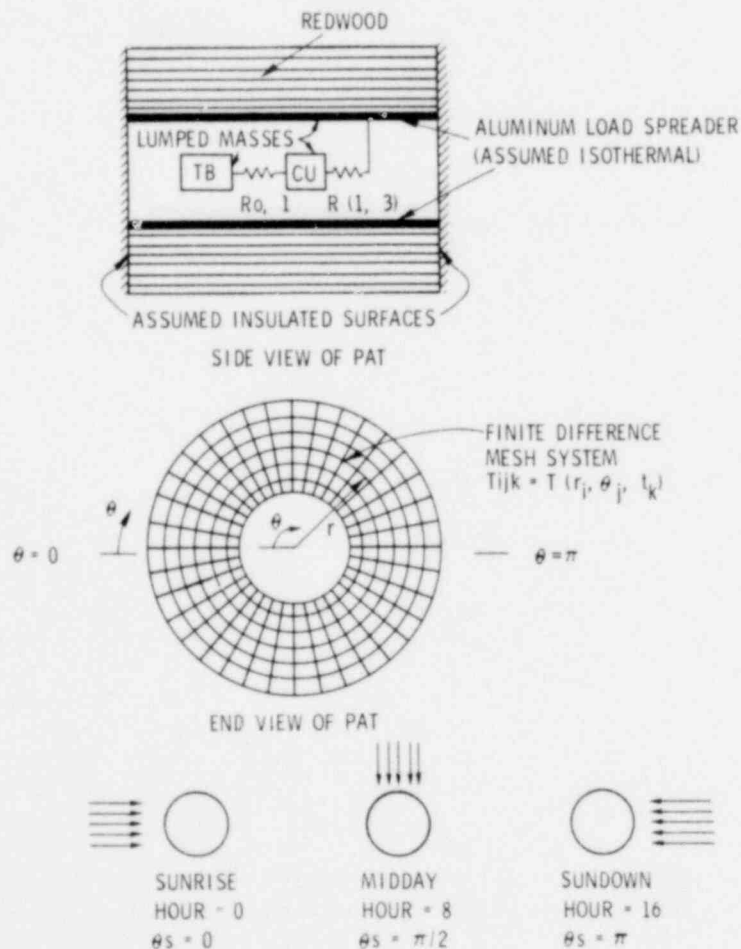
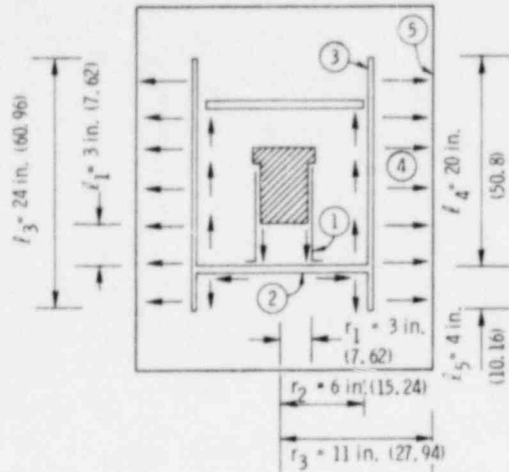


Figure 3.4-1. Schematic of Numerical Model Used to Assess Solar Heating



- 1 COPPER CYLINDER: $k_C = 220 \text{ (0.91)}$ $\delta = \text{THICKNESS INCHES (cm)}$
 $\delta = 0.25 \text{ (0.63)}$ $k = \text{CONDUCTIVITY}$ $\frac{\text{Btu}}{\text{hr/ft}^2\text{F}}$ $\left(\frac{\text{cal}}{\text{cm/s}^2\text{C}} \right)$
- 2 ALUMINUM PLATE: $k_A = 90 \text{ (0.37)}$
 $\delta = 1 \text{ in. (2.54)}$
- 3 ALUMINUM TUBE: $k_A = 90 \text{ (0.37)}$
 $\delta = 0.5 \text{ in. (1.27)}$
- 4 REDWOOD LINER: $k_W = 0.31 @ 200^\circ\text{F} \text{ (0.0013)}$
- 5 STAINLESS WALL: $k_S = 10 \text{ (0.04)}$

Figure 3.4-2. Schematic of Internal Heat Flow Path

TABLE 3.4-1

Experimentally Determined Thermal Resistances

Location	Thermal Resistance
TB-1 vessel and copper heat tube $R_{0,1}$	0.56°F/W
Copper heat tube and Al tube load spreader, $R_{1,3}$	0.36°F/W
Axial resistance in copper sleeve, R_1	0.1°F/W
Radial resistance in lower aluminum plate, R_2	0.05°F/W
Axial resistance in aluminum tube, R_3	0.19°F/W
Contact resistance Cu/Al and Al/Al joints, $R_{1,2} + R_{2,3}$	0.02°F/W
Through Redwood Liner (varies slightly with T), R_4	0.5°F/W
From TB-1 to outside surface, R_{TOT}	<u>1.4°F/W</u>

1567 198

3.4.1 Thermal Models

3.4.1.1 Steady-State Model

The outer wall temperature of the PAT-1 depends upon the external environment. A steady-state heat balance on the stainless-steel surface can be written as follows

$$Q + q_s \alpha_s A_s = \bar{h} A_c (T_s - T_\infty) \quad (1)$$

where Q is the decay heat; q_s is the incident solar flux; α_s is solar absorptivity; A_s is the area of the container projected normal to the solar flux; and A_c is the total surface area for convective and radiative exchange with the local surroundings.

The surface heat transfer coefficient \bar{h} includes both radiation and convection

$$\bar{h} = h_r + h_c \quad (2)$$

Data correlations for natural convection⁴ give the mean surface Nusselt number as a function of Grashoff and Prandtl Numbers

$$Nu = f(Pr, Gr) \quad (3)$$

where $Nu = h_c L/k$, L is a characteristic length (diameter), and k is the conductivity of air. Using properties of air at 130°F (54°C) and the package diameter of $D = 22$ in. (56 cm), the convection coefficient is found to be

$$h_c \simeq .08 (T_s - T_\infty)^{.25} \text{ (W/ft}^2\text{/}^\circ\text{F)} \quad (4)$$

where the fourth root dependence on temperature difference arises through the Grashoff number. The radiative heat-transfer coefficient h_r is defined as

$$h_r = q_r'' / \Delta T \quad (5)$$

where q_r'' is the net radiant heat flux as given by

$$q_r'' = \mathcal{E} \sigma (T_s^4 - T_\infty^4) \quad (6)$$

in which $\mathcal{E} \simeq 0.2$ is the mean surface emissivity (and absorptivity) in the long wavelength range and $\sigma = .1714 \times 10^{-8}$ (Btu/hr/ft²/°R⁴) is the Stefan-Boltzman constant. Combining the above equations (5) and (6), denoting $T_s = T_\infty + \delta$ and noting that $T_\infty \gg \delta$ for the conditions being considered here, the radiative heat transfer coefficient becomes, to the first order

$$h_r \cong 4 \epsilon \sigma T_\infty^3 = 0.08 \text{ (W/ft}^2/\text{°F)}$$

or

$$= 1.55 \text{ W/m}^2 \cdot \text{k} \quad (7)$$

There are two different environments of interest: (a) interior storage (building or vehicle) or external storage in shade, and (b) external exposure, which includes solar heating. In either case, the most severe conditions are encountered in hot, dry climates.

- a. Interior storage (building or vehicle) or external storage in shade: for interior storage or external storage in the shade, direct solar heating is absent. The surface area from Figure 3.4-2 for convective and radiative heat transfer to the surroundings is at least

$$A_c = 2\pi r_3 r_3 = 11.5 \text{ ft}^2$$

or

$$= 1.07 \text{ m}^2 \quad (8)$$

Thus, using Equations (1), (4), and (7), it was found that the temperature difference should not exceed

$$T_s - T_\infty = 10^\circ\text{F}$$

or

$$= -12^\circ\text{C} \quad (9)$$

Since the maximum air temperatures in storage are in the neighborhood of 150°F (66°C),⁵ the maximum temperature on the PAT-1 surface is:

$$T_s < 160^\circ\text{F}$$

or

$$< 71^\circ\text{C} \quad (10)$$

and the assumption used in deriving Equation (7) is verified since $\delta \cong 10^\circ\text{R}$ and $T_\infty \cong 610^\circ\text{R}$.

1567 200

If stored in an external 100°F (38°C) ambient environment:

$$T_s < 110^\circ\text{F}$$

or

$$< 43^\circ\text{C}$$

- b. External exposure which includes solar heating: when solar heating is present, the external surface of the PAT-1 may deviate significantly from the isothermal condition implied in Equation (1). Nevertheless, the average surface temperature \bar{T}_s can still be estimated. The most severe attitude occurs when the sun impinges directly on the cylindrical side of the package. An upper bound on \bar{T}_s can therefore be obtained by taking

$$A_c = 2\pi l_3 r_3 = 11.5 \text{ ft}^2$$

or

$$= 1.07 \text{ m}^2 \quad (11)$$

$$A_s = 2l_3 r_3 = 3.7 \text{ ft}^2$$

or

$$= 0.34 \text{ m}^2 \quad (12)$$

which conservatively neglects heat flow off the ends.

Then, for $q_s = 87 \text{ W/ft}^2$ (295 Btu/hr/ft^2 ; 930 W/m^2) $\alpha_s = 0.45$, and $T_\infty = 130^\circ\text{F}$ (54°C), the following estimates were obtained from Equations (1), (4), and (7):

$$\bar{T}_s < 180^\circ\text{F}$$

or

$$< 82^\circ\text{C} \quad (13)$$

$$T_{\text{TB}} < 215^\circ\text{F}$$

or

$$< 102^\circ\text{C} \quad (14)$$

The maximum temperature on the surface was estimated by considering a small element of surface area which lies normal to the impinging solar flux for which the approximate heat balance is

$$q_s \alpha_s dA = \bar{h}(T_s - T) dA \quad (15)$$

If \bar{h} is still taken at its mean value, then using (2), (4), (7), and (15)

$$(T_s)_{MAX} < 234^\circ F$$

or

$$112^\circ F \quad (16)$$

However, it is expected that circumferential conduction in the PAT-1 will reduce this upper bound estimate of surface temperature.

The foregoing analytical estimates are based on steady-state heat balance. It is likely that the heat capacity of the package will somewhat reduce the temperature rise caused by insolation, particularly since the sun passes over the package during the day and is absent during the night hours. The effect of these transients is addressed in the next paragraph.

3.4.1.2 Numerical Model

The transient temperature response of the PAT-1 was calculated using finite difference methods. The numerical model is shown schematically in Figure 3.4-1. Since the influence of solar flux is of primary interest, heat flow in the radial and circumferential directions was modeled, with temperature assumed uniform in the axial direction. This is equivalent to chopping off the ends of the package (at the end of the aluminum tube) and replacing this material with insulated planes. Such a model overpredicts the PAT-1 temperatures because internal heat and absorbed solar radiation are not lost to the surroundings from the end surfaces.

To further simplify the model, a few assumptions were made concerning the internal metallic components. The TB-1, the copper tube, and the aluminum load-spreader assembly were each treated as lumped masses of uniform temperature. The thermal resistances between these components were taken from the test results of Appendix 3A.1, which are shown in Table 3.4-1. These approximations have a negligible influence on the temperature distribution in the wood.

The energy equation which is applied to the redwood liner is the transient conduction equation

$$\rho c \frac{\partial T}{\partial t} = \frac{1}{r} \frac{\partial}{\partial r} \left(rk \frac{\partial T}{\partial r} \right) + \frac{1}{r} \frac{\partial}{\partial \theta} \left(k \frac{\partial T}{\partial \theta} \right) \quad (17)$$

in which c , k^{\parallel} , and k^{\perp} were taken as the temperature dependent functions given previously in Table 3.2-1 and the other parameters are illustrated in Figure 3.4-2. The boundary condition applied at the outer wall is as follows

$$-k^{\parallel} \frac{\partial T}{\partial r} = \bar{h}(T_{\infty} - T) + \alpha_s q_s \cos \beta \quad (18)$$

where

$$\cos \beta = \cos(\theta - \theta_s), \quad 0 < |\theta - \theta_s| < \frac{\pi}{2} \quad (19)$$

$$\cos \beta = 0 \quad \frac{\pi}{2} < |\theta - \theta_s| < \pi$$

θ_s is the angular location of the sun which varies during the day and θ is the angular coordinate on the surface, as noted in Figure 3.4-1. As the sun passes over the package, θ_s is gradually increased from $\theta_s = 0$ to $\theta_s = \pi$ during a 16-hr period, and then q_s is set to zero for the next 8 hr. The entire daily cycle was repeated until a periodic behavior was established. Because of the cylindrical shape of the package, the normal area projected to the insolation remains the same throughout the 16-hr period of sunlight. This is in contrast to the case of a flat plate for which the energy absorption varies approximately as a half sine wave due to geometric considerations.⁶ Thus, it is expected that the most severe attitude for the PAT-1 package is the one considered here, with the sun moving in the (r, θ) -plane.

The finite difference equations derived from (17) and (18) comprise a standard, explicit scheme. The nodal equations for the outer boundary include the heat capacity and the circumferential conduction in the stainless-steel wall as well as the convective and radiative exchange with the surroundings. Stability and sufficient accuracy were obtained using 9 radial divisions, 15 angular divisions, and a time step of 1/2 minute.

Before considering the effects of insolation, a test case was run corresponding to the conditions of the thermal test which was described in Appendix 3A.1. A comparison of experimental and numerical results is shown in Figure 3.4.1.2-1. The steady-state temperatures are in precise agreement because the coded expressions for redwood conductivity and resistance between metallic components are based on the test data. The transient behavior is in reasonably good agreement, with some minor deviations. The thermocouples which measure wall temperature were located on the ends of the PAT-1 and are therefore not in intimate contact with the redwood. The calculated wall temperature refers to the side wall where the temperature rise due to environmental heating is slowed by conduction into the redwood. The predicted internal temperatures increase somewhat faster than the experimental data, particularly in the early period. This is partly because the resistance heater was not in direct contact with the TB-1, thus causing an

initial time lag in the experimentally observed temperature rise. Also, the numerical model neglects axial spreading of the internal heat from the TB-1. None of these factors should have a significant impact on the calculations concerned with insolation.

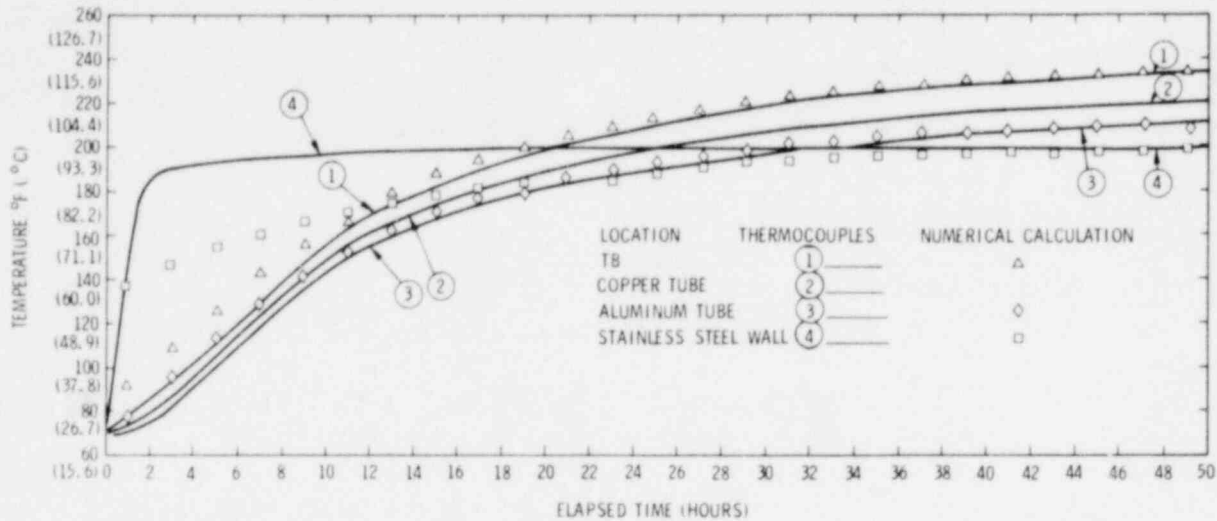


Figure 3.4.1.2-1. Results of Thermal Test (Solid Lines) and Comparison with Numerical Calculation (Symbols)

The response of PAT-1 was calculated for a solar flux of $q_s = 295 \text{ Btu/hr/ft}^2$ (930 W/m^2) passing over the cylindrical surface from $\theta_s = 0$ to $\theta_s = \pi$ in a 16-hr period, followed by 8 hr of darkness. The ambient temperature was held steady at 130°F (54°C) throughout the day. Calculation was continued for five consecutive days. After the third day the thermal cycle shown in Figure 3.4.1.2-2 was well established. It is seen that the representative temperatures increase steadily during the period of insolation, reaching maximum values at sunset or shortly after. Maximum values of the TB-1 temperature, the mean surface temperature \bar{T}_s , and the mean red-wood temperature \bar{T}_W are as follows:

$$T_{TB} < 212^\circ\text{F} (100^\circ\text{C})$$

$$\bar{T}_W < 182^\circ\text{F} (83^\circ\text{C}) \quad (20)$$

$$\bar{T}_s < 176^\circ\text{F} (80^\circ\text{C})$$

These values are only slightly less (3° to 4°F ; 1.7° to 2.2°C) than those obtained by the analytical estimates in Equations (13) and (14) of the previous section, indicating that 16 hr of insolation has almost brought the package to a quasi-steady state condition. This approach to a quasi-steady limit is also apparent in the flattening off of mean temperatures in Figure 3.4.1.2-2.

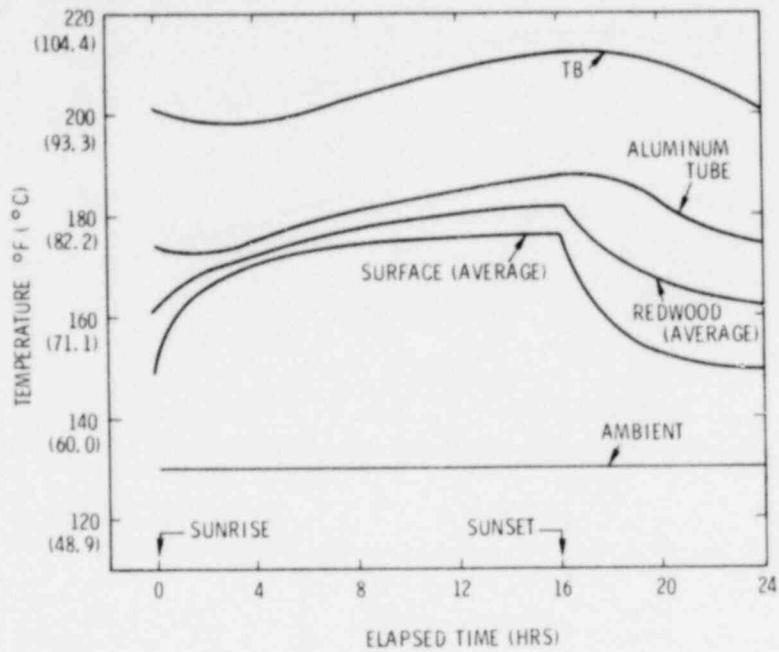


Figure 3.4.1.2-2. Daily Thermal Cycle of PAT-1 Subjected to Solar Radiation

The most severe temperature distribution in the redwood is shown in Figure 3.4.1.2-3. The peak temperature occurs at the surface near $\theta = \pi$, where the insolation impinges normal to the surface.

$$(T_s)_{\text{MAX}} < 224^\circ\text{F} (107^\circ\text{C}) \quad (21)$$

This is about 10°F (5.6°C) less than the analytical estimate in the previous section because circumferential conduction and transient effects are now included. Since the circumferential conductivity of the wood is small, it appears that the aluminum load spreader is playing a significant role in carrying heat from the hot side to the cold side of the package. Also, the temperature distribution is skewed slightly to the left of $\theta = \pi$ because that side has been subjected to greater solar flux in the preceding hours of the day.

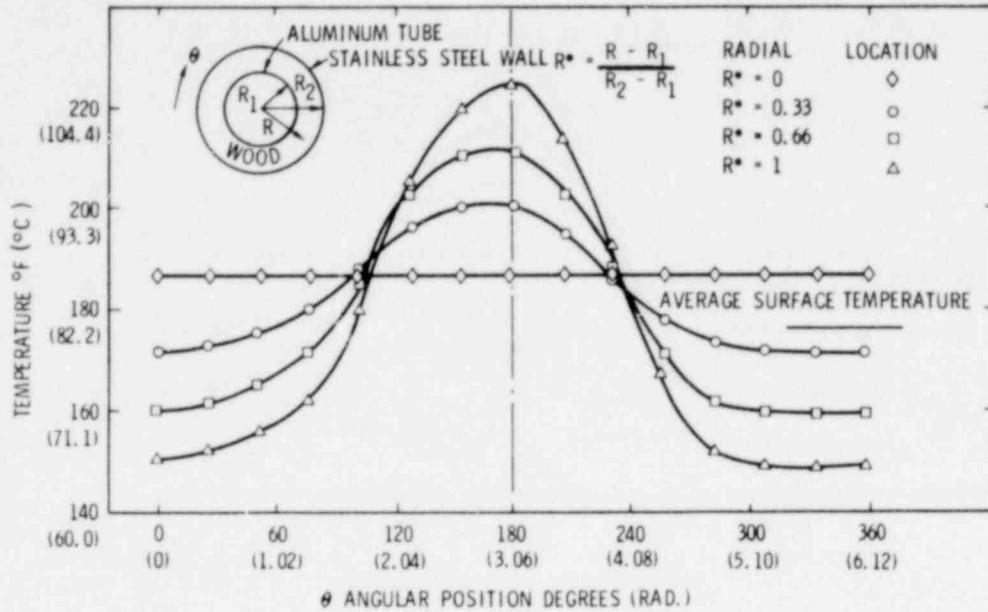


Figure 3.4.1.2-3. Temperature Distribution in Redwood Overpack Just Before Sundown (Most Severe Case)

Figure 3.4.1.2-4 shows the amount of the redwood overpack which is cooler than any given temperature. It is seen that 90 percent of the redwood is cooler than 200°F (93°C) even at the end of the day. This is a conservative estimate because the ends of the package, which are significantly cooler, have not been included in the analysis.

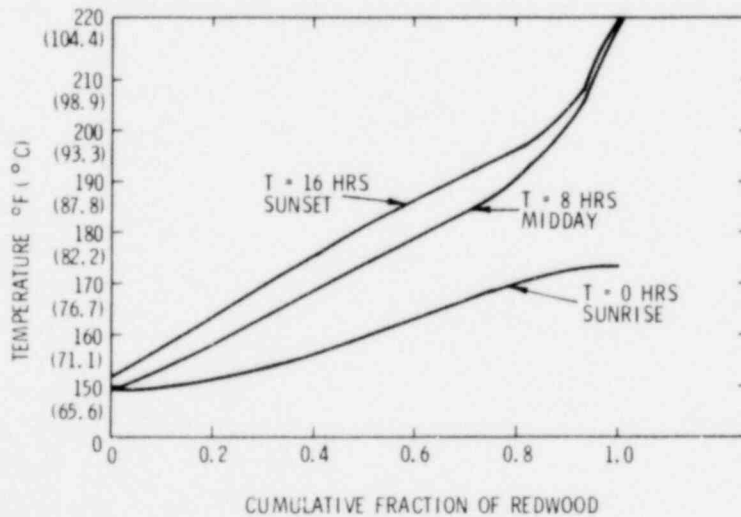


Figure 3.4.1.2-4. Temperature of PAT Redwood -- Severe Normal Environment

3.4.2 Maximum Temperatures

The foregoing analysis and testing of the PAT-1 package supports the estimates for maximum temperatures under normal conditions of transport as shown in Table 3.1-I. The conservatism (over-prediction) of Table 3.1-I estimates is emphasized by a review of modeling assumptions:

- a. Geometric orientation maximizes absorption of solar flux
- b. 16 hr of solar flux (295 Btu/hr/ft^2) (930 W/m^2)
- c. High ratio of solar absorptivity to surface emissivity
- d. Ambient temperature of 130°F (54°C), even at night
- e. No allowance made for heat loss from ends of PAT-1
- f. No wind to enhance convection cooling.

The thermal stresses and internal pressures in the TB-1 are negligible at these temperatures. Also, the characteristics of the redwood are not significantly affected by a temperature of 200°F as demonstrated in Reference 7.

3.4.3 Minimum Temperatures

In an external ambient of -40°F (-40°C) with no direct solar flux, the temperatures of the outer wall and the TB-1 are estimated as -30°F (-34°C) and $+5^\circ\text{F}$ (-15°C), respectively, for an internal heat load of 25 W and -40°F (-40°C) without an internal heat load. The associated thermal stresses and pressures at these temperatures pose no threat to the PAT-1 package.

3.4.4 Maximum Internal Pressure

For a TB-1 containment vessel at a temperature of 215°F (102°C) (2°F in excess of the Table 3.1-I value), the internal pressure is 34.3 psi (236 kPa) as discussed in paragraph 4.2.2.

3.4.5 Maximum Thermal Stresses

Temperature differences within the TB-1 should not exceed $\sim 10^\circ\text{F}$ (5.6°C) under normal conditions of transport. Corresponding stresses are insignificant.

3.4.6 Evaluation of Package Performance for Normal Conditions of Transport

The ability of the PAT-1 package to safely contain plutonium oxide under normal conditions of transport has been demonstrated by the evaluation in Chapter 2 which is supported by information in this paragraph (3.4). Over the range of normal operating temperatures [-40°F (-40°C) to 212°F (100°C)], the TB-1 design has sufficient capability to maintain its contents under leaktight conditions. Long-term performance of the stainless-steel vessel is unaffected by this range of temperatures. The copper gasket and elastomeric O-ring, over their periods of intended use (Chapter 8), are also unaffected by this normal operating temperature range.

The PC-1 product can, operating over essentially the same temperature range as the TB-1 vessel, demonstrated the ability to retain its contents without leakage. The roll-crimped, contact-adhesive and flexibilized-epoxy-overbonded PC-1 closure was unaffected by the normal-condition performance tests and will not be degraded during its use in the single-trip PC-1 containment system.

The metal components of the AQ-1 overpack are unaffected by the temperature range of normal transport [e. g., -40°F (-40°C) to 225°F (107°C) for the outer stainless-steel drum]. The mean temperature range for the redwood of -40°F (-40°C) to 182°F (83°C) has no detrimental effects on redwood material properties, and the redwood properties experience no long-term degradation upon being subjected to temperatures within this range.

3.5 10 CFR 71 -- Thermal Accident Evaluation

Compliance of the PAT-1 package to the requirements of 10 CFR 71 Appendix B was accomplished primarily by test. However, one assessment was required to establish that the maximum TB-1 temperature assumed in Chapter 4 is a reasonable value. Also, it is demonstrated in paragraph 3.6.2.2 that the test facility used to conduct the fire tests produced the environments required.

3.5.1 Thermal Models

3.5.1.1 PAT-1 Package Response in a 10 CFR 71 Fire Environment -- Analytical Model

The fire response of the TB-1 within the PAT-1 package can be calculated utilizing data of charring rates in wood.^{3,8,9} In Reference 3, the exposed surface of the wood was confined within steel skin similar to the condition of the PAT-1 package following the 30-ft (9-m) drops and puncture tests called for in 10 CFR 71 Appendix B. However, data were generated utilizing an external 1850°F (1010°C) blackbody radiation source rather than the 1475°F (802°C) radiation environment specified in 10 CFR 71 Appendix B. Figure 3.2-1b shows that after 30 minutes of fire exposure, a char depth in the range of 2.1 in. (5.3 cm) would be predicted in 22 lb/f² (352 kg/m³) density redwood typical to PAT-1. The amount of virgin redwood remaining between

the char front and the aluminum load-spreader tube at this time would be approximately 2.6 in. (6.6 cm). The char front is predicted by Figure 3, 2-1a to be moving at a velocity of about 0.28 ft/hr (.085 m/hr).

Several tests, including the PAT-1 package and other prototype packages, indicate that if the redwood is contained and remains in an integral condition following termination of the fuel fire, a curtailment of the char front progression occurs (demonstrated in paragraph 3.5.1.2). Since the PAT-1 package is essentially undamaged prior to the 10 CFR 71 fire test (refer to Chapter 2), charring terminates shortly after the fuel fire is extinguished. The temperature in front of the char front can be estimated for the equation,¹⁰

$$\frac{T - T_i}{T_c - T_i} = \exp\left(-\frac{vx}{\alpha_w}\right) \quad (22)$$

where T is the temperature at a distance x in front of the progressing char front (0.22 ft) (0.067 m), T_i is the initial internal temperature at x , v is the char front velocity (0.28 ft/hr) (0.085 m/hr), and T_c is the char front temperature, $\sim 550^\circ\text{F}$ (288°C).⁸ Based on the high-thermal resistivity of the uncharred redwood, the value chosen for T_i would not be expected to be much higher than the maximum normal operating temperatures ($\sim 200^\circ\text{F}$ (93°C), Table 3.1-1) at the load spreader. Thermal diffusivity ($\alpha_w = k/\rho c$) can be calculated from the values in Table 3.2-1 as $0.024 \text{ ft}^2/\text{hr}$ ($0.002 \text{ m}^2/\text{hr}$). The temperature of the wood adjacent to the load-spreader tube is calculated as

$$T \text{ redwood @ load spreader} = 227^\circ\text{F} (108^\circ\text{C}) \quad (23)$$

Since the physical condition of the PAT-1 package throughout the 10 CFR 71 accident condition performance tests assures that reasonable thermal contact between the TB-1 and the aluminum load spreader is maintained, the TB-1 temperature would also be at about this temperature.

3.5.1.2 Test Model - PAT-1 Performance During 10 CFR 71 Accident Condition Tests

Testing to the accident conditions of transport as specified by 10 CFR 71 Appendix B was accomplished on a PAT-1 package. In this sequence of tests, the TB-1 did not contain actual PuO_2 contents but 1.484 kg of UO_2 , a surrogate. As in all loadings of surrogate, 19.3 g of water was added to the UO_2 contents (see paragraph 4.3.2).

The thermal test requirement of 10 CFR 71 Appendix B calls for a heat input to the package of not less than would result from exposure of the whole package to a radiation environment of 1475°F (802°C) for 30 minutes with an emissivity coefficient of 0.9, assuming the surfaces of the package have an absorption coefficient of 0.8. The ability of the fire test facility to meet these requirements is discussed in paragraph 3.6.2.2. The performance of this specific fire test is shown in Table 3.5.1.2-1 and indicates that the 10 CFR 71 requirements were exceeded. The

duration of the fire was 52 minutes. It is seen in Figure 3.5.1.2-1 that the luminous flame zone extends essentially across the diameter at the top of the chimney. Internal package condition and char depth is shown in Figures 3.5.1.2-2 and -3. The maximum TB-1 temperature during the test was estimated to be just over 200°F (93°C); this temperature was estimated by posttest examination of Tempilaq coating painted on the external bottom and internal cover of the TB-1 vessel. The 200°F (93°C) coating on the exterior of the TB-1 was degraded (possibly by the effects of the water-submersion test) but indicated a temperature slightly exceeding 200°F (93°C) (the 300°F (149°C) coating was completely intact). The 200°F (93°C) coating inside the TB-1 cover was discolored but still intact confirming the 200°F (93°C) estimated temperature (a 300°F (149°C) coating was completely intact). Tempilabels placed on the surface of the PC-1 (indicating temperatures in 10°F (5.6°C) increments) indicated a PC-1 temperature between 170°F (77°C) and 180°F (82°C).

TABLE 3.5.1.2-I

10 CFR 71 Appendix B Burn Test

Observed average temperature on AQ-1 drum:	~1800°F
Observed flame temperatures in vicinity of PAT-1:	2200-2300°F
Duration of above temperatures:	52 minutes
Char depth in outer redwood:	3.825 in.
TB-1 temperature:	~200°F (> 170; < 210)
Cumulative char rate:*	< 0.37 ft/hr

* Total char depth observed was divided by 52 minutes; this is a severe assumption because char would persist beyond the 52 minute duration of the JP-4 fire. Char rate pretest prediction was 0.28 ft/hr (see paragraph 3.5.1.1).

The conclusion is that the fire test conducted in the accident condition of transport test series provides a significantly more severe thermal environment than that required by 10 CFR 71 Appendix B. Differences between the TB-1 temperature achieved in the test and that calculated by analysis (assuming maximum PAT-1 package normal operating temperatures (Table 3.1-I) as initial conditions) were minimal (<27°F, -15°C).

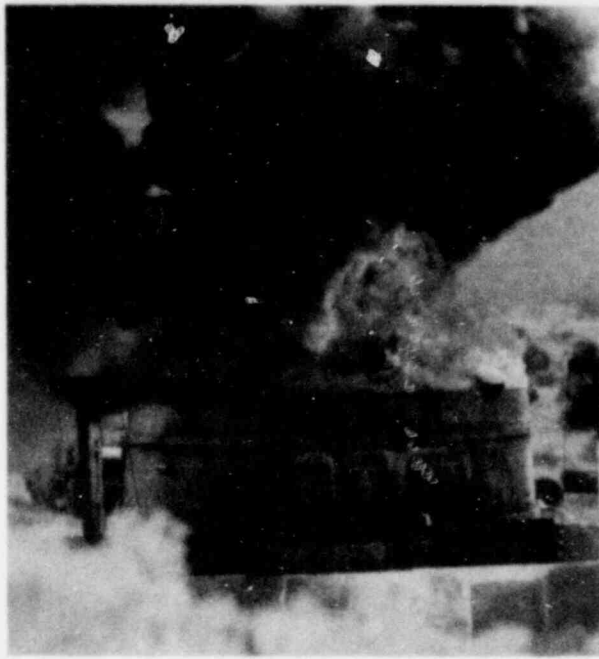


Figure 3.5.1.2-1. Luminous Flame Zone

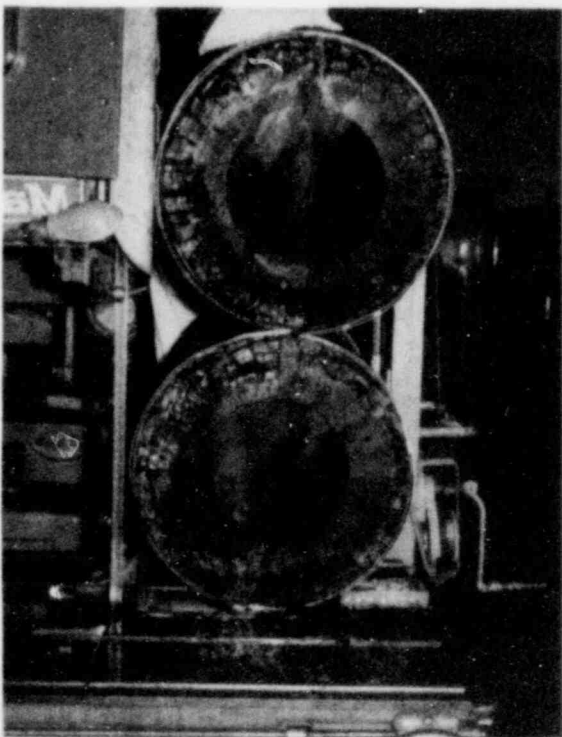


Figure 3.5.1.2-2. Internal Package Conditions

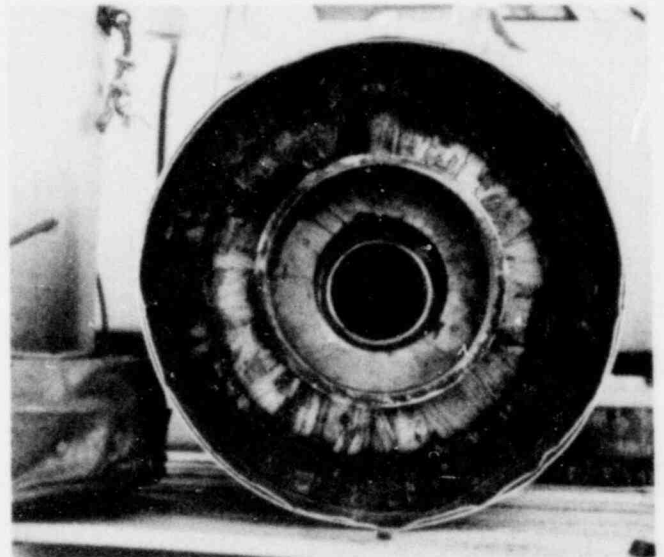


Figure 3.5.1.2-3. Char Depth

3.5.2 Package Conditions and Environment

The damage to the PAT-1 package resulting from five 30-ft free-drop tests and the puncture test was discussed in Chapter 2. The minor dents and scratches caused by these tests are assessed as no significant impact on the package performance during the thermal test.

3.5.3 Package Temperatures

The above analysis and testing of the PAT-1 package supports an estimate of $\sim 227^{\circ}\text{F}$ (108°C) for the maximum TB-1 temperature during the thermal performance tests of 10 CFR 71 Appendix B.

3.5.4 Maximum Internal Pressure

For a TB-1 containment vessel at 227°F (108°C), the internal pressure is 38.7 psi (269 kPa) as discussed in Chapter 4.

3.5.5 Maximum Thermal Stresses

Temperature differences within the TB-1 should not exceed 10°F (5.6°C) under 10 CFR 71 Appendix B, Accident Conditions of Transport Performance Tests. Corresponding stresses are insignificant.

3.5.6 Evaluation of Package Performance for the 10 CFR 71 Accident Conditions

The ability of the PAT-1 package to safely contain plutonium oxide under 10 CFR 71 accident conditions of transport has been demonstrated in Chapter 2 with supporting information provided by this paragraph (3.5). Maximum temperature predicted for the TB-1 (227°F , 108°C) only exceeds the peak of the normal operating range by 15°F (8.3°C); therefore, the demonstrated ability of this containment vessel to maintain its contents under leaktight conditions is not unexpected (considering that prefire structural damage to the PAT-1 is minimal). The maximum internal pressure associated with the 227°F (108°C) maximum temperature is 38.7 psi (267 kPa), 12 psi (83 kPa) less than the internal pressures generated in the 1-1/2 x maximum normal operating pressure test (Chapter 2). Testing the PAT-1 package to this pressure is routinely required in the containment system fabrication verification tests specified in Chapter 8. The elastomeric O-ring and copper gasket were not degraded under these performance test conditions.

The PC-1 product can was demonstrated to retain its contents without leakage. The roll-crimped and epoxy-overbonded PC-1 closure was also not visibly degraded by the 10 CFR 71 Appendix B environments.

The redwood within the AQ-1 overpack served its intended purpose. During the fire test the redwood located external to the aluminum load spreaders charred to a depth of about 4 in. (10 cm) (in agreement with an analytical assessment performed as indicated in paragraph 3.5.1.1). The redwood located within the load-spreader tube and discs, except for soot staining caused by the immersion test (Figure 3.5.1.2-3), was unaffected by the 10 CFR 71 Appendix B performance tests (Figure 3.5.1.2-4).

3.6 NRC Qualification Criteria -- Thermal Accident Evaluation

The compliance of the PAT-1 package to the requirements of the NRC qualification criteria was accomplished primarily by test demonstrations. The purpose of the assessment in this section, therefore, is to establish that the maximum TB-1 temperature assumed in paragraph 4.4.2 is a reasonable upper limit which would bound all test results.

3.6.1 Thermal Models

3.6.1.1 PAT-1 Package Response to the Fire Environment of the NRC Qualification Criteria -- Analytical Assessment

The PAT-1 packages subjected to the first test of the NRC qualification criteria were in a damaged condition -- the packages were impacted at > 422 fps (129 m/s), crushed with a 70,000-lb (311-kN) force, punctured with a 500-lb (187-kg) conical probe, and slashed with a 100-lb (37-kg) steel angle dropped from 150 ft (46 m). Such prefire test distortions of package geometry and alterations in physical properties of package materials (e. g., compressed redwood) limit any theoretical package thermal evaluation to a conservative bounding assessment.

The two ripping/slashing tests were specifically of interest since the resulting penetrations allowed a significant direct exposure of the redwood to the fuel fire environment. The main effect of this degradation was to allow continued charring of the redwood after the 1-hr fuel fires had terminated. Therefore, the effects of varying damage and geometric configurations resulting from impacts in five orientations (top, top corner, side, bottom, and bottom corner) became unimportant in the analytical assessment of maximum TB-1 temperatures achieved during the fire test. This conclusion hinged on the test-verified assumption that sufficient thermal insulation was still provided by the crushed/damaged outer redwood assemblies (exterior to the load-spreader tube) to protect the load spreader from direct exposure to the fuel fire.^{*} As indicated by the data correlation in Reference 3 and observed in test experience of Reference 3, redwood has similar insulation capabilities in its compressed and uncompressed states -- given that the mass of redwood contained within a constant area segment extending through the depth of protecting material remains constant. It is therefore demonstrated that sufficient thermal insulation is provided even in the postimpact PAT-1 package configurations to protect the loader spreader from exceeding melt temperatures.

^{*} Depending on the viability of the heat-conduction path between the load spreader and the TB-1 following the high-velocity impact and puncture tests, direct exposure of the load spreader could result in TB-1 temperatures approximately equal to the load-spreader temperature. In this event, maximum load-spreader temperature would be limited to the melting temperature range for the load-spreader material, Al 6061: 1080°F solidus, 1205°F liquidus.

Following impact of the package in the most damaging orientation (a side-on impact), the redwood remains entirely confined within the outer stainless-steel drum. At the point of minimum distance between the outer stainless-steel drum and the aluminum load spreader, approximately 1-in. compressed redwood separates these two materials. Although some redwood material was displaced tangentially in the distorted PAT-1 configuration (see figures in Chapter 2), the remaining compressed redwood, combined with the protection provided by the essentially integral outer stainless-steel drum, was sufficient, as verified by the test program, to provide the insulating effect of ~3 in. (~7 cm) of undamaged redwood. This amount of redwood prevents the load-spreader tube from reaching its melting point prior to termination of the 1-hr fuel fire.

Following the termination of the 60-min fuel fire, redwood burning/charring would continue. During development testing, the temperatures achieved during this postfuel fire burning were observed to vary in one of two ranges. If the redwood was contained within an essentially integral stainless-steel outer drum after the high-velocity impact test, any continued combustion of redwood occurred through the progression of a char front. This char front temperature as indicated in Reference 3 would be expected to exhibit a temperature range between 550°F (288°C) and 620°F (327°C). If, however, the breakup of the redwood was extensive and the damage to the outer stainless-steel drum allowed "open" glowing combustion of the charcoal, temperatures of ~1100°F (594°C) were experienced.

The PAT-1 package, specifically the outer stainless-steel drum, was designed to remain essentially integral following the high-velocity impact test. However, the ripping/slashing tests caused two ~5 in.² (0.003 m²) penetrations of the outer drum as illustrated in figures in Chapter 2. Therefore, the conclusion from this analytical assessment of package performance is that the maximum temperature to which the TB-1 will be directly exposed (during the NRC qualification-criteria-defined fire test) will be between the temperature of the redwood char front, 550°F (288°C) to 620°F (327°C), and the glowing combustion temperature of charcoal 1100°F (594°C). The TB-1 surface temperature would not be expected to vary significantly from these values (i. e., the temperature differential caused by the 25-W internal heat source would be inconsequential).

3.6.1.2 PAT-1 Package Response to the Fire Environment of the NRC Qualification Criteria -- Test Model

Testing to the accident conditions as specified in the NRC qualification criteria was accomplished by subjecting five different PAT-1 packages to the sequence of tests mentioned in paragraph 3.6.1.1.

In each PAT-1 package, the TB-1 contained from 1.05 to 1.25 kg of UO₂ surrogate. Water (19.3 g) was added to the surrogate loadings to simulate TB-1 containment vessel internal pressures as described in paragraph 4.4.2.

1567 214

The major variable in performing the series of sequential tests involved the package orientation with respect to the target at impact. Side, top, top corner, bottom, and bottom corner impacts were conducted followed by the crush, puncture, and slashing tests; then these packages were subjected to the specified fire test. The requirements for this fire test include exposure to luminous flames from a pool fire of JP-4 or JP-5 fuel for a period of at least 60 minutes. The luminous flames are to extend an average of at least 3 ft (1 m) and no more than 10 ft (3 m) beyond the package in all horizontal directions.

The ability of the fire test facility to meet these requirements is discussed in paragraph 3.6.2.2. The time/temperature records for the three fires for the five package tests are shown in Figures 3.6.1.2-1 through -9. The estimated average flame temperature at package height, estimated average package skin (AQ-1 drum) temperature, the duration of the fires, and the maximum TB-1 temperature during each test are indicated in Table 3.6.1.2-I. Actual thermocouple data plots from the tests have a fairly wide band of jitter; the temperatures in Figures 3.6.1.2-1 through -9 are averaged results. The estimates were made by posttest examination of Tempilaq coatings painted on the external bottoms and internal covers of the TB-1 vessels; the normal response of the Tempilaq was perturbed by the adjacent redwood char, and by the mechanical effects of the severe crash test, but a rough estimate indicated a response of about 1000°F (538°C) on each TB-1. Also, the postfire coloration of four of the five tested TB-1s was a dark blue, which is roughly indicative of about 1000°F (538°C) for PH13-8 Mo stainless steel when heated in an oxidizing atmosphere. The other TB-1 was a medium yellow color, roughly indicative of less than 1000°F (538°C).

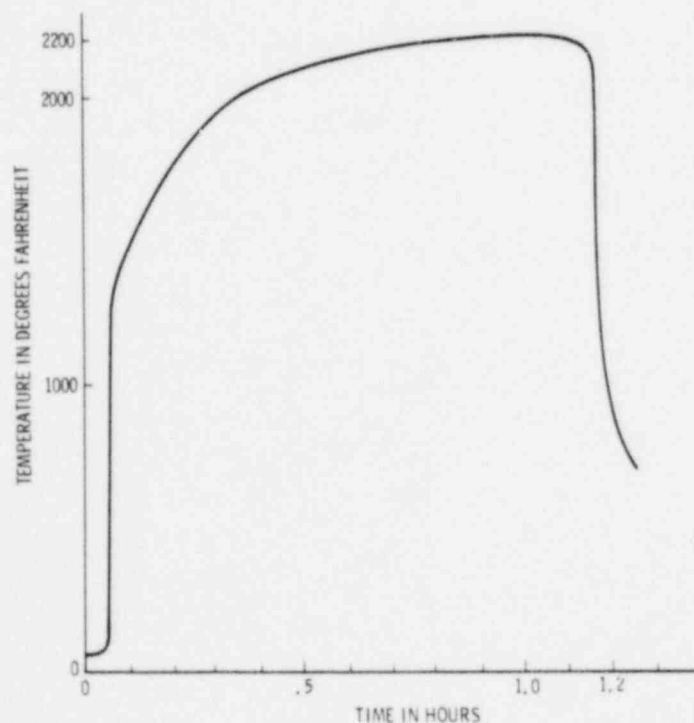


Figure 3.6.1.2-1. Flame Temperature at Package Level. (Fire test of top-corner-crashed and side-crashed PAT-1 package.)

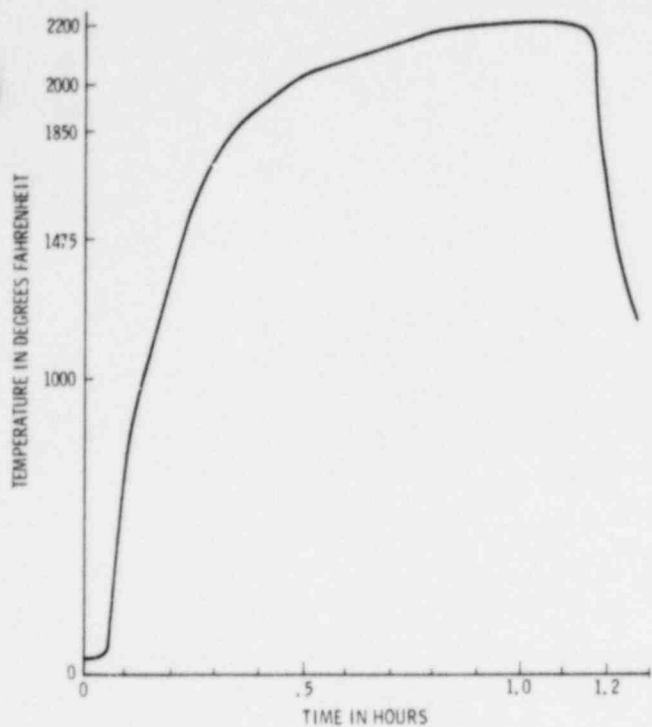


Figure 3.6.1.2-2. AQ-1 Drum Temperature.
(Fire test of side-crashed PAT-1 package.)

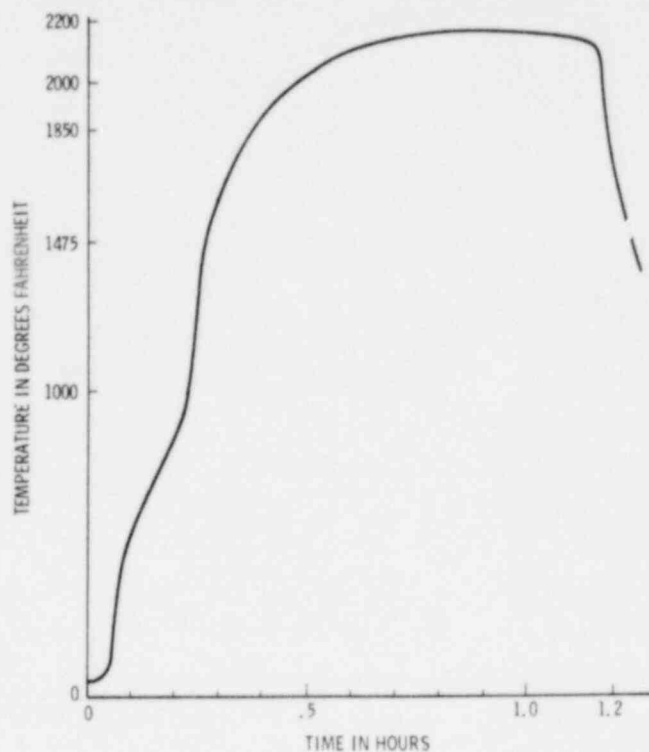


Figure 3.6.1.2-3. AQ-1 Drum Temperature.
(Fire test of top-corner-crashed PAT-1 package.)

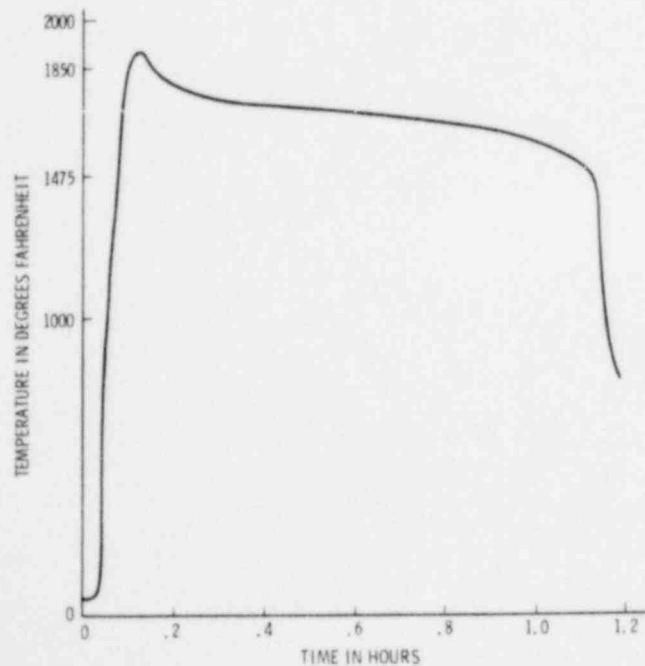


Figure 3.6.1.2-4. Flame Temperature at Package Level.
(Fire test of top-end-crashed and bottom-end-crashed PAT-1 packages.)

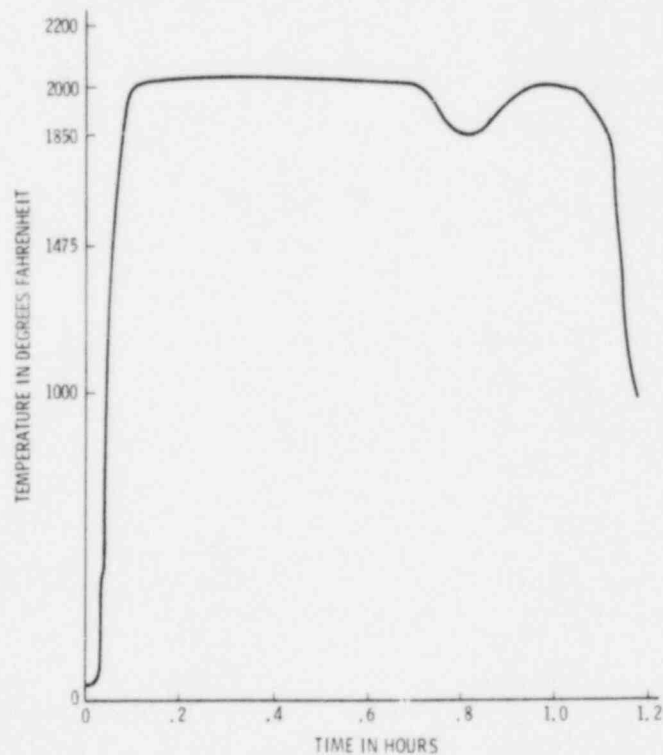


Figure 3.6.1.2-5. Flame Temperature 1-hr Below Package Level.
(Fire test of top-end-crashed and bottom-end-crashed PAT-1 packages.)

1567 216

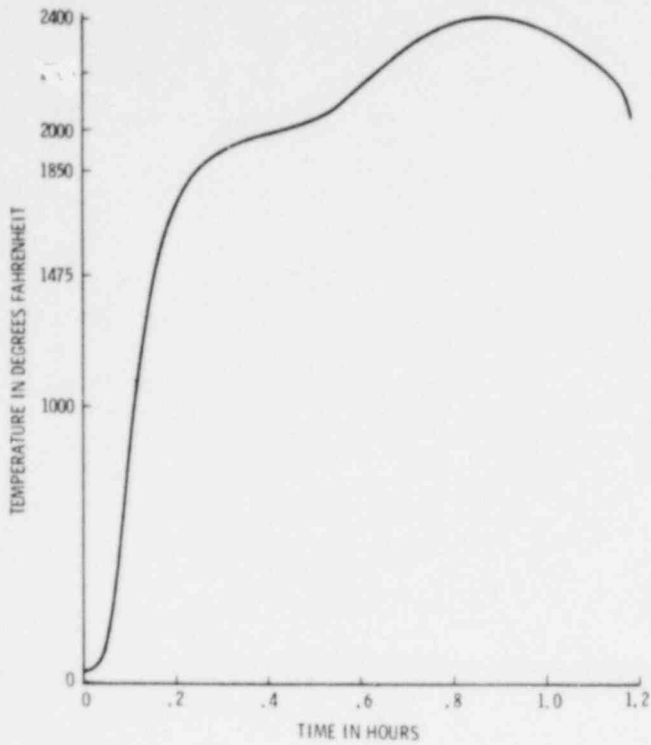


Figure 3.6.1.2-6. AQ-1 Drum Temperature. (Fire test of bottom-end-crashed PAT-1 package.)

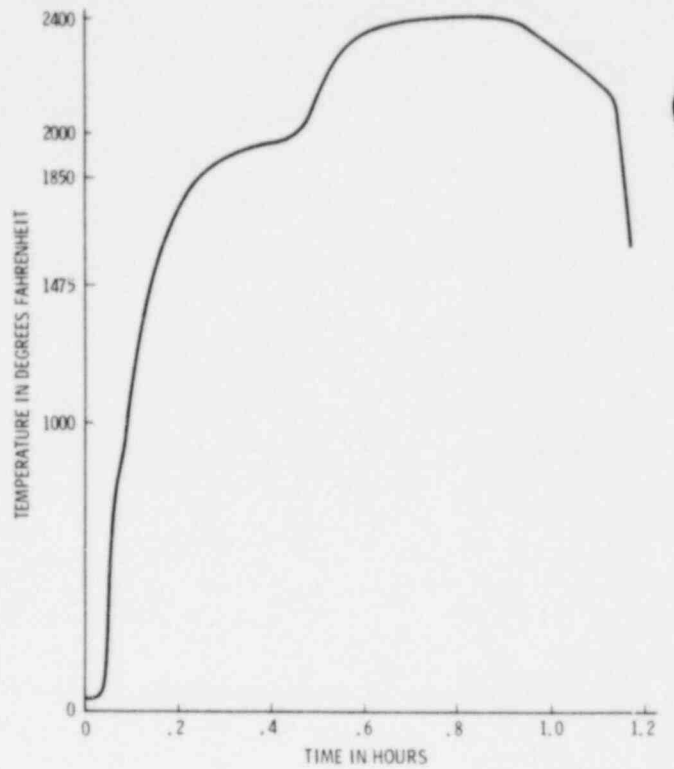


Figure 3.6.1.2-7. AQ-1 Drum Temperature. (Fire test of top-end-crashed PAT-1 package.)

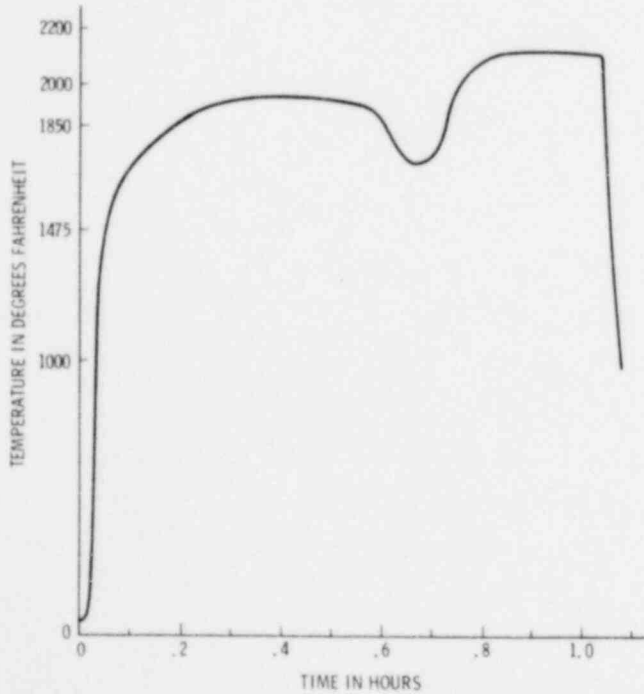


Figure 3.6.1.2-8. Flame Temperature at Package Level. (Fire test of bottom-corner-crashed PAT-1 package.)

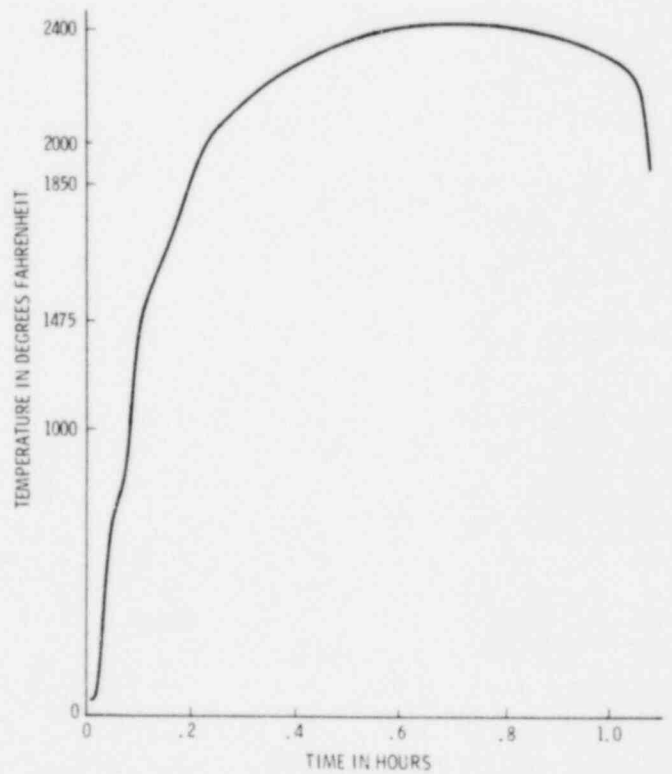


Figure 3.6.1.2-9. AQ-1 Drum Temperature. (Fire test of bottom-corner-crashed PAT-1 package.)

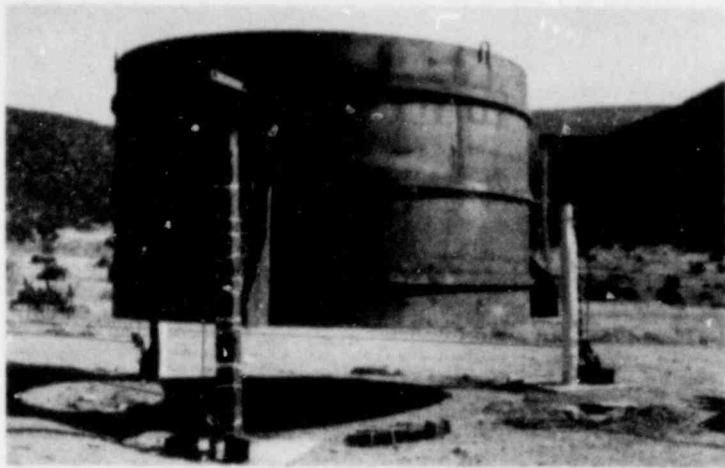


Figure 3.6.2.2-1. Steel-Tub Burn Pit

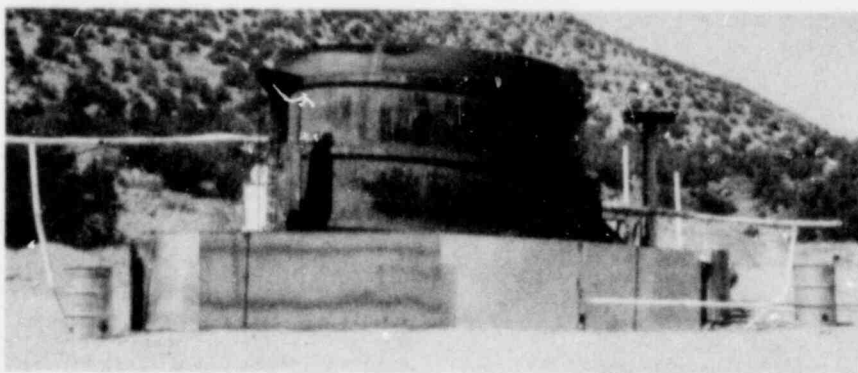


Figure 3.6.2.2-2. Noncombustible Fence Surrounds Chimney

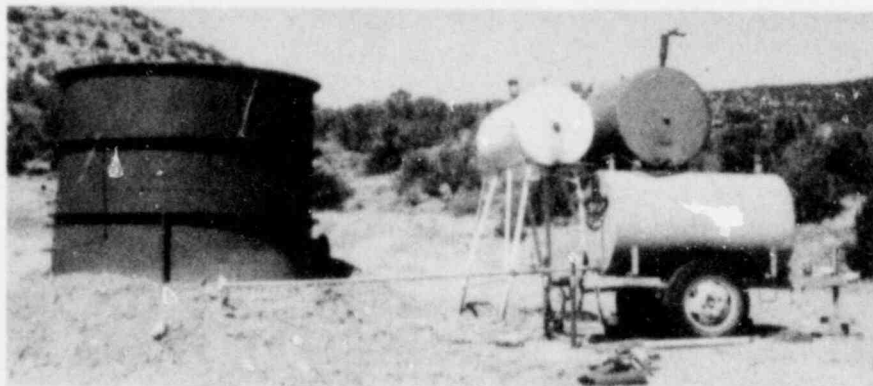


Figure 3.6.2.2-3. Storage Tanks for Water and JP-4 Fuel

TABLE 3. 6. 1, 2-1

Averaged Results -- NRC Qualification Criteria Fire Tests

PAT-1 Package Tests	Flame Temp. @ Package Level for Time Reported (°F)	Duration of Fire Above 1850°F (min)	Max. Temp. of AQ-1 Drum (°F)	Minimum Total Exposure Time to Engulfing JP-4 Flames (min)	Max. TB-1 Total (°F)
Top Impact	1850-2100 ^a	63	>2400	66	<1000
Top Corner Impact	1850-2100 ^b	58	2150	66	~1000
Side Impact	1850-2200 ^b	58	2200	66	~1000
Bottom Corner Impact	1700-2100 ^b	~50 ^c	>2400	63	~1000
Bottom impact	1850-2100 ^a	63	>2400	66	~1000

NOTES: ^aFlame temperature 6 in. below packages

^bFlame temperature at package median

^cShort-time dip below 1850°F during fire; package temperature continued to rise. Note Figures 3. 6. 1, 2-8 and -9.

3. 6. 2 Package Conditions and Environment

3. 6. 2. 1 Package Conditions

The damage to the PAT-1 packages resulting from the high-velocity impact, crush, puncture, and slashing environments of the NRC Qualification Criteria was discussed in Chapter 2. The damage from the high-velocity impacts, when combined with the openings in the outer drum of the AQ-1 produced by the puncture and two slashing tests, significantly deforms specific areas of redwood in the outer overpack. These prefire tests, in threatening the integrity of the outer stainless-steel drum, allow (1) limited direct exposure of the redwood to the fuel fire and (2) long-term charring of the redwood following fuel fire termination.

3. 6. 2. 2 Fire Test Facility Description (Figures 3. 6. 2. 2-1, -2, -3)

The fire test facility consists of a steel-tub burn pit approximately 10 ft in diameter (see Figure 3. 6. 2. 2-1). The tub is set into the ground and has minimum freeboard above the ground surface level. JP-4 aviation jet fuel is floated on water within the tub. A chimney, approximately 16 ft (5 m) in diameter and 10 ft (3 m) tall, fabricated from 1-in. (2.54-cm) thick mild steel plate, is centered over the burn pit. The chimney is suspended on wire ropes and can be lifted to provide draft for the fire (see Figure 3. 6. 2. 2-1). A 4-ft-high, noncombustible fence is situated about 3 ft (1 m) away from the draft opening and surrounds the chimney to lessen the effects of surface wind on flame characteristics (see Figure 3. 6. 2. 2-2).

The water level, the JP-4 fuel level, and the chimney draft are preset to attempt to achieve a minimum temperature of 1850°F (1010°C) at the median height of the PAT-1 test article. The PAT-1 packages are situated about 3 ft (1 m) above the fuel surface on a stand centered in the burn pit. Flame temperatures were measured with thermocouples at levels below, even with, and above the PAT-1. In addition, thermocouples are mounted on the external drum of the PAT-1. Evidence that the luminous flame extended approximately 5 ft (1.5 m) from any point on the package surface to the chimney surface was provided by these thermocouples and photographic coverage of the fire tests (indicating luminous flame completely envelops the enclosed area at the top of the chimney).

Water and JP-4 fuel are gravity-fed to the burner site from storage tanks (see Figure 3.6.2.2-3).

3.6.3 Package Temperatures

The analyses of 3.6.1.1 and the test results indicated in 3.6.1.2 support an estimate of approximately 1080°F (582°C) for the maximum TB-1 temperature during the thermal test of the NRC Qualification Criteria.

3.6.4 Maximum Internal Pressure

For a TB-1 containment vessel at 1080°F (582°C) the maximum internal pressure is 1253 psi (8.6 MPa) as discussed in Chapter 4.

3.6.5 Maximum Thermal Stresses

Substantiation that the thermal stresses in the TB-1 do not affect its containment integrity was provided by the testing of five PAT-1 packages to the required five performance tests. Temperatures on the TB-1 could vary depending on the progression of the redwood char front, but are equalized by the aluminum load spreader. The conductivity of the TB-1 stainless steel is such that significant temperature differences within a vessel would not be expected.

3.6.6 Evaluation of Package Performance for NRC Qualification Criteria Thermal Conditions

The ability of the PAT-1 package to safely contain plutonium oxide throughout the sequential testing required by the NRC Qualification Criteria has been demonstrated in Chapter 2 with supporting information provided by this section (3.6). Maximum temperatures reached by the TB-1s are typically 900°F (482°C) to 1100°F (593°C), assessed both analytically and by actual tests. Comparisons of pretest and posttest air leak rate measurements across the TB-1 seal indicate that leak tightness of the pristine containment vessel does change as a result of the severe environments imposed on the package. As indicated in Chapter 4, this change in leak rate had no effect on package safety since no surrogate material was lost from the containment vessel (to the limit of test instrument (fluorimeter) detectability, $\geq 10^{-8}$ g of uranium). An analytical correlation between posttest gas leakage and potential powder leakage indicated compliance with the acceptance criteria.

The PC-1 product can was still intact, a condition not required for the NRC qualification tests and not accounted for in the analytical assessment of leakage performed in Chapter 4. A maximum temperature of 1080°F (582°C) was utilized in establishing the maximum internal pressure used in the assessment of content leakage described in Chapter 4.

The redwood, as expected, was completely charred, a process which provided the required protection for the TB-1. The integrity of the char, especially internal to the aluminum load spreader, indicates that glowing combustion of this internal char did not take place. This test evidence further confirms the ability of the PAT-1 package to limit TB-1 temperatures below 1100°F (593°C) during the NRC Qualification Criteria fire test.

APPENDIX 3A

Test to Establish Thermal Resistance Values of PAT-1 Components

A thermal test was conducted to determine the thermal resistance values for PAT-1 components. A resistance heater was placed inside the TB-1 of a PAT-1 package, and thermocouples were attached at the locations noted in Table 3A.3.1-I.

TABLE 3A.3.1-I

<u>TC No.</u>	<u>Location</u>	<u>Designation on Figure 3.4.1.2-1</u>	<u>Steady-State Temperature (°F)</u>
2, 3, 4	Lid of TB	1	235
5, 6	Cu sleeve	2	221
7, 8	Al tube	3	212
9	Al plate (upper)	3	212
10, 11, 12	Outer SS wall	4	200

The test was run in a temperature-controlled chamber which was maintained in the neighborhood of 200°F (93°C). The power to the internal heater was maintained at 25 W using a variable resistance power supply. The transient response of the thermocouples is indicated by the solid lines in Figure 3.4.1.2-1. The symbols on this plot represent comparative numerical calculations which are discussed in paragraph 3.4.1.2.

The steady-state temperatures listed in Table 3A.3.1-I were used in conjunction with the known heat load of 25 W to calculate thermal resistances along the heat-flow path. The steady-state temperature difference between the TB-1 and the outer surface of the PAT-1 was written as follows:

$$T_{TB} - T_S = RQ \quad (A3-1)$$

where Q is the internal heating rate (25 W) and R is the overall thermal resistance of the primary conduction path shown in Figure 3.4-2. The overall resistance R is the sum of the separate resistances along the path. The axial heat flow at the ends was neglected since it contributes less than 15% to the total conductance.

The temperature difference between the TB-1 and the copper sleeve was 14°F (7.8°C). Since thermocouples 5 and 6 were located near the top of the copper sleeve, this temperature drop was attributed to the resistance $R_{0,1}$ of the fiberglass protective layer at the slip-fit joint between the TB-1 containment vessel and the cadmium-plated copper sleeve.

$$R_{0,1} = \frac{T_{TB} - T_{CU}}{Q} = 0.56^\circ\text{F/W}$$

or

$$= 0.3^\circ\text{C/W} \quad . \quad (\text{A3-2})$$

The measured temperature difference between the copper sleeve and the aluminum tube was 9°F (5°C), corresponding to a thermal resistance of

$$R_{(1,3)} = \frac{T_{AL} - T_{CU}}{Q} \approx 0.36^\circ\text{F/W}$$

or

$$\approx 0.2^\circ\text{C/W} \quad . \quad (\text{A3-3})$$

Since thermocouples 7 and 8 were located near the top of the aluminum tube, this resistance includes the axial resistance in the tube as well as the axial resistance of the copper sleeve, the radial resistance in the lower aluminum plate, and the contact resistance at the two joints

$$R_{(1,3)} = R_1 + R_2 + R_3 + R_{1,2} + R_{2,3} \quad . \quad (\text{A3-4})$$

The axial resistance in the copper sleeve is

$$R_1 = \frac{1}{2\pi r_1^2 k_c} \approx (0.1^\circ\text{F/W})$$

or

$$\approx 0.056^\circ\text{C/W} \quad (\text{A3-5})$$

where the parameters are defined in Figure 3.4-2, and the radial resistance in the lower aluminum plate is

$$R_2 \sim \frac{\ln(r_2/r_1)}{2\pi b \cdot 2k_A} \approx 0.05^\circ\text{F/W}$$

or

$$\approx 0.028^\circ\text{C/W} \quad . \quad (\text{A3-6})$$

As will be explained below, the axial resistance in the aluminum tube is on the order of

$$R_3 \approx 0.19^\circ\text{F/W}$$

or

$$\approx 0.106^\circ\text{C/W} \quad . \quad (\text{A3-7})$$

This leaves a total contact resistance of approximately

$$R_{1,2} + R_{2,3} \approx (0.02^\circ\text{F/W})$$

or

$$\approx 0.011^\circ\text{C/W} \quad (\text{A3-8})$$

for the copper/aluminum joint $R_{1,2}$ and the aluminum/aluminum joint $R_{2,3}$. Since these are jointed with metallic fasteners, a very small resistance was expected.

The measured temperature difference between the top of the aluminum tube and the outer wall was

$$\Delta T_{3,5} = 12^\circ\text{F} (6.7^\circ\text{C}) \quad . \quad (\text{A3-9})$$

Since this temperature drop is related to the thermal resistance of the wood liner, it provided a means for checking the redwood conductivity. The axial conduction in the aluminum cylinder was coupled with outward radial conduction along the grain of the wood. Thus, the fin equation was applicable provided the usual convection coefficient h was redefined as follows in terms of the radial conductance of the wood

$$h = \frac{k_w}{r_2 \ell \ln(r_3/r_2)} \quad . \quad (\text{A3-10})$$

Then, from the textbook solution,⁴

$$Q = \Delta T (h P k_A A)^{1/2} \left\{ \tanh \left[\frac{h P \ell_5^2}{k_A A} \right]^{1/2} + \tanh \left[\frac{h P \ell_4^2}{k_A A} \right]^{1/2} \right\} \quad (\text{A3-11})$$

in which ΔT is the temperature difference between the lower end of the aluminum tube (base of the fin) and the outer wall. Equation (11) was rearranged as follows

$$\Delta T = Q \frac{\ell_n(r_3/r_2)}{2\pi \ell_3 k_w} \Psi \left\{ \tanh \left[\Psi \frac{\ell_5}{\ell_3} \right] + \tanh \left[\Psi \frac{\ell_4}{\ell_3} \right] \right\}^{-1} \quad (\text{A3-12})$$

in which

$$\Psi = \left[\frac{k_w}{k_A} \frac{\ell_3^2}{r_3^5} \frac{1}{\ell_n(r_3/r_2)} \right]^{1/2} . \quad (\text{A3-13})$$

Also, the relationship between ΔT and $\Delta T_{3,5}$ was available from the solution of the fin equation [4]

$$\Delta T = \Delta T_{3,5} \cosh \left[\Psi \frac{\ell_4}{\ell_3} \right] . \quad (\text{A3-14})$$

Then, by combining (12) and (14),

$$\Delta T_{3,5} = Q \frac{\ell_n(r_3/r_2)}{2\pi \ell_3 k_w} \Psi \left\{ \sinh \left(\frac{\ell_4}{\ell_3} \Psi \right) + \cosh \left(\frac{\ell_4}{\ell_3} \Psi \right) \tanh \left(\frac{\ell_5}{\ell_3} \Psi \right) \right\}^{-1} . \quad (\text{A3-15})$$

Since Q , $\Delta T_{3,5}$ and the geometry were all known, the value of k_w is calculated from (13) and (15) as

$$k_w \approx 0.31 \text{ Btu/hr/ft/}^\circ\text{F}$$

or

$$\approx 1.76 \text{ W/m}^2 \cdot \text{k} . \quad (\text{A3-16})$$

This is in good agreement with published empirical expressions noted in Table 3.2-I.

The temperature drop along the aluminum tube was estimated using (14)

$$\Delta T_3 = \Delta T - \Delta T_{3,5} \approx 4.8^\circ\text{F} (\approx 2.7^\circ\text{C}) \quad (\text{A3-17})$$

and the corresponding thermal resistance was

$$R_3 = \frac{\Delta T_3}{Q} \approx 0.19^\circ\text{F/W}$$

or

$$\approx 0.106^\circ\text{C/W} \quad (\text{A3-18})$$

as given previously in Equation (7).

The thermal resistance of the redwood liner was evaluated as

$$R_4 = \frac{\Delta T_{3,5}}{Q} \approx 0.5^\circ\text{F/W}$$

or

$$\approx 0.278^\circ\text{C/W} \quad (\text{A3-19})$$

but this resistance decreases as the temperature increases due to temperature dependence of the redwood conductivity.

Contact resistance was neglected in the analytical model (fin approximation) which describes the heat flow from the aluminum tube to the outer wall. Nevertheless, the inferred value for redwood conductivity, $k_w \approx 0.31$, already exceeds the expected value based on published correlations. If contact resistance had been included, the inferred value of k_w would be even greater. This assessment appears to confirm that contact resistance is negligible at the wood/metal glue joints.

In summary, the overall thermal resistance R between the TB-1 and the outer stainless-steel drum wall consists of the three major contributions discussed separately above

$$R = R_{0,1} + R_{1,3} + R_4 \approx 1.4^\circ\text{F/W}$$

or

$$\approx 0.78^\circ\text{C/W} \quad (\text{A3-21})$$

Although the redwood conductivity varies with temperature, the total R changes by only 5% with a temperature change of 50°F (10°C). Thus, the steady-state temperature difference between the TB and the outer surface can be taken as

$$T_{TB} - T_S = QR \approx 35^\circ\text{F} (\approx 19^\circ\text{C}) \quad (\text{A3-22})$$

The experimental temperature measurements in the PAT-1 were found to be consistent with a simple analytical model of conduction heat flow. Contact resistance and redwood conductivity were estimated from these tests results.

References

1. Y. S. Youloukian, "Thermophysical Properties of High Temperature Solid Materials," Vol. 3, Macmillan, New York, 1967.
2. F. F. Wangaard, "Heat Transmissivity of Southern Pine Wood, Plywood, Fiberboard, and Particleboard," Wood Science, Vol. 2, No. 1, 54-60, 1969.
3. R. E. Berry, T. K. Hill, W. W. Joseph, and R. K. Clarke, Accident-Resistant Container: Materials and Structures Evaluation, SAND74-0010, August, 1975.
4. A. J. Chapman, Heat Transfer, third edition, Macmillan, New York, 1974.
5. MIL-STD-210B, Military Standard Climatic Extremes for Military Equipment, December, 1973.
6. J. A. Duffie and W. A. Beckman, "Solar Energy Thermal Processes," Wiley-Intersciences, New York, 1974.
7. W. A. Von Riesenmann and T. R. Guess, The Effects of Temperature on the Energy-Absorbing Characteristics of Redwood, SAND77-1589, Sandia Laboratories report, to be published.
8. E. L. Schaffer, "Review of Information Related to the Charring Rate of Wood," U.S. Forest Service Research Note FPL-0145, U.S. Department of Agriculture, November, 1966.
9. R. P. May, "Radiant Heat Test of Four Wood Samples," internal memo to J. A. Sisler and L. A. Dunn, Sandia Laboratories, Albuquerque, September, 1964.
10. E. L. Schaffer, "An Approach to the Mathematical Prediction of Temperature Rise Within a Semi-Infinite Wood Slab Subjected to High Temperature Conditions," Pyrodynamics, 2, 117-132, 1965.

CHAPTER 4
CONTAINMENT

4.1 Summary

The containment acceptance criteria for the PAT-1 package following the tests described in Chapter 2 are: (1) no release of radioactive material from the TB-1 containment vessel and PC-1 product can following the normal and accident condition tests of 10 CFR 71, and (2) release of no more than an A2 quantity of plutonium in one week from the TB-1 containment vessel following the tests prescribed in the NRC qualification criteria. An A2 quantity is defined in Table VII of the International Atomic Energy Agency regulations for the Safe Transport of Radioactive Materials (IAEA Safety Series No. 6); typical pertinent A2 quantities are tabulated in Appendix 4A.

Verification of TB-1 containment vessel compliance involved a direct measurement to detect if any surrogate contents* (UO_2) had escaped during the performance tests. The measurement procedure involved submitting standard health physics swipe samples, collected from the containment vessel at the completion of the sequential tests, to analysis with a fluorimeter capable of detecting $\geq 10^{-8}$ g U.

Another method of verifying containment involved a mass-spectrometer-type helium leak-detector measurement of helium gas leakage across the TB-1 containment vessel boundary. The leak-detection test was capable of detecting $\geq 10^{-10}$ cm^3/s helium. The leak-rate data are to be used to perform a bounding analytical/experimental correlation to establish upper bounds on possible plutonium release. This correlation involves experimental work on plutonium-oxide release at Battelle Pacific Northwest Laboratories (Refs. 2-6) and analytical work by a member of the USNRC staff.** It is not part of the Sandia Laboratories work in this report.

Summary results follow in Table 4.1-1

* Surrogate contents are defined in Appendix 4B.

** William R. Lahs, PAT-1 Program Manager, PuO_2 Container Certification, Division of Safeguards, Fuel Cycle, and Environmental Research, USNRC.

TABLE 4.1-1

PAT-1 Package Containment -- Posttest Results

<u>Component</u>	<u>Test Condition</u>	<u>Regulatory Acceptance Standard</u>	<u>Uranium Detection Measurement</u>	<u>Helium Leak Rate (cm³/s)</u>
TB-1	Normal conditions of transport (Appendix A of 10 CFR 71)	No release	No release ⁺	Less than 1×10^{-10} (leak tight)*
	Hypothetical accident conditions (Appendix B of 10 CFR 71)	No release	No release ⁺	Less than 1×10^{-10} (leak tight)*
	NRC Qualification	A2/week**	No release ⁺	Less than 4.5×10^{-5}
PC-1	Normal conditions of transport (Appendix A of 10 CFR 71)	No release	No release ⁺	-
	Hypothetical accident conditions (Appendix B of 10 CFR 71)	No release	No release ⁺	-

* Reference 6 - Regulatory Guide 7.4 and ANSI N14.5.

** For a typical mixture of a recycle plutonium-oxide powder, an A2 quantity is approximately 2.55 mg of plutonium.

⁺ No release above detection capability of 10^{-8} gm.

4.2 Containment Boundary

The containment boundary for all performance test environments is the TB-1 containment vessel. The PC-1 product can provides the separate inner container required by 10 CFR 71.42, effective June 17, 1978. The boundary provided by the PC-1 product can is required following the 10 CFR 71 normal and accident condition tests and is not required following the test sequences defined by the NRC qualification criteria.

4.2.1 TB-1 Containment Vessel

The TB-1 containment vessel is described in Chapter 1 and is shown in Figures 1.4 and 1.5; stress analyses, material properties, and tests with results are described in Chapter 2. Drawings and specifications are included in Appendix 9A.

4.2.2 PC-1 Product Can

The PC-1 product can is described in Chapter 1 and is shown in Figure 1.5; drawings and specifications are included in Appendix 9A.

4.2.3 Closure

Positive closure of the TB-1 containment vessel is provided by the twelve 1/2-in.-diam bolts which fasten the lid to the body of the vessel, acting through a ductile copper gasket in conjunction with a knife-edge sealing bead on both the body and lid. Bolt torquing procedures are described in Chapter 7. An elastomer O-ring seal between the TB-1 lid and body is also provided with details of this closure and seal shown in Figure 4.2.3-1.

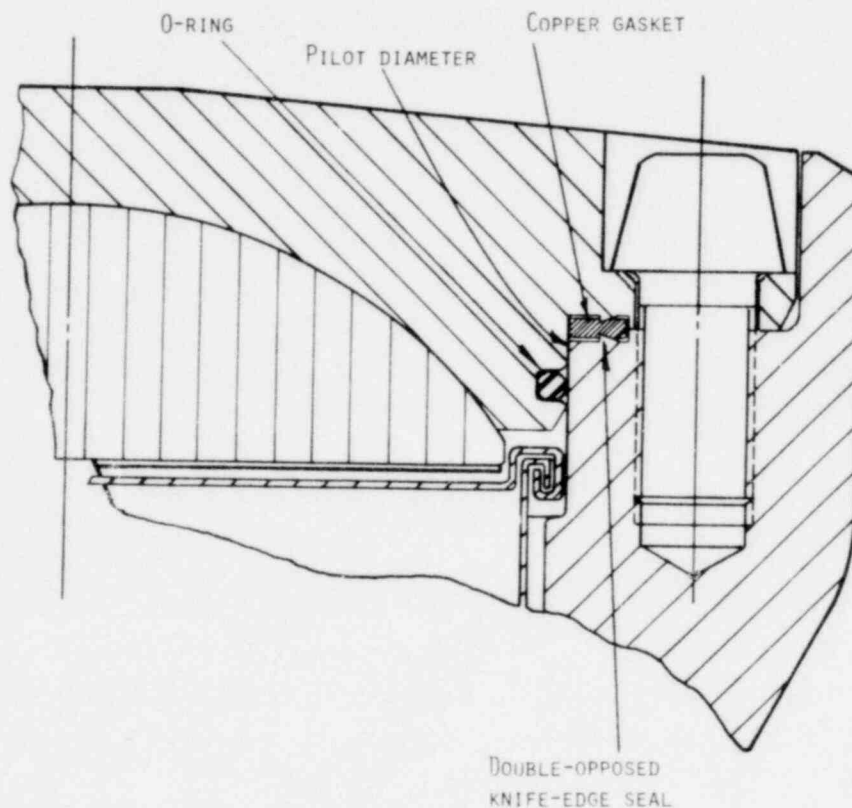


Figure 4.2.3-1. Cross Section of TB-1 Seals

The PC-1 closure is attained through a crimping of the can lid to the body and the application of a double coat of sealer material around the circumference of the crimped closure. There is also a contact-sealer material internal to the crimp joint.

4.3 Requirements for Normal Conditions of Transport 10 CFR 71

4.3.1 Release of Radioactive Contents

Through the use of the surrogate release and helium leak-detection methods described previously, it was verified that the TB-1 does not release radioactive contents under the defined normal conditions of transport. Specifically, (1) the uranium detection measurement confirmed

that no release of the surrogate contents (depleted UO_2) had occurred; and (2) the posttest gas leakage measurement established that the TB-1 vessel remained leaktight.*

The uranium detection method was used to demonstrate that the PC-1 product can meet the requirements of 10 CFR 71.42. Specifically, the uranium detection measurement confirmed that no release of the surrogate contents had occurred from the PC-1 into the leaktight TB-1.

4.3.1.1 Demonstration of TB-1 Containment Vessel Leaktightness

During assembly of the PAT-1 packages, the TB-1 containment vessels were backfilled with helium at ambient temperature and pressure, and were checked with a mass spectrometer-type helium leak detector for leaktightness. No leakage to the detection limit of the mass spectrometer ($10^{-10} \text{ cm}^3/\text{s}$) was ever observed.

The TB-1 and PC-1 product can were both subjected to a pretest uranium detection measurement which verified that no uranium-oxide surrogate contamination existed on either container to the limits of detectability -- $\geq 10^{-8}$ g of uranium.

After accomplishing the series of normal-condition performance tests (including a 1-1/2 times maximum normal-operating pressure test -- Chapter 2) and following PAT-1 disassembly, the TB-1 was subjected to a uranium detection measurement based on swipes of the TB-1 seal areas. No uranium dioxide was detected in this measurement (detectable limit $\geq 10^{-8}$ g of uranium).

The TB-1 containment vessel was then placed in the mass spectrometer and, by drawing a near-vacuum external to the TB-1, a measurement of helium leakage was made. Posttest helium leakage was undetectable (spectrometer capable of detecting leakage as low as $10^{-10} \text{ cm}^3/\text{s}$). Disassembly of the TB-1 confirmed that helium had remained in the vessel. It was, therefore, concluded that the TB-1 containment vessel remained leaktight throughout the normal condition of transport tests (including the 10 CFR 71.53(b) requirements).

4.3.1.2 Demonstration of PC-1 Product Can Integrity

Following the TB-1 posttest leakage measurement and TB-1 disassembly, the interior of the TB-1 and the exterior of the PC-1 product can were subjected to a uranium detection measurement. If UO_2 surrogate had been released from the PC-1 product can, it would have been contained within the leaktight TB-1. No uranium oxide surrogate was detected on any of the swipe samples (detectable limit $\geq 10^{-8}$ g of uranium).

* ANSI N14.5, Reference 7, defines that $q \leq 10^{-7} \text{ cm}^3/\text{s}$ is leaktight (where g = leakrate).

A verification test was also performed which demonstrated that this result was not dependent on the double-wrapped plastic bags which contained the UO_2 within the PC-1. These bags may have retained their integrity throughout the normal conditions of transport performance tests. The verification test, discussed in paragraph 4.4.1.2, involved packaging the UO_2 surrogate into a PC-1 without use of the plastic bags. The 10 CFR 71 accident condition of transport performance tests were then repeated on a PAT-1 package containing this PC-1. No uranium-oxide surrogate leakage was detected following these tests.

Therefore, based on these results, it is concluded that the PC-1 product can meet the intent of 10 CFR 71.42 requirements.

4.3.2 Pressurization of Containment Vessel

The TB-1 containment vessel and PC-1 product can were designed to hold a maximum of 3.15 kg PuO_2 powder with a maximum moisture content of 16 g of water. These contents are limited to generating a maximum 24 W of decay heat. The TB-1 is loaded at atmospheric pressure or less as described in Chapter 7.

After the PC-1 and TB-1 are sealed, a content loading which generates the maximum 25 W of internal decay heat, combined with the external environments specified in 10 CFR 71 [130° F (54° C) ambient temperature and solar heating], will cause the TB-1 to reach a maximum temperature of 215° F (102° C) with a corresponding higher internal pressure (see Chapter 3). This higher pressure is caused by the heated air and the vapor pressure of the contained moisture. With plutonium contents at 215° F (102° C), the vapor pressure for 16 g of water in a free volume of 715 cm^3 * is 15.6 psi (110 kPa). The pressure from the original 715 cm^3 of air is calculated to be 18.7 psi (130 kPa); the total internal pressure is 34.3 psi (240 kPa). Therefore, the requirement for testing at 1-1/2 times maximum normal operating pressure involved producing an internal PC-1 pressure \geq 51.4 psi (350 kPa).

The PAT-1 used in the normal condition of transport performance tests was loaded with 1.485-kg** UO_2 to which 19.3 g*** of water was added. Water vapor pressure at 215° F (120° C) is independent of water volume (since saturation conditions exist) and air pressure is essentially

* The approximate free volume is calculated by taking the PC-1 internal volume (1124 cm^3) and subtracting the volume of PuO_2 contents, assuming maximum particle density of 8 g/cm^3 (393 cm^3), and the original volume occupied by the H_2O (16 cm^3).

** The actual mass of UO_2 surrogate that can be loaded into a PC-1 is controlled by the density of the material and the space available.

*** As indicated in paragraph 4.5, the constant water loading in all PAT packages was established to produce the internal pressure which could occur during the accident conditions defined in the NRC qualification criteria.

independent of initial volume. Therefore, during the 10 CFR 71 heat test (Chapter 2) of the PAT-1 package, the internal container pressure of 34.3 psi (240 kPa) which could be associated with PuO₂ shipments was properly simulated.

To achieve the internal pressure required for 10 CFR 71.53(b), namely 51.4 psi (350 kPa), the TB-1 was subjected to a 255° F (124° C) temperature for 8 hr (see Chapter 2). At this temperature, water vapor pressure is 32.6 psi (220 kPa) and air pressure is 19.8 psi (140 kPa) or a total internal pressure of 52.4 psi (360 kPa). This pressure exceeds the required value of 51.4 psi (350 kPa).

4.4 Requirements for Accident Conditions of Transport 10 CFR 71

4.4.1 Release of Radioactive Contents

The two methods described previously (gas leakage and uranium detection) also verified that the TB-1 and PC-1 meet the containment requirements for radioactive contents under the accident conditions of transport defined by 10 CFR 71. Specifically, (1) the posttest gas leakage measurement established that the TB-1 vessel remained leaktight, and (2) the uranium detection measurement confirmed that no release of surrogate contents (depleted UO₂) had occurred throughout the prescribed test series.

The uranium detection method was also used to demonstrate that the PC-1 product can integrity was preserved intact as required by 10 CFR 71.42. Specifically, the uranium detection test confirmed that no release of surrogate contents had occurred from the PC-1 to the leaktight TB-1.

4.4.1.1 Demonstration of TB-1 Containment Vessel Leaktightness

During the assembly of the PAT-1 package prior to the performance tests representing the 10 CFR 71 accident conditions, TB-1 containment vessels were helium-filled and were checked for leaktightness with a helium-mass spectrometer. No leakage to the detection limit of the mass spectrometer (10^{-10} cm³/s) was ever observed. The TB-1 containment vessel and the PC-1 product can were also subjected to uranium detection measurements which verified no UO₂ surrogate contamination of either vessel (to detectability limits of $\geq 10^{-8}$ g of uranium).

After accomplishing the series of 10 CFR 71 accident condition performance tests and following PAT-1 disassembly, the TB-1 was subjected to uranium detection measurements for potential release of UO₂ surrogate. No UO₂ was detected in this measurement (detectable limit $\geq 10^{-8}$ g of uranium).

The TB-1 containment vessel was again placed in the mass spectrometer. Posttest helium leakage was undetectable (less than 10^{-10} cm³/s). Disassembly of the TB-1 containment vessel revealed a helium-rich internal atmosphere confirming the validity of the leak detection measurement.

It is therefore concluded that the TB-1 containment vessel/PAT-1 package meets the acceptance criteria of 10 CFR 71 and qualifies for consideration as a B(U) package under IAEA regulations (IAEA Safety Series No. 6).¹

4.4.1.2 Demonstration of PC-1 Product Can Integrity

Following the TB-1 posttest leakage measurement and disassembly, the interior of the TB-1 and the exterior of the PC-1 product can were subjected to a uranium detection measurement. If UO_2 surrogate had been released from the PC-1 product can, it would have been contained within the TB-1. No uranium oxide surrogate was detected on any of the swipe samples (detectability limit $\geq 10^{-8}$ g of uranium).

An added verification test was also performed which demonstrated the above measurement was not dependent on the doubled-wrapped plastic bags that contained the surrogate contents within the PC-1 and may have remained intact throughout the testing. This added test involved a second PAT-1 package which was subjected to the 10 CFR 71 Accident Condition performance test sequences. The contents within this product can included 606 g of UO_2 surrogate, 2545 g of No. 8 lead shot (used as ballast to attain a 3.15-kg content weight) and 19.3 g of water. This material was placed directly into the PC-1 without use of the double-wrapped plastic bags. Following completion of the test series, the TB-1 was disassembled and the entire interior surface of the TB-1 and exterior of the PC-1 were subjected to uranium detection measurements. No uranium oxide surrogate was detected. Therefore, based on these results, the PC-1 product can meets the intent of 10 CFR 71.42 requirements.

4.4.2 Pressurization of Containment Vessel

The TB-1 containment vessel and PC-1 product can were designed to contain a maximum 3.15 kg of PuO_2 powder with a maximum moisture content of 16 g of water. These contents are also restricted so as to generate a maximum 25 W of decay heat.

The TB-1 is loaded at atmospheric pressure or less as described in Chapter 7. After the PC-1 and TB-1 are sealed, the internal pressures rise as equilibrium temperatures are established throughout the PAT-1 package. To demonstrate compliance with the 10 CFR 71 accident conditions of transport, the peak internal TB-1 and PC-1 pressures reached during the 10 CFR 71 fire test were also evaluated.

As demonstrated in the PAT-1 package tests to the 10 CFR 71 Appendix B performance requirements (see Chapter 2), the structural damage caused by multiple 30-ft (9-m) drops and the puncture test was limited to minor dents to the outer stainless-steel drum.* The effects of PAT-1

* Further evidence of the structural toughness of the PAT-1 was demonstrated through an error in a test at the aerial cable facility when a PAT-1 package experienced a free fall of 155 ft (47 m) to the surface with only superficial damage.

package exposure to the 10 CFR 71 Appendix B, 1475° F (802° C) 1/2-hr fire are expected to be similar to those which would be experienced if an undamaged PAT-1 package was subjected to the fire. As indicated in Chapter 3, the peak TB-1 temperature which could be attained with heat-generating PuO₂ contents in the 10 CFR 71 fire environment has been calculated to be approximately 227° F (108° C).^{*} At this temperature the vapor pressure for 16 g of water in the minimum free volume of the PC-1 product can (715 cm³) is 19.6 psi (135 kPa) [see footnote^{*} for 4.3.2]. The pressure of the original 715 cm³ of air is calculated to be 19.1 psi (130 kPa); therefore, the maximum total pressure within the product can is 38.7 psi (270 kPa).

The maximum total pressure within the TB-1 cannot exceed the maximum pressure of the PC-1, in that the source of the vapor pressure is the moisture within the PC-1, and the only pressurization source outside of the PC-1 but within the TB-1 at this temperature is the additional air between the outside of the PC-1 and the inside of the TB-1, which would have the same value of 19.1 psi (130 kPa).

The first of the two PAT-1 packages used in the 10 CFR 71 accident condition of transport performance tests described in Chapter 2 was loaded with 1.484 kg of UO₂ to which 19.3 g of water was added (see footnote^{*} for 4.3.2). As indicated in Chapter 3, the fire test was an over-test for it was conducted in flame temperatures averaging over 2000° F (1093° C) rather than the specified 1475° F (802° C), and it extended for a time period of 52 minutes rather than the required 30 minutes. Measured TB-1 temperature in this test was ~200° F (93° C) (see Chapter 3). The water-vapor pressure at this temperature is 11.5 psi (79 kPa) and air pressure is 18.3 psi (130 kPa) for a total induced internal pressure of 29.8 psi (210 kPa).

The ~9 psi (62 kPa) pressure difference between maximum calculated pressure and the pressure attained in the 10 CFR 71 Appendix B test series is not considered significant for the following reasons:

- a. The calculated pressure is based on a conservative assessment of the maximum pressure attained within the TB-1; i.e., use of char depth and char front velocity data based on >1850° F (1010° C) external temperatures rather than 1475° F (802° C).
- b. The magnitude of the pressure difference is inconsequential for a PAT-1 package which experienced limited deformations within the AQ-1 and no permanent deformations of the TB-1 in the preceding impact and puncture

^{*} This calculation, because of lack of data at 1475° F (802° C), was conservatively based on data at 1850° F (1010° C) as discussed in Chapter 3.

tests (e.g., differential axial force on TB-1 bolts 11 lb (48.9 N)/bolt.* At these loadings, thread shear stress is insignificant).

- c. Furnace tests on a TB-1 indicated no seal failures until long-term exposure to a temperature of 1000° F (538° C) with 62.5 g of water deliberately introduced, causing 3330 psi (23 MPa) internal pressure [see paragraph 4.6.4].

As described in 4.4.1.2, an additional PAT-1 package was submitted to the 10 CFR 71 accident condition performance test sequences. The contents within this package included lead-shot ballast as well as UO₂ surrogate (to attain a 3.15-kg content weight) and 19.3 g of water which were placed directly into the PC-1 without the benefit of using two plastic bags. No significant difference in the evaluation of peak internal PC-1 pressure (~30 psi; 210 kPa) attained during the fire was indicated by the results of this testing.

4.5 Requirements for NRC Qualification Criteria

4.5.1 Release of Radioactive Contents

4.5.1.1 Summary

Uranium surrogate detection measurements were used to verify that TB-1 containment vessel plutonium containment acceptance criteria were achieved.

Also, gas leakage measurements were made across the TB-1 containment vessel boundary, to be used in correlation with experiments involving passage of PuO₂ powder through defined leaks under controlled conditions. Specifically, (1) the uranium detection measurement confirmed that no release of surrogate UO₂ contents occurred, and (2) the helium leak-rate measurements converted to air leak rates indicated that all TB-1 leak rates, posttest,** were $< 5 \times 10^{-5} \text{ cm}^3/\text{s}$.

4.5.1.2 Uranium Detection Measurements

During assembly of the five PAT-1 packages which were tested to the requirements of the NRC qualification criteria, the TB-1 vessels were subjected to uranium detection measurements which verified no UO₂ surrogate contamination (to detectability limit $\geq 10^{-8}$ g uranium).

After the sequential testing, the TB-1 containment vessels were again subjected to the uranium detection measurement for potential release of UO₂ surrogate. No UO₂ was detected in

* Based on total axial force (F) per bolt: $F = P\pi r^2/N$ where P = internal pressure, r = inside radius of TB-1, and N = number of bolts.

** Included all TB-1 vessels that were subjected to the impact, crush, puncture, slash, burn, and immersion tests required by the NRC qualification criteria.

these measurements. The limit of detectability is about five orders of magnitude below a typical mass of plutonium powder associated with an A2 quantity (Appendix 4A).

Upon disassembly, additional uranium detection measurements, not required by the NRC criteria, were made internal to the TB-1 containment vessels. Results of these additional measurements are presented in Appendix 4C. This additional evidence further demonstrates that release is controlled to less than an A2 quantity.

4.5.1.3 Gas Leak-Rate Measurements

During assembly of the five PAT-1 packages which were tested to the requirements of the NRC qualification criteria, the TB-1 containment vessels were backfilled with helium at ambient temperature and pressure. Each TB-1 was checked for leaktightness; no helium leakage was detected ($< 10^{-10}$ atm cm³/s). After experiencing the environments required by the NRC qualification criteria, the TB-1 vessels were again leak-tested. The results, when converted to air leakage, are indicated in Table 4.5.1.3-I; all leak rates are $< 5 \times 10^{-5}$ cm³/s.*

TABLE 4.5.1.3-I
Posttest TB-1 Air Leakage Rates

<u>Package Impact Orientation</u>	<u>Air Leakage Rate (cm³/s)*</u>
Top end (0°)	$< 4.5 \times 10^{-6}$
Top corner (30°)	$< 4.5 \times 10^{-5}$
Side (90°)	1.4×10^{-6}
Bottom corner (150°)	$< 5.5 \times 10^{-6}$
Bottom end (180°)	1.9×10^{-6}

* The measurements with a < sign are believed to include gases from redwood decomposition products (trapped in bolt holes), cleaning solution, and water vapor, all generated exterior to the TB-1 containment vessel. Wide-spectrum gas spectrometer leak-rate tests identified the presence of other gases, which was expected considering the combustion processes that took place adjacent to the TB-1 in the fire test.

* Experimental work with actual PuO₂ was conducted under NRC sponsorship at another laboratory (Refs. 2, 3, 4, 5, and 6), to correlate the observed helium leak rates with conservative bounding estimates of worst-case possible plutonium loss (again, no surrogate powder escaped). These conservative bounding assessments of plutonium loss were compared to IAEA "A2" quantities (Ref. 1) by the NRC staff. These assessments demonstrated successful performance of the PAT-1 package, satisfying the criteria for plutonium containment.

4.5.2 Pressurization of Containment Vessel

The TB-1 containment vessel was designed to contain a maximum of 3.15 kg of PuO₂ powder with a maximum moisture content of 16 g water (0.5% weight fraction of water). At the peak temperature attained in the NRC qualification fire test (~1080°F; 582°C) the internal pressure within the TB-1 would be 1253 psi (8.64 MPa). This total includes a contribution of 879 psi (6.06 MPa) from superheated steam at 1080°F (582°C), 49 psi (338 kPa) from the pressure of heated air within the TB-1, and 325 psi (2.2 MPa) from pressure of ethylene gas resulting from decomposition of the two polyethylene bags. These pressures were based on a calculated original free volume* of 1013 cm³. The PAT-1 packages used in the five NRC qualification criterial testing sequences included PC-1 product cans that contained from 1048 to 1254 g of UO₂. (Table 4.5.2-I), to which 19.3 g of water were added. Four of the TB-1s within these PAT-1 packages appeared to achieve temperatures approximating the estimated maximum of about 1080°F (582°C). Total internal TB-1 pressures attained in these qualification tests were calculated to range between 1144 psi (7.89 MPa) and 1183 psi (8.16 MPa). This total again includes contributions from superheated steam of 833 psi (5.74 MPa) to 867 psi (5.98 MPa), 49 psi (338 kPa) from the pressure of heated air, and 262 psi (1.81 MPa) to 267 psi (1.84 MPa) from decomposition of the polyethylene bags. These pressures were based on a calculated free volume ranging from 1235 to 1261 cm³. These calculated TB-1 vessel pressures would be slight underestimates of actual pressures achieved during the tests, since the UO₂ used as a surrogate had a small initial moisture content (<0.4 w/o or ~4 g of water per specification). This effect was not considered in the internal pressure calculation. The conclusion from the above calculations is that the internal pressures which were generated in the NRC qualification test PAT-1 packages provided a proper simulation of pressures which would have been experienced by a PAT-1 package loaded with maximum PuO₂ contents containing a maximum moisture content.

TABLE 4.5.2-I

Surrogate UO₂ Loadings in 5 PAT-1 Packages Tested
to NRC Qualification Criteria

<u>Impact Orientation</u>	<u>UO₂ Surrogate Loading (g)</u>
Top end	1346
Top corner	1048
Side	1205
Bottom end	1080
Bottom corner	1073

* The original free volume was calculated by taking the TB-1 internal volume (1460 cm³) and subtracting (1) the volume of the PC-1 product can (25 cm³), (2) the volume of the aluminum honeycomb spacer (13 cm³), (3) the volume of PuO₂ contents assuming maximum particle density of 8 g/cm³ (393 cm³), and (4) the original volume occupied by the H₂O (16 cm³); subtracting this volume for the space occupied by water makes the calculation conservative (higher calculated pressure) because 582°C is in the superheat region and no water would remain.

References

1. International Atomic Energy Agency IAEA Safety Series No. 6.
2. L. C. Schwendiman, et al, Quarterly Progress Report Study of Plutonium Oxide Leak Rates From Shipping Containers, October 1, 1976 - December 31, 1976, Battelle Pacific Northwest Laboratories Report No. BNWL-2260-1, January 1977.
3. L. C. Schwendiman, et al, Quarterly Progress Report Study of Plutonium Oxide Leak Rates From Shipping Containers, January 1, 1977 - March 31, 1977, Battelle Pacific Northwest Laboratories Report No. BNWL-2260-2, April 1977.
4. L. C. Schwendiman, et al, Quarterly Progress Report April 1, 1977 - June 30, 1977, Study of Plutonium Oxide Leak Rates From Shipping Containers, Battelle Pacific Northwest Laboratories Report No. BNWL-2260-3, July 1977.
5. L. C. Schwendiman, et al, Quarterly Progress Report, July 1, 1977 - September 30, 1977, Study of Plutonium Oxide Leak Rates from Shipping Containers, Battelle Pacific Northwest Laboratories Report No. BNWL-2260-4, October 1977.
6. L. C. Schwendiman, et al, Quarterly Progress Report October 1, 1977 - December 31, 1977, Study of Plutonium Oxide Leak Rates From Shipping Containers, Battelle Pacific Northwest Laboratories Report No. BNWL-2260-5, January 1978.
7. Regulatory Guide 7.4, Leakage Tests on Packages for Shipment of Radioactive Materials and ANSI N14.5, same title.
8. "Effect of Oxalate Precipitation on PuO₂ Microstructures," 6th International Materials Symposium, Berkeley, California, August 24-27, 1976. (Referenced in Appendix 4B)

APPENDIX 4A

IAEA (A2) Quantity Containment Requirements

Accident Conditions of Transport mg/wk	Normal Conditions of Transport $\mu\text{g/hr}$
^{238}Pu 0.176	0.000176
^{239}Pu 32.2	0.032
^{240}Pu 8.7	0.0087
^{241}Pu 0.9	0.0009
^{242}Pu 770	0.77
Typical Mixture 2.55 mg Pu/wk	0.002

APPENDIX 4B

Application and Characterization of Surrogate UO_2 Powder

Depleted sinterable UO_2 powder was used as a surrogate for PuO_2 during testing of the PAT-1 packages. Selection of this material was based primarily on its ability to replicate the aerosol characteristics of PuO_2 and the capability to detect very small quantities (10^{-8} gm) of this material. This detection capability was utilized as one of the two methods to demonstrate container compliance with the performance specifications. Other similarities of this UO_2 surrogate with PuO_2 include (1) U and Pu are both actinide rare earths with similar atomic properties; and, (2) UO_2 and PuO_2 have similar heat capabilities, surface tensions, and thermal conductivity. The bulk density of the UO_2 powder ($1 - 1.25 \text{ g/cm}^3$) is also similar to PuO_2 formed in the oxalate process ($1.2 - 1.5 \text{ g/cm}^3$).

All PAT-1 package analyses presented in this report assume a content weight of 3.15-kg PuO_2 . This weight represents a maximum mass payload of PuO_2 powder with a 2.8 g/cm^3 bulk density (could be formed in a peroxide process)* that could be contained in 100% of the 1124 cm^3 of the PC-1 product can. Chapter 2 indicates that the ability to package from 1.048 to 1.485 kg of UO_2 within the product cans in the tested packages does not affect the capabilities of the PAT-1 package to contain 3.15 kg of PuO_2 .

The depleted UO_2 powder used in the testing program was supplied by Eldorado Nuclear, Ltd., Port Hope, Ontario, Canada, as specification ENL-1-Issue 5--Depleted Sinterable UO_2 .

The powder was examined by the Nuclear Materials Division, Savannah River Laboratory (SRL), by agitating it in an isoton solution by ultrasonic means and then taking measurements with both an electron-beam microscope and a Coulter counter.

Eldorado reported the bulk density to be $1.00 \pm 0.25 \text{ g/cm}^3$ per ASTM-B329 (the 40,000-psi sintered density would be $5 \text{ to } 6 \text{ g/cm}^3$). SRL reported the particle size as

3.01 μ median

5.59 μ mean

52.74% of population < 1 micron

5.65% of volume < 1 micron

* Personal communication, L. S. Nelson, 5443, Sandia Laboratories to J. A. Andersen, 5433, Sandia Laboratories and also Reference 8.

For comparison purposes, SRL reports the following for an oxalate precipitation $^{239}\text{PuO}_2$ (direct strike); low (small particle) data group of four measured samples are

28.06 μ median

29.14 microns mean

No particles < 6 microns.

The above data show that the UO_2 examined was much finer than at least one specific PuO_2 powder examined by SRL; the individual PuO_2 powder grain was typically "briquette-like or straw-like,"* whereas the individual UO_2 powder grain was more nearly spherical or "sandlike". Additional information on PuO_2 microstructure may be found in Reference 8.

The particle size distribution of the UO_2 used in the PAT-1 qualification tests is given in Table 4B-1.

TABLE 4B-1

Particle Size Distribution of Depleted UO_2 Powder, PAT-1

μ Range	Volume %	Population %
0.63 - 0.79	2.60	33.23
0.79 - 1.00	3.05	19.51
1.00 - 1.26	5.77	18.42
1.26 - 1.59	7.24	11.56
1.59 - 2.00	10.41	8.31
2.00 - 2.52	12.50	5.00
2.52 - 3.17	11.03	2.20
3.17 - 4.00	10.75	1.07
4.00 - 5.04	9.45	0.47
5.04 - 6.35	6.22	0.16
6.35 - 8.00	4.07	0.05
8.00 - 10.08	2.88	0.02
10.08 - 12.70	2.94	0.009
12.70 - 16.00	3.28	0.005
16.00 - 20.16	2.43	0.001
20.16 - 25.40	1.70	0.0006
25.40 - 32.00	2.55	0.0005
32.00 - 40.32	0	0.0005
40.32 - 50.80	1.13	-----
	100.00	100.01615

* Telecon, 11/10/77, from James Scarbrough, Savannah River Laboratory Nuclear Materials Division, to J. A. Andersen, Division 5433, Sandia Laboratories.

APPENDIX 4C

Post-NRC-Qualification-Test Uranium Detection Measurements,
Internal to TB-1 Containment Vessel

A further indication of the ability of the PAT-1 package to meet the containment acceptance criteria following the NRC qualification criteria testing was provided by uranium measurements taken internal to the TB-1. These measurements, Table 4C-1, indicate that release of surrogate from the PC-1 to the internal environment of the TB-1 was limited to less than 10^{-5} g of uranium. This mass is 10^{-2} times the A2 quantity, which is the acceptable plutonium leakage limit from the TB-1 for typical recycled PuO_2 . The NRC qualification criteria did not require this double containment of the radioisotopic contents.

TABLE 4C-1

Posttest* Uranium Surrogate Measurements Internal to the TB-1

Package Impact Orientation	TB-1 Internal Surfaces (g)	PC-1 Factory Seam (g)	PC-1 Bonded Joint (g)
Top end	$<10^{-8}$	5.6×10^{-8}	$<10^{-8}$
Top corner	$<10^{-8}$	2.6×10^{-8}	3.4×10^{-8}
Side	1.2×10^{-8}	6.2×10^{-7}	9.5×10^{-7}
Bottom corners	$<10^{-8}$	$<10^{-8}$	3.4×10^{-8}
Bottom end	2.1×10^{-8}	6.8×10^{-8}	4.0×10^{-6}

* NRC Sequential Tests for Certification of a Plutonium Air Transportable Package.

Upon disassembly of the five TB-1 vessels from the NRC qualification test series, it was found that the PC-1 product cans, although severely deformed, exhibited no visible openings (see Figures 4C-1 through 4C-10). The residue visible in the photographs is decomposed aluminum honeycomb, decomposed Tempilaq (temperature indicating lacquer applied inside the TB-1 lid), decomposed Viton O-ring material, and decomposed identification and warning stickers from the PC-1 product can exterior (none is UO_2 powder). Figure 4C-1 indicates the general procedure followed in first opening all of the TB-1 containment vessels: handling precautions in the event UO_2 was openly present, immediate helium "sniffing" and gas sample collection, and health-physics-radiation monitoring preceding the swipe collections.

This TB-1 (Figure 4C-1) is from the top-end-impacted PAT-1 package following the entire test sequence of impact, crush, puncture, slash, burn, and immersion. Figure 4C-2 is the PC-1 product can from the top-end-impacted sequence. The following figures (4C-3 through 4C-10) show the TB-1 disassembly and details of the PC-1 condition following the full NRC qualification criteria test series that initiated with impact on the PAT-1 top corner, side, bottom corner, and bottom, in that sequence.

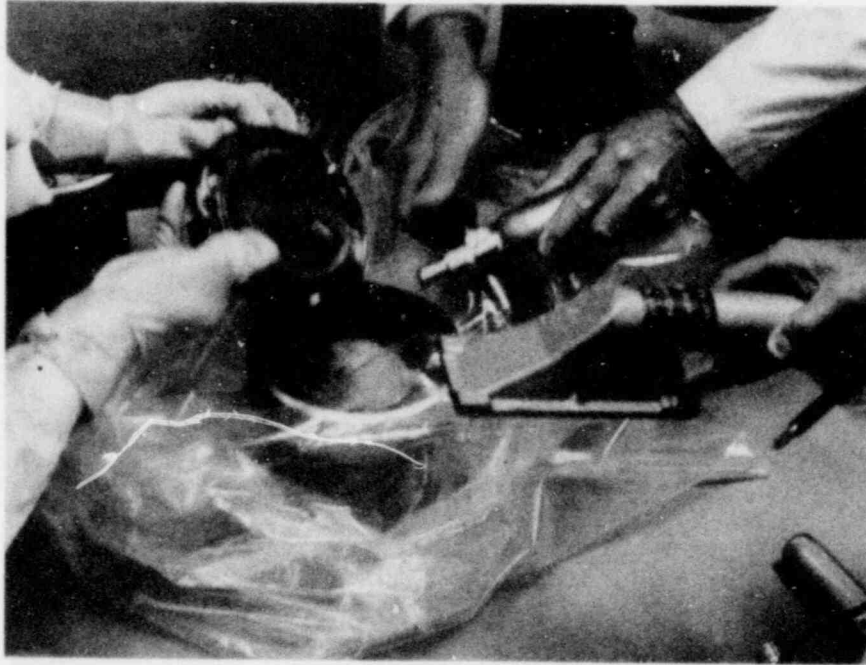


Figure 4C-1. First Opening of TB-1 Containment Vessel

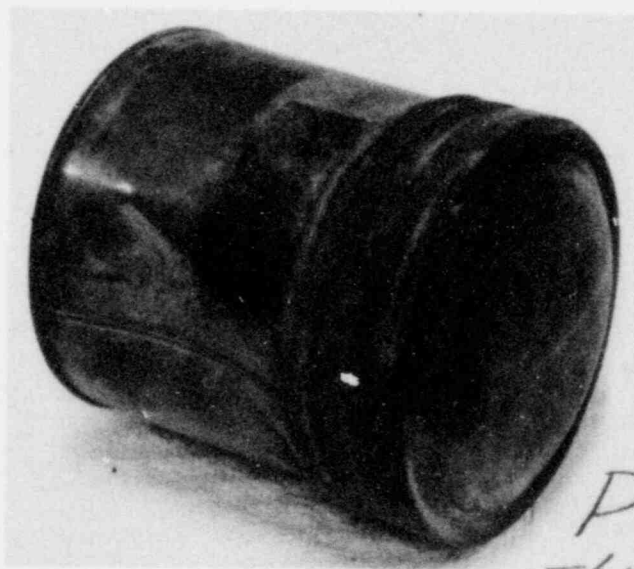


Figure 4C-2. Product Can From Top-End Impact Sequence

Figures 4C-3 through 4C-10. Series Showing TB-1 Disassembly and Details of PC-1 Condition

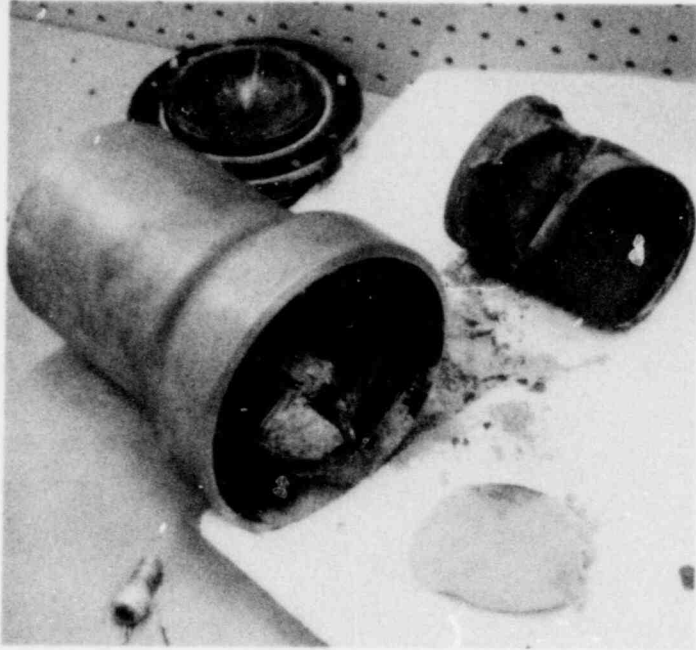


Figure 4C-3

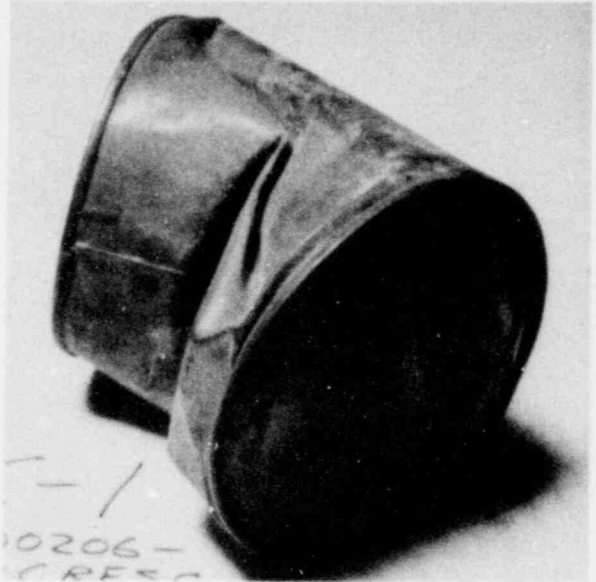


Figure 4C-4



Figure 4C-5

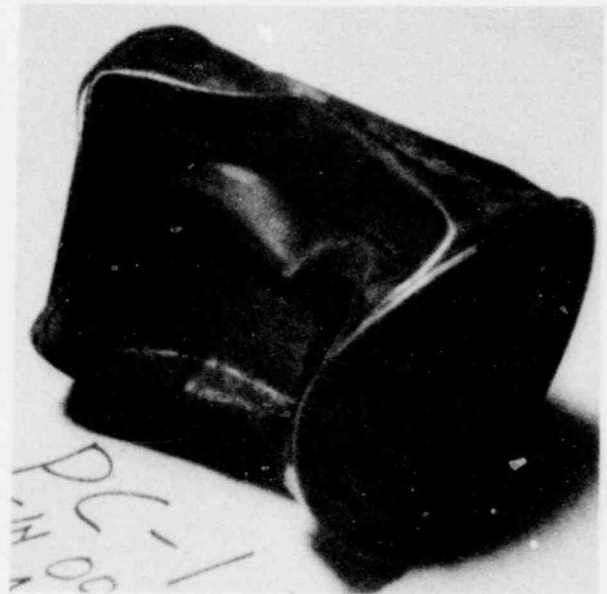


Figure 4C-6

POOR ORIGINAL

1567 246

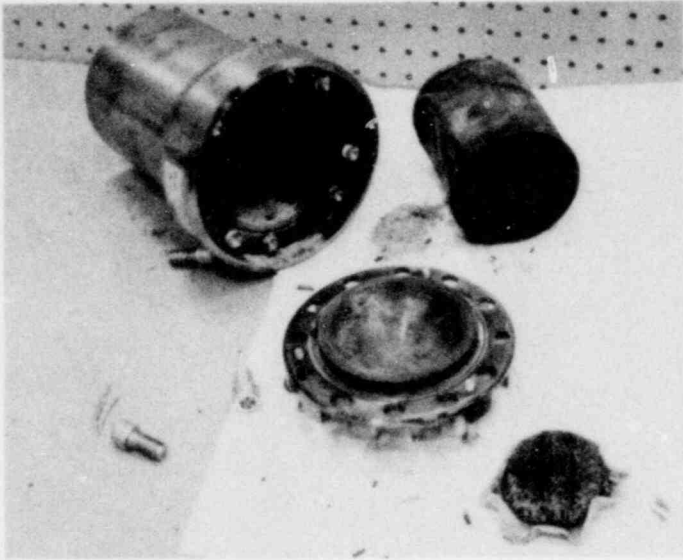


Figure 4C-7

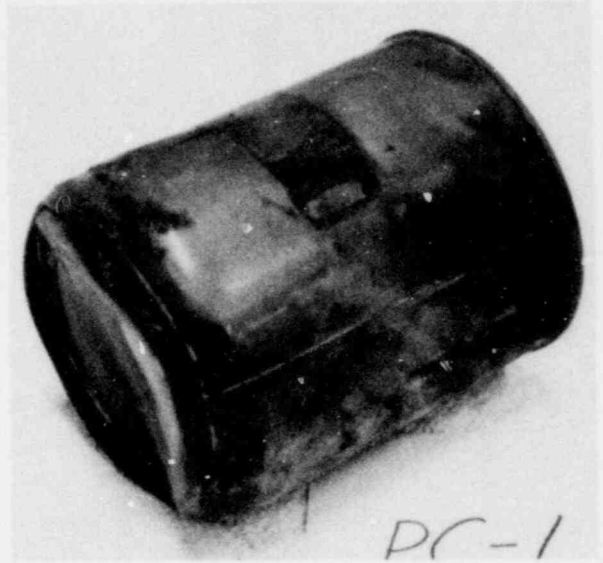


Figure 4C-8

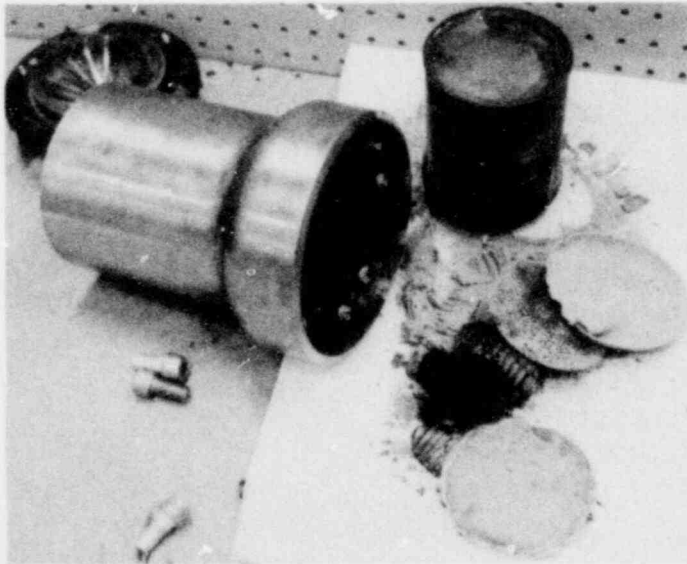


Figure 4C-9



Figure 4C-10

CHAPTER 5

RADIATION SHIELDING EVALUATION

5.1 Summary

The PAT-1 has been examined to determine the radiation environment external to the package when loaded with PuO_2 . A variety of isotopic mixtures of Pu have been considered and a specific mixture has been selected for use in determining the external dose rates. The source intensity for this mixture is unlikely to be exceeded by any real PuO_2 sample. The calculated dose rates, including the effect of ground scatter, indicate that the package meets all radiation requirements of 49 CFR 173.393 and 10 CFR 71.36. The calculated results for the normal operation and the post-accident radiation tissue dose rates are:

Normal Operation

Dose rate on the surface	Horizontal	30 mrem/hr
	Vertical	15 mrem/hr
Dose rate 3 ft from the surface	Horizontal	4 mrem/hr
	Vertical	1 mrem/hr

Postaccident Case

Dose rate 3 ft from the surface	Horizontal or Vertical	8 mrem/hr
---	---------------------------	-----------

5.2 Introduction

The purpose of this chapter is to show that the radiation levels external to the PAT-1 are within the regulatory limits set by 49 CFR 173 and 10 CFR 71.¹ The regulatory limit for normal operation specifies a maximum tissue dose rate of 10 mrem/hr at a distance of 3 ft (~ 1 m) from the accessible surface of the package and a maximum tissue dose rate of 200 mrem/hr on the surface of the package. The limit under accident conditions is 1000 mrem/hr at 3 ft from the package surface.

The radiation source in the PAT-1 is produced from the natural radioactivity of the Pu isotopes and their daughter products, from induced reactions with the oxygen in the PuO_2 , and from fissions induced in the Pu. The source strength is limited by the concurrent constraints assumed for the payload of the package: the mass of the PuO_2 may not exceed 3.15 kg and the thermal power of the payload may not exceed 25 W. The volume available for the payload is 1124 cm^3 .

1567 248

5.3 Source Definition

The thermal power and nuclear radiation emitted by the payload of the PAT-1 will depend on the isotopic mix of the plutonium. This, in turn, depends on the type of nuclear reactor, neutron flux and fluence, and uranium enrichment used to generate the Pu; the cooling time of the fuel prior to chemical extraction of the Pu; and the shelf life of the Pu after extraction. The neutron source strength also depends on the chemical form of the Pu, the oxide being more active than the metal per unit mass of Pu, and on the presence or absence of low-Z impurities such as B and F.

Generally the chemical extraction of Pu from its parent fuel results in relatively pure Pu. The presence of transplutonic actinides or of fission products, even in small quantities, would greatly increase the thermal and nuclear radiation sources in the Pu. In practice, levels of these materials in the extracted Pu are on the order of a few parts per million. The radiation environment for the PAT-1 has been considered only for "clean" Pu as has been produced in the past or is being produced at present (i. e., by the Purex process). The safeguard concept of using so-called "denatured" Pu, or of including selected fission products to increase the radiation source in order to thwart interveners (the Civex process), do not pertain in any way to the payload considered for the PAT-1.

The radiation characteristics of the different major isotopes of Pu and their daughter products, and their relative abundances in typical Pu mixtures, are discussed in Appendix 5A. Based upon the analysis described there, the range of PAT-1 source intensities from Pu-isotope mixtures that realistically could be expected to occur is somewhat limited. Therefore, a specific source has been selected for use in this study. No mixture of Pu isotopes that could be produced in quantity from existing sources, or from anticipated future sources, has been identified that would result in a significantly higher radiation source than that for the case selected. Additional conservatism in the source does not appear to be warranted.

The total neutron source strength for the selected isotopic mix, assuming the maximum payload in the PAT-1, is 2.1×10^6 n/s. About 20-30% of the neutrons emitted originate from spontaneous fission and 70-80% originate from (α, n) reactions. The actual division of the neutrons between the two sources varies with the shelf life of the sample. The energy spectrum of the spontaneous fission neutrons is well known² and is shown for specific energy-group structures in Section 5.4. The energy spectrum of the neutrons resulting from the (α, n) reaction varies with the energy of the α particle and the specific target nucleus. The neutron energy spectrum produced by the 5.5-MeV α from ^{238}Pu reacting with oxygen is given by Stoddard and Albenesius.³ The maximum neutron energy is given by Evans⁴ and by Arnold⁵ for a variety of reactions. The (α, n) neutron-energy spectrum used in this study is shown for a specific group structure in Section 5.4.

The gamma-ray source strength for the Pu-isotope mix selected for the present shielding study is shown in Table 5.3-1. This gamma source represents the maximum source identified in Appendix 5A and is based on 14.6-yr-old Pu (i. e., approximately one half-life of ^{241}Pu).

TABLE 5.3-1

Gamma-Ray Source Used in the Present Shielding Analysis

Energy Group	Average Energy (MeV)	Photons/s From Maximum Payload of Worst-Case PuO ₂
1	3.25	4.5×10^4
2	2.75	2.1×10^7
3	2.38	7.5×10^4
4	1.99	5.2×10^5
5	1.55	1.1×10^6
6	1.10	1.9×10^6
7	0.63	1.5×10^8
8	0.30	2.9×10^8
9	0.15	1.6×10^9
10	0.05	4.2×10^{12}

5.4 Shielding Calculations

A series of radiation-transport calculations was performed on the PAT-1 and the TB-1 to determine the radiation environments to be expected on the surface and 3 ft from the surface of the package. All one-dimensional calculations were performed with the ANISN discrete-ordinates code,⁶ Two-dimensional calculations were performed with the TWOTRAN-II discrete-ordinates code⁷ and with the MORSE-SGC Monte Carlo code.⁸ The geometries considered were as follows*:

a. One-Dimension, Normal Operation -- The PAT-1 was modeled in spherical geometry using layer thicknesses based on the minimum shielding path through the side of the package. For the neutron transport calculations, 3 ft of air was assumed external to the PAT-1 followed by a ~3-cm-thick water phantom. This geometry is shown in Figure 5.4-1 and Table 5.4-I. A water phantom is included in some of the present calculational models to account for perturbation of the radiation field by a human body. The results which include a water phantom are conservative since its effect is to increase the neutron dose rate slightly (~10%). No water phantom was used in the primary gamma-ray transport calculations because such a water phantom has very little effect on the gamma-ray dose rate.

*The discrete-ordinates (one- and two-dimensional) models were developed by S. H. Sutherland of Sandia Laboratories. Sutherland also performed the discrete-ordinates neutron and secondary-gamma transport calculations reported here.

This and the following three models assumed 2 kg of PuO_2 inside the TB-1 for the neutron transport calculations and 1.5 kg of PuO_2 for the gamma-ray transport calculations; the actual payload for the specific source used in the calculations was 1.5 kg. This represents the worst-case radiation source identified for the PAT-1 and is controlled by the 25 W thermal limit (see Appendix 5A). The payload mass has very little effect on the calculated neutron-dose rate but has a large effect on the calculated gamma-ray dose rate.

b. One-Dimension, Postaccident Conditions -- The worst case for a postaccident configuration of the PAT-1, based on the test results reported in Chapter 2, is for the outer surface of the TB-1 containment vessel to be located a few centimeters inside the crushed outer surface of the AQ-1 overpack. However, to simplify the postaccident model and ensure consideration of the worst-case conditions, a completely bare TB-1 was used for the postaccident dose-rate determination. The one-dimensional model consists of the TB-1 portion of Figure 5.4-1 surrounded by 3 ft of air. A water phantom was included for the neutron-transport calculations but not for the primary gamma-ray transport calculations. The geometry is shown in Table 5.4-II.

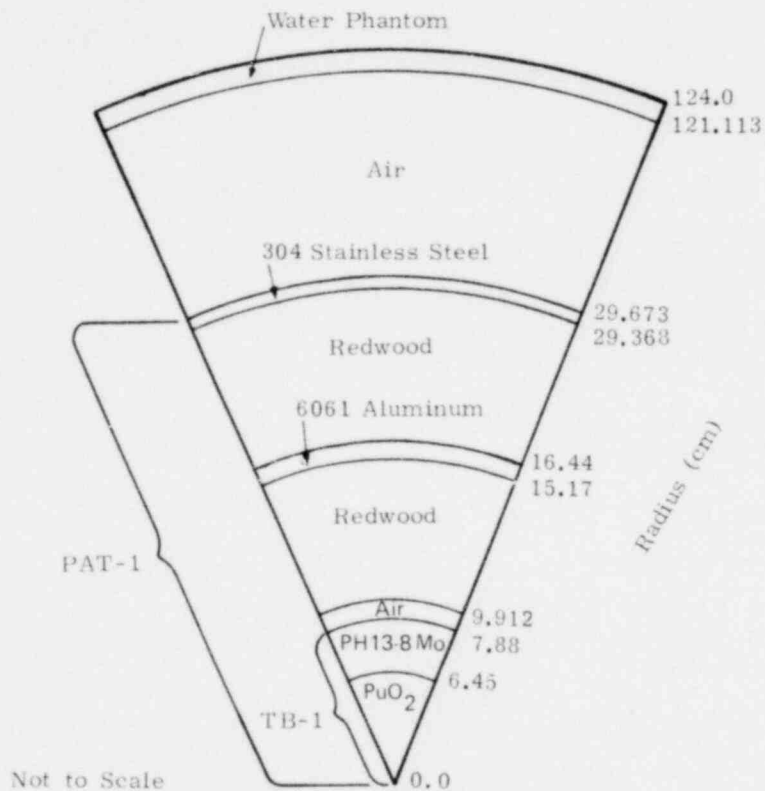


Figure 5.4-1. One-Dimensional Model of the PAT-1 (Normal Operation)

TABLE 5.4-I

One-Dimensional Model of the PAT-1 (Normal Operation)

Zone	Zone Outer Radius (cm)	Thickness (cm)	Material
1	6.450 ^a	6.450	PuO ₂
2	7.880	1.430 ^b	PH13-8 Mo stainless steel
3	9.912	2.032	Air gap
4	15.170	5.258 ^c	Redwood
5	16.440	1.270	6061 aluminum
6	29.368	12.928 ^c	Redwood
7	29.673	0.305	304 stainless steel
8	121.113	91.440	Air
9	124.000	2.887	Water

^aTB-1 volume 1124 cm³; contents of 2-kg PuO₂ used in the neutron transport calculations; 1.5-kg PuO₂ used in the primary gamma-ray transport calculations.

^bCombination of 0.033-cm-thick 304 stainless steel inner product can wall and 1.397-cm-thick PH13-8 Mo stainless steel TB-1 vessel wall.

^cIncludes two 0.152-cm-thick glue lines.

TABLE 5.4-II

One-Dimensional Model of the TB-1 (Postaccident Conditions)

Zone	Zone Outer Radius (cm)	Thickness (cm)	Material
1	6.450 ^a	6.450	PuO ₂
2	7.880	1.430 ^b	PH13-8 Mo stainless steel
3	99.320	91.440	Air
4	102.000	2.680	Water

^aTB-1 volume 1124 cm³; contents of 2-kg PuO₂ used in the neutron transport calculations; 1.5-kg PuO₂ used in the primary gamma-ray transport calculations.

^bCombination of 0.033-cm-thick 304 stainless steel inner product can wall and 1.397-cm-thick PH13-8 Mo stainless steel TB-1 vessel wall.

c. Two-Dimension Discrete-Ordinates Model, Normal Operation -- The finite (r, z) geometry of the TWOTRAN code was used to model the PAT-1 in an air-over-ground geometry. A substantially correct PAT-1 internal geometry was included as shown in Figure 5.4-2 and Table 5.4-III. This model was specifically developed to determine the effect on the external dose rates of the backscatter of neutrons in the ground. A water phantom was included both radially and axially. This introduces additional conservatism in the results by approximating a completely enclosed vault around the PAT-1. No primary gamma-ray transport calculations were performed using this model.

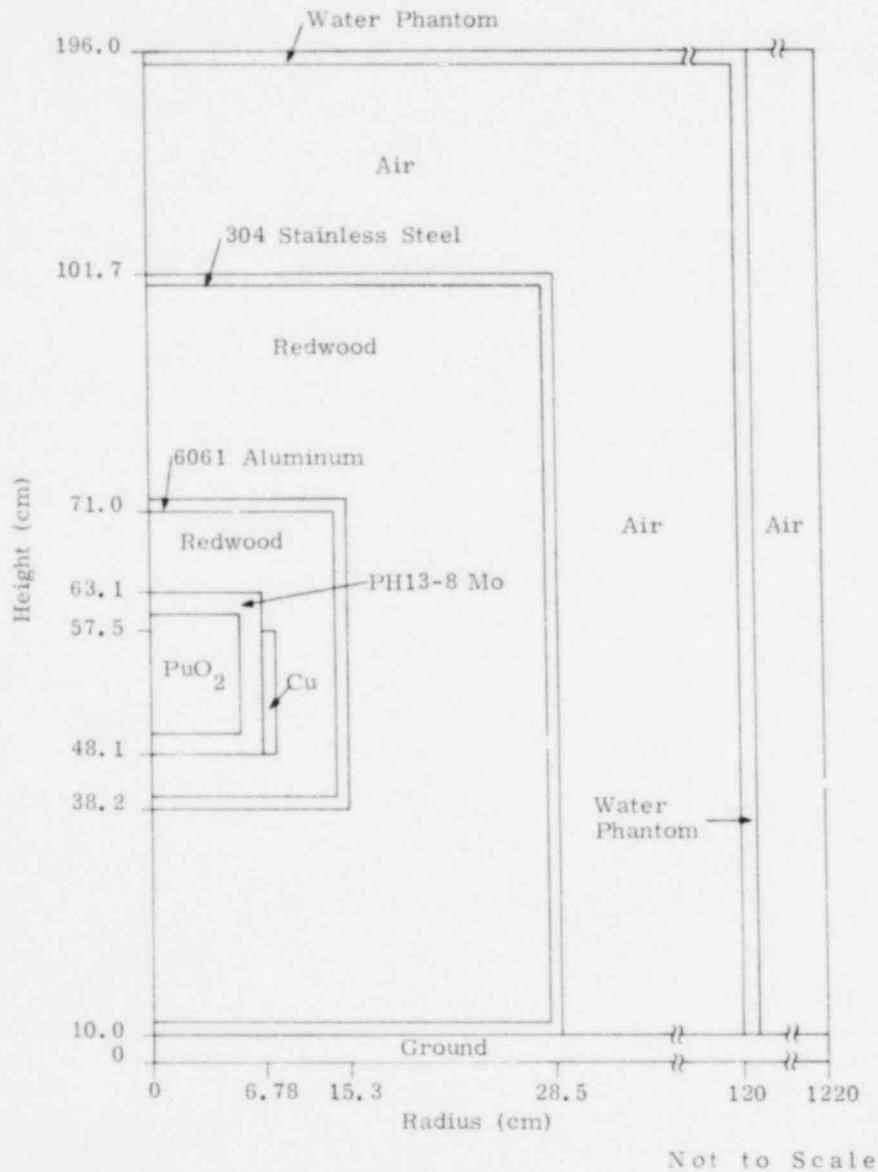


Figure 5.4-2. Two-Dimensional Discrete-Ordinates Model of the PAT-1 (Normal Operation) in an Air-Over-Ground Geometry

* All region boundaries are right circular cylinders.

TABLE 5.4-III

Two-Dimensional Discrete-Ordinates Model of the PAT-1
(Normal Operation) in an Air-Over-Ground Geometry

Radial Mesh			
Zone	Zone Outer Radius (cm)	Thickness (cm)	Material
1	5.3848	5.3848	PuO ₂ ^a
2	6.7818	1.3970	PH13-8 Mo stainless steel
3	7.5692	0.7874	Copper
4	14.0208	6.4516	Redwood
5	15.2908	1.2700	6061 aluminum
6	28.2194	12.9286	Redwood
7	28.5242	0.3048	304 stainless steel
8	119.9642	91.4400	Air
9	122.0	2.0358	Water
0	1220.0	1098.0	Air

Axial Mesh			
Zone	Zone Upper Boundary (cm)	Thickness (cm)	Material
1	10.0	10.0	Ground
2	10.3048	0.3048	304 stainless steel
3	38.1940	27.8892	Redwood
4	40.7340	2.5400	6061 aluminum
5	48.1254	7.3914	Redwood
6	49.5224	1.3970	PH13-8 Mo stainless steel
7	61.8612	12.7358	PuO ₂ ^a
8	63.0982	1.2370	PH13-8 Mo stainless steel
9	70.9976	7.8994	Redwood
10	73.5376	2.5400	6061 aluminum
11	101.4268	27.8892	Redwood
12	101.7316	0.3048	304 stainless steel
13	193.1716	91.4400	Air
14	196.0	2.282	Water

^aTB-1 volume 1124 cm³; contents of 2-kg PuO₂ used for self-shielding.

d. Two-Dimensional Discrete-Ordinates Model, Postaccident -- The bare TB-1 was modeled as a worst-case postaccident condition in an air-over-ground geometry. This model is shown in Table 5.4-IV. Neutron and secondary gamma-ray transport calculations were performed using this model.

e. Two-Dimensional Monte Carlo Model, Normal Operation -- A detailed model of the PAT-1, including a more accurate model of the TB-1 than was used in models 'c' and 'd', was developed in the MORSE combinatorial geometry. A cross section of the PAT-1 model, generated by the PICTURE code^{9,10} is shown in Figure 5.4-3. In addition to the PAT-1, the model included a 15-cm-thick ground underneath the package and 20 m of air both horizontally and vertically. No water phantom was used.

f. Two-Dimensional Monte Carlo Model, Postaccident -- The TB-1 portion of model 'e' was used over 15 cm of ground for the postaccident Monte Carlo calculations. This model also included 20 m of air horizontally and vertically.

TABLE 5.4-IV

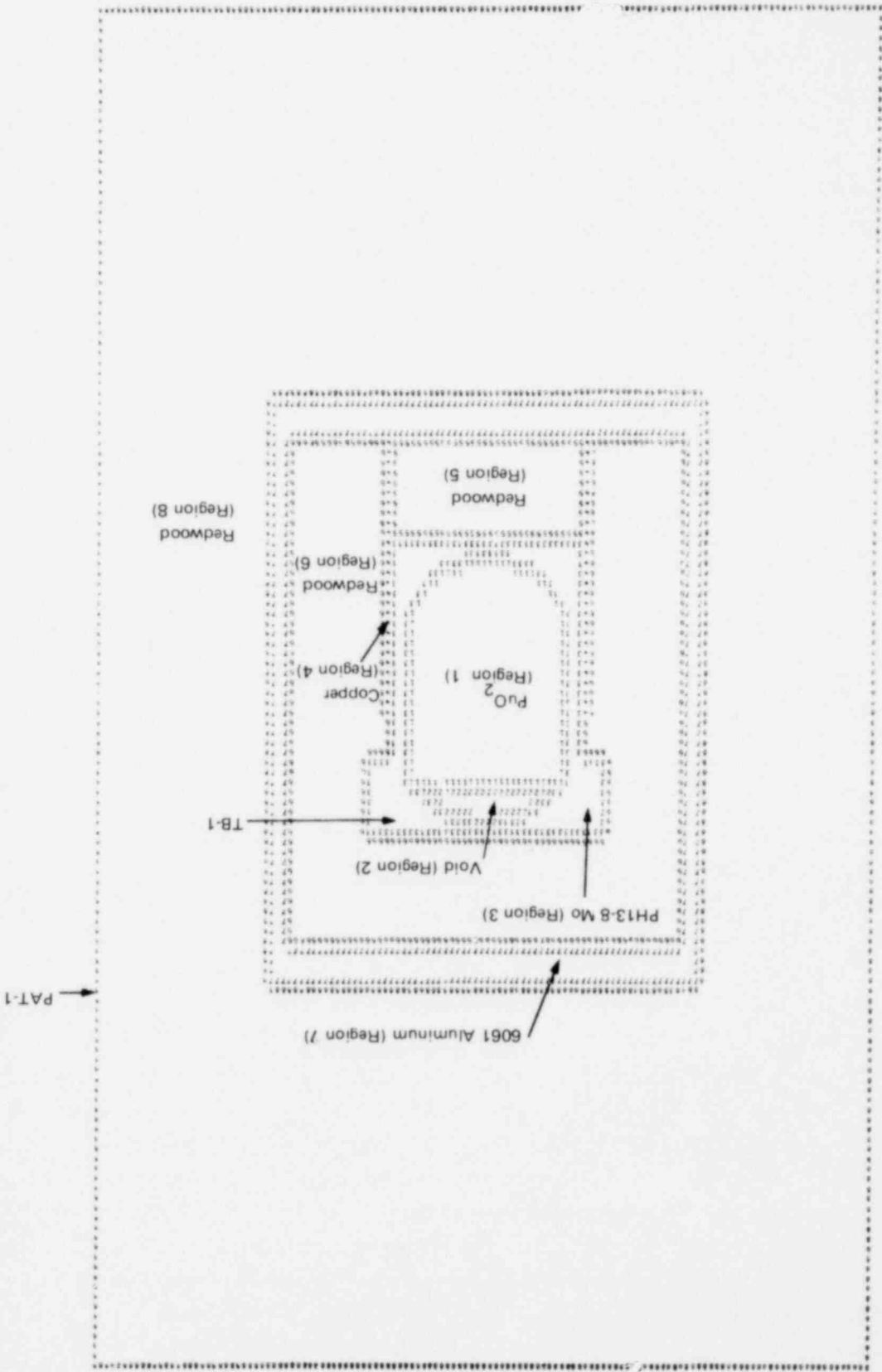
Two-Dimensional Discrete-Ordinates Model of the TB-1
(Postaccident Condition) in Air-Over-Ground Geometry

Radial Mesh			
Zone	Zone Outer Radius (cm)	Thickness (cm)	Material
1	5.385	5.385	PuO ₂ ^a
2	6.782	1.397	PH13-8 Mo stainless steel
3	98.222	91.440	Air
4	105.0	6.778	Water
5	1108.0	1003.0	Air

Axial Mesh			
Zone	Zone Upper Boundary (cm)	Thickness (cm)	Material
1	10.000	10.000	Ground
2	11.397	1.397	PH13-8 Mo stainless steel
3	23.736	12.339	PuO ₂ ^a
4	24.973	1.237	PH13-8 Mo stainless steel
5	116.413	91.440	Air
6	121.490	5.077	Water
7	1126.0	1004.510	Air

^aTB-1 volume 1124 cm³; contents of 2-kg PuO₂ used for self-shielding.

Figure 5.4-3. Picture Printout of the MORSE Monte Carlo Model of the PAT-1



The elemental compositions of the various materials used in the above models are shown in Table 5.4-V. The redwood composition was taken from the analyses of Matchette¹¹ and Erickson.¹² Only the major constituents (H, C, and O) were used in the calculations. The next most abundant element in redwood, Ca, has an atomic density of 8.7×10^{-7} atoms/b·cm. Although this Ca, along with other trace elements, will produce some secondary gamma radiation, its contribution will be negligible due to the extremely low atom densities involved. The compositions of 6061 aluminum and 304 stainless steel were taken from Ref. 13. The composition of PH13-8 Mo stainless steel is from Ref. 14. The soil composition was taken from Ref. 15 and represents extremely wet worst-case ground (30% water with a total density of 1.7 g/cm^3) based on data from Ref. 16.

TABLE 5.4-V

Elemental Compositions of Materials Used in Shielding Calculations

<u>Material</u>	<u>Density (g/cm³)</u>	<u>Composition (atoms/bar 1·cm)</u>	
PH13-8 Mo stainless steel	7.76	C	0.000195
		Al	0.001905
		Si	0.000166
		Cr	0.01168
		Fe	0.06304
		Ni	0.006368
Redwood	0.36	H	0.01242
		C	0.009131
		O	0.006034
6061 aluminum	2.70	Mg	0.000669
		Al	0.05825
		Si	0.000347
		Fe	0.000204
304 stainless steel	7.9	C	0.000317
		Si	0.001694
		Cr	0.01738
		Mn	0.001732
		Fe	0.05785
		Ni	0.008103
Soil	1.7	H	0.034
		O	0.0398
		Al	0.00881
		Si	0.00371
PuO ₂	1.33 ^a	²³⁹ Pu	0.002966
		O	0.005932

^aCorresponds to a payload of 1.5 kg PuO₂.

The calculations used several different PuO_2 compositions. The one-dimensional and two-dimensional discrete-ordinates neutron transport calculations assumed an oxide payload of 2 kg. Neutron self-multiplication from fissions in the oxide region was neglected in these calculations. Although the effect of including such fissions is small, they were included in the Monte Carlo calculations. The Monte Carlo neutron transport calculations assumed pure $^{239}\text{PuO}_2$ at maximum density (3.15 kg in 1124 cm^3) to maximize this self-multiplication. The Monte Carlo primary gamma-ray calculations assumed $^{239}\text{PuO}_2$ at the density of Case 2 of Table 5A-IV (1.5 kg in 1124 cm^3 , see Appendix 5A) in order to correctly account for the self-shielding of the gamma rays. The resulting atomic densities are shown in Table 5.4-V.

Four different cross-section sets were used for the various calculations reported here. Two separate sets were used to calculate simultaneous neutron and secondary gamma-ray transport. A third set was used for neutron transport only. Finally, the fourth cross-section set was used only for primary gamma-ray transport. The neutron (and neutron-induced gamma-ray) transport was separately analyzed from the primary gamma-ray transport because the energy spectrum of the secondary gamma rays is markedly different from that of the primary gamma rays. Significant computer time is saved without loss of accuracy by splitting the problem into two parts.

Most of the neutron and secondary gamma-ray calculations used a 20-group, P_3 set (12 neutron, 8 gammas, or '12-8') collapsed from the BUGLE¹⁷ set using the MALOCS¹⁸ code. The 12-8 group structure, tissue dose factors, and fission spectrum are shown in Table 5.4-VI. The dose factors for the cross-section sets were taken from Ref. 19.

The second cross-section set used in the present calculations was a 32-group, P_1 set (19 neutron, 13 gammas) collapsed from the DNA few-group library²⁰ using ANISN. The energy bounds, tissue dose factors, (α, n) neutron spectrum, and prompt-fission-neutron spectrum for this group structure are shown in Table 5.4-VII.

A single one-dimensional neutron dose rate calculation was performed using the 27-group, P_3 criticality library described in Chapter 6. Although not designed for shielding calculations, the library was used as a cross check on the accuracy of the smaller sets.

All primary gamma-ray transport calculations were performed using an 11-group, P_3 set generated with GAMLEG.²¹ The group bounds and tissue dose factors for this set are shown in Table 5.4-VIII. The energy bounds match those shown in Table 5A-I of Appendix 5A from group 5 through group 12.

*The results of the neutron transport calculations are not sensitive to the mass of the payload, its density, or its isotopic composition.

Table 5.4-VI

Group Structure and Data for the 12-8 Cross-Section Set

<u>Group Number</u>	<u>Upper Energy Bound (MeV)</u>	<u>Dose Factor</u> $\left(\frac{\text{mrem/hr}}{\text{particle/cm}^2 \cdot \text{s}}\right)$	<u>Fission Spectrum</u>
<u>Neutrons</u>			
1	17.33	0.1471	0.076
2	7.408	0.1559	0.186
3	2.725	0.1264	0.322
4	1.353	0.1308	0.161
5	0.863	0.1029	0.159
6	0.369	4.781×10^{-2}	0.073
7	0.111	1.514×10^{-2}	0.023
8	0.015	3.553×10^{-3}	0.0
9	1.234×10^{-3}	3.822×10^{-3}	0.0
10	1.013×10^{-4}	4.290×10^{-3}	0.0
11	1.068×10^{-5}	4.573×10^{-3}	0.0
12	4.140×10^{-7}	3.724×10^{-3}	0.0
	1.0×10^{-11}		
<u>Gammas</u>			
13	14.0	8.991×10^{-3}	
14	8.0	7.294×10^{-3}	
15	6.0	5.823×10^{-3}	
16	4.0	4.413×10^{-3}	
17	2.5	3.207×10^{-3}	
18	1.5	2.308×10^{-3}	
19	1.0	1.564×10^{-3}	
20	0.45	6.387×10^{-4}	
	0.01		

TABLE 5.4-VII

Group Structure and Data for the 19-13 Cross-Section Set

<u>Group Number</u>	<u>Upper Energy Bound (MeV)</u>	<u>Dose Factor</u> $\left(\frac{\text{mrem/hr}}{\text{particle/cm}^2 \cdot \text{s}}\right)$	<u>Fission Spectrum</u>	<u>(α, n) Spectrum</u>
		<u>Neutrons</u>		
1	10.0	0.1447	0.204	0.010
2	3.01	0.1268	0.236	0.321
3	1.83	0.1291	0.220	0.431
4	1.11	0.1162	0.196	0.178
5	0.55	0.0568	0.123	0.060
6	0.111	0.0179	0.021	0.0
7	5.25×10^{-2}	9.893×10^{-3}	0.0	0.0
8	2.48×10^{-2}	6.912×10^{-3}	0.0	0.0
9	2.19×10^{-2}	4.969×10^{-3}	0.0	0.0
10	1.03×10^{-2}	3.601×10^{-3}	0.0	0.0
11	3.35×10^{-3}	3.694×10^{-3}	0.0	0.0
12	1.23×10^{-3}	3.790×10^{-3}	0.0	0.0
13	5.83×10^{-4}	4.015×10^{-3}	0.0	0.0
14	1.01×10^{-4}	4.275×10^{-3}	0.0	0.0
15	2.90×10^{-5}	4.451×10^{-3}	0.0	0.0
16	1.07×10^{-5}	4.522×10^{-3}	0.0	0.0
17	3.06×10^{-6}	4.482×10^{-3}	0.0	0.0
18	1.13×10^{-6}	4.317×10^{-3}	0.0	0.0
19	4.14×10^{-7}	3.724×10^{-3}	0.0	0.0
	1.0×10^{-11}			
		<u>Gammas</u>		
20	14.0	8.991×10^{-3}		
21	8.0	7.634×10^{-3}		
22	7.0	6.899×10^{-3}		
23	6.0	6.155×10^{-3}		
24	5.0	5.388×10^{-3}		
25	4.0	4.578×10^{-3}		
26	3.0	3.625×10^{-3}		
27	2.0	2.926×10^{-3}		
28	1.5	2.308×10^{-3}		
29	1.0	1.736×10^{-3}		
30	0.7	1.125×10^{-3}		
31	0.3	5.297×10^{-4}		
32	0.1	5.822×10^{-4}		
	0.01			

TABLE 5.4-VIII

Group Structure and Data for the 11-Group Gamma-Ray Cross-Section Set

<u>Group Number</u>	<u>Upper Energy Bound (MeV)</u>	<u>Dose Factor</u> $\left(\frac{\text{mrem/hr}}{\text{gamma/cm}^2 \cdot \text{s}} \right)$
1	3.5	4.36×10^{-3}
2	3.0	4.00×10^{-3}
3	2.6	3.71×10^{-3}
4	2.2	3.24×10^{-3}
5	1.8	2.77×10^{-3}
6	1.35	2.30×10^{-3}
7	0.9	1.51×10^{-3}
8	0.4	0.83×10^{-3}
9	0.2	0.36×10^{-3}
10	0.1	0.37×10^{-3}
11	0.01	0.37×10^{-3}
	0.001	

Neutron dose-rate calculations were performed using both the prompt-fission source energy spectrum and the (α, n) energy spectrum. The difference in the external dose rate per source neutron was small for the two cases. The primary gamma-ray dose rate calculations used the source spectrum for Case 2 of Table 5A-IV for a 14.6-yr (one ^{241}Pu half-life) shelf life. This source spectrum is shown in Table 5.3-I.

5.5 Results

A number of radiation-transport calculations have been performed on the PAT-1 using the computer codes, cross sections, and geometries described in Section 5.4. As expected, the dose rates determined from two-dimensional calculations excluding the ground were lower than the worst-case one-dimensional results. However, ground scatter contributed significantly to the neutron dose rate at the side of the PAT-1; the two-dimensional results, which included this effect, were found to give the highest external dose rates obtained in this analysis. These results, then, based on the Case 2 source of Table 5A-IV (Appendix 5A), reflect the worst-case radiation environments for the PAT-1. The calculated total dose rates are shown in Table 5.5-I.

In the undamaged PAT-1, the amount of material located above or below the TB-1 greatly exceeds the amount located radially outside of the source. The top and bottom results in Table 5.5-I

reflect this additional shielding. The postaccident geometry is governed by the wall thickness of the TB-1, which is fairly uniform except for the thick flange at the top. Calculations without ground scatter included have shown very little difference between the dose rates produced in the radial or axial directions for the bare TB-1. When ground scatter is included, the dose rate at 3 ft is larger to the side of the TB-1 than overhead. Only this worst-case result is given for the postaccident case. All of the dose rates shown in Table 5.5-I are well within the regulatory requirements and Qualification Criteria for the PAT-1.

TABLE 5.5-I

Total Dose Rates External to the PAT-1 (in mrem (tissue)/hr)

Normal Operation				Postaccident
Dose Rate on Surface		Dose Rate at 3 ft		Dose Rate at 3 ft
Side	Top or Bottom	Side	Top or Bottom	Side
30	15	4	1	8

Tables 5.5-II and 5.5-III show a relatively complete matrix of results from the calculations performed and indicate the breakdown of the dose rates into neutron, secondary gamma-ray, and primary gamma-ray contributions. As mentioned in Section 5.4, use of the (α, n) spectrum results in a higher external neutron dose rate per source neutron than use of the fission spectrum, but the effect is small at 3 ft from the surface of the container. The one-dimensional neutron results are in good agreement with the two-dimensional results on the surface of the package, but the ground scatter effects greatly increase the neutron-dose component 3 ft radially outward from the package. The primary gammas are also increased by the ground scatter. Neither the neutron nor the gamma dose rates 3 ft vertically above the package are significantly affected by the ground.

The summary results of Table 5.5-I are taken from the worst-case results of Tables 5.5-II and 5.5-III. Specifically, the maximum dose rate during normal operation at 3 ft from the package surface is 2.4 mrem/hr from neutrons (two-dimensional Monte Carlo result plus one standard deviation; secondary gamma-rays are negligible) plus 1.1 mrem/hr from primary gamma rays (two-dimensional Monte Carlo result plus one standard deviation). The sum, 3.5, was rounded up to 4 as shown in Table 5.5-I. The one-dimensional result is the worst case for the dose rate on the radial surface of the PAT-1 during normal operation. The dose rates on the top surface and at 3 ft above the top surface were estimated by summing the one-dimensional primary gamma dose rates (11 and 0.6 mrem/hr, respectively) and the two-dimensional discrete-ordinates neutron and secondary-gamma results (3.6 and 0.6 mrem/hr, respectively). Finally, the postaccident dose rate at 3 ft was taken from the Monte Carlo results (plus one standard deviation) and again rounded to an integer.

1567 262

TABLE 5.5-II

Calculated Dose Rates External to the PAT-1 (Normal Operation)

One-Dimensional Results			Discrete Ordinates Two-Dimensional Results (ground scatter included)			Monte Carlo Two-Dimensional Results (ground scatter included)			
Source		Dose Rate (mrem/hr)	Source		Dose Rate (mrem/hr)				
Source Spectrum	Cross-Section Set				Side	Top			
Neutron			Neutron			n/a			
(Fission source spectrum, 12-8 cross sections)									
α, n	19-13	18			19	3.6			
α, n	12-8	20							
α, n	27	20							
Fission	19-13	14							
Secondary Gamma Ray (all spectral cases)			Secondary Gamma Ray			0.2	nil		
Primary Gamma Ray			Primary Gamma Ray			n/a	n/a		
Worst-Case Total		11	Worst-Case Total		30				

Source		Dose Rate (mrem/hr)	Source		Dose Rate (mrem/hr)		Source		
Source Spectrum	Cross-Section Set				Side	Top	Side	Top	
Neutron			Neutron			Neutron			
(Fission source spectrum, 12-8 cross sections)			(Fission source spectrum, 12-8 cross sections)			(Fission source spectrum, 12-8 cross sections)			
α, n	19-13	1.1			1.8	0.6	2.1 ± 0.3	n/a	
α, n	12-8	1.2							
α, n	27	1.2							
Fission	19-13	1.0							
Secondary Gamma Ray (all spectral cases)			Secondary Gamma Ray			nil	nil	0.03 ± 0.004	n/a
Primary Gamma Ray			Primary Gamma Ray			n/a	n/a	1.0 ± 0.1	0.2 ± 0.1
Worst-Case Total		0.6	Worst-Case Total		1.8		Total	3.1 ± 0.4	

Dose Rate
on the Surface
of the PAT-1Dose Rate at
3 ft From the
Surface of the
PAT-1

TABLE 5.5-III

Calculated Dose Rates External to the PAT-1 (Postaccident Configuration)

One-Dimensional Results			Discrete Ordinates Two-Dimensional Results (ground scatter included)			Monte Carlo Two-Dimensional Results (ground scatter included)		
Source		Dose Rate (mrem/hr)	Source		Dose Rate (mrem/hr) Side	Top		
Dose Rate on the Surface of the TB-1			Neutron			n/a		
Source Spectrum	Cross- Section Set		(Fission source spectrum, 12-8 cross sections)	350	340			
α, n	19-13	400						
Secondary Gamma Ray		nil	Secondary Gamma Ray	2	4			
Primary Gamma Ray		<u>270</u>	Primary Gamma Ray	n/a	n/a			
Total		670						
-----			-----			-----		
Dose Rate at 3 ft From the Surface of the TB-1			Neutron			Neutron		
Source Spectrum	Cross- Section Set	Dose Rate (mrem/hr)	(Fission source spectrum, 12-8 cross sections)			Dose Rate (mrem/hr) Side	Top	
α, n	19-13	1.9		n/a		5.3 ± 0.9	1.1 ± 0.2	
Secondary Gamma Ray		nil				0.03 ± 0.01	$(2.0 \pm 0.3) \times 10^{-3}$	
Primary Gamma Ray		<u>1.4</u>				<u>2.0 ± 0.1</u>	<u>0.3 ± 0.1</u>	
Total		3.3				Total	7.3 ± 1.0	1.4 ± 0.3

1567 264

The uncertainties in the results presented here stem from uncertainties in (1) the source terms; (2) the cross sections used; (3) the accuracy to which the computer models simulate the true PAT-1 geometry and material compositions; and (4) the accuracy of the computer solutions with regard to convergence, the finite-difference approximation, and the Monte Carlo statistics. Of these, the largest uncertainty is in the source definition. For the PAT-1 application a conservative source has been used and a realistic range of uncertainty is probably +25%, -90%.^{*} The cross sections used are based on the best available data and the cross sections for the specific materials used in the PAT-1 construction are reasonably well known; their probable uncertainty is $\pm 20\%$. The error in the computer solution is small-- $\pm 5\%$ for the discrete-ordinates calculations. Uncertainties in the Monte Carlo results are shown in Tables 5.5-II and 5.5-III and are included in the results reported in Table 5.5-1.

Including the cumulative uncertainties and ground scatter effects, the present analysis shows that the PAT-1 meets all regulatory requirements on radiation dose rates external to the package.

* No minimum loading is specified for the PAT-1, hence the lower limit in the source intensity is zero. In a practical sense, however, the smallest full-payload source identified in Appendix 5A is approximately 10% of the source used in the calculations described. Hence, a downside uncertainty of 90% is considered realistic.

References

1. Code of Federal Regulations, Title 49, paragraph 173. and Title 10, paragraph 71.
2. W. E. Selph and C. W. Garrett, "Sources of Radiation," Reactor Shielding for Nuclear Engineers, N. M. Schaeffer, ed., TID-25951, US Atomic Energy Commission, Office of Information Services, 1973, p 54.
3. D. H. Stoddard and E. L. Albenesius, "Radiation Properties of ^{238}Pu Produced for Isotopic Power Generators," DP-984, E. I. Du Pont de Nemours and Co., Savannah River Laboratory, Aiken, SC, 1965.
4. R. D. Evans, The Atomic Nucleus, McGraw Hill, New York, 1955, p 411.
5. E. D. Arnold, "Neutron Sources," Engineering Compendium on Radiation Shielding for Nuclear Engineers, R. G. Jaeger, ed., Vol. I, p 30, Springer-Verlag, NY, 1968.
6. W. W. Engle, Jr., "A User's Manual for ANISN," K-1693, Union Carbide Corp., Oak Ridge, TN, 1967.
7. K. D. Lathrop and F. W. Brinkley, "TWO TRAN-II: An Interfaced, Exportable Version of the TWO TRAN Code for Two-Dimensional Transport," LA-4848-MS, Los Alamos Scientific Laboratory, Los Alamos, NM, 1973.
8. S. K. Fraley, "User's Guide to MORSE-SGC," ORNL/CSD-7, Oak Ridge National Laboratory, Oak Ridge, TN, 1976.
9. D. C. Irving and G. W. Morrison, "PICTURE: An Aid in Debugging GEOM Input Data," ORNL-TM-2892, Oak Ridge National Laboratory, Oak Ridge, TN, 1970.
10. E. A. Straker, W. H. Scott, Jr., and N. R. Byrn, "The MORSE Code with Combinatorial Geometry," DNA 2860T, Science Applications, Inc., La Jolla, CA, 1972.
11. E. E. Matchette, Bendix Corp., Kansas City, MO, Ltr to J. A. Andersen, Sandia Laboratories, Albuquerque, NM, Aug. 2, 1976.
12. S. L. Erickson, "Analyses of PARC Redwood," Sandia Laboratories, Albuquerque, NM, Memo to J. A. Andersen, Aug. 5, 1973.
13. Metals Handbook, 8th Edition, Vol. I, "Properties and Selection of Metals," Taylor Lyman-Ed., American Society for Metals, Metals Park, OH, 1975.
14. Aerospace Materials Specification AMS-5629, Society of Automotive Engineers, Warrendale, PA.
15. J. E. Campbell and H. A. Sandmeier, "Radiation Transport in Air Over Ground and Air Over Seawater," NWEF-1102, Naval Weapons Evaluation Facility, Albuquerque, NM, 1973.
16. E. A. Straker, "The Effect of the Ground on the Steady-State and Time-Dependent Transport of Neutrons and Secondary Gamma Rays in the Atmosphere," Nucl Sci Eng 46, 334 (1971).

17. "BUGLE Coupled 45 Neutron, 16 Gamma-Ray, P3, Cross Sections for Studies by the ANS 6.1.2 Shielding Standards Working Group on Multigroup Cross Sections," DLC-47, Radiation Shielding Information Center, Oak Ridge, TN, 1977.
18. N. M. Greene, J. L. Lucius, L. M. Petrie, W. E. Ford, III, J. E. White, and R. Q. Wright, "AMPX: A Modular Code System for Generating Coupled Multigroup Neutron-Gamma Libraries from ENDF/B," ORNL/TM-3706, Oak Ridge National Laboratory, Oak Ridge, TN, 1977.
19. "American National Standard Neutron and Gamma-Ray Flux-to-Dose-Rate Factors," ANSI/ANS-6.1.1-1977 (N666), American Nuclear Society, Standards Committee, Working Group ANS-6.1.1, 1977.
20. D. E. Bartine, J. R. Knight, J. V. Pace III, and R. Roussin, "Production and Testing of the DNA Few Group Coupled Neutron-Gamma Cross-Section Library," ORNL/TM-4840, Oak Ridge National Laboratory, Oak Ridge, TN, 1977.
21. J. H. Renken and K. G. Adams, "An Improved Capability for Solution of Photon Transport Problems by the Method of Discrete Ordinates," SC-RR-69-739, Sandia Laboratories, Albuquerque, NM, 1969.

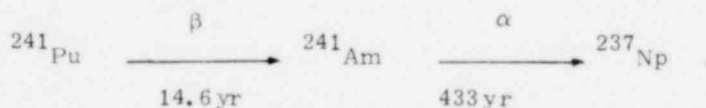
APPENDIX 5A

Derivation of Worst-Case Source Terms for the PAT-1

The radiation source originating within a given sample of PuO₂ depends upon the isotopic composition of the Pu at the time it was removed from its source fuel and the shelf life of the Pu after such removal. Determination of a realistic worst-case source for the PAT-1 therefore requires consideration of these variables and their quantitative impact on the source.

The radiation and thermal source strengths for Pu composed initially of pure isotopes are shown in Figures 5A-1 through 5A-3 as a function of shelf life; i. e., the length of time since the purification of the Pu. The results are based upon 1 kg of each isotope initially present; thus, the source in any actual sample of Pu will be given by the sum of this source per isotope times the mass (in kg) of the isotope initially in the sample.*

The most striking result shown in Figure 5A-1 is the increasing thermal source from the buildup of daughter products of ²⁴¹Pu as a function of shelf life. This increase is caused by the decay chain



The ²³⁷Np daughter product is long lived (half-life ~ 2.1 x 10⁶ yr) and it and its daughter products do not contribute to the buildup of the radiation-source strength. The 433-yr half-life of the ²⁴¹Am coupled with its high thermal-source strength, however, causes the decay heat from a sample of Pu, initially composed solely of ²⁴¹Pu, to reach a maximum after a shelf life of about 74 yr.¹ This maximum is more than an order of magnitude larger than the thermal source from the same mass of ²⁴¹Pu and its daughter products at a shelf life of one year. Thus, depending upon its isotopic mix at zero shelf life, the thermal source from a sample of Pu may increase with shelf life for the first 70 yr or so after extraction from its parent fuel. A quantity of PuO₂ that meets the PAT-1 25-W thermal limit at some point in time may therefore exceed the limit after further shelf life. Thus, using a PAT-1 to store PuO₂ for extended periods should be undertaken with caution.

* Small quantities of ²⁴⁴Pu are generated in nuclear reactors, but the total quantity produced is typically 6-7 orders of magnitude less than the quantity of ²³⁶Pu generated.

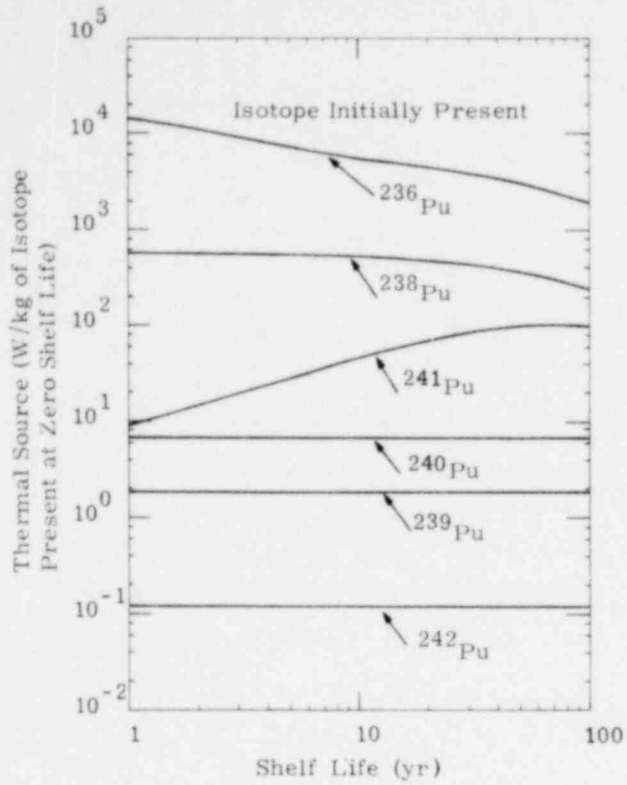


Figure 5A-1. Calculated Thermal Power Emitted by Pu Samples Consisting Initially of Pure Isotopes

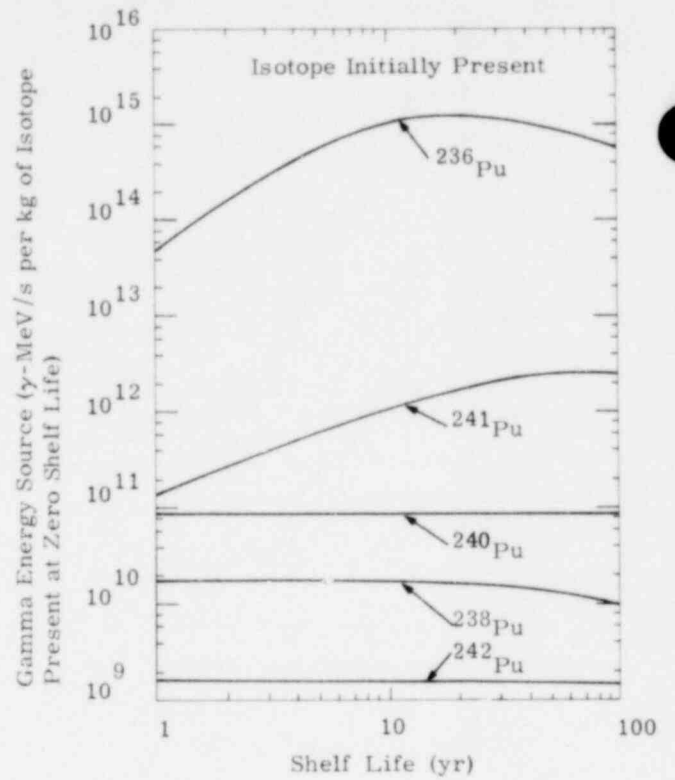


Figure 5A-2. Calculated Gamma-Ray Energy-Emission Rate From Samples of Pu Consisting Initially of Pure Isotopes

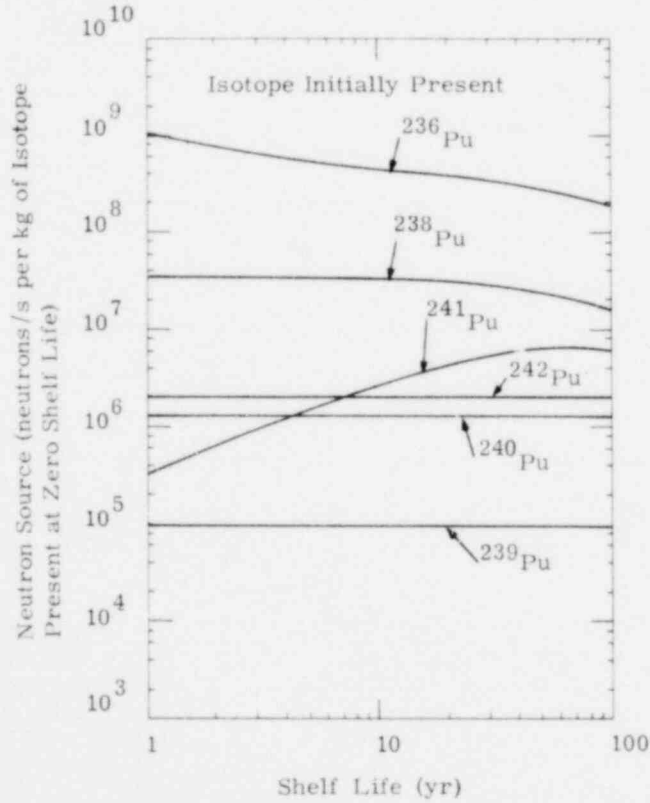
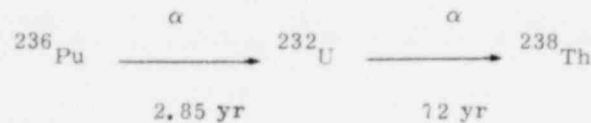


Figure 5A-3. Calculated Neutron-Emission Rate From Samples of Pu Consisting Initially of Pure Isotopes

The total gamma-ray energy-emission rate for Pu composed initially of a pure isotope is shown in Figure 5A-2. * ^{239}Pu and its daughter products are very low-intensity sources of gamma rays compared with those shown, emitting $\sim 10^8 \gamma\text{-MeV/s/kg}$ over the shelf life range shown. As was found for the total thermal power, the gamma source of an initially pure ^{241}Pu sample increases with shelf life due to the buildup of ^{241}Am , reaching a maximum after about 74 yr. In addition, the gamma source from an initially pure ^{236}Pu sample increases with time. The buildup from this latter isotope is caused by the decay chain which begins



The daughter products of ^{232}U are all short lived compared with 72y. Thus, the gamma source from ^{236}Pu and its daughter products reaches a maximum after a shelf life of approximately 14 yr.¹ The major gamma emitters in the ^{236}Pu decay chain are ^{212}Pb and ^{208}Tl .

Figure 5A-2 gives the total energy emitted per second in the form of gamma rays by Pu composed initially of a pure isotope. However, the energy of the gamma photons emitted must be known in order to determine which gamma rays from a particular isotope are capable of penetrating a given amount of shielding. The energy spectra of the gamma rays emitted by the initially pure Pu samples are shown in Table 5A-I.** The intensities shown reflect a shelf life of one ^{241}Pu half-life or 14.6 yr. The energy-group structure is that used in the ORIGEN² code. All gammas above group 6 ($E > 3 \text{ MeV}$) are from spontaneous fission.[†] The intensity of these gamma rays is extremely low and their presence can be neglected. The very large photon-source intensities below 150 keV are likewise of little importance in shielding analyses due to their low penetrating power.

Table 5A-I shows that not only does ^{236}Pu and its daughter products produce the greatest gamma-energy emission rate per unit mass of Pu isotope present at zero shelf life, but that these gammas are much more penetrating, on the average, than those of any of the other Pu isotopes and their daughter products. Thus, even small quantities of ^{236}Pu in a sample might contribute significantly to the total gamma source in the sample.

* Only gamma rays with energies above 20 keV are included in this analysis. Low energy x-rays are abundant in Pu but are easily shielded.

** Gamma-ray sources and spectral data are taken from the ORIGEN² data library as compiled by the Oak Ridge National Laboratory and released through the Radiation Shielding Information Center, ORNL (CCC-217). See also Heath,³ Stoddard and Albenesius,⁴ and Matlack and Metz.⁵

† Although ^{236}Pu and ^{239}Pu do undergo spontaneous fission,⁶ their rates are low and their high-energy gamma sources are much less than those shown for ^{238}Pu , ^{240}Pu , and ^{242}Pu .

TABLE 5A-1

Gamma-Ray Emission Spectra for the Major Isotopes of Plutonium and Their Daughter Products

Energy Group	Average Energy (MeV)	Gamma-Emission Rate at a Shelf Life of 14.6 yr (Photon/s/kg of Each Pu Isotope Present at Zero Shelf Life)					
		²³⁶ Pu	²³⁸ Pu	²³⁹ Pu	²⁴⁰ Pu	²⁴¹ Pu	²⁴² Pu
1	5.25	0.0	1.1×10^4	0.0	4.7×10^3	0.0	9.0×10^3
2	4.7	0.0	1.8×10^4	0.0	7.4×10^3	0.0	1.4×10^4
3	4.22	0.0	3.9×10^4	0.0	1.6×10^4	0.0	3.0×10^4
4	3.7	0.0	6.1×10^4	0.0	2.5×10^4	0.0	4.8×10^4
5	3.25	0.0	9.5×10^4	0.0	3.9×10^4	0.0	7.5×10^4
6	2.75	2.3×10^{14}	5.8×10^5	0.0	6.2×10^4	0.0	1.2×10^5
7	2.38	0.0	7.5×10^5	0.0	1.3×10^5	0.0	2.6×10^5
8	1.99	4.2×10^{12}	1.0×10^6	0.0	2.7×10^5	0.0	5.2×10^5
9	1.55	8.7×10^{12}	4.0×10^6	0.0	5.1×10^5	0.0	9.8×10^5
10	1.10	1.7×10^{13}	1.8×10^6	0.0	7.5×10^5	0.0	1.4×10^6
11	0.63	5.3×10^{14}	5.0×10^8	1.4×10^7	5.4×10^6	5.5×10^8	7.0×10^6
12	0.30	2.7×10^{14}	1.3×10^7	4.7×10^7	8.0×10^5	1.6×10^9	1.5×10^6
13	0.20	6.7×10^{14}	2.4×10^7	9.4×10^6	4.0×10^5	1.1×10^{10}	7.6×10^5
	$\sim 0.05^*$	1.9×10^{14}	2.6×10^{11}	2.3×10^8	2.2×10^{12}	2.4×10^{13}	3.9×10^{10}

* Photons with energies less than 20 keV are neglected.

Figure 5A-3 shows the neutron source by Pu isotope present at zero shelf life assuming an oxide matrix. The neutrons are produced by spontaneous fission and by (α, n) reactions with oxygen, particularly the reaction $^{17}\text{O}(\alpha, n)^{20}\text{Ne}$. The plotted results are for the sum of these two sources. The (α, n) neutrons have a slightly higher average energy than the spontaneous fission neutrons⁴ (~ 2.5 MeV compared with ~ 1.5 MeV). The portion of the total neutron source contributed by the two processes varies with the isotope undergoing spontaneous fission and/or α decay as shown in Table 5A-II. Because ^{232}U and ^{241}Am are important daughters of ^{236}Pu and ^{241}Pu , respectively, they are included in the table. It is apparent that the buildup of ^{232}U and ^{241}Am does not change the relative strength of the two neutron-source components. Most of the neutrons produced by the three dominant isotopes and their daughter products shown in Figure 5A-3 (initially pure ^{236}Pu , ^{238}Pu , and ^{241}Pu) are from (α, n) reactions.

TABLE 5A-II

Contributions of Spontaneous Fission and (α, n) Reactions
to Neutron Sources in the Major Pu Isotopes,
 ^{232}U , and ^{241}Am

Isotope	Fraction of Neutrons Due to	
	Spontaneous Fission	(α, n)
^{232}U	~ 0	~ 1.0
^{236}Pu	~ 0	~ 1.0
^{238}Pu	0.06	0.94
^{239}Pu	~ 0	~ 1.0
^{240}Pu	0.73	0.27
^{241}Pu	0	1.0
^{242}Pu	> 0.99	< 0.01
^{241}Am	~ 0	~ 1.0

The maximum neutron and gamma-ray source strengths per watt of thermal power of the major Pu isotopes and their daughter products are shown in Table 5A-III. The gamma ratios are taken at 14 and 70 yr of shelf life for initially pure ^{236}Pu and ^{241}Pu , respectively; the neutron ratio is taken at 70 yr for ^{241}Pu . All other ratios are taken at zero shelf life. Although this table does not apply to an actual payload that might be loaded into a PAT-1, it is informative concerning upper limit sources attainable in the PAT-1. The maximum source possible in a

PAT-1, assuming a payload consisting initially of each of the pure isotopes, is shown. Because of its very low power density and relatively high spontaneous-fission rate, ^{242}Pu at zero shelf life produces the highest neutron source achievable within the PAT-1 payload mass and thermal power restrictions. Correspondingly, the high gamma-source strength from the ^{236}Pu daughter products makes a payload based upon this isotope the worst case for gammas despite the high thermal-power density of the sample and its correspondingly small payload. Furthermore, from Table 5A-I it is apparent that the gamma radiation from the ^{236}Pu daughter products is the most penetrating emitted by any of the Pu decay chains, making this clearly the worst case for gamma rays.

TABLE 5A-III

Maximum Source Densities for the Major Plutonium Isotopes and Their Daughter Products

Isotope Present at Zero Shelf Life	Maximum Payload in PAT-1 ^a (kg of oxide)	Neutron Source			Gamma-Ray Source		
		Neutrons/s/kg	Neutrons/s/W of Thermal Power	Maximum Neutron/s Achievable ^b	γ -MeV/s/kg	γ -MeV/s/W of Thermal Power	Maximum γ -MeV/s Achievable ^b
^{236}Pu	1.7×10^{-3}	1.0×10^9	6.7×10^4	1.7×10^6	1.2×10^{15}	8.1×10^{10}	2.0×10^{12}
^{238}Pu	4.5×10^{-2}	3.5×10^7	6.2×10^4	1.6×10^6	1.7×10^{10}	3.0×10^7	7.6×10^8
^{239}Pu	3.15	9.5×10^4	5.0×10^4	3.0×10^5	9.0×10^7	4.7×10^7	2.8×10^8
^{240}Pu	3.15	1.3×10^6	1.9×10^5	4.1×10^6	8.9×10^{10}	1.3×10^{10}	3.8×10^{11}
^{241}Pu	0.25	6.2×10^6	6.2×10^4	1.6×10^6	2.6×10^{12}	2.6×10^{10}	6.5×10^{11}
^{242}Pu	3.15	2.0×10^6	1.6×10^7	6.3×10^6	1.5×10^9	1.4×10^{10}	4.7×10^9

^aMaximum source achievable is limited by the PAT-1 payload capacity of 3.15 kg of oxide or 25 W, whichever is reached first. For a power density of 7.9 W/kg or less, the full payload of 3.15 kg is possible.

Having examined the radiation source from hypothetical samples composed initially of pure isotopes of Pu, one can combine the results according to actual isotope mass fractions at zero shelf life to determine the source for any given sample of Pu. Isotopic enrichment is not practiced on bulk quantities of Pu. The initial isotopic mixture is therefore determined by the environment used to generate the Pu and the cooling time prior to chemical extraction of the Pu. A wide diversity of isotopic compositions is readily available. A few of the possible mixtures are shown in Table 5A-IV. The results shown in this table by no means exhaust the conceivable mixtures of Pu isotopes; however, they do provide a representative sampling of possible mixtures.

TABLE 5A-IV

Possible Isotopic Mixtures of Plutonium

Case No.	Mass Fractions of Pu Isotopes at Zero Shelf Life						
	1	2	3	4	5	6	7
Isotopes	Low Burnup (11 MWd/kg) LWR Spent Fuel ^a (3.3% ²³⁵ U enriched)	High Burnup (33 MWd/kg) LWR Spent Fuel ^a (3.3% ²³⁵ U enriched)	Hanford Pu (from low- enriched U, burnup 3 MWd/kg)	FFTF Recycle Pu ^b	CRBR Recycle Pu ^c	U-Recycle LWR Spent Fuel ^d (nominal)	U- and Pu- LWR Spent Fuel ^d (nominal)
²³⁶ Pu	$8 \times 10^{-10} - 8 \times 10^{-9}$	$7 \times 10^{-9} - 7 \times 10^{-8}$	2×10^{-8}	$3 \times 10^{-10} - 5 \times 10^{-9}$	$7 \times 10^{-10} - 2 \times 10^{-8}$	$8 \times 10^{-9} - 1 \times 10^{-8}$	$8 \times 10^{-9} - 1 \times 10^{-8}$
²³⁸ Pu	0.0021 - 0.0022	0.02	0.001	0.0015 - 0.0022	0.011 - 0.017	0.034 - 0.035	0.041
²³⁹ Pu	0.82 - 0.83	0.59 - 0.61	0.927	0.79 - 0.81	0.59 - 0.64	0.35	0.34
²⁴⁰ Pu	0.14	0.24 - 0.25	0.066	0.17 - 0.19	0.26 - 0.32	0.29	0.31
²⁴¹ Pu	0.02 - 0.03	0.08 - 0.11	0.006	0.010 - 0.017	0.030 - 0.064	0.17 - 0.18	0.16 - 0.17
²⁴² Pu	0.003	0.04	2×10^{-4}	0.003	0.033 - 0.038	0.15	0.14

Approximate Maximum Payload ^e (kg oxide)	3.15	1.5	3.15	3.15	1.8	0.9	0.8
Neutron Source (n/s for maximum payload)	1.2×10^6	1.9×10^6	6.4×10^5	1.3×10^6	2.1×10^6	2.0×10^6	2.0×10^6
Gamma-Ray Source (γ -MeV/s for maximum payload)	1.5×10^{11}	2.3×10^{11}	4.0×10^{10}	1.1×10^{11}	1.9×10^{11}	2.3×10^{11}	2.0×10^{11}

^aRanges refer to cooling times prior to extraction of the Pu and are from 6 mo to 10 yr.

^bThe Fast Flux Test Facility (FFTF) is an experimental LMFBR under construction at Hanford, WA. Range of composition refers to different burnups and cooling times.

^cThe Clinch River Breeder Reactor (CRBR) is included as being indicative of the composition to be expected from commercial LMFBR plutonium. Range of composition refers to different fuel cycles, burnups, and cooling times.

^dRanges refer to cooling times prior to extraction of the Pu and are from 1 to 2 yr.

^eMaximum payload is limited by the PAT-1 capacity of 3.15 kg of oxide or 25 W of thermal power whichever is reached first. Maximum payloads and sources assume a shelf life of 14.6 yr.

1567 274

Cases 1 and 2 represent Pu that could be extracted from commercial pressurized light-water reactor (LWR) spent fuel after 1- and 3-yr burnup, respectively. The isotopic compositions given also encompass the ranges expected for boiling-water reactor spent fuel. Case 3 is based on the irradiation sequence used at N Reactor,⁷ Hanford, WA. It represents Pu that could be obtained from low-burnup, low-enriched uranium fuel. Cases 4 and 5 represent Pu that might be extracted from two types of Liquid Metal Fast Breeder Reactor (LMFBR) spent fuel.⁸ Cases 6 and 7 represent the Pu mix to be expected from spent fuel after initiation of U recycle or U and Pu recycle in commercial LWRs, respectively. Each of these isotopic mixtures were obtained using the ORIGEN code.² ORIGEN computes both the burnup and decay of the feed fuel, the recovery of the Pu, and the decay of the Pu after recovery. The present results are in reasonable agreement with other calculations.^{8,9,10}

The maximum payload in the PAT-1, shown for each of the isotopic mixes in Table 5A-IV, was obtained using the maximum mass fractions given for all isotopes except ²³⁹Pu. The ²³⁹Pu mass fraction was then adjusted to make the total unity. Since not all of the resulting combinations are physically possible and the indicated payload may in fact produce a lower source than that shown, the sources are conservative from the present point of view.

Except for the Pu for Case 3 (which has an extremely low radiation intensity), the source strengths of the various Pu-isotopic mixtures are similar and produce about $1-2 \times 10^6$ n/s and about $1-2 \times 10^{11}$ γ -MeV/s, despite the fact that their payloads vary from 800 g to 3.15 kg of oxide. In every case, the gamma source is dominated by ²⁴¹Am while the neutron source is spread more or less uniformly among ²³⁸Pu, ²³⁹Pu, ²⁴⁰Pu, and ²⁴¹Am. The ²⁴²Pu isotope is important only in Cases 5 and 6. The ²³⁶Pu daughter products are important contributors of high-energy gamma rays.

The maximum source strengths shown at the bottom of the table were obtained in the same manner as the maximum payload. All of these results assume a shelf life of 14.5 yr (one ²⁴¹Pu half-life). As the shelf life increases, the maximum PAT-1 oxide payloads of the mixtures of Cases 2, 5, 6, and 7 decrease due to the buildup of ²⁴¹Am. This decrease in the permissible payload somewhat compensates for the increase in source strength per initial unit mass of ²⁴¹Pu. The use of a 14.6-yr shelf life already accounts for the gamma-ray source increase due to the buildup of the daughter products of ²³⁶Pu. The maximum PAT-1 payload mass of PuO₂, based on the 25-W thermal limit, and the corresponding neutron and gamma-ray source strengths for Case 2 oxide of Table 5A-IV, are shown in Figure 5A-4. For this case, the radiation sources continue to increase beyond a shelf life of 70 yr because of the increasing payload mass.

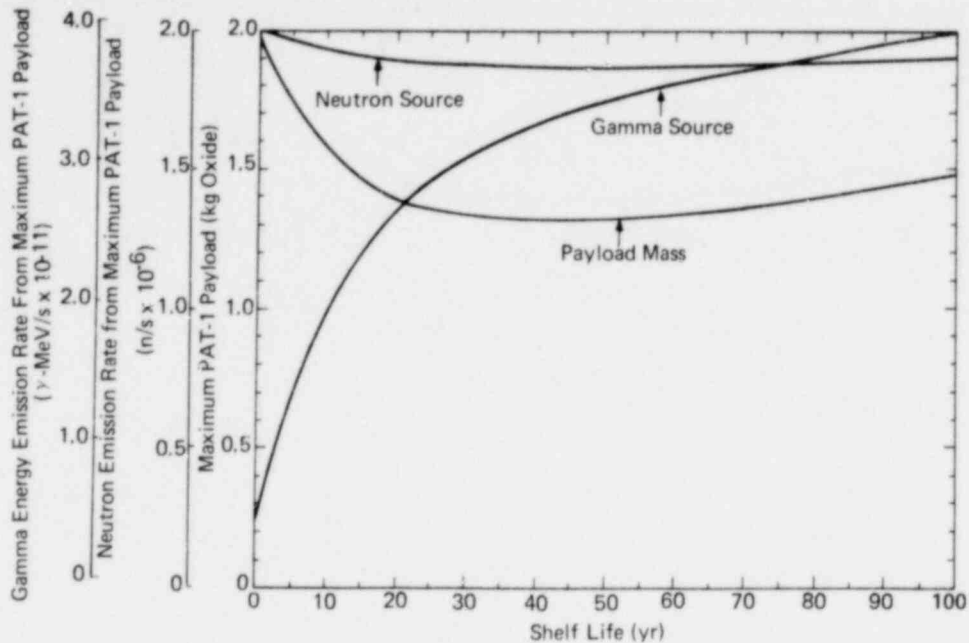


Figure 5A-4. Maximum PAT-1 Payload and Corresponding Neutron and Gamma Ray Energy Emission Rates for Case 2 PuO₂ as a Function of Shelf Life

The source strengths of Cases 2 and 6 are similar and constitute the worst-case gamma-radiation source for the PAT-1 of those shown in Table 5A-IV. Case 2 has a higher initial ²³⁶Pu mass fraction than Case 6, however, making it the worst-case of the two for the gamma source. The gamma-ray energy-emission rate for a maximum PAT-1 payload of Case 2 oxide continues to increase beyond 14.6 yr, as shown in Figure 5A-4. However, the average energy of these gamma rays, and thus their penetrating power, decreases with time. Therefore, a maximum payload of Case 2 oxide with a shelf life of 14.6 yr has been selected as the worst-case gamma source to be expected from any real payload of a PAT-1. The neutron source strength from the maximum PAT-1 payload of Case 2 oxide is relatively insensitive to shelf life, as indicated by Figure 5A-4, and is close to the maximum neutron source shown in Table 5A-IV. To insure use of worst-case conditions, the neutron source of Case 2 was scaled to 2.1×10^6 n/s to encompass the higher Case 5 results.

All of the sources of Table 5A-IV are based upon a series of conservative assumptions and it is extremely unlikely that any sample of PuO₂ loaded in the PAT-1 will emit as much radiation as the Pu mixture of Case 2. However, due to uncertainties in the ORIGEN data base, possible changes in the irradiation history of a particular reactor fuel element and the variation of the source strength in a given sample of PuO₂ with its shelf life, the uncertainty in this specific source term is probably on the order of ±25%.

References (App. A)

1. Irving Kaplan, Nuclear Physics, Addison-Wesley, Reading, MA, Second Edition, 1962, Ch. 10.
2. M. J. Bell, "ORIGEN - The ORNL Isotope Generation and Depletion Code," ORNL-4628, Oak Ridge National Laboratory, Oak Ridge, TN, 1973.
3. R. L. Heath, "Table of Isotopes," Handbook of Chemistry and Physics, R. C. Weast, ed., The Chemical Rubber Co., Cleveland, OH, 58th Edition, p. 8-270, 1977-78.
4. D. H. Stoddard and E. L. Albenesius, "Radiation Properties of ^{238}Pu Produced for Isotopic Power Generators," DP-984, E. I. du Pont de Nemours and Co., Savannah River Laboratory, Aiken, SC, 1965.
5. G. M. Matlack and C. F. Metz, "Radiation Characteristics of Plutonium-238," LA-3696, Los Alamos Scientific Laboratory, Los Alamos, NM, 1967.
6. E. D. Arnold, "Neutron Sources," Engineering Compendium on Radiation Shielding for Nuclear Engineers, R. G. Jaeger, ed., Vol. I, p 30, Springer-Verlag, NY, 1968.
7. "N Reactor Updated Safety Analysis Report," UNI-M-90, United Nuclear Industries, Richland, Wa. To be published, 1978.
8. S. A. Dupree and W. H. Schmidt, "LMFBR Spent Fuel Characterization for Shipping-Cask Application," SAND76-0602, Sandia Laboratories, Albuquerque, NM, 1977.
9. "Clinch River Breeder Reactor Project Preliminary Safety Analysis Report," Vol. 4, Project Management Corp., Oak Ridge, TN, 1977.
10. C. W. Kee, A. G. Croff, and J. O. Blomeke, "Updated Projections of Radioactive Wastes to be Generated by the US Nuclear Power Industry," ORNL/TM-5427, Oak Ridge National Laboratory, Oak Ridge, TN, 1976.

CHAPTER 6
CRITICALITY EVALUATION

6.1 Summary

A series of nuclear criticality calculations has been performed on the PAT-1 package and its PuO₂ contents. PAT-1 packages were considered both singly and in arrays. The results, summarized in Table 6.1-1, indicate that the PAT-1 package when fully loaded with 3.15 kg of PuO₂ powder qualifies as a fissile Class I package in accordance with 10 CFR 71.

TABLE 6.1-1

Results of Criticality Calculations That Establish the PAT-1
as a Fissile Class I Package
(Nominal payload: PuO₂ powder with density 2.8 g/cm³)

<u>Normal Conditions</u>	<u>Results</u>
Number of undamaged packages calculated to be subcritical	∞
k _{eff} of infinite array of undamaged packages*	0.22 ±0.005
Package size	Right circular cylinder: Diameter - 24 in. (61 cm) Height - 42.5 in. (108 cm)
<u>Accident Conditions</u>	
k _{eff} of infinite array of packages damaged by impact, redwood not consumed by fire, no water present	0.28 ±0.006
k _{eff} of infinite array of packages damaged by impact, redwood replaced with water	0.34 ±0.006
k _{eff} of array of 768 packages damaged by impact, redwood replaced with air, array externally water reflected	0.31 ±0.005
k _{eff} of a single TB-1 with water moderation of contents and full water reflection on all sides (10 CFR 71.33a)	0.62 ±0.008
Package size	See Figures 6.3-2 through 6.5-1

* Result is independent of water moderation between packages.

The dimensions of the undamaged packages were based on the design values; dimensions of the impact-damaged PAT-1's were obtained from measurements made on packages that had undergone sequential testing to the NRC Qualification Criteria. The neutronic interaction between adjacent damaged or undamaged packages was found to be small for cases in which the redwood was left in place or in which the redwood was replaced with water. The interaction increased when the redwood was replaced with air; however, none of these changes affected the conclusion regarding the criticality safety of the PAT-1 package.

Although water leakage into the TB-1 under the postulated accident environments is precluded by the package and vessel designs, calculations show that should the vessel (with worst-case fissile contents) become flooded by water and externally water reflected, the system remains critically safe.

6.2 Introduction

The federal regulatory agencies concerned with the handling and transportation of fissile materials do not specify a maximum neutron self-multiplication (k_{eff}) which a shipment will be permitted to reach. It is required, of course, that fissile material not become critical ($k_{eff} = 1$) under any normal or credible accident configuration. In practice, persons knowledgeable in criticality safety typically permit stationary assemblies to reach no more than $k_{eff} = 0.98$ under worst-case conditions when verified by experiment, or $k_{eff} = 0.95$ (including three standard deviations to envelope the 99% confidence level if Monte Carlo is used) when based on calculations.

When fissile material is to be moved, the maximum k_{eff} is commonly limited to about 0.95 under worst-case accident conditions. An analysis of the changes in k_{eff} incurred by the compression of the PuO_2 in a TB-1 during impact was performed by Lawrence and Marshall.¹ Their study shows that under worst-case conditions (422-ft/s impact of an unreflected sphere of PuO_2 at a density of 5 g/cm^3) and conservative mechanical assumptions (uniaxial strain and rigid-wall impact) the increase in k_{eff} due to compression is less than 0.1. Therefore, in order to limit the postaccident k_{eff} in the PAT-1 to 0.95, it is sufficient to limit the normal operation k_{eff} to about 0.85. The conditions under which the PAT-1 is to be handled and shipped in no way indicate the existence of extraordinary circumstances which would exclude it from accepted practical limits of criticality safety and control. Therefore, the above limits have been used as guidelines in this chapter.

6.3 Calculational Model

It is assumed that the payload of the PAT-1 consists of a maximum of 3.15 kg of PuO_2 , subject to the concurrent requirement that the contents generate no more than 25 W of thermal power. The scope of this report does not include Pu metal as contents of the package. The highest k_{eff} of the system will occur when a high percentage of the Pu in the payload is ^{239}Pu .*

* Although ^{241}Pu has a reactivity worth similar to that of ^{239}Pu , it never constitutes the dominant isotope in Pu (see, for example, Table 5A-IV).

In Chapter 5 it was shown that a maximum-weight payload of $^{239}\text{PuO}_2$ is possible without exceeding the thermal limit of 25 W. Therefore, for worst-case criticality conditions such a payload has been assumed. This assumption is conservative since even Hanford Pu is only 93 w/o ^{239}Pu (see Table 5A-IV).

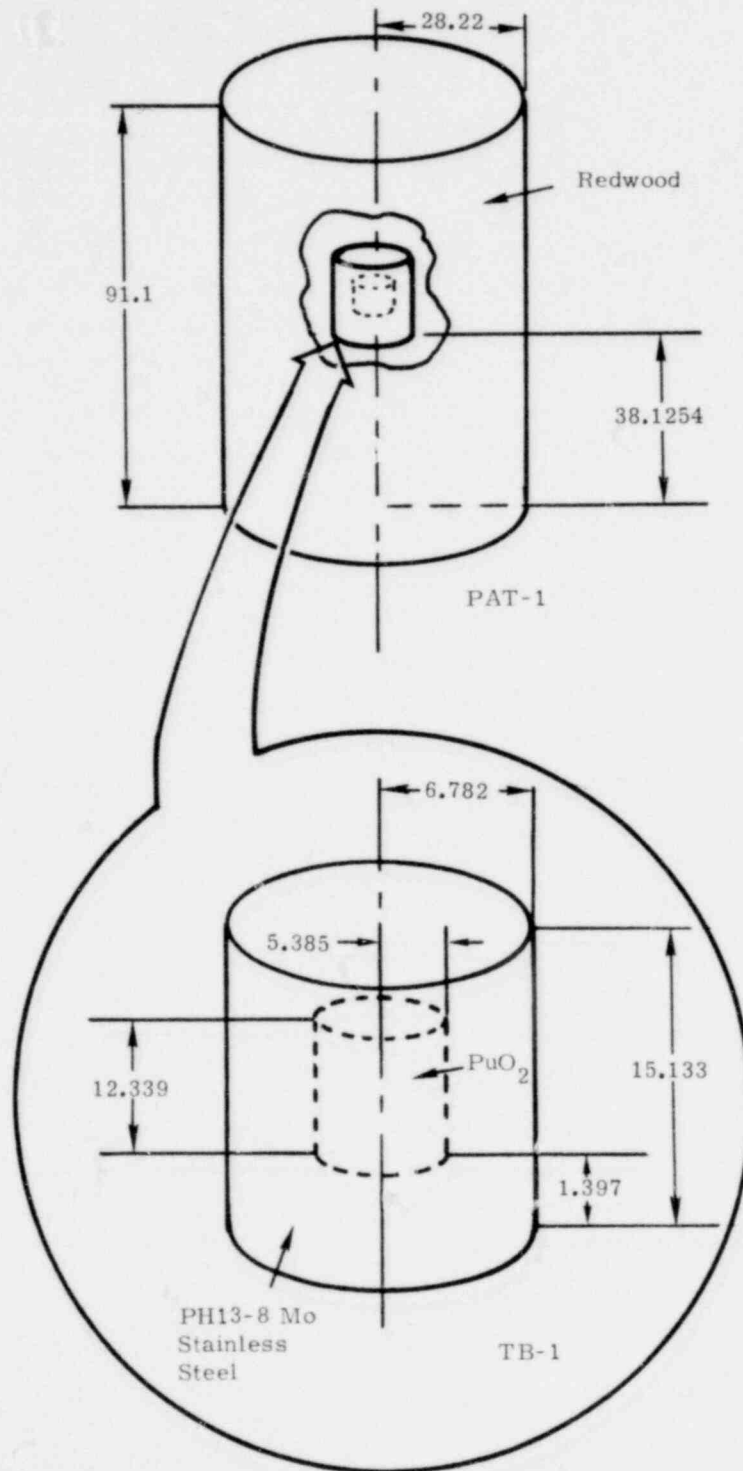
The nominal water content inside the payload section of the TB-1 is 16 g. The maximum amount of water that could theoretically be included with the oxide powder can be estimated from the crystal density of the oxide (11.5 g/cm^3), the mass of the oxide (3.15 kg), and the volume of the product can (1124 cm^3), as approximately 850 g. However, achieving a water content in excess of 16 g is considered possible only if the TB-1 is not properly sealed.

Most of the multiplication eigenvalue calculations performed in support of the present analysis used the KENO-IV code,² a Monte Carlo program designed specifically for performing criticality analyses. As a cross check, the MORSE-SGC code³ was used for a limited number of cases. The KENO geometry package was used even though certain details of the PAT-1 geometry were omitted. In the KENO geometry the TB-1 was modeled as a right circular cylinder with an interior volume of 1124 cm^3 . The radial and bottom wall thicknesses were 1.4 cm (0.55 in.); the top was 1.24-cm (0.49-in.) thick. Thus the curved bottom, Al honeycomb spacer, and wide flange at the top of the TB-1 were neglected. These features were, however, included in the MORSE geometry (see Figure 5.4-3). Comparisons between KENO and MORSE results for equivalent configurations, differing in their geometry approximations but using identical cross sections, showed differences in k_{eff} of less than the statistical standard deviations of the two calculations, indicating that the error introduced by the KENO geometry approximation is insignificant.

A number of calculations were made with both finite and infinite arrays of packages, with and without water filling the intervening spaces. The KENO geometry is well suited for this type of configuration, with either rectangular or hexagonal spacing of packages equally convenient. Use was made of reflecting boundary conditions to simulate the infinite arrays.

The KENO geometry models for the TB-1 and the undamaged PAT-1 are shown in Figure 6.3-1.⁴ The copper annulus, the aluminum load spreader, and the stainless-steel outer container of the PAT-1 were not included in this model; these features, included in the MORSE model, have little effect on the system k_{eff} . The material compositions used were the same as those used in Chapter 5 (see Table 5.4-V) except for the PuO_2 . For the nominal case, the payload was modeled as a minimum-density powder (2.80 g/cm^3 uniformly distributed in 1124 cm^3). The effect of changes in the payload density on the system k_{eff} are considered in Appendix 6A.

⁴The KENO models were developed and calculations performed by S. H. Sutherland of Sandia Laboratories.



Not to Scale

Figure 6.3-1. KENO Geometry Models for the PAT-1 and the TB-1, Normal Operating Conditions

To address the requirements of 10 CFR 71.33a, a criticality assessment was made of a single TB-1 including the effects of water moderation and reflection.* For the nominal, minimum-density powder payload the water was assumed to be homogeneously mixed with the oxide.

The worst-case postaccident configuration for the PAT-1 was determined experimentally. The most vulnerable impact is side-on and produces a final configuration in which the PAT-1 is crushed almost into a half-cylinder with the TB-1 located a few centimeters inside the flattened face. The present calculational model for this configuration, shown in Figure 6.3-2, neglects the overpack material remaining external to the TB-1 and assumes instead that the vessel is tangent to the flattened face. This model is conservative since it underestimates the shielding of neutrons between the payload and the external environment, and it minimizes the distance between TB-1's in an array of damaged packages. The aluminum load spreader and stainless-steel outer container are also neglected.

A separate geometry model was used to analyze a finite array of impact-damaged PAT-1's for which it was assumed that the redwood had been consumed by fire. This model is shown in Figure 6.3-3. In this case, the carbon residue or ash from the burned redwood has been neglected and the space created filled with air. The aluminum load spreader was included as a 1.27-cm (0.5-in.)-thick annulus immediately outside the TB-1 with 2.54-cm (1-in.)-thick aluminum plates on the top and bottom. Thus, the mass of the load spreader was underestimated, which is conservative for determining the system k_{eff} . The 0.3048-cm-thick stainless-steel outside drum was also included. The outer dimensions of the drum are the same as those in Figure 6.3-2. The array contains 768 damaged PAT-1's, each containing the maximum payload of $^{239}\text{PuO}_2$, and is externally water reflected. To maximize the system k_{eff} , the damaged packages have been arranged in an approximately cubic volume. The array exceeds the regulatory requirement for postaccident criticality safety of Fissile Class I packages (10 CFR 71, which requires that an array of at least 250 such packages be shown to be critically safe) by approximately a factor of three.

*For practical purposes, an infinite water reflector can be approximated to a high degree of accuracy by 15 cm of water.

1567 282

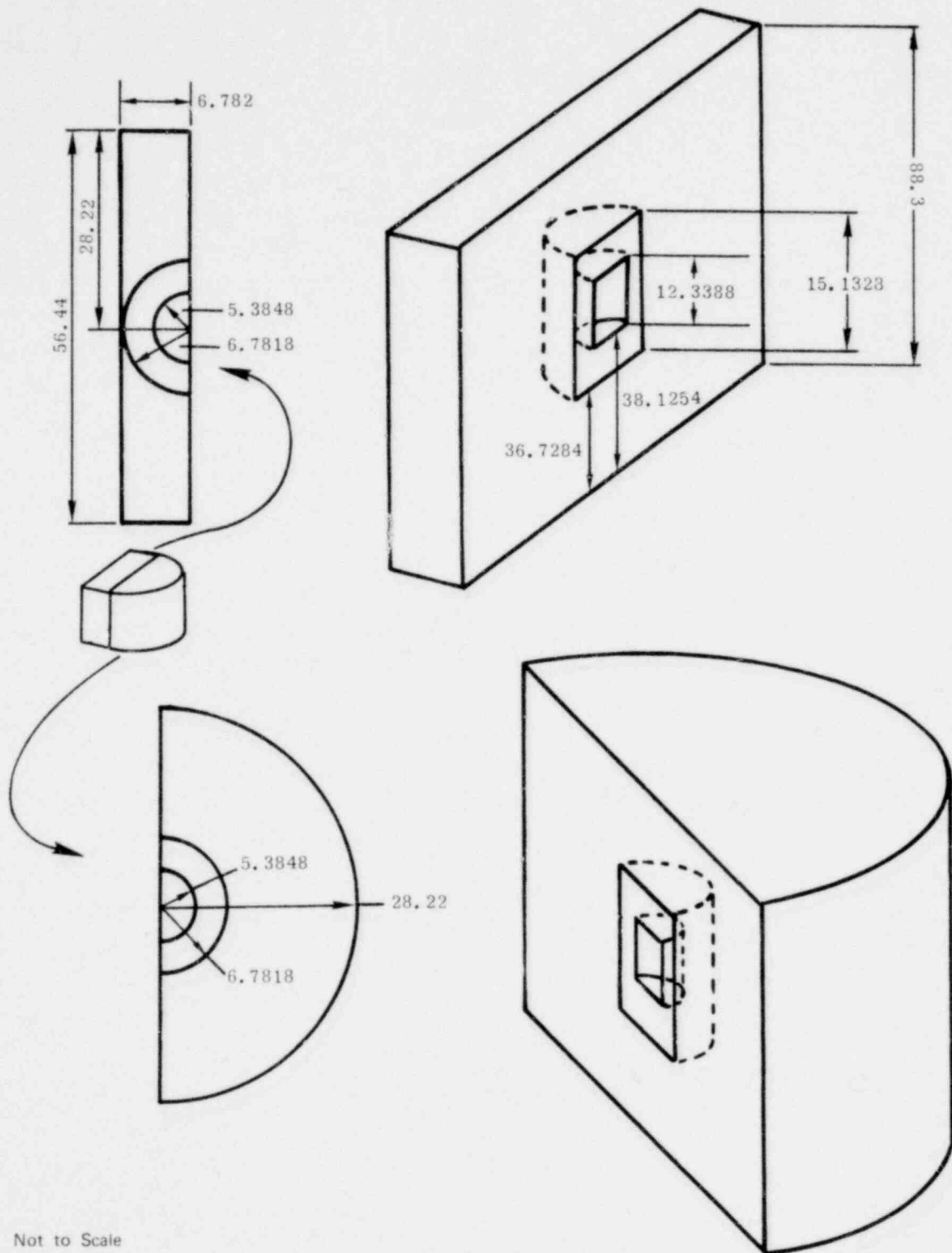
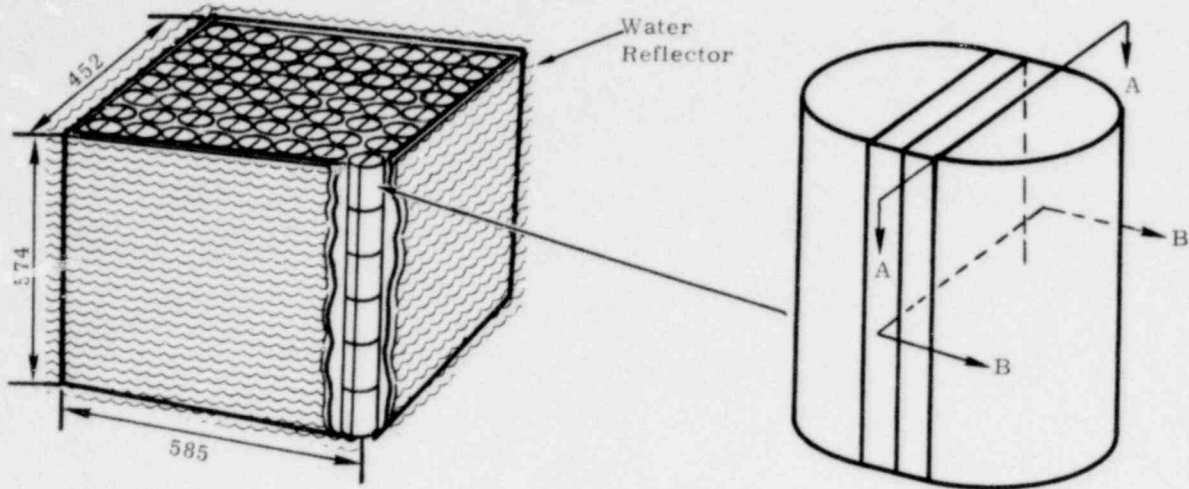
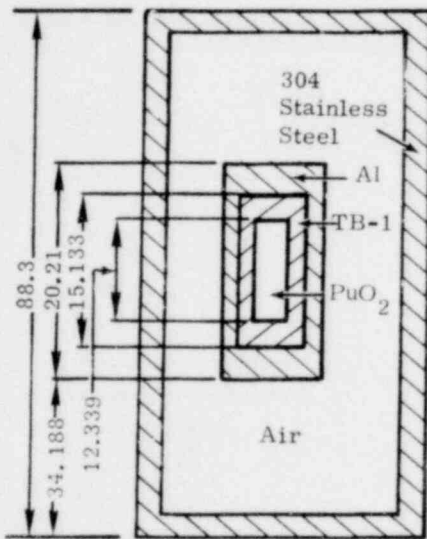


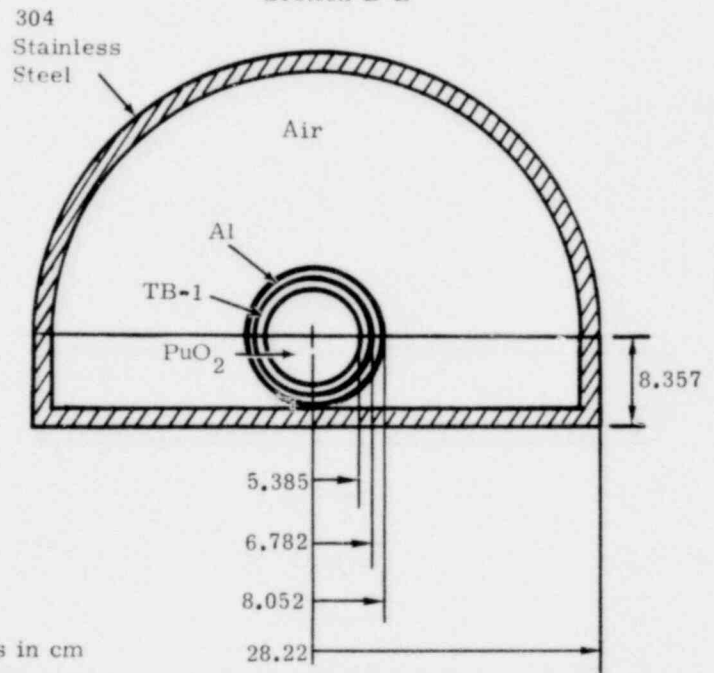
Figure 6.3-2. Postaccident KENO Calculational Model for the PAT-1



Section A-A



Section B-B



Dimensions in cm

Not to Scale

Figure 6.3-3. Finite Array of 768 Impact-Damaged PAT-1's, Redwood Replaced With Air, Externally Water Reflected

A special 27-group cross-section set was generated for the criticality calculations reported here. The P_3 , 218-group Criticality Safety Research Library⁴ was collapsed, using the MALOCS⁵ code, into 27 groups. Resonance parameters were processed with NITAWL,⁵ a Nordheim integral processor.⁶ Analyses by Westfall et al⁶ have shown that this group structure, which includes 16 thermal groups, reproduces the results obtained from use of the full 218-group library and the results so obtained agree with experiments to a high degree of accuracy for problems involving significant amounts of Pu. The 27-group structure is shown in Table 6.3-I.

TABLE 6.3-I
Energy Structure of the 27-Group Neutron Cross-Section Set Used
for Criticality Analyses of the PAT-1

Energy Group	Upper Energy Bound (eV)	Fission Spectrum	Dose Factor ^{**} (mrem/hr per n/cm ² ·s)
1	20×10^6	0.0261	1.471×10^{-1}
2	6.434×10^6	0.2034	1.533×10^{-1}
3	3×10^6	0.2175	1.252×10^{-1}
4	1.85×10^6	0.1227	1.281×10^{-1}
5	1.4×10^6	0.1609	1.306×10^{-1}
6	900×10^3	0.1716	1.057×10^{-1}
7	400×10^3	0.0840	4.961×10^{-2}
8	100×10^3	0.0129	1.428×10^{-2}
9	17×10^3	0.0009	3.572×10^{-3}
10	3×10^3	0.0	3.676×10^{-3}
11	550	0.0	3.951×10^{-3}
12	100	0.0	4.263×10^{-3}
13	30	0.0	4.458×10^{-3}
14	10	0.0	4.567×10^{-3}
15	3.05	0.0	4.562×10^{-3}
16	1.77	0.0	4.521×10^{-3}
17	1.3	0.0	4.488×10^{-3}
18	1.13	0.0	4.467×10^{-3}
19	1.0	0.0	4.436×10^{-3}
20	0.8	0.0	4.345×10^{-3}
21	0.4	0.0	4.200×10^{-3}
22	0.325	0.0	4.105×10^{-3}
23	0.225	0.0	3.895×10^{-3}
24	0.1	0.0	3.675×10^{-3}
25	0.05	0.0	3.675×10^{-3}
26	0.03	0.0	3.675×10^{-3}
27	0.01	0.0	3.675×10^{-3}
	10^{-5}		

^{**}The dose factors were used in calculations reported in Chapter 5. See Reference 19 of that chapter.

*The cross sections were collapsed and processed by P. J. McDaniel of Sandia Laboratories.

All of the Monte Carlo results quoted in this chapter include a best-estimate of the one standard deviation uncertainty. This is a statistical quantity and does not account for nonstatistical sources of uncertainty such as geometry approximations, cross sections, and material compositions. Thus, the quoted statistical standard deviations overestimate the accuracy to which the system k_{eff} values are known. However, the additional uncertainty introduced by the nonstatistical factors may be concluded as small due to the agreement achieved with KENO, using the 27-group cross sections, in comparisons with benchmark results (Section 6.4), and the fact that the cross sections of the most important materials in the problem (^{239}Pu , O, H, Fe, Cr, Ni, and Mo) are reasonably well-known. A more conservative estimate of the uncertainty in the reported k_{eff} values would be two or three times the amounts shown. Certain tests made to verify problem convergence in KENO are discussed in Appendix 6D.

The calculated results presented in this chapter are shown to three significant digits in order to facilitate making certain comparisons and to indicate trends. Although the statistical standard deviation quoted with each number generally warrants this level of numerical precision, the actual level of accuracy to which the neutron self-multiplication is known does not justify use of the third significant digit.

6.4 Benchmark Calculations

To verify that the 27-group cross sections are adequate for the type of problem of interest in this study, the neutron self-multiplications of two benchmark critical assemblies have been calculated. These assemblies consisted of rectangular parallelepipeds of PuO_2 , one unmoderated⁷ and one moderated.⁸ Both assemblies used 15-cm-thick plexiglas reflectors. The PuO_2 was placed in a polystyrene matrix providing H/Pu atom ratios of 0.04 and 15 for the unmoderated and moderated cases, respectively. Thus, the benchmark problems encompass a range of neutron spectra of interest to the current PAT-1 analysis.

The isotopic composition of the Pu for the two experiments, along with the critical densities and dimensions, are shown in Tables 6.4-I and 6.4-II. The experimental uncertainties in the quantities shown were on the order of 0.5 to 1.0%. The nominal dimensions were used in KENO. The neutron self-multiplications calculated were 1.003 ± 0.008 for the unmoderated configuration and 0.991 ± 0.008 for the moderated configuration. Both results are based on 50 neutron generations of 300 neutrons per generation. These results validate the calculational method and the accuracy of the KENO-IV code (used with the 27-group cross section set) for application to criticality evaluations of the type presented below.

TABLE 6.4-1

Configuration of Criticality Benchmark Calculation
Using Unmoderated PuO₂
(see Reference 7)

Experiment Critical Dimensions (cm)

Reflector thickness (plexiglas) *	15.0
Length **	25.65 ± 0.01
Width **	25.65 ± 0.01
Height **	10.03 ± 0.01

Critical Mass

38.3 ± 0.3 kg Pu

Calculational Composition of Fuel Region

PuO₂ - polystyrene mixture

Element	Density	
	Atoms/b·cm	g/cm ³
Pu	1.450 x 10 ⁻²	5.762
O	3.094 x 10 ⁻²	0.822
H	5.511 x 10 ⁻⁴	0.00091

Pu Isotopic Composition

Isotope	Atom %
²³⁹ Pu	7.53 x 10 ⁻¹
²⁴⁰ Pu	1.97 x 10 ⁻¹
²⁴¹ Pu	5.01 x 10 ⁻²

Calculated k_{eff} = 1.003 ± 0.008

* Plexiglass composition:

Element	Density (Atoms/b·cm)
O	1.422 x 10 ⁻²
H	5.688 x 10 ⁻²
C	3.555 x 10 ⁻²

** Excluding reflector.

TABLE 6.4-II
 Configuration of Criticality Benchmark Calculation
 Using Moderated PuO₂
 (see Reference 8)

<u>Experiment Critical Dimensions (cm)[†]</u>	
Reflector Thickness (plexiglas) [*]	15.0
Length ^{**}	51.31 ± 0.03
Width ^{**}	68.25 ± 0.03
Height ^{**}	10.36 ± 0.03

Critical Mass[†]
 38.09 ± 0.11 kg Pu

Calculational Composition of Fuel Region

PuO₂ - polystyrene mixture

<u>Element</u>	<u>Density</u>	
	<u>Atoms/b·cm</u>	<u>g/cm³</u>
Pu	2.763 x 10 ⁻³	1.098
O	5.481 x 10 ⁻³	0.146
H	4.144 x 10 ⁻²	0.0694
C	3.942 x 10 ⁻²	0.785

Pu Isotopic Composition

<u>Isotope</u>	<u>Atom %</u>
²³⁹ Pu	9.12 x 10 ⁻¹
²⁴⁰ Pu	8.06 x 10 ⁻²
²⁴¹ Pu	7.50 x 10 ⁻³

Calculated k_{eff} = 0.991 ± 0.008

* See note to Table 6.4-I for plexiglas composition.

** Excluding reflector.

† Stated uncertainty is from least-squares analysis and does not reflect additional experimental uncertainty.

6.5 Results of Criticality Calculations

The neutron self-multiplication of a single PAT-1 under normal operating conditions, containing 3.15 kg of dry $^{239}\text{PuO}_2$ powder at the minimum density of 2.8 g/cm^3 , has been calculated to be 0.220 ± 0.005 . The difference in k_{eff} for dry oxide powder and for the oxide plus the nominal 16 g of water inside the TB-1 is negligible (see Appendix 6B). Stacking undamaged PAT-1 packages, all with payloads of 3.15 kg of $^{239}\text{PuO}_2$, in an infinite rectangular array increases k_{eff} less than one standard deviation whether or not water is assumed to fill the intervening spaces. Thus, the AQ-1 overpack is an efficient neutron decoupler and each oxide-filled, undamaged PAT-1 can be treated independent of any number of other PAT-1 packages; i. e., the presence or absence of additional containers external to a given PAT-1 in no way influences the k_{eff} of the PAT-1.

The postaccident model of the PAT-1 is shown in Figure 6.3-2. The k_{eff} of a single package in this configuration with a full payload of dry $^{239}\text{PuO}_2$ powder of minimum density, the redwood still in place, and no neutron reflection external to the damaged package has been calculated to be 0.219 ± 0.006 . If the single damaged PAT-1 with this fuel loading is submerged in water, the self-multiplication increases to 0.277 ± 0.005 . If the redwood is replaced with water (package still assumed to be externally water reflected) as might be the case following a fire, the system k_{eff} becomes 0.334 ± 0.007 . If the redwood is assumed burned and replaced with air, the k_{eff} of the package becomes 0.198 ± 0.003 .

The k_{eff} of an array of damaged PAT-1 packages depends on the detail of their configuration. Several stacking arrangements have been proposed, the most straightforward of which is the infinite array shown in Figure 6.5-1. If the impact-damaged redwood is assumed to remain in place, the k_{eff} calculated for this array, each PAT-1 containing the maximum payload of $^{239}\text{PuO}_2$ powder at the minimum density, is 0.279 ± 0.006 .^{*} If the redwood is replaced with water, the system k_{eff} becomes 0.343 ± 0.006 .

Performing calculations on different geometries for arrays of damaged PAT-1 packages may enable one to identify configurations that produce a higher or lower k_{eff} than that of Figure 6.5-1. However, even if the TB-1's are permitted to move freely about inside the volume of the damaged PAT-1's (permitting locally increased densities of oxide by moving TB-1's to adjacent corners in the array of Figure 6.5-1), the infinite array of damaged packages still remains critically safe. Specifically, in the configuration of Figure 6.5-2, an infinite array of clusters of TB-1's, each cluster containing 8 vessels and each vessel containing 3.15 kg of $^{239}\text{PuO}_2$ as a minimum density powder, is considered. All intervening spaces are filled with redwood. The resulting system has a k_{eff} of 0.521 ± 0.006 .

^{*}The neutron self-multiplication factors calculated for other stacking arrangements are similar in magnitude to this result (see Reference 9).

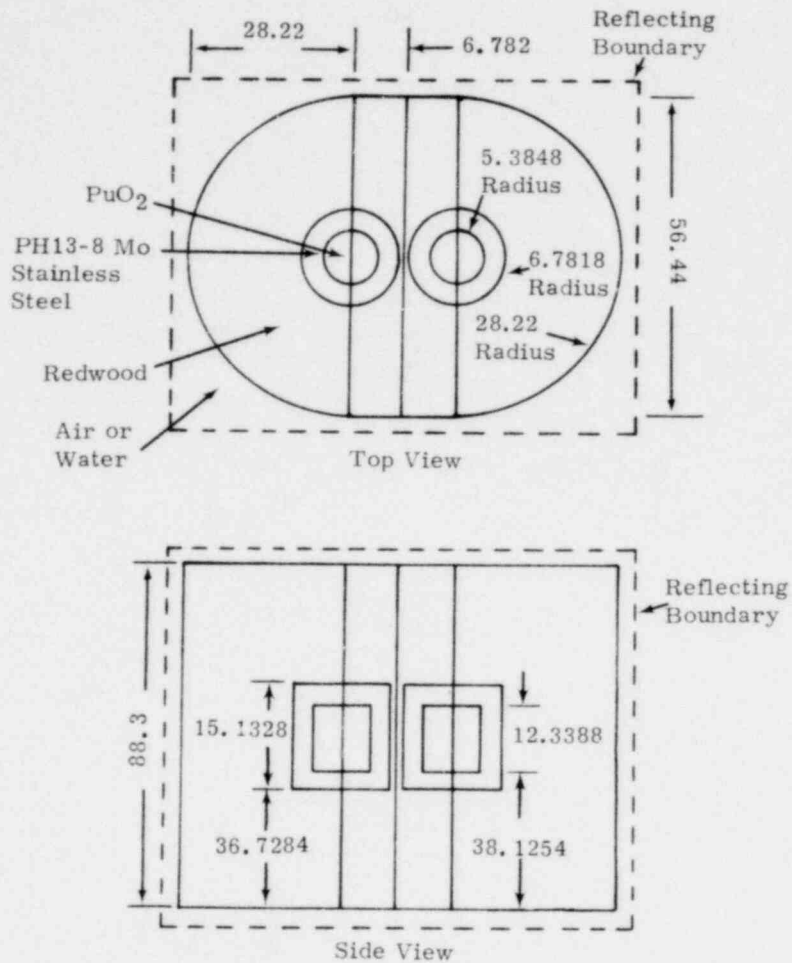


Figure 6.5-1. Calculational Model for an Infinite Array of Postaccident PAT-1 Packages

Although a carbonaceous residue remains after redwood is burned, a criticality calculation was performed on a finite array of impact-damaged PAT-1's in which the redwood was replaced with air. This configuration (shown in Figure 6.3-3) consisted of 768 PAT-1's, or approximately three times the number required (250) by 10 CFR 71 to qualify a package as Fissile Class I. The array was externally water reflected. The neutron multiplication for this array, each TB-1 containing 3.15 kg of $^{239}\text{PuO}_2$ as a minimum density powder, was calculated to be 0.312 ± 0.005 .

The results of this section (see also Appendix 6A) provide a high degree of confidence in the conclusion that it is not possible to assemble any credible number of damaged or undamaged PAT-1 packages in such a way as to make them critically unsafe, independent of their payloads, provided that such payloads meet the concurrent criteria of 3.15-kg PuO_2 and 25 W of thermal power maximum.

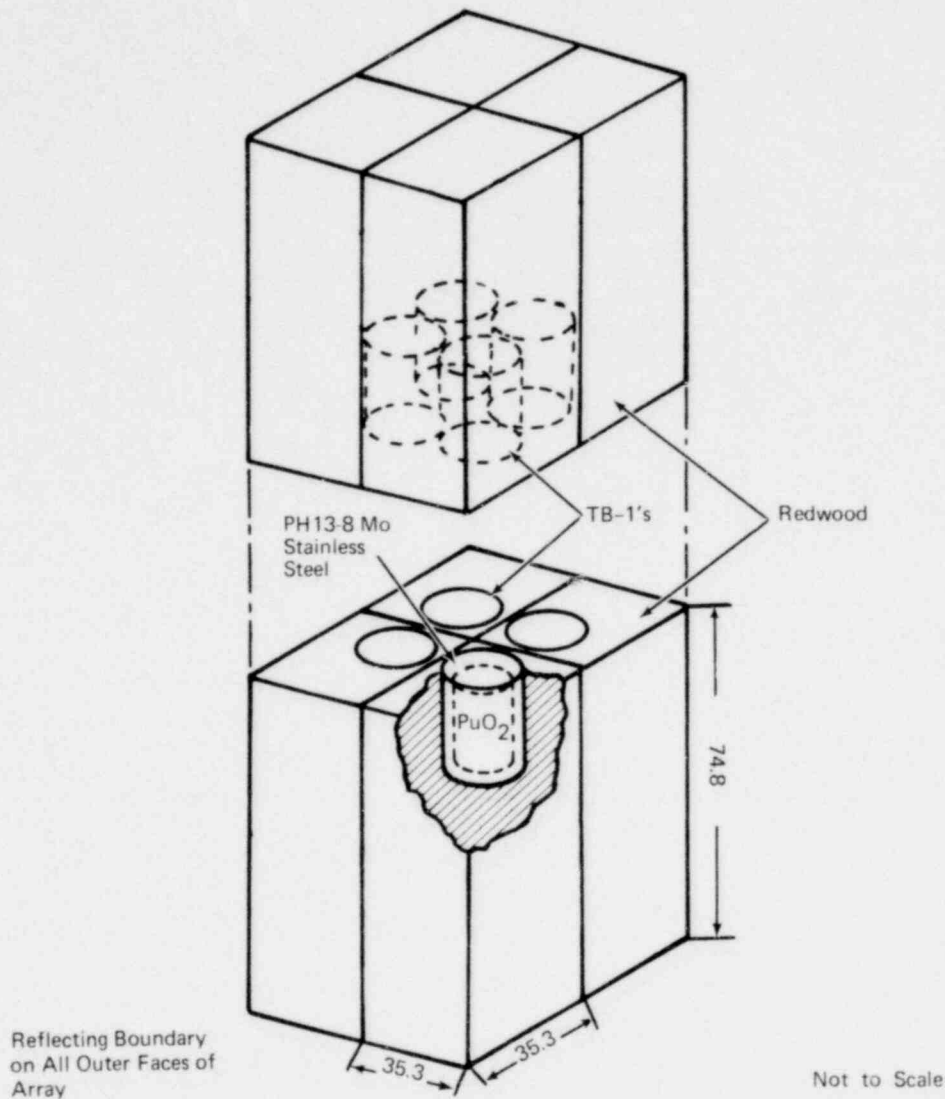


Figure 6.5-2. Calculational Model for infinite Array of Impact-Damaged PAT-1's in Which the TB-1's are Arranged in Clusters of Eight

The neutron self-multiplication of a single TB-1 with water moderation of the contents and full water reflection on all sides was calculated as required by 10 CFR 71.33a. A payload of 3.15 kg of $^{239}\text{PuO}_2$ in the form of a minimum density (2.8 g/cm^3) powder was assumed along with 850 g of water. These conditions represent the maximum k_{eff} for a single TB-1 since this is the theoretical maximum amount of water that can be added without displacing the oxide contents. The system k_{eff} was calculated to be 0.617 ± 0.008 .

The present analysis indicates the PAT-1 package meets all requirements for a Fissile Class I package, as defined in 10 CFR 71, and has been found critically safe under any normal or credible accident condition.

References

1. R. J. Lawrence and A. C. Marshall, The Effect of Densification on Reactivity of Plutonium-Based Reactor Materials in an Air-Transportable Package During High-Speed Impact, SAND77-1516, Sandia Laboratories, Albuquerque, NM, 1978. (See also A. C. Marshall and C. R. Marotta, "The Effect of Compression on Reactivity of Plutonium-Based Materials," paper presented at the 5th International Symposium on Packaging and Transportation of Radioactive Materials, May 7-12, 1978, Las Vegas, NV.)
2. L. M. Petrie and N. F. Cross, KENO IV—An Improved Monte Carlo Criticality Program, ORNL 4938, Oak Ridge National Laboratory, Oak Ridge, TN, 1975.
3. S. K. Fraley, User's Guide to MORSE-SGC, ORNL/CSD-7, Oak Ridge National Laboratory, Oak Ridge, TN, 1976.
4. W. E. Ford, III, C. C. Webster, and R. M. Westfall, A 218-Group Neutron Cross-Section Library in the AMPX Master Interface Format for Criticality Safety Studies, ORNL/CSD/TM-4, Oak Ridge National Laboratory, Oak Ridge, TN, 1976.
5. N. M. Greene, J. L. Lucius, L. M. Petrie, W. E. Ford, III, J. E. White, and R. Q. Wright, AMPX: A Modular Code System for Generating Coupled Multigroup Neutron-Gamma Libraries from ENDF/B, ORNL TM-3706, Oak Ridge National Laboratory, Oak Ridge, TN, 1977.
6. R. M. Westfall, W. E. Ford, III, and C. C. Webster, "Design Criteria for the 218-Group Criticality Safety Reference Library," presented at the RSIC Seminar-Workshop on Multigroup Cross Sections, March 14-16, 1978, sponsored by the Radiation Shielding Information Center, Oak Ridge National Laboratory, Oak Ridge, TN. Proceedings to be published. Also personal communication, R. M. Westfall, 1978.
7. S. R. Bierman and E. D. Clayton, "Critical Experiments with Unmoderated Plutonium Oxide," Nucl Tech **11**, 185 (1971).
8. C. R. Richey, J. D. White, E. D. Clayton, and R. C. Lloyd, "Criticality of Homogeneous Plutonium Oxide-Plastic Compacts at $H:Pu = 15$," Nucl Sci Eng **23**, 150 (1975).
9. W. H. Schmidt, "Results from Nuclear Criticality and Shielding Calculations for Damaged and Undamaged Plutonium Air Transportable (PAT) Packages," paper presented at the 5th International Symposium on Packaging and Transportation of Radioactive Materials, May 7-12, 1978, Las Vegas, NV.

APPENDIX 6A

Effect of Oxide Density on Neutron Self-Multiplication in the PAT-1

The neutron self-multiplication of a mass of fissile material depends on the density and geometry of the material as well as its relation to nearby matter. The results of criticality calculations reported in Chapter 6 assumed the 3.15-kg PuO₂ PAT-1 payload to be in the form of a powder with a density of 2.8 g/cm³. This is the minimum density that will permit a full-weight payload to be carried in the TB-1 and reflects the original impetus of the PARC project. However, compaction techniques exist which can produce PuO₂ in densities close to the crystal density of 11.5 g/cm³.

To determine the effect of payload density on the criticality safety of the PAT-1 package, a model of the TB-1 and the PAT-1 was developed in which the payload was assumed to be a sphere of 3.15 kg of ²³⁹PuO₂ with a density of 11.5 g/cm³. This provides an extreme upper limit to the neutron self-multiplication that might be possible in the PAT-1 from unrestricted forms and configurations of PuO₂ subject to the concurrent constraints of 3.15 kg and 25 W thermal maximum.

Table 6A-I shows the effect on the quantities reported in Table 6.1-I of changing the payload from a minimum-density powder to a maximum-density sphere. The water moderated TB-1 result (10 CFR 71.33a) again assumes the maximum 850 g of water inside the vessel. The water is assumed to occupy the space not occupied by the oxide. The sphere of PuO₂ is assumed to be located at the center of the TB-1.

Although most of the results shown in Table 6A-I are higher than the corresponding values shown in Table 6.1-I, they all reflect safe levels for criticality control. Thus, the PAT-1 package meets all requirements for a Fissile Class I package, as defined in 10 CFR 71, independent of the density and geometry of its PuO₂ payload, provided such payload meets the concurrent requirements of 3.15 kg and 25-W thermal maximum.

TABLE 6A-1

Results of Criticality Calculations on the PAT-1
(PuO₂ payload in the shape of a sphere with density
11.5 g/cm³)

<u>Normal Conditions</u>	<u>Results</u>
Number of undamaged packages calculated to be subcritical	∞
k _{eff} of infinite array of undamaged packages*	0.51 ± 0.005
<u>Accident Conditions</u>	
k _{eff} of infinite array of packages damaged by impact, redwood not consumed by fire, no water present	0.54 ± 0.006
k _{eff} of infinite array of packages damaged by impact, redwood re- placed with water	0.56 ± 0.005
k _{eff} of 768 packages damaged by impact, redwood replaced with air, array externally water reflected	0.55 ± 0.005
k _{eff} of single TB-1 with water moderation of contents and full water reflection on all sides (10 CFR 71.33a)	0.61 ± 0.007

* Result is independent of water moderation between packages.

APPENDIX 6B

Effect of Water Inside a TB-1 on Neutron Self-Multiplication in the PAT-1

The nominal water content in the TB-1 is 0.5 w/o of the oxide, or 16 g for the maximum 3.15-kg payload. Water leaking into a properly sealed TB-1 is not credible—no TB-1 vessel has ever leaked water in the tests of packages to the Qualification Criteria. However, the question has been raised as to what effect the presence of water would have on the results presented in Chapter 6 and in Appendix 6A; a series of calculations has been performed to answer it. The results reported in this section are theoretical studies of hypothetical configurations of PAT-1's. The values produced are not required by any federal regulation to be part of the documentation supporting an application for a Certificate of Compliance from the Nuclear Regulatory Commission, or the operational use of the PAT-1.

Figure 6B-1 shows the neutron self-multiplication of a single undamaged PAT-1 containing 3.15 kg of $^{239}\text{PuO}_2$ as a function of the amount of water inside the TB-1. Results are shown for the oxide in the form of a minimum-density powder and as a maximum-density sphere (see Appendix 6A).^{*} The difference between k_{eff} of a single undamaged PAT-1 and of an infinite array of such PAT-1's is small. Note that although the k_{eff} of the system is considerably different for the powder and the solid oxide cases when the TB-1 is dry, the difference decreases with increasing water content and is small when the maximum amount of water is included. It is also apparent from the figure that the difference in k_{eff} between the dry and nominal (16 g) water cases is negligible.

It was mentioned in the body of Chapter 6 that the k_{eff} of a single impact-damaged PAT-1 carrying the worst-case minimum-density powder payload was calculated to be 0.219 ± 0.006 when unreflected and 0.277 ± 0.005 when water reflected. If the maximum amount of water is added inside the TB-1, the reflected system k_{eff} increases to 0.545 ± 0.005 . If the payload of the PAT-1 is in the form of a maximum-density, 3.15-kg $^{239}\text{PuO}_2$ sphere, the postaccident k_{eff} in the dry (no water inside the TB-1), unreflected (a vacuum assumed external to the PAT-1) configuration

^{*}For the oxide in the form of a minimum-density powder, the water and the PuO_2 are assumed mixed homogeneously. For the oxide in the form of a maximum-density sphere, the water is assumed to occupy the space inside the product can not occupied by the PuO_2 and the sphere is located at the center of the TB-1. This assumption is conservative since it maximizes the reactivity effect of the water. The theoretical upper limit for the amount of water that can be placed inside the TB-1 without displacing the oxide is 850 g.

is 0.497 ± 0.004 . If this damaged PAT-1 were submerged in water, k_{eff} would increase to 0.528 ± 0.009 . Finally if one assumes, in addition, that the maximum 850 g of water is placed inside the TB-1, the system k_{eff} becomes 0.594 ± 0.007 .

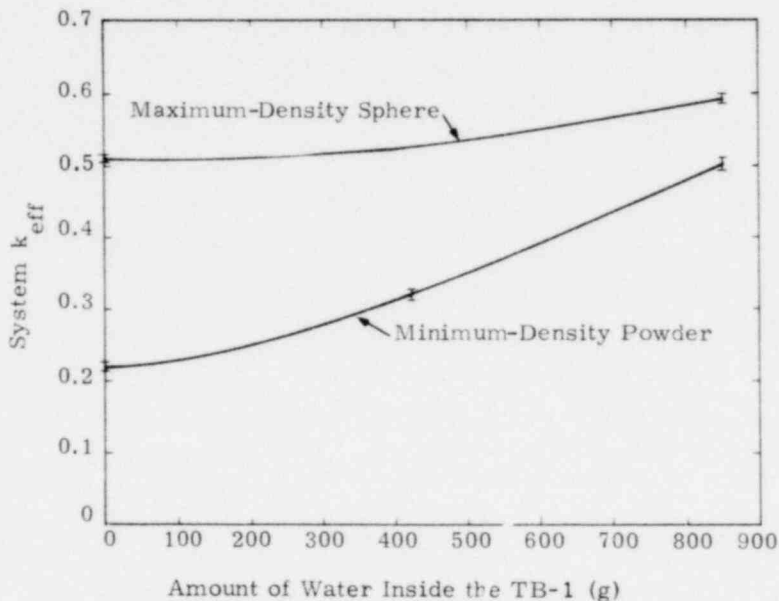


Figure 6B-1. Neutron Multiplication in the PAT-1, Normal Operation

For the infinite array of impact-damaged PAT-1's shown in Figure 6.5-1, the system k_{eff} was found to be 0.279 ± 0.006 (worst-case powder payload). If, in addition, 850 g of water were added to each of the TB-1's, the k_{eff} would increase to 0.570 ± 0.007 . If the PuO_2 were in the form of a maximum-density sphere in each of the PAT-1's, the k_{eff} of the array of Figure 6.5-1 would be 0.544 ± 0.006 . If the maximum amount of water were then added inside the TB-1's, the system k_{eff} would increase to 0.627 ± 0.007 .

In the configuration of Figure 6.5-2, in which the TB-1's are clustered in groups of eight, the k_{eff} of an infinite array of impact-damaged PAT-1's was found to be 0.521 ± 0.006 if the oxide is in the form of a minimum-density powder. If the oxide is in the form of a solid sphere, the system k_{eff} becomes 0.664 ± 0.009 . If, in addition, the TB-1's each contain the maximum amount of water, the system k_{eff} 's become $0.895 \pm 0.009^*$ and 0.720 ± 0.008 for powder and solid oxide, respectively.

*The safe k_{eff} limit of 0.85 discussed in Section 6.2 is assumed to apply to the PAT-1 under normal operating conditions. The present hypothetical configuration would be considered post-accident and, hence, be subject to a criticality safety limit of 0.95.

For the 768-package postaccident array of Figure 6.3-3 the system k_{eff} was found to be 0.312 ± 0.005 for minimum-density oxide powder and 0.548 ± 0.005 for solid oxide spheres. If the maximum amount of water is placed in the TB-1's, the neutron self-multiplications increase to 0.636 ± 0.007 and 0.622 ± 0.006 for the respective PuO_2 configurations.

The presence of water inside the TB-1's increases the k_{eff} of the system studied here. The impact of the water is greatest when the oxide payload is in the powder form. However, in every case examined, the system remains critically safe when water is added inside the TB-1's independent of the density of the oxide.

APPENDIX 6C

Criticality Analysis of Arrays of Bare TB-1's

The only time that a TB-1 containing PuO_2 should be outside the AQ-1 overpack is during the loading or unloading of the PAT-1's. Each facility handling PuO_2 operates under its own criticality guidelines, an area outside the scope of this study. However, delineation of the neutronic characteristics of bare TB-1's containing worst-case PuO_2 payloads may be of interest to the PAT-1 user community. The k_{eff} of a single dry, unreflected TB-1 containing 3.15 kg of $^{239}\text{PuO}_2$ in the form of a minimum-density powder is 0.198 ± 0.003 . Under the same conditions but with the PuO_2 as a solid sphere, the k_{eff} is 0.499 ± 0.005 . Finally, if the oxide is in the shape of a solid rod extending along the axis of the TB-1, the k_{eff} is 0.439 ± 0.004 . Thus, the neutron self-multiplication is sensitive to the geometry of the oxide but even the worst-case is critically safe.

The effect of adding water internal or external to the TB-1 containing 3.15 kg of $^{239}\text{PuO}_2$ is shown in Figure 6C-1.* This figure shows that when the water content exceeds 850 g and the oxide is displaced, the system k_{eff} decreases. The maximum k_{eff} for a single TB-1, containing the maximum payload of $^{239}\text{PuO}_2$ (in the form of a minimum-density powder), the maximum amount of water internally, and fully water reflected, is 0.617 ± 0.008 . The k_{eff} of a fully reflected, internally dry TB-1 under the same payload conditions is 0.334 ± 0.007 . The corresponding values for a maximum-density sphere of $^{239}\text{PuO}_2$ are 0.612 ± 0.007 (maximum water internal, fully reflected) and 0.565 ± 0.005 (dry internal, fully reflected).** Thus, the geometry details of the oxide become relatively unimportant under water-flooded conditions.

The k_{eff} of an array of TB-1's is sensitive not only to their payload compositions and masses, their oxide geometries, and their water contents, but also to their spacing or pitch.† Figure 6C-2 shows the results of changing the pitch of three different rectangular arrays of TB-1's, each containing the maximum payload of $^{239}\text{PuO}_2$. Results are shown both for the oxide in the form of a

* When the oxide is in the form of a powder, the model used here assumes the PuO_2 and the water to be homogeneously mixed; when the oxide is in the form of a maximum-density solid, the water is assumed to occupy the space inside the product can not occupied by the PuO_2 . The oxide sphere is assumed located at the center of the TB-1.

** The reactivity worth of ^{241}Pu was claimed to be similar to that of ^{239}Pu . In the present case, if the sphere were $^{241}\text{PuO}_2$ instead of $^{239}\text{PuO}_2$, the system self-multiplications would be 0.628 ± 0.006 (maximum water internal, fully reflected) and 0.521 ± 0.005 (dry internal, fully reflected) instead of as stated in the text.

† Horizontal pitch is defined as the distance between centerlines of adjacent vessels. The minimum horizontal pitch is the diameter of the vessels.

minimum-density powder and as a maximum-density sphere. The 8-vessel array assumes two layers of four TB-1's each while the 12-vessel array includes a third layer of four. As was found for the single TB-1, the dense form of the oxide results in a higher k_{eff} for these arrays than the powder form when no water is present. Moderation of the neutron spectrum by placing water internally or externally increases the system k_{eff} for both fuel densities, but has a much larger effect on the powder than on the solid. The k_{eff} of a water-reflected array of TB-1's, each vessel also containing the maximum amount of water internally, is not highly sensitive to the geometry of the oxide and the sensitivity decreases with increasing pitch.

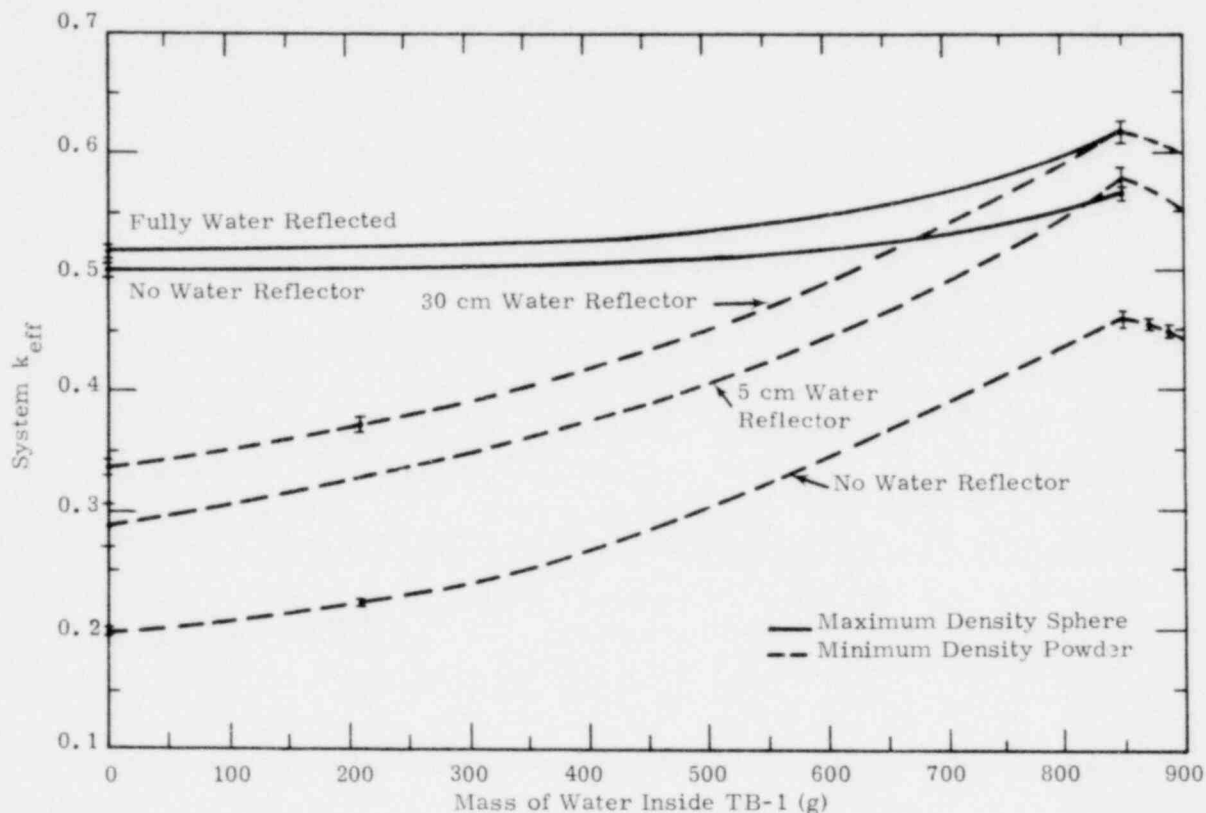


Figure 6C-1. Neutron Multiplication in a Single TB-1

Water added internally to a TB-1 containing a payload with a high ^{239}Pu content always has a positive reactivity effect as long as no oxide is displaced. The reactivity worth of water added externally to the TB-1's, either singly or in an array, is also positive provided the total number of TB-1's in the array, or the spacing between them, is not too great. As the number of TB-1's in an array or the spacing between them increases, at some point the water begins to act as an absorber and produces a negative reactivity effect. However, a large number of TB-1's (several hundred) in a tight-packed array, or a spacing that is on the order of the PAT-1 dimensions (~ 60 cm), is required before this effect appears.

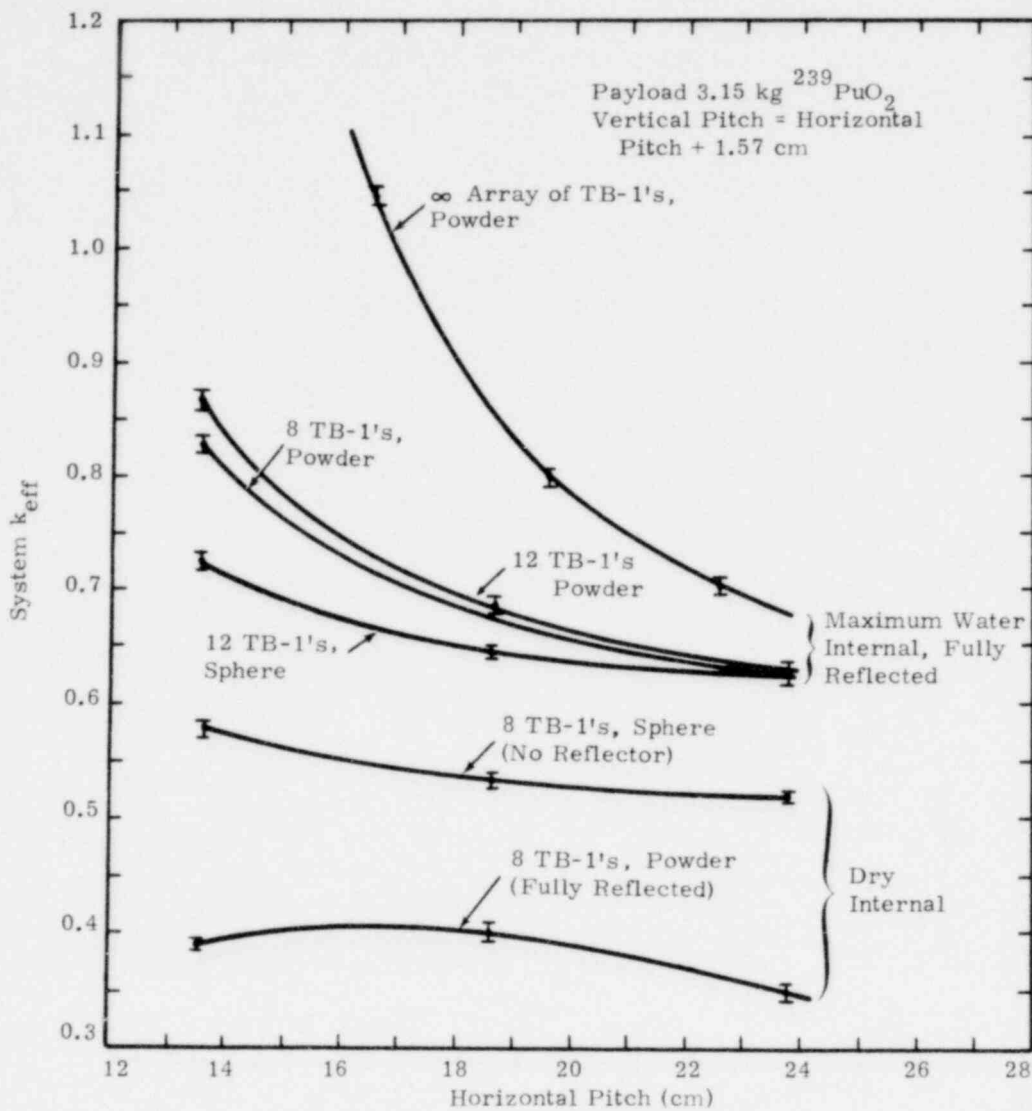


Figure 6C-2. Effect of Pitch on Neutron Self-Multiplication in Rectangular Arrays of TB-1's

The array of eight TB-1's containing dry, minimum-density $^{239}\text{PuO}_2$ powder but externally water reflected (bottom curve in Figure 6C-2) reaches a maximum k_{eff} of approximately 0.41 at a nonzero separation between the cans. This is because the closest-packed configuration is undermoderated. Increasing the spacing and, therefore, the amount of water between vessels softens the neutron spectrum and increases k_{eff} . By further increasing the spacing between the vessels, however, the probability of a neutron leaving one vessel and entering another declines and k_{eff} begins to decrease. This phenomenon does not occur when the maximum amount of water is present inside the TB-1's. An infinite rectangular array of TB-1's, each containing the maximum amount of water internally and externally reflected (top curve of Figure 6C-2) is unsafe* at a pitch of approximately 17.5 cm or less. The rectangular arrays of 8 and 12 TB-1's are unconditionally safe.

* This hypothetical array of bare TB-1's is stationary and, hence, assumed subject to a calculated criticality safety limit of $k_{\text{eff}} \leq 0.95$.

Figure 6C-3 (upper curve) shows the k_{eff} of a hexagonal closest-packet array of TB-1 vessels (intervening spaces filled with water), each vessel containing 3.15 kg of $^{239}\text{PuO}_2$ in powder form along with 850 g of water, vs the number of vessels in the array. The effect of changing the oxide density is small in this case since all vessels are assumed to be flooded with water. Under this noncredible condition, nine TB-1's are still safe; ten or more are no longer safe under current assumptions. Note, however, that the neutron self-multiplication is reduced significantly if the array is changed from hexagonal to rectangular (lower curve in Figure 6C-3). In the later case, 15 worst-case TB-1's (3 layers of 5 vessels) produce a k_{eff} of 0.942 ± 0.009 .

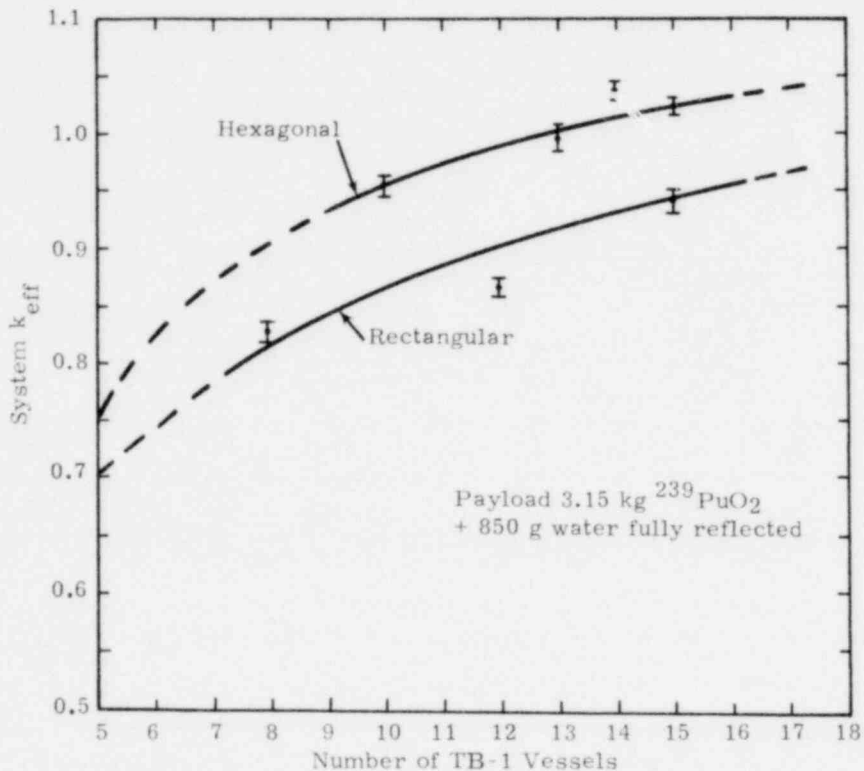


Figure 6C-3. Neutron Self-Multiplication of a Worst-Case Finite Array of Bare TB-1's

The reactivity worth of a worst-case TB-1 decreases rapidly as it is separated physically from an array of similar vessels, and the presence of water inside a TB-1 in amounts greater than the nominal 16 g is an extremely unlikely occurrence. Therefore, the above results indicate that the probability is vanishingly small that any reasonable number (15 or less) of bare TB-1's, containing PuO_2 which meets the concurrent requirements of 3.15 kg and 25 W thermal maximum and stacked or arranged in any manner, will pose a criticality safety hazard unless there are significant amounts of fissile materials not sealed inside TB-1 vessels also located in the vicinity.

APPENDIX 6D

Tests of the Convergence of KENO Criticality Results

The statistical standard deviation calculated by KENO is an important and generally reliable test of the convergence of the neutron self-multiplication predicted. However, under certain circumstances, reliance on this quantity alone to assure convergence may not be justified. In particular, a case in which the fissile material is present in discrete lumps that are widely distributed may not converge reliably unless a sufficiently large number of neutrons per generation and/or number of generations are used. Several of the problems examined in Chapter 6 and its Appendixes are of this nature.

Most of the results reported in Section 6.5 were obtained using 300 neutrons per generation for 50 generations.^{*} The MORSE code was used on a small number of cases as a cross check. In each such case the two results differed by less than one standard deviation.^{**} In addition, in several KENO calculations the number of neutrons per generation were varied. Three of these cases are summarized in Table 6D-1. In each case the agreement between the 300 and 400 neutrons per generation results was satisfactory, indicating that the statistical standard deviation is a reasonable estimate of the calculational uncertainty in these results.

The final test applied to verify convergence of the KENO result was to examine the cofactor k matrix.¹ This matrix provides an estimate of the reactivity worth of the different components in the geometry by printing an estimate of what the k_{eff} would be if the component were omitted.[†] If a fundamental spatial flux mode has been reached, the cofactor k values for symmetric components should be similar and the values for components containing fissile material and located near the center of the geometry should be smaller (reflecting a greater reactivity worth) than similar components located near the outer edge of the geometry. Furthermore, any component not undergoing fission should have a cofactor k value roughly equal to the k_{eff} of the system. Examination of the matrix of cofactors allows the KENO user to verify that fissions are occurring where they should and that the spatial distribution of fissions is reasonable.

^{*}The calculations actually included 53 generations but the results from the first 3 were discarded to account for the fact that the input source did not have the fundamental mode spatial distribution.

^{**}Because of this agreement, the MORSE results were not reported.

[†]The result is only an estimate since the calculation assumes that the spatial dependence of the neutron flux is not affected by removal of the component. Computer run time and core requirements are increased when the cofactor k matrix is calculated; hence, normally this diagnostic tool is not used on a regular basis.

TABLE 6D-I

Effect on KENO Results of Variation in Neutrons per Generation

Problem Description	Calculated k_{eff} ^a	
	300 Neutrons/ Generation	400 Neutrons/ Generation
8 TB-1's, Rectangular array ^{b,c}	0.626 ± 0.009	0.625 ± 0.006
12 TB-1's, Rectangular array ^{b,c}	0.631 ± 0.009	0.630 ± 0.007
15 TB-1's, Rectangular array [†]	0.874 ± 0.008	0.871 ± 0.005

^a All calculations were run for 53 generations; k_{eff} was based on the last 50 generations. The k_{eff} 's for the 8- and 12-vessel arrays are plotted in Figure 6C-2; the 15-vessel array corresponds to the rectangular-array data point plotted in Figure 6C-3 except that the present results include no water external to the TB-1's.

^{b,c} All vessels and intervening spaces flooded with water.

[†] All vessels fully flooded; no water was assumed external to the TB-1's.

The cofactor k matrix for the third case of Table 6D-I with 400 neutrons per generation is shown in Table 6D-II. In each case the nonfissioning regions (voids, designated V) give $k_{eff} \approx 0.87$, which is close to the 50-generation average value of 0.871 ± 0.005 . The values for the symmetric regions such as the central TB-1 value for layers 1 and 3 are similar and the centrally located vessel (center of layer 2) has the smallest cofactor value shown. Thus the problem has apparently converged properly and the calculated k_{eff} appears to be correct.

TABLE 6D-II

Cofactor k Matrix for Array of 15 TB-1's in a Rectangular Configuration

Layer ^a	Geometry ^{b,c}			Cofactor k [†]		
	V	TB-1	V	0.8698	0.8604	0.8699
1	TB-1	TB-1	TB-1	0.8592	0.8389	0.8614
	V	TB-1	V	0.8699	0.8597	0.8699
	V	TB-1	V	0.8699	0.8420	0.8695
2	TB-1	TB-1	TB-1	0.8435	0.7569	0.8443
	V	TB-1	V	0.8695	0.8501	0.8696
	V	TB-1	V	0.8696	0.8587	0.8697
3	TB-1	TB-1	TB-1	0.8582	0.8320	0.8584
	V	TB-1	V	0.8696	0.8580	0.8696

^a Configuration consists of three layers of 5 TB-1's each.

^{b,c} "TB-1" designates TB-1 containing 3.15-kg $^{239}\text{PuO}_2$, "V" designates void. Spaces between TB-1's were assumed to be voids.

[†] Average $k_{eff} = 0.871 \pm 0.005$ based on 50 generations.

Reference (App. 6D)

1. L. M. Petrie and N. F. Cross, KENO IV- An Improved Monte Carlo Criticality Program, ORNL 4938, Oak Ridge National Laboratory, Oak Ridge, TN, 1975.

1567 304

CHAPTER 7
OPERATING PROCEDURES

The information in this chapter presents recommendations to the NRC reviewing staff regarding operating procedures applicable to the PAT-1 package.

7.1 Procedures for Loading the PAT-1 Package

7.1.1 Loading of PuO₂ Into the PC-1 Product Can

A procedure for loading PuO₂ into the PC-1 product can is described in Appendix 7A. The specific requirements would be as follows:

- a. Any filler material used within the PC-1 (e.g., to fill space resulting from a short load) must be restricted to those which will not decompose at $\leq 1100^{\circ}\text{F}$ (593°C), except for two plastic bags and a necessary amount of tape which are for initial plutonium-oxide powder packaging.
- b. The PC-1 must be roll-crimped to the PC-1 body and double-sealed by the application of an overcoating of a room-temperature-curing impact-resistant rubber-modified epoxy sealant.

7.1.2 Loading the PC-1 Into the TB-1 Containment Vessel

A detailed procedure for loading the PC-1 into the TB-1 containment vessel, described in Appendix 7B, includes the following:

- a. Load the PC-1 product can into the TB-1 containment vessel.
- b. Place the aluminum honeycomb spacer on top of the PC-1 product can.
- c. Grease the O-ring with silicone grease (see Table 7B-1) and insert onto TB-1 lid.
- d. Verify the presence of the copper gasket and inspect for major damage to the copper.
- e. Place TB-1 lid into TB-1 body and install two of the twelve 1/2-20 socket-head cap screws. These two screws should be 180° apart.

- f. Install remainder of cap screws fingertight and then tighten all 12 screws to 50 ft-lb in the following order (by screw number): 1-7, 4-10, 2-8, 11-5, 3-9, 12-6.
- g. Repeat step f. to a torque level as indicated in Table 7.1.2-1.
- h. Attach the lifting sling to the TB-1 lid.

TABLE 7.1.2-1

<u>Assembly or TB-1 Copper Seal Use No.</u>	<u>Second Torque Level (ft-lb)</u>
1 (First use of seal)	75
2 (Second use of seal)	75
3 (Third use of seal)	75
4 (Fourth use of seal)	80
5 (Fifth use of seal)	80
6 (Sixth use of seal)	80
7 (Seventh use of seal)	85
8 (Eighth use of seal)	85
9 (Ninth use of seal)	85

Note: After its ninth use, the TB-1 copper seal must be replaced. Refer to example replacement procedure of 7.1.5.

7.1.3 Loading the TB-1 Containment Vessel Into the AQ-1 Overpack

A detailed procedure is described in Appendix 7C and includes the following:

- a. Lower the TB-1 into the AQ-1 overpack.
- b. Insert the small redwood plug.
- c. Insert the 11-in. -diam aluminum load-spreader plate.
- d. Insert the large outer redwood plug.
- e. Place the large insulation pad on the plug.
- f. Insert the inner liner cover (line up index marks).
- g. Place the insulation pad on the inner cover.

- h. Insert the outer cover, lining up index marks.
- i. Install the clamp ring by lining up index marks and holes and using twenty-three 3/8-24 UNF hexagon-head screws. Start screws at index mark and proceed on alternate sides, towards the gap in the ring.
- j. Torque hexagon-head screws to 15 ft-lb.
- k. Install the clamp-ring bolt and lock nut; install security wire, if required.

7.1.4 Loading the AQ-1 Overpack Onto a Packing Skid

The PAT-1 package may be steel-banded to a packing skid (which is provided with the AQ-1 overpack) for transportation and handling.

A design of such a skid is indicated in Figure 7.1.4-1. Federal Standard QQ-5-781 describes the proper strapping and fasteners.

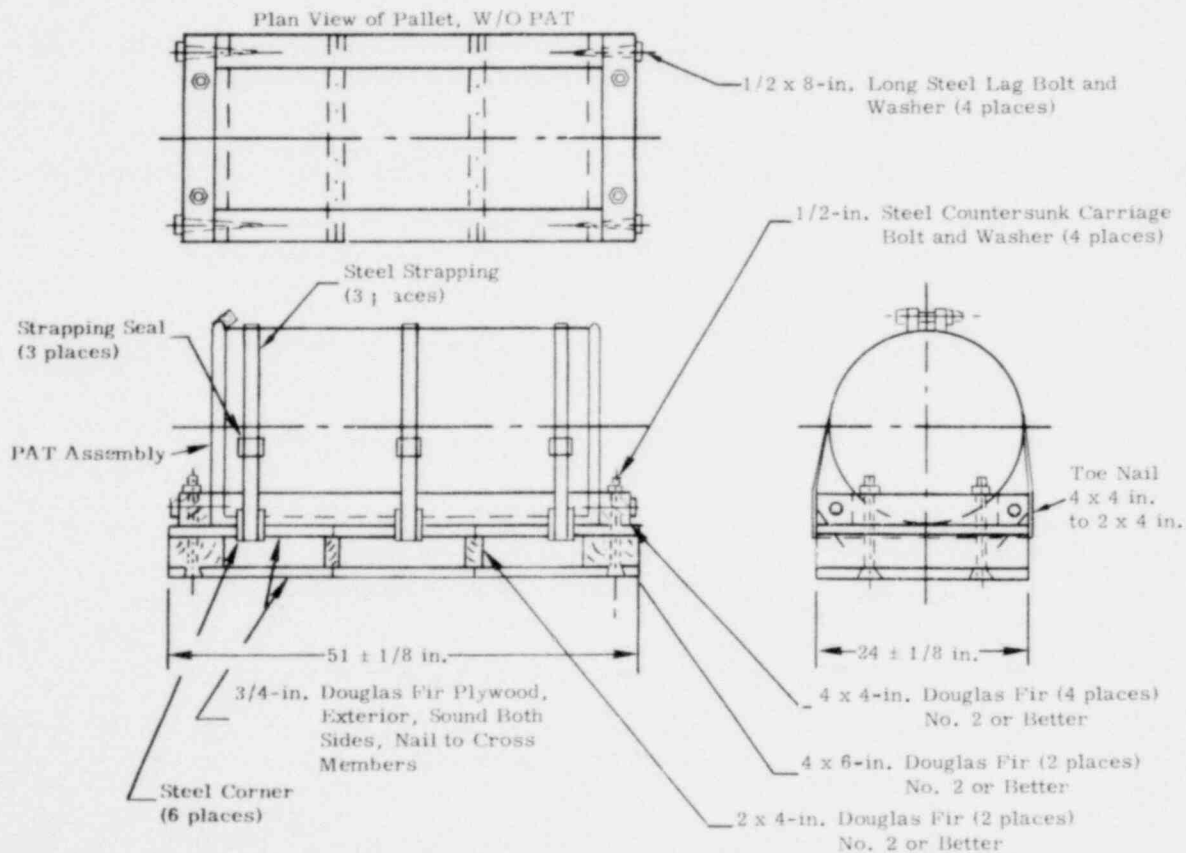


Figure 7.1.4-1. Shipping Configuration

1567 307

7.1.5 Replacement Operations for Copper Seal

Replacement of the copper seal is required after its ninth use as noted in Table 7.1.2-1. When the copper gasket becomes firmly imbedded within the groove on the TB-1 lid, it is difficult to remove; however, it can be removed by the careful use of a small, sharp machinist's chisel and a small machinist's hammer. Take great care not to mark the stainless-steel lid in any manner with the chisel. Hold the flat cutting edge of the chisel parallel to the flat sealing surface of the lid (the flat region that the 12 bolt holes pass through); gently hammer the chisel into the edge thickness of the copper gasket. This is done in an inward, radial direction. Once the chisel edge has a "bite" in the copper, pry up on the copper by pushing down on the chisel. Repeat this operation at twelve points (in between each bolt hole). If the copper gasket is not pryed out by the twelfth attempt, repeat the entire operation, imbedding the chisel slightly deeper each time, until the copper gasket pries out.

The O-ring may be removed by pushing slack to one point, then grasping it, and pulling it out.

Clean the lid with a suitable solvent and disposable wipes.

Fit a new copper gasket, part No. R00637-000, into the mating groove on the lid. Make sure the gasket fits in a flat and centered manner. The gasket is loose prior to the first closure of the TB-1 lid onto the TB-1 body (it is tightened by applying torque to the 12 closure bolts). After the first closure, the copper gasket will pinch into the groove on the lid. Lubricate a new O-ring, Parker V 747-75-242, with silicone grease (see Table 7B-1), and install it in the O-ring groove on the TB-1 lid.

7.2 Procedures for Unloading the Package

- a. Remove the PAT-1 from the skid, if present.
- b. Remove the security wire and seal, if present.
- c. Remove the twenty-three 3/8-24 UNF hexagon-head screws.
- d. Remove the clamp-ring bolt and lock nut.
- e. Remove the clamp ring by grasping the lugs in either hand and pulling the ring apart while lifting.
- f. Remove the cover.
- g. Remove the insulation pad.

- h. Remove the inner cover by lifting from the two finger holes provided.
- i. Remove the outer redwood plug by lifting from the two finger holes provided.
- j. Remove the 11-in. -diam aluminum load-spreader plate by lifting from the two finger holes provided.
- k. Remove the inner redwood plug by lifting from the two finger holes provided.
- l. Remove the TB-1 by grasping the lifting sling and lifting.
- m. Remove the lifting sling from the TB-1.
- n. Remove the twelve 1/2-20 socket-head cap screws from the TB-1.
- o. Remove the TB-1 lid. This can be done by installing three screws 1/4-28 UNF x 1-in. - long and turning them evenly until the lid releases. There may be some pressure relief action.
- p. Remove the aluminum honeycomb top spacer.
- q. Remove the PC-1 product can with contents by carefully tilting the TB-1 until the product can slides out.

CAUTION: When returning empty PAT-1 packaging with an empty TB-1, the assembly steps of paragraph 1.2 should be followed, except that the twelve TB-1 1/2-20 socket-head cap screws should be torqued to a nominal mechanic's feel.

APPENDIX 7A

Operating Procedures for Loading of PuO₂ Into the PC-1 Product Can

The process for loading plutonium into the PC-1 product can is expected to proceed under the following conditions: The PC-1 loading operation would be performed in a glove box or controlled exhaust hood with less than ambient atmospheric air pressure, with adequate exhaust filtration, and with appropriate control of surface cleanliness. The plutonium-oxide powder would be double-wrapped in polyethylene bags (for PuO₂ with low decay heat) or in special high-temperature plastic bags (for PuO₂ with high decay heat) with each bag taped shut individually. The bags and tape would be weighed and the data recorded prior to shipment. Appropriate processing and handling would be implemented to maintain an uncontaminated exterior surface on the second bag. A PC-1 product can, without the lid, could be used as a form in filling the bags so that the finished double-bagged product will fit easily into another clean PC-1 selected for actual shipment. The PC-1 can, having a round bottom, should be supported in a work stand to provide stability.

The PC-1 selected for use within the TB-1 should be serialized, identified, appropriately marked as to its contents, and visually inspected to assure cleanliness and freedom from defects. The PC-1 can body and mating lid should, likewise, be inspected and may be weighed for accountability control. These data should be recorded.

If any filler material is used within the PC-1 (e. g., to fill space resulting from a short load), the material is restricted to that which will not decompose at $\leq 1100^{\circ}\text{F}$ (593°C). The two plastic bags and the necessary amount of tape are the only low-temperature-decomposing materials permitted within the PC-1.

The double-bagged plutonium oxide, with clean exterior, would then be loaded into the clean PC-1 selected for use. The PC-1 lid must then be roll crimped to the PC-1 body by using a standard canning tool or machine. The stainless steel can lid and body material is more difficult to form into place than ordinary can materials, requiring extra care and attention. Several small stages of forming, with each set of roller tools, is recommended. The exterior of the PC-1 should be cleaned and then inspected by standard health physics swipe tests for plutonium contamination.

The gross weight of the loaded PC-1 should be measured and recorded, and the net weight of PuO₂ contents calculated and marked on appropriate labels on the PC-1.

The crimped-lid seam of the stainless-steel PC-1 product can must be double-sealed by the application of an overcoating of a room-temperature-curing, impact-resistant rubber-modified epoxy sealant. A formulation equivalent to that specified in Table 7A-I is to be applied all around the roll-crimped joint by the use of a disposable plastic syringe.

TABLE 7A-I

Formulation for Rubber-Modified Epoxy Sealant

<u>Proprietary Designation</u>	<u>Chemical Type</u>	<u>Parts by Wt.</u>
Dow Chemical XD7575-02*	CTBN (carboxy-terminated-butadiene-nitrile) rubber-modified epoxy	110
B. F. Goodrich ATBN	ATBN (amine-terminated butadiene-nitrile) rubber	50
Jefferson Chemical Co. T403	Polyoxypropylene-triamine	45
Jefferson Chemical Co. Accelerator 398	Amine accelerator	4.5

* or manufacturer's recommended substitute

Care should be taken to leave no gaps or voids in the bond region. The bonded PC-1 can with contents should be permitted to cure at room temperature for 24 hr, or longer if necessary to be tack free. Sixteen hours at 75° F (24° C) has been a typical cure condition.

The parts and material needed for the PC-1 product-can loading are listed in the Table 7A-2. These parts are to be visually inspected for major imperfections or damage, and for cleanliness.

TABLE 7A-II

Parts List for PC-1 Loading

<u>Quantity</u>	<u>Item</u>	<u>Part Number</u>
1 ea	Body, can	R00633-000
1 ea	Lid, can	R00634-000
2 ea	Plastic bags 6 x 12 in.	
As reqd	Tape	
As reqd	Nuclear material labels	
As reqd	Identification labels	
As reqd	Rubber-modified epoxy sealant	
1 ea	Can assembly	R00631-000*

* The part results from joining the body and lid.

APPENDIX 7B

Loading the PC-1 Product Can Into the TB-1 Containment Vessel

7B.1 Introduction

The parts and materials required for loading the PC-1 into the TB-1 are listed in Table 7B-I. These parts should be visually inspected for major imperfections or damage, for cleanliness, and for the presence of the correct part number.

TABLE 7B-I

Parts List for TB-1 Loading

<u>Quantity</u>	<u>Item</u>	<u>Part Number</u>
1 ea	Body, TB-1	R00635-000
1 ea	Lid, TB-1	R00636-000
1 ea	Spacer, top	R00632-000
1 ea	Gasket, copper	R00637-000
1 ea	O-ring (Viton)	Parker No. V747-75-242
12 ea	Bolt, socket head, special 0.500-20	R00638-000
1 ea	Sling, lifting	R00619-000
1 ea	PC-1 product can, loaded	
3 ea	Screw, cap, hex head, 0.250-28 x 0.750 in. long	MS90726-6
3 ea	Washer, steel, 0.281 I.D. x 0.625 x 0.065 in.	MS27183-10
As reqd	Silicone grease	General Electric G-624 (MIL-S-8660) or Dow Corning DC-4 (MIL-S-8660)
As reqd	Labels, nuclear material	
As reqd	Labels, identification	
1 ea	Containment vessel, TB-1*	R00630-000

* This part results from the assembly sequence.

The step-by-step loading procedure is given in paragraph 7B.2.

7B.2 TB-1 Containment Vessel Assembly Procedure

Step 1. The first step of the loading procedure is to insure that all necessary parts are available. Figure 7B-1 shows the parts needed to load the PC-1 product can.

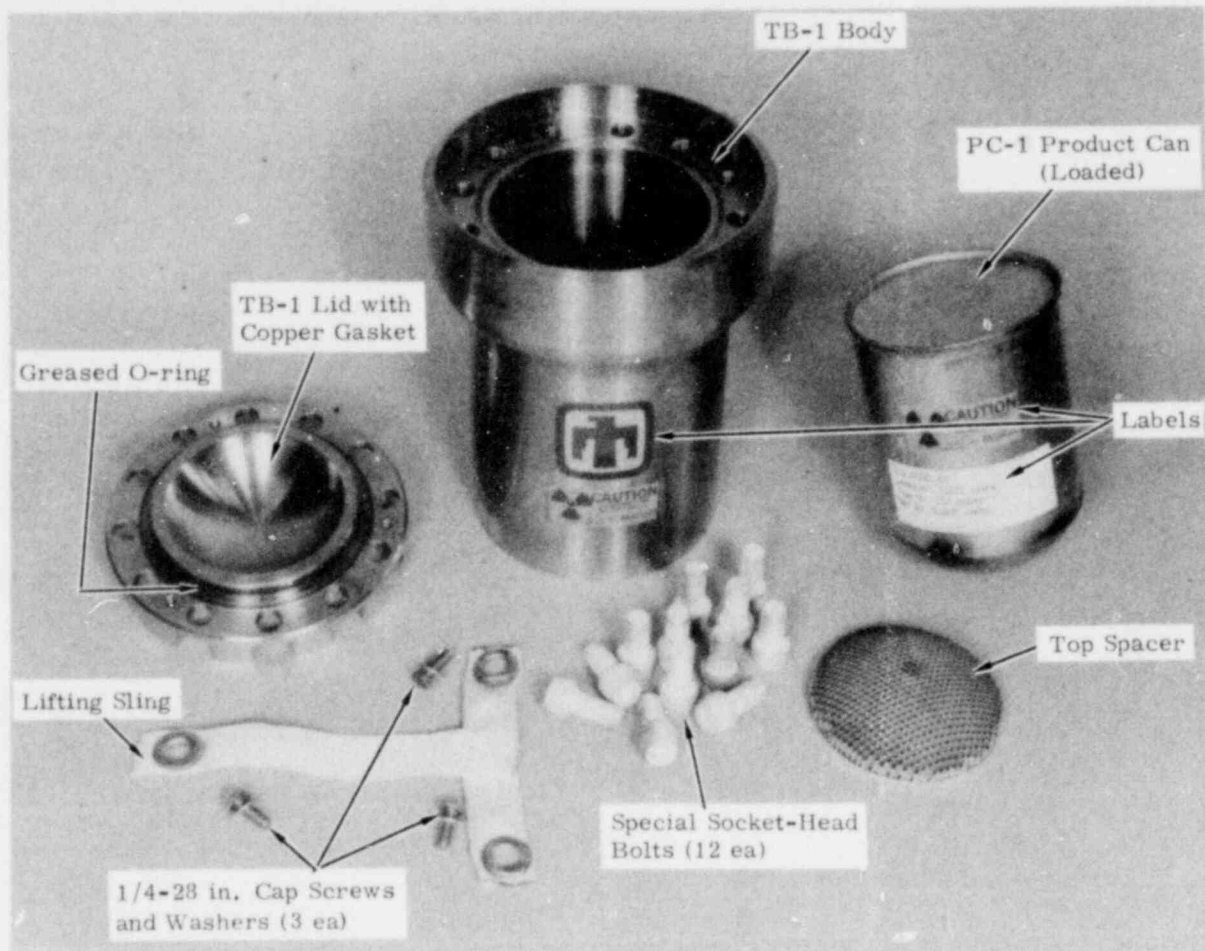


Figure 7B-1. Parts for Loading PC-1 Product Can

POOR ORIGINAL

Step 2. Place the product can and top spacer into the TB-1 body (Figure 7B-2).

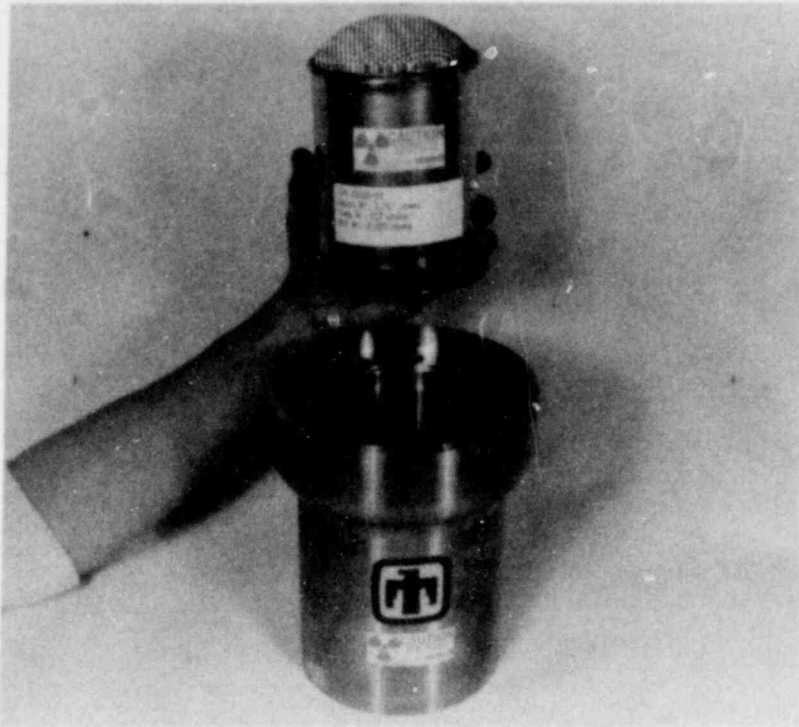


Figure 7B-2
Step 2

Step 3. Grease the O-ring with the required silicone grease (General Electric or Dow Corning) and put the O-ring into the groove in the TB-1 lid. Verify the presence of the copper gasket firmly imbedded in its groove in the lid. Visually inspect for any major damage to the copper. The small circular groove all around the copper gasket is proper and acceptable. Small scratches in the copper are acceptable (Figure 7B-3).

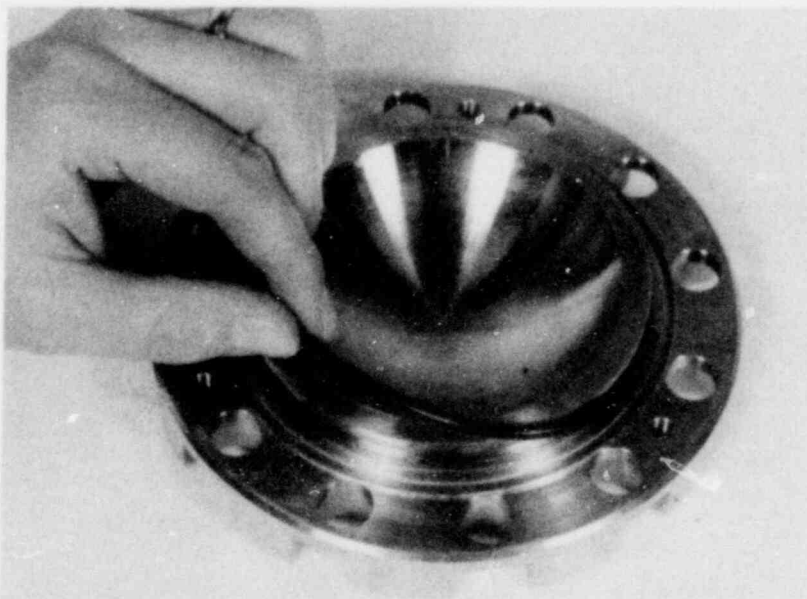


Figure 7B-3
Step 3

POOR ORIGINAL

1567 314

Step 4. Place the TB-1 lid in the TB-1 body, lining up the screw holes by eye (Figure 7B-4). Take care not to disturb the O-ring or the top spacer. Install two of the twelve big cap screws fingertight, as shown. Install the rest of the big cap screws fingertight.

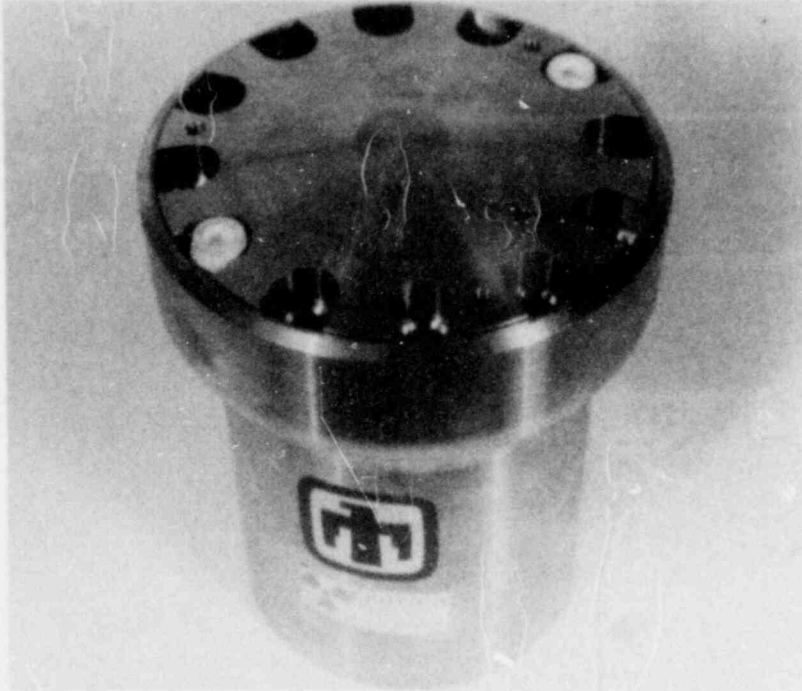


Figure 7B-4
Step 4

Step 5. Put the TB-1 Containment Vessel in a vise (Figure 7B-5), with screw No. 12 on top. The screws must be tightened two times with a torque wrench.

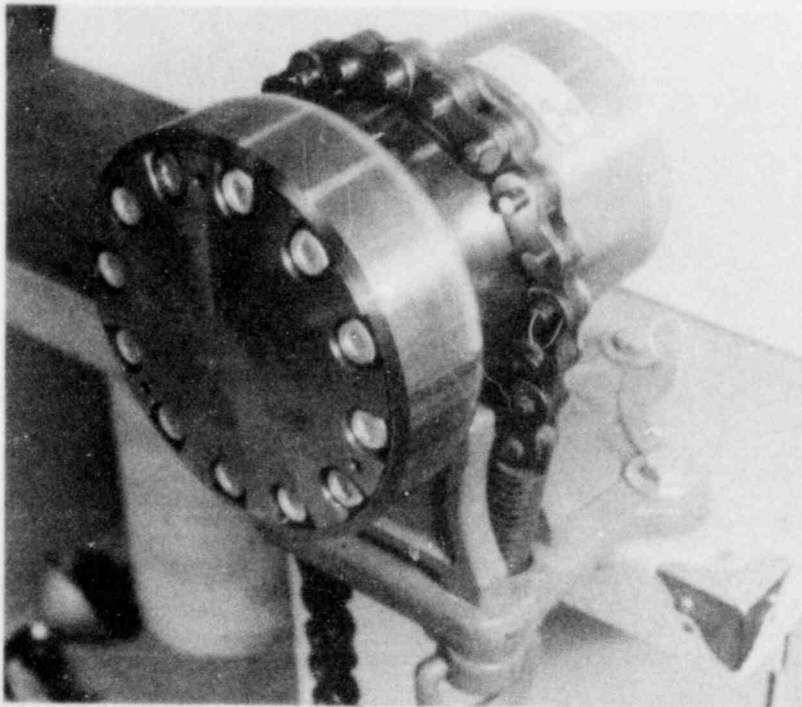


Figure 7B-5
Step 5

Step 6. For the first torque, set the torque wrench to 50 ft-lb, and tighten all twelve screws in the following order (by screw number).

1-7 4-10 2-8 11-5 3-9 12-6

Step 7. For the second torque, find the first line (from the top), in the list below, that has not been used. Use the torque level in that line for the second torque.

<u>Assembly No.</u>	<u>Second Torque Level (ft-lb)</u>	<u>Name</u>	<u>Organization</u>	<u>Date</u>
1	75	_____	_____	_____
2	75	_____	_____	_____
3	75	_____	_____	_____
4	80	_____	_____	_____
5	80	_____	_____	_____
6	80	_____	_____	_____
7	85	_____	_____	_____
8	85	_____	_____	_____
9	85	_____	_____	_____

Note: After assembly No. 9, the containment vessel copper seal must be replaced, as described in paragraph 7.1.4.

Tighten the screws in the following order:

1-7 4-10 2-8 11-5 3-9 12-6

Write your name, organization, and date on the line next to the torque-level you just used.

Step 8. Using the three small screws and washers, attach the lifting sling as shown (Figure 7B-6). Tighten the screws fingertight, then tighten very slightly with a wrench. Do not over-tighten.

Note: Always use the lifting sling when carrying the containment vessel.

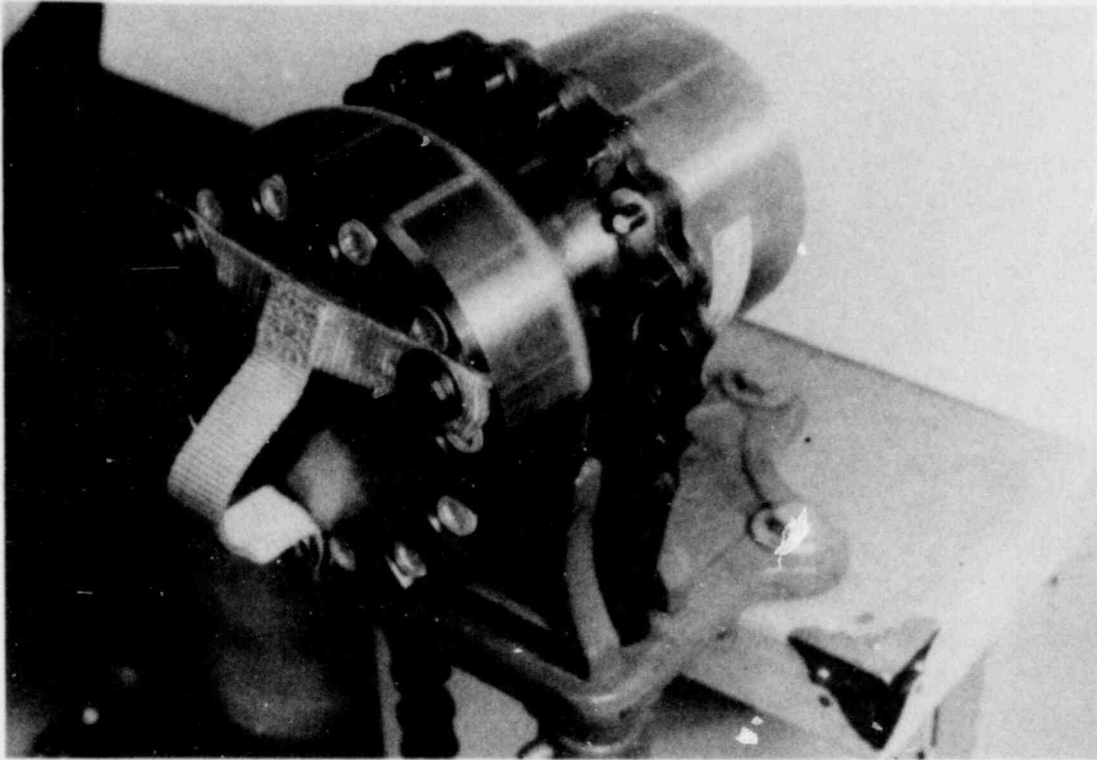


Figure 7B-6. Step 8

Step 9. Loosen the vise and remove the TB-1 containment vessel. The TB-1 containment vessel is now ready to be placed in the AQ-1 overpack.

POOR ORIGINAL

APPENDIX 7C

Loading the TB-1 Containment Vessel Into the AQ-1 Overpack

7C.1 Introduction

The parts and material required for loading the TB-1 containment vessel into the AQ-1 overpack are listed in Table 7C-1. These parts are to be visually inspected for major imperfections or damage and for general cleanliness.

TABLE 7C-1
Parts List for AQ-1 Loading

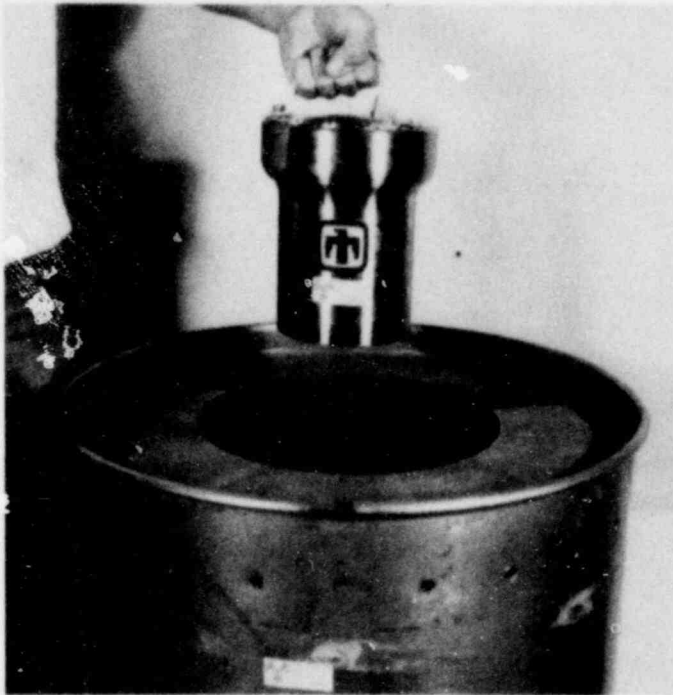
<u>Quantity</u>	<u>Item</u>	<u>Part Number</u>
1 ea	Container subassembly	R00629-001
1 ea	Removable wood plug (small inner plug)	R00627-000
1 ea	Removable disc	R00625-000
1 ea	Removable wood plug (large outer plug)	R00625-000
1 ea	Liner cover (furnished with 23 floating nut plates)	R00624-000
1 ea	Modified cover (furnished with gasket and plug)	R00618-000
1 ea	Modified clamp ring (furnished with 5/8 -11 x 4 in. long draw bolt and lock nut)	R00621-000
1 ea	Insulation pad	R00628-000
1 ea	Insulation pad	R00639-000
23 ea	Hex-head cap screw 3/8 in. -24	MS90726-60
As reqd	Security wire and seal	
1 ea	Assembled TB-1 containment vessel	R00630-000

The step-by-step loading procedure follows in paragraph 7C.2.

1567 318

7C.2 AQ-1 Overpack Loading Procedure (Loading the TB-1 Containment Vessel Into the AQ-1 Overpack)

Step 1. Place the TB-1 containment vessel into the AQ-1 overpack (shipping package), seating it all the way down (Figure 7C-1).



Figures 7C-1 through 7C-14.
Loading Procedure for TB-1 Con-
tainment Vessel Into the AQ-1

Figure 7C-1
Step 1

Step 2. Insert the small redwood plug. Twist it to ensure that the notches in the bottom of the plug clear the lifting sling screws in the TB-1, and that the plug is all the way down.



Figure 7C-2
Step 2

Step 3. Insert the aluminum plate, seating it all the way down (Figure 7C-3).

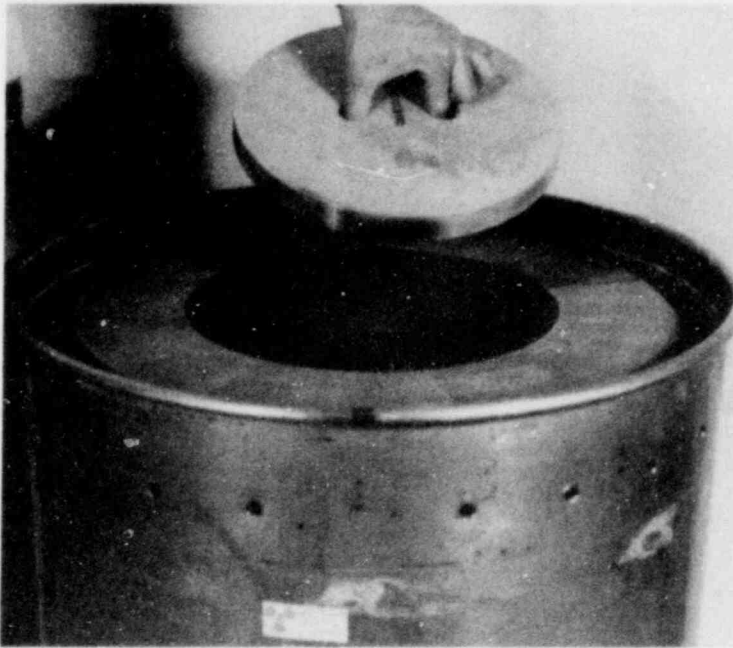


Figure 7C-3
Step 3

Step 4. Insert the big redwood plug, seating it all the way down (Figure 7C-4).



Figure 7C-4
Step 4

Step 5. Center the big pad on top of the big redwood plug (Figure 7C-5).



Figure 7C-5
Step 5

Step 6. Insert the inner cover, lining up the index marks (Figure 7C-6).

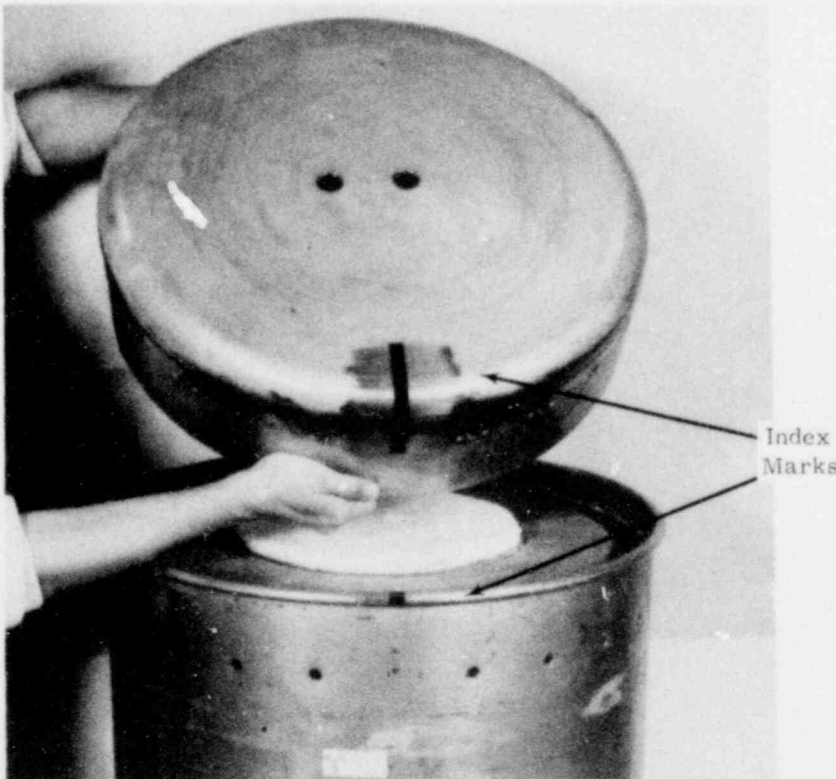


Figure 7C-6
Step 6

Step 7. Center the small pad on the inner cover (Figure 7C-7).

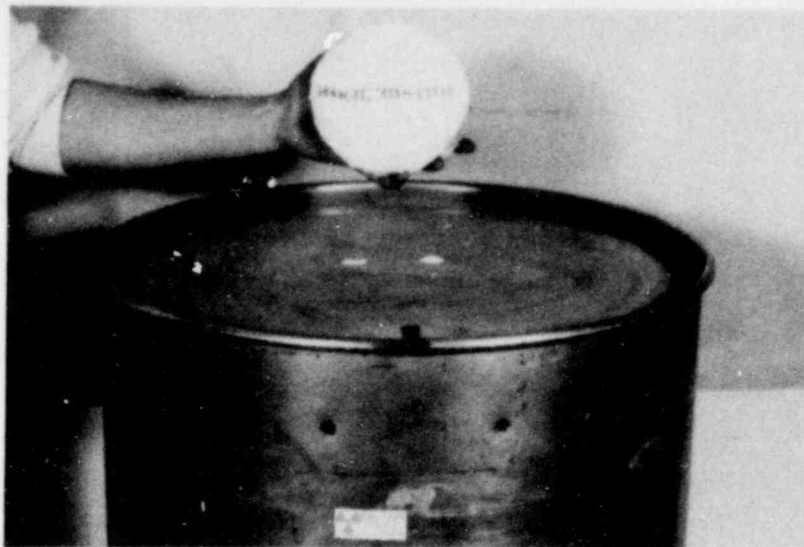


Figure 7C-7
Step 7

Step 8. Insert the outer cover, lining up the index marks (Figure 7C-8).



Figure 7C-8
Step 8

POOR ORIGINAL 1567 322

Step 9. Install the clamp ring, lining up the index marks (Figure 7C-9).

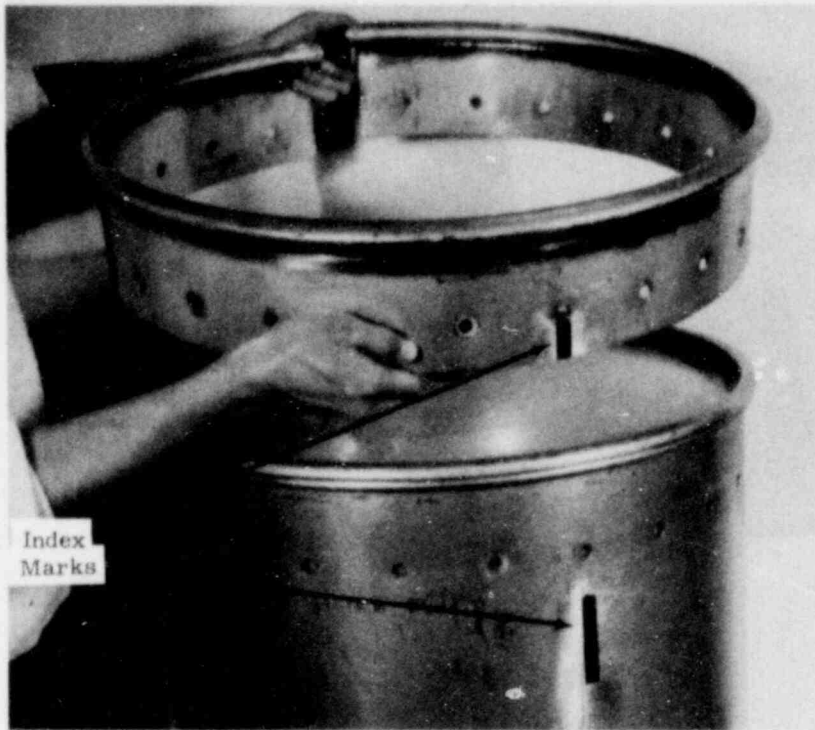


Figure 7C-9
Step 9

Step 10. Using a tapered pin, line up the holes by the index marks so that you can thread one of the 23 screws through the holes (Figure 7C-10).

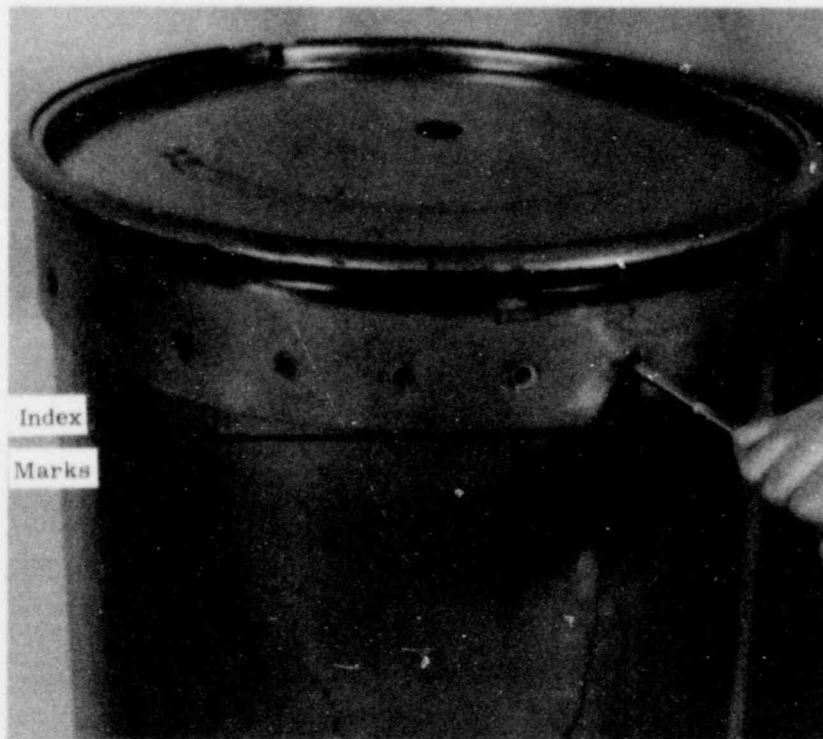


Figure 7C-10
Step 10

Step 11. Thread one hex-head screw into the hole by the index mark, and tighten it fingertight (Figure 7C-11).

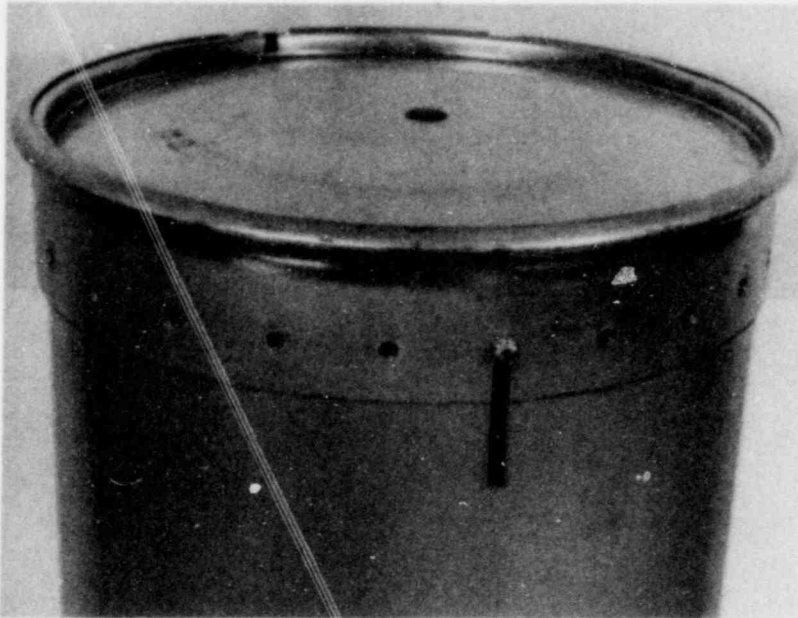


Figure 7C-11
Step 11

Step 12. Install the remaining hex-head screws one by one: one to the left of the first screw, then one to the right of the first screw, working back and forth toward the gap in the clamp ring (Figure 7C-12). Use the tapered pin to help line up the holes for the screws. (If some of the screws are faulty and won't screw in, replace them with new ones.)

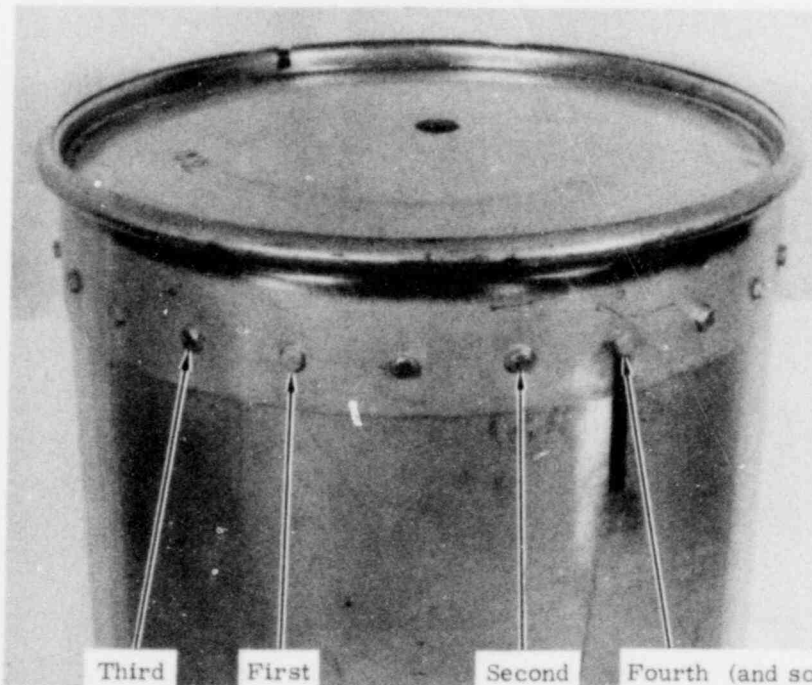


Figure 7C-12
Step 12

Step 13. When all the screws are threaded in, torque them to 15 ft-lb.

Step 14. Install the 4-in.-long hex-head screw in the clamp ring and torque it to 50 ft-lb (Figure 7C-13).



Figure 7C-13. Step 14

Step 15. Install the nut on the 4-in.-long screw. Hold a wrench on the screw to keep it from turning, and torque the nut to 30 ft-lb.

Step 16. A security wire and seal may be installed through the holes provided in the lugs on the clamp ring (Figure 7C-14).



Figure 7C-14. Step 16

This completes the assembly of the shipping package. The assembly of the TB-1 containment vessel into the AQ-1 overpack forms a PAT-1 package.

POOR ORIGINAL

1567 326

303-304

CHAPTER 8

ACCEPTANCE TESTS AND MAINTENANCE PROGRAM

The Product Specification, Plutonium Air Transportable (PAT) Package, PS-R00602-000, as presented in Chapter 9, Appendix A, is the authoritative statement establishing the requirements for manufacture and manufacturer's acceptance of those Model PAT-1 packages that were produced for Sandia Laboratories and that were used in the tests documented throughout this report. Additional information in this chapter is recommended to the NRC staff as possible instructions for users of the PAT-1 package.

8.1 Acceptance Tests to be Performed Prior to First Use of Each Package

8.1.1 Visual Inspection

Note: The following steps are not necessarily in sequential order. To accomplish a complete visual inspection, the TB-1 and AQ-1 must be disassembled in accordance with paragraph 7.2.

8.1.1.1 AQ-1 Overpack

- a. Check that there are no indentations deeper than 1/2 in. in the visible interior redwood assemblies.
- b. Check that there are no large, obvious breaks in the fiberglass covering of the innermost tubular member (copper heat-conductor tube).
- c. Check that there are no indentations or damage points deeper than 1/2 in. in the outer steel drum and covers.
- d. Check that the 23 bolt-head covers are in place around the bottom of the drum.
- e. Check that the twenty-three 3/8-24 bolts are in place around the top end of the drum (when AQ-1 is assembled).
- f. Check that the 5/8-in. -diam x 4-in. -long clamp-ring bolt and lock nut are in place at the top of the drum (when AQ-1 is assembled).
- g. Check that the Caplug vent plugs are in place on the drum bottom and on the drum lid.

8.1.1.2 TB-1 Containment Vessel

- a. Check that the copper gasket is in place on the TB-1 lid and that it is free of any major gouge or irregularity (the circular groove all around is correct).
- b. Check that the O-ring is in place on the TB-1 lid, free of large obvious gouges, and lightly lubricated with the specified silicone grease.
- c. Check for visible damage to the small circular knife-edge in the TB-1 body (the lid knife-edge will normally be hidden by the copper gasket).
- d. Check for the presence of the 12 socket-head bolts and the nylon lifting sling with 3 bolts and washers (when TB-1 is assembled).

8.1.1.3 Replacement Parts

Missing parts may be replaced if (a) the replacement part meets the design requirements as described in the drawings of Chapter 9, Appendix A, and (b) no other damage to the PAT-1 package is evident as a result of the missing part.

8.1.1.4 Rejection

Mechanical damage as described in paragraphs 8.1.1.1 and 8.1.1.2 is cause for rejection. Damage to the knife-edge or copper gasket is cause to perform a leakage test as described in paragraph 8.1.3 to demonstrate TB-1 vessel acceptability.

8.1.2 Structural, Pressure, and Leak-Rate Tests of the TB-1 Containment Vessel

Each TB-1 containment vessel before its first use must be demonstrated to remain leak-tight* when assembled as for shipment and subjected to an internal pressure 50 percent higher than maximum normal operating pressure ($1.5 \times 34.3 \text{ psi} = 51.4 \text{ psi}$).

Structural and pressure tests beyond this leakage test and those described in paragraph 8.1.3 are not required.

8.1.3 Leak Testing of PC-1 Product Can

To demonstrate that before first-use the PC-1 product can meets the requirements pertaining to single-trip containment systems, at least one PC-1 product can from each lot or one of each 20 PC-1 containers (whichever results in the highest test frequency) will be assembled as for use with actual contents. This PC-1 must be leak-tested. This leakage test shall have a

* $10^{-7} \text{ cm}^3/\text{s}$ per USNRC Regulatory Guide 7.4 which references ANSI N14.5.

sensitivity of at least 10^{-4} cm³/s and indicate leakage less than 10^{-3} cm³/s in the assembled PC-1. (An acceptable test would be one in which the PC-1 is placed in a closely fitting chamber, a vacuum is rapidly drawn, and any subsequent rise in chamber pressure is correlated with leak rate.)

8.2 Tests to Verify Proper Assembly Prior to Each Shipment

8.2.1 PC-1 Product Can

Prior to loading the PC-1 product can (with contents) into the TB-1 containment vessel, a leakage test shall be completed on the PC-1. This leakage test shall have a sensitivity of at least 10^{-4} cm³/s and indicate leakage less than 10^{-3} cm³/s in the assembled PC-1. (An acceptable test would be one in which the PC-1 is placed in a closely fitting chamber, a vacuum is rapidly drawn, and any subsequent rise in chamber pressure is correlated with leak rate.)

8.2.2 TB-1 Containment Vessel

As part of preparation for each actual shipment, the TB-1 containment vessel will be assembled in accordance with the procedure described in paragraph 7B-2 and a leakage test shall be completed on the TB-1 together with its radioactive contents. This leakage test shall have a sensitivity of at least 10^{-4} cm³/s and indicate leakage $<10^{-3}$ cm³/s for the assembled TB-1. (An acceptable test would be one in which the TB-1 is placed in a closely fitting chamber, a vacuum is rapidly drawn, and any subsequent rise in chamber pressure is correlated with leak rate.)

8.3 Periodic Test and Maintenance

8.3.1 TB-1 Containment Vessel

After every third use of a TB-1 containment vessel, or if a leaktest as described in paragraph 8.1.3 has not been performed within the preceding 12-mo period, the TB-1 shall be subjected to the leak test as described in paragraph 8.1.3 before further use is permitted.

8.3.2 PC-1 Product Can

If a leaktest as described in paragraph 8.1.3 has not been performed within the preceding 12-mo period, a PC-1 shall be subjected to such a leaktest before further use is permitted.

8.3.3 Replacement of Gaskets on Containment Vessel

The only components of the TB-1 having a replacement schedule are the copper gasket and the Viton O-ring. The copper-gasket-replacement schedule is indicated in Table 7.1.2-I as occurring after the ninth full torquing of the closure bolts. Prior to the tenth use of the TB-1 containment vessel, the copper gasket and the O-ring must be replaced as described in paragraph 7.1.5.

CHAPTER 9
QUALITY ASSURANCE

9.1 Discussion

This chapter identifies the quality assurance requirements that were used for Sandia Laboratories' design, purchase, fabrication, and test of the Model PAT-1 package, and recommends certain requirements^{*} applicable to users of the PAT-1 package. In the areas of design and environmental test, the preceding chapters of this report provide full information regarding tests and most of the design information; Appendix 9A of this chapter provides a complete design definition. The material presented in the remainder of this chapter applies to the quality assurance program utilized for the fabrication and manufacturing of the specific Model PAT-1 packages addressed in this report, meeting the intent of 10 CFR 71, Appendix E.

9.2 Quality Assurance Program

An effective quality assurance program is maintained at both of the Department of Energy (DOE) agencies involved: Sandia Laboratories (responsible for package design and test) and the Bendix Corporation, Kansas City Division (responsible for package fabrication). The quality assurance programs assure that adequate quality control is maintained from the time of material procurement through the receipt, identification, stocking, and issue of material, and through the entire PAT-1 fabrication process. All materials which are procured from suppliers outside the DOE system are subjected to adequate quality controls and inspections to assure conformance to specification requirements. The program forestalls the procurement or manufacture of defective material, and provides that defects or other unsatisfactory conditions are discovered at the earliest practical point. The program provides readily available recorded evidence of quality in the form of inspection and test results.

The specific quality assurance provisions for the Model PAT-1 package are cited in the attached Product Specification, Plutonium Air Transportable (PAT) Package, PS-R00602-000, Section 4, Quality Assurance Provisions. This covers inspection per MIL-I-45208, calibration per MIL-C-45662, serial numbers, test records, test conditions, rejected units, certification of compliance, tolerances, in-process inspection and testing, final acceptance testing, function and fit, leak rate, and drawing compliance.

^{*}Specifically, sections 9.2.13, 9.2.14, and 9.2.15.

9.2.1 Organization

The Quality Assurance Program for the design, fabrication, and test of the Model PAT-1 package falls within the guidance of Department of Energy (DOE) directives. For the Model PAT-1 package, Sandia Laboratories, Albuquerque (SLA) was the design agency vested with all jurisdiction over design and testing. The Bendix Corporation, Kansas City Division (BKC) was the production agency for the PAT-1 packages pertinent to this report with the responsibility for fabricating the PAT-1 packages to the design requirements. In both companies, the administration, coordination, and evaluation of the quality program is vested in a responsible, authoritative element able to ensure objective decisions by contractor management.

The responsible organizations are staffed by technically competent personnel with freedom to make appropriate objective judgments, recommendations, and decisions consistent with delegated authority. Copies of organizational charts for both companies can be obtained which indicate the level of authority and independence delegated to the quality assurance function.

9.2.2 Design Control

Sandia Laboratories has overall responsibility for the design of the Model PAT-1 package. The project manager is responsible for validation and application of all analysis used in the design phase of the package.

However, the NRC performance criteria were of sufficient severity that complete reliance on analysis was not possible and the overall design adequacy of the PAT-1 was verified by a comprehensive, environmental test program. The specifications for the PAT-1 require assurance of conformity of all materials which, through design and design reviews, are necessary to the proper performance of the PAT-1 with respect to the NRC qualification criteria. Calibration systems are directly traceable to the National Bureau of Standards (NBS). All inspection tools used are to be within this calibration system.

Within the DOE this traceability is maintained by a Primary Standards Laboratory within SLA. All standards are periodically recertified by the NBS. A secondary standards laboratory is maintained at BKC which periodically recertifies their standards against those of the Sandia Primary Standards Laboratory. Periodic audits of the system are performed by Primary Standards personnel as well as personnel from the DOE.

A design definition system was formalized and controlled by EP401219, Definition Control for Plutonium Air Transportable (PAT) Package, an engineering procedure issued specifically for this task, from which excerpts are as follows:

- a. Drawing Definitions: The drawing control and drawing numbers are described in D10521, "Nonweapon Drawing Set". The 9-digit part number system applies to all parts on this program, providing for precise part identification referenced to design definition.

- b. A List of Data (LD) drawing that lists the drawings by issue which are required for procurement of the PAT-1 will be maintained by the SLA specifications engineer. This drawing may be used to authorize specific development-build definitions. (The implementation of this requirement is LD-R00602-000, List of Data, Plutonium Air Transportable (PAT) Package.)
- c. Release: All drawings will be initially released after preliminary design and review by a Development Engineering Release (DER). The DER shall also be used to authorize specific engineering actions during the development contract. SLA Department 5430 shall release drawings by DER for drawings located at SLA or BKC.
- d. Change: After release of the drawings by DER, specific changes to the design will be made by change order. The change order may authorize specific engineering action during the development contract. The class of change will be "development" (DEV). Changes to the drawings may be by either Advance Change Order (ACO) or Final Change Order (FCO). ACOs are issued prior to drawing changes being incorporated in a new drawing issue; FCOs identify a change document issued after the drawing changes are incorporated in a new drawing issue. If the drawing originals are located at BKC, Bendix has the responsibility for originating changes; if the drawing originals are located at SLA, Department 5430 has responsibility for originating changes.
- e. Approvals: The applicable 5430 project engineer and project engineering division supervisor, or his authorized delegate, approve all DERs and those changes originated at SLA. For changes originated at BKC, Bendix obtains verbal approval from the SLA project engineer and so states that approval on the change order.
- f. Distribution: The distribution of both release and change orders shall be SLA No. 1, * the buyer, the 9633 specifications engineer, the 5430 project engineer, and others as determined by the project engineer.
- g. Processing of Release and Change Orders at SLA: The specifications engineer at SLA is responsible for preparation of release and change orders originating at SLA.
- h. Relation to Development Contract: Change orders originated at SLA will be processed through the Sandia buyer in addition to the project engineering group. The change order is processed by the Product Definition Drawing Distribution Control Section.

* This is an internal Sandia Laboratories distribution list.

- i. Deviating Material: Deviation from development-build definitions must be confirmed in writing, on an SE (Specification Exception) document. SLA-originated deviations will be transmitted through the buyer.
- j. Disposition of Original Tracings: At the end of the development contract, SLA will transfer all drawing originals located at BKC by DTER to SLA for final retention. Aperture cards will be prepared and retained at Sandia and the project engineering division will authorize archiving by Archive Engineering Release.

9.2.2 Procurement Document Control

Engineering Procedure EP401219, Definition Control for Plutonium Air Transportable (PAT) Package, attached as an Appendix, is the authoritative procurement document control for the development contract and drawing definitions.

Product Specification PS-R00602-000 cites all documents required for PAT-1 quality and fabrication control.

9.2.4 Instructions, Procedures, and Drawings

Instructions, procedures, and drawings are as cited in the previously referenced Engineering Procedure EP401219 and Product Specification PS-R00602-000, and in the List of Data, Plutonium Air Transportable (PAT) Package, LD-R00602-000 (provided in attached Appendix). Instructions for users are in Chapters 7 and 8 of this report.

9.2.5 Document Control

The complete set of specifications, drawings, and control documents for the PAT-1 package are included as Appendix 9A, as cited in 9.2.3, above.

9.2.6 Control of Purchased Material

The BKC purchasing documents will specify the requirements of the contract via use of engineering drawings with the noted design requirements and by citing specifications in purchase orders. Assurance that these requirements are maintained is accomplished by inspection upon receipt of material. All material must conform to the drawing requirements. Any discrepant material is either rejected to the supplier or, if useable, approved for use via a nonconforming approval system. Any nonconforming approval request is processed to the applicable design engineer for his approval or rejection.

Certification of compliance is required on critical items (refer to paragraph 4.1.5 of PS-R00602-000 (see Appendix)).

9.2.7 Identification and Control of Material Parts and Components

All material received within BKC is properly bagged or tagged to allow referral to appropriate specifications and inspections. During fabrication of these materials into a PAT-1, records are generated to allow traceability to any previous analysis or inspection. These data are maintained for use by any appropriate organization.

Each PAT-1, AQ-1, and TB-1 is permanently marked with a serial number in ascending numerical order corresponding to the sequence of manufacture. Once assigned, a serial number is not assigned to another item.

9.2.8 Control of Special Processes

All special processes are controlled and accomplished by qualified personnel using qualified procedures in accordance with specifications included in the Appendix to this section.

Special Specifications were issued as follows:

SS-R00602 Material Specification, Redwood for PAT Package.

SS-R00621 Welding Corrosion-Resistant Steel, PAT Package.

SS-R00630 Testing, Leak Rate, Mass Spectrometer, PAT Package.

SS-R00645 General Requirements, PAT Package.

Compliance with these specifications is required on the drawings and in the overall Product Specification PS-R00602-000. Copies of these specifications are included in the Appendix.

9.2.9 Inspection

All inspections are performed in accordance with MIL-I-45208 by qualified personnel who utilize calibrated inspection devices and standard inspection techniques in accordance with MIL-C-45662. All inspection personnel are assigned to the inspection organization which is functioning independently.

Specific inspection details (final acceptance testing) are cited in paragraph 4.3 of PS-R00602-000, attached in Appendix 9A.

9.2.10 Test Control

Test control for environmental tests is per the Test Protocol, PAT-1 (Plutonium Air Transportable) Package, Model 1, included as Appendix 2H, and per the facility descriptions presented in Appendix 2J. Tests required in manufacturing are specified in the applicable drawings and specifications.

9.2.11 Control of Measuring and Test Equipment

The quality assurance program described above embodies the control of MIL-C-45662 for calibration, MIL-I-45208 for inspection, and MIL-Q-9858 for quality control, as specified in PS-R00602-000, included within Appendix 9A.

9.2.12 Handling and Related Functions

No special measures to control handling, storage and shipping, cleaning and preservation of materials and equipment are required beyond those previously addressed in this section.

9.2.13 Inspection, Test, and Operating Status

Appropriate markings, tags, labels, routing cards, or other suitable means of assuring satisfactory completion of the inspections, tests, and replacements described in Chapters 7 and 8 must be provided by the user of the Model PAT-1. This should include a user's torque-record card for the TB-1.

9.2.14 Nonconforming Materials, Parts, or Components (in service)

Appropriate measures shall be established by the Model PAT-1 package user to assure that nonconforming parts are not inadvertently used.

9.2.15 Corrective Action

Measures applicable to design, fabrication, and test have been addressed previously in this section. Measures required during package transport operations must be identified by the user.

9.2.16 Quality Assurance Records

The provisions for maintaining sufficient records of design, fabrication, and test activities have been addressed previously in this section.

9.2.17 Audits

A comprehensive system of planned and periodic audits is included in the authority delegated to the quality assurance organizations at SLA and BKC under DOE directives. A comprehensive program must also be provided by the user of the Model PAT-1 package.

9.3 Certification of Compliance

The Bendix Corporation Certificate of Compliance letter appears as Appendix 9B. The referenced Specification Exceptions are on file with the Sandia Laboratories Department 5430 Project Engineer.

APPENDIX 9A

Hierarchical Index to
PAT-1 Specification and Drawing System

LD-R00602 - List of Data

EP-401219 - Definition Control

PS-R00602 - Product Specification

SS-R00602 - Material Specification, Redwood

SS-R00621 - Welding

SS-R00630 - Leak Testing

SS-R00645 - General Requirements

R00602 - PAT Assy.

R00603 - AQ Overpack

R00604-001 - Gasket

R00618 - Modified Cover*

R00620 - Cover Skirt

R00621 - Modified Clamp Ring*

R00623 - Ring Skirt

R00624 - Liner Cover*

R00625 - Removable Wood Plug

R00626 - Removable Disc

R00627 - Removable Wood Plug

R00628 - Insulation Pad*

R00629 - Container Subassembly

R00604-001 - Drum

R00605 - AQ Subassembly

R00607 - Liner Cylinder

R00609 - Wood Cylinder

R00610 - Wood Cylinder

R00611 - Fixed Wood Plug

R00612 - Load Spreader Assembly

* Called out twice

R00613 - Load Spdr. Tube
R00614 - Fixed Disc
R00615 - Heat Conductor Tube

R00616 - Wood Cylinder
R00617 - Fixed Wood Plug

R00618 - Modified Cover
R00621 - Modified Clamp Ring
R00624 - Liner Cover
R00628 - Insulation Pad (12" dia.)
R00639 - Insulation Pad (6" dia.)
R00639 - Insulation Pad

R00630 - TB Containment Vessel

R00635 - TB Body

R00643 - TB Body Forging

R00636 - TB Lid

R00644 - TB Lid Forging

R00637 - Cooper Gasket
R00619 - Lifting Sling
R00638 - Spl. Bolt

R00632 - Top Spacer
R00631 - Can Assy.

R00633 - Can Body
R00634 - Can Lid

Note: Do not use drawings R00606 - Drum Liner, R00608 - Liner Cap,
R00622 - Mod. Drum

FSCM NO. 14213
FCO 772915SC-DEV
P.R.OWENS 9633 PRO 12/2-173
J.A.ANDERSEN 5433
LEX/140

LD-R00602
-000

Page 1 of 3

LIST OF DATA, PLUTONIUM AIR TRANSPORTABLE (PAT) PACKAGE

Page 1 2 3
Issue F E E

<u>Document No.</u>	<u>Issue</u>	<u>Title</u>
EP401219	B	Definition Control for Plutonium Air Transportable (PAT) Package
PS-R00602	F	Product Specification, Plutonium Air Transportable (PAT) Package
SS-R00602	B	Material Specification, Redwood for PAT Package
SS-R00621	A	Welding, Corrosion Resistant Steel, PAT Package
SS-R00630	B	Testing, Leak Rate, Mass Spectrometer, PAT Package
SS-R00645	B	General Requirements, PAT Package
R00602	C	PAT Assembly
R00603	C	Overpack, AQ
R00604	C	Drum
R00605	C	Subassembly, AQ
RG0607	C	Cylinder, Liner

<u>Document No.</u>	<u>Issue</u>	<u>Title</u>
R00609	B	Cylinder, Wood
R00610	C	Cylinder, Wood
R00611	B	Plug, Wood, Fixed
R00612	B	Load Spreader Assembly
R00613	B	Tube, Load Spreader
R00614	B	Disc, Fixed
R00615	B	Tube, Heat Conductor
R00616	B	Cylinder, Wood
R00617	B	Plug, Wood, Fixed
R00618	B	Cover, Modified
R00619	B	Sling, Lifting
R00620	B	Skirt, Cover
R00621	B	Clamp Ring, Modified
R00623	B	Skirt, Ring
R00624	B	Cover, Liner
R00625	B	Plug, Wood, Removable
R00626	B	Disc, Removable
R00627	B	Plug, Wood, Removable
R00628	B	Pad, Insulation
R00629	C	Container, Subassembly
R00630	B	Containment Vessel, TB
R00631	A	Can Assembly
R00632	B	Spacer, Top
R00633	B	Body, Can

<u>Document No.</u>	<u>Issue</u>	<u>Title</u>
R00634	B	Lid, Can
R00635	B	Body, TB
R00636	B	Lid, TB
R00637	B	Gasket, Copper
R00638	A	Bolt, Socket HD, Special, 0.500-20
R00639	A	Pad, Insulation
R00643	B	Forging, TB Body
R00644	B	Forging, TB Lid

ENGINEERING PROCEDURE	DWG CLASSIFICATION LEVEL	LEX-A-894
-----------------------	--------------------------	-----------

DESIGN AGENCY CONTROL NO.	REVISIONS		
	ISSUE	DESCRIPTION	PREPARED BY

B	FCO 772632SC	R. M. HAWK	9636	11/18/77
---	--------------	------------	------	----------

1 GENERAL.

1.1 Purpose. This procedure establishes the design definition system to be used for development units of the Plutonium Air Transportable (PAT) Package, and the release and change procedures for that definition. The responsible project engineering group for PAT is the Nuclear Fuel Cycle Technology Development Department, 5430.

1.2 Development Contract. The development contract with Bendix, Kansas City (BKC) is the controlling document for:

- a. Scope of work
- b. Quantities
- c. Price
- d. Deliveries
- e. Administrative conditions
- f. General terms and conditions of contract

The development contract shall call for this engineering procedure for the purposes described.

2. DRAWING DEFINITIONS. The drawing control and drawing numbers are described in D10521 (see reference 1). The 9-digit part number system will apply to all parts on this program.

An LD (List of Data) drawing that lists the drawings by issue which are required for procurement of the PAT will be maintained by the SLA specifications engineer. This drawing may be used (through the buyer) to authorize specific development build definitions.

SHEET	SHEET																			
	ISSUE																			
INDEX	SHEET	1	2	3																
	ISSUE	B	B	B																

AGENCY APPROVALS			TITLE		
ORG	DATE	INITIALS	DEFINITION CONTROL FOR PLUTONIUM AIR TRANSPORTABLE (PAT) PACKAGE		
DWG CLASSIFICATION LEVEL			SIZE	CODE IDENT NO.	DWG NUMBER
UNCLASSIFIED			A	14213	EP401219
					SHEET 1 OF 3

SA 5300 AC(3-77)

ENGINEERING PROCEDURE

DWG. CLASSIFICATION LEVEL

3. DRAWING RELEASE AND CHANGE SYSTEM.

3.1 Release. All drawings will be initially released after preliminary design and review by a Development Engineering Release (DER). The DER shall also be used to authorize specific engineering actions during the development contract. SLA Department 5430 shall release drawings by DER whether the drawings are located at SLA or BKC.

3.2 Change. After release of the drawings by DER, specific changes to the design will be made by change order.

The change order may authorize specific engineering action during the development contract. The class of change will be DEV. Changes to the drawings may be by either Advance Change Order (ACO) or Final Change Order (FCO). ACO's are issued prior to drawing changes being incorporated in a new drawing issue and FCO's identify a change document issued after the drawing changes are incorporated in a new drawing issue. If the drawing originals are located at BKC, Bendix has the responsibility for originating changes; if the drawing originals are located at SLA, Department 5430 has responsibility for originating changes.

3.3 Approvals. The applicable 5430 project engineer and project engineering division supervisor or his authorized delegate approves all DER's and those changes originated at SLA. For changes originated at BKC, Bendix shall obtain verbal approval from the SLA project engineer and so state that approval on the change order.

3.4 Distribution. The distribution of both release and change orders shall be SLA #1, the buyer, the 9633 specifications engineer, the 5430 project engineer, and others as determined by the project engineer.

3.5 Responsibility for Release and Change Orders at SLA. The specifications engineer at SLA is responsible for preparation of release and change orders originated at SLA. Change orders originated at SLA will be routed to the Sandia buyer in addition to the project engineering group. Section 9631-1 processes the releases and change orders.

4. DEVIATING MATERIAL. Deviation from development build definitions must be agreed to in conversations and confirmed in writing, as an SE (specification exception) document. SLA originated deviations will be transmitted through the buyer.

ISSUE	B			DWG. CLASSIFICATION LEVEL	SIZE	CODE IDENT. NO.	DWG. NUMBER
				UNCLASSIFIED	A	14213	EP401219
							SHEET 2 OF

SA 5300-ABD (11-76)

1567 342

ENGINEERING PROCEDURE	DWG. CLASSIFICATION LEVEL	
-----------------------	---------------------------	--

5. DISPOSITION OF ORIGINAL TRACINGS. At the end of the development contract, SLA will request transfer of all drawing originals located at BKC to SLA for final retention. If and when there is no longer a need for the original tracings, the project engineering division will authorize archiving the drawings and specifications by an Archive Engineering Release.

6. REFERENCES.

1. D10521, "Nonweapon Drawing Set".

ISSUE	B		DWG. CLASSIFICATION LEVEL	SIZE	CODE IDENT. NO	DWG. NUMBER
			UNCLASSIFIED	A	14213	EP401219
					SHEET 3 OF 3	

SA 5300-ABD (11-76)

FSCM NO. 14213
FCO772915SC-DEV
P.R.OWENS 9633 PPU 12/177
J.A.ANDERSEN 5433
LEX/CASSETTE NO. 123

PS-R00602
-000

Page 1 of 11

PRODUCT SPECIFICATION, PLUTONIUM AIR TRANSPORTABLE (PAT) PACKAGE

Page	1	2	3	4	5	6	7	8	9	10	11
Issue	F	D	D	E	D	E	F	F	E	D	D

1. GENERAL.

- 1.1 Scope. This specification establishes the requirements for manufacture and acceptance of the Plutonium Air Transportable (PAT) Package.
- 1.2 Item Description. The Plutonium Air Transportable Package covered by this specification is a packaging system suitable for use in transporting (including transportation by air) limited quantities of plutonium and similar material. It is designed to meet the requirements of CFR 10, Part 71, and CFR 49, Parts 170 through 178, and newly emerging Nuclear Regulatory Commission (NRC) accident criteria.

The Total Package, PAT, drawing number R00602, is made up of the following major components.

- a. Overpack, AQ, drawing number R00603.
- b. Containment Vessel, TB, drawing number R00630.
- c. Spacer, drawing number R00632.

2. DOCUMENTS.

The following documents form a part of this specification to the extent specified herein. Unless otherwise specified the latest issues shall be used. In the event of conflict between documents referenced herein and the contents of this specification, the contents of this specification shall be a superseding requirement.

1567 344

323

2.1 DOCUMENTS.

Specifications:

Federal:

QQ-S-781 Steel Strapping, Flat

Military:

MIL-C-45662 Calibration System Requirements

MIL-I-45208 Inspection System Requirements

MIL-Q-9858 Quality Control System Requirements

Sandia Laboratories:

SS-R00602 Material Specification, Redwood for PAT Package

SS-R00645 General Requirements, PAT Package

SS-R00621 Welding, Corrosion Resistant Steel, PAT Package

SS-R00630 Testing, Leak Rate, Mass Spectrometer, PAT Package

Standards:

Military:

MIL-STD-129 Marking For Shipment and Storage

Drawings:

LD-R00602 List of Data, PAT

Other Publications:

Regulations:

10CFR 71 Packaging of Radioactive Material For Transport and Transportation of Radioactive Material Under Certain Conditions

CFR 49 Transportation

2..1 continued

Procedures:

EP40219

Definition Control for Plutonium Air
Transportable (PAT) Package

3. REQUIREMENTS.

The provisions of SS-R00645 shall apply.

3.1 Performance. The PAT shall provide a sealed, accident resistant packaging system suitable for use in transporting plutonium by air.

3.2 Construction.

3.2.1 Production Drawings. The PAT shall be fabricated and assembled in accordance with the drawings, material lists, and other documents listed on LD-R00602, and the additional documents specified therein.

3.2.2 Standards Of Manufacture.

3.2.2.1 Quality Control. Unless otherwise specified, the requirements of MIL-Q-9858 shall apply.

3.2.2.2 Workmanship. The provisions of SS-R00645 shall apply.

3.2.2.3 Welding Methods. Welding and fabrication shall be in accordance with SS-R00621.

3.2.2.4 Glued Assemblies. The provisions of SS-R00602 shall apply.

a. In gluing wood pieces together (wood to wood), polyvinyl acetate resin emulsion per MMM-A-180 shall be used. As an alternate, glue per 3.2.2.4.b may be used, unless otherwise specified.

b. In gluing wood to metal, or metal to metal parts, the bond material shall be a mixture of the following, by weight.

100 parts Uniroyal B635 resin

15 parts Benzoflex 988 plasticizer

9 parts Uniroyal 3080 hardener

1567 346

3.2.2.4.b continued

The material shall be processed as follows: Upon receipt of the five gallon cans of Uniroyal B635, heat them for 12 hours at $130 \pm 10^{\circ}\text{F}$ and then shake them for 30 minutes in a paint shaker. This is necessary because the material will freeze at close to room temperature. Before use, the material shall be a clear, high viscosity liquid. If it is cloudy, lumpy, or resembles an "icy slush", repeat the heating and shaking process.

After withdrawing B635 material from the can, the air space above the material should be thoroughly flushed with dry nitrogen, and the can tightly sealed. If moisture in the air is allowed to react with this material, a crystalline layer will form on its surface. This can be removed, and the material used, but it is best to prevent this from happening.

In mixing, first blend the B635 and the Benzoflex 988 plasticizer together, next add the 3080 hardener and mix thoroughly. For small batches of 100 to 200 grams, two minutes of vigorous hand mixing with a spatula will be satisfactory. For larger batches, mix thoroughly to insure uniformity. To extend the pot life of the adhesive, mixing should be done as rapidly as possible.

- c. Glue lines, resulting from the dimensions of finished mating parts, shall be 0.001 to 0.100 inch.

3.2.2.5 Part Number Marking. Product marking shall be per Section 3.5 of SS-R00645.

3.3 Preproduction Sample. Preproduction samples are required.

3.3.1 Sample Items. The preproduction sample shall consist of the following items which have been manufactured and assembled by the supplier using the same continuous production processes, procedures, and equipment which will be used in fulfilling the production contract.

one (1) Package, PAT, part number R00602-001.

one (1) Product Can, part number R00631-000.

one (1) Spacer, part number R00632-000.

The sample shall be accompanied by certificates of compliance in accordance with 4.1.5.

- 3.3.2 Sample Testing. The preproduction sample shall be subjected to the tests specified in 4.3.
- 3.3.3 Sample Rejection. If any assembly or component fails to comply with any of the applicable requirements, the preproduction sample shall be rejected. In the event of rejection, the supplier shall take corrective action and submit new preproduction samples until such time as an acceptable sample is submitted. Until the first preproduction sample is accepted, the supplier is not authorized to begin or resume regular production, unless otherwise directed.

4. QUALITY ASSURANCE PROVISIONS.

- 4.1 General. The supplier responsible for the manufacture of the PAT is responsible for the accomplishment of all of the tests and inspections specified herein. Inspection shall be in accordance with MIL-I-45208. Calibration shall be in accordance with MIL-C-45662.
 - 4.1.1 Serial Numbers. Each PAT, AQ, and TB shall be permanently marked with a serial number in ascending numerical order corresponding to the sequence of manufacture. Once assigned, a serial number shall not be assigned to another item.
 - 4.1.2 Test Records. The supplier shall maintain records of all tests performed per 4.3. Copies shall be distributed as required by the contract or purchase order.
 - 4.1.3 Test Conditions. Unless otherwise specified, all measurements and tests shall be performed at standard ambient conditions.
 - 4.1.4 Rejected Units. Units that fail any test shall be rejected. Rejected units shall not be reworked, unless otherwise directed, and shall be marked in red to prevent accidental use.
 - 4.1.5 Certificate of Compliance. The supplier of the PAT shall obtain and supply, as requested, certificates of compliance from subcontractors verifying that the following materials used in fabrication of the PAT are in accordance with the applicable drawings and specifications.
 - a. The stainless steel for the Overpack, AQ, see R00603.
 - b. The redwood for the AQ, per SS-R00602.
 - c. The 7075 aluminum for the load spreader discs, see R00614 and R00626.

4.1.5 continued

- d. The 6061 aluminum for the tubular load spreader, see R00613.
- e. The copper for the heat conductor tube, see R00615.
- f. The cadmium plating for the copper heat conductor tube, see R00615.
- g. The stainless steel forgings for the TB, see R00643 and R00644.
- h. The 0.500-20 bolts for the TB, see R00638. Certify bolt material, silver plating, and 30,000 # ultimate T.S.
- i. The copper for the TB gasket, see R00637.
- j. The rubber for the TB O-ring, per assembly drawing R00630.
- k. The stainless steel for the product can, see R00633 and R00634.
- l. The aluminum honeycomb for the spacer, see R00632.

4.1.6 Tolerances. Limiting values specified in the drawings and specifications shall be absolute, as defined in SS-R00645.

4.2 In-Process Inspection and Testing. The supplier shall perform such in-process inspection and testing as he deems necessary to obtain product which meets the requirements of this specification.

4.3 Final Acceptance Testing. The following tests and inspections shall be performed on all units. Tests may be performed in any sequence, as appropriate.

4.3.1 Function and Fit. The PAT shall be visually and mechanically inspected to assure that all of the component parts fit into the assembly properly, as specified in the drawings.

4.3.2 Leak Rate. The TB shall be leak tested utilizing mass spectrometer leak rate measurement methods in accordance with SS-R00630. Helium leak rates, when present, shall be converted to equivalent air leak rates. The leak rate shall not exceed 1×10^{-7} ATM cc/sec (air).

4.3.3 Drawing Compliance. The PAT assembly and component parts shall be inspected, either by open set-up or gaging methods, to assure that the dimensional requirements specified on the applicable drawings are met, as follows.

4.3.3.1 Overpack, AQ, Drawing No. R00603.

- a. The 3/8 inch bolts (item 15) in place (23 required).
- b. The 5/8 inch clamp ring bolt in place.
- c. Marking as specified for both impression stamping and painted index marks.
- d. The 23 covered bolts at bottom, in place.
- e. The two end cover caplugs, in place.
- f. Verify that the bottom clamp ring lugs have been removed and the ring reworked per Note 6 of drawing R00629.

4.3.3.2 TB Body, Drawing No. R00635.

- a. The 4.250 +0.001, -0.002 diameter at gasket location (first 1/2 inch).
- b. The 0.030 \pm 0.010 radius, two places.
- c. The 20 \pm 1' angle and sharp corner.
- d. The 0.022 \pm 0.002 dimension.
- e. The 0.047 \pm 0.002 dimension.
- f. The 32 rms finish, three places.
- g. The 5.375 TP diameter bolt circle, the threaded hole locations, and the 0.500-20 UNF-2B thread size.
- h. The 4.810 +0.005, -0.000 diameter.
- i. The 4.559 \pm 0.002 diameter.
- j. The 5.350 \pm 0.010 diameter.
- k. The 63 rms finish and the flatness tolerance on that surface.
- l. The 6.250 \pm 0.010 diameter.
- m. Marking as specified.

4.3.3.3 TB Lid, Drawing No. R00636.

- a. The 4.247 +0.000, -0.001 diameter.
- b. The 4.559 \pm 0.002 diameter.
- c. The 20' \pm 1' angle and sharp corner.
- d. The 4.810 +0.005, -0.000 diameter.
- e. The 0.022 \pm 0.002 dimension.
- f. The 0.047 \pm 0.002 dimension.
- g. The 32 rms finish, two places.
- h. The 5.375 TP diameter bolt circle, the size and location of the 0.530 holes.
- i. The 4.028 +0.000, -0.002 diameter.
- j. The 6.220 \pm 0.010 diameter.
- k. The 63 rms finish and the flatness tolerance on that surface.

4.3.3.4 Gasket, Copper, Drawing No. R00637.

- a. The 4.808 +0.000, -0.005 diameter.
- b. The 4.252 \pm 0.002 diameter.
- c. The 0.080 \pm 0.002 dimension.
- d. The 63 rms finish.
- e. The concentricity specified for the inside and outside diameters.

4.3.3.5 Bolt, socket head, special, 0.500-20, R00638.

- a. The 0.780/0.790 diameter.
- b. The 0.073/0.063 radius.
- c. The 1.015/.985 length dimension.
- d. The "maximum two incomplete threads" requirement.

5. PREPARATION FOR DELIVERY.

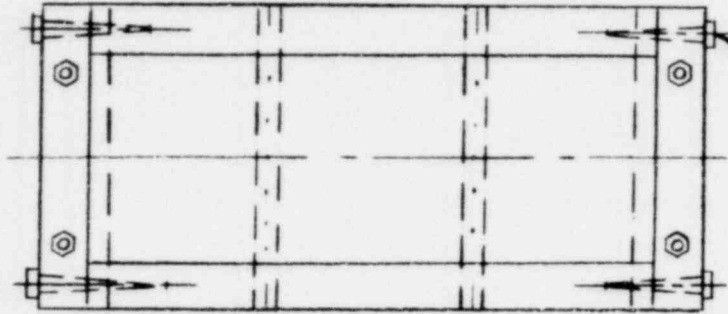
- 5.1 Preservation and Packaging. The PAT shall be packaged for shipment as specified in Figure 1.
- 5.2 Marking. Marking for shipment shall be in general accordance with the requirements of MIL-STD-129 and shall have the following minimum information legibly marked or labeled:
- a. Contractor's Part Number.
 - b. Contractor's Name.
 - c. Serial Number.
 - d. Purchase Order Number.
 - e. Quantity.

6. NOTES.

Procurement documents shall specify the following:

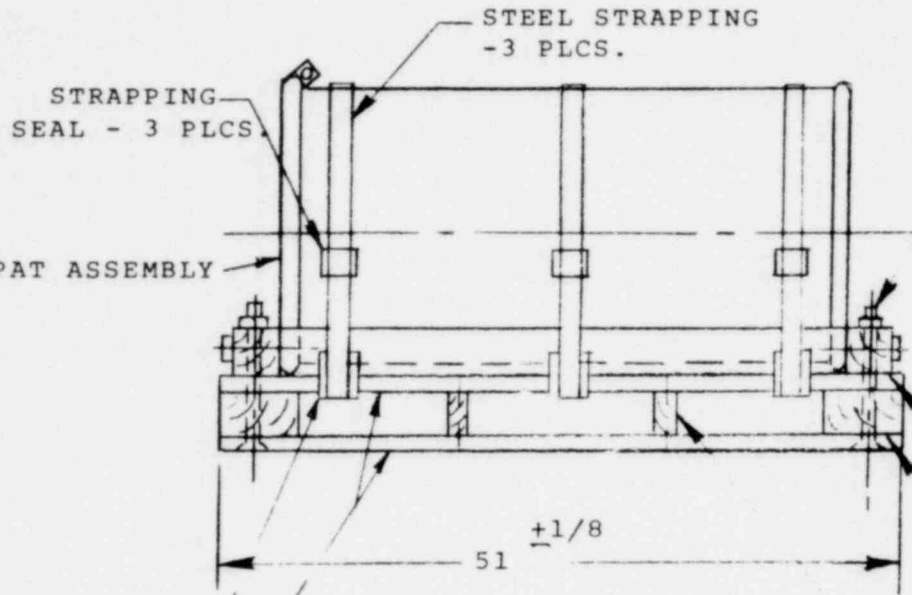
- a. Title, number, and date of this specification.
- b. Applicability of Preproduction Sample Approval (paragraph 3.3).
- c. Any exceptions to this specification.

PLAN VIEW OF PALLET, W/O PAT



1/2 x 8 LONG STEEL LAG BOLT AND WASHER - 4 PLCS.

1/2 STEEL COUNTERSUNK CARRIAGE BOLT AND WASHER - 4 PLCS.



STEEL STRAPPING - 3 PLCS.

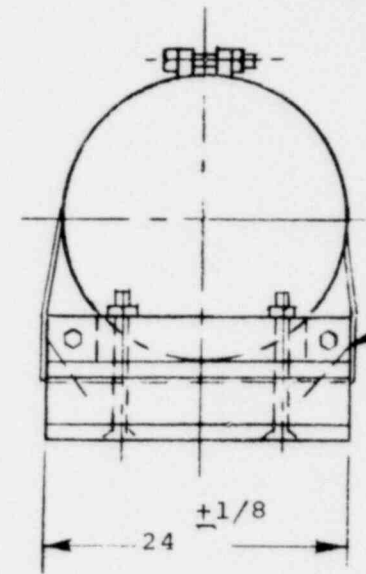
STRAPPING SEAL - 3 PLCS.

PAT ASSEMBLY

51 ± 1/8

3/4 DOUGLAS FIR PLYWOOD, EXTERIOR, SOUND BOTH SIDES, NAIL TO CROSS MEMBERS

STEEL CORNER - 6 PLCS.



TOE NAIL
4 x 4 TO
2 x 4

24 ± 1/8

4 x 4 DOUGLAS FIR - 4 PLCS. NO. 2 OR BETTER

4 x 6 DOUGLAS FIR - 2 PLCS. NO. 2 OR BETTER

2 x 4 DOUGLAS FIR - 2 PLCS. NO. 2 OR BETTER

FIGURE 1 - SHIPPING CONFIGURATION

Notes for Figure 1:

1. All dimensions are in inches.
2. Nails shall be cement coated.
3. Hardware shall be galvanized or black oxide coated.
4. Strapping shall be 1 1/4 x 0.035 minimum thickness, steel per QQ-S-781, Class 1, Type I, Finish A.
5. The 4 x 4's shall fit snugly against the Pat at sides and ends.

FSCM NO. 14213
DEF 770185SC
P.R.OWENS 9633
J.A.ANDERSEN 5433
LEX/

SS-R00602
-000

Page 1 of 3

MATERIAL SPECIFICATION, REDWOOD FOR PAT PACKAGE

Page 1 2 3
Issue B A A

1. GENERAL.

1.1 Scope.

This specification defines the requirements for the redwood material used in fabrication of the Plutonium Air Transportable (PAT) Package.

1.2 Definitions. Definitions of terms used in this specification may be found in the document listed in 2.1.

2. DOCUMENTS AND EQUIPMENT.

The following documents and equipment form a part of this specification to the extent specified herein. Unless otherwise specified the latest issues shall be used. In the event of conflict between documents referenced herein and the contents of this specification, the contents of this specification shall be a superseding requirement.

2.1 Documents.

"Standard Specification for Grades of California Redwood Lumber", published by Redwood Inspection Service, San Francisco, California

2.2 Equipment.

Moisture Register, Model L, made by the Moisture Register Co. Alhambra, Calif., or approved equivalent.

3. REQUIREMENTS.

3.1 Material Description.

- a. The material to be used shall be clear, kiln dried redwood, free of defects, as defined in para. 104 of the "Standard Specifications" document. Knots are not permissible.
- b. Assemblies shall be fabricated of one inch or greater nominal thickness.
- c. Moisture content shall not exceed 12%. The material shall be protected, as necessary, to assure this condition.
- d. Finger-joined and edge-glued lumber is acceptable.
 - (1) Parts shall be assembled in accordance with the applicable drawings, using polyvinyl acetate resin emulsion per MMM-A-180, or Resorcinal adhesive per MMM-A-181.
 - (2) Glue lines shall be 0.030 inch maximum.

- 3.2 Grain Defects. Burls and birdseyes of less than 0.375 inch diameter are acceptable, providing there are not more than six such defects in a six inch diameter, in a maximum of 5% of the lumber in a subassembly.

4. QUALITY ASSURANCE PROVISIONS.

- 4.1 Visual Inspection. All material shall be visually inspected to assure that it meets the requirements of Section 3 of this specification.
- 4.2 Moisture Content.

The material shall be inspected, after final machining and just before application of sealant, to assure that the moisture content specified in 3.1.c is not exceeded. Inspection shall be conducted as follows.

- a. Zero the Moisture Register in accordance with the manufacturer's instructions.
- b. Twenty percent of the material in each subassembly shall be checked for moisture content, using the Moisture Register per the manufacturer's instructions. The Register readings shall not exceed 24.

5. PREPARATION FOR DELIVERY.

The lumber to be used shall be packaged by the subcontractor so that it will meet the requirements of this specification after processing by the fabricator of the PAT. Vapor barriers shall be used in packaging to maintain the minimum moisture content requirement specified.

FSCM NO. 14213
DEF 770185SC
OWENS 9633 *PL 1-3/77*
ANDERSEN 5433 *PL*
LEX/

SS-R00621
-000

Page 1 of 4

WELDING, CORROSION RESISTANT STEEL, PAT PACKAGE

Page 1 2 3 4
Issue A A A A

1. GENERAL.

1.1 Scope. This specification defines the fabrication and inspection requirements for the welding of corrosion resistant steel parts used on the Plutonium Air Transportable (PAT) Package.

1.2 Definitions.

1.2.1 Welding Terms and Definitions. Welding terms and definitions used in this specification shall be in accordance with AWS A2.0, except for the following:

Porosity. Voids in the weld metal of approximately spherical shape.

1.2.2 Welding Symbols. Welding symbols used on the product drawings shall be in accordance with AWS A2.0.

2. DOCUMENTS.

The following documents form a part of this specification to the extent stated herein. Unless otherwise specified use latest issues.

AWS A 2.0-58

Welding Symbols

AWS A 3.0-51

Welding Terms and Definitions

MIL-I-6866B

Inspection, Penetrant Method of

3. REQUIREMENTS.

- 3.1 Welding Process. Welding shall be done by any of the arc welding processes, using manual, semiautomatic, or automatic techniques.
- 3.2 Weld Preparation. Loose scale, slag, rust, grease, oil, and other foreign matter shall be removed from surfaces to be welded. Beveling and weld preparation may be done by flux-oxygen cutting, provided cracking does not occur in the metal and provided at least 0.125 inch of metal is removed from all cut edges by mechanical means, grinding, etc.
- 3.3 Weld Defects. Imperfections that exceed the limits specified in Table 1 shall be considered defects and are unacceptable, except as specified below.
- 3.4 Repair of defects. Repair of defects is permissible if the required weldment, the repair weld itself, and the adjacent parent metal meet the requirements of the original weldment. A repaired weldment shall be reinspected in the same manner as the original weldment.

4. QUALITY ASSURANCE PROVISIONS.

4.1 General.

- 4.1.1 Responsibility for Inspection. The Supplier performing the welding shall be responsible for the performance of all tests and inspections specified herein.
- 4.1.2 Inspection Records. The Supplier shall maintain records of all inspections performed per 4.2. Copies shall be distributed as specified in the contract or purchase order.
- 4.1.3 Inspection Sequence. Weldments may be inspected at any time after the weld preparation and cleaning requirements of Section 3 have been met.
- 4.1.4 Rejected Units. Parts that fail to meet any of the requirements of this specification shall be rejected. Some rework, as defined in 3.4, is permissible.

4.2 Product Inspection and Testing. The following inspections shall be performed on the weldments on parts of the PAT Package on which welding is performed.

- 4.2.1 100% Visual Inspection. Parts shall be visually inspected 100% for the imperfections defined in Table 1. No magnification is required.

4.2.2 Penetrant Inspection. Each Clamp Ring, Modified, part number R00621-000, shall be penetrant inspected in accordance with MIL-I-6866B. See Table 1 for acceptance criteria.

5. PREPARATION FOR DELIVERY.

Not applicable.

6. NOTES.

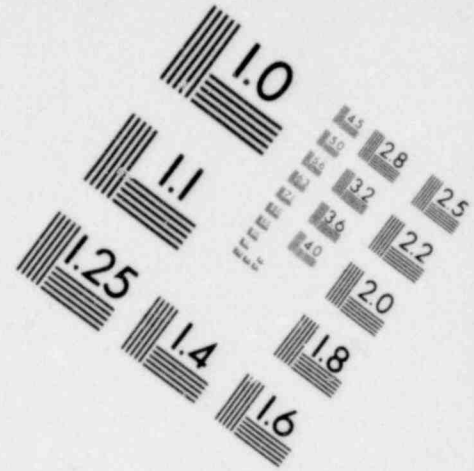
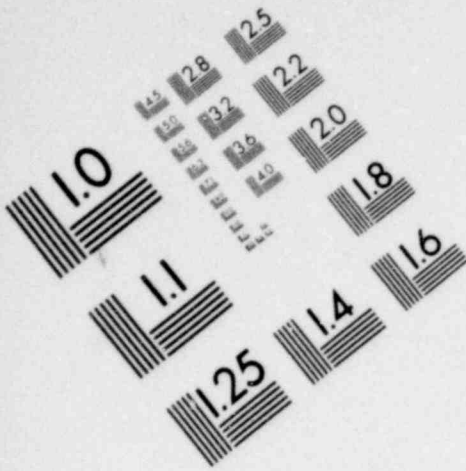
Not applicable.

TABLE 1 - LIMITS OF IMPERFECTIONS IN ACCEPTABLE WELDS

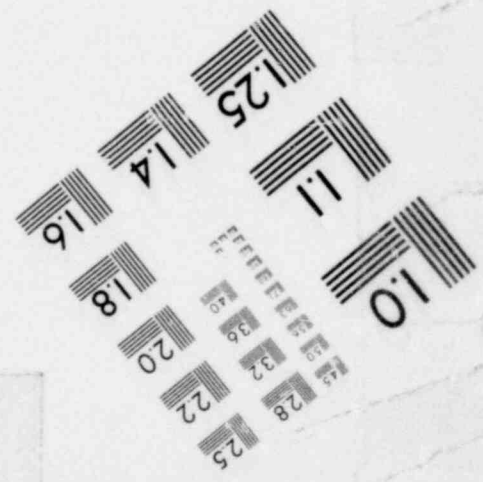
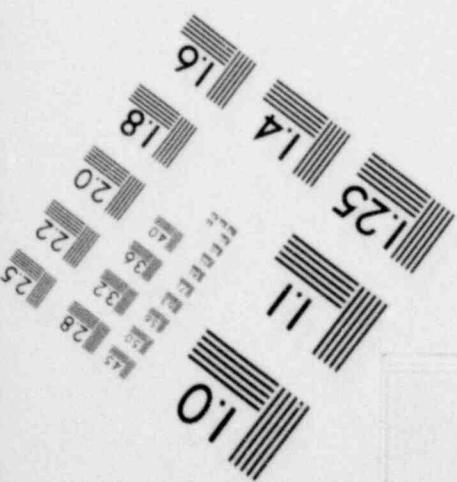
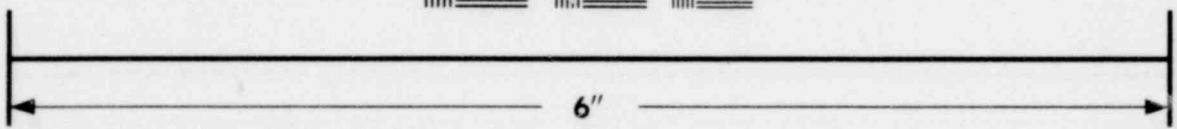
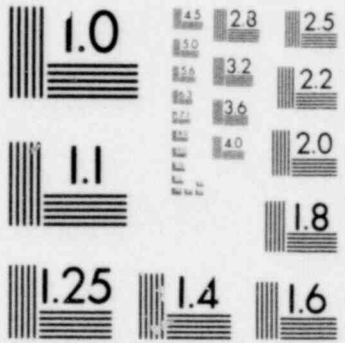
IMPERFECTION	LIMIT	
Cracks in weld bead	Unacceptable	
Cracks in parent metal	Unacceptable	
Crater cracks	Unacceptable	
Incomplete fusion and inadequate joint penetration	The aggregate length of the imperfections shall not exceed $1\frac{1}{2}T$ in a weld length of $6T$, and the length of any individual imperfection shall not exceed $1/2T$. If the weld length is less than $6T$, the aggregate length of the imperfections shall not exceed $1/4$ the weld length, and the length of any individual imperfection shall not exceed $1/12$ the weld length. (See Note 1)	
Porosity (Internal)	Not applicable	
Inclusions (Internal)	Not applicable	
Undercut	Unacceptable	
Overlap	Unacceptable	
Concavity	Unacceptable in butt welds. In fillet welds, actual throat shall be not less than the theoretical throat for specified weld size.	
Convexity of butt welds on either side	<u>Weld Size</u>	<u>Max. Reinforcement Height</u>
	Up to 0.125 inch	0.050 inch
	0.125 to 0.500 inch	25% of weld size
	0.500 inch and larger	0.125 inch
Size of fillet welds	Specified weld size (length of legs) +50%, -0.	

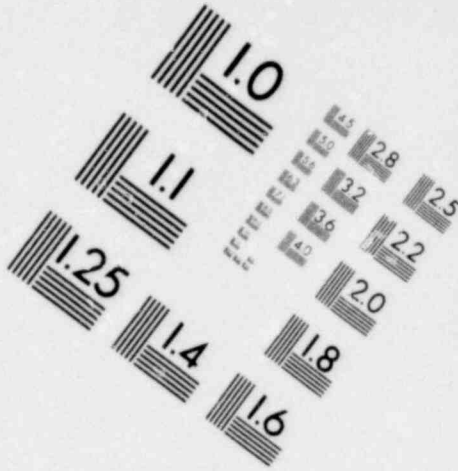
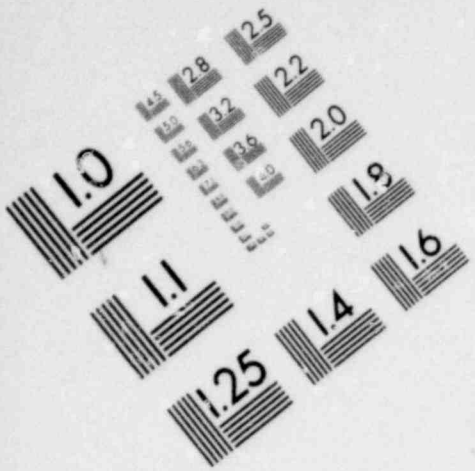
NOTE:

- (T) is the specified weld size.

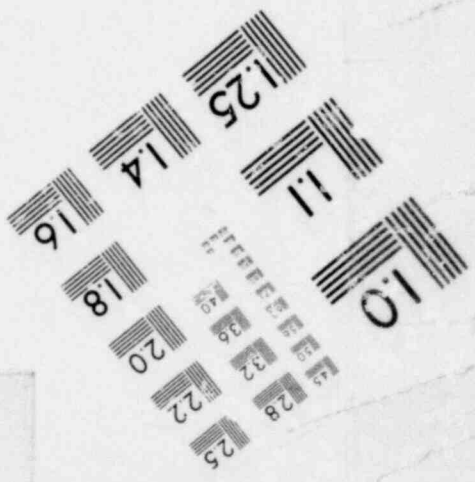
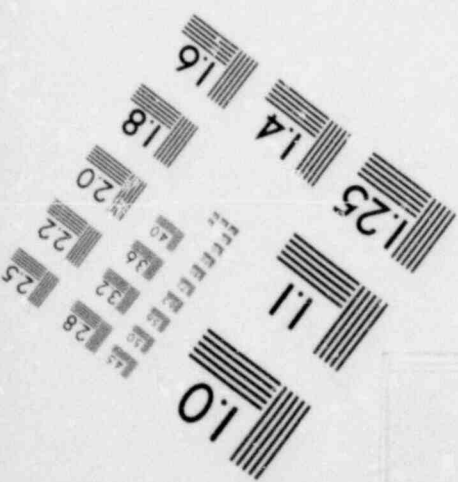
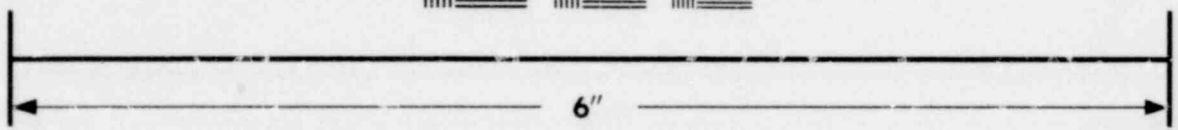
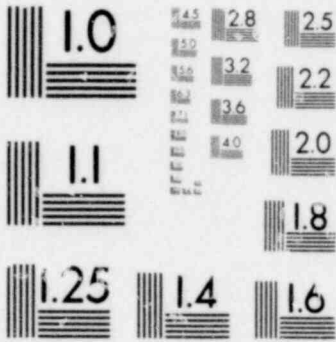


**IMAGE EVALUATION
TEST TARGET (MT-3)**





**IMAGE EVALUATION
TEST TARGET (MT-3)**



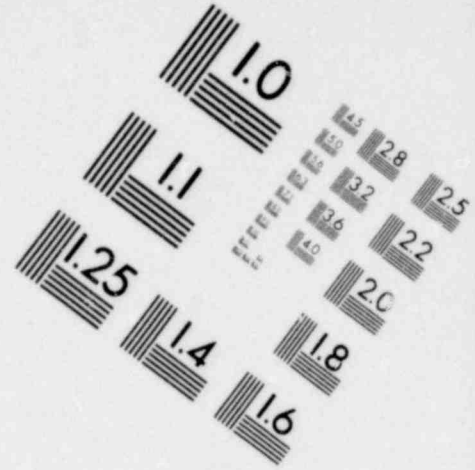
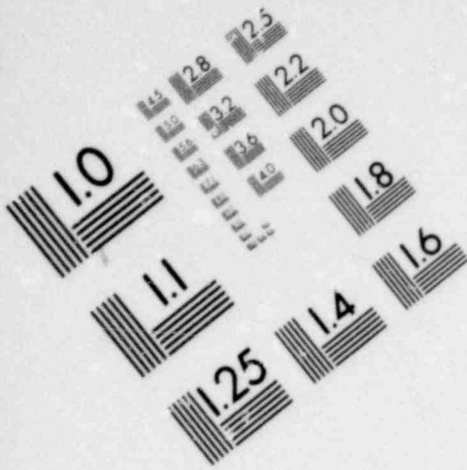
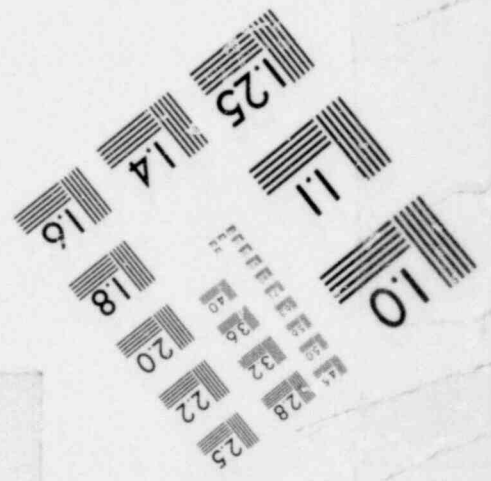
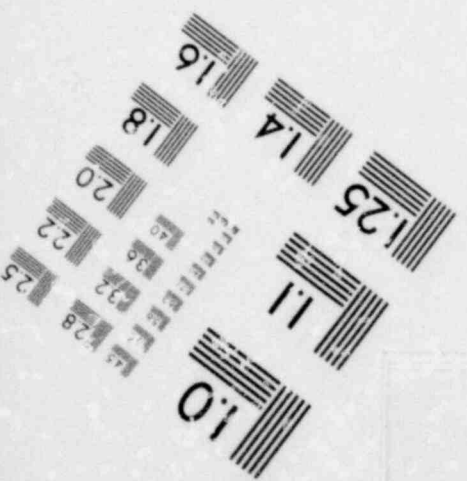
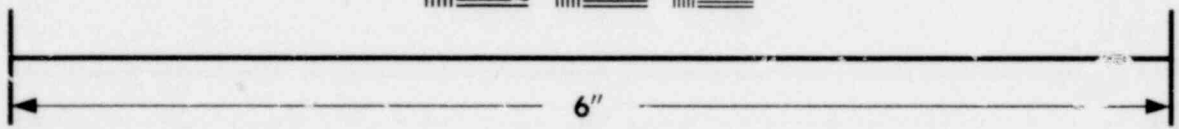
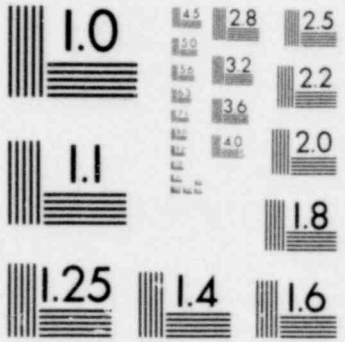


**IMAGE EVALUATION
TEST TARGET (MT-3)**



FSCM NO. 14213
FCO 772210SC-DEV
P. R. OWENS 9633
J. A. ANDERSEN 5433
LEX/CASSETTE NO. 140

SS-R00630
-000

Page 1 of 6

TESTING, LEAK RATE, MASS SPECTROMETER, PAT PACKAGE

Page	1	2	3	4	5	6
Issue	B	A	A	A	B	A

1. GENERAL.

1.1 Scope. This specification defines the requirements for the quantitative measurement of the leak rate of a sealed component of the Plutonium Air Transportable (PAT) Package. A mass spectrometer type leak detector is used.

1.2 Product Description. The item to be leak tested per this specification is the Containment Vessel, TB, part number R00630-000, which is a major component of the PAT Package, R00602-001. The detail parts of the Containment Vessel, TB, are:

TB Body, R00635-000

TB Lid, R00636-000

Copper Gasket, R00637-000

Rubber O-Ring

Bolt, Socket Head, Special, .500-20 UNF, R00638-000 (12 required)

1.3 Definitions.

1.3.1 Background. Test system background is included in the leak rate result. This may be spurious output of the leak detector expressed in suitable terms, due to the response to all gases other than the actual leakage of tracer gas from the product being tested and/or the known leak. The background may be inherent in the detector or extraneous, and includes absorbed tracer gas.

1.3.2 Units.

1.3.2.1 Pressure Units.

- a. Millimeter of Mercury (mmHg). A unit of pressure corresponding to a column of mercury exactly 1 millimeter high at 0°C under standard gravity acceleration of 980.665 Cm/sec².
- b. Micron of Mercury (uHg). A unit of pressure equal to 1/1000 of the millimeter of mercury pressure unit.
- c. Torr. A unit of pressure equal to 1/760 of a standard atmosphere; differs by only one part in 7 million from a millimeter of mercury. Torr is the preferred pressure unit for low pressure (vacuum) measurement.

1.3.2.2 Leak Rate Units.

- a. CC/sec. STP (Cubic Centimeter Per Second, Standard Temperature and Pressure). A flow rate of gas in terms of cubic centimeters per second in which the gas volume is reduced to standard temperature and pressure. 1.315 cc/sec. = 1 Torr-liter/sec.

1.3.3 STP (Standard Temperature and Pressure). Defined as 0°C and 760 Torr.

1.3.4 K Factor. A factor used to convert from a tracer gas leak rate obtained under the specified test conditions to an equivalent air leak rate at those specific test conditions. For purposes of this specification:

$$K = \sqrt{\frac{\text{Molecular weight of helium}}{\text{Molecular weight of air}}} = \sqrt{\frac{4}{29}}$$

$$K = 0.372$$

1.3.5 Sealed Product. A product which is capable of maintaining, or of being sealed by special fixtures to maintain, an internal pressure or vacuum.

- 1.3.6 Tracer Gas. A gas that is used to measure the leak rate of the product being tested.
- 1.3.7 Leak Rate. The quantity of gas flowing in unit time into or out of the product under test, reduced to units of volume at standard temperature and pressure.
 - 1.3.7.1 Tracer Gas Leak Rate. The leak rate test result, calculated without application of a K factor, from the leak detector readings.
 - 1.3.7.2 Total Gas Leak Rate. An estimate of the product leak rate, obtained by multiplying the tracer gas leak rate by the specified K factor.
 - 1.3.7.3 Maximum Permissible Leak Rate. The maximum total gas leak rate limit allowable for product acceptance.
- 1.3.8 Known Leak. A calibrated device from which tracer gas is emitted at a known rate.

2. DOCUMENTS

The following documents, of the exact issue shown, form a part of this specification to the extent specified herein.

Specifications:

Federal:

BB-H-1168b Helium, Technical

3. REQUIREMENTS.

3.1 Equipment Capability.

- 3.1.1 Leak Detector System. The system shall consist of a mass spectrometer type leak detector together with a suitable test chamber that will completely enclose the product, auxiliary pressurization equipment, and instrumentation necessary for performance of the test under the specified conditions.

- 3.1.2 Location of Known Leak. The known leak shall be connected directly to the vacuum system as closely as possible to that point at which the test item will be connected.
- 3.1.3 Vacuum Gages. Gages used to ascertain that the pressure in the test chamber or fixture is not greater than the specified maximum shall be suitably located to read the pressure of the test chamber or fixture. If leak detectors having gages capable of reading pressures indicated below are available, it is permissible to use these gages provided:
- a. An indicated test pressure of 5×10^{-5} Torr (mmHg) or lower is used for helium.
 - b. An essentially short direct connection is maintained between the leak detector and the test chamber or fixture.

Under the present state-of-the-art, calibration of vacuum gages below one micron of mercury is not guaranteed by Primary Standards and; therefore, is not required.

- 3.1.4 Attenuation Setting On Leak Detector. The leak detector shall be operated on the most sensitive readable scale.
- 3.2 Gases. The tracer and fill gas used shall be helium per BB-H-1168b, Type I, Grade A.
- 3.3 Calibration of Known Leak. The known leaks used shall be calibrated by the Primary Standards Laboratory specified in the contract or purchase order. Calibration shall be performed prior to initial use and at intervals thereafter in accordance with policies established by the Primary Standards Laboratory.
- 3.4 Procedure (Leak Rate Measurement).
- 3.4.1 General.
- a. Readability of the leak detector output meter shall be checked per 3.1.3.
 - b. Pressures at which a test is to be performed shall not exceed 5×10^{-4} Torr (mmHg) helium.
- 3.4.2 Product Leak Test.
- 3.4.2.1 The TB to be leak tested will be received disassembled, and it will be necessary to assemble the unit as the leak test progresses, as follows.

3.4.2.1 continued

- a. Invert the TB Body and place it on the edge of a clean work surface, with approximately one-fourth the interior diameter of the Body extending out from the work surface.
- b. Insert the nozzle of the helium tracer gas line into the interior of the TB Body, and flood the interior with helium for a period of at least 20 seconds.
- c. Remove the nozzle and, with the TB still in the inverted position, place the TB Body in position over the TB Lid (the copper gasket and lubricated rubber O-ring should be in place at this time). While holding the Lid firmly against the Body, invert both and place them in the up-right position on the work surface.
- d. Align the holes in the Lid with the threaded holes in the Body (orientation optional) and install the 12 socket head bolts onto the unit. Using a suitable strap-type holding device and torque wrench, torque the bolts to 50 ± 5 foot-pounds.
- e. Place the assembled TB in the chamber of the mass spectrometer leak tester. Two readings shall be taken from the leak detector output meter for each test, as follows:

R_1 = Background

R_2 = Background + Known Leak

R_3 = Product Leak + Background

- 3.4.2.2 Leak Rate Calculation. Readings R_1 , R_2 , and R_3 , as obtained in e. above, permit calculation of the total gas leak rate as follows:

$$L = \frac{(C)(K)(R_3 - R_1)}{R_2 - R_1}$$

Where:

L = Total gas leak rate

C = Calibrated value of known leak

K = See 1.3.4

3.4.2.3 Maximum Permissible Leak Rate. The leak rate for the TB shall not exceed 1×10^{-7} ATM cc/sec (air).

3.4.3 Test Records. The following information shall be recorded by the testing laboratory. Copies of test records shall be distributed as specified in the contract or purchase order.

- a. Product part number and serial number.
- b. Purchase order or contract number.
- c. Make and model number of leak detector used.
- d. Value of known leaks used.
- e. Test pressures (internal and external).
- f. Tracer gas and concentration used.
- g. Fill gas used.
- h. Leak detector output readings per 3.4.2.1.e.
- i. Calculated total gas leak rate.
- j. Date of test.

4. QUALITY ASSURANCE PROVISIONS.

Not applicable.

5. PREPARATION FOR DELIVERY.

Not applicable.

6. NOTES.

Not applicable.

FSCM NO. 14213
DER 770185SC
P. R. OWENS 9633 *PRO 1/2-1/11*
J. A. ANDERSEN 5433 *AA*
LEX/

SS-R00645
-000

Page 1 of 10

GENERAL REQUIREMENTS, PAT PACKAGE

Page	1	2	3	4	5	6	7	8	9	10
Issue	B	A	A	A	A	A	A	B	B	B

1. GENERAL.

- 1.1 Scope. This specification defines the general requirements for product fabrication and inspection of parts and assemblies used on the Plutonium Air Transportable (PAT) Package, R00602. It also provides interpretation of certain requirements specified on the product drawings. Specific requirements on the product drawings shall take precedence over these general requirements and interpretations.

2. DOCUMENTS.

The following documents form a part of this specification to the extent specified herein. Unless otherwise specified, the issues shown shall be used.

ANSI Y14.5-1973	Dimensioning and Tolerancing
ANSI B1.1-1974	Unified Inch Screw Threads (UN and UNR Thread Form)

3. REQUIREMENTS.

- 3.1 Drawing Interpretation. The product drawings utilize the "True Position" drawing system, as defined in ANSI Y14.5. An understanding of the provisions in the ANSI document is essential for the proper interpretation of the dimensions and tolerances on the PAT drawings.

1568 007

- 3.2 Dimensions, Tolerances, and Measurements. The product is defined using customary (inch) dimensions.
- 3.2.1 Absolute Tolerance Concept. Design requirements are based on the absolute tolerance concept, which means the true value of the characteristic shall be within the tolerance stated. An acceptable degree of conformance of product to the intent of absolute tolerances is required. To judge the degree of conformance, consideration shall be given to the inherent measurement uncertainty in relation to the specified tolerances. Information concerning production process distribution (both centering and dispersion), if available, may also be used in determining conformance.
- 3.2.2 Decimal Places. As many (or as few) decimal places are used as are needed to express design requirements.
- 3.2.3 Interpretation of Dimensional Limits. Regardless of the number of decimal places, the maximum and minimum limits are considered to be followed by a single (implied) zero. Any measurement made beyond this implied zero reading shall be disregarded; rounding is not applicable. There is no need to measure past the single implied zero.
- 3.2.4 Measurement Temperatures. Physical measurements of a product are considered to apply only at a temperature of 68°F. If referee measurements are required, the measurement shall be made at 68°F or adjusted to 68°F to account for differences in thermal expansion or contraction in the material of the gage and/or parts. The tolerance on the 68°F temperature is controlled by the degree of accuracy required for the measurement being made.
- 3.2.5 Counterbores. In curved surfaces or on flat surfaces where the hole axis is not perpendicular to the surface, the depth of a counterbore is the minimum distance from the bottom of the rim as shown in Figure 1. The interior corner at the bottom of a counterbore produced by a standard tool is acceptable.
- 3.2.6 Countersinks. In curved surfaces or on flat surfaces where the hole axis is not perpendicular to the surface, the diameter of a countersink is the diameter of the lowest point on the rim in a plane perpendicular to the hole axis. See Figure 1. Countersink for flat head screws to allow head of screw to be flush to .010 below the surface.

3.2.7 Stock Material Tolerances. When the drawing specifies nominal cross-sectional dimensions for material used to fabricate the part, but does not specify tolerances for these dimensions, the widest tolerances applicable to the material, form, and process may be used.

3.3 Manufacturing Practices.

3.3.1 Removing Burrs and Sharp Edges. All burrs and sharp edges shall be removed to the extent that material fragments are not visible and sharpness cannot be felt. Either a .010 maximum x .010 maximum chamfer or .010 maximum radius is satisfactory treatment in breaking edges and deburring. Only those edges that appear to exceed these limits upon visual inspection need be measured for conformance to these dimensions. If it is necessary to break sharp edges or to deburr after application of chemical surface treatment, the bared metal shall be touched up as required. Flash on molded plastic parts that does not cause the part to exceed maximum dimensional limits need not be removed. These requirements do not apply to rough and semi-finished metal castings and forgings.

3.3.2 Free-State Variations. If material flexibility or normal internal stresses can be expected to cause parts to be out of tolerance, appropriate inspection procedures shall be obtained prior to the manufacture of parts.

3.3.3 Holes Called for on Assembly Drawings. Where holes are called out on assembly drawings, they may be provided in the detail parts, either full size or less than full size, as required to facilitate manufacture. Inspection of such holes is not required, however, until final assembly, at which point the holes must meet all assembly drawing requirements.

3.3.4 Machine or Molded Diameters. Where no concentricity requirement (position or runout tolerance) is specified, any two or more diameters having a common axis (including hole countersinks, counterbores) shall be concentric within a full indicator movement (FIM) of one-half the arithmetic sum of their size tolerance. The diameter having the smallest tolerances shall be the datum feature for all related diameters. If size tolerance values are equal, the diameter having the longest axis shall be used as the datum feature.

3.3.5 Threaded Parts.

3.3.5.1 Form and Class of Fit. All threads shall conform to the requirements of ANSI B1.1.

3.3.5.2 Appearance. All threads shall be free from burrs, nicks, and rough or chattered surfaces, that are visible without magnification.

3.3.5.3 Gaging.

- a. Measurement Over Wires. Thread wires and measurement indicators may be used.
- b. "GO" Gages. When "GO" gages are used, the product shall allow the "GO" gage to enter or to be entered the specified full length or depth of the thread; however, the thread must be functional.
- c. "NOT GO" Gages. Threads are acceptable as within material limits if, when plug ring thread gages are used, the "NOT GO" plug gage does not enter or the "NOT GO" ring gage is not entered. Threads may be accepted if all complete threads can enter in or be entered by the "NOT GO" gage provided a definite drag results from metal-to-metal contact on or before the third turn of entry. For threads having three or fewer turns, the drag shall occur on or before the first one-half turn of actual thread engagement. "NOT GO" gaging procedures for extremely ductile materials shall be as specified by the Design Agency. Neither working nor final inspection "NOT GO" gages should be forced after the drag is definite.
- d. Three-Roll Indicating-Type Gage Readings. When this type gage is used on Class 2A or 3A threads, the gage reading may not exceed the basic pitch diameter by more than 1/8 turn of the screw providing the maximum gage reading does not exceed the basic pitch diameter by more than 50 percent of the difference between basic pitch diameter and minimum 2A or 3A pitch diameter, as applicable (See 3.3.5.6.c).
- e. Threads in Installed Commercial Hardware and Inserts. Thread size and class of fit callouts may appear on assembly drawings in conjunction with installed commercial hardware and inserts. Unless such callouts are modified by reference to specific notes on the assembly drawing, the size and class of fit shown are for information purposes only and the commercial part thread limits shall be governed by the limits of the commercial part specified on the assembly drawing.

3.3.5.4 Assembly. When two or more threaded fasteners are used to attach a part, a sequential tightening pattern shall be established that will equalize fastener load throughout the part.

3.3.5.5 Torque Wrenches.

- a. When torque limits are specified for threaded assemblies or fasteners, the torque wrench used shall be selected so that the limits specified for each feature will fall within approximately the middle 75 percent of the wrench scale.
- b. A procedure for the routine periodic calibration and repair of all torque wrenches used to assemble items to specified limits shall be established and maintained.
- c. Torque wrench readings shall be taken in a direction that will tighten the part.

3.3.5.6 External Threads.

- a. Thread Length. Dimensions of axial thread length shown on drawings indicate minimum required length of complete threads. When the dimensioned thread length terminates at a shoulder and an undercut is not specified, the two threads next to the shoulder may be incomplete.
- b. Chamfer. The leading end of externally threaded parts shall be chamfered. The resulting incomplete threads are included in the measurement of thread length but must not exceed two pitches in length.
- c. Coated Class 2A Threads. Class 2A threads to which metallic plating, chemical-film coatings, resin bonded dry film lubricants, or any combination thereof have been applied may be gaged with basic "GO" gages in determining conformance to maximum size limits.

3.3.5.7 Internal Threads.

- a. Tap Drills. Select a standard tap drill size that will assure approximately 75% of full thread.
- b. Blind Hole Depth. The tap drill point shall not break through or deform the surface opposite the mouth of the hole.
- c. Thread Depth. Dimensions of axial thread depth shown on drawings indicate minimum required depth of complete threads.

3.3.5.7 continued

- d. Perpendicularity. The perpendicularity or normality of threaded holes in flat or curved surfaces shall be within $1^{\circ}0'$.
- e. Chamfer. The leading ends of internal threads shall be chamfered as shown in Figure 2. If accessible, both ends of through-tapped holes shall be chamfered. Chamfering shall not result in elimination of more than one pitch of thread depth. For the purpose of determining the number of complete threads from the surface adjacent to the hole, the chamfered thread may be counted.

3.3.6 Metal Heat Treatment.

- a. When necessary to facilitate fabrication, parts made from heat-treatable alloys, for which material is specified in terms of the final temper or condition required, may be fabricated from raw stock of a temper or condition different from the final temper and then heat-treated to the specified temper or condition.
- b. After the completion of in-process heat-treatment, sample parts from each heat-treat lot shall be tested to determine that the material properties influenced by heat-treatment conform to the applicable material specification requirements. If tests of actual parts are impractical, suitable samples of the same alloy and starting condition as the parts shall be heat-treated with the lot and tested for conformance to the applicable requirements.
- c. Parts specified to be made from a work-hardened temper of a non-heat-treatable alloy must be fabricated from material of the required temper or condition.
- d. Thermal treatments such as hot forming, stress-relieving, drying, bonding, and baking, other than those specifically permitted by the product drawings, shall not be used.

3.4 Requirements for Cleaning, Protection, and Identification of Raw Material, Parts, and Assemblies.

3.4.1 Protection. All parts and assemblies shall be adequately protected from accumulation of foreign matter, corrosion, physical damage or deterioration. This requirement shall apply to all manufacturing operations from receipt of raw material to completion of a finished product, to product held in any storage area, and to product prepared for shipment.

- a. Protective measures used during processing, fabricating, and packaging must not only guard against obvious damage and deterioration but also against the creation of latent conditions that may later cause unsatisfactory performance, accelerating deterioration, or malfunction.
- b. Raw material and parts at all levels of production shall be kept adequately segregated and identified at all times. Parts shall be transported in a manner which will assure adequate protection from damage.
- c. All items such as raw material, parts, subassemblies, assemblies, etc., not in immediate use, shall be adequately packaged, identified, and stored.

3.4.2 Cleanup of Parts and Assemblies. All finished parts and subassemblies shall be adequately cleaned before final assembly. Final assembly and necessary subassembly shall be performed in an environment appropriate to the type of product. All parts and assemblies shall be thoroughly cleaned to remove foreign and manufacturing waste material such as:

Superfluous hardware, wire, and insulation clippings.

Chips, filings, abrasives, machining lubricants.

Soldering, brazing, and welding fluxes, solder droppings, weld spatter, slag, and welding rod ends.

Drippings of lubricants, adhesives, and sealing compounds.

Paint droppings, splatter, and overspray.

Residues from liquid baths used in plating and chemical treatments.

Temporary tags and packaging.

3.5 Part Number Marking.

- a. All finished parts, assemblies, and subassemblies shall be permanently marked with the applicable part number, e.g., R00615-000, using ink marking with covercoat. The vertical height of characters shall be not less than 0.12 inch.
- b. Part numbers shall be located in any readily observable location which does not affect function.

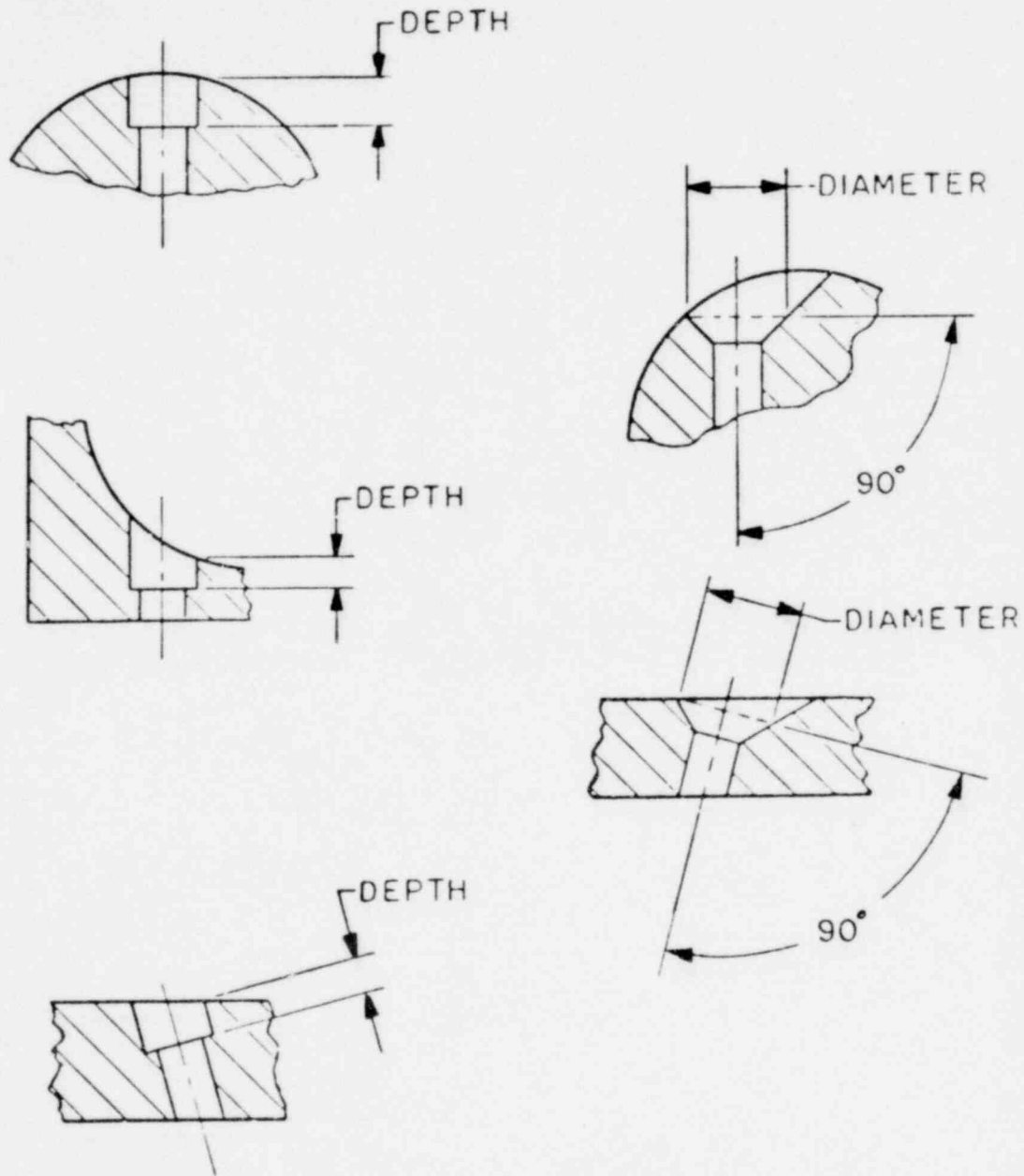


FIGURE 1 - COUNTER BORES AND COUNTERSINKS

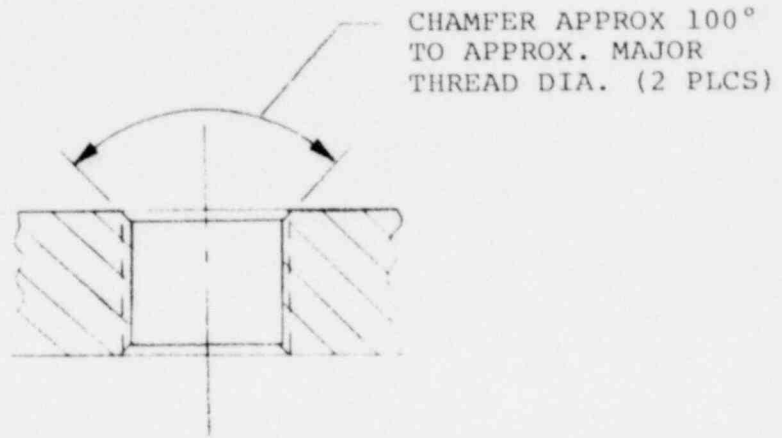
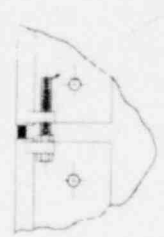
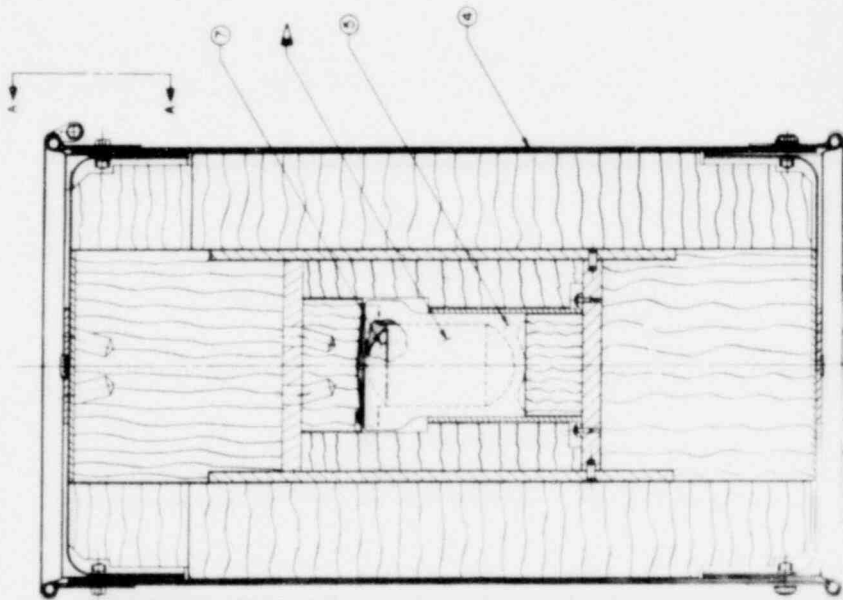


FIGURE 2 - INTERNAL THREAD CHAMFER

NOTES
 1. FINISHING PRODUCTION ASSEMBLY
 2. TRANSPORTABLE UNIT INCLAS 15-100-0000
 3. DIMENSIONS SHOWN ARE IN INCHES
 4. DIMENSIONS IN PARENTHESES ARE IN MILLIMETERS
 5. DIMENSIONS IN BRACKETS ARE IN METERS

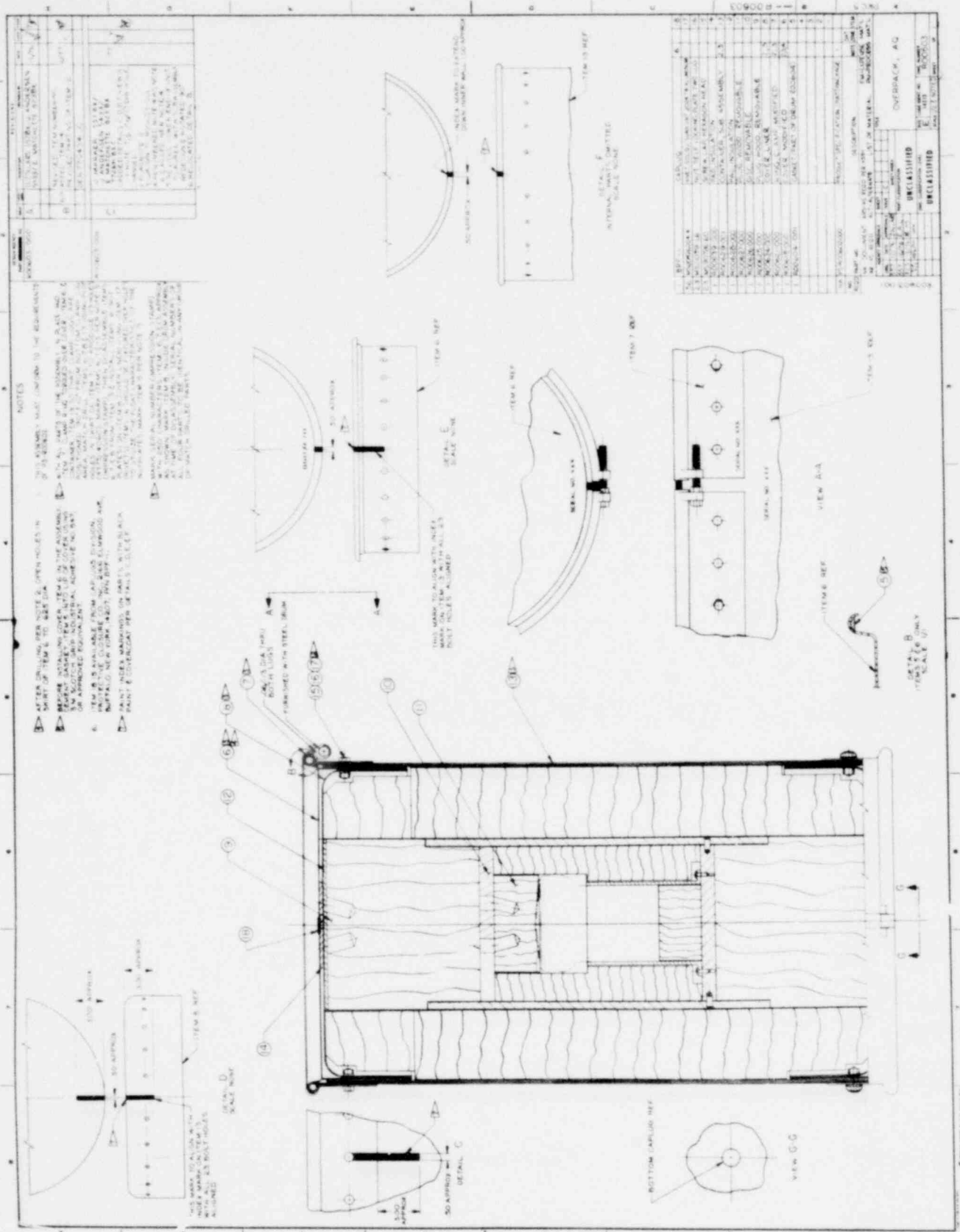
REV	DATE	DESCRIPTION
A	15 MAR 1977	INITIAL DESIGN
B	15 MAR 1977	REVISED TO INCLUDE DIMENSIONS
C	15 MAR 1977	REVISED TO INCLUDE DIMENSIONS

1. FINISHING PRODUCTION ASSEMBLY
 2. TRANSPORTABLE UNIT INCLAS 15-100-0000
 3. DIMENSIONS SHOWN ARE IN INCHES
 4. DIMENSIONS IN PARENTHESES ARE IN MILLIMETERS
 5. DIMENSIONS IN BRACKETS ARE IN METERS



MIN. 1/8" ROUNDED CORNERS UNLESS NOTED OTHERWISE

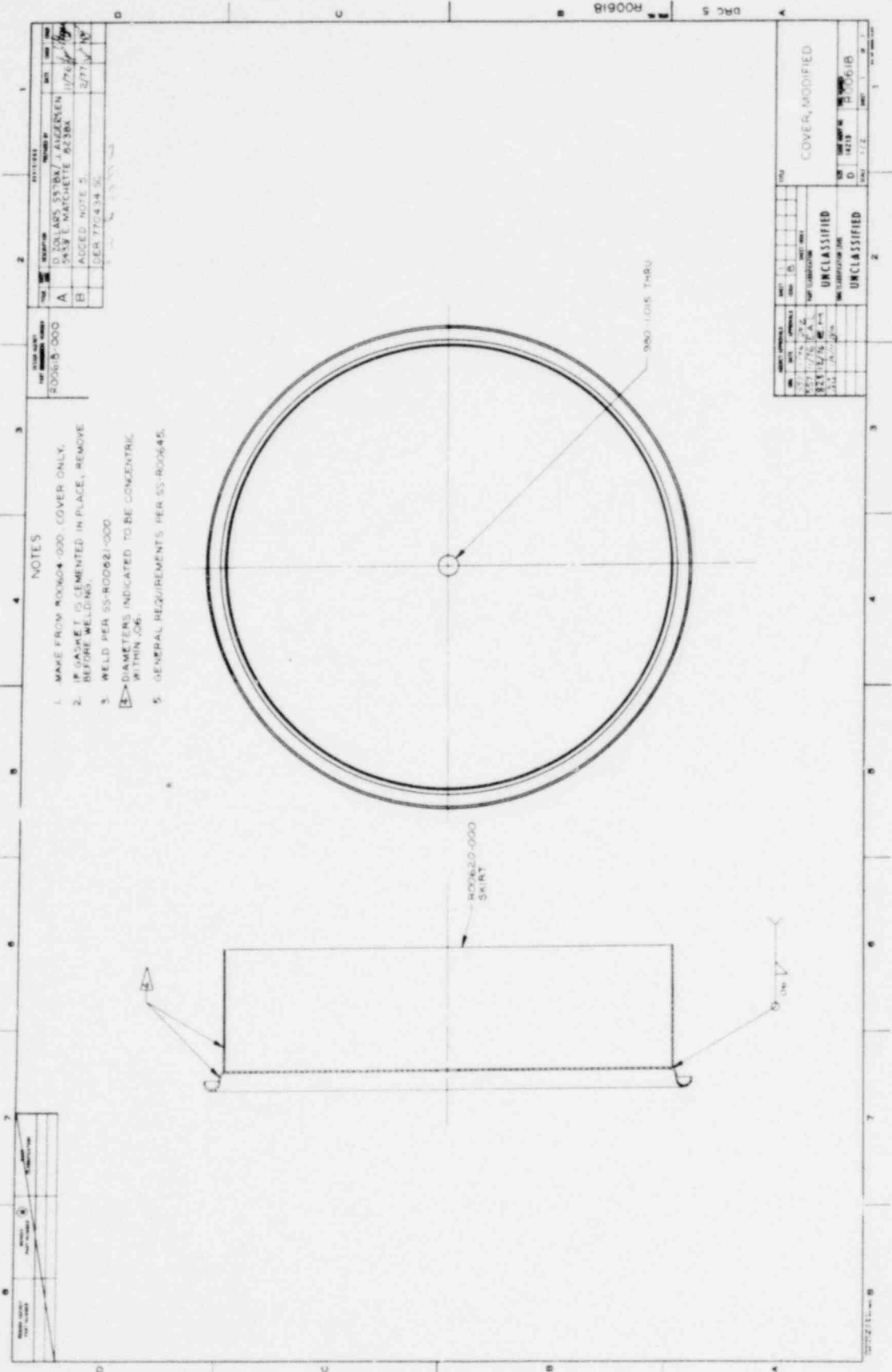
NO. 15-100-0000	UNIT ASSEMBLY
NO. 15-100-0001	UNIT ASSEMBLY
NO. 15-100-0002	UNIT ASSEMBLY
NO. 15-100-0003	UNIT ASSEMBLY
NO. 15-100-0004	UNIT ASSEMBLY
NO. 15-100-0005	UNIT ASSEMBLY
NO. 15-100-0006	UNIT ASSEMBLY
NO. 15-100-0007	UNIT ASSEMBLY
NO. 15-100-0008	UNIT ASSEMBLY
NO. 15-100-0009	UNIT ASSEMBLY
NO. 15-100-0010	UNIT ASSEMBLY
NO. 15-100-0011	UNIT ASSEMBLY
NO. 15-100-0012	UNIT ASSEMBLY
NO. 15-100-0013	UNIT ASSEMBLY
NO. 15-100-0014	UNIT ASSEMBLY
NO. 15-100-0015	UNIT ASSEMBLY
NO. 15-100-0016	UNIT ASSEMBLY
NO. 15-100-0017	UNIT ASSEMBLY
NO. 15-100-0018	UNIT ASSEMBLY
NO. 15-100-0019	UNIT ASSEMBLY
NO. 15-100-0020	UNIT ASSEMBLY
NO. 15-100-0021	UNIT ASSEMBLY
NO. 15-100-0022	UNIT ASSEMBLY
NO. 15-100-0023	UNIT ASSEMBLY
NO. 15-100-0024	UNIT ASSEMBLY
NO. 15-100-0025	UNIT ASSEMBLY
NO. 15-100-0026	UNIT ASSEMBLY
NO. 15-100-0027	UNIT ASSEMBLY
NO. 15-100-0028	UNIT ASSEMBLY
NO. 15-100-0029	UNIT ASSEMBLY
NO. 15-100-0030	UNIT ASSEMBLY
NO. 15-100-0031	UNIT ASSEMBLY
NO. 15-100-0032	UNIT ASSEMBLY
NO. 15-100-0033	UNIT ASSEMBLY
NO. 15-100-0034	UNIT ASSEMBLY
NO. 15-100-0035	UNIT ASSEMBLY
NO. 15-100-0036	UNIT ASSEMBLY
NO. 15-100-0037	UNIT ASSEMBLY
NO. 15-100-0038	UNIT ASSEMBLY
NO. 15-100-0039	UNIT ASSEMBLY
NO. 15-100-0040	UNIT ASSEMBLY
NO. 15-100-0041	UNIT ASSEMBLY
NO. 15-100-0042	UNIT ASSEMBLY
NO. 15-100-0043	UNIT ASSEMBLY
NO. 15-100-0044	UNIT ASSEMBLY
NO. 15-100-0045	UNIT ASSEMBLY
NO. 15-100-0046	UNIT ASSEMBLY
NO. 15-100-0047	UNIT ASSEMBLY
NO. 15-100-0048	UNIT ASSEMBLY
NO. 15-100-0049	UNIT ASSEMBLY
NO. 15-100-0050	UNIT ASSEMBLY



ITEM NO.	DESCRIPTION	QUANTITY	UNIT
1
2
3
4
5
6
7
8
9
10
11
12
13
14
15
16
17
18
19
20
21
22
23
24
25
26
27
28
29
30
31
32
33
34
35
36
37
38
39
40
41
42
43
44
45
46
47
48
49
50

ITEM NO.	DESCRIPTION	QUANTITY	UNIT
1
2
3
4
5
6
7
8
9
10
11
12
13
14
15
16
17
18
19
20
21
22
23
24
25
26
27
28
29
30
31
32
33
34
35
36
37
38
39
40
41
42
43
44
45
46
47
48
49
50

DRAWING NO. 1568 018
 SHEET NO. 1 OF 1
 DATE 11/1/71
 BY [Signature]
 CHECKED BY [Signature]
 APPROVED BY [Signature]
 TITLE: [Blank]
 PROJECT: [Blank]
 ORGANIZATION: [Blank]
 DRAWING NO. 1568 018
 SHEET NO. 1 OF 1
 DATE 11/1/71
 BY [Signature]
 CHECKED BY [Signature]
 APPROVED BY [Signature]
 TITLE: [Blank]
 PROJECT: [Blank]
 ORGANIZATION: [Blank]



NOTES

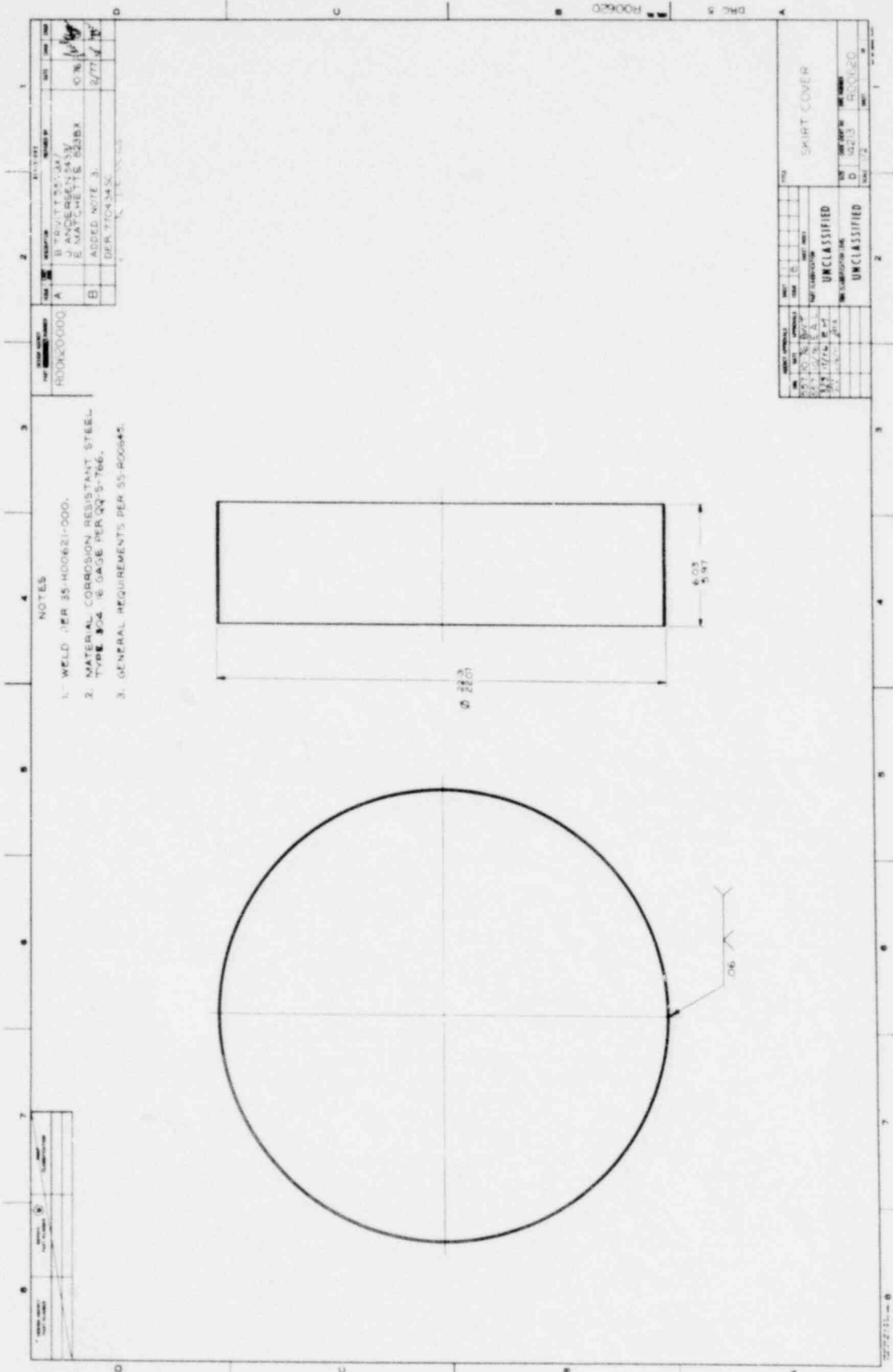
1. MAKE FROM R00604-000 COVER ONLY.
2. IF GASKET IS CEMENTED IN PLACE, REMOVE BEFORE WELDING.
3. WELD PER SS-R00621-000.
4. DIAMETERS INDICATED TO BE CONCENTRIC WITHIN JOB.
5. GENERAL REQUIREMENTS PER SS-R00645.

REV	DESCRIPTION	DATE	BY	CHK
A	COLLARS SYSTEM / JANDERSEN	1/76	JJ	
B	353 L'INCHETTE 863BA	2/77	NY	
	ADDED NOTE 5			
	DER 77-434-5C			

ITEM NO.	QTY	UNIT	DESCRIPTION
R00618-000			

REV	DESCRIPTION	DATE	BY	CHK
D	COVER, MODIFIED	1/78	JJ	
	UNCLASSIFIED			
	UNCLASSIFIED			

R00618 DRC 5

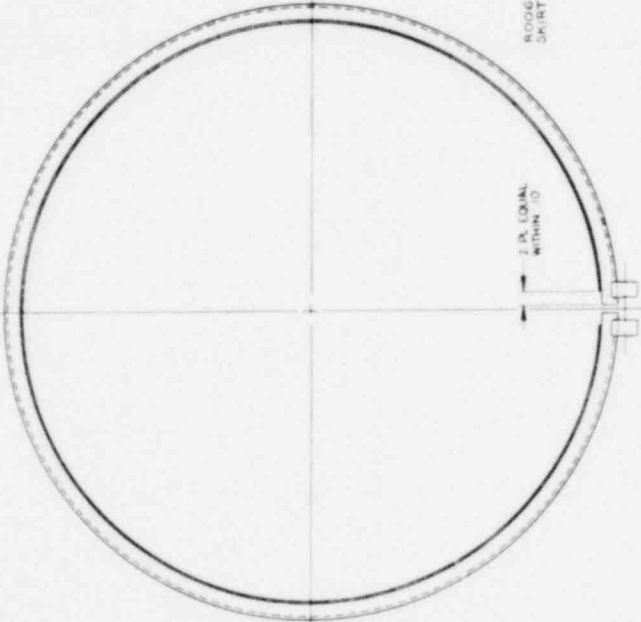
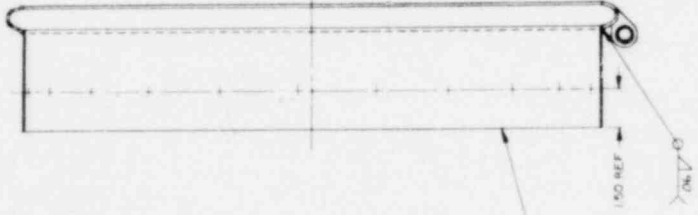


REV	DATE	DESCRIPTION	BY	CHK
A	11/11/53	D. COLLARS 55RIN (J ANGLE 2/54)		
		5433 E. MATCHETTE, 6238		
		ADDED DIM 1.50 REF		
		ADDED NOTE 4.		
		RELOCATED ROW OF PLOT HOLES		
		DEP 377434		

RO0621-000

NOTES

1. MAKE FROM RO0604-000, CLAMP RING.
2. RO0623-000 MAY BE PERFORMED TO FACILITATE ASSEMBLY.
3. WELD PER 55-RO0621-000.
4. GENERAL REQUIREMENTS PER 55-RO0645.



REV	DATE	DESCRIPTION	BY	CHK
D	11/11/53	UNCLASSIFIED		
D	11/11/53	UNCLASSIFIED		

RING, CLAMP, MODIFIED

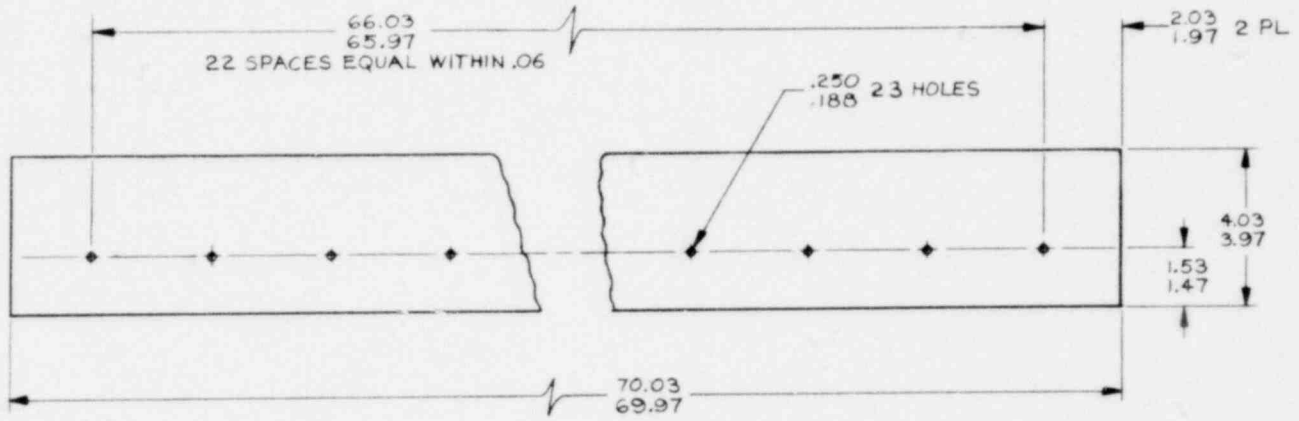
RO0621

DESIGN AGENCY PART NUMBER	BENCH PART NUMBER	PART CLASSIFICATION

NOTES

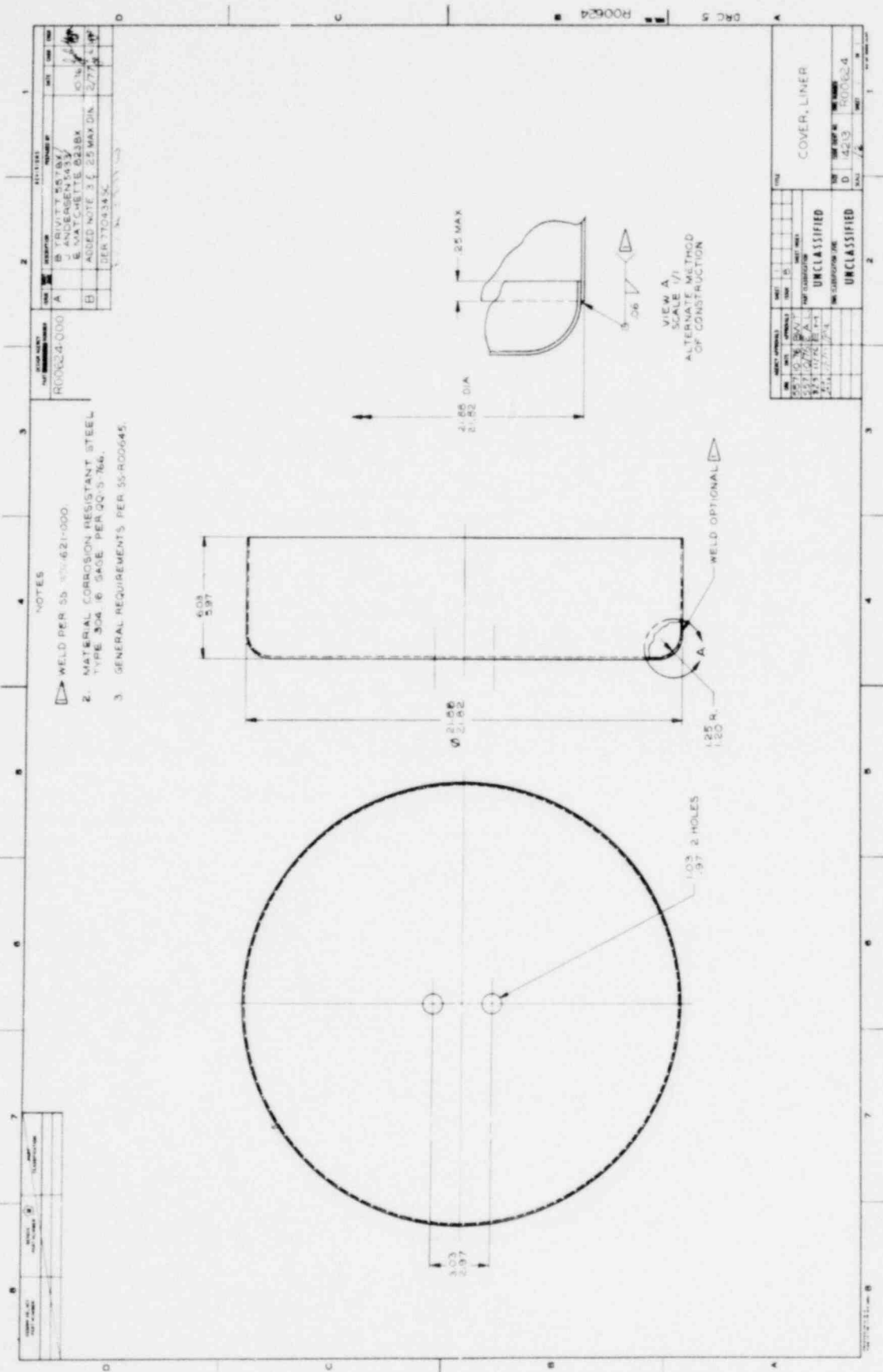
1. MATERIAL: CORROSION RESISTANT STEEL
TYPE 304, 16 GAGE PER QQ-S-766.
2. GENERAL REQUIREMENTS PER SS-R00645.

DESIGN AGENCY PART NUMBER	DESCRIPTION	PREPARED BY	DATE	CHKD	ENGR
R00623-000	A B TRIVITT 557 BX/ J ANDERSEN 5433/ E MATCHETTE 823 BX		1/76	<i>Handwritten initials</i>	<i>Handwritten initials</i>
	B ADDED NOTE 2. 1.53/1.47 WAS 2.03/1.97		2/77	<i>Handwritten initials</i>	<i>Handwritten initials</i>
	DER 770434 SC				



DRC 5
REV NO R00623

AGENCY APPROVAL	DATE	INITIALS	TITLE
<i>Handwritten initials</i>	1/23/76	<i>Handwritten initials</i>	SKIRT, RING
<i>Handwritten initials</i>	1/27/76	<i>Handwritten initials</i>	UNCLASSIFIED
<i>Handwritten initials</i>	1/27/76	<i>Handwritten initials</i>	UNCLASSIFIED



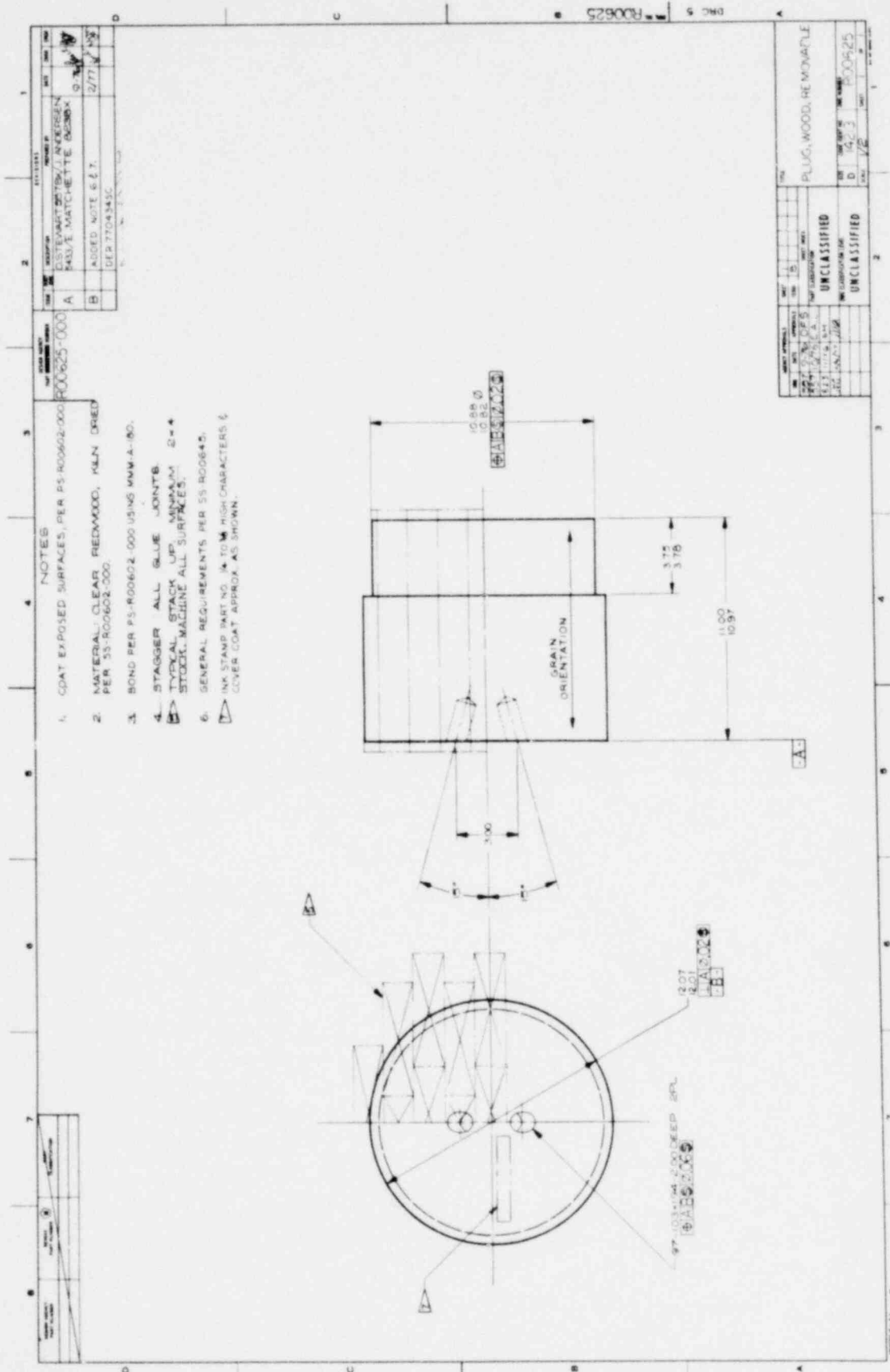
REV	DESCRIPTION	DATE	BY	CHK
A	TRIVITT BOSTON			
J	ANDERSON			
E	MATCHELLE			
B	ADDED NOTE 3. 25 MAX DIA. 2.774			

NOTES
 1. WELD PER SS 304-621-000
 2. MATERIAL CORROSION RESISTANT STEEL TYPE 304. 6 SAGE PER QQ-S-764.
 3. GENERAL REQUIREMENTS PER SS-R00645.

REV	DESCRIPTION	DATE	BY	CHK
A	TRIVITT BOSTON			
J	ANDERSON			
E	MATCHELLE			
B	ADDED NOTE 3. 25 MAX DIA. 2.774			

REV	DESCRIPTION	DATE	BY	CHK
A	TRIVITT BOSTON			
J	ANDERSON			
E	MATCHELLE			
B	ADDED NOTE 3. 25 MAX DIA. 2.774			

1568 023



NOTES

1. COAT EXPOSED SURFACES, PER PS-R00602-000 R00625-000
 2. MATERIAL: CLEAR REDWOOD, KLN DRED PER 35-R00602-000.
 3. BOND PER PS-R00602-000 USING MVM-A-180.
 4. STAGGER ALL BLUE JOINTS
 5. TYPICAL STACK UP, MINIMUM 2-4 STOCK, MACHINE ALL SURFACES.
 6. GENERAL REQUIREMENTS PER 55 R00645.
- INK STAMP PART NO. 14-TOM HIGH CHARACTERS & COVER COAT APPROX. AS SHOWN.

REV	DATE	DESCRIPTION
A	2/77	ESTIMATE 2/78/1/INKERGEN 343/1 MATCHETTE 2/28/8X
B	2/77	ADDED NOTE 6 & 7. DEP 7704343C

REV	DATE	DESCRIPTION
UNCLASSIFIED		
UNCLASSIFIED		

PLUG, WOOD, RE-MONABLE

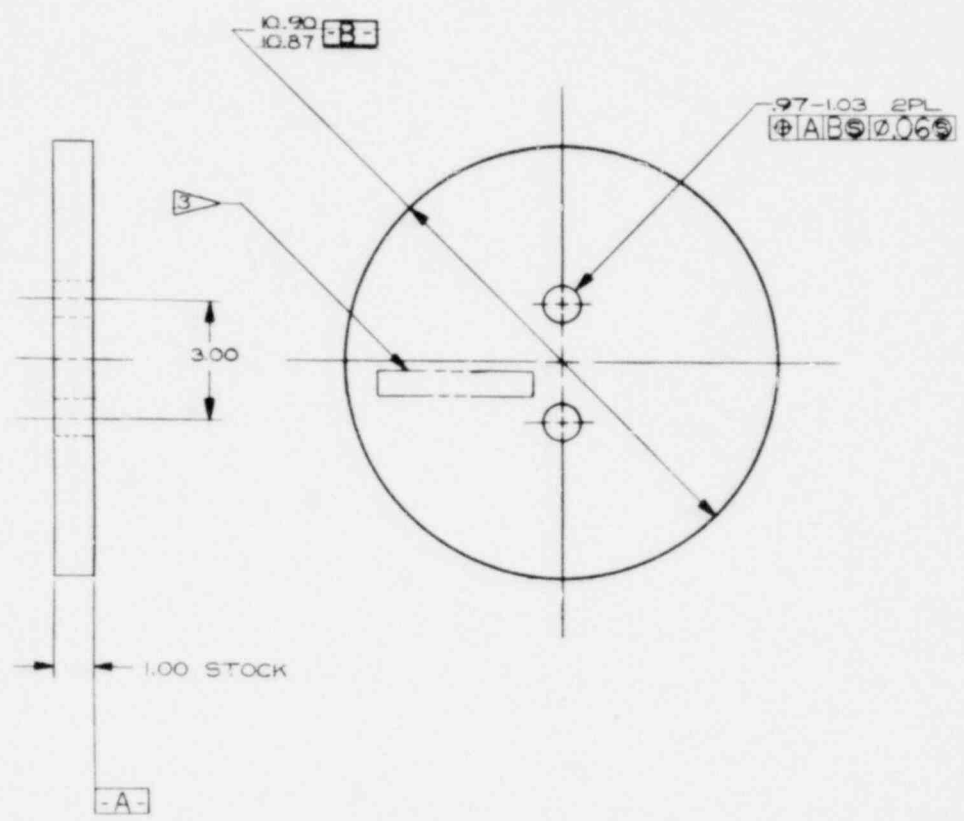
D 1423 R00625

DESIGN AGENCY PART NUMBER	BENDIS PART NUMBER	WWT CLASSIFICATION

NOTES

1. MATERIAL: ALUMINUM PLATE 7075-T6 PER QQ-A-250/12.
2. GENERAL REQUIREMENTS PER SS-R00645.
3. INK STAMP PART NO. 1/4 HIGH CHARACTERS & COVER COAT APPROX. AS SHOWN.

REV	DESCRIPTION	PREPARED BY	DATE	CHKD	ENGR
A	D STEWART 507BX/J ANDERSEN 5433/E MATCHETTE 823BX		8-76		
B	ADDED NOTE 2 & 3.		2/77		
UER 770434 5C R. Stewart 3-8-77 W					



1568 025

365

DRC 5
REV NO R00626

AGENCY APPROVALS			SHEET	TITLE
DATE	INITIALS	WWT	NO.	
11/76	[Signature]	[Signature]	1	DISC, REMOVABLE
11/76	[Signature]	[Signature]		
11/76	[Signature]	[Signature]		
11/76	[Signature]	[Signature]		
DESIGNATION LEVEL			SCALE	FIG. NO. / SHEET
UNCLASSIFIED			1/4	14213 / R00626
UNCLASSIFIED				

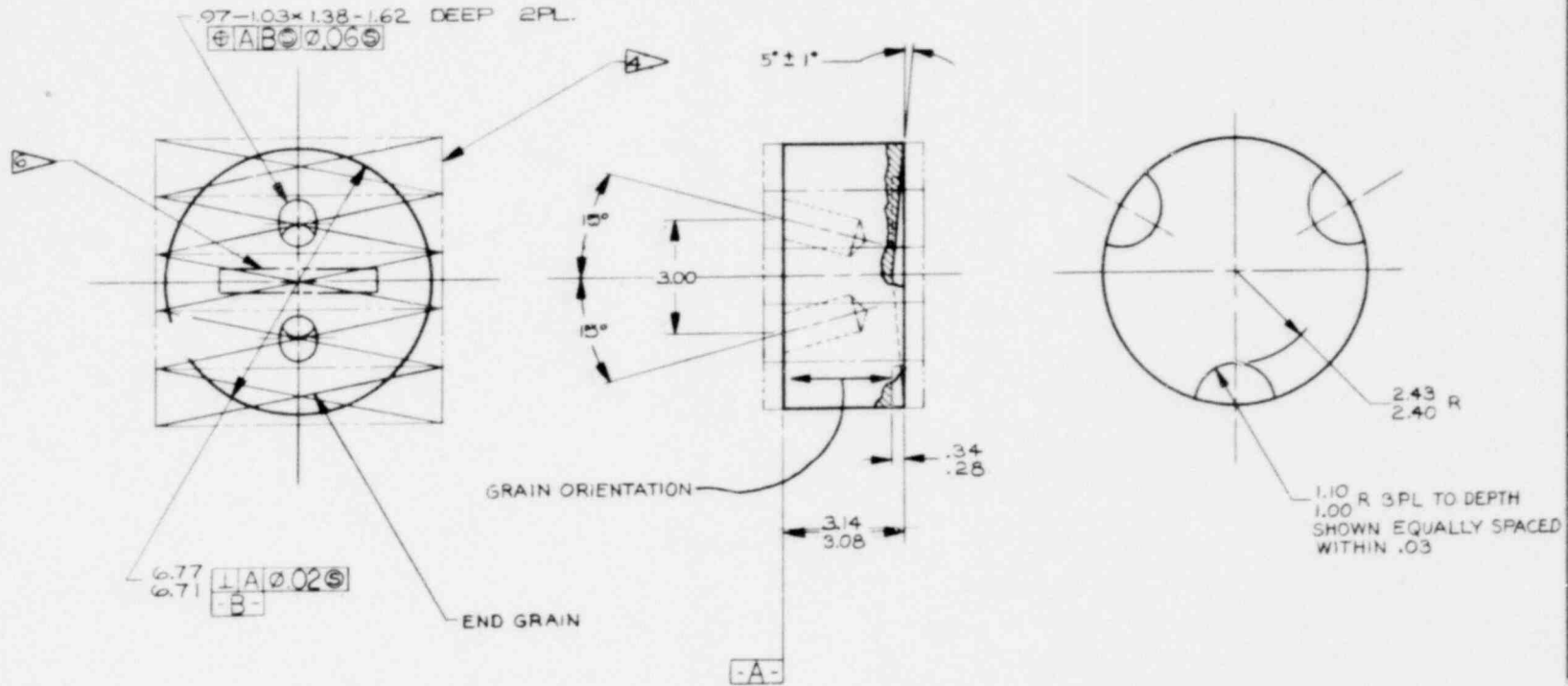
DESIGN AGENCY PART NUMBER	BENCH PART NUMBER	AGENCY CLASSIFICATION

NOTES

1. COAT EXPOSED SURFACES PER PS-R00602-000.
2. MATERIAL: CLEAR REDWOOD, KILN DRIED PER SS-R00602-000.
3. BOND PER PS-R00602-000 USING MMM-A-180.
4. TYPICAL STACK UP. MINIMUM 2x8 STOCK. MACHINE ALL SURFACES.
5. GENERAL REQUIREMENTS PER SS-R00645.

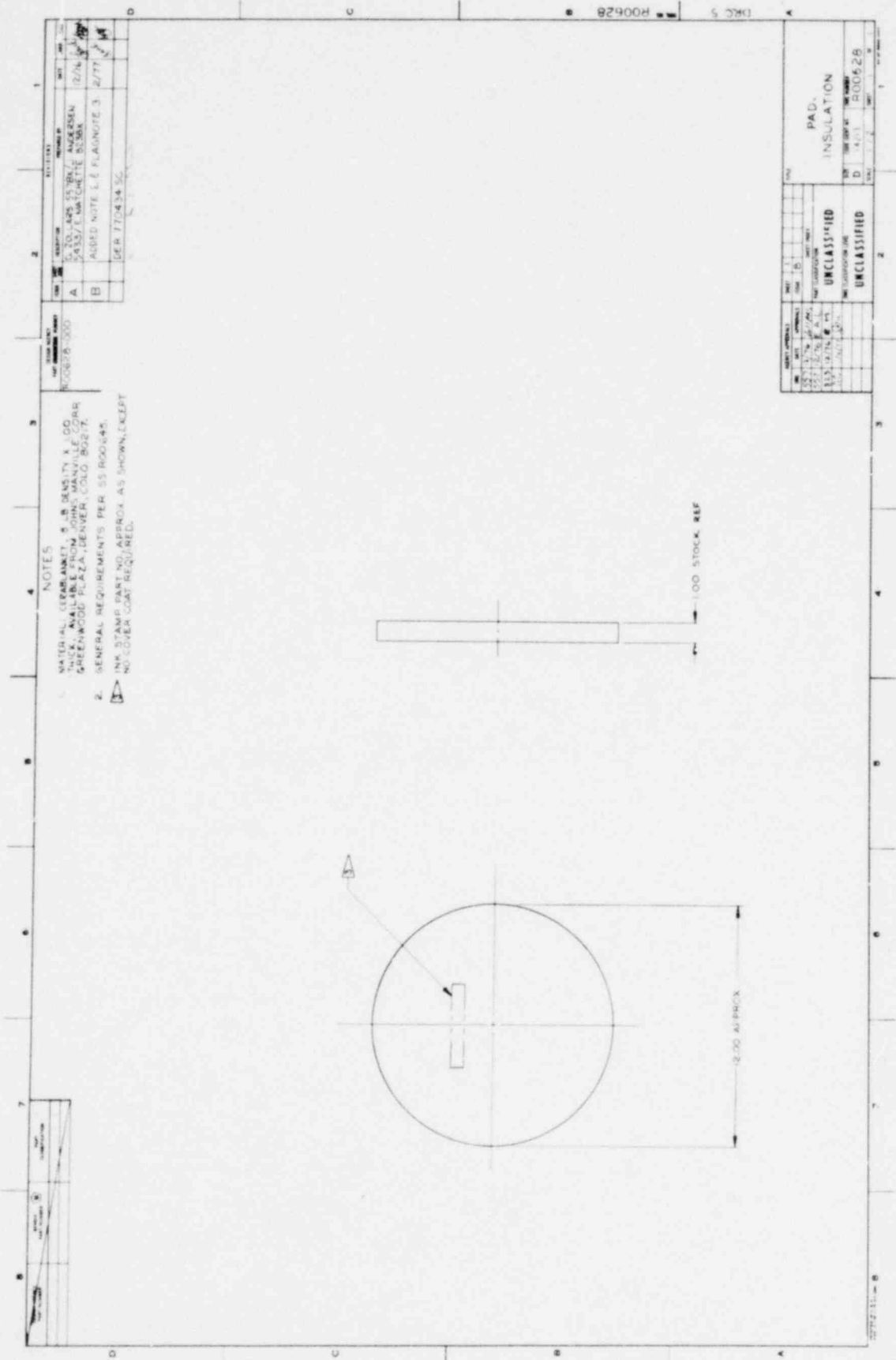
INK STAMP PART NO. 1/4 TO 3/8 HIGH CHARACTERS & COVER COAT APPROX. AS SHOWN.

REV	DESCRIPTION	PREPARED BY	DATE	CHECK	ENGR
A	D. STEWART/557EX/JANDERSEN 5433/E MATCHETTE 823EX		9-76		
B	ADDED NOTE 5 & 6. DER 770434 SC		2/77		



DRC 5
DER 770434 SC
R00627

AGENCY APPROVALS		SHEET	TITLE
DATE	BY	NO.	PLUG, WOOD, REMOVABLE
10/76	EAL	1	
11/76	EAL		
1/77	EAL		
2/77	EAL		
UNCLASSIFIED		TIME CLASSIFICATION	REV
UNCLASSIFIED			1213
		SHEET	R00627
		OF	2



REV	DATE	BY	DESCRIPTION
A	02/14/75	BR. ANDERSEN	ISSUED FOR CONSTRUCTION
B	02/14/75	BR. ANDERSEN	ADDED NOTE 1, 2, 3, 4

1. MATERIAL: GERBANKET, 8" SENSITIVITY, 1.00" THICK, AVAILABLE FROM JOHN'S MANVILLE CORR GREENWOOD PLAZA, DENVER, COLO. 80217.
 2. GENERAL REQUIREMENTS PER SS 800645.

INK STAMP NOT TO APPROX. AS SHOWN, KEPT NO COVER CAP REQUIRED.

12.00 AT PRIC.
 1.00 STOCK REF.

1568 027

367

1568 027

367

1568 027

367

1568 027

367

1568 027

367

1568 027

367

1568 027

367

1568 027

367

1568 027

367

1568 027

367

1568 027

367

1568 027

367

REV	DATE	BY	DESCRIPTION
A	02/14/75	BR. ANDERSEN	ISSUED FOR CONSTRUCTION
B	02/14/75	BR. ANDERSEN	ADDED NOTE 1, 2, 3, 4

12.00 AT PRIC.
 1.00 STOCK REF.

1568 027

367

1568 027

367

1568 027

367

1568 027

367

1568 027

367

1568 027

367

1568 027

367

1568 027

367

1568 027

367

1568 027

367

1568 027

367

1568 027

367

1568 027

367

1568 027

367

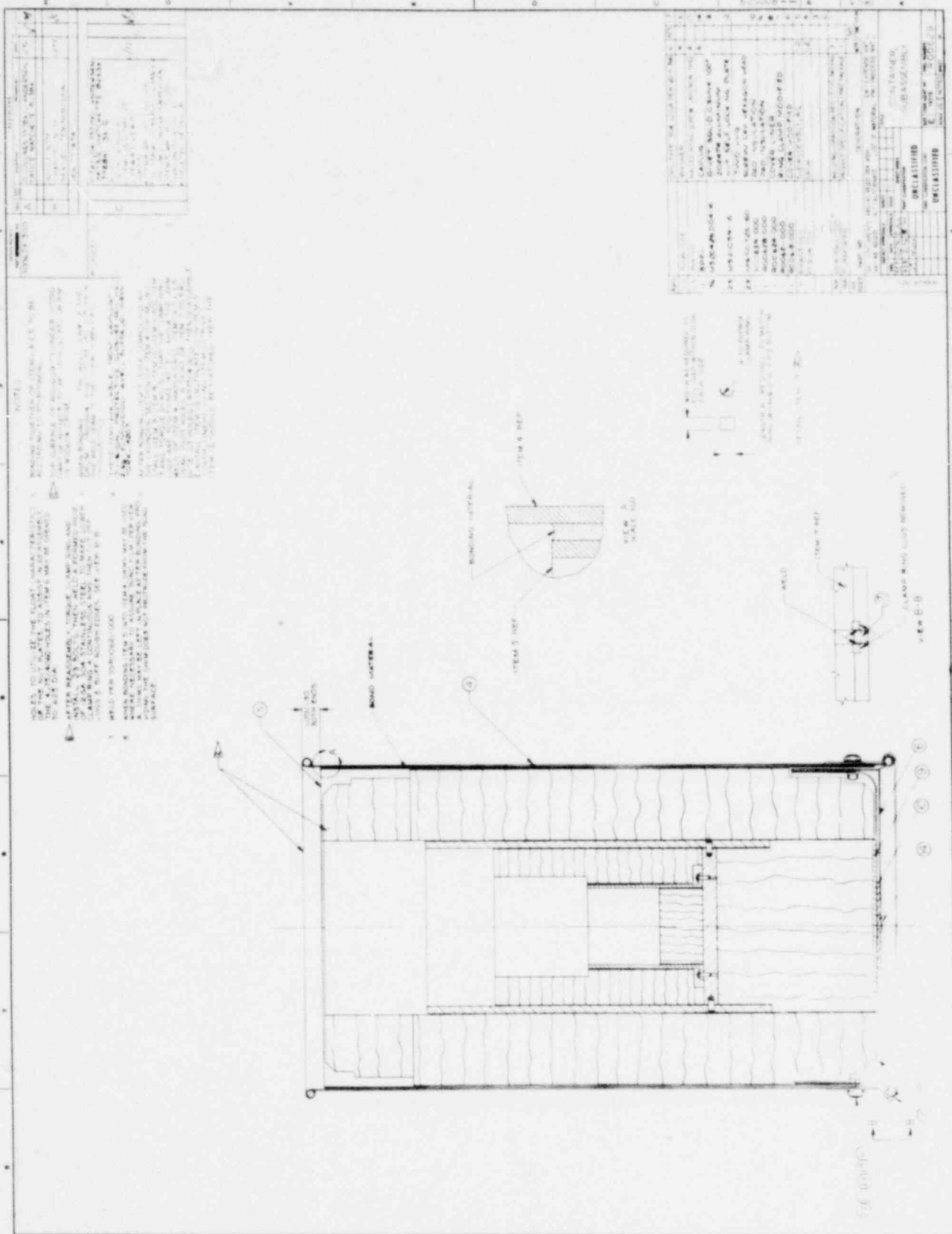
1568 027

367

1568 027

367

1568 027

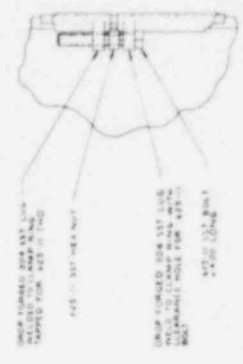
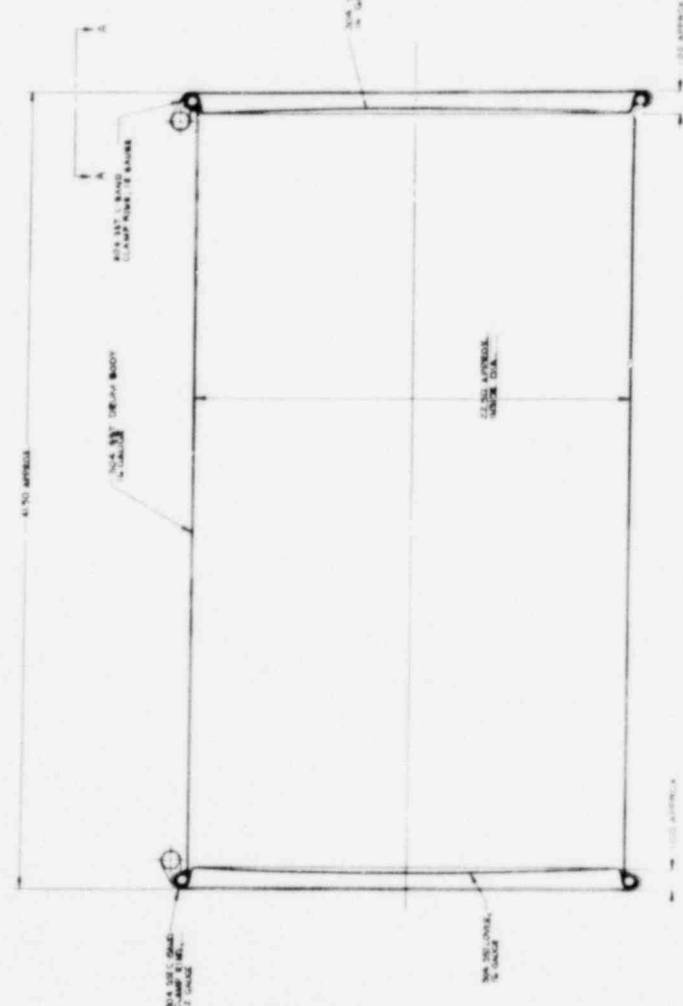
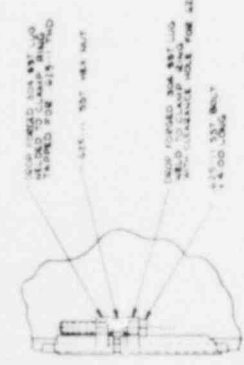


NO.	DESCRIPTION	QTY.	UNIT	REMARKS
1	ROOFING MATERIAL		SQ. FT.	
2	WALLING MATERIAL		SQ. FT.	
3	FLOORING MATERIAL		SQ. FT.	

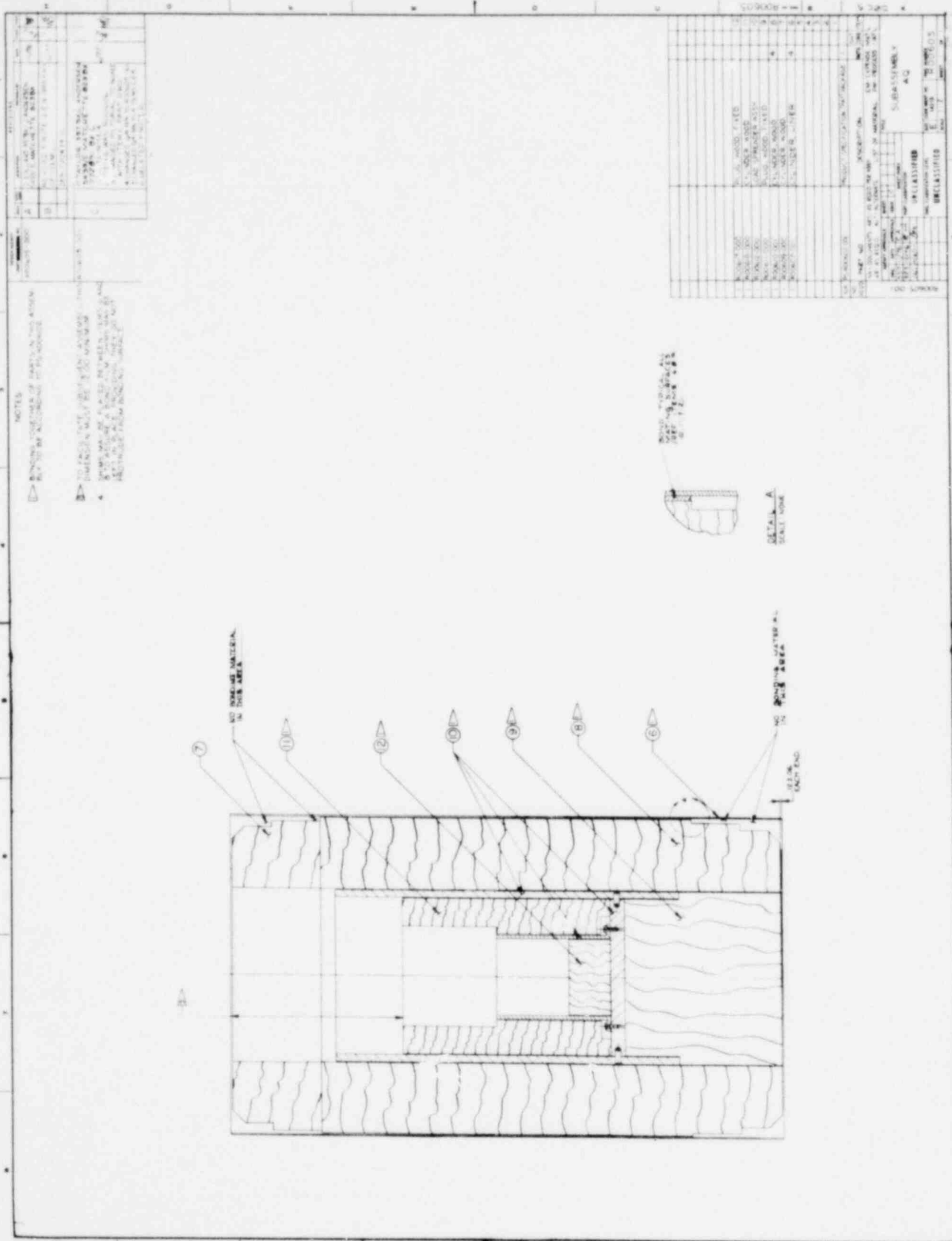
NO.	DESCRIPTION	QTY.	UNIT	REMARKS
4	MASONRY MATERIAL		SQ. FT.	
5	FLOORING MATERIAL		SQ. FT.	
6	STAIRCASE		SQ. FT.	
7	ROOFING MATERIAL		SQ. FT.	
8	WALLING MATERIAL		SQ. FT.	
9	FLOORING MATERIAL		SQ. FT.	
10	STAIRCASE		SQ. FT.	

NO. 1	NO. 2	NO. 3	NO. 4	NO. 5	NO. 6	NO. 7	NO. 8	NO. 9	NO. 10
1	2	3	4	5	6	7	8	9	10

1. FABRICATE AND ASSEMBLE IN STEEL PLATE, STAINLESS STEEL, 304, 1/2" THICK, 18" X 18" X 1/2" (SEE DRAWING FOR DIMENSIONS). THE FABRICATOR SHALL BE RESPONSIBLE FOR THE FABRICATOR'S WORK AT ALL TIMES.
2. DIMENSIONS AND TOLERANCES SHOWN ARE APPROXIMATE.
3. USE 304 STAINLESS STEEL, SHEET, PER MIL-SPEC-201.
4. FABRICATE AND ASSEMBLE TO DIMENSIONS SHOWN.



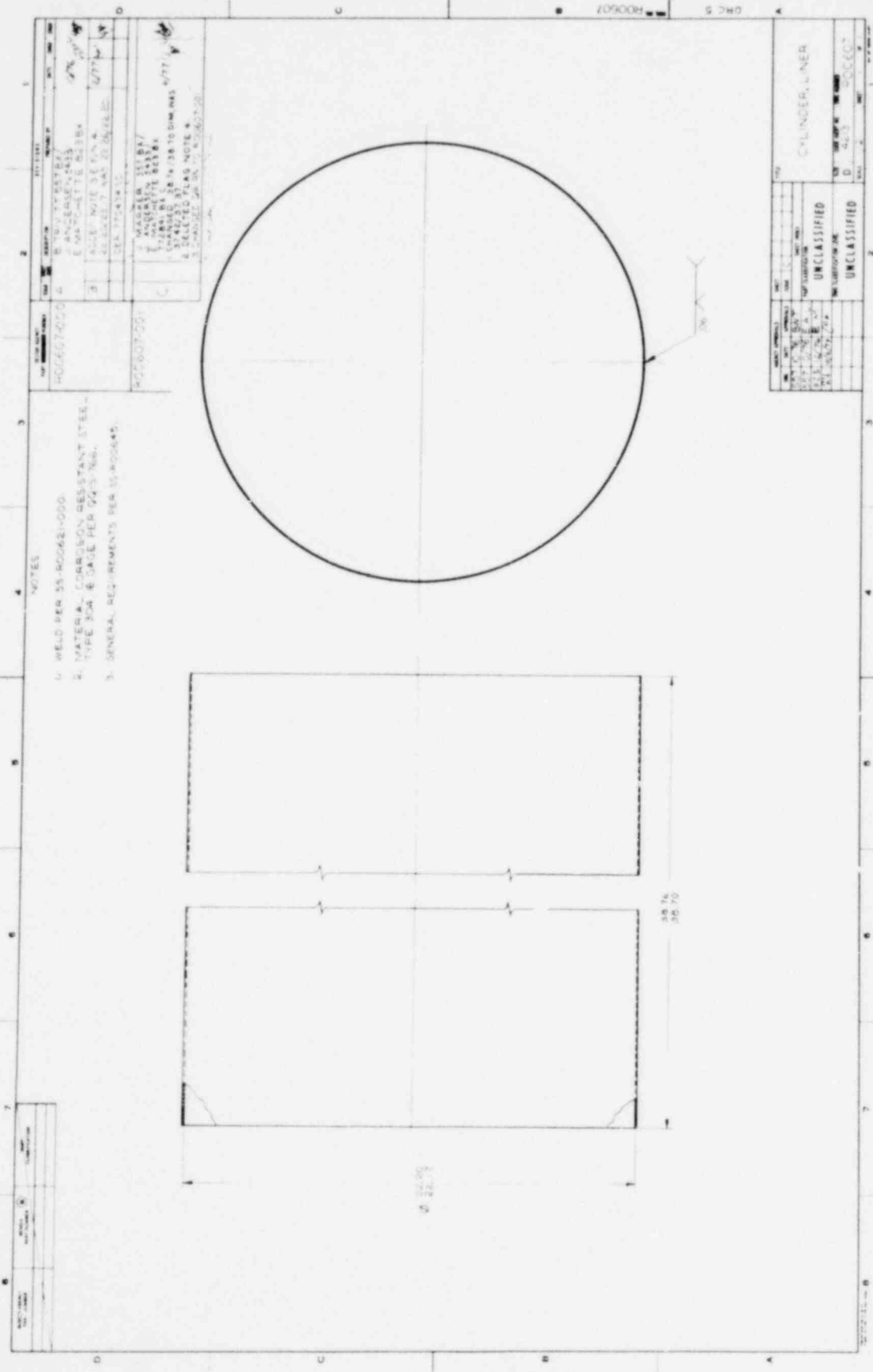
NO. 1	NO. 2	NO. 3	NO. 4	NO. 5	NO. 6	NO. 7	NO. 8	NO. 9	NO. 10
1	2	3	4	5	6	7	8	9	10



NOTES
 1. REFER TO DRAWING OF PARTIAL SECTION
 2. REFER TO DRAWING OF PARTIAL SECTION
 3. REFER TO DRAWING OF PARTIAL SECTION
 4. REFER TO DRAWING OF PARTIAL SECTION
 5. REFER TO DRAWING OF PARTIAL SECTION
 6. REFER TO DRAWING OF PARTIAL SECTION
 7. REFER TO DRAWING OF PARTIAL SECTION
 8. REFER TO DRAWING OF PARTIAL SECTION

NO.	REVISION	DATE
1	ISSUED FOR CONSTRUCTION	11/15/54
2	REVISED TO SHOW INSULATION	11/15/54
3	REVISED TO SHOW INSULATION	11/15/54
4	REVISED TO SHOW INSULATION	11/15/54
5	REVISED TO SHOW INSULATION	11/15/54
6	REVISED TO SHOW INSULATION	11/15/54
7	REVISED TO SHOW INSULATION	11/15/54
8	REVISED TO SHOW INSULATION	11/15/54

NO.	REVISION	DATE
1	ISSUED FOR CONSTRUCTION	11/15/54
2	REVISED TO SHOW INSULATION	11/15/54
3	REVISED TO SHOW INSULATION	11/15/54
4	REVISED TO SHOW INSULATION	11/15/54
5	REVISED TO SHOW INSULATION	11/15/54
6	REVISED TO SHOW INSULATION	11/15/54
7	REVISED TO SHOW INSULATION	11/15/54
8	REVISED TO SHOW INSULATION	11/15/54



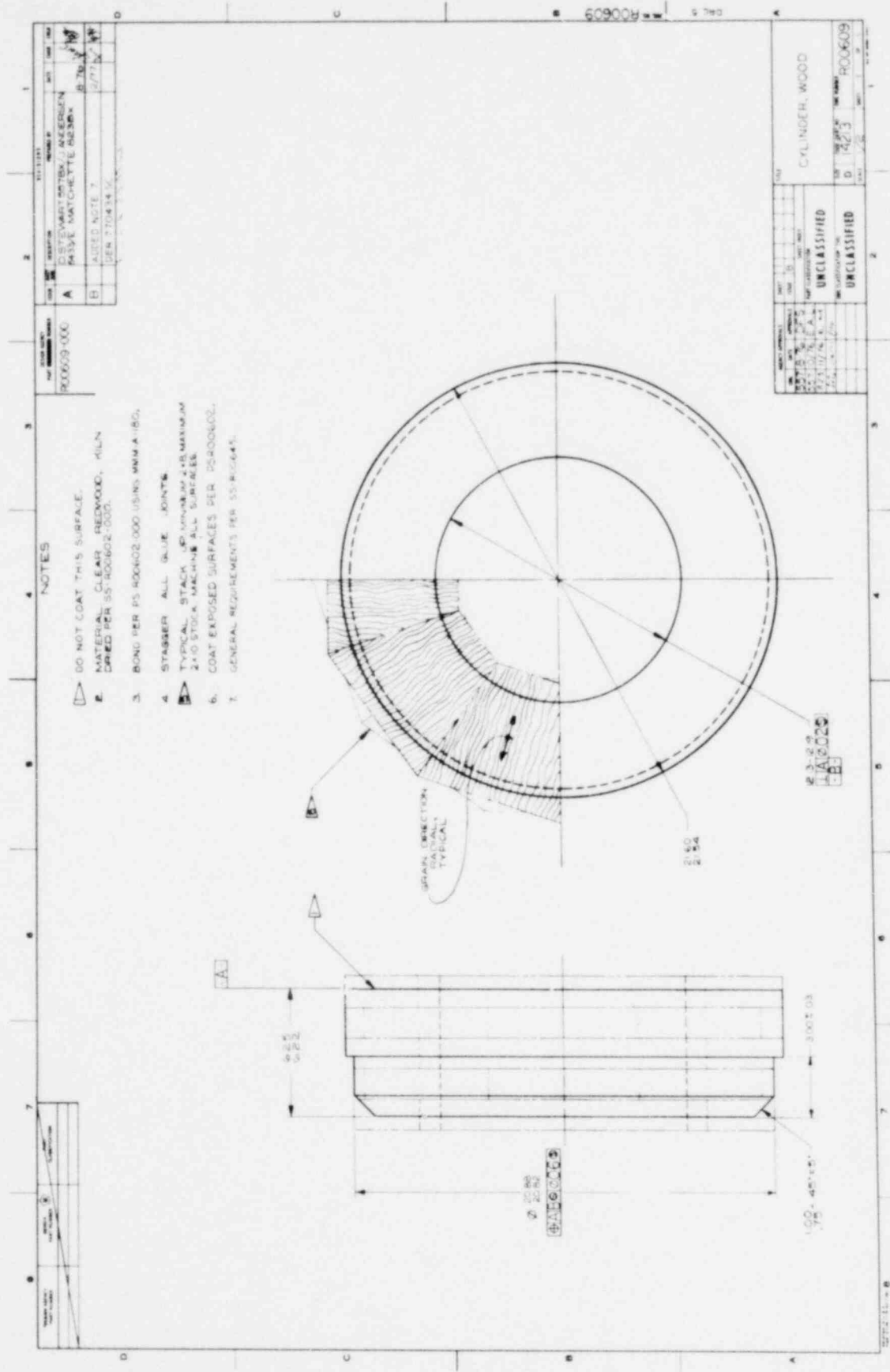
REV	DATE	BY	CHKD	DESCRIPTION
1	07/11/81	W. J.
2
3
4
5
6
7

1. WELDED TO ...
 2. ...
 3. ...
 4. ...
 5. ...
 6. ...
 7. ...

- NOTES
- WELD PER SS-R0062-000.
 - MATERIAL CORROSION RESISTANT STEEL TYPE 304. 6 GAUGE PER 64'S 788.
 - GENERAL REQUIREMENTS PER SS-R0064'S.

REV	DATE	BY	CHKD	DESCRIPTION
1
2
3
4
5
6
7

1. ...
 2. ...
 3. ...
 4. ...
 5. ...
 6. ...
 7. ...



NOTES

1. DO NOT COAT THIS SURFACE.
2. MATERIAL: CLEAR BEECHWOOD, 41LN DRIED PER SS-R00602-000.
3. BOND PER PS-R00602-000 USING MM-A-180.
4. STAGGER ALL GLUE JOINTS.
5. TYPICAL STACK JOINTS SHOWN AS MINIMUM 2x0 STOCK MACHINE ALL SURFACES.
6. COAT EXPOSED SURFACES PER PS-R00602-000.
7. GENERAL REQUIREMENTS PER SS-R00644-000.

REV	DESCRIPTION	DATE	BY	CHK
A	REVIEWED PARTS BY PHYL MATCHETT DESIGN	8/7/77	PH	PH
B	ADDED NOTE 7	8/7/77	PH	PH
	GEN 2108143			

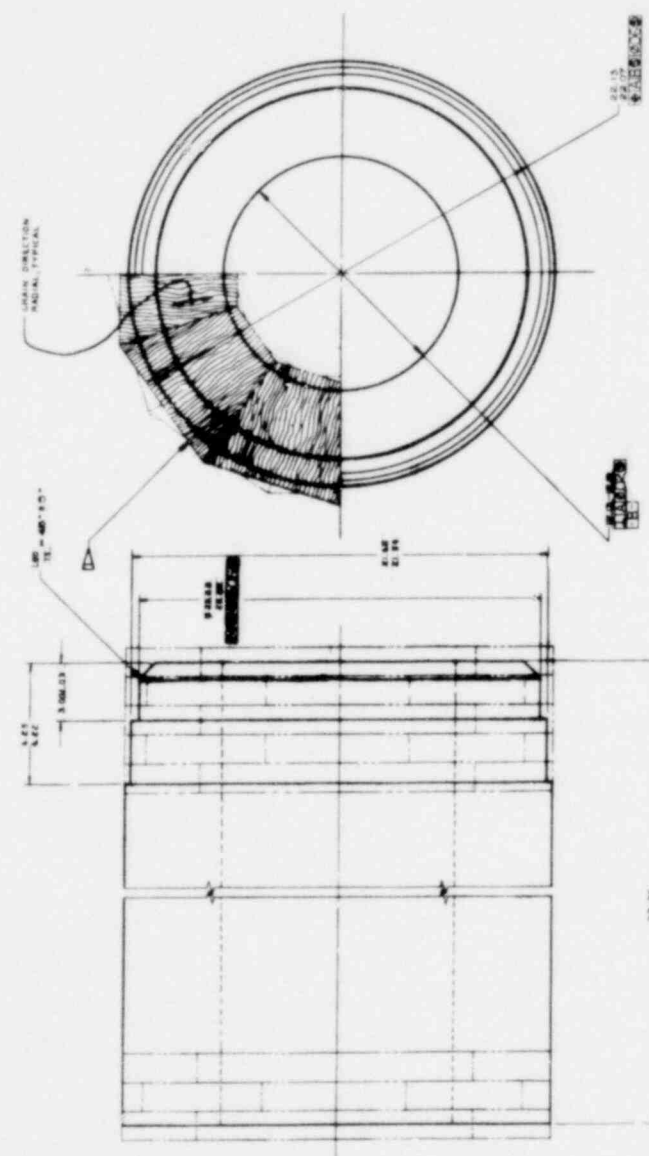
900609-000

REV	DESCRIPTION	DATE	BY	CHK
D	UNCLASSIFIED			
D	UNCLASSIFIED			

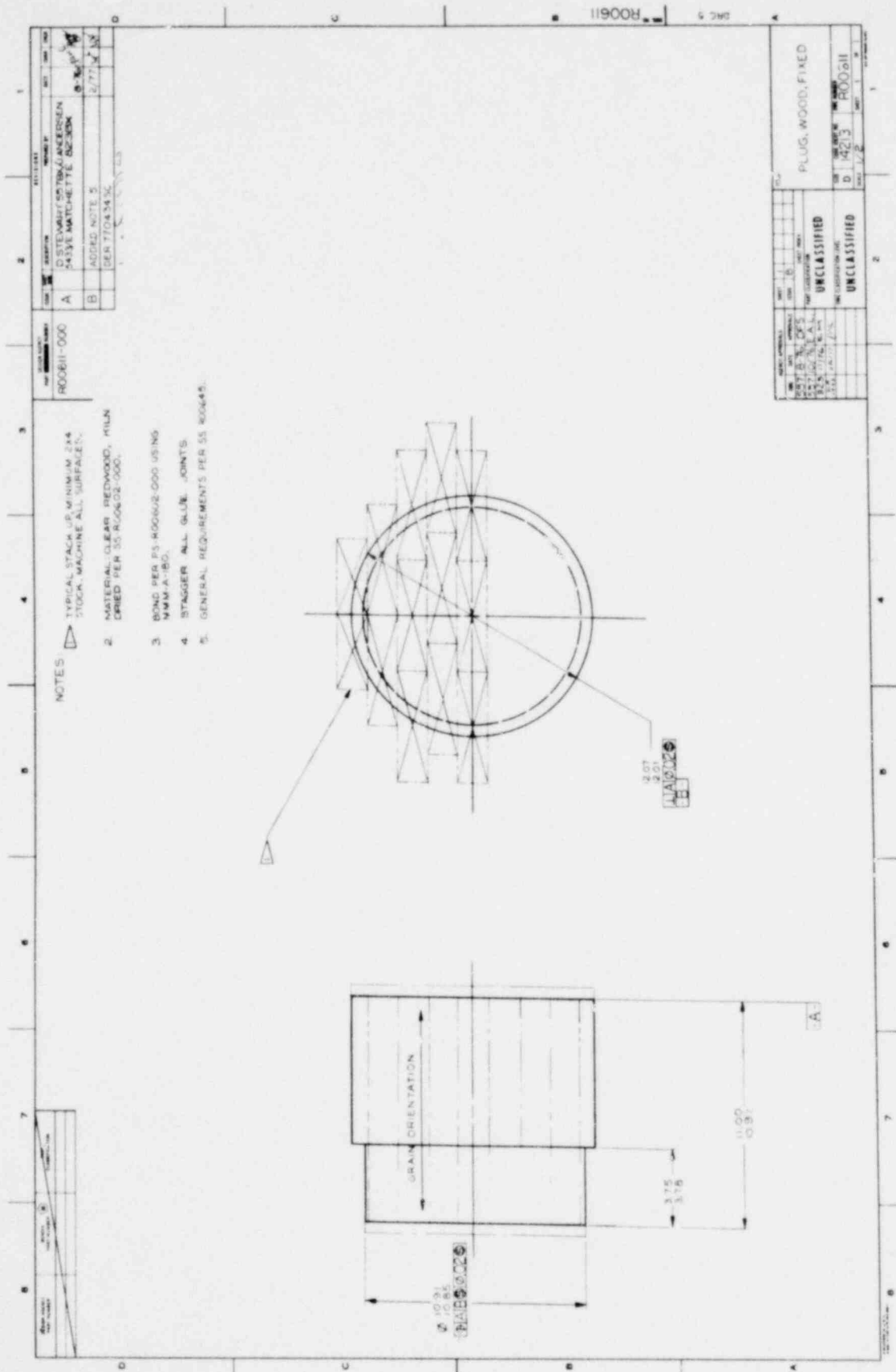
CYLINDER, WOOD
D 14213 R00609

REV	DATE	BY	CHKD	DESCRIPTION
A				ISSUED FOR CONSTRUCTION
B				ISSUED FOR CONSTRUCTION
C				ISSUED FOR CONSTRUCTION

- NOTES
1. TYPICAL UNITS OF MEASUREMENT SHALL BE AS SHOWN ON DRAWING.
 2. MATERIALS SHALL BE AS SPECIFIED IN THE NOTES AND SHALL BE SUBJECT TO INSPECTION AND APPROVAL BY THE CONTRACTOR.
 3. FINISH SHALL BE AS SPECIFIED IN THE NOTES AND SHALL BE SUBJECT TO INSPECTION AND APPROVAL BY THE CONTRACTOR.
 4. STAIRS SHALL BE AS SPECIFIED IN THE NOTES AND SHALL BE SUBJECT TO INSPECTION AND APPROVAL BY THE CONTRACTOR.
 5. GENERAL REQUIREMENTS SHALL BE AS SPECIFIED IN THE NOTES AND SHALL BE SUBJECT TO INSPECTION AND APPROVAL BY THE CONTRACTOR.



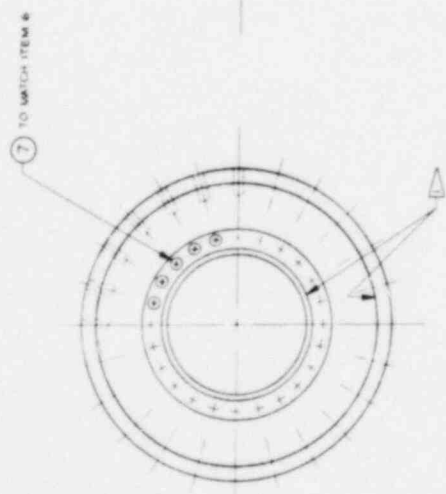
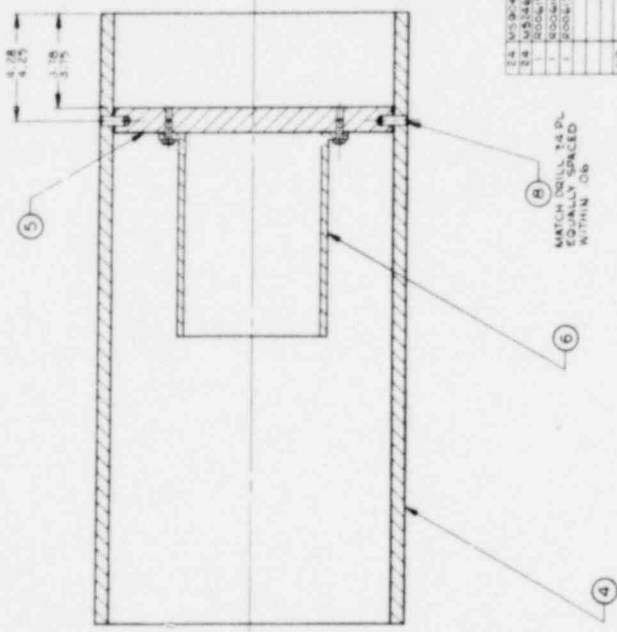
REV	DATE	BY	CHKD	DESCRIPTION
A				ISSUED FOR CONSTRUCTION
B				ISSUED FOR CONSTRUCTION
C				ISSUED FOR CONSTRUCTION



REV	DATE	DESCRIPTION
A	05/15/62	DESIGN MATCHED TO DRAWING 1568-035-0000
B	07/17/62	ADDED NOTE 2.
C	08/14/62	DESIGN MATCHED TO DRAWING 1568-035-0000

NOTES

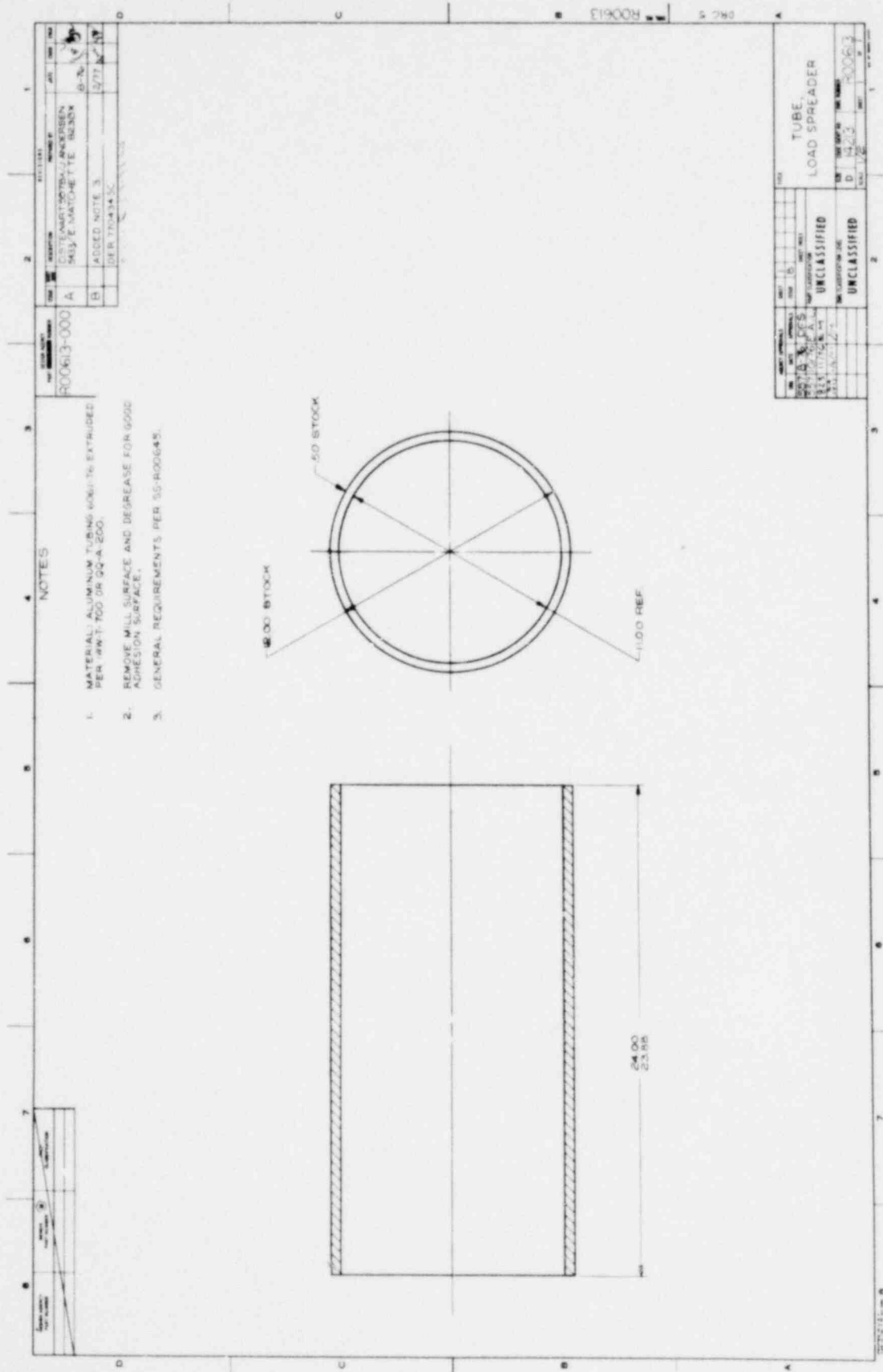
1. THESE DIAMETERS TO BE CONCENTRIC WITHIN 0.1.
2. GENERAL REQUIREMENTS PER SS-R00645.



REV	DATE	DESCRIPTION
1	05/15/62	DESIGN MATCHED TO DRAWING 1568-035-0000
2	07/17/62	ADDED NOTE 2.
3	08/14/62	DESIGN MATCHED TO DRAWING 1568-035-0000

REV	DATE	DESCRIPTION
1	05/15/62	DESIGN MATCHED TO DRAWING 1568-035-0000
2	07/17/62	ADDED NOTE 2.
3	08/14/62	DESIGN MATCHED TO DRAWING 1568-035-0000

REV	DATE	DESCRIPTION
1	05/15/62	DESIGN MATCHED TO DRAWING 1568-035-0000
2	07/17/62	ADDED NOTE 2.
3	08/14/62	DESIGN MATCHED TO DRAWING 1568-035-0000



820 8291

1568 037

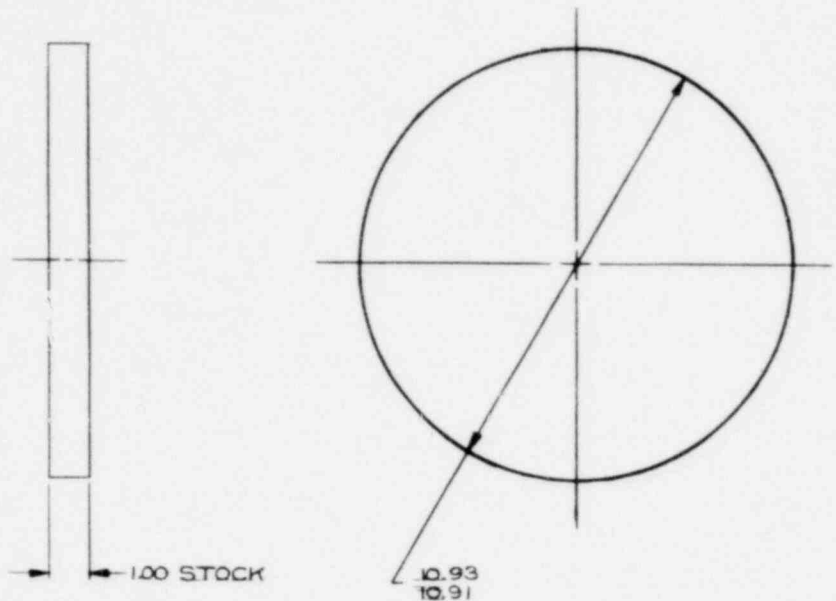
377

DESIGN AGENCY PART NUMBER	DESIGN PART NUMBER	PART CLASSIFICATION

NOTES

1. MATERIAL: ALUMINUM PLATE 7075-T6 PER QQ-A-250/12.
2. REMOVE MILL SCALE AND DEGREASE STOCK SURFACES FOR GOOD ADHESION SURFACE.
3. GENERAL REQUIREMENTS PER SS-R00645.

R0064-000	REVISIONS	DATE	CHKD	APPD
	DESCRIPTION	PREPARED BY		
A	D STEWART 557BX/J ANDERSEN 5433/E MATCHETTE 823BX	8-76	[Signature]	[Signature]
B	ADDED NOTE 3. DER 7704345C	2/77	[Signature]	[Signature]



1568 037 R00614

DAC 5

AGENCY APPROVALS			SHEET	TITLE
DATE	INITIALS	INITIALS	NO.	DISC, FIXED
11/76	[Signature]	[Signature]		
11/76	[Signature]	[Signature]		
2/77	[Signature]	[Signature]		
PART CLASSIFICATION			DESIGN NUMBER	
UNCLASSIFIED			C 14213	R00614
DESIGNATION			REV	
UNCLASSIFIED			1/2	

PRINTED IN U.S.A.

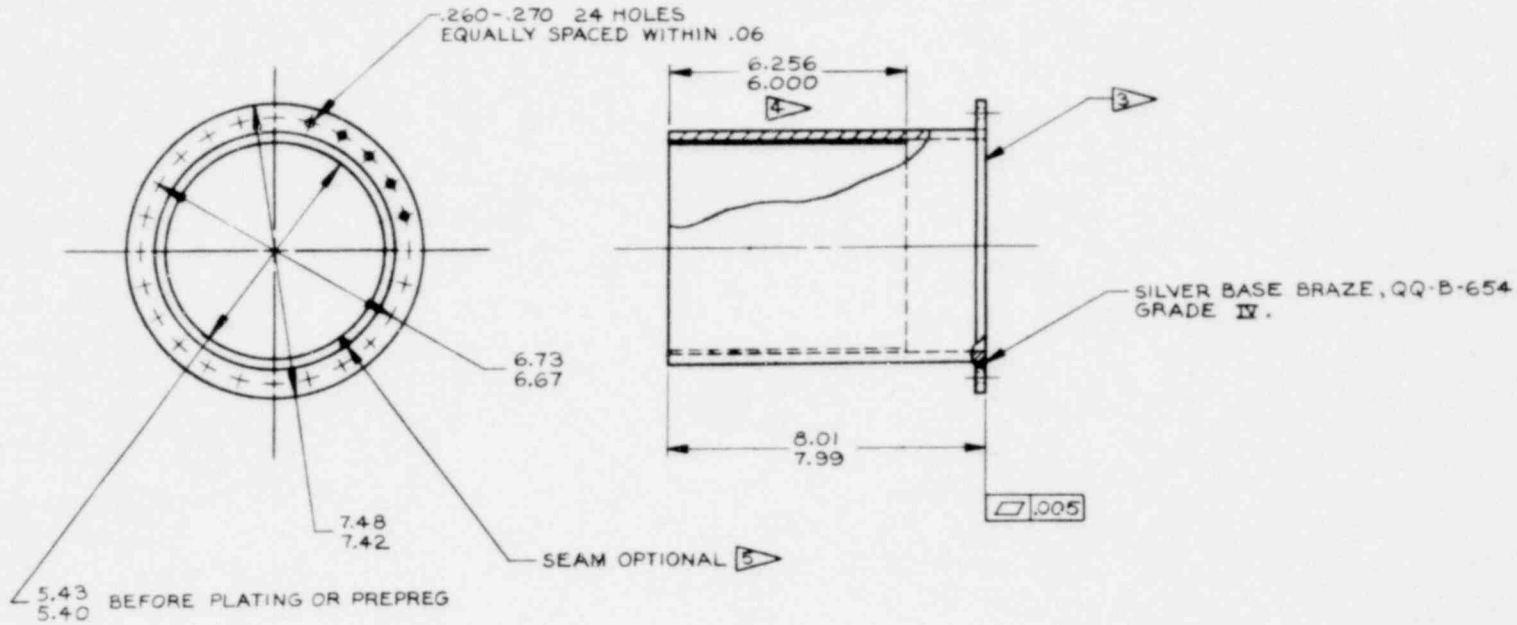
DESIGN AGENCY PART NUMBER	BENDIS PART NUMBER	ARMY CLASSIFICATION

NOTES

- MATERIAL: .25 INCH COPPER STOCK, NUMBER 110 ETP, PER QQ-C-576.
- CADMIUM PLATE AFTER DRILLING PER QQ-P-416, TYPE I, FULL COVERAGE ALL OVER.
- CADMIUM PLATE PER QQ-P-416, TYPE I, CLASS I MIN. THICKNESS REQUIRED ON THIS SURFACE.
- AFTER CAD. PLATE, LINE INSIDE WITH FIBERGLASS-EPOXY PREPREG, TYPE 120 FERROCORDO, CE 3201, .007 THICK, AS PURCHASED FROM FERRO CORP, CULVER CITY, CALIF., OR APPROVED EQUIVALENT 100% ADHESION REQUIRED.
- GTAW USING COMMERCIALY PURE COPPER WIRE.

6. GENERAL REQUIREMENTS PER SS-RO0645.

DESIGN AGENCY PART IDENTIFICATION NO.	DESCRIPTION	PREPARED BY	DATE	CHKD	ENGR
RO0615-000	A STEWART 557BX/LANDEPSEN 5433E.MATCHETT 323		9/76		
	B REVISED NOTES & FLAG NOS.		2/77		
	DER 770434 SC				



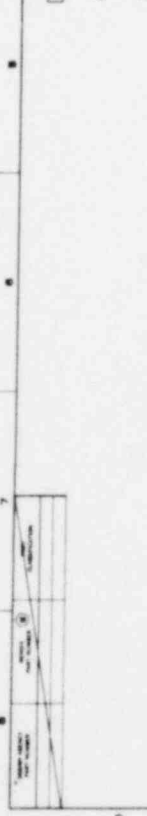
AGENCY APPROVALS		SHEET	TITLE	
DATE	INITIALS	NO. 5	TUBE, HEAT CONDUCTOR	
9/76	SM	UNCLASSIFIED		
2/77	SM	UNCLASSIFIED	SCALE 1/2"	SHEET 1 OF 1

DER 770434 SC
DRC 5
RO0615

DATE	DESCRIPTION	BY	CHKD
10/11/51	DESIGN	W. J. J.	
10/11/51	REVISION		
A	DESIGN BY STEPHEN W. J. J. / ANGERSMAN		
B	ADDED NOTE 6.		
	USE R 7704 54 5C.		

NOTES

1. COAT INDICATED BY RALES PER PS R00602-000.
2. MATERIAL: CLEAR PIEDWOOD, FINISHED PER PS R00602-000.
3. BOND PER PS R00602-000 USING MAM-A-180.
4. STAGGER ALL GLUE JOINTS.
5. TYING: STACK UP MINIMUM 2-4 STOCK MACHINE ALL SURFACES.
6. GENERAL REQUIREMENTS PER PS R00645.



DATE	DESCRIPTION	BY	CHKD
10/11/51	DESIGN	W. J. J.	
10/11/51	REVISION		
A	DESIGN BY STEPHEN W. J. J. / ANGERSMAN		
B	ADDED NOTE 6.		
	USE R 7704 54 5C.		

DATE	DESCRIPTION	BY	CHKD
10/11/51	DESIGN	W. J. J.	
10/11/51	REVISION		
A	DESIGN BY STEPHEN W. J. J. / ANGERSMAN		
B	ADDED NOTE 6.		
	USE R 7704 54 5C.		

DATE	DESCRIPTION	BY	CHKD
10/11/51	DESIGN	W. J. J.	
10/11/51	REVISION		
A	DESIGN BY STEPHEN W. J. J. / ANGERSMAN		
B	ADDED NOTE 6.		
	USE R 7704 54 5C.		

DATE	DESCRIPTION	BY	CHKD
10/11/51	DESIGN	W. J. J.	
10/11/51	REVISION		
A	DESIGN BY STEPHEN W. J. J. / ANGERSMAN		
B	ADDED NOTE 6.		
	USE R 7704 54 5C.		

DATE	DESCRIPTION	BY	CHKD
10/11/51	DESIGN	W. J. J.	
10/11/51	REVISION		
A	DESIGN BY STEPHEN W. J. J. / ANGERSMAN		
B	ADDED NOTE 6.		
	USE R 7704 54 5C.		

DATE	DESCRIPTION	BY	CHKD
10/11/51	DESIGN	W. J. J.	
10/11/51	REVISION		
A	DESIGN BY STEPHEN W. J. J. / ANGERSMAN		
B	ADDED NOTE 6.		
	USE R 7704 54 5C.		

DATE	DESCRIPTION	BY	CHKD
10/11/51	DESIGN	W. J. J.	
10/11/51	REVISION		
A	DESIGN BY STEPHEN W. J. J. / ANGERSMAN		
B	ADDED NOTE 6.		
	USE R 7704 54 5C.		

DATE	DESCRIPTION	BY	CHKD
10/11/51	DESIGN	W. J. J.	
10/11/51	REVISION		
A	DESIGN BY STEPHEN W. J. J. / ANGERSMAN		
B	ADDED NOTE 6.		
	USE R 7704 54 5C.		

DATE	DESCRIPTION	BY	CHKD
10/11/51	DESIGN	W. J. J.	
10/11/51	REVISION		
A	DESIGN BY STEPHEN W. J. J. / ANGERSMAN		
B	ADDED NOTE 6.		
	USE R 7704 54 5C.		

DATE	DESCRIPTION	BY	CHKD
10/11/51	DESIGN	W. J. J.	
10/11/51	REVISION		
A	DESIGN BY STEPHEN W. J. J. / ANGERSMAN		
B	ADDED NOTE 6.		
	USE R 7704 54 5C.		

1568 039

379

020 844

DESIGN AGENCY PART NUMBER	BENDS PART NUMBER	DMS CLASSIFICATION	NOTES	DESIGN AGENCY PART NUMBER R00617 000	REV. DESCRIPTION A D. STEWART 557BX/J. ANDERSEN 5433'E. MATCHETTE B238X B ADDED NOTE 4. DER 770434 SC <i>Revised 3-5-77 W</i>									
			<p>1. TYPICAL STACK UP, MINIMUM 2X6 STOCK. MACHINE ALL SURFACES.</p> <p>2. MATERIAL: CLEAR REDWOOD, KILN DRIED PER SS-R00602-000.</p> <p>3. BOND PER PS-R00602-000 USING MMM-A-180.</p> <p>4. GENERAL REQUIREMENTS PER SS-R00645.</p>		<table border="1" style="width:100%; border-collapse: collapse;"> <tr> <th>DATE</th> <th>CHKD</th> <th>ENGR</th> </tr> <tr> <td>8-76</td> <td><i>[Signature]</i></td> <td><i>[Signature]</i></td> </tr> <tr> <td>2/77</td> <td><i>[Signature]</i></td> <td><i>[Signature]</i></td> </tr> </table>	DATE	CHKD	ENGR	8-76	<i>[Signature]</i>	<i>[Signature]</i>	2/77	<i>[Signature]</i>	<i>[Signature]</i>
DATE	CHKD	ENGR												
8-76	<i>[Signature]</i>	<i>[Signature]</i>												
2/77	<i>[Signature]</i>	<i>[Signature]</i>												

GRAIN ORIENTATION

2.94
2.88

END GRAIN

5.31
5.28

LA0020

-B-

AGENCY APPROVALS		SHEET	TITLE
DATE	INITIALS	OF	PLUG, WOOD, FIXED
12/25/76	<i>[Signature]</i>	1	
1/25/77	<i>[Signature]</i>		
CLASSIFICATION LEVEL		REV. NO.	REV. DATE
UNCLASSIFIED		C	12/13
		REV. NO.	REV. DATE
		1/2	
		SHEET	OF

DRC 5 | R00617



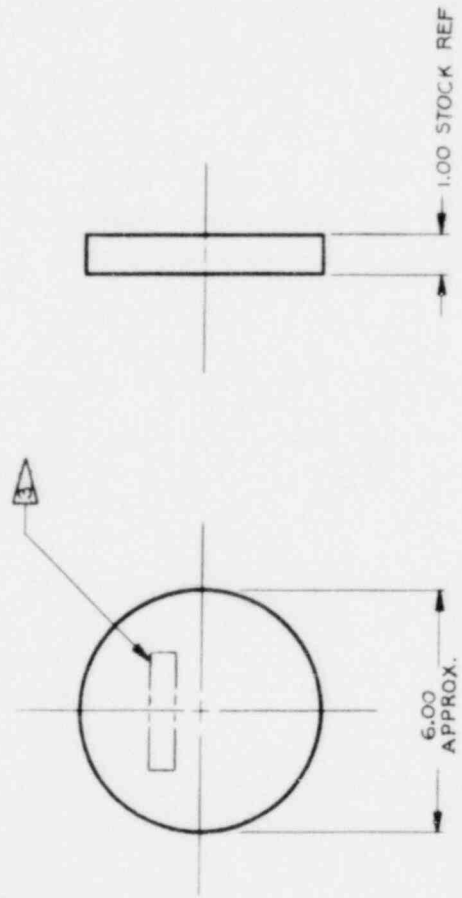
GROUP AGENCY PART NUMBER	GROUP AGENCY PART NUMBER	DESCRIPTION	DATE	BY
R00639-000	A	LANE 557BX/JANDERSEN 5439/ E.MATCHETTE 8239X DER 770434 SC	2/77	JW

NOTES

- MATERIAL: CERABLANKET, 8LB DENSITY X 1.00 THICK, AVAILABLE AT RENLER CO., INC., 5401 PRINCE ST, BOX 1220, LITTLETON, CO., 80120.
- GENERAL REQUIREMENTS PER SS-R00645.



INK STAMP PART NO. APPROX. AS SHOWN, EXCEPT NO COVER COAT REQUIRED.



DWG 5

R00639

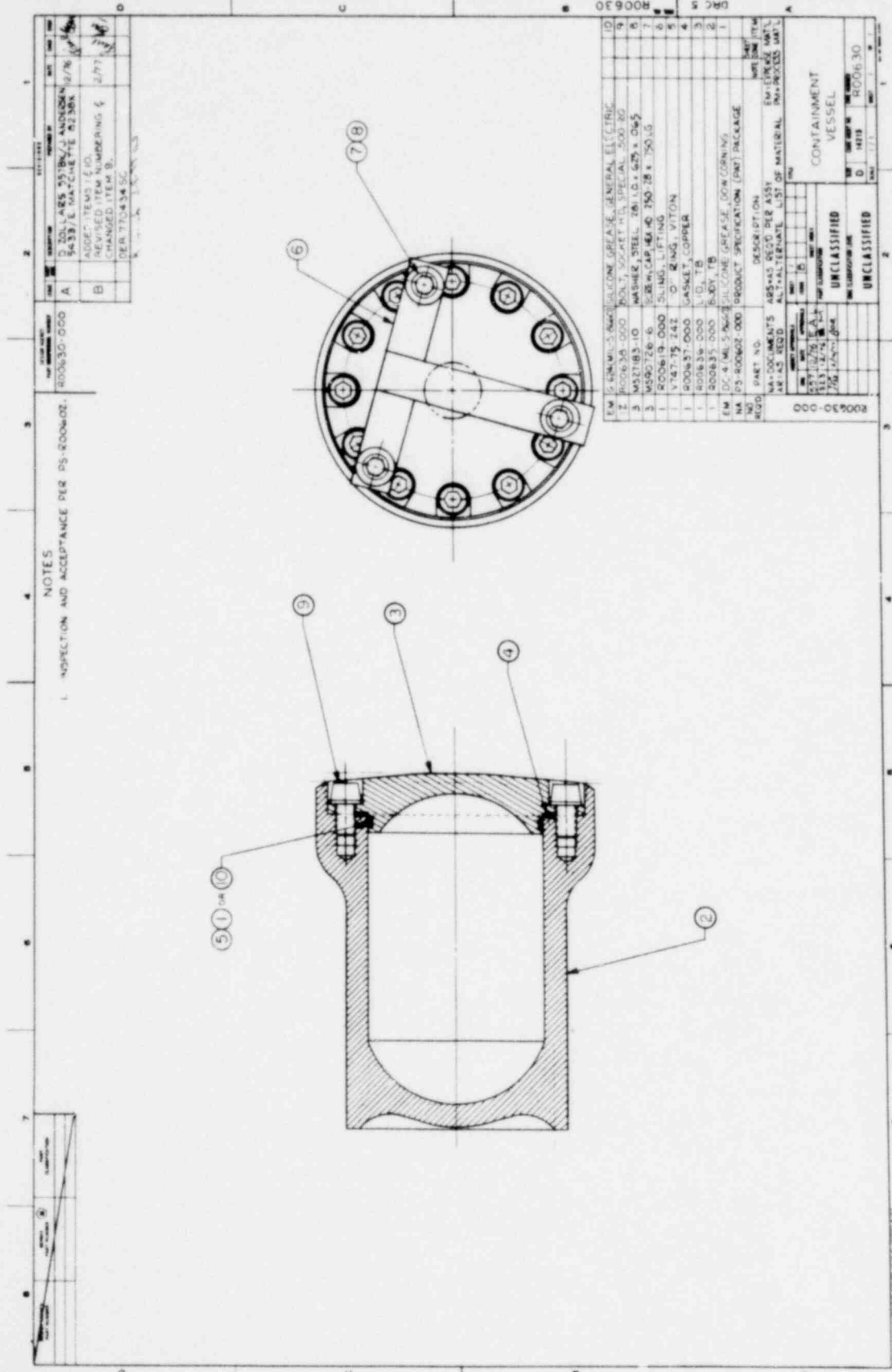
GROUP AGENCY PART NUMBER	GROUP AGENCY PART NUMBER	DESCRIPTION	DATE	BY
R00639-000	A	LANE 557BX/JANDERSEN 5439/ E.MATCHETTE 8239X DER 770434 SC	2/77	JW

PAD, INSULATION

UNCLASSIFIED

UNCLASSIFIED

1568 041



REV	DATE	DESCRIPTION
1	10/10/50	ISSUED FOR FABRICATION
2	11/15/50	REVISIONS
3	12/15/50	REVISIONS
4	1/15/51	REVISIONS
5	2/15/51	REVISIONS

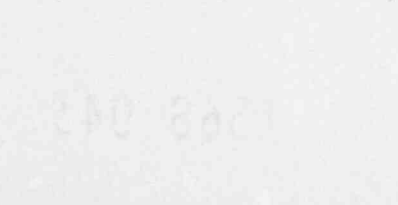
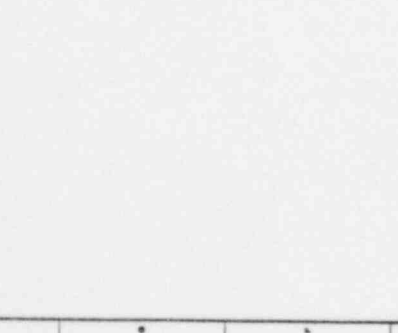
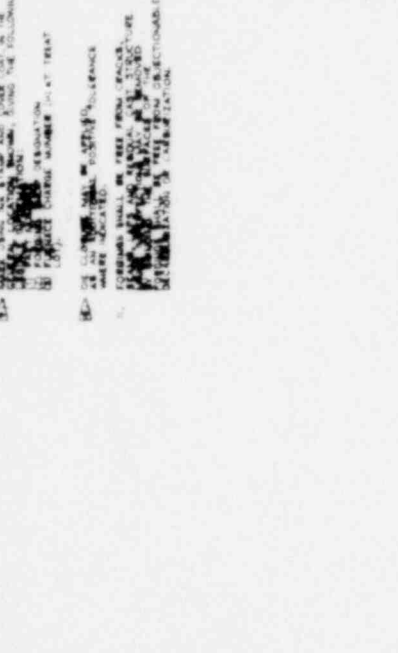
NOTES
 1. MATERIAL, FORM AND FINISH SPECIFICATIONS SHALL BE AS SHOWN ON DRAWING. ALL WORK SHALL BE DONE IN ACCORDANCE WITH THE BOARD'S SPECIFICATIONS.
 2. DIMENSIONS SHALL BE IN INCHES UNLESS OTHERWISE SPECIFIED.
 3. ALL DIMENSIONS SHALL BE TO UNLESS OTHERWISE SPECIFIED.
 4. ALL DIMENSIONS SHALL BE TO UNLESS OTHERWISE SPECIFIED.
 5. ALL DIMENSIONS SHALL BE TO UNLESS OTHERWISE SPECIFIED.

1. HEAT TREATMENT SPECIFICATIONS SHALL BE AS SHOWN ON DRAWING. ALL WORK SHALL BE DONE IN ACCORDANCE WITH THE BOARD'S SPECIFICATIONS.
 2. DIMENSIONS SHALL BE IN INCHES UNLESS OTHERWISE SPECIFIED.
 3. ALL DIMENSIONS SHALL BE TO UNLESS OTHERWISE SPECIFIED.
 4. ALL DIMENSIONS SHALL BE TO UNLESS OTHERWISE SPECIFIED.

5. ALL DIMENSIONS SHALL BE TO UNLESS OTHERWISE SPECIFIED.
 6. ALL DIMENSIONS SHALL BE TO UNLESS OTHERWISE SPECIFIED.
 7. ALL DIMENSIONS SHALL BE TO UNLESS OTHERWISE SPECIFIED.
 8. ALL DIMENSIONS SHALL BE TO UNLESS OTHERWISE SPECIFIED.

9. ALL DIMENSIONS SHALL BE TO UNLESS OTHERWISE SPECIFIED.
 10. ALL DIMENSIONS SHALL BE TO UNLESS OTHERWISE SPECIFIED.
 11. ALL DIMENSIONS SHALL BE TO UNLESS OTHERWISE SPECIFIED.
 12. ALL DIMENSIONS SHALL BE TO UNLESS OTHERWISE SPECIFIED.

13. ALL DIMENSIONS SHALL BE TO UNLESS OTHERWISE SPECIFIED.
 14. ALL DIMENSIONS SHALL BE TO UNLESS OTHERWISE SPECIFIED.
 15. ALL DIMENSIONS SHALL BE TO UNLESS OTHERWISE SPECIFIED.



REV	DATE	DESCRIPTION
1	10/10/50	ISSUED FOR FABRICATION
2	11/15/50	REVISIONS
3	12/15/50	REVISIONS
4	1/15/51	REVISIONS
5	2/15/51	REVISIONS

NOTES
 1. MATERIAL, FORM AND FINISH SPECIFICATIONS SHALL BE AS SHOWN ON DRAWING. ALL WORK SHALL BE DONE IN ACCORDANCE WITH THE BOARD'S SPECIFICATIONS.
 2. DIMENSIONS SHALL BE IN INCHES UNLESS OTHERWISE SPECIFIED.
 3. ALL DIMENSIONS SHALL BE TO UNLESS OTHERWISE SPECIFIED.
 4. ALL DIMENSIONS SHALL BE TO UNLESS OTHERWISE SPECIFIED.

5. ALL DIMENSIONS SHALL BE TO UNLESS OTHERWISE SPECIFIED.
 6. ALL DIMENSIONS SHALL BE TO UNLESS OTHERWISE SPECIFIED.
 7. ALL DIMENSIONS SHALL BE TO UNLESS OTHERWISE SPECIFIED.
 8. ALL DIMENSIONS SHALL BE TO UNLESS OTHERWISE SPECIFIED.

9. ALL DIMENSIONS SHALL BE TO UNLESS OTHERWISE SPECIFIED.
 10. ALL DIMENSIONS SHALL BE TO UNLESS OTHERWISE SPECIFIED.
 11. ALL DIMENSIONS SHALL BE TO UNLESS OTHERWISE SPECIFIED.
 12. ALL DIMENSIONS SHALL BE TO UNLESS OTHERWISE SPECIFIED.

13. ALL DIMENSIONS SHALL BE TO UNLESS OTHERWISE SPECIFIED.
 14. ALL DIMENSIONS SHALL BE TO UNLESS OTHERWISE SPECIFIED.
 15. ALL DIMENSIONS SHALL BE TO UNLESS OTHERWISE SPECIFIED.

16. ALL DIMENSIONS SHALL BE TO UNLESS OTHERWISE SPECIFIED.
 17. ALL DIMENSIONS SHALL BE TO UNLESS OTHERWISE SPECIFIED.
 18. ALL DIMENSIONS SHALL BE TO UNLESS OTHERWISE SPECIFIED.

REV	DATE	BY	APP
1	10/1/54
2
3

NOTES

1. MATERIAL: 15-20 PHOSPHOR BRONZE, C15200, UNSPECIFIED GRADE, 15% PHOSPHOR, 20% COPPER, BALANCE BRONZE.

2. FINISH: ALL SURFACES TO BE FINISHED TO A 63 R.M.S. FINISH UNLESS OTHERWISE SPECIFIED.

3. DIMENSIONS: ALL DIMENSIONS ARE IN INCHES UNLESS OTHERWISE SPECIFIED.

4. TOLERANCES: UNLESS OTHERWISE SPECIFIED, TOLERANCES SHALL BE AS FOLLOWS:

5. SURFACE FINISH: UNLESS OTHERWISE SPECIFIED, ALL SURFACES SHALL BE FINISHED TO A 63 R.M.S. FINISH.

6. MARKING: THE PART SHALL BE MARKED WITH THE PART NUMBER AND THE DATE OF MANUFACTURE.

7. INSPECTION: THE PART SHALL BE INSPECTED AND FOUND TO CONFORM TO THE DRAWING BEFORE BEING ACCEPTED FOR DELIVERY.

1. HEAT TREATMENT: SOLUTION ANNEAL AT 1000°F FOR 1 HOUR, WATER COOL, AND STRESS RELIEF AT 600°F FOR 1 HOUR.

2. DIMENSIONS: ALL DIMENSIONS ARE IN INCHES UNLESS OTHERWISE SPECIFIED.

3. TOLERANCES: UNLESS OTHERWISE SPECIFIED, TOLERANCES SHALL BE AS FOLLOWS:

4. SURFACE FINISH: UNLESS OTHERWISE SPECIFIED, ALL SURFACES SHALL BE FINISHED TO A 63 R.M.S. FINISH.

5. MARKING: THE PART SHALL BE MARKED WITH THE PART NUMBER AND THE DATE OF MANUFACTURE.

6. INSPECTION: THE PART SHALL BE INSPECTED AND FOUND TO CONFORM TO THE DRAWING BEFORE BEING ACCEPTED FOR DELIVERY.

1. MATERIAL: 15-20 PHOSPHOR BRONZE, C15200, UNSPECIFIED GRADE, 15% PHOSPHOR, 20% COPPER, BALANCE BRONZE.

2. FINISH: ALL SURFACES TO BE FINISHED TO A 63 R.M.S. FINISH UNLESS OTHERWISE SPECIFIED.

3. DIMENSIONS: ALL DIMENSIONS ARE IN INCHES UNLESS OTHERWISE SPECIFIED.

4. TOLERANCES: UNLESS OTHERWISE SPECIFIED, TOLERANCES SHALL BE AS FOLLOWS:

5. SURFACE FINISH: UNLESS OTHERWISE SPECIFIED, ALL SURFACES SHALL BE FINISHED TO A 63 R.M.S. FINISH.

6. MARKING: THE PART SHALL BE MARKED WITH THE PART NUMBER AND THE DATE OF MANUFACTURE.

7. INSPECTION: THE PART SHALL BE INSPECTED AND FOUND TO CONFORM TO THE DRAWING BEFORE BEING ACCEPTED FOR DELIVERY.

1. MATERIAL: 15-20 PHOSPHOR BRONZE, C15200, UNSPECIFIED GRADE, 15% PHOSPHOR, 20% COPPER, BALANCE BRONZE.

2. FINISH: ALL SURFACES TO BE FINISHED TO A 63 R.M.S. FINISH UNLESS OTHERWISE SPECIFIED.

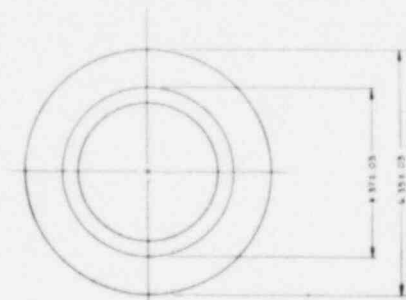
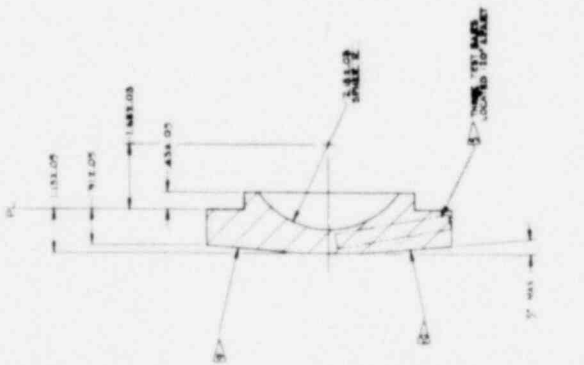
3. DIMENSIONS: ALL DIMENSIONS ARE IN INCHES UNLESS OTHERWISE SPECIFIED.

4. TOLERANCES: UNLESS OTHERWISE SPECIFIED, TOLERANCES SHALL BE AS FOLLOWS:

5. SURFACE FINISH: UNLESS OTHERWISE SPECIFIED, ALL SURFACES SHALL BE FINISHED TO A 63 R.M.S. FINISH.

6. MARKING: THE PART SHALL BE MARKED WITH THE PART NUMBER AND THE DATE OF MANUFACTURE.

7. INSPECTION: THE PART SHALL BE INSPECTED AND FOUND TO CONFORM TO THE DRAWING BEFORE BEING ACCEPTED FOR DELIVERY.

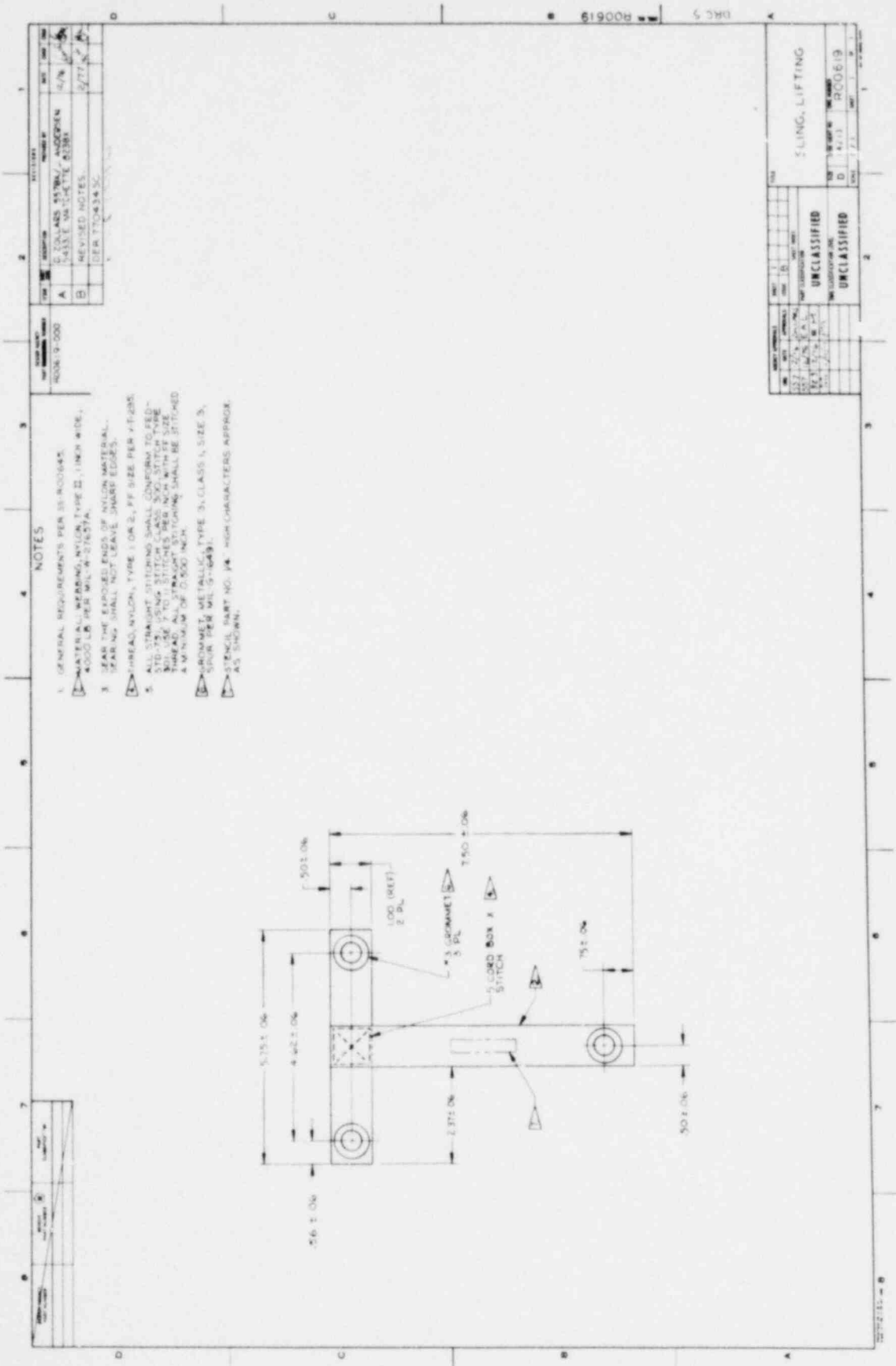


REV	DATE	BY	APP
1	10/1/54
2
3

FORGING, 15 L10

DECLASSIFIED

DECLASSIFIED



REV	DESCRIPTION	DATE	BY	CHK
A	5. CLASS 15 NYLON, UNOPENED INSIDE 1/4 INCH WIDE BEBET	4/78		
B	REVISED NOTES. DER 7704343C.	3/77		

REV	DESCRIPTION	DATE	BY	CHK
UNCLASSIFIED				
UNCLASSIFIED				
SLING, LIFTING				
D 4/13 1000000				
D 4/13 1000000				

ROOM 5 100619

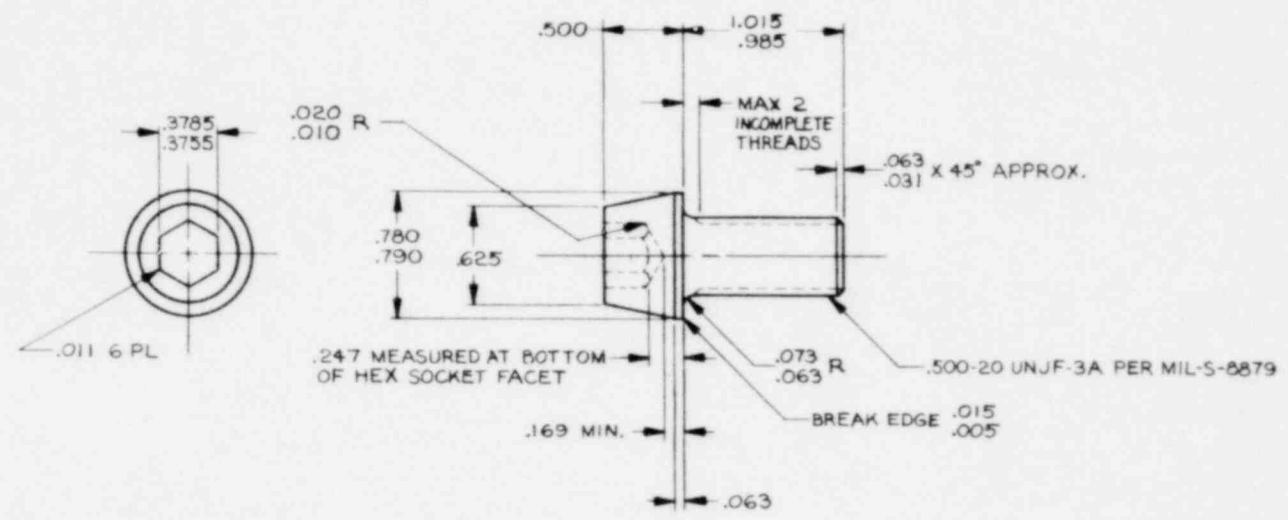
DESIGN AGENCY PART NUMBER	BENDIX PART NUMBER	PART CLASSIFICATION

NOTES

7. BREAK SHARP EDGES .003-.015 X 45°
8. CHAMFER PLUS INCOMPLETE THREADS NOT TO EXCEED 2 PITCHES.
9. DIMENSIONS IN INCHES.

1. MATERIAL: A-286 PER AMS 5731.
2. HEAT TREAT: 180 KSI BOLT TENSILE STRENGTH, RC 36 MIN.
3. FINISH: SILVER PLATE PER AMS 2410.
4. CONCENTRICITY: HEAD DIAMETER TO BE CONCENTRIC TO THE THREAD PITCH DIA. WITHIN .010 T.I.R. SOCKET TO BE CONCENTRIC WITH HEAD DIA. WITHIN .012 T.I.R.
5. SURFACE TEXTURE: PER ANSI B46.1 UNLESS OTHERWISE SPECIFIED, THE SURFACE TEXTURE SHALL NOT EXCEED 125 MICROINCHES.
6. MECHANICAL PROPERTIES: RATED ULTIMATE TENSILE STRENGTH IS 30000 LBS. DOUBLE SHEAR REQUIREMENTS ARE NOT APPLICABLE. TENSILE TESTING SHALL BE PERFORMED USING A TENSILE BAR ENGAGED AS FULLY AS POSSIBLE. FATIGUE TESTING IS WAIVED.

DESIGN AGENCY PART OR CONTROL NO.	REV#	DESCRIPTION	PREPARED BY	DATE	CHKD	ENGR
R00638-000	A	LANE 557BX/JANDERSEN 5433/ E.MATCHETTE 823BX		2/77		
		DER 770434 SC				



1568 049

389

DWG. NO. R00638
DRC 5

AGENCY APPROVALS		SHEET	TITLE
DATE	INITIALS	NO. OF SHEETS	BOLT, SOCKET HD, SPECIAL .500-20
DATE	INITIALS	NO. OF SHEETS	
UNCLASSIFIED		UNCLASSIFIED	SCALE 2/1
UNCLASSIFIED		UNCLASSIFIED	SHEET 1 OF 1

DESIGN AGENCY PART NUMBER	REVISIONS	DATE	BY
RO0631-000	A	2/77	[Signature]
DESCRIPTION LANE 557BX/LANDERSEN 5433/ E. MATCHETTE 823 BX DER 770434 SC			

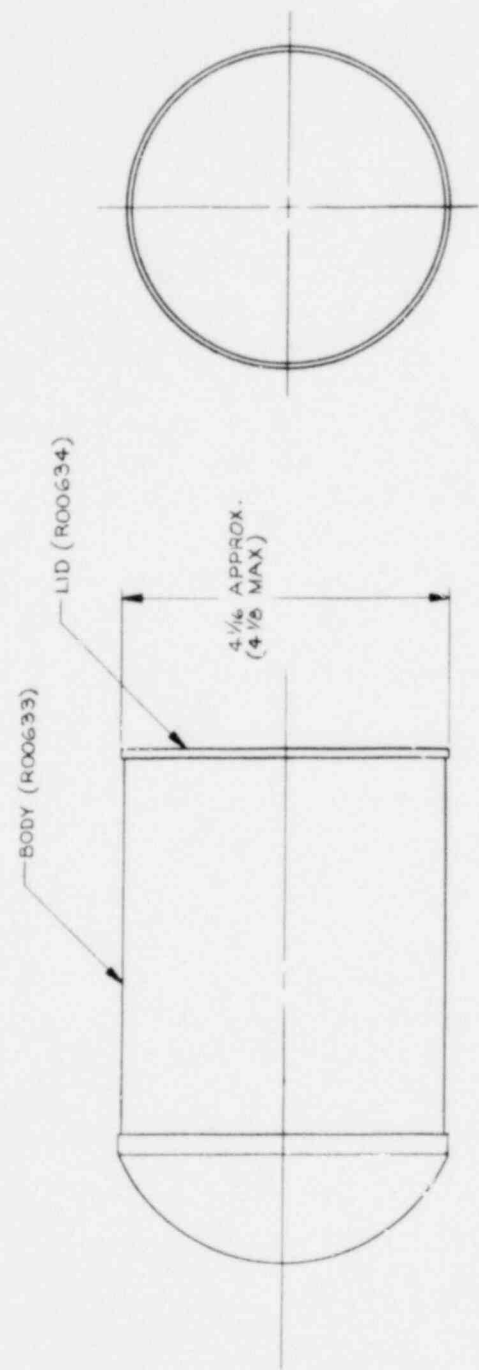
DESIGN AGENCY PART NUMBER	REVISIONS	DATE	BY
RO0631-000	A	2/77	[Signature]

NOTES

1. THIS DRAWING IS INTENDED TO BE USED FOR ASSEMBLY INFORMATION ONLY, FOLLOWING INSERTION OF CONTENTS INTO THE CAN BODY.

2. ASSEMBLE CAN LID, PART NO. RO0634, TO CAN BODY, PART NO. RO0633, IN A SECURE & WORK-MANLIKE MANNER, USING A CONVENTIONAL DOUBLE ACTION CANNING TOOL OR MACHINE.

DESIGN AGENCY PART NUMBER	REVISIONS	DATE	BY
RO0631-000	A	2/77	[Signature]



DESIGN AGENCY PART NUMBER	REVISIONS	DATE	BY
RO0631-000	A	2/77	[Signature]
DESCRIPTION LANE 557BX/LANDERSEN 5433/ E. MATCHETTE 823 BX DER 770434 SC			

DESIGN AGENCY PART NUMBER	REVISIONS	DATE	BY
RO0631-000	A	2/77	[Signature]
DESCRIPTION LANE 557BX/LANDERSEN 5433/ E. MATCHETTE 823 BX DER 770434 SC			

DRG NO R00631

CAN ASSEMBLY

UNCLASSIFIED

UNCLASSIFIED

1568 051

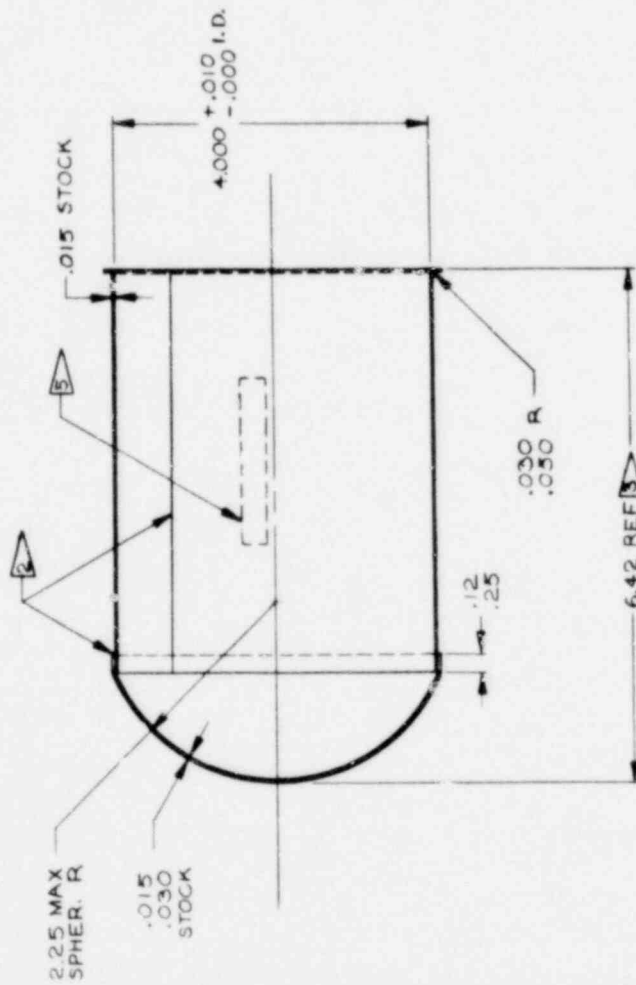
1288-001

DESIGN AGENCY PART NUMBER	REVISED PART NUMBER	CLASSIFICATION	DATE	BY	CHKD
RO0633-000	RO0633-000		12/76		
REVISIONS			DATE	BY	CHKD
A LANE 557 BX/JANDERSEN 5433/ E.MATCHETTE 823BX DER 770434 SC			8/77	Hand	
B LANE 557 BX/JANDERSEN 5433/ E.MATCHETTE 823BX 774255 BX DEY I. REVISED PHOTO 5 & PART MARKING OUTLINE. 2. 4.250 ± .010 WAS 4.25 APPROX. 3. 4.000 ± .008 I.D. WAS 4.00 MIN I.D. 4. .030 ± .005 R WAS .015 MAX R. 5. 6.42 REF FLAG 3 WAS FLAG 3. 6. DELETED NOTE 4.					

NOTES

- MATERIAL: CORROSION RESISTANT STEEL TYPE 304 PER QQ-S-769.
- SEAM OPTIONAL, BEAM WELD OR SILVER SOLDER.
- THIS DIMENSION TO BE SUCH THAT WHEN THE LID IS ROLLED ON, THE DISTANCE FROM THE OUTSIDE OF THE SPHER. END TO THE OUTSIDE OF THE LID FLAT, REF RO0634, WILL BE 6.30 TO 6.33.

INK STAMP PART NO. & COVERCOAT APPROX. AS SHOWN, ON OUTSIDE SURFACE.



DRG 5 R00633

DESIGN AGENCY PART NUMBER	REVISED PART NUMBER	CLASSIFICATION	DATE	BY	CHKD
RO0633-000	RO0633-000		12/76		
REVISIONS			DATE	BY	CHKD
A LANE 557 BX/JANDERSEN 5433/ E.MATCHETTE 823BX DER 770434 SC			8/77	Hand	
B LANE 557 BX/JANDERSEN 5433/ E.MATCHETTE 823BX 774255 BX DEY I. REVISED PHOTO 5 & PART MARKING OUTLINE. 2. 4.250 ± .010 WAS 4.25 APPROX. 3. 4.000 ± .008 I.D. WAS 4.00 MIN I.D. 4. .030 ± .005 R WAS .015 MAX R. 5. 6.42 REF FLAG 3 WAS FLAG 3. 6. DELETED NOTE 4.					

BCDY, CAN

UNCLASSIFIED

UNCLASSIFIED

14213

14213

UNCLASSIFIED

UNCLASSIFIED

1288-001

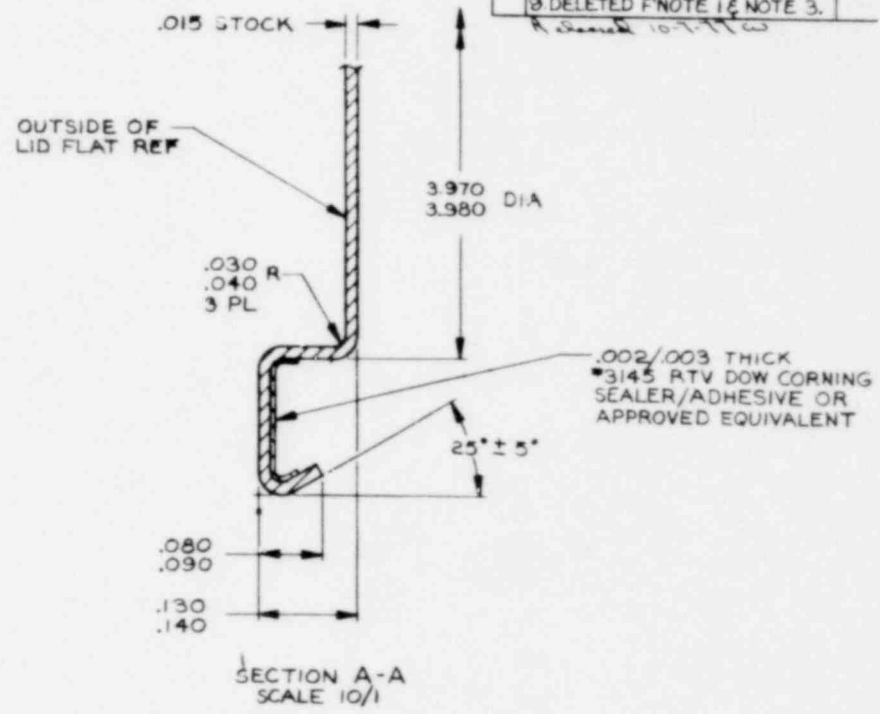
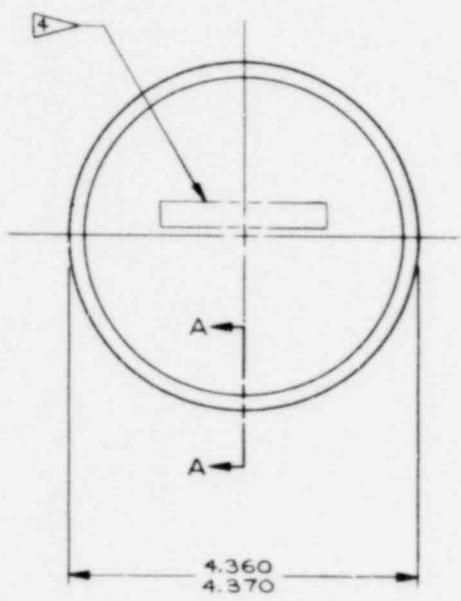
DESIGN AGENCY PART NUMBER	DESIGN PART NUMBER	PART CLASSIFICATION

NOTES

1. INK STAMP PART NO. & COVERCOAT APPROX. AS SHOWN.

2. MATERIAL: CORROSION RESISTANT STEEL TYPE 304 PER QQ-S-766.

ITEM NO.	DESCRIPTION	PREPARED BY	DATE	CHKD	APPD
001	LANE 557/J.ANDERSEN 5433/ E.MATCHETTE 823 BX DER 770434 SC		2/77		
002	LANE 557 BX/J.ANDERSEN 5433/ E.MATCHETTE 823 BX 774256 BX DEV		8/77		



SECTION A-A
SCALE 10/1

DRC 5
REV # RO0634

1568 053

393-394

AGENCY APPROVALS	SHEET	TITLE
DESIGNED BY: J.A.A. DRAWN BY: J.A.A. CHECKED BY: J.A.A.	SHEET: A PART CLASSIFICATION: UNCLASSIFIED THIS CLASSIFICATION IS: UNCLASSIFIED	TITLE: LID, CAN QTY: C UNIT: 14213 PART NO: R00634

APPENDIX 9B



**Kansas City
Division**

December 11, 1977

TO: John Andersen
Organization 5433
Sandia Laboratories

FROM: E. E. Matchette

SUBJ: Certification of Compliance - PAT Assembly - R00602


RE: SLA Order No. 05-3057 for twenty-four (24) R00602 Pat Assemblies

DRAWINGS: LD-R00602


REQUIREMENTS: PS - R00602 - Product Specification, Plutonium Air
Transportable (PAT) Package
SS - R00602 - Material Specifications, Redwood for
PAT Package
SS - R00630 - Testing Leak Rate, Mass Spectrometer,
PAT Package
SS - R00645 - General Requirements, PAT Package
SS - R00621 - Welding Corrosion Resistant Steel, PAT
Package

EXCEPTIONS: Specification exceptions for PAT Package per SE-001,
SE-002, SE-003, SE-004, SE-005, SE-006 and SE-007

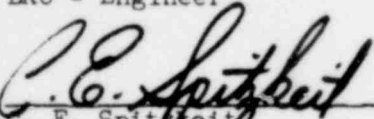
PAT Packages, Units 101 thru 124, inclusive are hereby certified to
conform to all requirements and drawings as set forth above except
for deviations as listed in Specification Exceptions SE-001 through
SE-007.



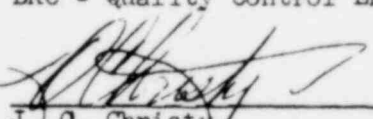
E. E. Matchette
BKC - Engineer



W. D. Schultz
BKC - Quality Control Engineer



C. E. Spitzke
BKC - Engineering Supervisor



J. O. Christy
BKC - Quality Control Supervisor

ATT: SE-001 thru SE-007

1568 054

DISTRIBUTION:

US Nuclear Regulatory Commission
(246 copies for RT)
Division of Document Control
Distribution Services Branch
7920 Norfolk Avenue
Bethesda, MD 20014

US Nuclear Regulatory Commission (10)
Washington, DC 20555
Attn: W. Laha (5)
Office of Nuclear Regulatory Research
Div. of Safeguards, Fuel Cycle, and
Environmental Research
C. E. Macdonald (5)
Office of Nuclear Material Safety and
Safeguards
Div. of Fuel Cycle and Material Safety

Los Alamos Scientific Laboratory (3)
P. O. Box 1663
Los Alamos, NM 87545
Attn: D. R. Smith
Nuclear Criticality Safety Officer
R. J. Batholomew, WX-8
G. W. Meinze, SP-4

Dr. D. Sellinschegg
Head, Physical Protection R&D
Nuclear Research Center
Fernforschungszentrum
Karlsruhe,
Federal Republic of Germany

Mr. Tetsuo Goto
Nuclear Industry Development Department
Japan Atomic Industrial Forum
No. 1-13, 1-Chome, Shimbashi, Minato-Ku
Tokyo, Japan

Battelle Pacific Northwest Lab
P. O. Box 999
Richland, WA 99352
Attn: L. C. Schwendiman

The Bendix Corporation
Kansas City Division
P. O. Box 1159
Kansas City, MO 64141
Attn: E. E. Matchette

State of New York
Department of Law
Two World Trade Center
New York, NY 10047
Attn: J. Y. Willen

R. A. Blythe
Central Electricity Generating Board
Generation Development and Consultation Div.
Barnwood
Gloucester
England

K. R. Shultz
Atomic Energy Control Board
P. O. Box 1046
Ottawa, Canada
KIP 5S9

R. S. Butterfield
United Kingdom Atomic Energy Authority
Risley Nuclear Power Development
Establishment
Warrington
Cheshire
WA36AT
England

C. B. G. Taylor MA
Manager, Isotope Production Unit
The Radiochemical Centre
Amersham
Buckinghamshire
England

Pierre Grandperret
C. E. N. Fontenay
Departement de Securite des Matieres
Nucleaires
B. P. No. 6 - 92260 Fontenay Aux Roses
France

A. Cricchio
Commission of the European Communities
DG XII - D-1
200 Rue de la Loi
1049 Brussels
Belgium

P. Rocco
Commission of the European Community
Joint Research Center
ISPRA Establishment
21020 ISPRA (VA)
Italy

J. L. Ridihaigh, President
Ridihaigh, Eggers, & Associates
Nuclear and Thermal Energy Systems Consultants
2112 Iuka Ave.
Columbus, OH 43201

Dr. Kazuo Ikeda
General Manager, Structural Engineering Lab
Kobe Steel, Ltd.
Doi - Cho
Amagasaki
Japan

Nuclear Fuel Services, Inc.
P. O. Box 218
Erwin, TN 37650
Attn: A. Maxin

DISTRIBUTION: (Cont)

A. Onodera
Manager, Nuclear Design
Hitachi Co., Ltd.
3-40 Sakurajima 1-Chome
Konohana-Ku
Osaka
Japan

Yoshikuni Fujise
Project Manager, Development Department
Mitsubishi Heavy Industries, Ltd.
5-1 Marunouchi, 2-Chome, Chiyoda-Ku
Tokyo 100
Japan

Osamu Terada
Headquarters, Technical Research and
Development Lab.
Applied Mechanics Research Station, Tamano
Mitsui Engineering & Shipbuilding Co., Ltd.
Tamano Works
16-1 Tamahara 3-Chome, Tamano
Okayama - Pref.
Japan

MSCE. Yasuro Maki
Senior Researcher
Civil Engineering Laboratory
Central Research Institute of Electric Power
Industry
1646, Abiko City
Chiba
Japan

Saburo Sakamaki
Supervising Sales Engineer
Special Representative Office
Mitsui Engineering & Shipbuilding Co., Ltd.
Suite 2029, One World Trade Center
New York, NY 10048

John Thomas Daniels
Brookwood
14 Whalley Road
Hal
Cheshire
England

Jean F. Fradin
92, 270 Bois-Colombes
France

Jens Quist
Master Mechanical Engineer
Riso National Laboratory
Fåborgvej 34
DK 4000
Roskilde
Denmark

1282 J. D. McClure
1336 J. K. Cole
5400 A. W. Snyder
5430 R. M. Jefferson (10)
5431 W. A. Von Rieseemann
5433 R. B. Pope (10)
5433 J. A. Andersen (10)
5433 B. J. Joseph
8266 E. A. Aas
3141 T. L. Werner (5)
3151 W. L. Garner (3)
For DOE/TIC (Unlimited Release)
DOE/TIC (25)
(R. P. Campbell, 3172-3)

F1

2

782190281

1568 057